

The design and synthesis of probe molecules to validate the inhibition of epigenetic mechanisms for phenotypic responses

PhD Thesis - 2014

Thomas G Hayhow

Epinova Discovery Performance Unit, GlaxoSmithKline

Department of Pure & Applied Chemistry, University of Strathclyde

Supervised by:

Colin J Suckling



Philip G Humphreys



Declarations of Authenticity and Author's Rights

This thesis is the result of the author's original research. It has been completed by the author and has not been previously submitted for examination which has led to the award of a degree.

The copyright of this thesis belongs to GSK in accordance with the author's contract of employment with GSK under the terms of the United Kingdom Copyright Acts. Due acknowledgement must always be made of the use of any material contained in, or derived from, this thesis.

Signed:

Date:

Thomas Hayhow

Acknowledgements

It is a pleasure to thank those who have made this thesis possible. Without support and encouragement from those around me I never would have got as far as I have.

First of all, I would like to thank Prof. Colin J. Suckling for his guidance and patience in helping me down this academic route after spending a considerable time in industry. His proof reading and supervision from the preliminary to the level I am now have been invaluable.

I am deeply grateful to Dr. Philip G. Humphreys who has been tireless in giving me help at every single level since starting this programme. He has diligently enabled me to think about topics in a more philosophical manner as well as proof reading many drafts. His effort to critique the document and return it to me within days has been superhuman.

I am indebted to all of those within my workgroup who have helped me by making some of the compounds commented on in this thesis. Without you there would not be the breadth of SAR available to me and my time in the laboratory would be much less pleasant: Alex Preston, Jack Brown, Sue Westaway, Jessica Renaux, Neil Garton and Mike Barker, Stephen Atkinson and Katherine Jones. Special thanks go to the students I have supervised who have enabled me to synthesise more compounds than I could do on my own: Matthew Teasdale and Diego Barrios. Special thanks go to Stephen Atkinson and Emmanuel Demont for proof reading and providing comments.

Many thanks go to those in other disciplines who have produced data for me and explained, in simple terms, how the assays work. Also without the X-ray crystallographers and computational chemists much of the SAR could not be understood so my gratitude is extended to them. Individuals at Cellzome ran all of the chemoproteomic experiments that enabled the PCAF programme to be successful.

Finally, I would like to thank my wife Laura. Thank you for being so understanding in my being away from the house or locked in the office and never once complaining. It's not always been easy with getting married, moving house and having Daniel during this time but thank you for letting me take the time to complete this thesis.

1 Abstract

The work described in this thesis concerns the design and synthesis of probe molecules for epigenetic proteins. In many cases, it is unclear what the effect of selective inhibition of epigenetic proteins would achieve in biological systems. This lack of understanding is in part due to the novelty of the area and suitable tool molecules would significantly enable further investigation. Probe molecules have been designed for two epigenetic targets using fragment based drug discovery techniques to grow the templates using structure based design.

For the Jumonji D2 family of enzymes, a pyridopyrimidinone core with poor cellular penetration was grown at two positions to identify hydrogen bonding interactions between the ligand and the protein to increase the potency of the series. This resulted in selective compounds with approximately micromolar cellular activity.

Two chemically distinct templates were investigated to discover probes for the PCAF bromodomain. Phthalazinone compounds were found to be selective for PCAF, although they had poor aqueous solubility. Improving the solubility of the molecules either abolished potency at PCAF or brought in unwanted off-target activity and work on this series was halted. Using a pyridazinone core, probe compounds for the PCAF bromodomain were found starting from an unselective molecule. Through identification of a putative salt bridge interaction, highly selective and potent compounds were accessed and shown to be capable of displacing PCAF from chromatin.

The compounds identified were found to engage their respective targets in cellular systems and are suitable for phenotypic investigation of the inhibition of these epigenetic mechanisms.

Contents

1	Abstract.....	4
2	Abbreviations.....	10
3	Introduction.....	14
3.1	The current state of the pharmaceutical industry.....	14
3.1.1	Screening strategies for drug discovery.....	16
3.1.2	New targets for drug discovery.....	17
3.2	Epigenetics.....	18
3.2.1	Packing of DNA.....	18
3.2.2	The histone code.....	20
3.2.3	Writers.....	20
3.2.4	Readers.....	21
3.2.5	Erasers.....	22
3.2.6	Current epigenetic treatments.....	23
3.3	Target validation challenges.....	23
3.3.1	Properties of chemical probes.....	24
3.3.2	Historical chemical probes.....	26
4	JmjC containing proteins.....	29
4.1.1	Lysine demethylase families.....	30
4.1.2	The function of JmjC domains.....	31
4.1.3	Known inhibitors of JmjC domains.....	33
4.2	Inhibition of JmjD2 lysine demethylases.....	35
4.2.1	Identification of lead molecules.....	36
4.3	Screening cascade.....	39
4.4	Identification of a JmjD2 family hit compound.....	41
4.5	Investigation of 6,7 and 6,5 sized ring systems.....	46
4.5.1	Synthesis of test compounds.....	46

4.5.2	Discussion of SAR of 6,7 and 6,5 sized ring systems and intermediates	48
4.6	Alternative 6,6-bicyclic systems.....	51
4.6.1	Investigation into changes of the pyrimidinone ring.....	51
4.6.2	Movement of Tyr136	55
4.6.3	Investigation into changes of the pyridine ring	56
4.7	Substitution at the 2-position of the pyridopyrimidinone core.....	58
4.7.1	General synthesis.....	58
4.7.2	SAR of pyridopyrimidinone 2-substituted with small aliphatic groups	62
4.8	Substitution at the 2-position of the pyridopyrimidinone core with 6-membered aryl rings.....	64
4.8.1	The synthesis of 5-(4-oxo-3,4-dihydropyrido[3,4- <i>d</i>]pyrimidin-2-yl)picolinamide (4.055)	64
4.8.2	SAR of pyridopyrimidinone 2-substituted with aryl rings.....	66
4.8.3	Biological rationale for the movement observed	70
4.8.4	SAR trend explained by Mode 2	72
4.8.5	H-bonding interactions	73
4.9	Substitution at the 2-position of the pyridopyrimidinone core with H-bond donors and acceptors.....	75
4.9.1	Synthesis of ethers.....	75
4.9.2	Analysis of the SAR of pyridopyrimidinone compounds 2-substituted with H-bond donors and acceptors	77
4.10	8-Substitution of the pyridopyrimidinone core with heteroaryl groups	81
4.10.1	Building the rings	83
4.10.2	Cross coupling methodology	90
4.10.3	SAR of 8-substituted pyridopyrimidinones	101
4.11	2-Substitution of the pyridopyrimidinone core with heteroatoms	105
4.11.1	Synthesis of 2-substituted ether linked pyridopyrimidinones.....	108

4.11.2	Probe compounds for the JmJD2 family	109
4.12	JmJD2 inhibitors conclusion	112
5	PCAF	115
5.1	Protein-protein interactions	115
5.2	Introduction to bromodomains	116
5.2.1	Links between bromodomains and disease.....	121
5.2.2	Small molecule inhibitors of BET bromodomains.....	122
5.1.3	Structural features of BET inhibitors	126
5.3	Inhibiting non-BET family bromodomains	129
5.3.1	Introduction to PCAF.....	132
5.3.2	Screening cascade.....	133
5.3.3	Rationale for achieving BET selectivity	135
5.3.4	Known inhibitors of PCAF	136
5.3.5	Bromodomain assays.....	139
5.3.6	Assay development.....	140
5.3.7	Comparing pIC ₅₀ values across assays	142
5.3.8	Compounds identified from a knowledge based screen	144
5.4	Phthalizinone series	145
5.4.1	Development of a higher yielding route to carboxylic acid 5.027.....	148
5.4.2	Synthesis of phenolic ether 5.032 and aniline 5.033.....	149
5.4.3	Synthesis of substituted benzylamine 5.034	152
5.4.4	Synthesis of benzyl ether 5.035.....	153
5.4.5	Assay results of phthalizinones with alternative linkers.....	154
5.4.6	Synthesis of compounds with amide linkers	155
5.4.7	Addition of solubilising basic groups to the phthalizinone core.....	157
5.4.8	Assay results of phthalizinones with solubilising groups.....	162
5.4.9	Phthalizinone conclusion	163

5.5	Aminopyridazinone series.....	165
5.5.1	Benzylic aminopyridazinones.....	168
5.5.2	Fragments bound to X-ray crystal structure of PCAF	173
5.5.3	Changes at the 2-position of the aminopyridazinone	175
5.5.4	Synthesis of analogues at the 5-position of the 4-methyl-5-aminopyridazinone	178
5.5.5	SAR of analogues at the 5-position of the 4-methyl-5-aminopyridazinone .	182
5.5.6	Variations of the tetrahydroisoquinoline containing 5.105	184
5.5.7	Generation of an improved PCAF assay reagent	191
5.5.8	Improving selectivity.....	195
5.5.9	Basic aminopyridazinones	202
5.5.10	Examination of chiral examples of 3-aminopiperidine and 3-aminoazepane pyridazinones.....	207
5.5.11	Substitution from the 3-piperidine	216
5.6	Selection of tool molecules.....	221
5.7	Further profiling of PCAF probe compounds	227
5.8	Conclusion.....	233
6	Experimental	235
6.1	General experimental abbreviations	235
6.2	NMR abbreviations	235
6.3	General methods	236
6.4	Procedures	245
6.4.1	6,7- and 6,5- sized ring systems.....	245
6.4.2	Pyridopyrimidinones.....	249
6.4.3	Schofield type compounds	262
6.4.5	Phthalizinones.....	286
6.4.6	Aminopyridazinones	308

7	References	337
Appendix A	Phthalizinone amide compounds.....	354
Appendix B	Copyright permissions	358

2 Abbreviations

2-MeTHF – 2-methyltetrahydrofuran
2-OG – 2-oxoglutarate
9-BBN – 9-borabicyclo[3.3.1]nonane
Ac-CoA – Acetyl-coenzyme A
AMP – artificial membrane permeability
ARID – AT-rich interaction domain
BACT – branched chain aminotransferase
Bcl-2 – B-cell lymphoma-2
BCP – bromodomain containing proteins
BET – bromo and extra terminal
BINAP – 2,2'-bis(diphenylphosphino)-1,1'-binaphthalene
Boc – *N-tert*-butoxycarbonyl
BRET – bioluminescence resonance energy transfer
cAMP – cyclic adenosine monophosphate
CDI – 1,1'-carbonyldiimidazole
COX – cyclooxygenase
CPME – cyclopentylmethyl ether
CPP – cyanopyrazolopyrimidinone
CREB – cAMP response element-binding protein
CREBBP – CREB binding protein
DBAD – di-*tert*-butyldiazodicarboxylate
DCC – *N,N'*-dicyclohexylcarbodiimide
DCM – dichloromethane
DDQ – 1,2-dichloro-4,5-dicyanobenzoquinone
DIAD – diisopropyl azodicarboxylate
DIPEA – diisopropylethylamine
DMA – *N,N*-dimethylacetamide
DMAP – *N,N*-dimethylaminopyridine
DMCC – dimethylcarbamoyl chloride
DMF – *N,N*-dimethylformamide
DMSO – dimethylsulfoxide
DNA – deoxyribonucleic acid

ELISA – enzyme-linked immunosorbent assay
EGLN3 – egl nine homolog 3
FAD – flavin adenine dinucleotide
FDA – U. S. Food and Drug Administration
FP – fluorescence polarisation
FRET – fluorescence resonance energy transfer
GCN5 – general control nondepressible 5
GSK – GlaxoSmithKline
HAT – histone acetyl transferase
HIV – human immunodeficiency virus
HDAC – histone deacetylase
HTS – high throughput screen
HxKy – histone x lysine y (where x and y are numbers)
IFN – interferon
IL – interleukin
IPA – 2-propanol
Jmj – Jumonji
Jak – Janus kinase
KAT – lysine acetyl transferase
KDM – lysine demethylase
KHMDS – potassium hexamethyldisilamide
KMT – lysine methyl transferase
LCMS – liquid chromatography - mass spectrometry
LDA – lithium diisopropylamide
LE – ligand efficiency
LiHMDS – lithium hexamethyldisilazide
LPS – lipopolysaccharide
LSD1 – lysine specific demethylase 1
LTR – long terminal repeat
MAPK – mitogen-activated protein kinases
MHC – major histocompatibility complex
MHz – megahertz
MIDA – *N*-methyliminodiacetic acid

NBS – *N*-bromosuccinimide
NMC – nuclear protein in testes midline carcinoma
NMR – nuclear magnetic resonance
NMP – *N*-methylpyrrolidinone
NF- κ B – nuclear factor kappa-light-chain-enhancer of activated B cells
NSAID – non steroidal anti inflammatory drug
NUT – nuclear protein in testis
p – page
P-TEFb – positive transcription elongation factor
PB1 – polybromodomain-1
PBMC – peripheral blood mononuclear cell
PCAF – p300/CBP-associated factor
Pd/C – palladium on carbon
pDC – plasmoidal dendritic cell
PI3K – phosphoinositide 3-kinase
PID – P-TEFb-interacting domain
PMB – para-methoxybenzyl
PPI – protein-protein interaction
pTSA – para-tolylsulfonic acid monohydrate
pyr – pyridyl
RNA - ribose nucleic acid
SAHA – suberoylanilide hydroxamic acid
SAR – structure activity relationship
SCX – strong cation exchange
SEM – 2-(trimethylsilyl)ethoxymethyl
SGC – Structural Genomics Consortium
siRNA – short interfering RNA
SLE - systemic lupus erythematosus
T_H – T helper cell
T3P® – propylphosphonic anhydride
TBAF – tetrabutylammonium fluoride
TBDMS – *tert*-butyldimethylsilyl
TBDPS – *tert*-butyldiphenylsilyl

TFA – trifluoroacetic acid

THF – tetrahydrofuran

TIPS – triisopropylsilyl

TNF – tumour necrosis factor

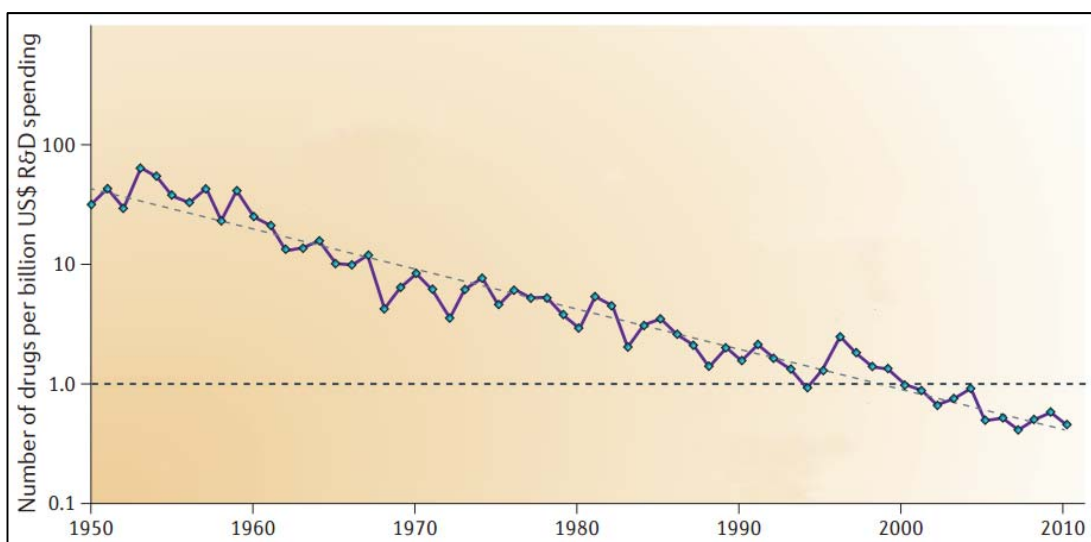
Tyk2 – tyrosine kinase 2

VCD – vibrational circular dichroism

3 Introduction

3.1 The current state of the pharmaceutical industry

Currently, the pharmaceutical industry is in a state of flux. Payers, such as medical insurance companies and governments who buy medicines for patients are, quite rightly, increasingly looking for value for money. Organisations such as England's National Institute for Health and Clinical Excellence perform cost/benefit analyses of drugs and if medicines do not provide sufficient value for money then they will not be purchased and used in patient populations.¹ At the same time as payers are expecting increased value for money, the total cost of having a drug launched on to the market is increasing exponentially. Over the last sixty years increasing amounts of money has been spent on R&D but this has resulted in a decrease in the number of drugs approved year on year.² In fact, the number of new drugs approved per billion US dollars spent has halved roughly every nine years since 1950 (Graph 1).³



Graph 1: The number of drugs approved by the FDA per billion US dollar spent over time. Adapted with permission from Macmillan Publishers Ltd, copyright 2012.³

This decrease in the number of drugs being approved is at odds with major advances in the field of pharmaceutical research and development.³ Combinatorial chemistry has increased the number of drug like molecules possible to be synthesised by a chemist by about 800-fold in a given time period. DNA sequencing is now over a billion times faster than when the first genome was sequenced. High throughput screening has resulted in a tenfold reduction in the cost of testing of compound libraries against protein targets since the

1990s.³ Even with these advances, the numbers of drugs being approved are falling. This decrease is thought to be due to a range of causes.⁴ For example, new drugs must have an advantage over existing ones and be safer, with fewer side effects than the previous generation.

Once a drug has been discovered and approved, it is marketed and sold by a single company until the patent expires, usually after 20 years.⁵ At this point the drug becomes generic and is often available at a greatly reduced price as other manufacturers can synthesise it without the need to recoup research and development costs. For a medicine to find a market for an already treatable disease it needs to show a demonstrable advantage over the other drugs on the market, including proven, well understood and cheaper generic pharmaceuticals.

In the field of anti-ulcerants there are two classes of highly effective and safe drugs on the market: histidine H₂ receptor antagonists such as ranitidine (**3.001**) and proton pump antagonists such as omeprazole (**3.002**), both of which are now generic (Fig. 1).

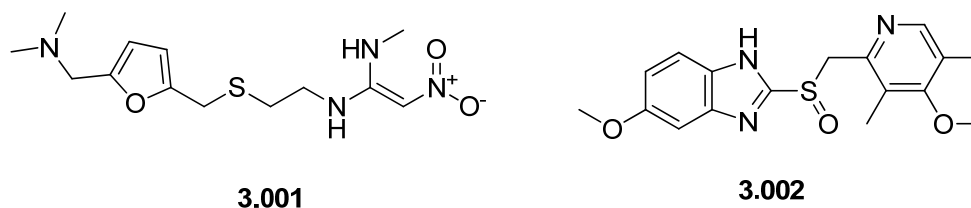


Figure 1: Structures of ranitidine (**3.001**) and omeprazole (**3.002**).

A novel class of anti-ulcerants, known as potassium competitive acid blockers, probably would have been safe and effective. If they had been discovered before ranitidine (**3.001**) and omeprazole (**3.002**) then they would have been blockbusters, selling more than one billion US dollars worth per year. However, with the existence of cheap, safe and proven alternative anti-ulcerants they did not make it to market. This was despite advantages over the previous generation of drugs.⁶ The potassium competitive acid blockers were treating an already solved problem. A payer will only buy the more expensive drug if patients fail to respond to cheaper, generic medicines thus limiting the market for a new class.³

Many other indications such as hypertension and cholesterol management already have good treatments. New medicines need to be better than the existing drugs for a disease. Regulatory agencies are growing more cautious and drugs need increasingly good safety

profiles to be approved. This is relaxed somewhat for severe diseases that have an unmet medical need. For example drugs for oncology can have a worse safety profile than anti-ulcerants. The lower barrier to entry for approval for oncology drugs from the regulatory agencies is due to the life threatening nature of cancer.

Therefore, with drug approvals per billion US dollars spent falling and higher requirements needed for new treatments, the pharmaceutical industry must consider what can be done to discover safer, more effective drugs in a less expensive manner.

3.1.1 Screening strategies for drug discovery

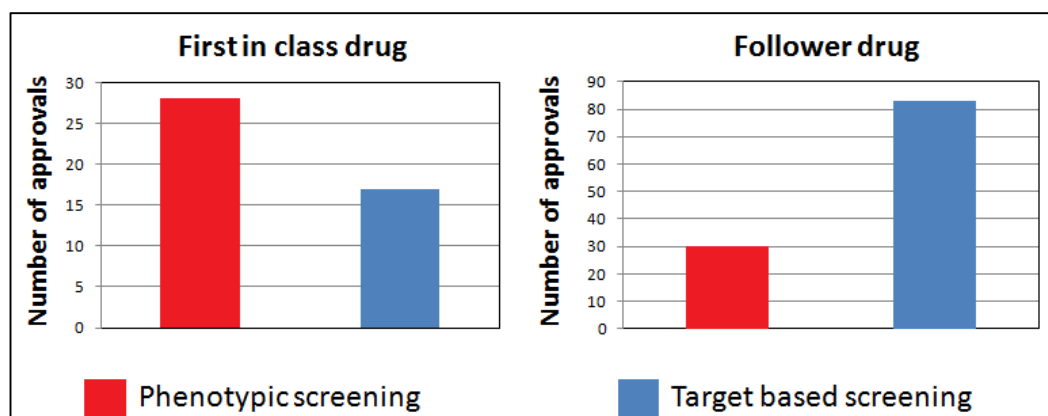
Over the last 100 years, two types of screening have dominated early stage drug discovery, phenotypic screens and target based screens. Phenotypic screening examines the effects that compounds have on cells, tissues or whole organisms. Target based screening investigates the effects that compounds have on a purified target protein in an *in vitro* system.⁷

Historically, phenotypic screening has been the mainstay of drug discovery. However, starting in the 1980s, advances in molecular biology and genomics led to a reduction in the use of phenotypic screening and a greater reliance on target based screening.⁷ The major advantage of moving to target based screening is that it allows a much higher throughput compared to phenotypic screening.⁸ The perceived benefit is that if more compounds are screened then there is a higher likelihood that a new drug would be discovered. However, as there is movement away from an entire organism, to isolated cells, to purified target protein, there is also a decrease in validation between the target disease and the system being screened. If the protein targeted by small molecules has no relevance to the disease in question then even the best ligand for that protein will have no effect on the disease.

Some researchers have wondered whether an over-reliance on target based screening has contributed to the decline in the number of new medicines being approved per billion US dollars spent.⁹ It is considered that overconfidence in the understanding of genomics and hence target based screening may have led to less effective target validation. Thus, by prosecuting some targets that are not linked to diseases, fewer successful drugs have been launched.

Analysis of first in class drugs, medicines that interact with a new biological target, between 1999 and 2008 have shown some interesting results.⁹ Drug discovery programmes that

used phenotypic screening had more success in getting drugs to market than those that used target based screening (Graph 2). However, for follower drugs, medicines that interact with a previously drugged protein, target based screening was more effective.



Graph 2: Number of new treatments approved for first in class and follower drugs between 1999 and 2008.⁹

The findings, summarised in Graph 2, show that once a protein has been validated for a disease, target based screening is very effective.

Establishing a link between a target and a disease is crucial for clinical success of a drug molecule. A recent examination of the reasons for project termination within AstraZeneca illustrates that once drug candidates enter the clinic the largest cause of failure is a lack of efficacy.¹⁰ The biggest reason for the lack of efficacy is having no link between the disease and the protein targeted by the clinical candidate. Hence, initially choosing a relevant target is extremely important.

3.1.2 New targets for drug discovery

For the pharmaceutical industry to reverse the decline seen in Graph 1 (p 14), one strategy to adopt is to treat diseases in a different manner by interacting with new biological targets. A class of proteins that has not been thoroughly investigated are epigenetic proteins. The term epigenetics derives from the Greek epi – meaning above, so literally termed as “above or near genetics”. Epigenetic changes do not alter the DNA itself, but what genes can be transcribed from DNA. To understand epigenetics it is important to know how DNA is stored in the nuclei of cells.

3.2 Epigenetics

3.2.1 Packing of DNA

There are 1.8 metres of DNA in each human cellular nucleus¹¹ and for this to be contained there must be efficient packing. Humans have twenty three chromosomes in their nuclei and these consist of negatively charged DNA wrapped around positively charged protein octamers called histones.¹² This protein-DNA complex is known as a nucleosome and is a monomer for chromatin.¹³

The initial level of chromatin organisation consists of wrapping 147 base pairs around the octameric histone protein core. This short length of DNA encircles each histone complex approximately one and three quarter times, with variable lengths of DNA between each protein octamer. The histone octamer is comprised of two molecules of each histone protein H2A, H2B, H3 and H4 (Fig. 2).¹²

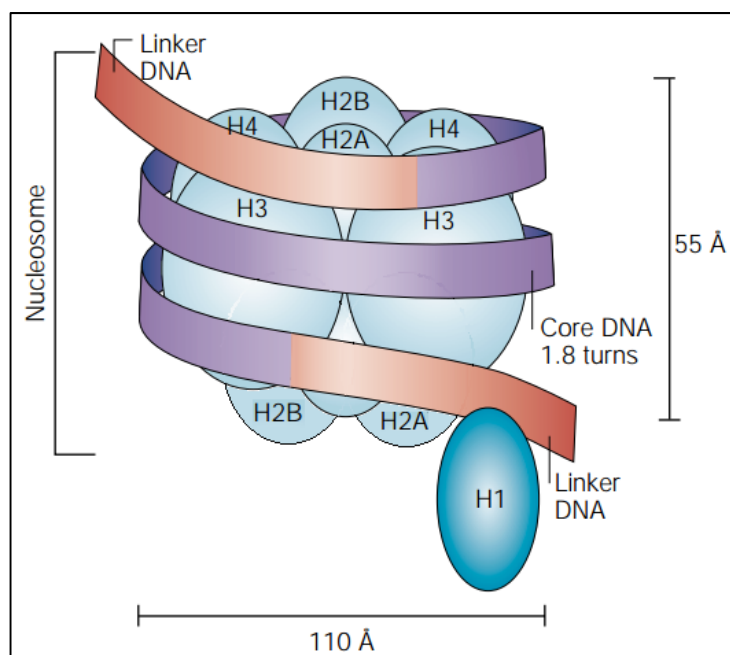


Figure 2: A schematic of a histone octamer. Adapted with permission from Macmillan Publishers Ltd, copyright 2002.¹³

Chromatin exists in two forms, loosely packed euchromatin, which resembles beads on a string, and the next level of packing, tightly bound heterochromatin. When the complex is in the heterochromatin form, DNA transcription cannot take place. However, when the complex relaxes to euchromatin, the transcription of DNA is possible (Fig. 3).¹⁴

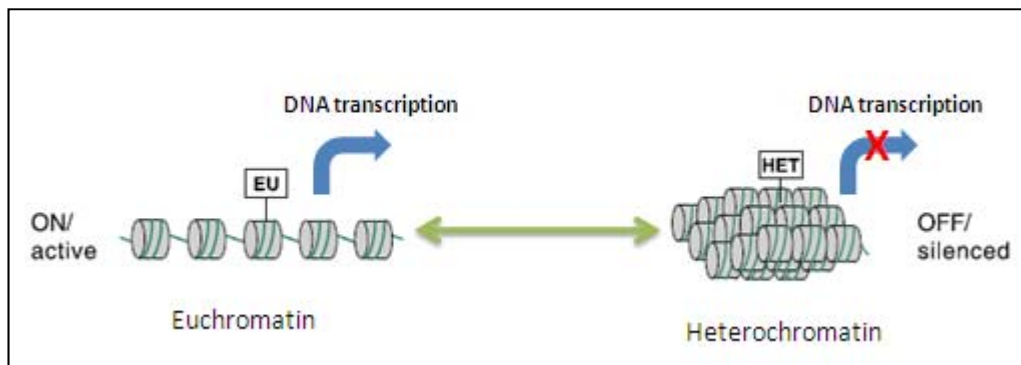


Figure 3: Relaxed euchromatin and tightly bound heterochromatin. Adapted.¹⁵

In the formation of heterochromatin another histone protein, H1, binds to the linker DNA and causes a higher order structure to form the 30 nm wide chromatin fibre with the H1 proteins found internally.^{16,12} The next levels of chromatin organisation to eventually form a chromosome are much less clear, although it is thought to involve the recruitment of scaffold proteins (Fig. 4).¹⁷

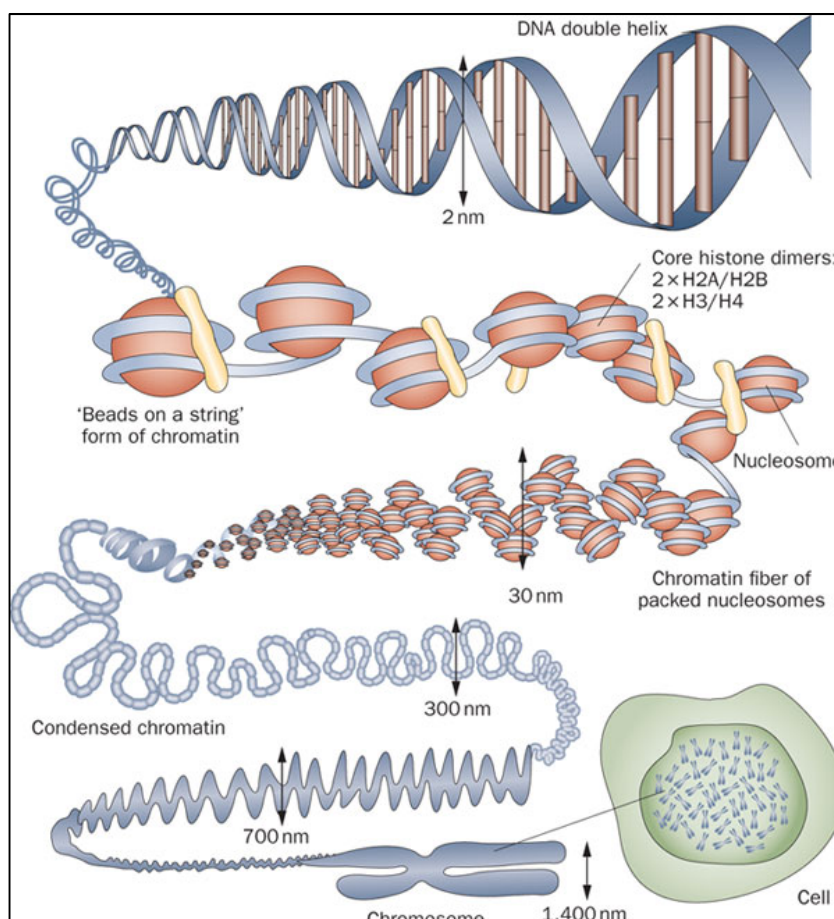


Figure 4: Packing of DNA from double helix to chromosome. Reprinted with permission from Macmillan Publishers Ltd, copyright 2010.¹⁸

3.2.2 The histone code

Although all cells in an organism inherit the same genetic material, they must be differentiated to become a particular type of tissue. Changes in the packaging of the chromatin can dictate changes in protein expression which leads to cell type. One mechanism for the chromatin complexes to transition between heterochromatin and euchromatin is by the modification of peptide chains originating from the histone proteins. These peptide chains are known as histone tails and can be modified in a multitude of ways. For example, residues in the histone tails can be acetylated, methylated or a combination of both as well as other modifications such as phosphorylation or ubiquitination.¹⁴ The addition or removal of these covalent modifications causes the chromatin to transition between heterochromatin and euchromatin. The change of these marks is known as epigenetic modification. The alteration of the proteins around which DNA is wrapped causes changes to which gene is transcribed. Lysine is one residue to which methyl and acetyl marks can be added, removed or read and particular families of enzymes carry out these changes (Fig. 5).¹⁴

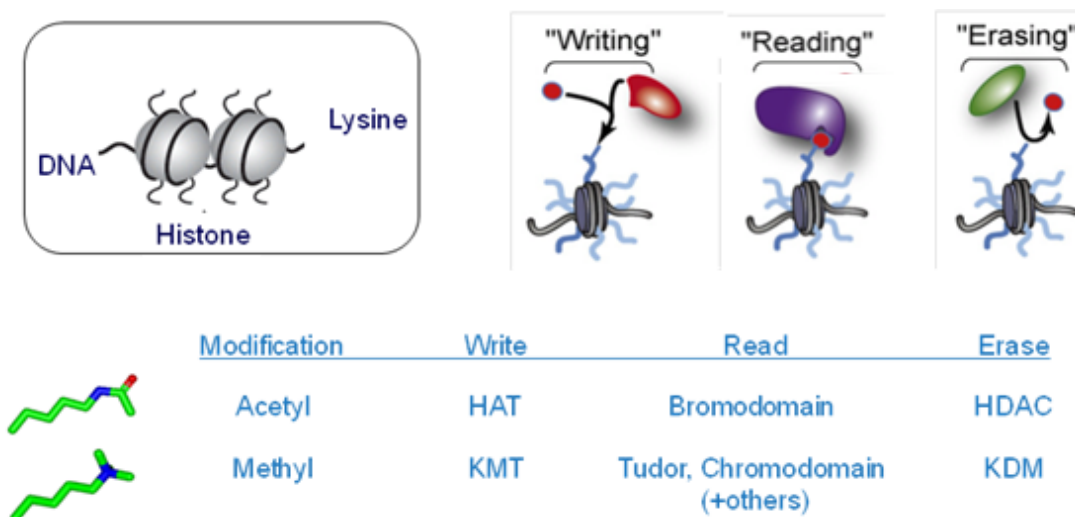
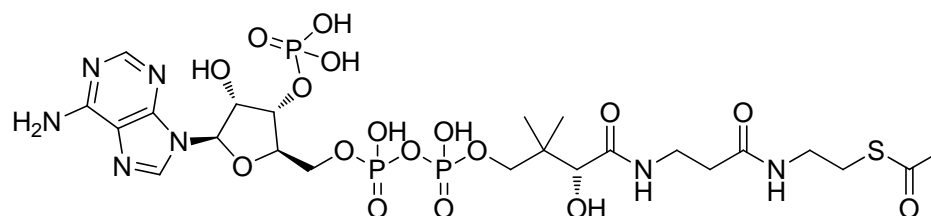


Figure 5: Families of epigenetic proteins which add, remove and read lysine marks on histone tails.

3.2.3 Writers

Histone acetyl transferases (HAT) acetylate lysines on histone tails¹⁹ and are broadly split into different families based on their primary structure homology.²⁰ Lysines are acetylated using acetyl - coenzyme A (Ac-CoA) (**3.003**) (Fig. 6) as a co - factor.²⁰

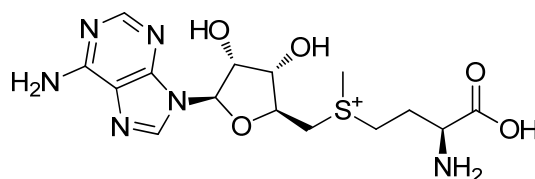


3.003

Figure 6: The structure of acetyl - coenzyme A (**3.003**).

Lysine acetylation is seen generally as a gene activating mark.²¹ This is thought to be due to the neutralisation of positive charge, which weakens the interactions between negatively charged DNA and the histone octamer.²²

Methylation of histone lysines can be either activating or repressing for gene transcription depending on the specific lysine residue on either histone H3 or H4 that is methylated.²³ For some processes, methylation on the same site can lead to different outcomes depending on the number of methyl groups added.²⁴ The methylation of lysines is catalysed by SET or DOT1L proteins using S-adenosyl-L-methionine (**3.004**) as a methyl group donor (Fig. 7).^{25,26}



3.004

Figure 7: Structure of S-adenosyl-L-methionine (**3.004**).

3.2.4 Readers

Bromodomains “read” by binding to acetylated lysines and are the only known protein domain to do this.²⁷ Bromodomain containing proteins (BCP) are often part of larger protein complexes, which can contain transcription factors and therefore facilitate transcriptional initiation and elongation.²¹ This causes genes to be activated and transcribed. Selectively inhibiting the PCAF bromodomain is part of the focus of this thesis.

There is a much wider range of proteins that read methylated lysines compared to acetylated lysines. The number of methylated lysine readers is estimated to be greater

than 170 and these readers are from several different families, for example the so-called chroma and tudor domains.²⁸ The large number of methyl lysine readers may indicate why there is a range of repressive and activating activities for different states of lysine methylation.

3.2.5 Erasers

Histone deacetylases (HDAC) remove acetyl groups from lysines on a histone tail and are linked with the repression of gene expression.²⁹ There are four main classes of HDAC, three of these contain zinc,³⁰ which is used in the enzymatic process to remove the acetyl group.³¹ The last class of HDACs includes sirtuins which have a requirement for NAD⁺ (**3.005**) to remove acetyl groups from lysines (Fig. 8).³⁰

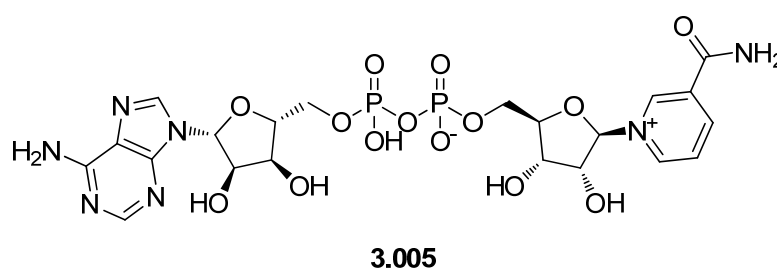


Figure 8: The structure of NAD⁺ (**3.005**).

Lysine demethylases (KDM) remove methyl groups from histone lysines.³² There are two known types of histone demethylases, those which use 2-oxoglutarate (2-OG, **3.006**) and those which use flavin adenine dinucleotide (FAD, **3.007**) as co-substrates in the removal of methyl groups from lysines (Fig. 9).³² Those demethylases that use 2-OG as a co-factor also require the presence of an iron (II) ion to catalyse the reaction.³³ Selectively inhibiting KDM enzymes is part of the focus of this thesis.

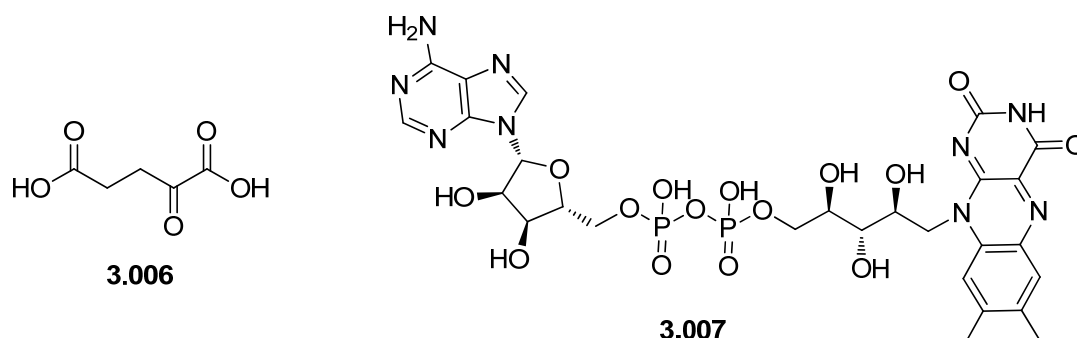


Figure 9: The structures of 2-OG (**3.006**) and FAD (**3.007**).

3.2.6 Current epigenetic treatments

The approach of inhibiting epigenetic mechanisms has had success with the approval of suberoylanilide hydroxamic acid (SAHA, **3.008**)³⁴ and romidepsin (**3.009**) for oncology (Fig. 10).³⁵ These compounds are histone deacetylase (HDAC) inhibitors which prevent the removal of acetyl groups from histone tails, which modulate the production of oncogenic proteins.³⁶

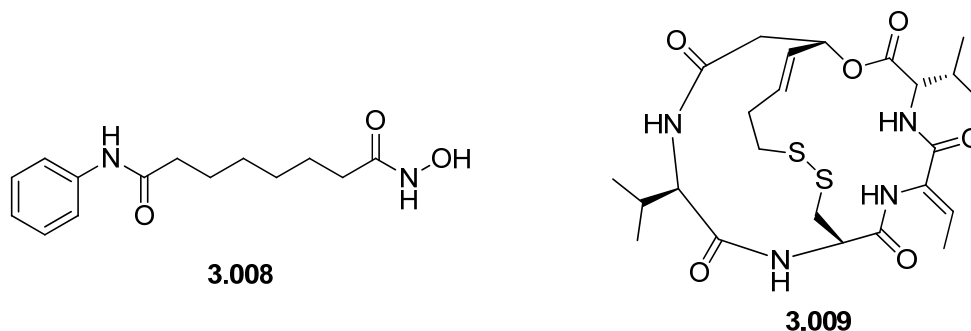


Figure 10: Structures of SAHA (**3.008**) and romidepsin (**3.009**).

Building on evidence that cancers can be modified through manipulating histone deacetylases, the aim of the research reported upon is to show that by modulating other epigenetic mechanisms, a phenotype can be observed in an *in vitro* system. However, as many epigenetic proteins have only recently been discovered there are often no known small molecule inhibitors of these proteins. To identify if these epigenetic proteins are potential drug targets, it needs to be established if interacting with these targets has a desirable biological effect.

3.3 Target validation challenges

A strategy to determine the biological role of a protein is to reduce or halt the expression of that specific protein. By doing this it is possible to observe what happens to the phenotype compared to a control experiment.³⁷ This can be performed with short interfering RNA (siRNA) which can be designed to bind selectively to mRNA and prevent expression of a specific protein.³⁸ If this is targeted towards an epigenetic protein the effects of inhibiting that protein can be investigated.

However, this approach removes all expression of the protein and epigenetic proteins often contain multiple binding domains which have different functions. For example CREB-binding protein (CREBBP) has eight different domains: a HAT domain, a bromodomain, a

plant homeodomain (PHD) finger, as well as five protein interaction domains.³⁹ It should be clear that inhibiting, for example, just the bromodomain may have a considerably different effect from removing the protein altogether. On removal of the entire protein, the HAT domain will no longer be able to acetylate histone tails and the protein complex that CREBBP is a part of might be significantly different, potentially altering the other function of other proteins in the complex. However, selectively antagonising the bromodomain would leave the other domains in CREBBP functional. Therefore, the identification of small molecule inhibitors that selectively bind to a single domain in the protein will enable the determination of a phenotype for the inhibition of that specific domain. Additionally, complete inhibition of the target of interest may not be desirable and small molecules allow a way to attenuate biological activity without complete blockade of the domain. These molecules are known as chemical probes.

3.3.1 Properties of chemical probes

Using chemical probes for target validation is different from “typical” drug discovery and different attributes can be required from an eventual chemical probe. A probe molecule requires more stringent selectivity requirements than a drug, as polypharmacology cannot be tolerated.⁴⁰ The lack of acceptance for polypharmacology is due to needing to associate any phenotype observed with binding to a single biological domain.

Building from principles articulated by Frye for chemical probe qualification,⁴¹ Bunnage *et al.*⁴² have recently disclosed their philosophy around the identification of chemical probes for target validation which was based upon a retrospective review of drug programmes. Programmes which reached phase 2 of clinical trials found three common themes amongst those which showed efficacy: sufficient exposure at the site of action; proof of target engagement and expression of functional pharmacological activity.⁴³ These themes were termed “The three pillars of survival” and a molecule possessing all these attributes has a high correlation with achieving a positive proof of concept and advancing the candidate into phase 3 of clinical trials.⁴² Bunnage *et al.* considered these “pillars” a good framework for desirable properties in chemical probes and adapted them into the following attributes necessary for a chemical probe:

1. Cellular penetration,
2. Target engagement and selectivity,
3. Expression of functional pharmacology,

4. Expression of a relevant phenotype.

Cellular penetration is generally required for a molecule to have biological effects as many target proteins are intracellular and thus molecules have to penetrate the cell to reach the desired target. This is especially true of epigenetic modulators where the molecules must also penetrate the nucleus to engage the target. However, molecules with molecular weights of less than 5000 Da diffuse into the nucleus so quickly that if a molecule can penetrate the cell it can be considered typically freely available within the nucleus.⁴⁴

A chemical probe needs to be able to bind to the target of interest and ideally be as selective as possible for that target compared to binding sites in other proteins. The selectivity requirement for a probe should be more stringent than for drug candidates. While “safe” promiscuity may enhance the efficacy of a drug molecule it can confuse the output of an assay if the chemical probe hits multiple targets.⁴² However, Bunnage *et al.* suggest that even with the most stringent biochemical selectivity it is likely that a given probe will have unknown off-target activity. Thus, they advocate the discovery and use of multiple, structurally distinct chemical probes, which would have alternative unknown off-target activity as well as an inactive or much less active close analogue as a negative control.⁴² The purpose of this is to identify polypharmacology by making a small change to a probe molecule which significantly lowers the potency of the compound at the target of interest while keeping the properties of the molecule, for example the lipophilicity, as unchanged as possible. While this has a major effect at the target being investigated it is hoped that it would give only a subtle change in potency at any unknown proteins. Hence, if the negative control shows the same biological activity as the chosen chemical probe then the target of interest is not driving the observed biological activity. A good example of this is in the discovery of I-BET762 (**3.010**).⁴⁵ It was found that the opposite enantiomer of I-BET762, **3.011** was inactive in the phenotypic assay providing a perfect control for non-specific activity (Fig. 11). The discovery of I-BET762 (**3.010**) will be discussed in more detail later (p 124).

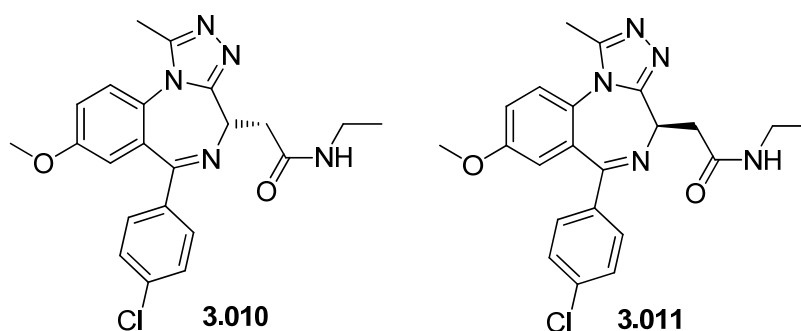


Figure 11: The structures of I-BET762 (**3.010**) and the inactive control **3.011**.

Chemoproteomics is a method in which an active ligand is attached to a solid support and used to pull down interacting proteins from cell lysates, and the interacting proteins can then be identified by mass spectrometry.⁷ Advances in chemoproteomics allow for an understanding of target engagement, both on-target and off-target for probe molecules under physiological conditions by investigating relevant cellular lysates. Hence, using chemoproteomics technology based on a probe molecule can demonstrate binding to the target of interest and “pull back” off-target proteins as well.

Identification of relevant cell based systems is a core principle of pillars 3 and 4. Cells derived from a patient with the disease of interest can be the best system for probing functional pharmacology as these can capture post-translational modifications lacking in other cell lines.⁴² However, this assumes knowledge of the disease of interest and might not be relevant in a disease agnostic approach. Equally important is the measure and identification of a relevant phenotype in these systems. Some of the measurable biomarkers associated with the disease could be symptoms rather than the cause itself and in these cases chemical probes could be found that affect a symptomatic phenotype, but have no impact on modifying the disease. However, the necessity of a disease affected cell line and identification of a relevant phenotype will depend on the knowledge of the cellular system and an understanding of the disease itself.

3.3.2 Historical chemical probes

Some historical probes have not complied with the four attributes needed for a chemical probe, predominantly selectivity.⁴² Examples of historical chemical probes have been identified by phenotypic screening. In one case b-AP15 (**3.012**) was shown to induce an apoptosis pathway.⁴⁶ It was considered that this was *via* a deubiquitination pathway, inhibited by b-AP15 (**3.012**). However, there was no investigation into other targets that

could be interacting with b-AP15 (**3.012**). Considering the chemical structure, it is likely that it binds promiscuously due to the presence of multiple Michael acceptors and nitro groups (Fig. 12).⁴⁷

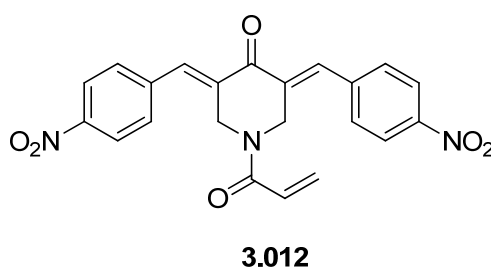


Figure 12: Structure of b-AP15 (**3.012**).⁴⁶

Another example of poor target validation comes from work to link Tyk2 (Tyrosine kinase 2) with skin inflammation.⁴⁸ In a series of experiments, mice with the gene Tyk2 knocked out were found to suffer from IL-23 induced inflammation less than wild-type mice. To investigate if Tyk2 inhibition in wild-type mice would have a similar effect to knocking out the Tyk2 gene, tyrphostin A1 (**3.013**), a reported Tyk2 kinase inhibitor, was dosed.⁴⁹ Inflammation was induced in wild-type mice with IL-23 and dosing tyrphostin A1 (**3.013**) did reduce the inflammation. However, the selectivity of tyrphostin A1 (**3.013**) was not well investigated. While selectivity was found against the Jak family of kinases, no other proteins were investigated. As seen for b-AP15 (**3.012**), there is a likelihood of tyrphostin A1 (**3.013**) acting as a Michael acceptor (Fig. 13).

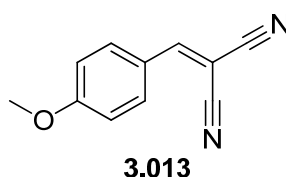


Figure 13: Structure of tyrphostin A1 (**3.013**).⁴⁸

Another issue is often the lack of negative controls. LY294002 (**3.014**, Fig. 14), discovered in 1994, is a widely used phosphoinositide 3-kinase (PI3K) probe molecule.⁵⁰ PI3Ks are involved in cell migration, metabolism and survival and were therefore thought to be attractive targets for oncology.⁵¹ However, a number of studies found PI3K independent effects using the inactive control LY303511 (**3.015**, Fig. 14). Through using chemoproteomics it was found that LY294002 (**3.014**) and LY303511 (**3.015**) bind to the BET

family of bromodomains, the same target that I-BET762 (**3.010**, Fig. 11, p 26) was found to inhibit. Therefore, some of the biological effects associated with PI3K could be due to inhibition of the BET family of bromodomains where negative controls have not been used.⁵²

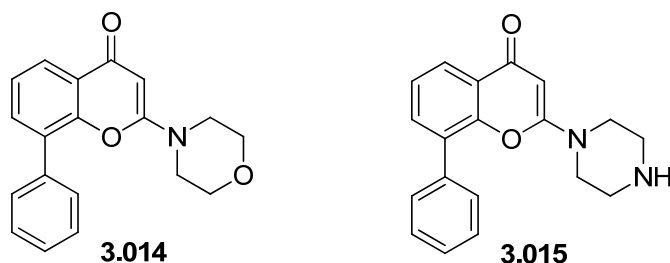


Figure 14: Structures of LY294002 (**3.014**) and LY303511 (**3.015**)

In the present work, with the four fundamental attributes that probe molecules require in mind (Section 3.3.1, p 24), an investigation was begun to identify inhibitors for epigenetic proteins and related inactive controls. Probe compounds were designed and synthesised for proteins covering two epigenetic mechanisms: a lysine demethylase (Section 4, p 29), and a bromodomain (Section 5, p 115). The molecules had to conform to the four attributes needed for a chemical probe and an inactive or considerably less active control identified. Once identified, the probe compounds would be tested in cells to determine whether a phenotype could be identified.

4 JmjC containing proteins

A jumonji (Jmj) gene was first discovered in 1995 in mice.⁵³ It was found that mouse embryos which had a mutation in this gene developed a cross-like structure in their growing brains. Jumonji is literally translated as cruciform in Japanese and hence the name arose.⁵³ JmjC containing proteins demethylate *N*-methylated lysines on histones tails. They are part of a wider family of enzymes that hydroxylate substrates.⁵⁴ Histone lysine demethylation is broadly associated with transcriptional activation, although there are some exceptions, which depend on the specific lysine methylated and the number of methyl groups added.⁵⁵

JmjC containing proteins often contain other protein-protein interaction domains⁵⁶ and are thought as having a scaffolding role in addition to functioning as part of transcriptional or chromatin protein complexes.⁵⁴ The JmjC containing KDMs (Lysine demethylase) are split into six different families based on sequence homology. There is a high degree of homology within the JmjC domains for different proteins and a phylogenetic tree can be drawn to compare the levels of similarity (Fig. 15).⁵⁷ The higher the sequence similarity of the JmjC domains the closer the branch point between the individual domains is.

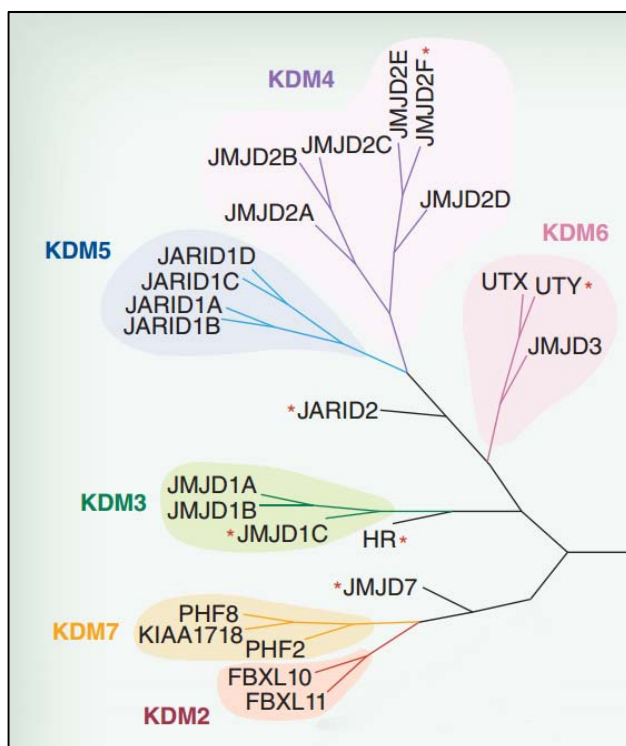


Figure 15: Phylogenetic tree for human JmjC containing KDM proteins. The asterisks indicate proteins for which no enzymatic activity has yet been determined. Adapted.⁵⁴

4.1.1 Lysine demethylase families

The KDM families, while having sequence similarities with each other, also appear to share common substrates. However, an individual KDM may demethylate more than one substrate. Both members of the KDM2 family, FBXL10 and FBXL11, demethylate methylated histone 3 lysine 36 (H3K36) with one or two methyl marks present. However, FBXL10 can also demethylate H3K4 with three methyl marks present.⁵⁸ The enzymes in this family have been linked to leukaemia, pancreatic cancer and implicated in the immune response through regulation of NFκB, which is a transcription factor for both innate and adaptive immune response.^{54,59}

The KDM3 family is known to demethylate H3K9 with one or two methyl groups present. However, substrates for JmjD1c and HR are currently unknown.⁶⁰ This family of enzymes is found to be overexpressed in a range of cancers including bladder, lung and prostate cancers. However, a range of cancers have also found enzymes from this family to be deleted, which may suggest some members could be tumour suppressors.⁵⁴

The KDM4 (JmjD2) family of enzymes with known substrates all demethylate tri- and dimethylated H3K9. The a, b and c JmjD2 proteins can also demethylate H3K36 in both the tri- and dimethylated forms.⁶¹ The KDM4 family has a role in the progression of prostate and breast cancers as well as some proteins being overexpressed in some breast cancers.⁵⁴ JmjD2d has been linked to gene transcription in immune cells and may have role in autoimmune diseases.⁶²

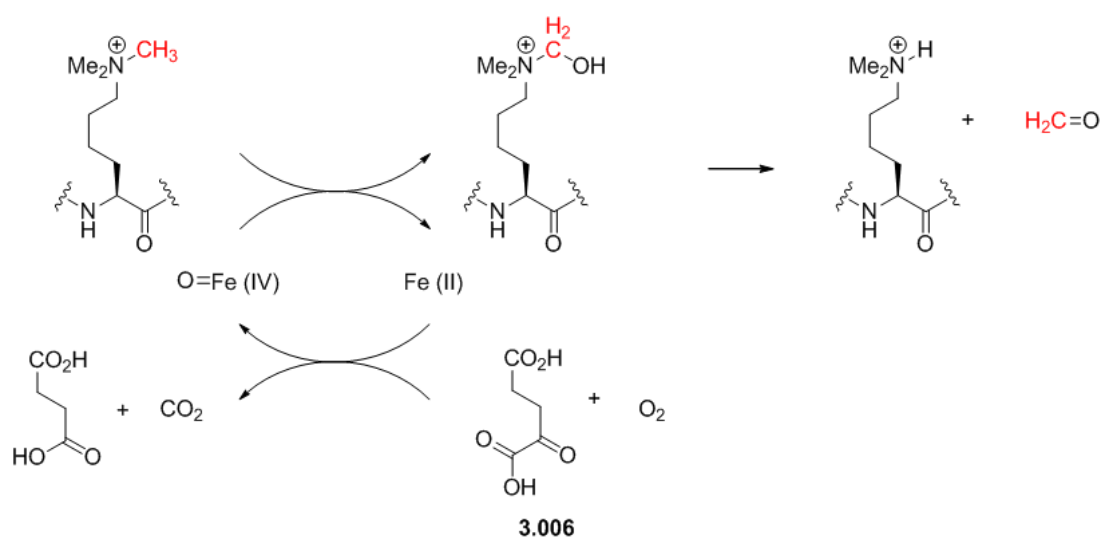
The KDM5 family of proteins, in addition to containing a JmjC domain also have AT-rich interaction domains (ARID) present, which are DNA binding features.⁶³ Mono-, di- and trimethylated lysines on H3K4 are demethylated by this family of KDMs. This family of JmjC containing proteins is implicated in the regulation of tumour suppression and JARID1D is deleted in half of prostate cancers.⁵⁴ JARID1a is associated with susceptibility to ankylosing spondylitis,⁶⁴ an immune disease which causes fusion of bones in the spine.⁶⁵

The KDM6 family of proteins are known to demethylate H3K27 in the tri- and di-methylated forms.⁶⁶ These enzymes are involved in cancer by inactivating mutations in multiple tumour types and have links to tumour suppression through other pathways. In inflammatory disease they assist with proinflammatory gene regulation and T helper cell development.⁵⁴

Finally, the KDM7 family of enzymes all demethylate dimethylated H3K9. PHF8 can additionally demethylate monomethylated H3K9 and monomethylated H4K20. KIAA1718 additionally demethylates monomethylated H3K9 and mono- and dimethylated H3K27.⁶⁷ The KDM7 family is involved in leukaemia⁶⁸ and control of proinflammatory gene expression.⁶⁹

4.1.2 The function of JmjC domains

All these families demethylate *N*-methylated lysines using molecular oxygen and 2-oxoglutarate (2-OG, **3.006**) as a co - factor (Scheme 1).⁷⁰



Scheme 1: Mechanism of demethylation of a trimethylated lysine.

For each demethylation, molecular oxygen associates to Fe (II). The oxygen oxidises 2-OG (**3.006**) to succinate and carbon dioxide and in doing so, Fe(II) is oxidised to a reactive Fe(IV) ferryl-oxo species. The ferryl-oxo species hydroxylates a methyl group on a methylated lysine thus generating an unstable hemiaminal intermediate, which subsequently fragments to the demethylated lysine and formaldehyde.⁷⁰ The process can be repeated until the lysine is fully demethylated with the appropriate enzyme for the substrate.

In the JmjC containing proteins different residues can surround the iron, which hold it in place, for example in KIAA1718 a glutamic acid common to many JmjC proteins in Fig. 16 is replaced with an aspartic acid.⁷¹ Each JmjC domain folds into eight β -sheets forming an enzymatically active pocket which coordinates Fe(II) and 2-oxoglutarate (2-OG, **3.006**) (Fig. 16). Most of the proteins also contain a JmjN domain which interacts extensively with the JmjC domain and provides structural integrity.^{54,72}

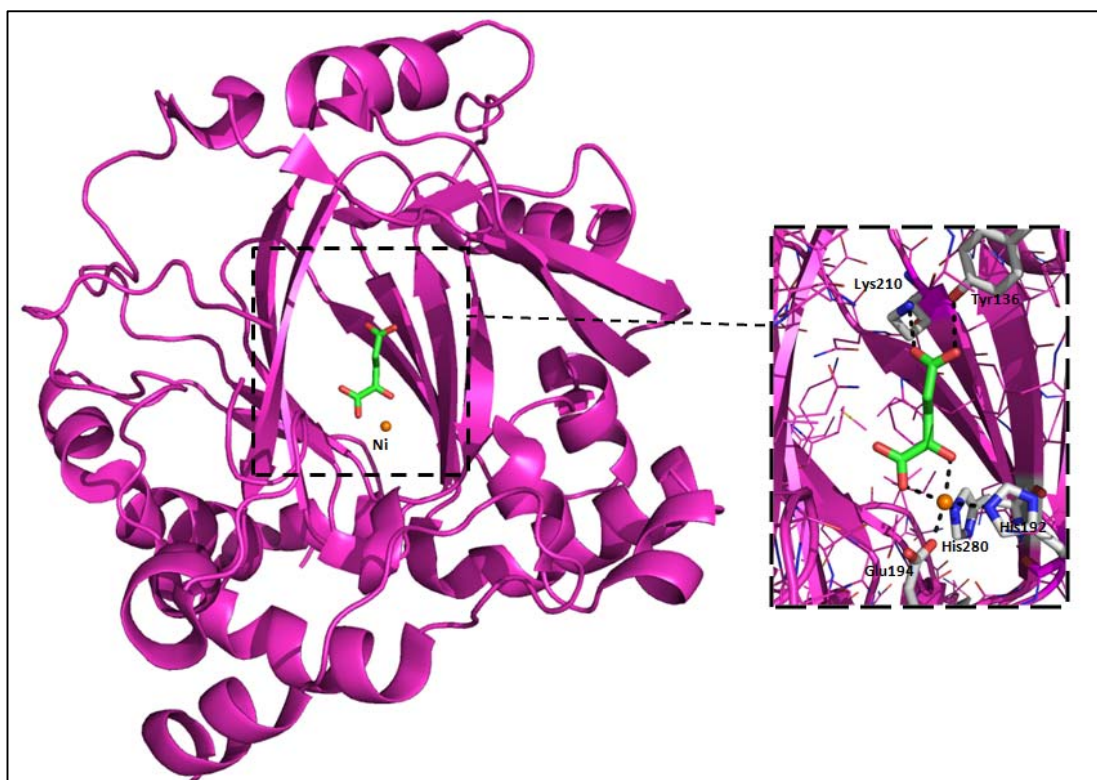


Figure 16: Tertiary structure of JmjD2d (magenta) with Ni(II) (orange) and 2-OG (green, **3.006**) bound, resolution = 1.8 Å.⁷³ The Ni(II) is a surrogate for Fe(II) that renders the protein catalytically inactive.

4.1.3 Known inhibitors of JmjC domains

A number of molecules which inhibit JmjC domains have been identified, all of which are competitive with the natural substrate 2-OG (**3.006**) (Fig. 17), and therefore are able to inhibit the demethylation of *N*-methylated histones.

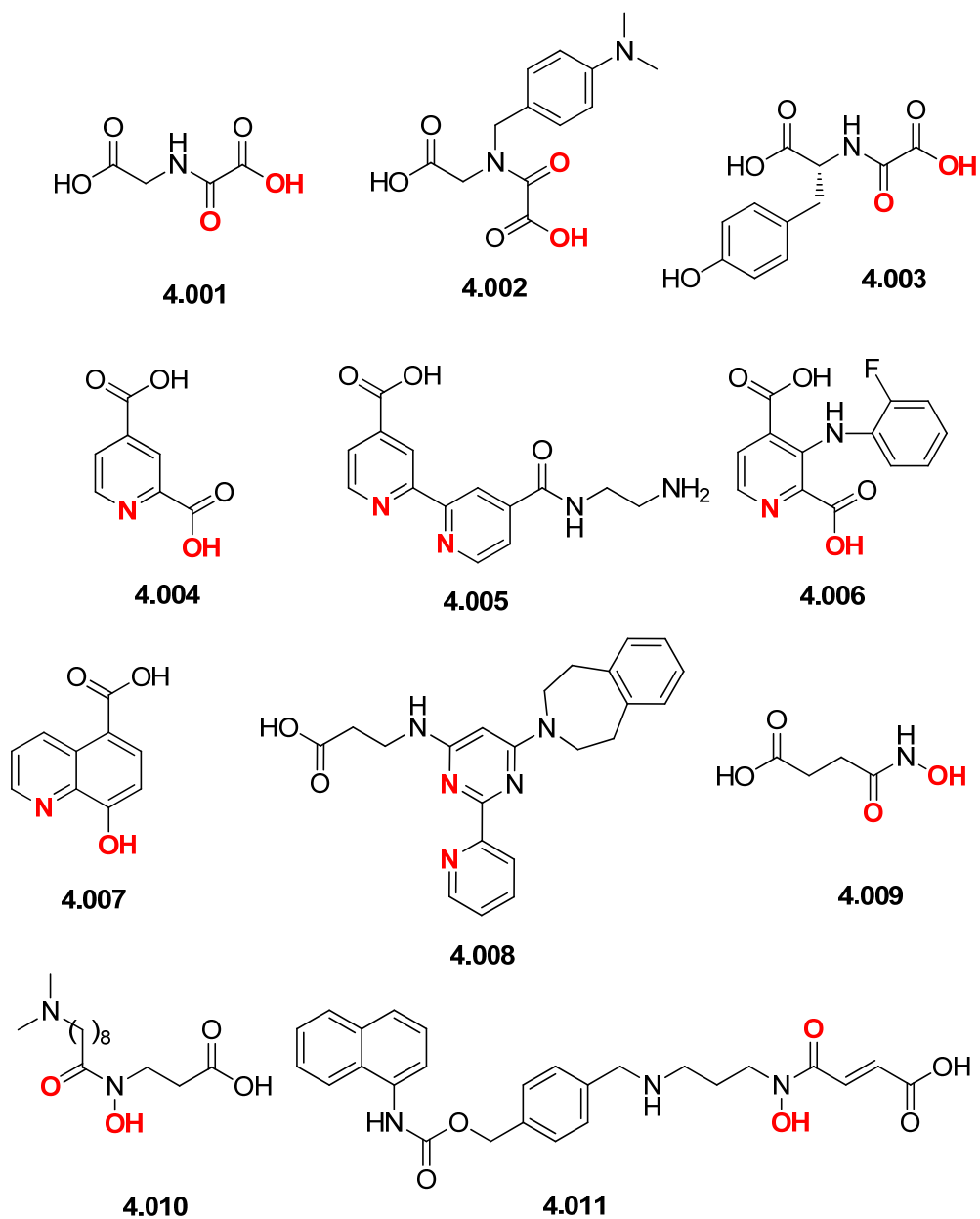


Figure 17: Reported inhibitors of JmjC domains. The atoms that chelate iron (II) are highlighted in red.

One of the earliest inhibitors *N*-oxalylglycine (NOG, **4.001**) is a catalytically inert analogue of 2-OG (**3**).⁷⁴ **4.002** is an analogue of NOG, which in addition to binding competitively with 2-

OG (**3.006**), has a benzyl spacer that places the *N*-dimethyl group in the methylated lysine binding pocket.⁷⁵ **4.003** is another NOG mimetic although this example is not targeted to fill the methylated lysine binding pocket.⁷⁶ The pyridine 4-carboxylic acid based inhibitors **4.004**,⁷⁷ **4.005**⁷⁰ and **4.006**⁷⁸ were found to inhibit JmjC domains by chelating to the catalytic iron present in JmjC domains through the pyridine nitrogen. Hydroxyquinoline **4.007** was screened against a wide range of 2-OG oxygenases and was found to inhibit all the enzymes it was tested against, with a shift in the active site iron compared to the natural ligand 2-OG (**3**).⁷⁹ Biheteroaryl **4.008** was found to selectively inhibit JmjD3 and similarly to hydroxyquinoline **4.007** causes a shift of the bound metal, cobalt in the JmjD3 X-ray crystallography system.⁸⁰ The hydroxamic acid containing **4.009**,⁸¹ **4.010**⁸² and **4.011**⁸³ were found to bind to JmjC containing proteins co-ordinating to the catalytic iron through the two oxygens of the hydroxamic acid. The larger examples of the hydroxamic acid containing compounds **4.010** and **4.011** were designed to mimic the peptide substrates while simultaneously binding to the iron.^{82,83}

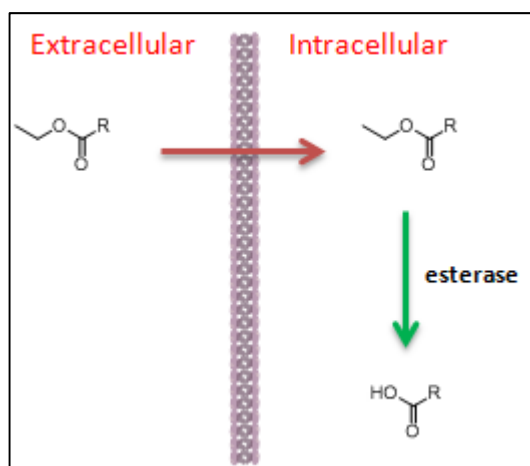


Figure 18: An ester pro-drug enters a cell and the ester is cleaved, revealing the active carboxylic acid.

All of the compounds discussed contain carboxylic acids and in many cases an ester pro-drug approach is used to enable cellular penetration and investigate biological activity in the cell. Within the cell, esterases cleave the ester and unmask the active carboxylic acid (Fig. 18). Only hydroxamic acid **4.011**, when dosed as the methyl ester analogue has shown an IC_{50} value less than 10 μ M.

4.2 Inhibition of Jmjd2 lysine demethylases

The KDM4 family of JmjC containing enzymes has been implicated in gene transcription in immune cells, in particular Jmjd2d (p 30).⁶² Jmjd2a, b, c and d have been found to demethylate H3K9⁵⁶ and high levels of H3K9 methylation has been shown to correlate with inhibition of the production of type I interferons (IFN), which are inflammatory cytokines.⁸⁴ Hence, the inhibition of H3K9 demethylation should reduce the amount of IFN production in the body and thereby help those with autoimmune diseases which display heightened levels of IFN, such as systemic lupus erythematosus (SLE).⁸⁵ It was hypothesised that inhibiting these enzymes in the body could reduce the amount of IFN produced. If less IFN is produced it could provide a treatment for SLE and other autoimmune diseases.⁸⁶

Jmjd2a and c share the highest homology within the JmjC domains and Jmjd2d is the most structurally divergent of the protein family. Beyond the JmjC domain, Jmjd2d is considerably different from the other members of the Jmjd2 family. It is a shorter protein than Jmjd2a, b or c and only contains a JmjC domain. The other members of the Jmjd2 family also contain a PHD (plant homeodomain) sequence, a methylated lysine binding motif,⁸⁷ and Tudor domains, which read di- and tri-methylated lysines as well as methylated arginines (Fig. 19).⁸⁸ There are two possible other members of the Jmjd2 family, Jmjd2e and f. The genes that code for these proteins are currently believed to be pseudogenes,⁸⁹ genes which have lost their protein coding ability or are not expressed in the cell.⁹⁰

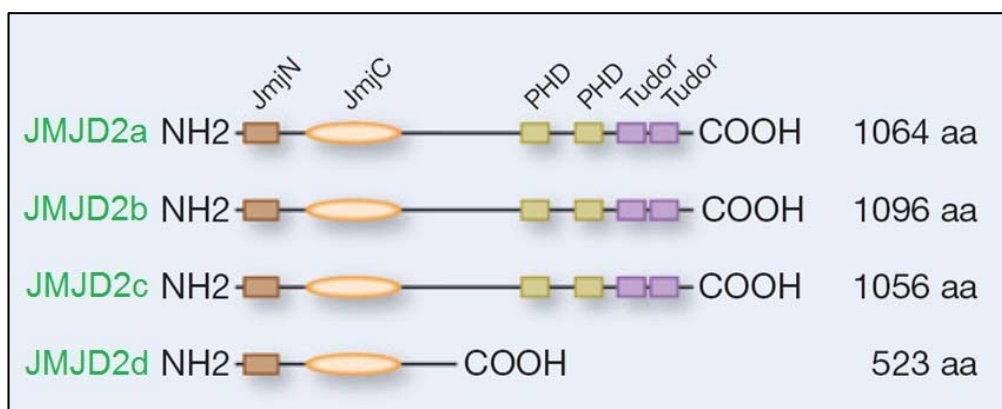


Figure 19: Schematic diagram of the Jmjd2 family showing the domains present and length of amino acid chain. Adapted⁷²

Ideally, a selective Jmjd2 inhibitor would be identified that would inhibit only one of the Jmjd2 family members as this would simplify any biological outcomes observed on dosing

the probe compound. However, due to the high homology between the JmjC domains in the JmjD2 family, especially within the methylated lysine binding pocket,⁵⁶ this would be difficult to achieve and is not a focus of the project (Table 1).

JmjD	a	b	c	d	e	JmjD	a	b	c	d	e
a	1.00	0.82	0.73	0.60	0.59	a	1.00	0.81	0.82	0.73	0.73
b	0.82	1.00	0.76	0.68	0.66	b	0.81	1.00	0.85	0.76	0.74
c	0.73	0.76	1.00	0.60	0.59	c	0.82	0.85	1.00	0.74	0.73
d	0.60	0.68	0.60	1.00	0.80	d	0.73	0.76	0.74	1.00	0.91
e	0.59	0.66	0.59	0.80	1.00	e	0.73	0.74	0.73	0.91	1.00

Table 1: Levels of homology of the JmjD2 family. Left: The first 387 aa residues. Right: The 169 aa residue sequence which contains the Fe and 2-OG interacting residues.

However, selectivity, in addition to other attributes, is required for the KDM4 or JmjD2 family over the other KDM families and the compounds described earlier (Fig. 17, p 33) do not provide the required profile, with many of them being pan-inhibitors of 2-OG using enzymes.^{76,77} Therefore, a body of work was initiated to identify compounds to provide probe compounds for the JmjC domain of the JmjD2 family of enzymes. Based on literature evidence, it was anticipated this would lead to down regulation of anti-inflammatory cytokines such as type I IFN, which would be of value for an SLE indication.⁸⁵

Therefore, a programme of work was undertaken to identify probe molecules that were potent, selective for JmjD2 lysine demethylases and could engage the endogenous enzyme in the nuclei of cells. Upon the identification of such molecules, they would be tested in cellular systems to determine if a phenotype could be identified.

4.2.1 Identification of lead molecules

Previously, in our laboratories, there had been an interest in the identification of a JmjD3 inhibitor and a high throughput screen (HTS) using the compound collection available in our laboratories had been undertaken. Following up the results from the HTS ultimately led to the discovery of biheteroaryl **4.008** (Fig. 17, p 33), a selective JmjD3 compound.⁸⁰ The output from the JmjD3 HTS was reinvestigated and hits were cross screened through a JmjD2 RapidFire™ assay.⁹¹ In a RapidFire™ assay a solution of the molecule of interest at different concentrations is incubated with one of the Jumonji enzymes and a trimethylated peptide substrate then added. The mixture is allowed to stand for either 45 or 60 minutes and then the enzyme is denatured with a TFA solution halting the demethylation. The

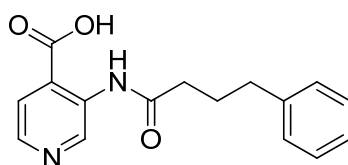
mixtures are then sampled by mass spectrometry and the remaining trimethylated lysine peptide substrate ARTAQTARKSTGGIA is quantified by looking for the molecular ion and compared against the ions of the di-methylated peptides. This is possible through integrating the peak areas of the ions. Comparing the amounts of tri- and di-methylated peptide from the different concentrations of inhibitor compound allows an IC₅₀ to be determined.

Molecules found from the Jmjd3 screen needed to have certain properties to be taken forward as hits for Jmjd2 family inhibitors:

- < 10 µM inhibition at a Jmjd2 family enzyme
- Evidence of selectivity over Jmjd3 or EGLN3
- > 500 mV redox potential

Less than 10 µM inhibition at the Jmjd2 family was required to have a reasonable level of potency that could be realistically optimised up to the required levels for a probe compound (p 39). Evidence of selectivity over other JmjC containing domains was required. Thus, Jmjd3 and EGLN3 (Egl nine homolog 3) were chosen as representative JmjC domain containing proteins to show selectivity against and previous efforts to find inhibitors of these proteins within our laboratories meant that assays already existed for these targets.^{80,92} The requirement to have a redox potential of greater than 500 mV was necessary to ensure the compounds were inhibiting the binding of 2-OG rather than reducing or oxidising the iron to a non-catalytic oxidation state.

By applying these principles in analysing the HTS dataset, amide containing 4-pyridine carboxylic acid **4.012** was identified (Table 2).



4.012

Jmjd2a/c pIC ₅₀ (LE)	5.7 (0.37)/ 6.4 (0.43)
Jmjd3 pIC ₅₀	5.9
EGLN3 pIC ₅₀	≤ 4.5
Oxidative stability mV	> 1320

Table 2: Properties of **4.012**.

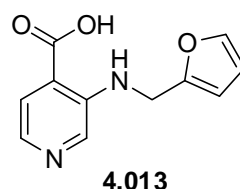
The numbers in brackets represent the ligand efficiency (LE) of the compound. LE is a concept which relates the amount of binding energy per non-hydrogen atom or heavy atom (HA).⁹³ By including a multiplication factor of 1.37 the amount of binding energy each atom is providing can be shown in kcal mol⁻¹ (Equation 1).⁹⁴

$$LE = \frac{1.37 \times pIC_{50}}{HA}$$

Equation 1: Calculation of LE.

Kuntz *et al.* have shown that the maximal affinity per HA for organic compounds is 1.5 kcal mol⁻¹.⁹⁵ The average LE of a marketed drug is around 0.3.⁹⁶ When identifying a starting fragment to work from and elaborate it is useful to start with as high an LE as possible because the ligand efficiencies of compounds can fall as they are grown from a fragment. Having stated this, maintaining or increasing LE is highly desirable as one proceeds through optimisation of a given lead.

Amide containing 4-pyridine carboxylic acid **4.012** was a good, ligand efficient starting point and a package of work was undertaken against it. This work eventually led to compounds, for example furan containing **4.013**, which were greater than one hundred-fold selective over JmjD3 and showed potency in a JmjD2c cell assay (Table 3). However, there was a one hundred-fold reduction in potency between the JmjD2c RapidFire™ assay and the JmjD2c cell assay. This was believed to be linked to the low permeability, measured using an artificial membrane, of carboxylic acid **4.013** (Table 3). The low permeability, in the artificial membrane permeability assay (AMP), shows that **4.013** is likely to diffuse into cells slowly. Charged molecules permeate cell membranes slowly through passive diffusion,⁹⁷ and the carboxylic acid present in **4.013** has a negative charge at biological pH of 7.4.⁹⁸ The permeability of a compound can be measured in a high throughput manner using an artificial membrane bilayer, which has been correlated with passive diffusion of compounds into cells.⁹⁹



JmjD2c/d pIC ₅₀ (LE)	6.9 (0.59)/6.8 (0.58)
JmjD3 pIC ₅₀	4.8
JmjD2c cell assay pIC ₅₀	5.2
AMP nm s ⁻¹	< 3

Table 3: Properties of **4.013**.

In an attempt to improve the cellular permeability of the compounds, esters were made of the carboxylic acids. These esters showed no activity in the JmjD2c cell assay, presumably due to the ester not being cleaved to the active carboxylic acid. Therefore, a search for non-carboxylic acid containing cellular inhibitors of the JmjD2 family was undertaken to investigate if inhibiting the JmjD2 family of enzymes could inhibit IFN production or show another phenotypic response. The removal of the carboxylic acid functionality was designed to improve cellular penetration of the probe molecules.

4.3 Screening cascade

In order to identify a suitable probe compound certain criteria needed to be met and hence a screening cascade was put into place (Fig. 20).

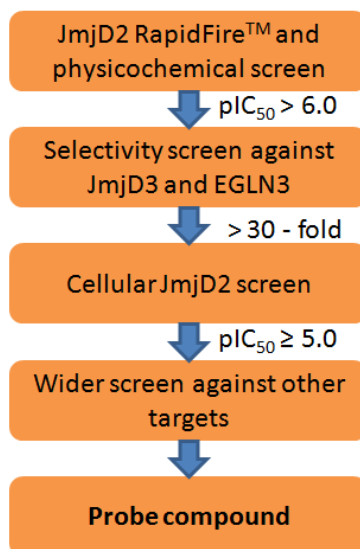


Figure 20: Screening cascade for JmjD2 family inhibitors.

To progress to the next level of the screening cascade the test compounds had to meet certain criteria that would facilitate identification of a probe molecule. Initially, the compounds need acceptable physicochemical properties with a LogP of between 1 – 3 and a molecular weight of < 400 Da as this has been demonstrated to be an acceptable range in order to obtain cellular penetration.¹⁰⁰ While increasing the lipophilicity of the compounds could aid cellular penetration, it is likely to cause wider issues. For example, compounds with high lipophilicity have been linked with promiscuity, poor PK and toxicology issues, often discovered later in development.¹⁰¹ These properties can be calculated prior to synthesis of the compound. However, the potency of the molecule cannot be calculated and the compound must be synthesised and screened in the RapidFire™ assay. Here a pIC₅₀ value of > 6.0 was thought to be sufficient for progression to the next level of the screening cascade along with AMP ≥ 30 nm s⁻¹ and aqueous solubility of ≥ 50 µg mL⁻¹.

Greater than 30-fold selectivity was required over both Jmjd3 and EGLN3 compared to the Jmjd2 family to provide selective compounds. Jmjd3 and EGLN3 had been investigated previously in our laboratories and there was already experience in running these assays. Selectivity over two other JmjC containing proteins gave confidence that test compounds were not inhibiting all of the JmjC containing proteins. Compounds that inhibit all known proteins of a family or class are known as pan - inhibitors.

Selectivity in the biochemical RapidFire™ assays allowed compounds to progress to the Jmjd2c cell assay where a pIC₅₀ value of ≥ 5.0 was needed for further progression. In the Jmjd2c cellular assay, cells are caused to overproduce Jmjd2c while being incubated with different concentrations of test compound for 24 hours. During this period of time the Jmjd2c can demethylate H3K9 present in the nucleus. The cells are rendered inactive with a solution of formaldehyde and incubated with a trimethylated - H3K9 antibody which can be used to measure the levels of inhibition by the compound.¹⁰² Positive activity in the cell assay also proves target engagement of the test compounds with Jmjd2c.

Finally, the compounds should be tested against a wide range of non-related drug and liability targets to ensure that any phenotype seen is not due to off-target activity. Once a test compound has passed all these criteria a probe compound for the Jmjd2 family will have been identified.

4.4 Identification of a JmjD2 family hit compound.

The amide containing 4-pyridine carboxylic acid **4.012** (Table 2, p 37) was simplified to isonicotinic acid (**4.014**, Table 4, p 43). Isonicotinic acid (**4.014**) was screened against JmjC containing enzymes and was found to be selective for the JmjD2 family compared to JmjD3 (Entry 1, Table 4, p 43). This provided a small fragment to begin the search for a JmjD2 family probe molecule. Isonicotinic acid (**4.014**) has an undesired carboxylic acid present and this needed to be removed to find a cellularly penetrant probe molecule.

An X-ray crystal structure was obtained for isonicotinic acid (**4.014**) bound in JmjD2d and this was compared to the crystal structure of 2-OG (**3.006**) bound in JmjD2d (Fig. 21).¹⁰³ The crystallography systems employed in this study use nickel or cobalt in place of the catalytic iron in the natural protein. In JmjD2d, the key interactions for isonicotinic acid (**4.014**) are between the carboxylate acting as an H-bond acceptor for Lys210 and Tyr136 and the pyridine nitrogen chelating to the iron. Additionally, there is a possibility of an aromatic face to face interaction between isonicotinic acid (**4.014**) and Phe189. The same interactions are seen across the JmjD2 family, albeit with the numbering of the residues changing. When comparing the overlay with 2-OG (**3.006**) (Fig. 16, p 32) there is no significant change in the conformation of the residues in the JmjC domain. The H-bonds are maintained between the protein and the ligand for both 2-OG (**3.006**) and isonicotinic acid (**4.014**). There are some minor changes around the chelation to the metal as 2-OG (**3.006**) binds in a bidentate fashion while isonicotinic acid (**4.014**) chelates in a monodentate manner (Fig. 21).

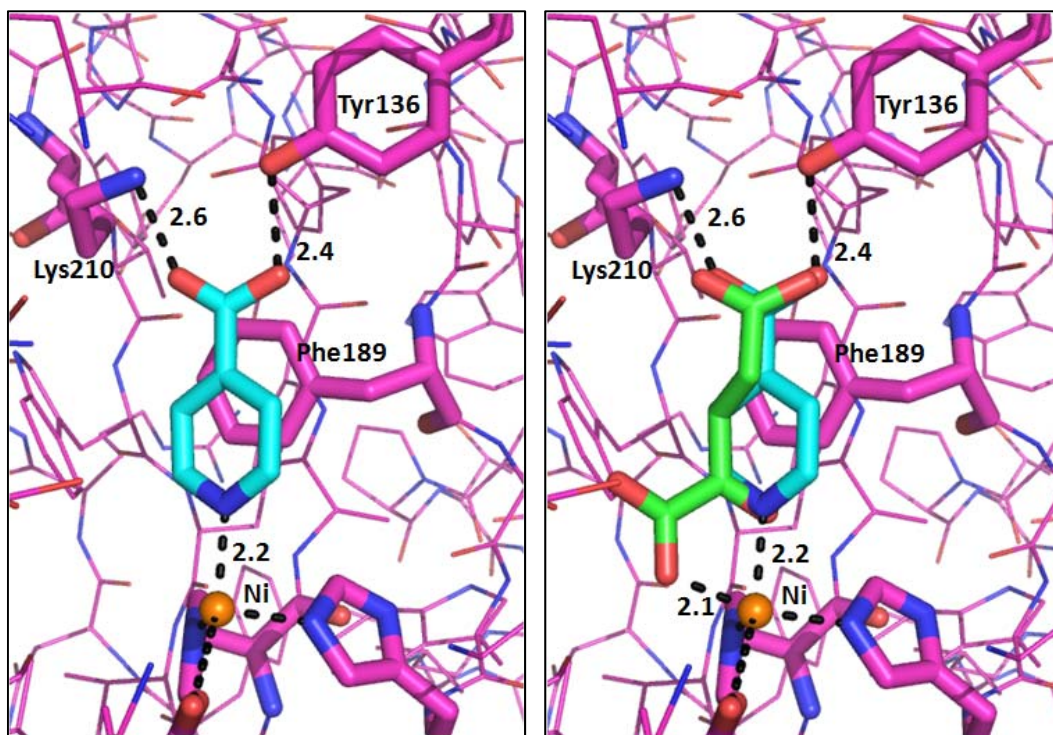


Figure 21: Left X-ray crystal structure of isonicotinic acid (**4.014**) shown in cyan in JmjD2d, resolution = 2.0 Å. Right Overlaid with 2-OG (**3.006**) in green (right), resolution = 1.8 Å.⁷³

Given the very limited success of using a pro-drug strategy for JmjC containing proteins (p 34) a search of similar compounds without the carboxylic acid moiety was undertaken using the compound collection available in our laboratories.¹⁰⁴ It was reasoned that the compounds selected would make the same interactions with the JmjD2 family proteins as isonicotinic acid (**4.014**) did. The results of the search were screened through the JmjD2 family and selectivity assays (Table 4).

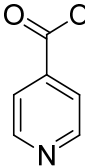
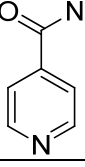
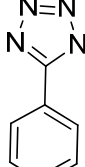
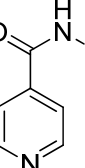
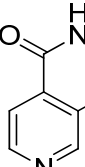
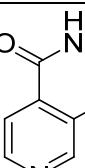
Entry	Number	Structure	JmjD2c pIC ₅₀ (LE)	JmjD2d pIC ₅₀ (LE)	JmjD2e pIC ₅₀ (LE)	JmjD3 pIC ₅₀	EGLN3 pIC ₅₀
1	4.014		5.9 (0.90)	5.3 (0.81)	5.4 (0.82)	< 4.0	-
2	4.015		< 4.0	< 4.0	< 4.0	< 4.0	< 4.3
3	4.016		4.1 (0.51)	3.6 (0.45)	-	-	-
4	4.017		5.8 (0.79)	4.8 (0.66)	5.1 (0.70)	5.3	< 4.0
5	4.018		< 4.0 ^a	< 4.0 ^a	< 4.0 ^a	< 4.0	4.4
6	4.019		5.7 (0.71)	5.0 (0.62)	5.1 (0.64)	< 4.0	< 4.3

Table 4: Comparison of the potencies of JmjD2 test compounds. ^a) Assay carried out with 10x concentration of JmjD2 enzyme, incubating for 8 min.

Primary amide containing **4.015** (Entry 3), as a close analogue to isonicotinic acid (**4.014**) was expected to retain some binding affinity, although upon testing it displayed pIC₅₀ values of < 4.3 at the enzymes of interest. Tetrazole is a known isostere of carboxylic acid^{105,106} and thus tetrazole containing **4.016** was selected for investigation. Compared to isonicotinic acid (**4.014**) tetrazole containing **4.016** was found to be 50 to 100-fold less active at JmjD2c and JmjD2e, respectively, which can be rationalised by examining Fig. 21 (p 42). Assuming that the pyridine nitrogen chelates to the metal, Lys210 and Tyr136 would have to move to avoid steric clash with the tetrazole, which is disfavoured energetically, causing a decrease in the binding potency. Hydroxamic acid is another known carboxylic

acid isostere¹⁰⁶ and therefore **4.017** was investigated. The potency of hydroxamic acid containing **4.017** was similar to isonicotinic acid (**4.014**) which was promising. However, the compound was equipotent at JmjD3 which made it an unsuitable starting point for a JmjD2 selective probe. This lack of selectivity could be due to hydroxamic acids being chelators for a wide range of transition metals^{107,108} and an X-ray crystal structure for hydroxamic acid containing **4.017** in JmjD2d shows a different binding mode (Fig. 22).¹⁰³

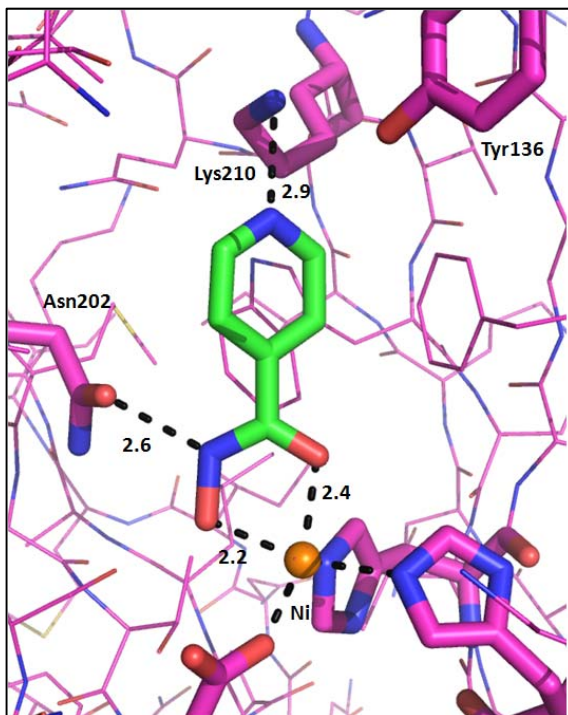


Figure 22: X-ray crystal structure of hydroxamic acid compound **4.017** in JmjD2d, resolution = 2.1 Å.

Compared to the X-ray crystal structure of isonicotinic acid (**4.014**) (Fig. 21, p 42) hydroxamic containing **4.017** has been inverted, with the hydroxamic acid chelating, in a bidentate fashion, to the metal. The hydroxamic acid also makes an H-bond to Asn202, which is not implicated in the binding of isonicotinic acid (**4.014**). The final interaction between the ligand and the protein is the pyridine nitrogen acting as an H-bond acceptor for Lys210. Tyr136 has not moved significantly even though it is not making an interaction with hydroxamic containing **4.017**.

Naphthyridone **4.018** universally had pIC_{50} values of < 4.0 at the JmjD2 family and was of no further interest as a template. However, introduction of a nitrogen into the core provided pyridopyrimidinone **4.019**, which gave a very attractive profile to work from being only approximately two and a half-fold less potent than isonicotinic acid (**4.014**) whilst its binding to JmjD3 and EGLN was below the limit of quantification. The difference in potency between naphthyridone **4.018** and pyridopyrimidinone **4.019** will be discussed later (Table 7, p 53). An X-ray structure of pyridopyrimidinone **4.019** shows it makes the same interactions as isonicotinic acid (**4.014**) (Fig. 23).¹⁰³

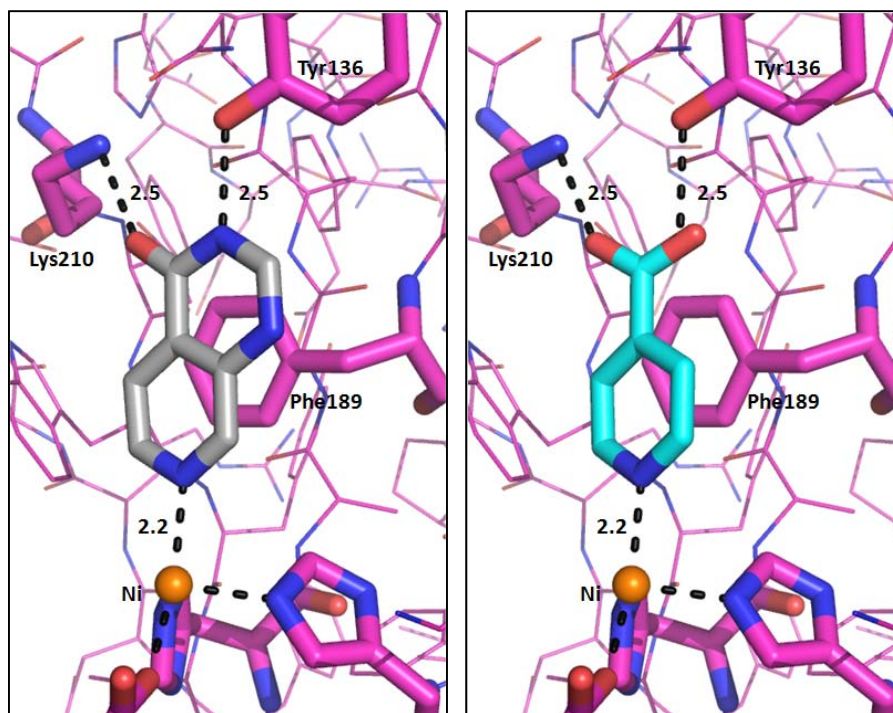
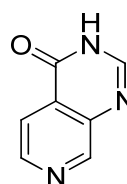


Figure 23: Comparison of the X-ray crystal structures of pyridopyrimidinone **4.019** (grey) and isonicotinic acid (**4.014**) (cyan) in JmjD2d, resolution for both = 2.0 Å.

The amide oxygen behaves as an H-bond acceptor for Lys210, the amide nitrogen is an H-bond donor for Tyr136 and the nitrogen of the pyridine ring chelates to the nickel. Additionally there is a face to face aromatic ring interaction with Phe189 (Fig. 23). Due to the high homology of the JmjD2 family, the lysine and tyrosine residues that pyridopyrimidinone **4.019** interacts with in JmjD2d are conserved in the other proteins of the JmjD2 family (Table 1, p 36). Therefore, selectivity for an individual member of the JmjD2 family will be very challenging to achieve. As the levels of inhibition for individual

members of the JmjD2 family have shown to be largely similar over a large number of compounds only JmjD2d RapidFire™ data will be presented routinely.



JmjD2c/d/e pIC ₅₀ (LE)	5.7 (0.71) / 5.0 (0.62) / 5.1 (0.64)
JmjD3 pIC ₅₀	< 4.0
EGLN3 pIC ₅₀	< 4.3
Oxidative stability mV	719
Molecular weight Da	147
cLogP	- 0.7
Aqueous solubility µg mL ⁻¹	≥ 68
pK _a	8.3
AMP nm s ⁻¹	69

Table 5: Properties of pyridopyrimidinone **4.019**.

As mentioned earlier, the potency of the molecule was at an acceptable level to work from with good selectivity between JmjD3 and the JmjD2 family. The compound was found to be oxidatively stable and had a low molecular weight and cLogP that were amenable to growing the fragment and looking for other interactions with the target enzymes. Pyridopyrimidinone **4.019** had acceptable levels of aqueous solubility in an assay determining this from a DMSO solution. This combined with pyridopyrimidinone **4.019** being, at a physiological pH of 7.4, largely uncharged gives it a higher chance of passively crossing the cell membrane compared to isonicotinic acid (**4.014**) as shown by the AMP data (Table 5). It was from pyridopyrimidinone **4.019** that work in this chapter originated.

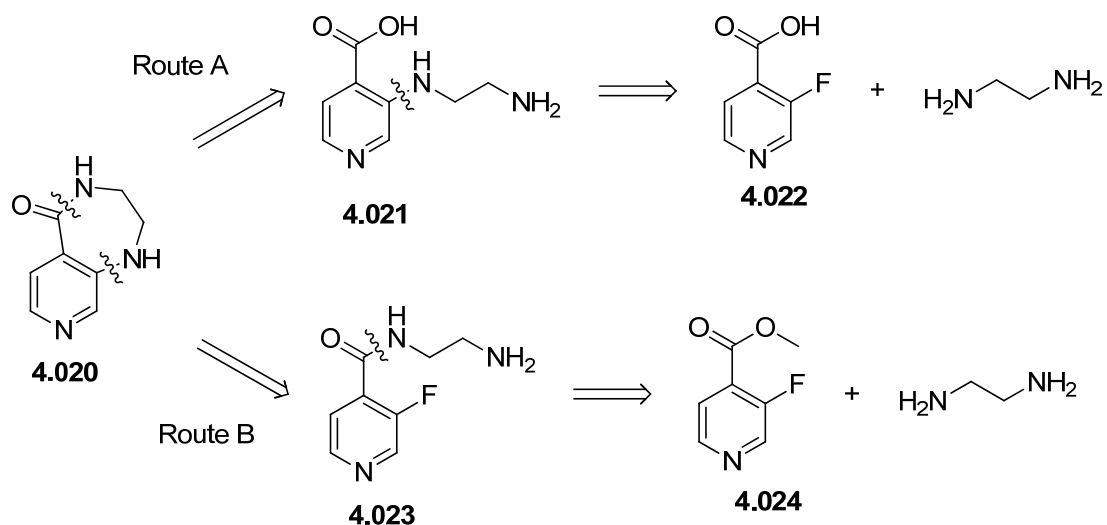
The synthesis of the compounds in this thesis was a team effort and bespoke compounds synthesised by other members of the research group will be noted with an asterisk (*).

4.5 Investigation of 6,7 and 6,5 sized ring systems

4.5.1 Synthesis of test compounds

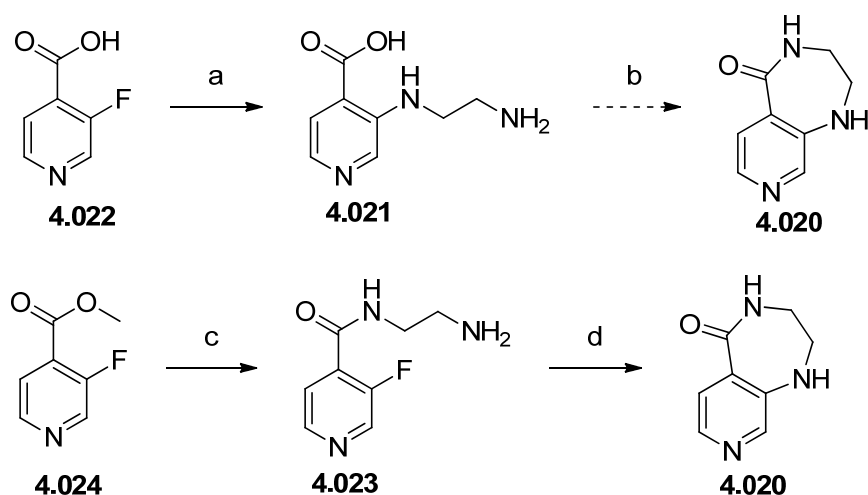
The first area investigated was to determine the effects of changing the ring size on the potency of the molecules. One of the first compounds to be synthesised was a homologated, saturated version of pyridopyrimidinone **4.019** which breaks the aromaticity in the pyrimidinone ring of the bicycle. Compound **4.020** was designed to investigate different vectors around the amide, to determine how this would affect the H-bonding to

Lys210 and Tyr136 in JmjD2d and whether a non-planar molecule would be tolerated within the active site. Two synthetic approaches were considered to give the desired material. Accordingly, there were two key bonds to disconnect (Scheme 2).



Scheme 2: Disconnections to **4.020**.

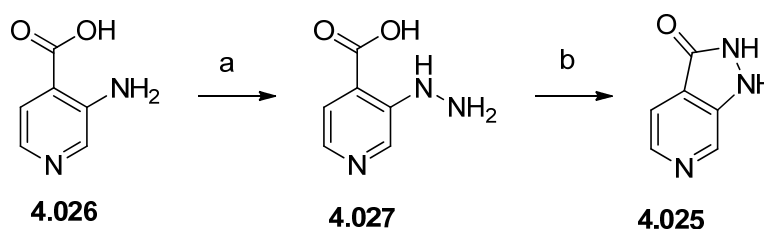
These initial disconnections were between the C-N bond of the amide (Route A) or the pyridyl ring-N bond (Route B). Historically, a number of molecules in the isonicotinic acid series such as furan containing **4.013** (Table 3, p 39) had been made by S_NAr of aliphatic amines with 3-fluoroisonicotinic acid (**4.022**) and there are further examples of S_NAr reactions with fluoro substituted electron deficient aromatic rings.¹⁰⁹ The 7-exo-trig cyclisation¹¹⁰ was then expected to deliver diazepinone containing **4.020** via an amide coupling (Scheme 3).^{111,112}



Scheme 3: Reagents and conditions: a) $H_2NCH_2CH_2NH_2$, 150 °C, microwave, 41%; b) H_2SO_4 , EtOH, 0%; c) $H_2NCH_2CH_2NH_2$, EtOH, 100 °C, microwave, 30%; d) DMSO, 160 °C, 21%.

The S_NAr reaction with fluoropyridine containing **4.022** using ethylenediamine as solvent gave amino acid **4.021**. The cyclisation of amino acid **4.021** was unsuccessful on heating in ethanol with sulfuric acid as neither the ethyl ester, a possible intermediate, or the desired product were observed. In contrast, diazepinone containing **4.020** was successfully accessed by the direct amide formation from methyl ester **4.024** to give amide **4.023** in 30% yield and the subsequent S_NAr cyclisation gave the desired product **4.020** in a yield sufficient for biological assays (Scheme 3).

Another compound of interest was pyridopyrazolone **4.025** which contracted the pyrimidinone ring of pyridopyrimidinone **4.019** to a pyrazolone. This probes a different ring size at the top of the molecule while retaining aromaticity allowing access to different vectors within the protein compared to the six membered ring ligands. The synthesis of **4.025** began with the diazotisation of 3-aminoisonicotinic acid (**4.026**) and subsequent reduction of the resulting diazonium salt by aqueous sodium sulfite, generated by passing gaseous sulfur dioxide through water, to give aryl hydrazine **4.027**. Aryl hydrazine **4.027** was subsequently cyclised to give pyridopyrazolone **4.025** by refluxing in dilute aqueous hydrogen chloride (Scheme 4).¹¹³



Scheme 4: Reagents and conditions a) conc. HCl, NaNO₂, sat. aq. SO₂, 0 °C to 20 °C, 66%; b) aq. HCl, reflux, 45%.

4.5.2 Discussion of SAR of 6,7 and 6,5 sized ring systems and intermediates

Diazepinone containing **4.020**, when tested at JmjD2d, was found to be inactive, indicating that a seven membered ring is not tolerated in this position (Table 6, Entry 6). This could be due to a number of factors: the protein is not sufficiently mobile in this area to incorporate the new vectors around the amide to interact with Lys210, Tyr136 or the face to face aromatic interaction between the ligand and Phe189 may not have sufficient overlap. Additionally, the aromatic face to face interaction with Tyr136 may be disrupted by the introduction of the sp³ centres. Another possibility is that the amide may not be suitably

acidic. The pK_a of the amide is predicted to be 13.4 and is considerably higher than the pK_a of fragment **4.019** which has a measured pK_a of 8.3 (Table 5, p 46). The distance between Phe189 and the original fragment **4.019** is 3.7 Å, which is within the range of distances for a diverse range of aromatic face to face interactions.¹¹⁴ Hence, the steric clash between the sp^3 centres of diazepinone containing **4.020** and Phe189 may be disrupting this important interaction and cause the binding of **4.020** not to be energetically favourable.

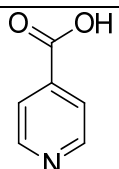
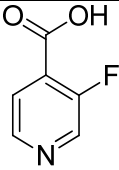
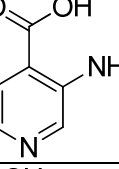
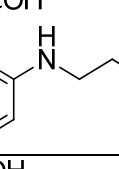
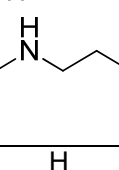
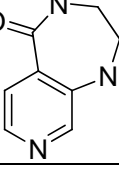
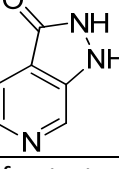
Entry	Number	Structure	JmjD2d pIC ₅₀ (LE)	cLogP ^a
1	4.014		5.3 (0.81)	0.8
2	4.022		4.6 (0.63) ^b	0.6
3	4.026		5.8 (0.78)	0.8
4	4.021		< 4.0	-1.0
5	4.028*		5.7 (0.56)	-0.6
6	4.020		< 4.0 ^b	-0.6
7	4.025		< 4.0	0.0

Table 6: JmjD2d RapidFire™ potencies for test compounds. ^a) Calculated using Daylight cLogP v4.81. ^b) Assay carried out 10x concentration of JmjD2 enzyme, incubating for 8 min.

3-Fluoroisonicotinic acid (**4.022**) and amino acid **4.021** (Entries 2 and 4, Table 6) were also submitted for test, but were found to be less active than isonicotinic acid (**4.014**) at JmjD2d. This five-fold drop in potency for 3-fluoroisonicotinic acid (**4.022**) may be due to the pyridine lone pair being less able to chelate to the iron as the electronegativity of the fluorine decreases the electron density in the ring. 3-Aminoisonicotinic acid (**4.026**) is 20-fold more potent than 3-fluoroisonicotinic acid (**4.022**) against JmjD2d. As the JmjD2d potency of the isonicotinic acids is ranked **4.026** > **4.014** > **4.022** and these respectively have electron donating, neutral and electron withdrawing groups, it lends weight to the hypothesis that as electron density within the pyridine ring increases so does the binding strength to the iron. A study by Rodgers on the binding strength of substituted pyridines to alkali metal ions supports this as aminopyridines are better binders to metal ions than unsubstituted pyridine.¹¹⁵ Also, the pyridine-metal bond of 2- and 4-aminopyridines is stronger than that of 3-aminopyridine as more electron density can be placed on the ring nitrogen by the mesomeric effect when the amino group is in the 2 or 4 positions.¹¹⁵ Why the activity of amino acid **4.021** is less than 3-aminoisonicotinic acid (**4.026**) (Entries 4 and 3) is unclear and for a definitive answer an X-ray crystal structure may be required. The ethylamine chain of amino acid **4.021** is clearly making a deleterious interaction, however, information from related crystal structures it is not obvious what this interaction is. One possibility is the aliphatic amine is too close to Lys245 at a distance of about 6 Å (Fig. 24). At physiological pH both Lys245 and the aliphatic amine will be positively charged and electrostatic repulsion between these two groups causes the drop in activity for ethylamine containing **4.021**. The amine moiety of ethylamine analogue **4.021** is near to Asp139 in JmjD2d. Propylamine analogue **4.028**, synthesised in the efforts that identified furan containing **4.013** (p 39), shows an increase in potency of at least 50-fold at JmjD2d compared to ethylamine containing **4.021** (Table 6). The X-ray crystal structure of propylamine compound **4.028** in JmjD2d suggests it is caused by a salt bridge between the aliphatic amine and Asp139 (Fig. 24).¹⁰³

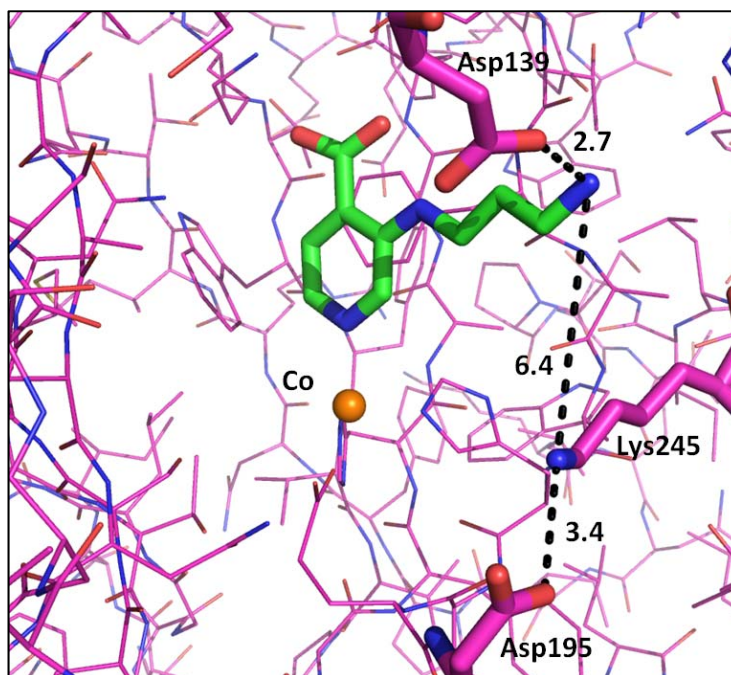


Figure 24: X-ray structure of **4.028** in JmjD2d, resolution = 1.9 Å.

The amine chain in amino acid **4.021** may not be able to form the salt bridge with Asp139 due to the shorter alkyl chain than comparatively homologated **4.028**. Pyridopyrazolone **4.025** (Entry 7, Table 6, p 49) had a pK_{50} value of < 4.0 possibly indicating that the interactions between the ligand and Lys210 and Tyr136 have been disrupted.

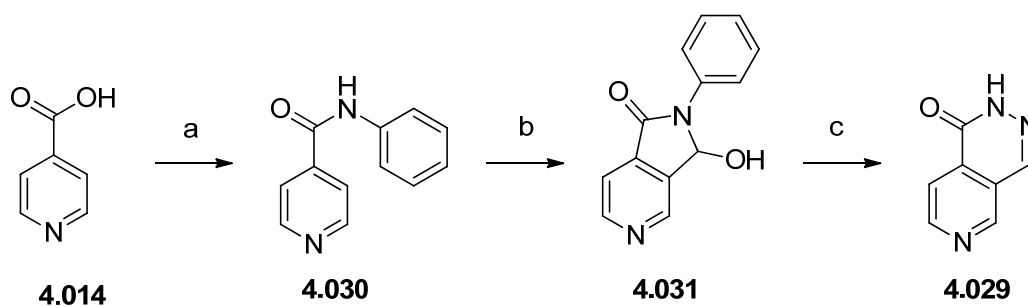
As there was precedent for activity with 6,6-bicycles and other ring systems, 5,6- and 7,6-bicycles (Table 6, p 49) showed no activity, it was decided to investigate both the pK_a s and potential alternative binding modes through changing the 6,6-bicyclic system.

4.6 Alternative 6,6-bicyclic systems

Both the pyrimidinone and pyridine rings were investigated. The modification of the pyrimidinone ring will be discussed first.

4.6.1 Investigation into changes of the pyrimidinone ring

Pyridopyridizinone **4.029** (Scheme 5) was a molecule of interest as it was predicted to have a lower pK_a than the corresponding inactive pyridopyridinone **4.018** (Table 7, p 53), although not as low as pyridopyrimidinone **4.019**. Pyridopyridizinone **4.029** was hypothesised to bind more strongly to the JmjD2 proteins as it would better mimic the carboxyl group in the isonicotinic acid (**4.014**). Based on this, pyridopyridizinone **4.029** was synthesised according to a literature procedure (Scheme 5).¹¹⁶



Scheme 5: Reagents and conditions: a) CDI, PhNH₂, 2-MeTHF, 50 °C, 83%; b) i) n-BuLi, THF, -70 – 0 °C; ii) DMF, -70 – 20 °C, 4%; c) 35% aq. NH₂NH₂, 120 °C, 8%.

After the amide formation to give aryl amide **4.030**, the addition of two equivalents of n-BuLi initially deprotonates the amide NH and then directed ortho-lithiation occurs.¹¹⁷ The anion adjacent to the amide group on the pyridine ring is initially quenched by DMF to give an aldehyde, which is isolated as hemiaminal **4.031**. Stirring hemiaminal **4.031** in refluxing 35% aq. hydrazine hydrate initially causes the formation of the hydrazone which then reacts, displacing aniline to give pyridopyridizone **4.029**. Pyridopyridizone **4.029** was found to be inactive at all enzymes of interest (Entry 3, Table 7).

Upon comparison of the measured pK_as of pyridopyridinone **4.018** and pyridopyridizinone **4.029** it was observed that having the additional electronegative nitrogen adjacent to the amidic nitrogen does lower the pK_a (Entries 3 and 2, Table 7). However, the lack of inhibition by pyridopyridizinone **4.029** could be due to the molecule still not being sufficiently acidic or the lack of H-bond acceptors at the 4-position of the pyridazinone ring. The lack of an H-bond acceptor may cause unfavourable interactions with the water network around this area of the active site rendering the compound inactive (Table 7). This potential disruption of the water network and necessity of an H-bond acceptor could be an additional factor in why pyridopyrazolone **4.025** (Entry 7, Table 6, p 49) was also found not to inhibit JmjD2 proteins.

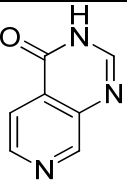
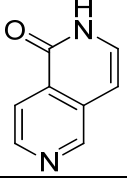
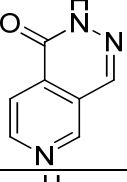
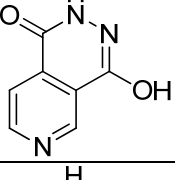
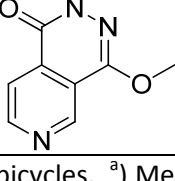
Entry	Number	Structure	JmjD2d pIC ₅₀	Measured pK _a ^a
1	4.019		5.0 (0.62)	8.3
2	4.018		< 4.0 ^b	> 12
3	4.029		< 4.0	10.6
4	4.032*		4.6 (0.53)	4.4
5	4.033*		< 4.0	10.9

Table 7: RapidFire™ activities of 6,6 bicycles. ^a) Measured using a Sirius T3. ^b) Assay carried out with 10x concentration of JmjD2 enzyme, incubating for 8 min.

The closely related molecule **4.032** was successfully crystallised in JmjD2d and an X-ray structure derived.¹⁰³ The crystal structure shows Lys245 is actively H-bonding with hydroxypyridopyridazinone **4.032** and Tyr136 has moved in comparison with pyridopyrimidinone **4.019**, while the remainder of the protein is comparatively static (Fig. 25).

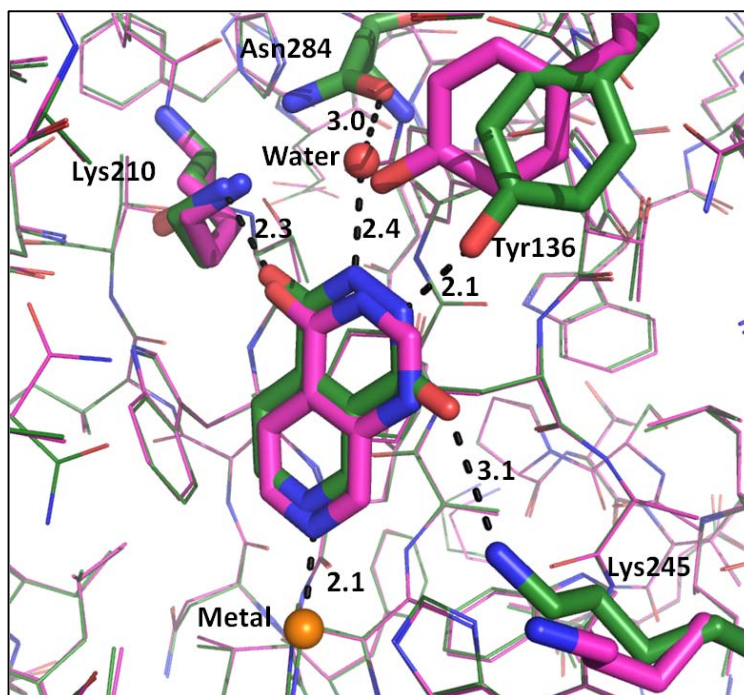
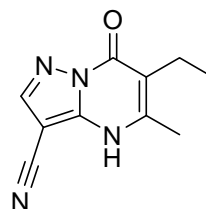


Figure 25: Overlay of two X-ray crystal structures in JmjD2d. Pyridopyrimidinone **4.019** (magenta), resolution = 2.0 Å, and hydroxypyridopyridazinone **4.032** (green), resolution = 2.5 Å. The water replacing the oxygen of Tyr136 is the red sphere labelled water below Asn284.

Interestingly, water occupies the same site as the oxygen of Tyr136 in pyridopyrimidinone **4.019** and makes an H-bond to Asn284 in an analogous manner to Tyr136. Lys245 is another residue in the active site which has moved, in this case closer to hydroxypyridopyridazinone **4.032** making an H-bond 3.1 Å long between the protonated nitrogen of Lys245 and the nearby oxygen of hydroxypyridopyridazinone **4.032**. Methoxy analogue **4.033** was found to be inactive. This could be caused by the disruption of the H-bond between Lys245 and the nearby oxygen due to steric hindrance around the oxygen by the methyl group. As methoxy containing **4.033** has a higher pK_a than pyridopyrimidinone **4.019** and is inactive, it appears that activity is partially driven by pK_a and above a certain value, lack of acidity may prevent binding of the molecules in the active site. The effect of pK_a may have a smaller effect on the potency of the molecule compared to having an accessible H-bond acceptor on the right hand side of the molecule for these bicycles. One hypothesis is that molecules which do not contain an H-bond acceptor on the right hand side of the molecule cause disruption of a water network in this area of the active site. This in turn causes a reduction in the activity of the molecules without this moiety.

4.6.2 Movement of Tyr136

The movement of the protein shown in Fig. 25 was intriguing and was also seen for another chemical series that was worked on by the JmjD2 chemistry team. This was in an attempt to produce a second JmjD2 inhibitor chemical series structurally distinct from the series based on pyridopyrimidinone **4.019**, as suggested by the probe philosophy (Section 3.3.1, p 24). The second series is exemplified by cyanopyridopyrimidinone **4.034** (Table 8).



JmjD2c/d/e pIC ₅₀ (LE)	5.6 (0.51) / 5.2 (0.47) / 5.4 (0.49)
JmjD3 pIC ₅₀	< 4.0
EGLN3 pIC ₅₀	< 4.3
Oxidative stability mV	892
Molecular weight Da	202
cLogP	0.2
Aqueous solubility µg mL ⁻¹	74
AMP nm s ⁻¹	< 3

Table 8: Properties of cyanopyridopyrimidinone **4.034**.

However, the desired probe profile was not achieved through this series and will not be discussed beyond this section. An X-ray crystal structure of cyanopyridopyrimidinone **4.034** in JmjD2d was obtained (Fig. 26).¹⁰³

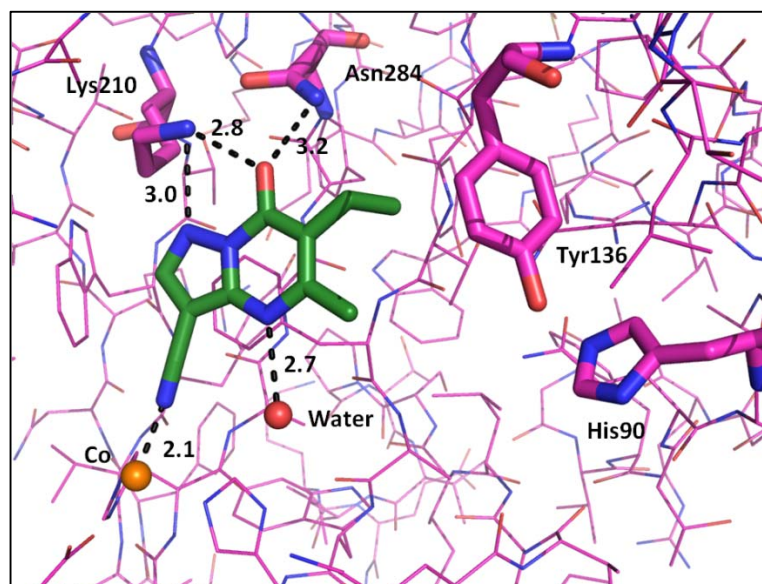


Figure 26: X-ray crystal structure of cyanopyridopyrimidinone **4.034** bound in JmjD2d, resolution = 2.1 Å.

Examination of the X-ray crystal structure of cyanopyridopyrimidinone **4.034** in JmjD2d shows the interactions between cyanopyridopyrimidinone **4.034** and the JmjD2d protein (Fig. 26). The nitrogen lone pair of the nitrile group chelates with the metal. The carbonyl oxygen and the nitrogen at the 1-position both make H-bonding interactions with Lys210, and the N-H in the pyrimidinone ring appears to make an H-bonding interaction with a conserved water. The oxygen of the carboxamide, in addition to the H-bond with Lys210, makes an H-bonding interaction with Asn284. It is in this position that the oxygen of Tyr136 in the X-ray crystal structure of pyridopyrimidinone **4.019** (Fig. 23, p 45) and the water highlighted in the X-ray crystal structure of hydroxypyridopyridazinone **4.032** sit (Fig. 25, p 54). This highlights that Tyr136 is capable of moving and therefore new interactions or binding pockets could be found for potential probe compounds to interact with. It also indicates that having an oxygen in this position is highly desirable as it is present from a tyrosine (Fig. 23, p 45), a water (Fig. 25, p 54) or the oxygen of a carboxamide (Fig. 26).

4.6.3 Investigation into changes of the pyridine ring

Returning to alterations of the 6,6-bicyclic system; changes to the pyridine portion of pyridopyrimidinone **4.019** were investigated *via* a number of alternative, nitrogen containing aromatic ring systems. Examples from the compound collection available in our laboratories were screened against the enzymes of interest (Table 9). These compounds were identified through substructure searching.¹⁰⁴

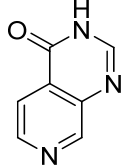
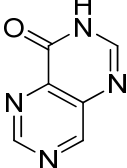
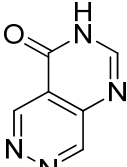
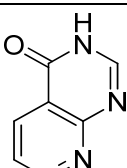
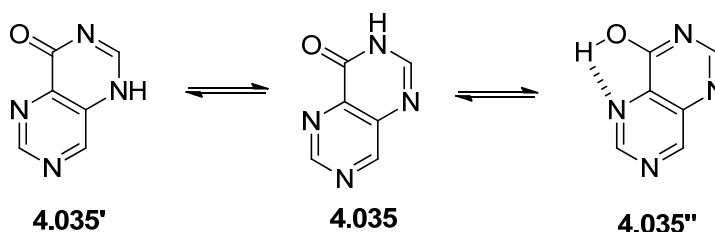
Entry	Number	Structure	JmjD2d pIC ₅₀ (LE)	Measured pK _a ^a
1	4.019		5.0 (0.62)	8.3
2	4.035		< 4.0 ^{b,c}	7.5
3	4.036		4.7 (0.59)	6.9
4	4.037		5.2 (0.65)	7.5

Table 9: RapidFire™ activities of analogues of **4.019** containing an additional nitrogen. ^{a)} Measured using a Sirius T3. ^{b)} Assay carried out with 10x concentration of JmjD2 enzyme, incubating for 8 min. ^{c)} pIC₅₀ = 5.6 on 1 test occasion, inactive on 4 other occasions.

Pyrimidine containing **4.035** (Entry 2) was found to be inactive at JmjD2d whilst the pyridazine analogues **4.036** and **4.037** (Entries 3 and 4) show similar levels of potency to pyridopyrimidinone **4.019**. The inactivity of pyrimidine compound **4.035** may be due to the metal binding properties of pyrimidines. The binding of pyrimidine to alkali metals has been shown to be less energetically favourable than the binding of alkali metals to pyridine and pyridazine.¹¹⁸ Alternatively, the binding of pyrimidine containing **4.035** to JmjD2 enzymes could be altered depending on which tautomer is energetically favoured (Scheme 6).



Scheme 6: Tautomers of **4.035**.

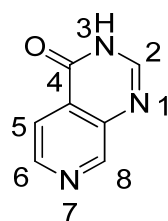
Tautomers **4.035** and **4.035'** can continue to bind Lys210 through the carbonyl group, however, the form represented by **4.035''** can form an internal hydrogen bond with the pyrimidine nitrogen at the 5-position (Scheme 6). While there are currently no small molecule X-ray crystal structures of **4.035** or its analogues, internal hydrogen bonds of the type shown in **4.035''** have been observed in 8-hydroxyquinolines.¹¹⁹ If **4.035''** is the preferred tautomer, this will further explain the loss in activity of **4.035** at JmjD2d as hydroxyl groups are poorer H-bond acceptors than carbonyl groups.¹²⁰ Hence, the key H-bonding interaction between Lys210 and **4.035** is weaker and the inhibitory effect is not detected.

Armed with the knowledge that the residues in the active site are capable of moving, exemplified by the X-ray crystal structures of hydroxypyridopyridazine **4.032** (Fig. 25, p 54) and cyanopyridopyrimidinone **4.034** (Fig. 26, p 55) in JmjD2d, an array of compounds with variation at the 2-position was planned to probe the SAR in this area. This work was carried out based on the pyridopyrimidinone core (**4.019**) as synthesis of analogues around the pyridazine templates **4.036** and **4.037** was more synthetically challenging and offered no significant benefits to potency.

4.7 Substitution at the 2-position of the pyridopyrimidinone core

4.7.1 General synthesis

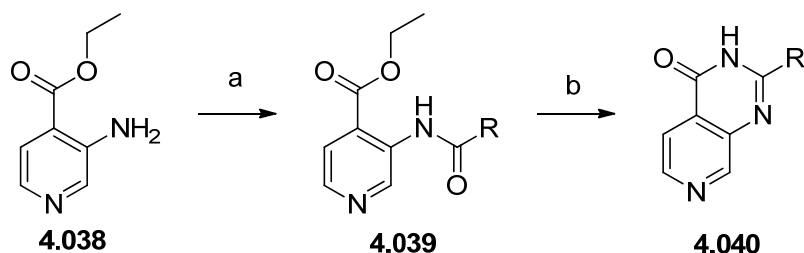
In the previous section, the X-ray crystal structure of hydroxypyridopyridazinone compound **4.032** bound in JmjD2d showed movement of Tyr136 (Fig. 25, p 54) compared with the X-ray crystal structure of pyridopyrimidinone **4.019** bound in JmjD2d. In this section the chemistry to synthesise pyridopyrimidinone analogues with substitution at the 2-position will be examined. The work was undertaken to determine if the potency of pyridopyrimidinone **4.019** could be improved upon and increased to the point where compounds could be screened in cellular assays if they were selective against JmjD3 and EGLN3. The IUPAC numbering of pyrido[3,4-*d*]pyrimidin-4(3*H*)-one is as shown below (Fig. 27).



4.019

Figure 27: Fragment **4.019** showing the numbering of pyrido[3,4-*d*]pyrimidin-4(3*H*)-one

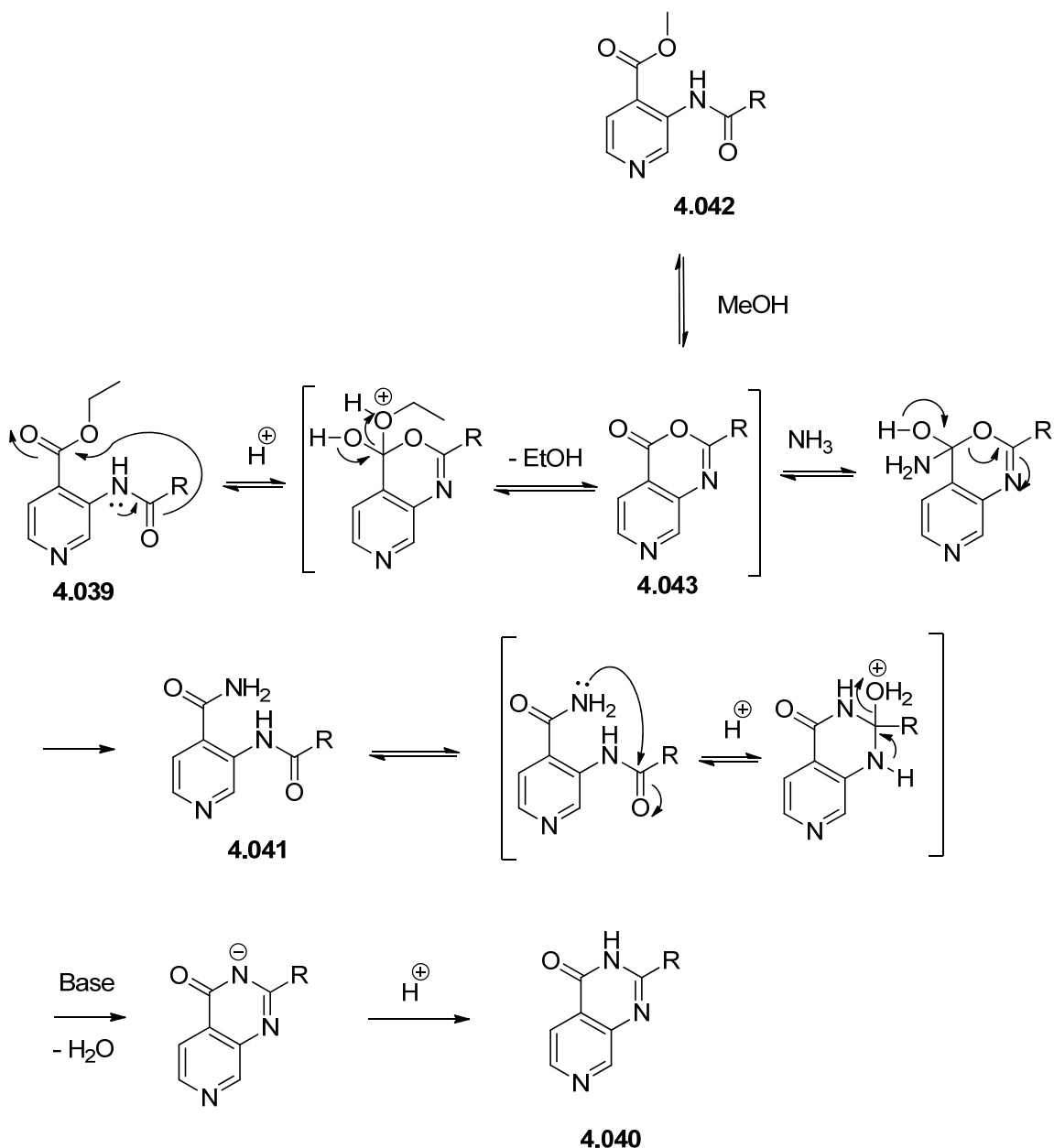
Initial exploration at the 2-position of the pyridopyrimidinone core was limited to small groups to investigate which substituents could be tolerated in this region of the molecule. Examining the crystal structure of pyridopyrimidinone **4.019** in JmjD2d showed limited space between the 2-position of **4.019** and Tyr136. To accommodate groups larger than one atom at the 2-position, Tyr136 would have to move. However, the evidence of hydroxypyridopyrimidinone **4.032** and cyanopyrazolopyrimidinone **4.034** causing significant movement of Tyr136 (Fig. 26, p 55), encouraged bold approaches to challenge the conformation of the protein. To test this hypothesis, an array of compounds with diversity at the 2-position of the pyridopyrimidinones was prepared (Scheme 7).



Scheme 7: Generic approach to the synthesis of pyridopyrimidinones: Reagents and conditions: a) RCO_2H , $(\text{COCl})_2$, DMF, NEt_3 , DCM, 20°C or RCO_2H , T3P[®], DIPEA, DCM, 20°C ; b) i) NH_3 , MeOH ii) NaOH , H_2O .

A variety of amide coupling agents were tested (CDI, T3P[®], HATU). However, the use of oxalyl chloride and DMF was the most used reagent system to activate the carboxylic acid for amide coupling with a wide range of alkyl or aryl R-substituents. Triethylamine and the ester **4.038** were then added to the activated acid *in situ* which, after purification, gave a range of amide analogues (**4.039**). Stirring some examples of amide containing **4.039** in a solution of 7 M methanolic ammonia caused cyclisation to pyridopyrimidinone analogues **4.040** at room temperature. When the cyclisation did occur, it generally took over twelve hours and the cyclisation was not successful for some analogues with only intermediate primary amides **4.041** formed (Scheme 8). After some experimentation, it was found that

the addition of sodium hydroxide greatly accelerated the ring forming reaction of primary amide **4.041** to 2-substituted pyridopyrimidinone **4.040**. The effect of base has been employed elsewhere to cyclise similar amide analogues of primary amide **4.041** after their isolation to give analogues of 2-substituted pyridopyrimidinone **4.040**.¹²¹ Several examples have shown the need for elevated temperatures for the reaction to be complete in a matter of hours and alternative bases to sodium hydroxide have also been used.^{122,123,124} However, with this pyridine template under the conditions outlined in Scheme 7, the cyclisation is complete in a matter of hours at room temperature.



Scheme 8: Proposed mechanism for formation of **4.040**.

During the cyclisation of ester **4.039** to give 2-substituted pyridopyrimidinone **4.040** a number of chemical transformations take place and several of these distinct chemical entities are observable by LCMS analysis (Fig. 28).

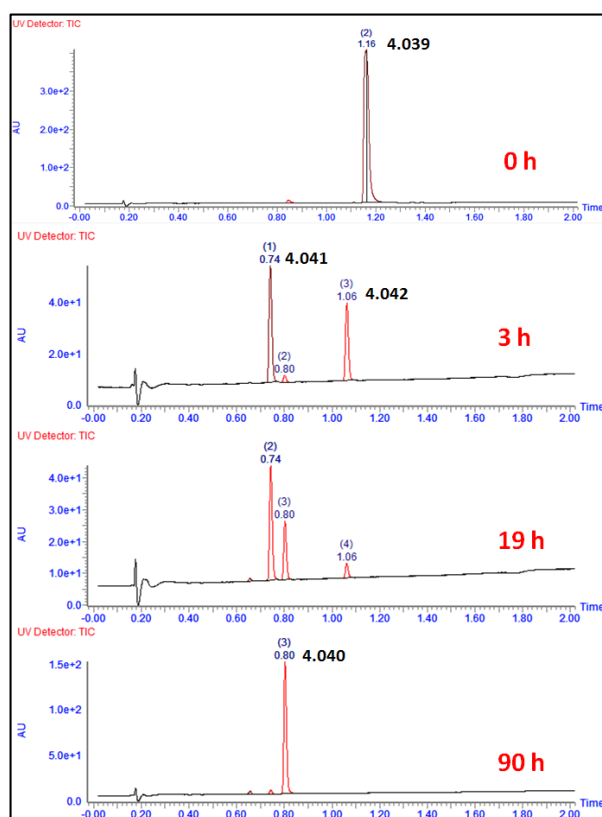


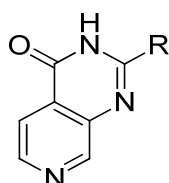
Figure 28: LCMS analysis of the formation of cyclohexyl containing **4.044** (Entry 8, Table 10, p 62) at different time points.

From the observation of these intermediates, a proposed mechanism is illustrated (Scheme 10). The formation of the primary amide, which typically would not be expected to take place at room temperature,¹²⁵ is thought to occur due to anchimeric assistance caused by the adjacent amide and ester groups to form oxazine **4.043**. Analogues of oxazine **4.043** have been isolated by co-workers and in the literature as well as other closely related cores and used to make analogues of pyridopyrimidinone **4.040**.^{126,127} Both the methyl ester **4.042** and the primary amide **4.041** are formed by reaction by nucleophilic addition to oxazine **4.043** by either methanol or ammonia. Primary amide **4.041** forms at a slower rate than methyl ester **4.042**, although it is generally the major component after a few hours as oxazine **4.043** undergoes nucleophilic attack by ammonia to irreversibly form primary amide **4.041**. Primary amide **4.041** can be isolated, although the addition of base, in this case sodium hydroxide, causes clean, rapid cyclisation to 2-substituted pyridopyrimidinone

4.040 so isolation and purification of intermediates of the primary amide analogues **4.041** are not necessary. The addition of a strong base may cause rapid cyclisation by deprotonating 2-substituted pyridopyrimidinone **4.040**, which has a measured pK_a of 13 in water, removing it from the equilibrium and forcing the reaction towards 2-substituted pyridopyrimidinone **4.040**. The methodology was used to make a variety of 2-substituted pyridopyrimidinones (Table 10).

4.7.2 SAR of pyridopyrimidinone 2-substituted with small aliphatic groups

A series of small 2-aliphatic substituted pyridopyrimidinones were synthesised and the RapidFire™ potencies for these compounds are shown below. Unsubstituted pyridopyrimidinone **4.019** is included for comparison (Table 10).



Entry	Number	R	JmjD2d pIC_{50} (LE)
1	4.019	H	5.0 (0.62)
2	4.045*	Me	< 4.0
3	4.046*	Et	< 4.0
4	4.047		5.1 (0.54)
5	4.048*		5.0 (0.43)
6	4.049*		4.7 (0.46)
7	4.050*		4.4 (0.40)
8	4.044		≤ 4.1 (0.31)
9	4.051*		≤ 4.2 (0.32)

Table 10: RapidFire™ potencies of aliphatic compounds.

The 2-methyl and 2-ethyl substituted pyridopyrimidinones (Entries 2 and 3, Table 10) showed a significant reduction in potency compared to unsubstituted pyridopyrimidinone **4.019**, possibly due to steric clash with Tyr136. Replacing the terminal methyl with a Cl in **4.047** or CF_3 in **4.048** causes an increase in potency compared to the 2-methyl and 2-ethyl substituted pyridopyrimidinones. This may be caused by the greater electronegativity of these groups compared to the aliphatic **4.046** and **4.045**^{128,129} making the ring system more electron poor and thus increasing the acidity of the amide NH. This in turn would cause the

molecule to behave more like carboxylic acid **4.026** (Table 6, p 49), having stronger interactions to the Lys210 and Tyr136 (Graph 3, p 107). An X-ray crystal structure of chloro containing **4.047** shows there is no evidence of a covalent bond being formed (Fig. 29).¹⁰³

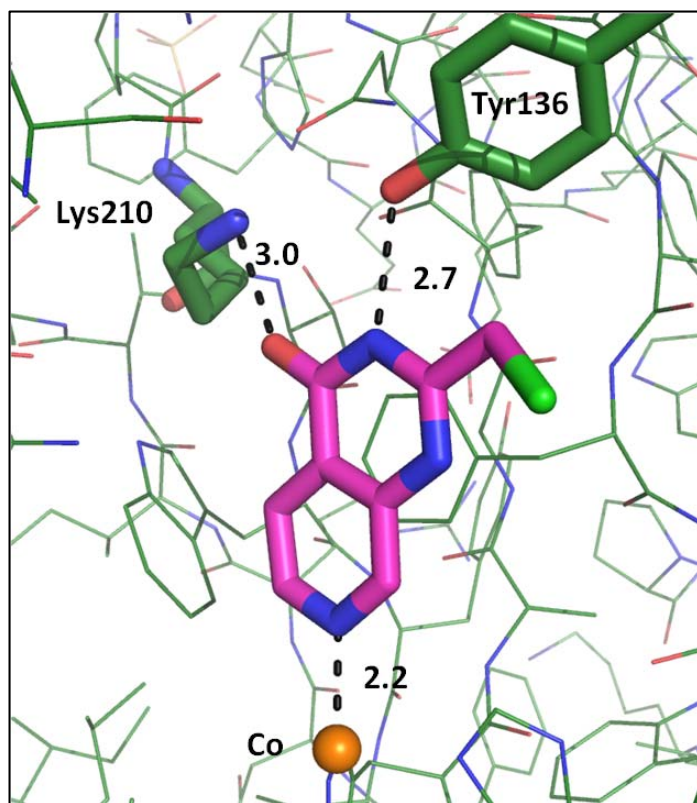


Figure 29: X-ray crystal structure of chloro **4.047** in JmjD2d with an implied chlorine atom, resolution = 2.1 Å.

While the 2-ethyl substituted pyridopyrimidinone **4.046** was inactive, the addition of one further carbon to make the 2-*n*-propyl substituted pyridopyrimidinone **4.049** causes a measurable potency increase of at least one log unit relative to that of ethyl **4.046** to give a RapidFire™ pIC₅₀ value of 4.7 at JmjD2d. This rise in potency cannot be solely explained by the increase in logP due to the hydrophobic effect, where ligand binding can be increased by adding lipophilicity to a molecule. This occurs due to the increase in lipophilicity causing the ligand to partition into the relatively hydrophobic protein compared to the polar solvent, usually water.¹³⁰ Even if the potency of ethyl analogue **4.046** was only 3.9, the increase in logP due to the homologation can only explain an increase in potency of about threefold.¹³¹ Thus, it must be concluded that the final methyl in the chain of *n*-propyl **4.049** must be in a hotspot for potency, although with the crystal structure evidence currently available, it is unclear what is causing this increase. To further explore this result,

cyclopropyl compound **4.050** and cyclohexyl analogue **4.044** were prepared, which show that as the substituent is made progressively more bulky, from *n*-propyl **4.049** to cyclopropyl **4.050** to cyclohexyl **4.044**, the level of potency decreases with a substantial drop in LE. The decrease in potency as the substituent gets bigger suggests there is limited space to fill in this area. X-ray crystallography of related compounds does not fully indicate why this would be, although the cyclopropyl **4.050** and cyclohexyl **4.044** compounds could be disrupting a water network within the enzymes and thereby reducing the potency of the molecules. The benzyl group of **4.051** removes some of the steric hindrance by flattening out the cyclohexyl to the aromatic phenyl, although this has no effect on JmjD2d potency. With the aim of driving potency higher, a number pyridopyrimidinone compounds with directly attached aromatic rings were synthesised (Scheme 7, p 59) to probe this sensitive region of the enzyme.

4.8 Substitution at the 2-position of the pyridopyrimidinone core with 6-membered aryl rings

The same methodology was used to synthesise 2-aryl substituted pyridopyrimidinones. For certain exemplars, some problems were encountered (Fig. 30).

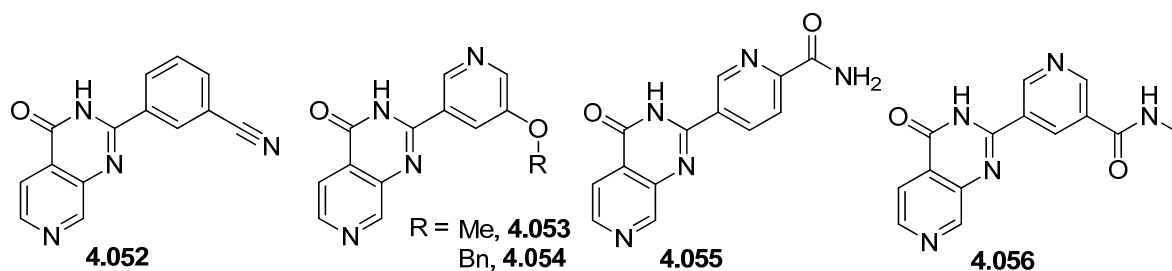


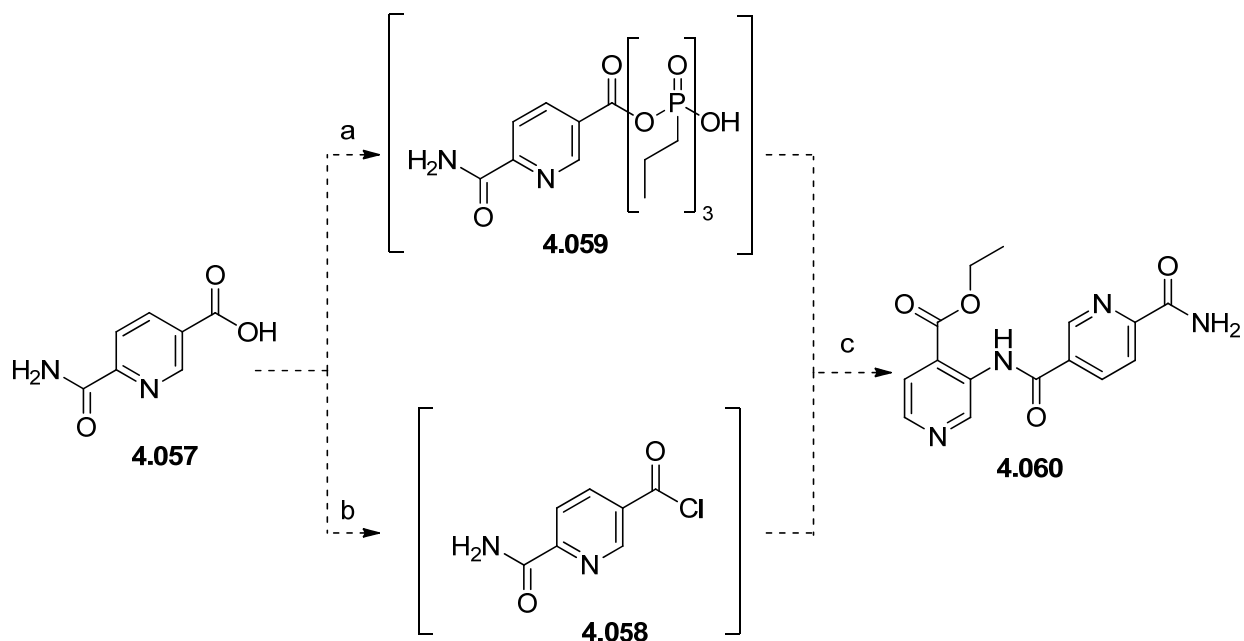
Figure 30: Molecules of interest to be accessed using the sequence shown in Scheme 7 (p 59).

Although nitrile compound **4.052**, secondary amide **4.056**, and ether analogues **4.053** and **4.054** were prepared smoothly using the methodology shown in Scheme 7 (p 59), primary amide containing **4.055** could not be accessed directly and a protecting group strategy was employed.

4.8.1 The synthesis of 5-(4-oxo-3,4-dihydropyrido[3,4-*d*]pyrimidin-2-yl)picolinamide (**4.055**)

The initial amide couplings activating the acid **4.057** with either the Vilsmeier-Haack reagent, generated through the reaction between oxalyl chloride and DMF, to the acid

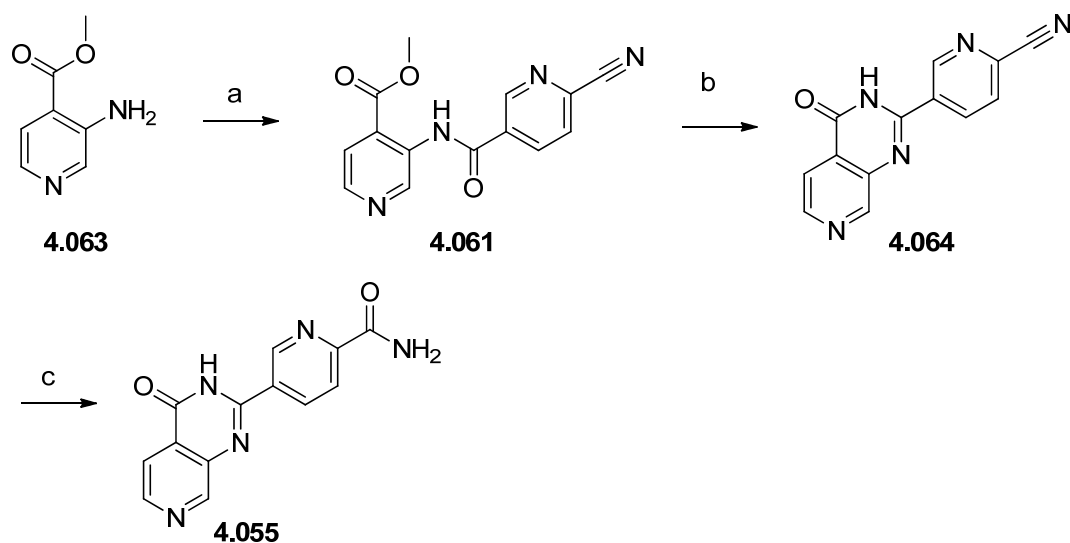
chloride (**4.058**) or T3P® to the phosphinic anhydride (**4.059**) gave none of the desired amide **4.060** upon addition of **4.038** (Scheme 9).



Scheme 9: Reagents and conditions: a) DIPEA, T3P®, DCM 20 °C 0%; b) (COCl)₂, DMF, NEt₃, DCM, 20 °C, 0%; c) **4.038**, 0%

As reactions on similar molecules had proven successful it was thought that there must be a problem with forming the activated acid species with the primary amide in place. Thus, masking the primary amide as a group which could be converted into the amide in one mild step was sought. Hydrolysis of nitriles to primary amides and acids is well known and the suitability was investigated with the aim of providing primary amide containing **4.055**.¹³² Classically, this hydrolysis is performed in the presence of acids or metal oxides as basic conditions can lead to over reaction to the carboxylic acid. However, Katritzky and *et. al.* have reported mild selective hydrolysis conditions using potassium carbonate and hydrogen peroxide in DMSO.^{132,133} Hence, amide **4.061** was prepared using the Vilsmeier-Haack reagent generated *in situ*, coupling together 6-cyanonicotinic acid (**4.062**) and aminopyridine **4.063** (Scheme 10). Due to the delicate nature of the nitrile group, the rate of the cyclisation step could not be accelerated by the addition of sodium hydroxide as in a trial reaction this was found to cause degradation of the cyclised product to a number of unidentified impurities. Hence, an alternative procedure was employed relying on the cyclisation taking place in just the 7 M methanolic ammonia which was left for three days at

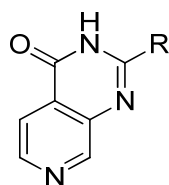
room temperature to yield **4.064**. Subsequent hydrolysis by hydrogen peroxide and potassium carbonate in DMSO gave the desired amide **4.055** (Scheme 10).¹³²



Scheme 10: Reagents and conditions: a) **4.062**, (COCl)₂, DMF, NEt₃, DCM, 20 °C, 30%; b) 7 M methanolic ammonia, 20 °C, 45%; c) aq. H₂O₂, K₂CO₃, DMSO, 0 °C, 57%.

4.8.2 SAR of pyridopyrimidinone 2-substituted with aryl rings

A number of molecules containing aromatic and heteroaromatic rings in the 2-position of pyridopyrimidinone **4.019** were synthesised as previously described. In order to determine if an increase in JmjD2 potency could be achieved through heteroaryl substitution at the 2-position (Scheme 7, p 59) the compounds were assayed against JmjD2d (Table 11).



Entry	Number	R	JmjD2d pIC ₅₀ (LE)
1	4.019	H	5.0 (0.62)
2	4.065*		5.0 (0.40)
3	4.066*		< 4.0
4	4.067*		5.1 (0.41)
5	4.068*		4.8 (0.39) ^a
6	4.069*		< 4.0 ^a

Table 11: RapidFire™ potencies of 2-aryl pyridopyrimidinones. ^a) Assay carried out with 10x concentration of JmjD2 enzyme, incubating for 8 min.

An X-ray crystal structure was obtained for 3-pyridyl pyridopyrimidinone **4.067** (Entry 4, Table 11) and showed some intriguing results. The first crystal structure obtained with an aromatic ring present at the 2-position of the pyridopyrimidinone showed rotation of Tyr136, a more subtle movement than had been seen previously (Fig. 31).¹⁰³

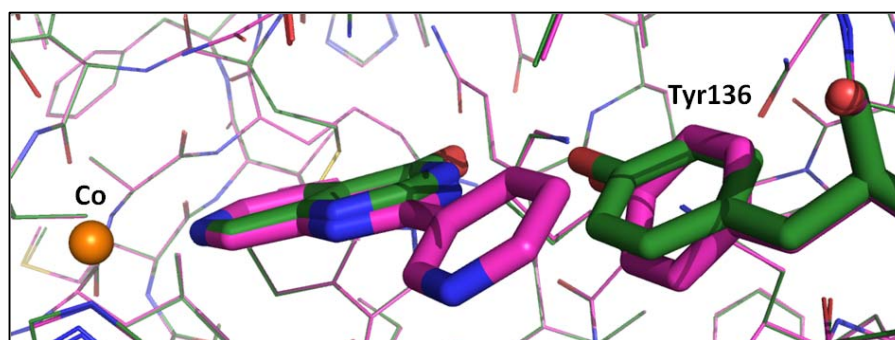


Figure 31: Overlay of pyridopyrimidinone **4.019**, resolution = 2.0 Å, in green and 3-pyridyl **4.067**, resolution = 1.9 Å, in magenta showing the movement of Tyr136 when the 2-position of the pyridopyrimidinone is substituted with a 6-membered aryl.

The initial phenyl substituted compound **4.065** retained potency against JmjD2d, when compared to pyridopyrimidinone **4.019**, which gave encouragement to further investigate with heteroaryl compounds. Comparing the 2-, 3- and 4-substituted pyridyl containing compounds, 2-pyridyl analogue **4.066** is inactive whilst 3-pyridyl example **4.067** and 4-pyridyl compound **4.068**, have a similar level of potency as phenyl substituted **4.065**. As 3-pyridyl containing **4.067** and 4-pyridyl analogue **4.068** were tolerated while 2-pyridyl example **4.066** was not, it was postulated that this might be due to the positioning of the basic nitrogen of the 2-pyridyl substituent. The nitrogen of the 2-pyridyl substituent in **4.066** can H-bond with the acidic proton of the pyrimidone core forming a pseudo 5-membered ring and thereby causing the molecule to be planar (Fig. 32).

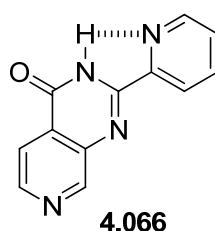


Figure 32: Possible pseudo 5-membered internal H-bond causing 2-pyridyl pyridopyrimidinone **4.066** to be planar.

To test the hypothesis that planarity has a negative effect, 5-methyl pyridine compound **4.069** (Entry 11, Table 12, p 73) was designed and synthesised to induce a twist. However, this compound was found to be inactive at the enzymes of interest. This can be explained by the ortho methyl group having a significant impact on the dihedral angle between the pyridopyrimidinone and the pyridine containing ring causing it to be driven out of the plane too far. This could cause a steric clash with Tyr136 and so methyl pyridine compound **4.069** is not tolerated in the JmjD2 family of enzymes.

However, through further examination of the electron density data of the X-ray crystal structure of 3-pyridyl pyridopyrimidinone **4.067** in JmjD2d showed there was an alternative conformation of JmjD2d (Fig. 33).¹⁰³

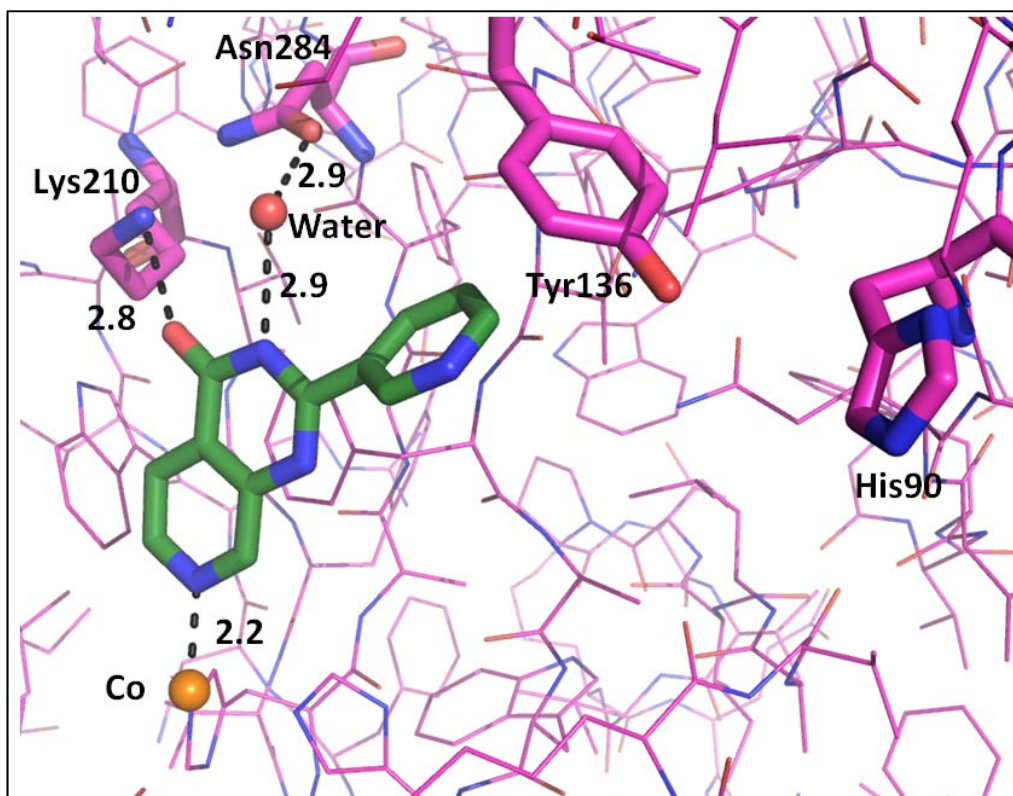


Figure 33: Alternative binding conformation (Mode 2) of JmjD2d with **4.067** present, resolution = 2.4 Å.

In this conformation, henceforth known as Mode 2, Tyr136 has pivoted away from H-bonding with the pyridopyrimidinone and in doing so His90 has also pivoted similarly. This is comparable to the X-ray crystal structure obtained for cyanopyridopyrimidinone **4.034** (Fig 26, p 55). A water molecule, labelled in Fig. 33, now occupies the position where the hydroxyl of Tyr136 was and the water H-bonds to Asn284. A direct comparison of the two binding modes shows the movement of Tyr136 and His90 (Fig. 34).

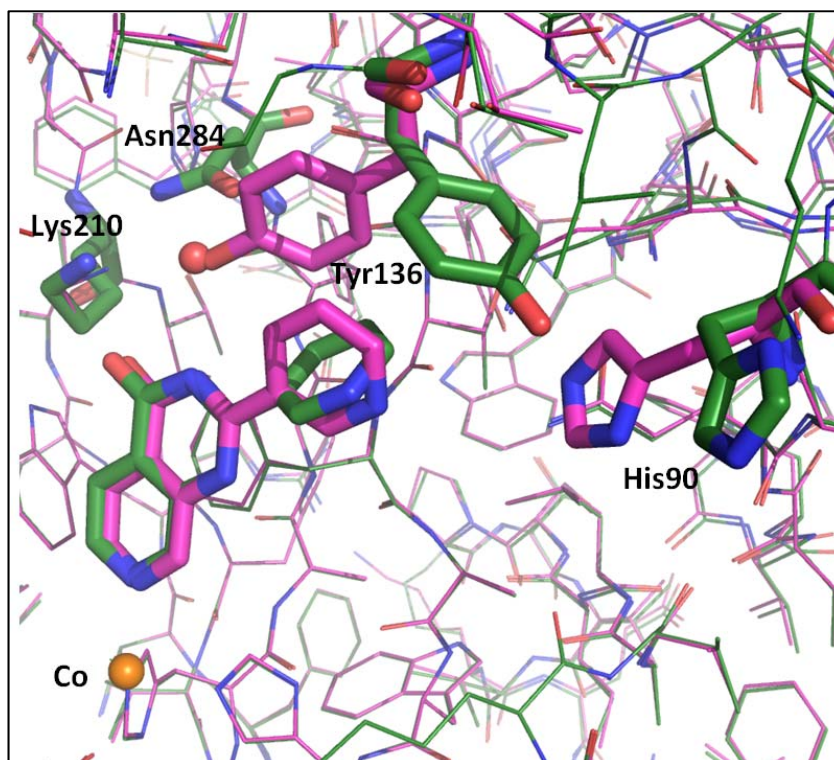


Figure 34: Comparison of the two conformations of JmjD2d with 3-pyridyl **4.067** present. The first observed conformation is in magenta, resolution = 2.0 Å, and Mode 2 shown in green, resolution = 2.4 Å.

As these tyrosine and histidine residues in the protein have been shown to flip, an interesting question is whether this movement has any biological relevance. Other types of protein have been shown to undergo conformational change while binding substrates and either enzymatically altering their structure, such as kinases,¹³⁴ or binding strongly to a substrate, such as streptavidin to biotin.¹³⁵

4.8.3 Biological rationale for the movement observed

A hypothesis for the biological relevance of the tyrosine and histidine movement in the JmjD2 family of enzymes is that the movement of the tyrosine and histidine residues may aid the decomplexation of the H3 peptide out of the JmjC domain once a demethylation event has taken place. In the crystal structure of JmjD2d with a truncated, trimethylated H3 peptide tail and 2-OG present there is a clear hydrogen bond between Tyr136 and 2-OG. In turn 2-OG is co-ordinated to the Fe (II) holding this sub-complex in a rigid position (Fig. 35). The proximity of the methylated lysine to the 2-OG co-factor allows the oxidative demethylation to occur.

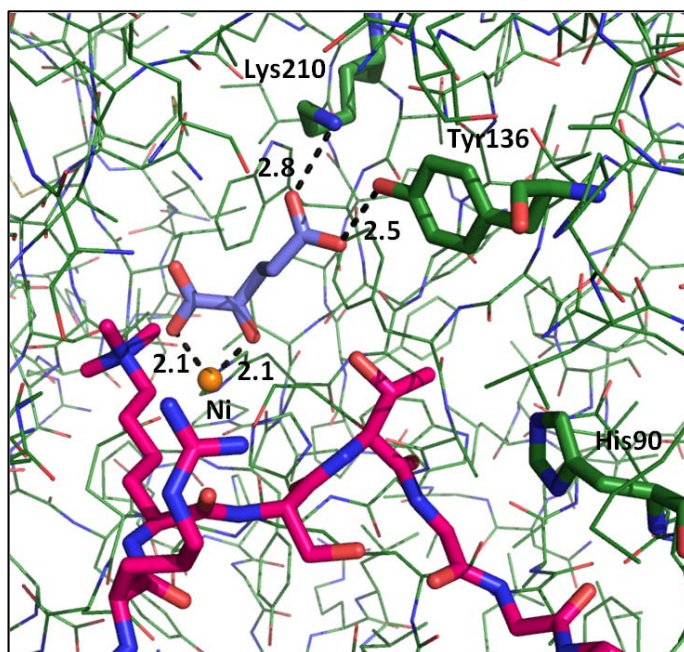


Figure 35: X-ray crystal structure of a truncated H3 peptide (magenta) and 2-OG (blue) bound in the active site of JmjD2d, resolution = 1.8 Å.⁷³

Upon oxidation of one of the methyl groups to formaldehyde, succinate is formed from 2-OG (**3.006**) (Scheme 1, p 31) which is less well bound to the Fe (II), compared to 2-OG (**3.006**). This could loosen the sub-complex, which allows Tyr136 and subsequently His90 to change conformation to Mode 2, ejecting the H3 peptide and allowing a new 2-OG molecule access to the active site for further oxidations. There is crystallographic evidence for movement of Tyr136 upon binding 2-OG as the Apo X-ray crystal structure of JmjD2d shows Tyr136 in an intermediate position between Mode 1 and Mode 2 (Fig. 36).

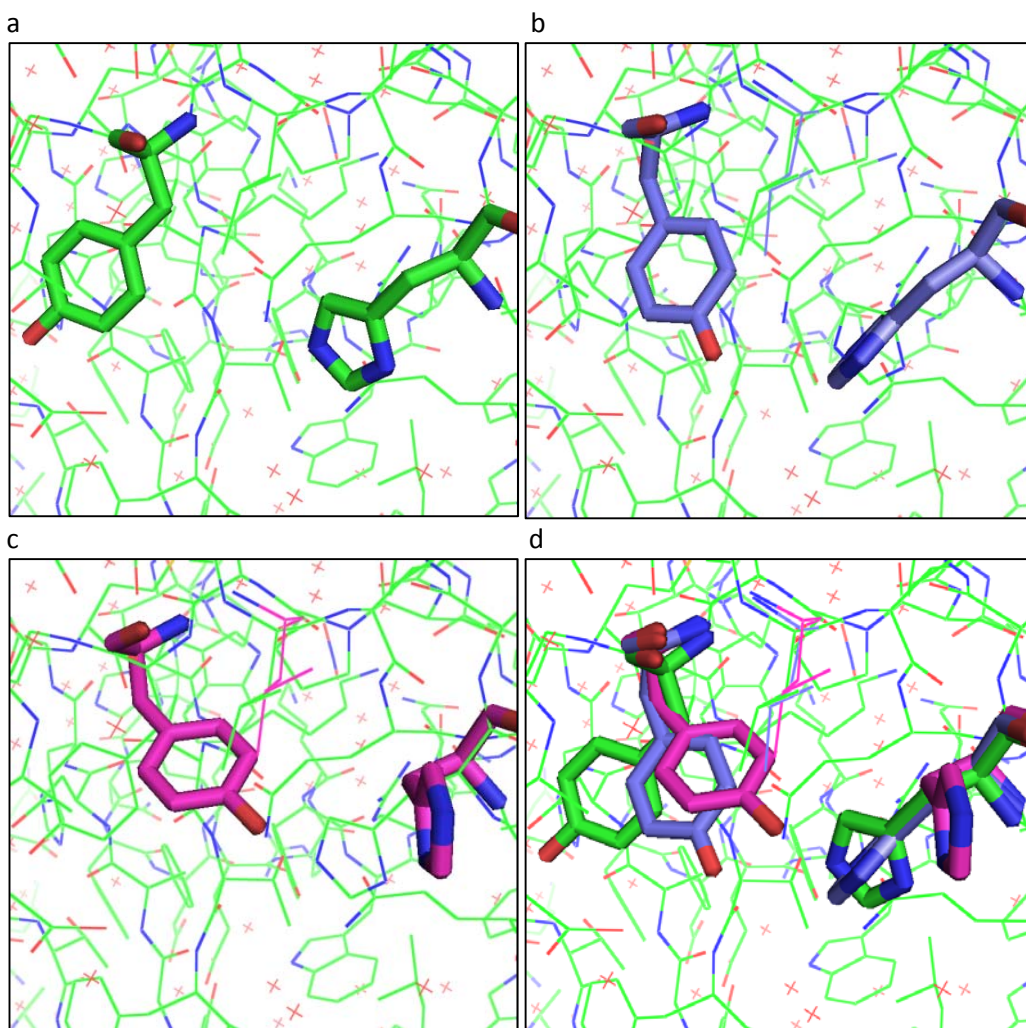


Figure 36: X-ray crystal structures JmjD2d highlighting the positions of Tyr136 and His90 in (a) Mode 1 (green), resolution = 2.0 Å, (b) in the JmjD2d apo structure (blue), resolution = 1.8 Å,⁷³ (c) Mode 2 (magenta), resolution = 2.4 Å, and (d) in overlay.

4.8.4 SAR trend explained by Mode 2

Having hypothesised the potential biological relevance for the movement of the Tyr136 and His90 into Mode 2, it was found that this conformation could be used to explain some of the SAR observed (Table 12).



Entry	Number	R	JmjD2d pIC ₅₀ (LE)
1	4.067*		5.1 (0.41)
2	4.070*		5.8 (0.44)

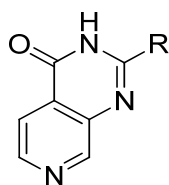
Table 12: RapidFire™ potencies of substituted aryl compounds.

Mode 2 is believed to enhance the potency of 3-pyridine containing **4.067** due to the increased polarity of the C-H σ -bond between the nitrogens of the pyrimidine ring making an interaction with the aromatic ring of the tyrosine. The polarised C-H bond is pointing towards the electron rich π -cloud of Tyr136 and makes a positive binding interaction. On the basis of this hypothesis, fluoropyridine analogue **4.070** (Table 12) was accessed *via* the method discussed earlier (Scheme 7, p 59).

The C-H bond in fluoropyridine compound **4.070** (Entry 1, Table 12) is adjacent to both the pyridine nitrogen and the fluorine, further polarising the σ -bond. This combination gives one of the most potent compounds investigated with a 2-substituted aryl example. However, merely exploring the 2-position with directly attached aryl rings did not provide the necessary sub-micromolar potency at the JmjD2 enzymes for a cellular probe. Therefore a series of compounds that could form polar interactions between the ligand and the protein was designed.

4.8.5 H-bonding interactions

Based on the observations noted above in relation to differential binding modes, a range of compounds that could investigate the area of the protein from the 2-position of the pyridopyrimidinone were designed. These compounds incorporated substituents capable of forming H-bonding interactions with the protein or any conserved water molecules (Table 13).



Entry	Number	R	JmjD2d pIC ₅₀ (LE)
1	4.067*		5.1 (0.41)
2	4.052		≤ 4.8 (0.35)
3	4.064		5.4 (0.39) ^a
4	4.055		< 4.0
5	4.053		≤ 4.5 (0.32)
6	4.056		4.1 (0.27)
7	4.054		4.3 (0.24)

Table 13: RapidFire™ potencies of substituted aryl compounds. ^a) Assay carried out with 10x concentration of JmjD2 enzyme, incubating for 8 min.

Benzonitrile compound **4.052** (Entry 2, Table 13) does not show any improvement compared to 3-pyridine example **4.067**. However, it does reinforce the evidence that benzonitrile is a bioisostere for pyridine H-bonded to a water due to the similar directionality and positioning of the lone pairs (Fig. 37).¹³⁶

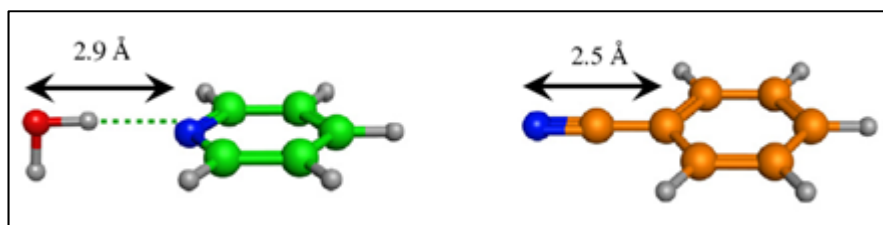


Figure 37: Benzonitrile is an isostere of water H-bonded to a pyridine nitrogen.

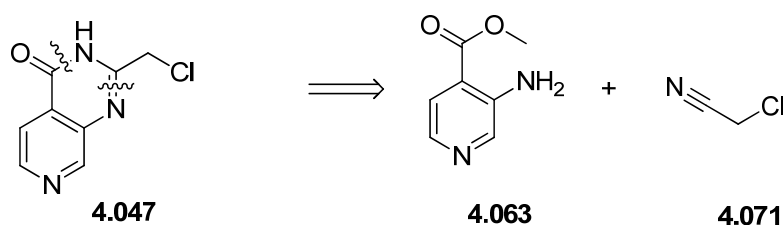
Comparing primary amide **4.055** and nitrile **4.064** (Entries 3 and 4) illustrates that while H-bond acceptors are tolerated in this area of the protein, H-bond donors are not. Against JmjD2d, ten-fold potency has been lost in adding an H-bond donor as observed by comparing primary amide **4.055** with 3-pyridyl containing **4.067** (Entries 4 and 1). The low potency of secondary amide example **4.056** indicates that H-bond donors are not tolerated in the 3-position of the pyridyl ring. 3-Aryl ether compounds **4.053** and **4.054** (Entries 5 and 7) indicate that electron donating groups do not improve the potency, although there is ample space for expansion.

As can be noted from Tables 11 – 13 (p 67 – 74), it was not possible to significantly improve the potencies at JmjD2d by directly attaching aryl groups to the 2-position of the pyridopyrimidinone core. Hence different strategies were employed and the first of these was to introduce H-bond donating and accepting groups branching out from the 2-position.

4.9 Substitution at the 2-position of the pyridopyrimidinone core with H-bond donors and acceptors

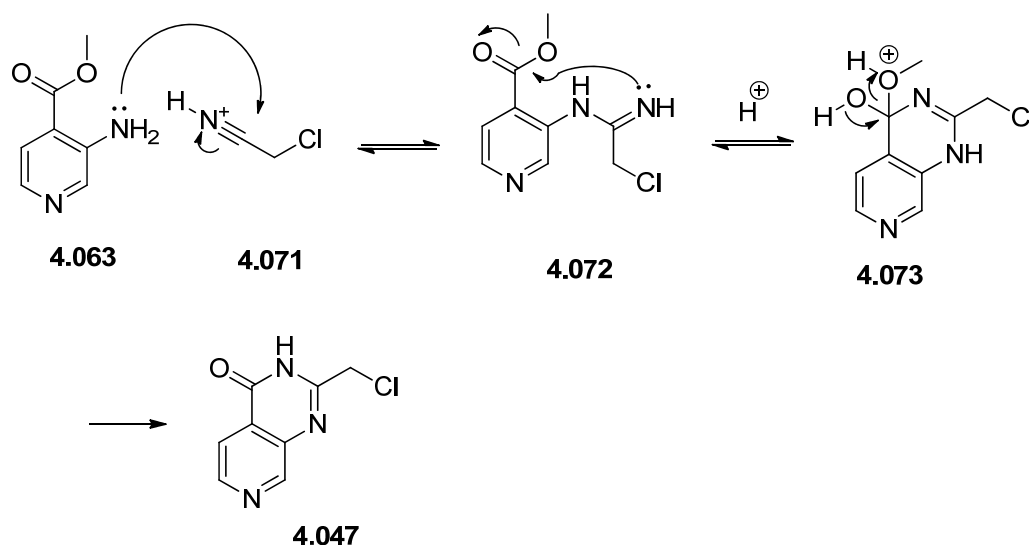
4.9.1 Synthesis of ethers

To easily probe the SAR around the 2-position with ethers, a late stage intermediate which could be used to synthesise target compounds in one or two synthetic steps was required. Chloride **4.047** was identified as one such intermediate and this could be made in one step using chloroacetonitrile (**4.071**) and amino ester **4.063** (Scheme 11).



Scheme 11: Retrosynthesis of intermediate **4.047**.

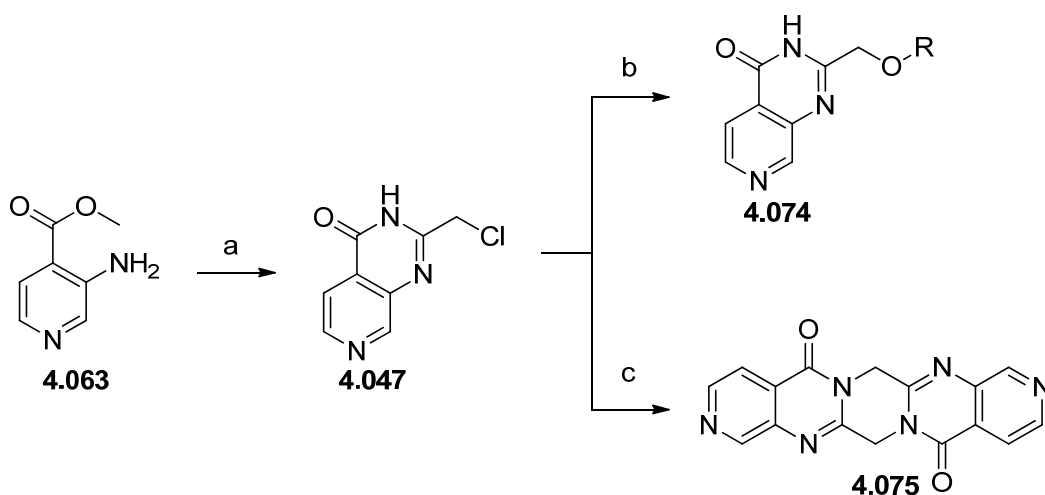
The key bond forming step is the reaction of nitrile **4.071** with the amino ester **4.063** in the presence of hydrogen chloride, which has been employed in the synthesis of similar molecules.¹³⁷ This methodology was not used for target molecules mentioned previously due to the relatively harsh conditions that could cause functional group incompatibility and the relative scarcity of readily available cyanopyridines was another. In the first step, HCl catalyses the formation of the amidine by reaction between amino ester **4.063** and protonated **4.071'**. The methyl ester subsequently undergoes nucleophilic attack by the amidine forming the ring and producing methanol as the condensation product (Scheme 12).



Scheme 12: Mechanism for the formation of **4.047**.

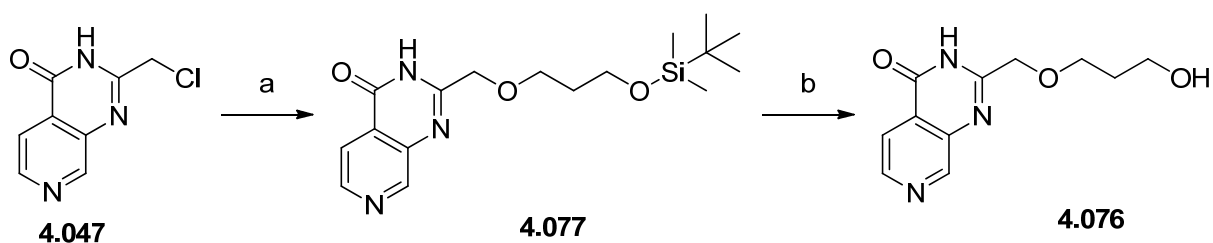
Methyl 3-aminoisonicotinate (**4.063**) was heated with stirring in the presence of 2-chloroacetonitrile in a solution of 4 M hydrogen chloride in 1,4-dioxane to give **4.047**.^{137,138} **4.047** could be further elaborated to molecules of interest through alkylation of alcohols and subsequent deprotection where necessary to give ethers of type **4.074** (Scheme 13).¹³⁹

The alkylation by reaction of chloro compound **4.047** with an alcohol in the presence of sodium hydroxide was problematic. The original attempts to alkylate alcohols using the solvents DMF, water or *tert*-butyl alcohol with a variety of different alcohols gave no evidence of the desired products. Performing the reaction in acetone at 0.1 M concentration using potassium carbonate as base formed pentacycle analogue **4.075**, formed through the dimerisation of two alkyl chloride monomer units (Scheme 13).



Scheme 13: Reagents and conditions: a) ClCH_2CN , 4 M HCl in 1,4-dioxane, 50 °C, 45%; b) NaOH, R-OH, 100 °C; c) K_2CO_3 , acetone, $\text{HO}(\text{CH}_2)_3\text{OTBDMS}$, reflux, 5%.

The reaction was completed successfully upon using the alcohol starting material as the solvent and sodium hydroxide as the base, furnishing hydroxy ethyl compound **4.083** and *n*-butyl containing **4.084**.¹³⁹ Whilst *n*-butyl analogue **4.084** was intended to be synthesised eventually, it was inadvertently formed whilst searching for appropriate conditions for the alkylation outlined in Scheme 13. *tert*-Butyl alcohol was supposed to be used as the solvent and *n*-butyl alcohol was inadvertently used instead. Compound **4.076** was synthesised in this manner in 7% yield over two steps with the hydroxy propyl group installed as the TBDMS ether **4.077** and subsequently deprotected (Scheme 14).

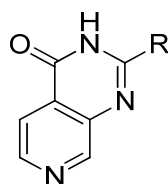


Scheme 14: Reagents and conditions: a) NaOH, $\text{HO}(\text{CH}_2)_3\text{OTBDMS}$, 90 °C, 10%; b) TBAF, THF, 20 °C, 70%.

4.9.2 Analysis of the SAR of pyridopyrimidinone compounds 2-substituted with H-bond donors and acceptors

It was unknown whether H-bond acceptors or donors would be tolerated at the 2-position of the pyridopyrimidinone or what the ideal distance from the core would be for these

groups because of the inherent movement of the protein (Fig. 36, p 72). Thus, a selection of molecules to answer these key questions were synthesised (Table 14).



Entry	Number	R	JmjD2d pIC ₅₀ (LE)
1	4.078*		< 4.0 ^a
2	4.079*		≤ 4.0 (0.42)
3	4.080*		< 4.0 ^a
4	4.081*		4.8 (0.47)
5	4.082*		5.3 (0.38)
6	4.083		4.8 (0.41)
7	4.076		4.6 (0.37)
8	4.084		≤ 4.7 (0.38)

Table 14: RapidFire™ potencies of 2-substituted compounds containing H-bond accepting and donating groups. ^a) Assay carried out with 10x concentration of JmjD2 enzyme, incubating for 8 min.

Primary amide **4.078** and alcohol **4.079** (Entries 1 and 2, Table 14) have both H-bond accepting and donating features and a pIC₅₀ value of ≤ 4.0 at JmjD2d. As dually H-bonding acceptors and donors were not tolerated at JmjD2d, the purely donating primary amine **4.080** and the purely accepting ether **4.081** were synthesised. Charged amine **4.080** has a pIC₅₀ value of < 4.0 at JmjD2d which indicates that basic groups, and by extension, purely donating groups are not well tolerated in this area of the protein. H-bond accepting ether **4.081** shows at least an eightfold increase of potency at JmjD2d compared to the H-bond donating examples **4.078** and **4.080**. This illustrates an H-bond acceptor to be well tolerated at this position. The addition of the phenyl ring in **4.082** compared to the methyl in **4.081** does increase JmjD2d potency by five-fold. This increase in potency can be rationalised through molecular modelling (Fig. 38).

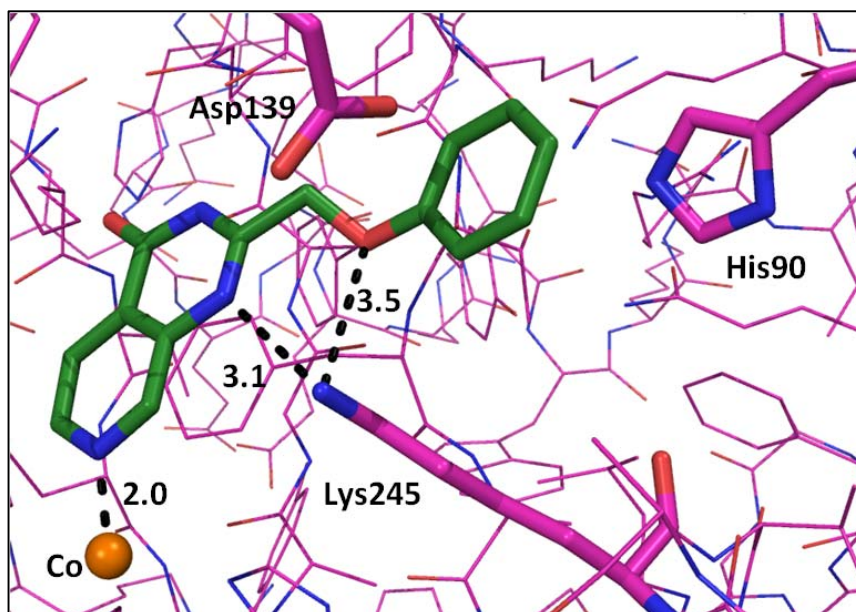


Figure 38: Glide¹⁴⁰ docking of phenyl ether **4.082** in JmjD2d.

Using this model, the ether oxygen and the 1-nitrogen on the pyridopyrimidinone core can be seen to be acting as H-bond acceptors and are interacting with the positively charged Lys245. The increase in potencies observed with phenyl ether **4.082** versus methyl ether **4.081** at JmjD2d can be explained by the potential of a face to face aromatic interaction of the phenyl ring with His90 in JmjD2d. To further exploit and probe this interaction, biaryl or bicyclic rings could be envisaged from the ether linker to achieve a larger overlap with His90. Ring systems such as benzoxazole, indazole or quinoline could be used to investigate this.

As can be seen from Fig. 38, Asp139 is sufficiently close to potentially design an H-bonding interaction with. This has already been attempted, with basic groups meeting only limited success, possibly due to charge-charge repulsion with Lys245 (p 50). Thus, hydroxyl groups attached to different length linkers were examined with ethyl hydroxyl compound **4.083**. If an interaction was successfully observed through either a boost in potency or *via* X-ray crystallography, the molecule would be conformationally restrained through cyclisation with an aim to further improve potency by preorganisation of the ligand.¹⁴¹ However, comparison of ethyl hydroxyl ether **4.083** with *n*-butyl ether **4.084** (Entries 5 – 7, Table 14), shows there is no significant difference in potency with the incorporation of a hydroxyl group. Therefore, it is unlikely the hydroxyl is engaged in an H-bonding interaction with Asp139.

None of the C-linked 2-pyridopyrimidinone molecules mentioned exhibited sufficient RapidFire™ potency of > 6.0 to be progressed into a cell assay. While work, not discussed here, has shown that substitution at the 5- and 6- positions of the pyridopyrimidinone core are not tolerated there had been little effort investigating the 8-position. If elaboration at the 8-position improves the potency it could be combined with 2-substituents that also give an enhancement in potency. These disubstituted combination molecules have the potential to be more potent than either just the 2- or 8-substituted molecule if the SAR is additive (Fig. 39).

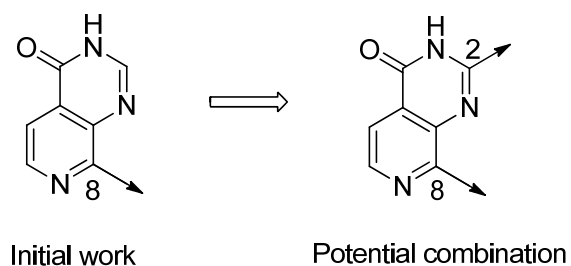


Figure 39: The SAR investigation examined in the next section and the potential combination of 2,8-disubstituted molecules to be synthesised if 8-substitution is advantageous.

4.10 8-Substitution of the pyridopyrimidinone core with heteroaryl groups

Research from Schofield *et al.*⁷⁷ has identified that substitution at the 2-position of pyridine-4-carboxylic acid is tolerated against Jumonji D2 enzymes when the substituent is carboxylic acid **4.004** (Fig. 17, p 33) or 2-pyridyl-4-carboxylic acid **4.085** (Table 15). Further work from Schofield *et al.* showed that incorporating ethane 1,2-diamine to form amide **4.005** was one of the most potent compounds they found against JmjD2e.⁷⁰ These compounds were remade and the results from the in house RapidFire™ assay are summarised below (Table 15).

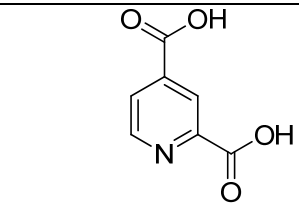
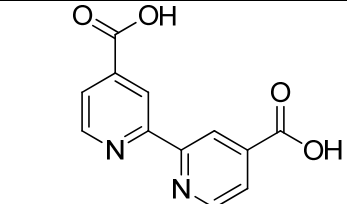
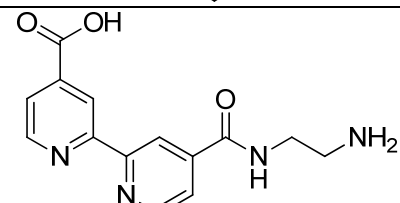
Entry	Number	Structure	JmjD2c pIC ₅₀ (LE)	JmjD2d pIC ₅₀ (LE)	JmjD2e pIC ₅₀ (LE)	AMP nm s ⁻¹
1	4.004		6.8 (0.78)	6.6 (0.75)	6.8 (0.78)	-
2	4.085		4.6 (0.35) ^a	5.3 (0.40) ^a	4.8 (0.37) ^a	-
3	4.005*		6.9 (0.45) ^a	6.4 (0.42) ^a	7.1 (0.46) ^a	< 10

Table 15: RapidFire™ potencies for compounds identified by Schofield *et al.*⁷⁰ ^a) Assay carried out with 10x concentration of JmjD2 enzyme, incubating for 8 min.

As seen before, the potencies for the JmjD2 enzymes are similar to each other and only JmjD2d data will be quoted. Starting from dicarboxylic acid containing **4.004**, replacing the 2-carboxylic acid with the pyridine carboxylic acid to give symmetrical compound **4.085** is not optimal as there is a loss of potency across all the JmjD2 family members assayed. The loss in potency is likely due to the conformation the compound will adopt in the protein for the metal to co-ordinate with both of the pyridine nitrogens. In the low energy conformation of symmetrical **4.085** the nitrogens of the pyridine rings are on opposite sides of the molecule thereby minimising steric clash with the peri hydrogens of the two rings.

Both nitrogens co-ordinating with the metal will cause an approximately 180° rotation of one of the rings, causing steric clash between the two peri hydrogens and moving the conformation away from the energy minima (Fig. 40).

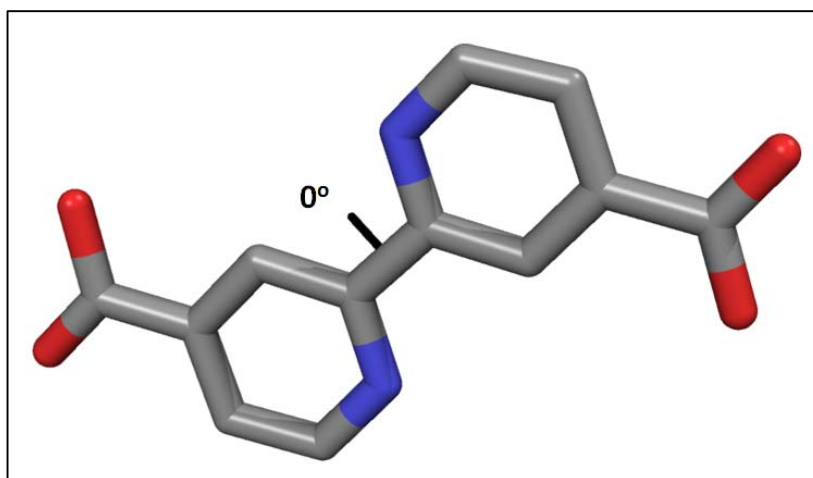


Figure 40: Low energy conformation of **4.085** calculated using force field MMFF94x.¹⁴²

From consideration of this initial data, it may appear that the bipyridyl motif is not an ideal scaffold to work from. However, by building out from one of the carboxylic acids with a basic amine to give amine **4.005** over one hundred-fold potency can be gained at JmjD2c and e and tenfold at JmjD2d compare to the symmetrical compound **4.085**. Schofield *et al.* have reported a crystal structure with amine **4.005** bound in JmjD2a (Fig. 41).⁷⁰ The crystal structure shows amine **4.005** binds in a similar manner to propylamine compound **4.028** (Fig. 24, p 51) with the basic amine making a salt bridge with Asp135 (Asp139 in JmjD2d). This interaction is believed to cause the large rise in potency across JmjD2c, d and e. The two pyridine rings are slightly out of plane with each other with a dihedral angle of 11°. Having the nitrogen on the same face was expected from the complexation of the metal but the molecule is not planar presumably due to the steric clash between the peri-hydrogens. Interestingly, there is a pseudo 7-membered ring caused by the basic amine H-bonding back to the carbonyl of the amide. This decreases the entropic penalty that would be caused if the amine was entirely conformationally free. Amine **4.005** has the level of potency that is desired for a probe compound. However, due to the presence of the carboxylic acid, as with the isonicotinic acids, no membrane penetration was observed in the AMP assay.

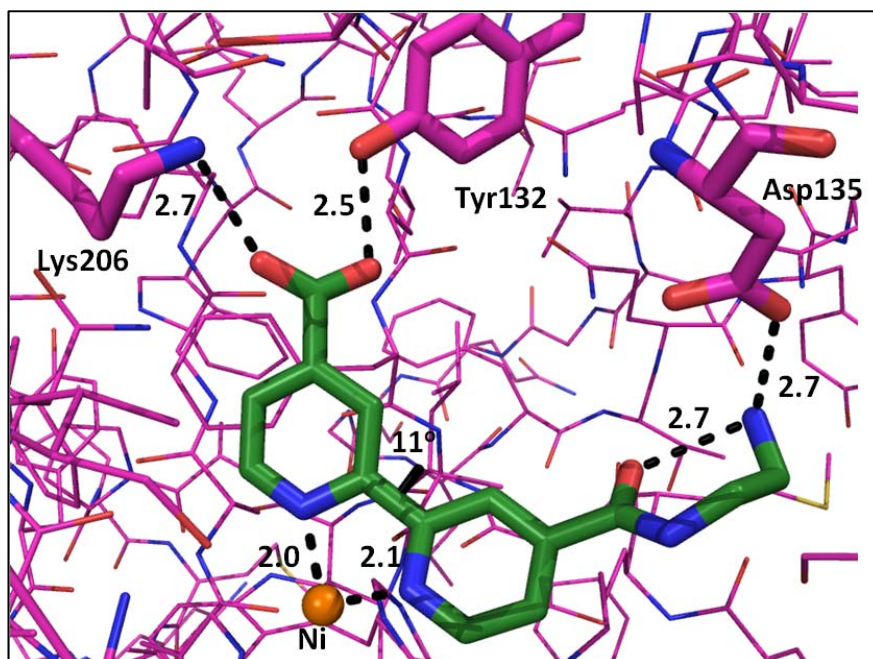
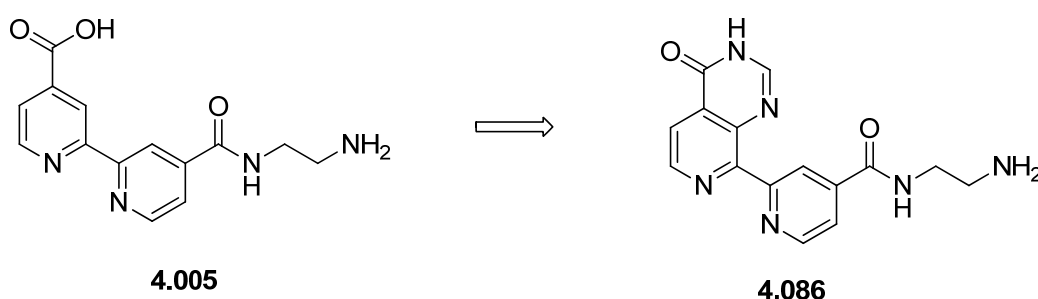


Figure 41: X-ray crystal structure of **4.005** bound in JmjD2a, resolution = 2.0 Å.⁷⁰

Given the success in replacing isonicotinic acid with the pyridopyrimidinone **4.019** it was hypothesised that the same replacement could be made with **4.005** to give **4.086** (Scheme 15). The change was predicted to improve the cellular penetration as compound **4.005** can be both positively and negatively charged.

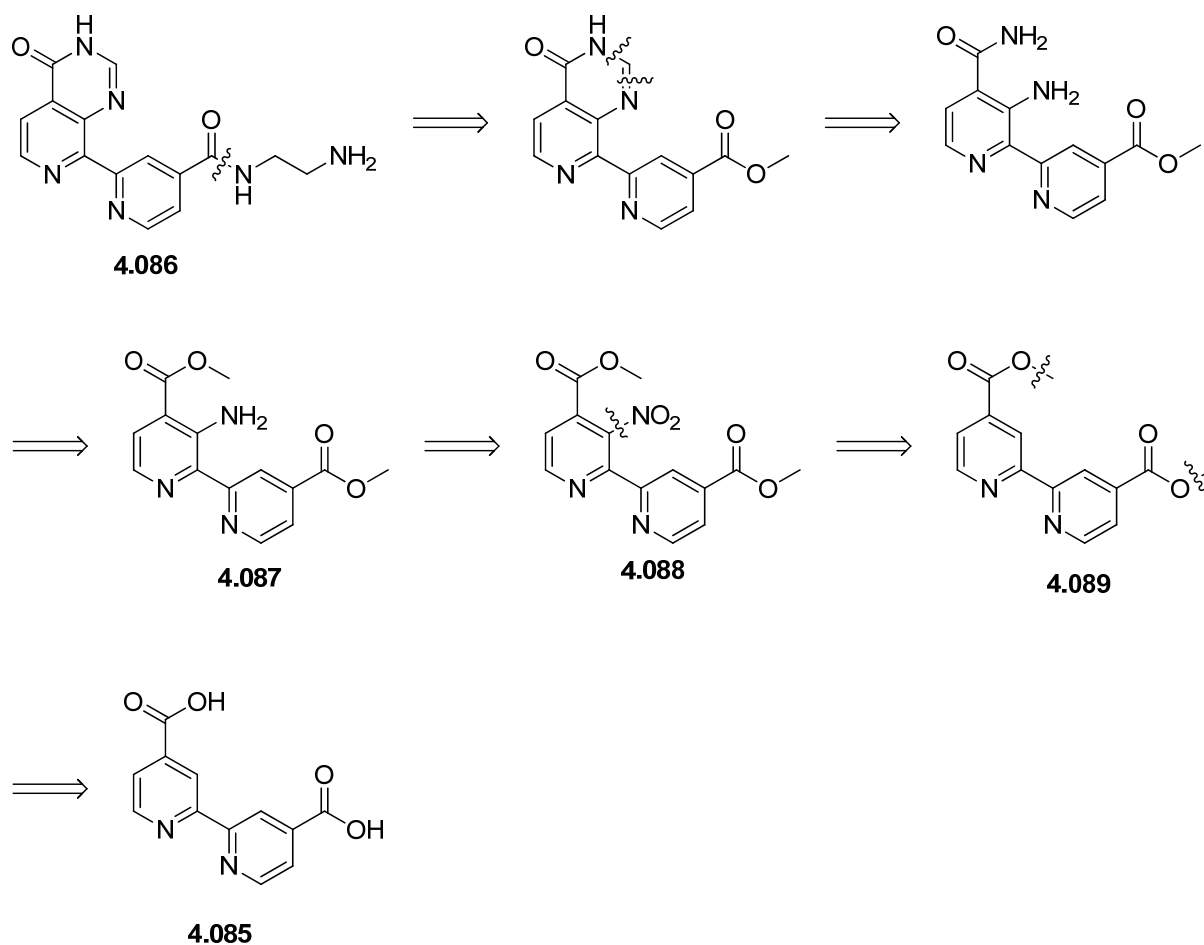


Scheme 15: Proposed scaffold hop to remove carboxylic acid.

4.10.1 Building the rings

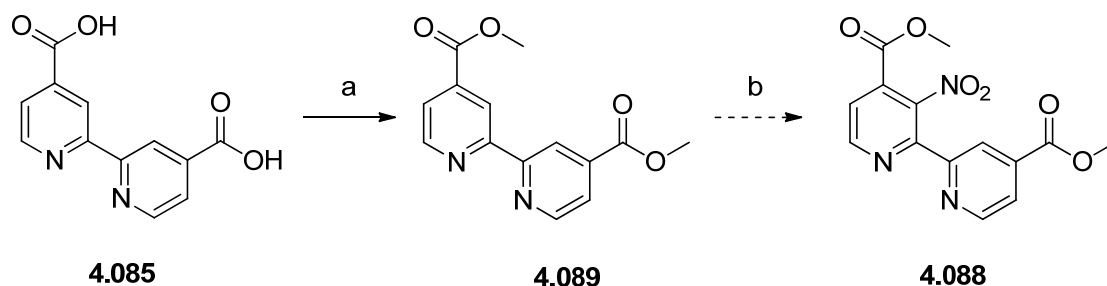
The bond perceived to be most difficult to form was the pyridine-pyridine bond. One of the most prevalent methods to form aryl-aryl bonds is the Suzuki reaction.^{143,144} The reaction, generally, takes place between an aryl-boronic acid or ester and an aryl-halide or pseudo halide in the presence of base and a palladium based catalyst. However, due to the lack of air stability of 2-pyridyl boronic acid and the tendency of 2-pyridyl boronic species to undergo protodeboronation,¹⁴⁵ it was desirable to have the pyridine-pyridine bond already

in place. To this end, a retrosynthetic analysis of pyridopyrimidinone **4.086** was undertaken reverting back to bipyridyl containing **4.085** (Scheme 16).



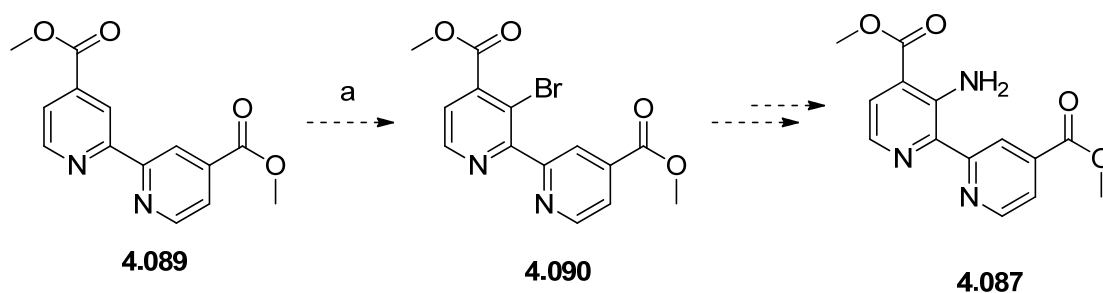
Scheme 16: Retrosynthetic analysis of **4.086** to **4.085**.

Diacid **4.085** was commercially available and treatment with thionyl chloride in methanol gave dimethyl ester **4.089**.¹⁴⁶ Work by Bakke and Raney suggested that treating dimethyl ester **4.089** with nitronium tetrafluoroborate and sodium hydrogen sulfate in nitromethane would give **4.088** as it had been shown to be successful on a range of 4-substituted pyridines (Scheme 17).¹⁴⁷



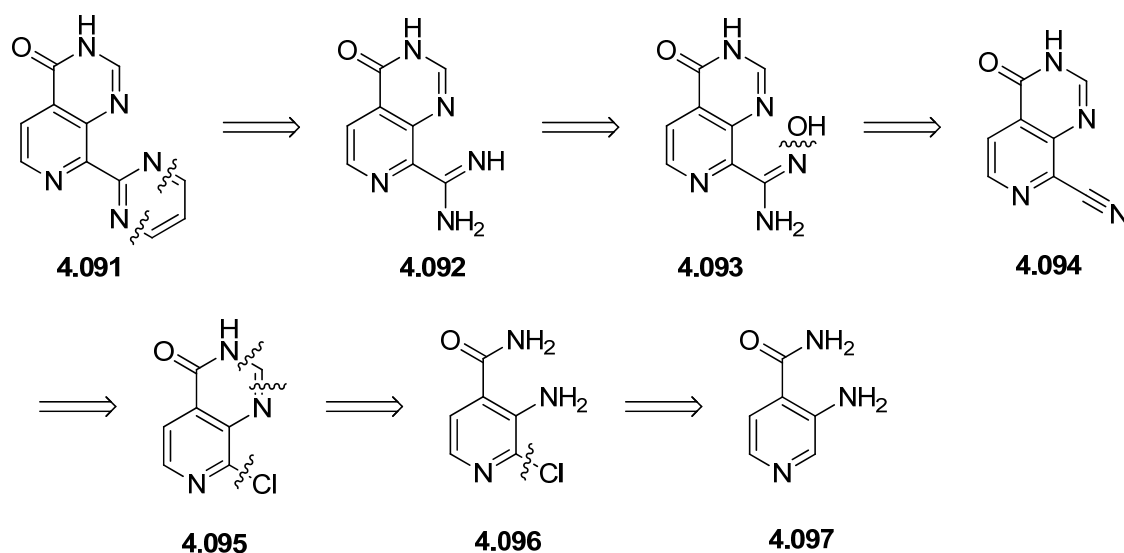
Scheme 17: Reagents and conditions: a) SOCl_2 , MeOH, 65 °C, 65%; b) NO_2BF_4 , NaHSO_3 , MeNO_2 , 20 °C, 0%.

Unfortunately, no desired nitro analogue **4.088** was isolated from the reaction mixture. An unsuccessful attempt was made to brominate diester **4.089** with *N*-bromosuccinimide to give 3-substituted example **4.090**. The planned forward reaction was to aminate bromo compound **4.090** to give amine analogue **4.087** via a palladium catalysed Buchwald-Hartwig coupling (Scheme 18).



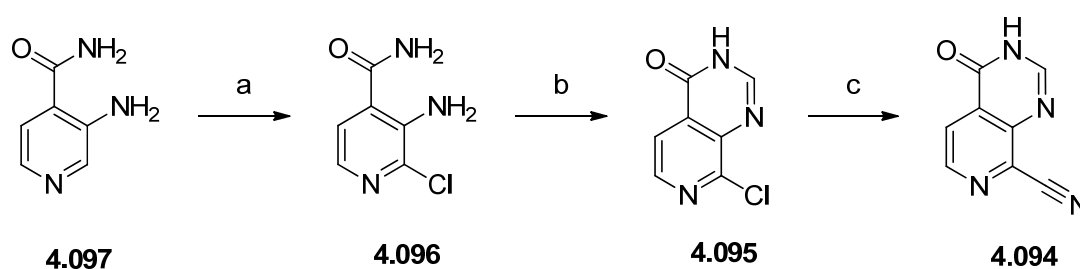
Scheme 18: Alternative route to amine containing **4.087**. Reagents and conditions: a) NBS, acetic acid, acetone, 20 – 90 °C, 0%

The strategies to elaborate diester **4.089** both failed at the first step with and given the lack of literature precedent for transformations of diester **4.089** it was decided that building up a heteroaryl ring to form the biheteroaryl metal binding moiety was a more feasible proposition (Scheme 19). Building the ring in this fashion would grant access to pyrimidine containing **4.091** which does not have peri hydrogens and thus will be less sterically hindered. This allows the biheteroaryl moiety to lie more in plane with each other and thereby suffer less of a penalty when co-ordinating the iron in the enzymes of interest.



Scheme 19: Retrosynthetic analysis of pyrimidine compound **4.091**.

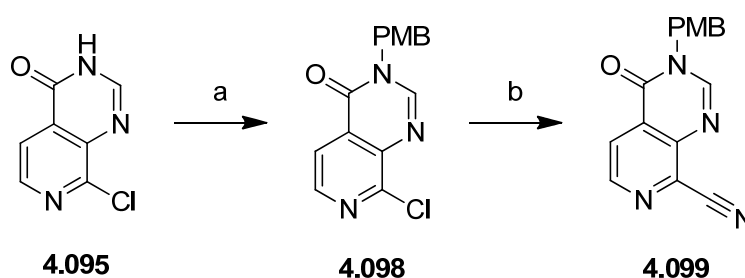
The retrosynthetic analysis of **4.091** illustrates the need for a halogen in the 2-position of the substituted pyridine (Scheme 19). Bakke and Riha have demonstrated the chlorination of primary amide **4.097** via the *in situ* oxidation of HCl to chlorine with hydrogen peroxide to give chloro containing **4.096**.¹⁴⁸ Applying these conditions furnished chloro analogue **4.096** and dichlorinated 3-amino-2,6-dichloroisonicotinamide by-product. These could be separated via silica gel chromatography to isolate pure mono-chloro example **4.096**. The pyrimidinone ring could be closed to form pyridopyrimidinone **4.095** using triethylorthoformate and pTSA.¹⁴⁹ 8-Chloropyridopyrimidinone **4.095** was a key intermediate and was used extensively in the synthesis of the 8-substituted pyridopyrimidinones (Scheme 20).



Scheme 20: Reagents and conditions a) 35% aq. H₂O₂, fuming HCl, 20 °C, 24%; b) CH(OEt)₃, pTSA.H₂O, 85 °C, 95%; b) Zn(CN)₂, 6% Pd(PPh₃)₄, DMF, 90 °C, 72%.

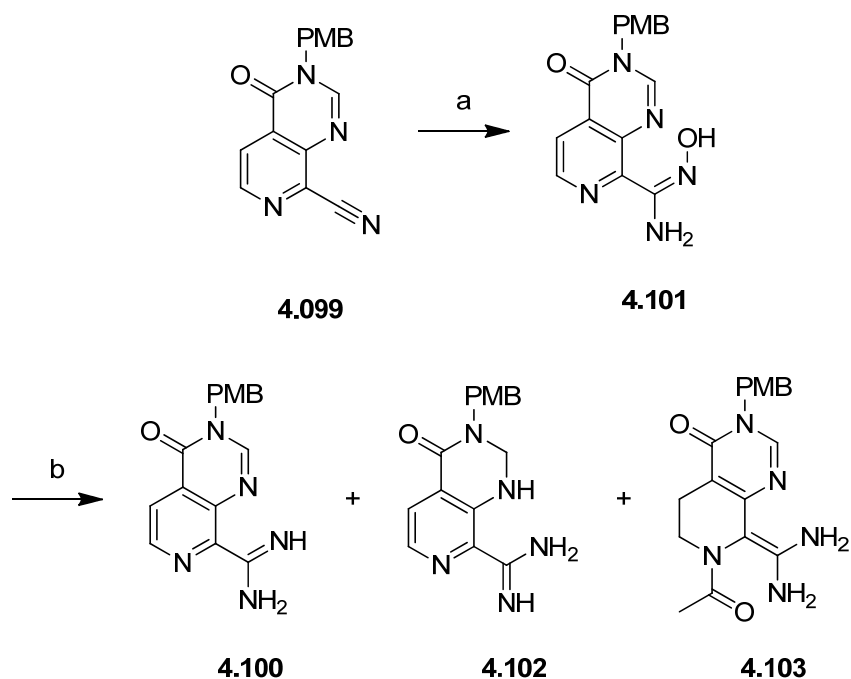
The initial coupling between 8-chloropyridopyrimidinone **4.095** and zinc cyanide was effective in providing 8-cyanopyridopyrimidinone **4.094**, but due to the lack of solubility in

organic solvents and water of both 8-chloropyridopyrimidinone **4.095** and 8-cyanopyridopyrimidinone **4.094** the compound could not be effectively purified.¹⁵⁰ The cyanation reaction provided **4.094** in 72% yield correcting for impurities, the largest being the unreacted starting material **4.095**. In order to access the required pure 8-chloropyridopyrimidinone **4.095**, a decision was made to use a protecting group strategy with the aim of providing more soluble intermediates. The inclusion of a PMB protecting group to 8-chloropyridopyrimidinone **4.095** gave PMB-protected **4.098** and subsequent cyanation provided 8-cyano **4.099**, which was considerably more soluble in organic solvents than des-PMB **4.094**. This improved solubility was thought to be due to both the removal of an H-bond donor and a significant increase in lipophilicity (Scheme 21).



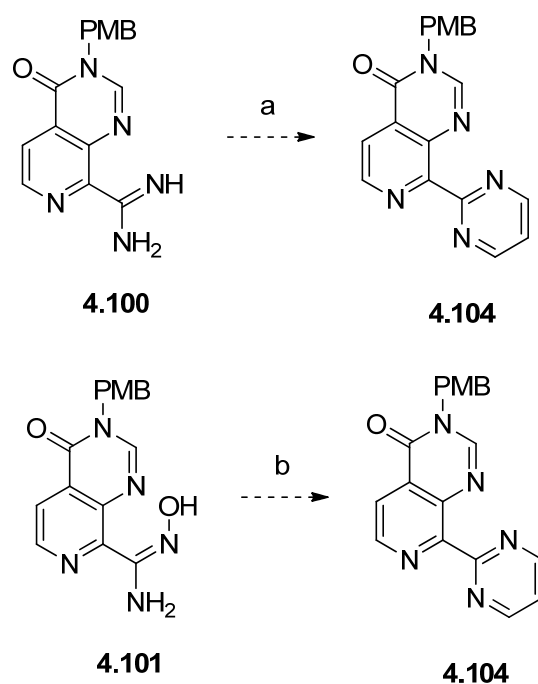
Scheme 21: Reagents and conditions a) K_2CO_3 , PMB-Cl, KI, acetone, 50 °C, 86%; b) $Zn(CN)_2$, 10% $Pd(PPh_3)_4$, DMF, 90 °C, 89%.

The key intermediate to the pyrimidine containing **4.091** (Scheme 20, p 86) was the amidine **4.100** which was accessed *via* hydroxyamidine **4.101** (Scheme 22). Hydroxylamine hydrochloride was added to **4.099** and, when neutralised with sodium hydroxide, attacked the nitrile of **4.099** in a nucleophilic manner to give hydroxyamidine compound **4.101**.^{151,152} Hydroxyamidine example **4.101** could be reduced to amidine containing **4.100** through initial treatment with acetic anhydride in acetic acid and hydrogenation in the presence of 10% palladium on carbon.¹⁵³ This transformation not only gave the desired product, but also two by-products in similar yield (Scheme 22).



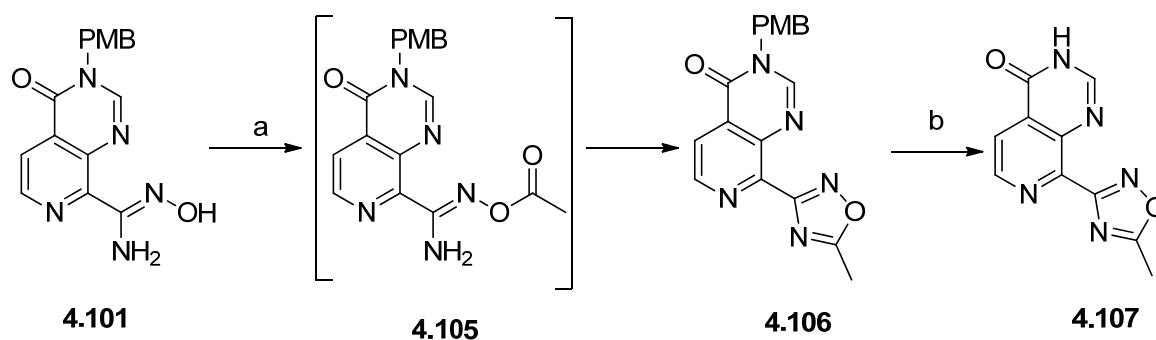
Scheme 22: Reagents and conditions a) H₂NOH.HCl, NaOH, EtOH, 60 °C, 84% b) Ac₂O, 10% Pd/C, H₂ 1 atm, AcOH, 20 °C, **4.100** 19%, **4.102** 23%, **4.103** 29%.

Dihydropyrimidinone containing **4.102** and acetamide example **4.103** are over reduction products. Acetamide example **4.103** has undergone a further amidation reaction with excess acetic anhydride in the reaction mixture. Reductions of *N*-alkylated pyrimidinone containing molecules with hydrogen and a metal catalyst are reasonably well known although many examples have required more than one atmosphere of hydrogen.^{154,155,156,157} Hydrogenation of pyridines is also well known with subsequent amide formation on the formed amine,^{158,159} although the diaminomethylene group is obscure. Reaction of amidine **4.100** with 3-dimethylaminoacrolein gave none of the desired pyrimidine **4.104** and neither did reaction of hydroxyl amidine **4.101** with acrolein (Scheme 23).¹⁶⁰



Scheme 23: Reagents and conditions a) $\text{Me}_2\text{NCH}_2\text{CHO}$, NaOMe, MeOH, 0%; b) H_2CCHCHO , pTSA, PhMe, 80 °C, 0%.

However, it was possible to access an oxadiazole, an alternative heteroaryl to the pyrimidine which may be able to provide a hydrogen bonding partner for Lys245 in addition to providing a metal binding motif. Hydroxyamidine containing **4.101** was stirred in acetic acid with acetic anhydride, first at room temperature to form acetylated compound **4.105** and then at 100 °C to form oxadiazole analogue **4.106** (Scheme 24).¹⁶¹ Attempted PMB deprotection with DDQ¹⁶² gave no reaction either at room temperature or with heating and the starting material **4.106** was recovered in quantitative yield. The next conditions used TFA as solvent and heating at 70 °C for one hour, which gave final compound **4.107** in 35% yield (Scheme 24).¹⁶³



Scheme 24: Reagents and conditions a) Ac_2O , AcOH , $20\text{ }^\circ\text{C}$ then $100\text{ }^\circ\text{C}$, 91%; b) TFA , $70\text{ }^\circ\text{C}$, 36%.

At this time efforts to access pyrimidine compound **4.091** were halted due to lack of success and a renewed focus was placed on introducing pyridine at the 8-position of the pyridopyrimidinone.

4.10.2 Cross coupling methodology

Despite initial misgivings about the challenge of forming the key pyridine-pyridine bond *via* cross coupling, pyridine containing **4.108** was targeted by this approach (Fig. 42). If pyridine compound **4.108** showed a pIC_{50} of > 4.0 at JmjD2d then fully elaborated **4.086** (Scheme 22, p 88) will be targeted as this should give a 10 to 100-fold jump in potency if the SAR of the Schofield compounds correlated with this series (Table 15, p 81).

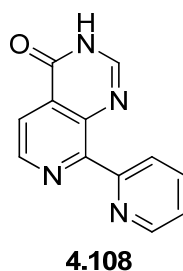
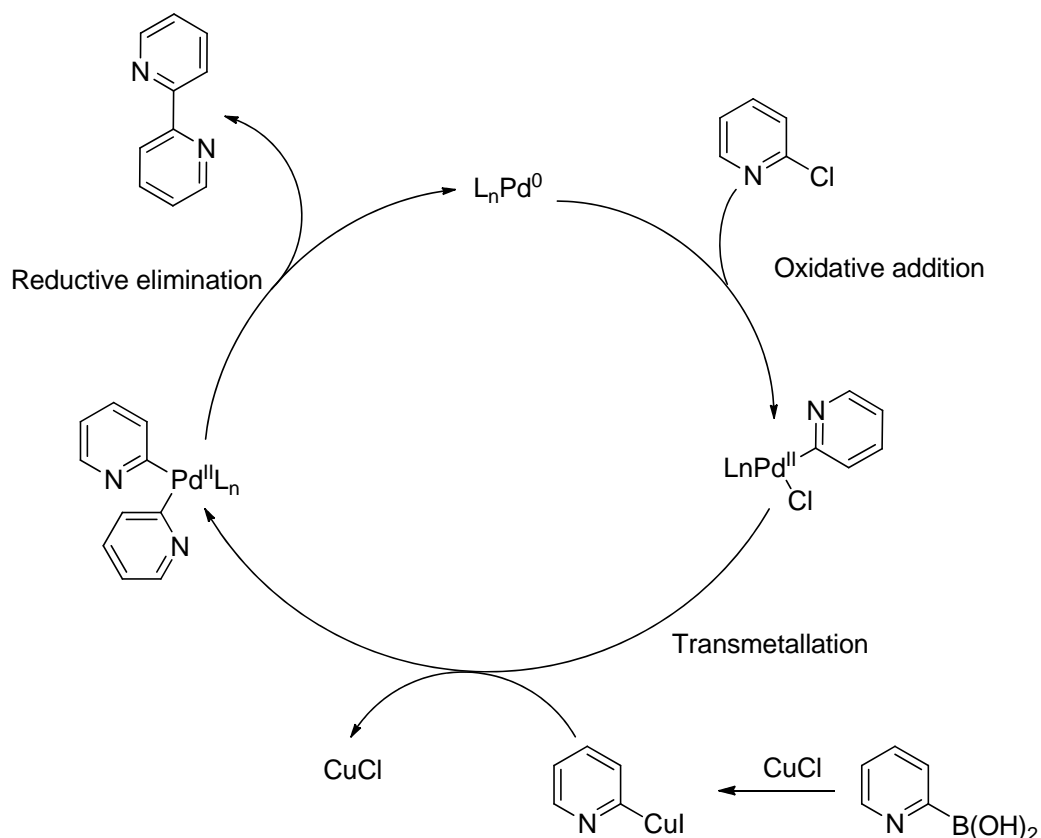


Figure 42: Initial target to model Schofield-like compounds.

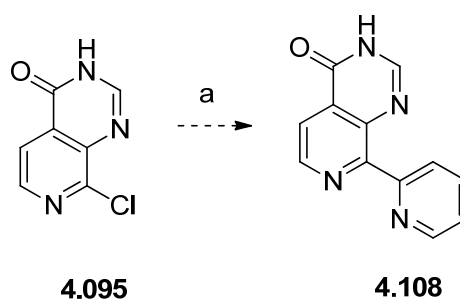
The first method attempted was the direct Suzuki coupling of chloro compound **4.095** with 2-pyridineboronic acid. The Suzuki reaction is a mild reaction with wide functional group tolerance which, in this example, should allow the introduction of an elaborated pyridine ring to make a late stage intermediate for the synthesis of amine containing **4.086**. 2-Pyridineboronic acid is a known difficult substrate to couple, believed to be due to the slow

rate of transmetalation from boron to palladium, which allows competitive protodeboronation. A group from Merck have had success in adding stoichiometric quantities of copper halides to their Suzuki reaction mixtures, increasing yields from less than 5% without copper chloride to much improved yields of 46 - 88%.¹⁶⁴ It was proposed in their examples that the pyridine boronic ester initially transmetalates to the copper at a much faster rate than compared to palladium. The copper-pyridine complex then transmetalates to palladium and proceeds through the remainder of the Suzuki mechanism to give the desired cross-coupled product (Scheme 25).



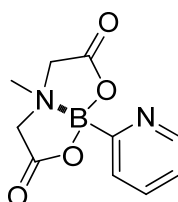
Scheme 25: Proposed mechanism of the copper mediated Suzuki cross coupling.¹⁶⁴

However, on attempting the copper mediated conditions, neither the desired product **4.108** or the des-chloro compound **4.019** were observed suggesting that no oxidative addition took place (Scheme 26).



Scheme 26: Reagents and conditions a) $(\text{HO})_2\text{B-2-pyr}$, CuCl , $\text{Pd}(\text{OAc})_2$, Cs_2CO_3 , DMF , $100\text{ }^\circ\text{C}$, 0%.

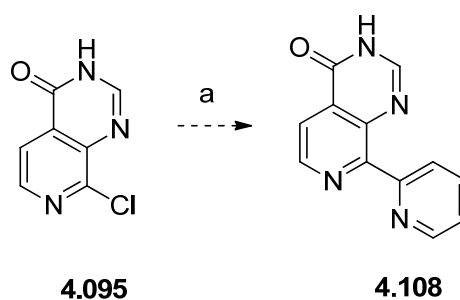
A recent strategy to reduce the issues of protodeboronation with 2-heteroaryl boronic acids and esters is to replace them with a MIDA boronate (Fig. 43).



4.109

Figure 43: Structure of 2-pyridyl MIDA boronate (**4.109**).

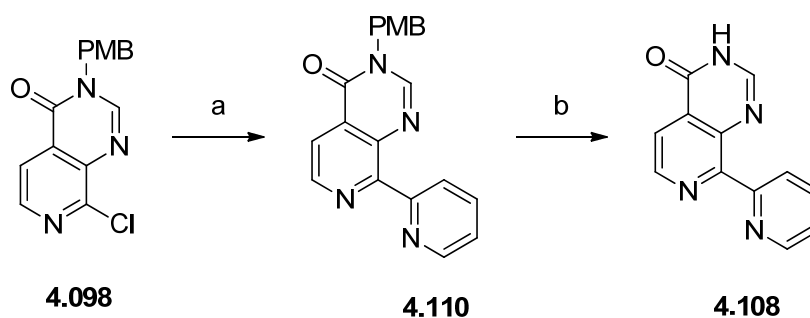
These MIDA boronates have the advantage of being air stable while many 2-heteroaryl boronic acids and esters are not.¹⁶⁵ While MIDA boronates are hydrolysed rapidly to boronic acids by strong bases such as sodium hydroxide, tripotassium phosphate causes only slow hydrolysis and it is believed this small quantity of boronic acid formed *in situ* is rapidly transmetallated by the palladium species which is in relative excess. The 2-pyridyl MIDA boronate (**4.109**) was used in conjunction with a palladium precatalyst developed by the Buchwald group, which is unmasked by base under the reaction conditions to give a palladium species which has proven effective in cross-coupling 2-heteroaryl boronic acids.¹⁶⁶ However, even given these advantages none of the desired coupled product **4.108** or the des-chloro compound **4.019** were observed (Scheme 27).



Scheme 27: Reagents and conditions a) **4.109**, XPhos palladacycle, K_3PO_4 , THF, H_2O , $60\text{ }^\circ\text{C}$, 0%.

The lack of any reaction at all led to questions regarding whether any form of cross-coupling was possible. The conditions in Schemes 26 and 27 were tried again with the PMB protected pyridopyrimidinone **4.098**, in case a lack of solubility of the 8-chloro pyridopyrimidinone **4.095** was a cause for the reactions to fail. Even with the more soluble PMB-protected **4.098** in the reaction mixture, none of the desired cross coupled product was observed.

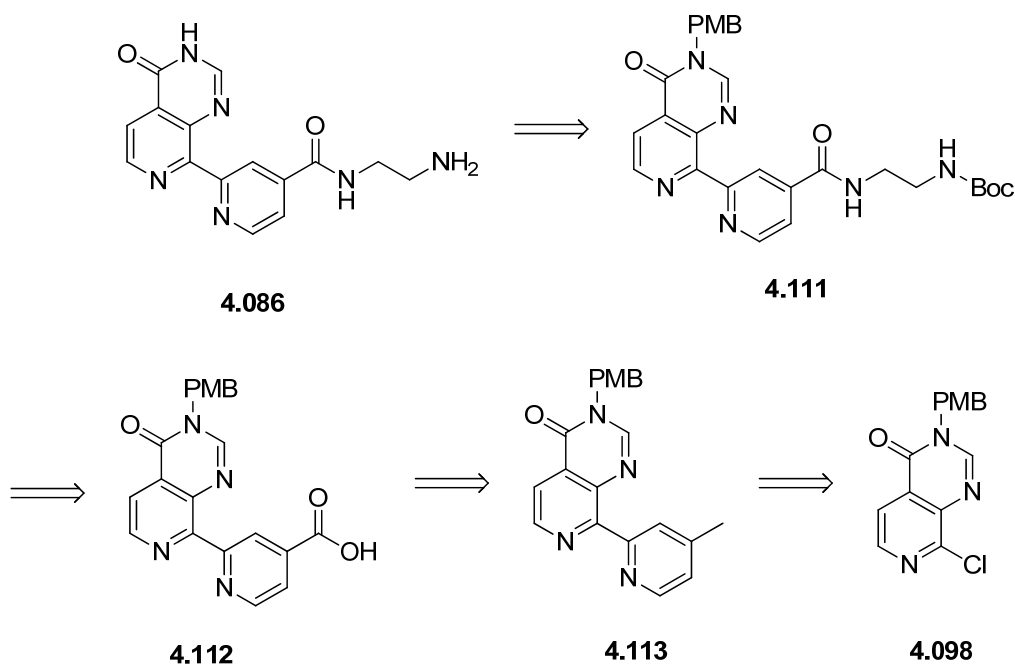
The success of the cyanation with zinc cyanide and tetrakis triphenylphosphine palladium to synthesise 8-cyanopyridopyrimidinone **4.099** (Scheme 21, p 87) gave a degree of confidence that a Negishi coupling to introduce the 2-pyridyl group would be successful. To this end, a Negishi coupling was trialled using 2-pyridylzinc bromide and tetrakis triphenylphosphine palladium in THF.¹⁶⁷ The coupling was successful in a modest yield of 36% to give bipyridyl **4.110**. The final step was the PMB deprotection which, given the ease of deprotection of PMB protected oxadiazole containing **4.106** to give unprotected **4.107**, (Scheme 24, p 90) was expected to be complete in short order. However, the reaction to remove the PMB group from 8-pyridyl pyridopyrimidinone **4.110** was considerably slower than the analogous reaction with the 8-oxadiazole (Scheme 24, p 90). After 4 days at reflux in TFA approximately half of protected **4.110** had been converted to unprotected **4.108**. The reaction was removed from the heat and purified at this point as impurities were beginning to form, which ultimately provided **4.108** in 31% yield (Scheme 28).



Scheme 28: Reagents and conditions a) pyr-2-ZnBr, 10% Pd(PPh₃)₄, THF, reflux, 36% b) TFA, reflux, 31%.

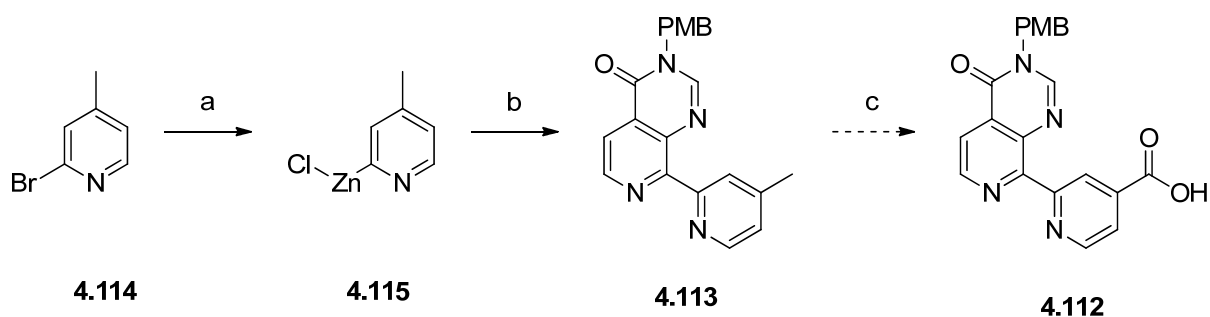
The hypothesis for the change in the rate of deprotection to provide oxadiazole **4.107** and pyridyl **4.108**, is the difference in the electron density in the pyridopyrimidinone ring system. Oxadiazole containing **4.106** is more electron deficient overall, due to the larger number of heteroatoms in the 8-substituted oxadiazole ring, than pyridine containing **4.110** and this causes the removal of the PMB group to occur at a faster rate.¹⁶⁸

When tested at the JmjD2 enzymes (Table 16, p 101), 8-pyridyl compound **4.108** had a pIC₅₀ value at JmjD2d of ≤ 4.3 which gave confidence to prosecute the synthesis of the pyridopyrimidinone analogue of the Schofield compound **4.086** (Scheme 15, p 83), the pyridopyrimidinone analogue of the most active compound in the Schofield paper.⁷⁰ Given the success of the Negishi coupling compared to the other methods evaluated in respect to introducing the 2-pyridyl moiety, this was the key step that would be used to synthesise amino pyridopyrimidinone **4.086**. Using similar methodology that Schofield *et al.* used to synthesise the carboxylic acids **4.085** and **4.005** (Table 15, p 81), a retrosynthesis using a 4-methylpyridyl substrate was undertaken (Scheme 29).⁷⁰



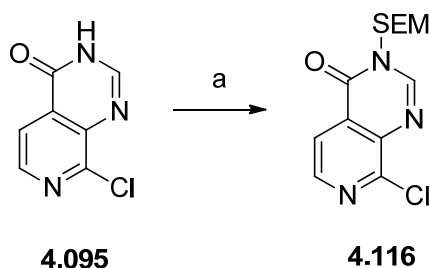
Scheme 29: Retrosynthesis to **4.086**.

Focussing on the forward synthesis, (4-methylpyridin-2-yl)zinc chloride (**4.115**) was synthesised as a solution in THF by treating 2-bromo-4-methylpyridine (**4.114**) first with a solution of isopropylmagnesium chloride in diethyl ether, followed by a solution of zinc chloride in THF.¹⁶⁹ Negishi coupling of aryl zinc compound **4.115** in THF with PMB protected compound **4.098** using tetrakis triphenylphosphine palladium gave bipyridyl analogue **4.113** in 22% yield.¹⁶⁷ Bipyridyl example **4.113** was dissolved in concentrated sulfuric acid and chromium trioxide added. This forms a solution of chromic acid which should be capable of oxidising methyl containing **4.113** to the corresponding carboxylic acid **4.112**. The chromic acid methodology is used to oxidise 4,4'-dimethyl-2,2'-bipyridine to form dicarboxylic acid **4.085** and was therefore considered likely to succeed.¹⁷⁰ However, when used on the methyl substituted pyridine **4.113** a multicomponent mixture was generated containing none of the desired acid **4.112** or PMB deprotected analogue (Scheme 30).



Scheme 30: Reagents and conditions a) $i\text{PrMgCl}$, ZnCl_2 , THF, 0 – 20 °C; b) **4.098**, 10% $\text{Pd}(\text{PPh}_3)_4$, reflux, 22% over 2 steps; c) CrO_3 , H_2SO_4 , 20 °C, 0%.

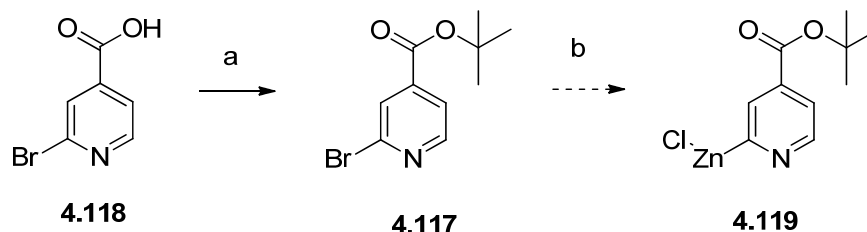
Therefore another synthetic strategy needed to be undertaken. Given the difficulty in removing the PMB protecting group from bipyridyl **4.110** (Scheme 28, p 94) an alternative protecting group was required. SEM was selected as it should be stable to the reaction conditions in the planned synthesis and can be removed using milder conditions than the PMB group such as in the presence of fluoride ions. The SEM group was appended to 8-chloropyrido[3,4-*d*]pyrimidin-4(3*H*)-one (**4.095**) using analogous conditions to those used to form PMB protected **4.098** (Scheme 21, p 87). In this particular case, DMF was added as a co-solvent to aid solubility and this gave **4.116** in 82% yield (Scheme 31).



Scheme 31: Reagents and conditions a) SEM-Cl, K_2CO_3 , acetone, DMF, 50 °C, 82%.

To enter at the appropriate oxidation state to access the carboxylic acid it was decided to protect the acid as a *tert*-butyl ester. The hypothesis was that the *tert*-butyl ester would be less likely to react with isopropyl magnesium chloride than smaller, less sterically hindered esters during the formation of the organozinc. *tert*-Butyl esters have been proved to be stable to isopropyl magnesium chloride at room temperature.¹⁷¹ Also, *tert*-butyl esters can be removed under mild conditions such as using silica in toluene which will leave the SEM group intact.¹⁷² *tert*-Butyl 2-bromoisonicotinate (**4.117**) was formed through the reaction of 2-bromoisonicotinic acid (**4.118**) with *tert*-butyl alcohol in the presence of DCC and DMAP in 58% yield.¹⁷³ Using the same conditions as were utilised to form organozinc

4.115, gave none of the desired product **4.119**. Even after adding further equivalents of isopropyl magnesium chloride, to rule out complexation of the Grignard reagent with either the pyridyl nitrogen or the ester oxygens, the starting material was only partially consumed and many side products were observed (Scheme 32).¹⁷⁴

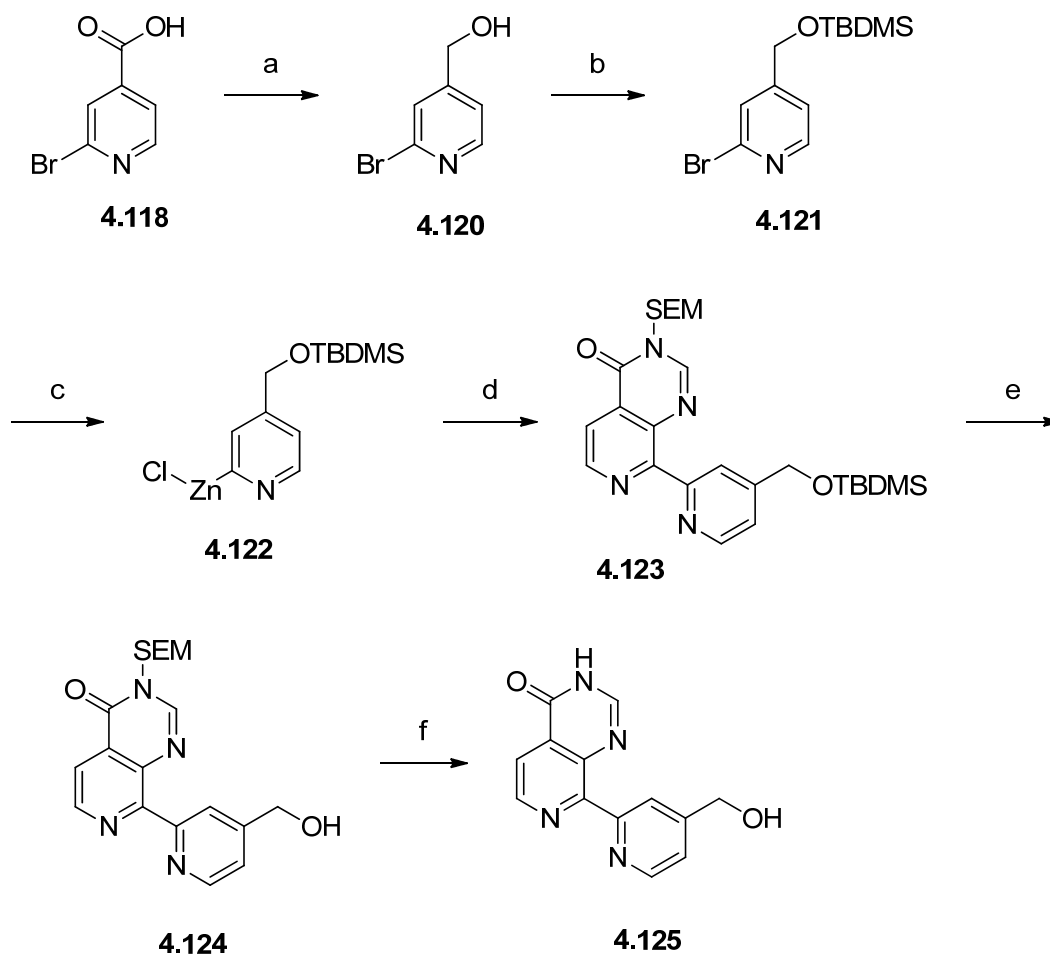


Scheme 32: Reagents and conditions a) DCC, ^tBuOH, DMAP, DCM, DMF, 20 °C, 58%; b) ⁱPrMgCl, ZnCl₂, THF -70 – 20 °C, 0%.

The reaction profile indicated it would not be possible to couple with a compound at the desired oxidation state using this method, so a route starting at the alcohol oxidation state, cross-coupling and then oxidising to the carboxylic acid for subsequent amide formation was selected (Scheme 33). Pyridyl carboxylic acid **4.118** was reduced to alcohol **4.120** with borane:THF complex. 1 M Sodium hydroxide was added and the mixture refluxed to disassociate residual boron complexes from the desired product to give alcohol **4.120** in 26% yield.¹⁷⁵ Primary alcohol **4.120** was protected with TBDMS to give silyl ether **4.121** and from this, organozinc **4.122** was formed.¹⁷⁴ Organozinc **4.122** was successfully cross coupled with SEM-protected chloro pyridopyrimidinone **4.116** using Negishi cross-coupling conditions to give bipyridyl compound **4.123**.¹⁶⁷

During the initial synthesis of bipyridyl **4.123** the material was loaded on to an SCX ion exchange column and after elution with 2 M methanolic ammonia two products were observed; fully protected desired product bipyridyl compound **4.123** and des-TBDMS analogue **4.124**. This suggested that while in contact with the sulfonic acid stationary phase of the SCX column the acid had selectively deprotected the TBDMS group. The original synthetic strategy was to globally deprotect bipyridyl **4.123** and carry out subsequent chemistry on the unalkylated pyridopyrimidinone. However, if the TBDMS could be selectively deprotected in the presence of the SEM this would make the handling of the intermediates significantly easier due to the previous experience of unprotected pyridopyrimidinones being poorly soluble in organic solvents. To test a more convenient

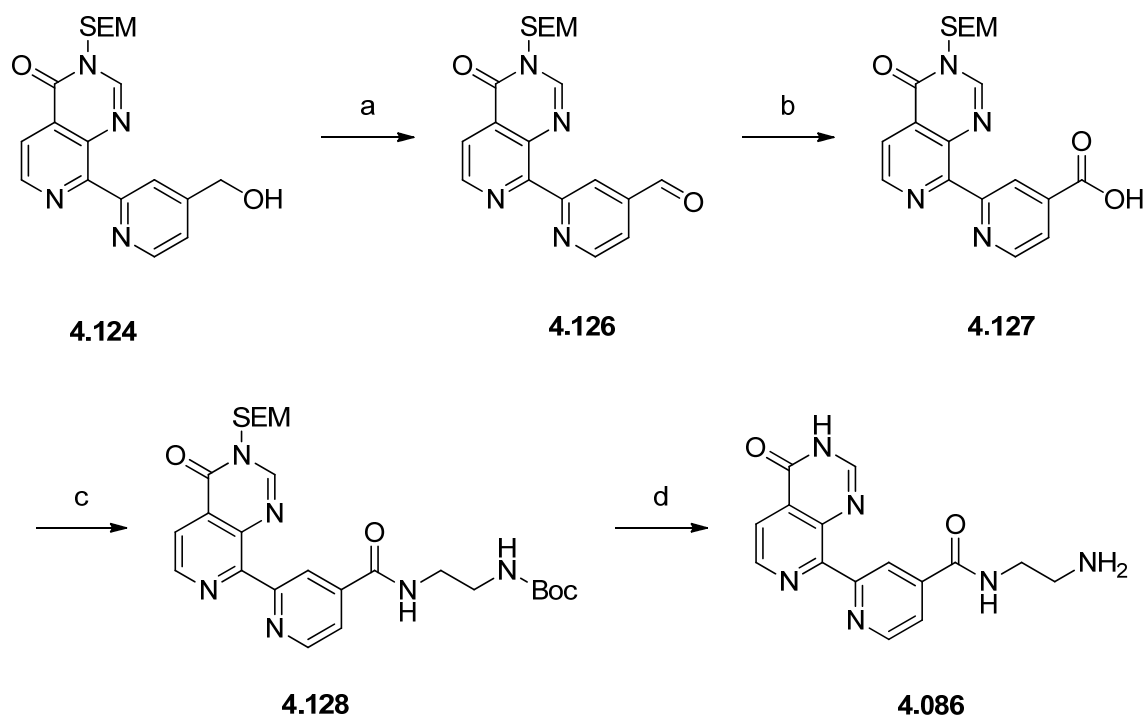
way of selectively removing the TBDMS group than leaving it in contact with the SCX stationary phase, bipyridyl **4.123** was stirred in THF at room temperature and a solution of 1 M TBAF in THF added. After 1 hour the bipyridyl **4.123** had been entirely converted to des-TBDMS **4.124**. After a further 4 days stirring at room temperature no SEM deprotection was detected. As expected, heating the reaction mixture to 60 °C overnight removed the SEM group to give fully deprotected **4.125** (Scheme 33).



Scheme 33: Reagents and conditions a) THF.BH₃, THF 0 – 60 °C, 26%; b) TBDMS-Cl, imidazole, DMF, 96%; c) ⁱPrMgCl, ZnCl₂, THF, 0 – 20 °C; d) **4.116**, 10% Pd(PPh₃)₄, reflux; e) TBAF, THF, 20 °C, 50% over 3 steps; f) TBAF, THF, 60 °C, 55%.

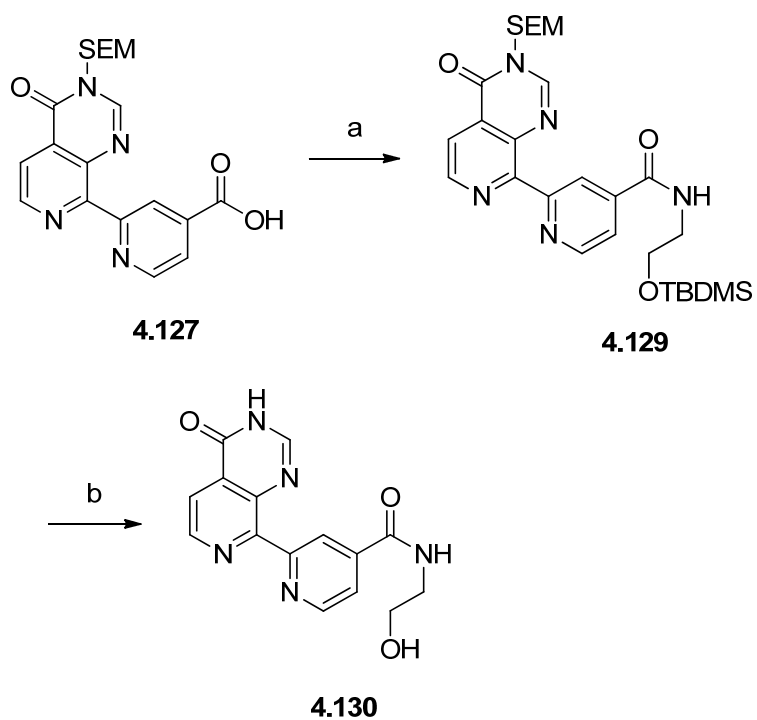
Alcohol **4.124** was oxidised to aldehyde **4.126** in 80% yield using a Swern oxidation (Scheme 34).^{176,177} Aldehyde containing **4.126** was then oxidised *via* a Pinnick oxidation to give carboxylic acid analogue **4.127** in 47% yield.¹⁷⁸ The acid chloride was generated with oxalyl chloride and catalysed by DMF forming the Vilsmeier reagent, chloromethylenedimethylammonium chloride, *in situ*. The crude acid chloride was

evaporated to dryness, redissolved in DCM and *N*-Boc-ethylenediamine added with triethylamine to form amide **4.128** in 86% yield. A solution of 5 M HCl in IPA was added to doubly protected **4.128** and after 2 hours it was noted that the Boc group had been removed but only a small amount of final product **4.086** had been formed, with the major species present in the reaction mixture being the des-Boc **4.128**. The reaction mixture was heated to 60 °C for 3 hours whereupon only desired final product **4.086** could be seen in the reaction mixture, which was isolated in 91% yield (Scheme 34).



Scheme 34: Reagents and conditions a) DMSO, (COCl)₂, NEt₃, -78 °C – 20 °C, 81%; b) NaClO₂, NaH₂PO₄, CH₃CHC(CH₃)₂, ^tBuOH, H₂O, 58%; c) i) (COCl)₂, DMF, DCM, 20 °C; ii) NH₂(CH₂)₂NHBOC, NEt₃, DCM, 20 °C, 86%; d) HCl, IPA, 20 – 60 °C, 91%.

In silico modelling had previously suggested that Asp139 in JmjD2d would make stronger interactions with an alcohol rather than an amine and thus improve the potency compared to amine containing **4.086**. Therefore, an analogous amide coupling was undertaken with TBDMS protected ethanolamine, which gave silyl ether **4.129** which could be deprotected with TBAF in THF. As previously observed the TBDMS group was removed first at 50 °C. However, the SEM group proved stubborn to remove and required heating at 110 °C under microwave conditions for 6 hours to give alcohol **4.130** in 14% yield (Scheme 35).

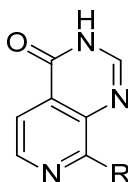


Scheme 35: Reagents and conditions a) i) $(\text{CO})_2\text{Cl}_2$, DMF, DCM, 20 °C; ii) $\text{NH}_2(\text{CH}_2)_2\text{OTBDMS}$, NEt_3 , DCM, 20 °C 35%; b) 1 M TBAF in THF, 110 °C, 14%.

Overall, synthetically challenging 8-substituted pyridopyrimidinones amino **4.086** and hydroxyl **4.130** were accessed in 3.6% and 0.2% overall yield, respectively, both over nine linear steps starting from 3-aminoisonicotinamide (**4.097**).

4.10.3 SAR of 8-substituted pyridopyrimidinones

If the SAR was to track as it did with compounds dicarboxylic acid **4.085** and amine **4.005** giving a 100-fold increase in potency (Table 15, p 81), then it would be expected that moving from 8-pyridyl **4.108** or benzyl alcohol **4.125** to amine **4.086** would give a similar shift in potency. However, this is not the case for this particular example (Table 16).



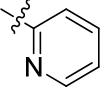
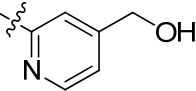
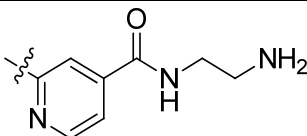
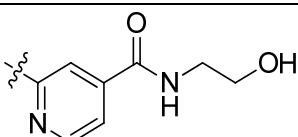
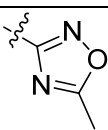
Entry	Number	R	JmjD2d pIC ₅₀ (LE)
1	4.019	H	5.0 (0.62)
2	4.108		≤ 4.3 (0.34)
3	4.125		< 4.0
4	4.086		4.9 (0.29)
5	4.130		< 4.0
6	4.107		< 4.0
7	4.095	Cl	< 4.0 ^a

Table 16: RapidFire™ potencies of compounds. ^a) Assay carried out with 10x concentration of JmjD2 enzyme, incubating for 8 min.

While there is an increase in potency moving from 8-pyridyl **4.108** and benzyl alcohol **4.125** to amine **4.086**, it is considerably smaller than the 10 to 100-fold increase that were seen for the Schofield compounds. This is, ultimately, disappointing as there is no increase in potency from pyridopyrimidinone **4.019** and nearly a halving of the LE. However, from the difference in potencies between amine **4.086** and alcohol **4.130** it can be inferred that the terminal primary amine is making a more favourable interaction with the protein, possibly a salt bridge with Asp139, than the primary alcohol. The inactivity of 8-chloropyrido[3,4-

d]pyrimidin-4(3*H*)-one (**4.095**) and the diazole containing **4.107** can be explained by the electron withdrawing nature of the groups in the 8-position of the pyridopyrimidinone. The chlorine and the diazole remove electron density from the pyridine ring and thus decrease the binding interaction between the lone pair of the pyridine nitrogen and the Fe (II).

The reason for the decrease in potency of the 8-pyridyl substituted compounds is not clear. However, there are some reasons why the potency for amino **4.086** may be lower than expected. First of all there is a reasonable probability that the lowest energy conformation of amino **4.086** is not with the nitrogens of the pyridine preorganised to chelate the iron. The lowest energy conformations of the two possible pyridopyrimidinone tautomers show the lowest energy conformer will not give bidentate chelation (Fig. 44).

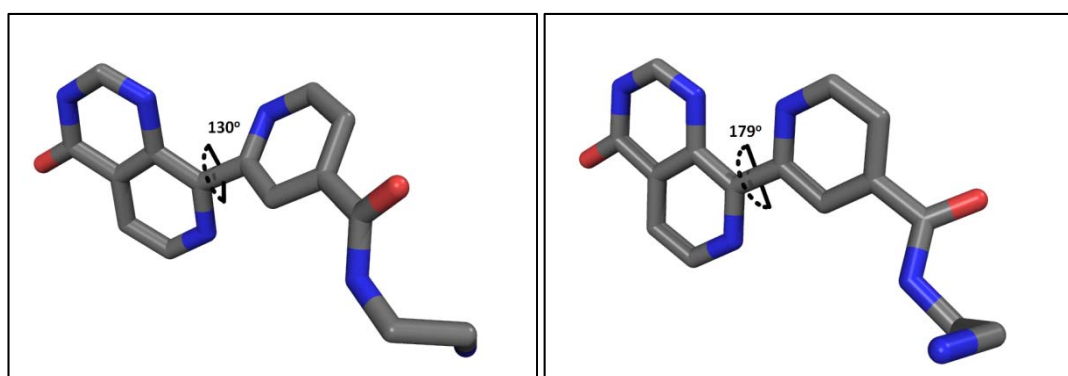


Figure 44: Left: Lowest energy conformer of **4.086** of the pyridopyrimidinone using force field MMFF94x.¹⁴² Right: Lowest energy conformer of **4.086** with an internal H-bond.

Due to steric clash between the peri-hydrogen of the pyridine and the nitrogen of the pyrimidone portion in the pyridopyrimidinone, the dihedral angle between the pyridopyrimidinone and the pyridine ring is 130° from the ideal 0° angle. If the 4-pyrimidinone tautomer of the pyridopyrimidinone is favoured then an internal hydrogen bond can be formed. This creates a pseudo 6-membered ring which holds the aromatic portion of amino **4.086** flat and would need to flip 180° to chelate in a bidentate manner to a metal. To compare with the conformation of amino **4.086** in JmjD2d an X-ray crystal structure was obtained for amino **4.086** in JmjD2d (Fig. 45).

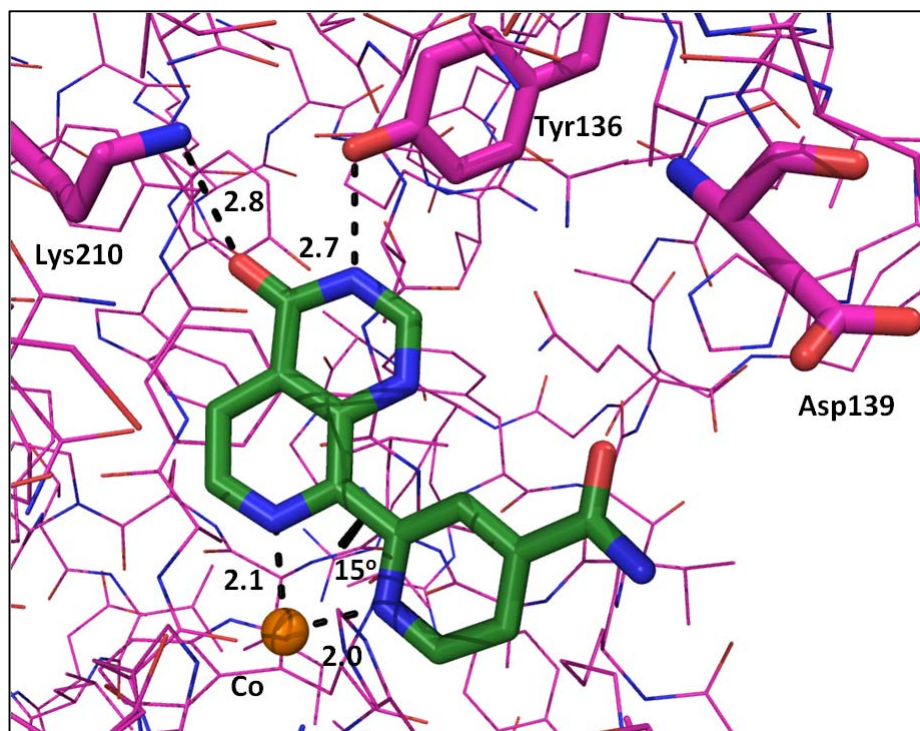
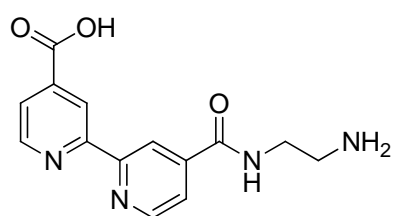
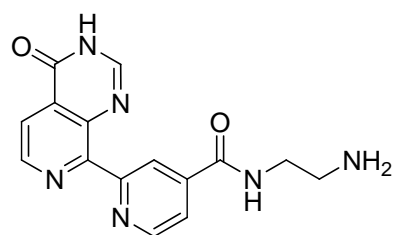


Figure 45: X-ray crystal structure of **4.086** in JmjD2d. Electron density for the pendant amine was not observed.

The ethylamine portion of the molecule cannot be seen in the crystal structure indicating it is in a disordered state throughout the crystal and thus not involved in a strong salt bridging interaction with Asp139. The dihedral angle between the pyridine rings is 15° which is comparable with the bipyridyl dihedral angle of 11° in the most potent compound from Schofield *et al.*, which is carboxylic acid **4.005** (Fig. 41, p 83). The energy needed to adopt the binding conformation rather than the low energy conformation is 10 kcal mol^{-1} greater for pyridopyrimidinone **4.086** than carboxylic acid **4.005** and thus rather than seeing a 10 to 100-fold increase in potency as was expected, only a threefold to fivefold increase was observed (Fig. 46).¹⁷⁹ The higher energy need to lay the pyridine ring in a position where it can chelate the iron in a bidentate manner is due to a steric clash between the peri-hydrogen in the 8-pyridyl position and the 1-N in the pyridopyrimidinone ring system.



4.005



4.086

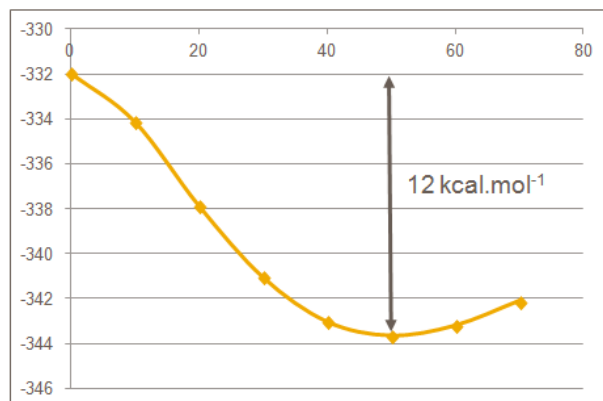
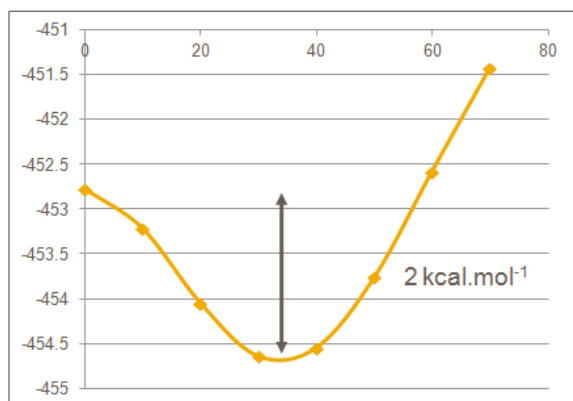
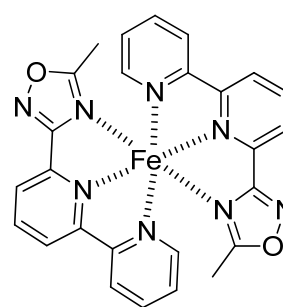
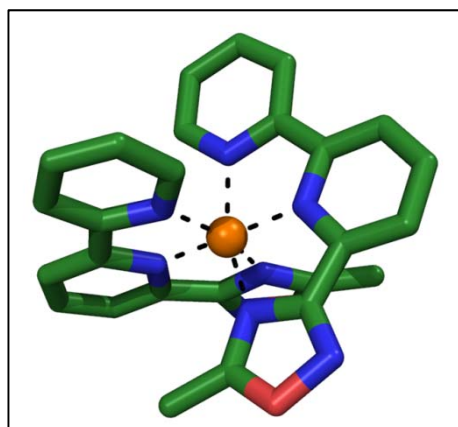


Figure 46: Biaryl torsion angle potential energies calculated using MMFF94s for **4.005** and **4.086**.

In contrast, oxadiazole example **4.107** should be planar due to the adjacency of the 5 and 6-membered aromatic rings (Fig. 33, p 69) and therefore set up to co-ordinate to the metal in the JmJD2 family enzyme. Similar substructures are known to co-ordinate iron (II) in small molecule crystal structures such as tricyclic **4.131** (Fig. 47).¹⁸⁰



4.131

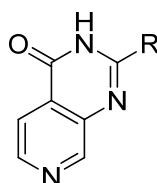
Figure 47: X-ray crystal structure of **4.131** co-ordinating to an iron (II) ion. Counter ions are not shown.

It may be that oxadiazole substituted pyridopyrimidinone **4.107** does not co-ordinate well to the iron in the JmjD2d enzyme as the oxadiazole is removing electron density from the pyridopyrimidinone ring system (p 94). The lowered electron density could reduce the binding between the iron and the pyridine nitrogen lone pair as hypothesised for 8-chloropyridopyrimidinone **4.095**.

Substitution at the 8-position of the pyridopyrimidinone core appears to lower potency when compared to fragment **4.019** which has no substitution. Thus, this will not provide the desired profile of increasing or at least retaining potency while generating a molecule which could be used to probe the phenotypic effects of inhibiting the JmjD2 family. However, substitution from the 2-position of the pyridopyrimidinone with heteroatoms was being pursued which showed some positive results.

4.11 2-Substitution of the pyridopyrimidinone core with heteroatoms

Screening compounds identified by substructure searches of the compound collection available within our laboratories with just a heteroatom at the 2-position of the pyridopyrimidinone, did not provide the desired increase in potency. However, when compounds were synthesised with substitution from the heteroatom interesting results were seen (Table 17).

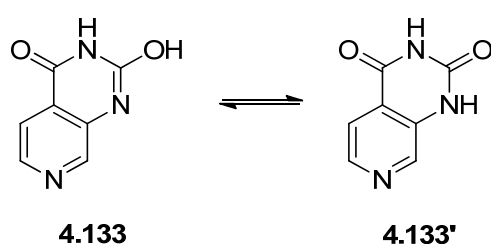


Entry	Number	R	JmjD2d pIC ₅₀ (LE)
1	4.019	H	5.0 (0.62)
2	4.045*	Me	< 4.0
3	4.132	NH ₂	4.6 (0.53)
4	4.133	OH	≤ 4.2 (0.48)
5	4.049*	n-Pr	4.7 (0.46)
6	4.134*	NHEt	5.1 (0.50)
7	4.135*	OEt	6.2 (0.61)

Table 17: RapidFire™ potencies of 2-substituted pyridopyrimidinones with heteroatoms.

While the initial 2-amino **4.132** compound and 2-hydroxyl substituted **4.133** pyridopyrimidinones (Entries 3 and 4, Table 17) were more potent than 2-methyl substituted **4.045** (Entry 2), there was no improvement in potency compared to the

unsubstituted pyridopyrimidinone **4.019**. When *N*-ethyl example **4.134** and *O*-ethyl **4.135** containing (Entries 6 and 7) were tested, a significant increase in potency was observed when compared to *n*-propyl analogue **4.049** (Entry 5). *O*-Ethyl compound **4.135** was the first compound to give sub-micromolar potency at JmjD2d. The 100-fold increase in potency between unsubstituted **4.133** (Entry 4) and ethyl substituted ether **4.135** (Entry 7) was thought to be due to substituting the oxygen forcing the resulting molecule into a more active tautomer **4.133** (Scheme 36). **4.133** could be more active than **4.133'** because of the H-bond acceptor at the 1-position of the pyridopyrimidinone ring. Having an H-bond acceptor at this position was seen to be positive for binding for a number of molecules previously (Table 7, p 53).

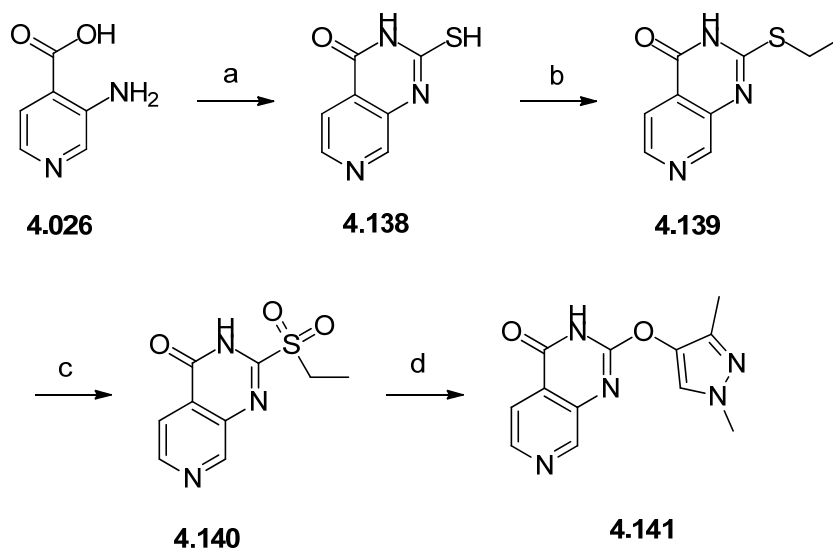


Scheme 36: Tautomers of **4.133**.

The improvement of the RapidFire™ potencies may be partially due to an increase in acidity of the amide N-H in the molecules. However, the nature of the pendant substituent will affect the potency as seen for the 2-carbon substituted pyridopyrimidinones. This is because it can affect the conformation of the JmjD2 family protein as seen by the changing conformation of the protein (Fig. 36, p 72). The pK_as of a range of pyridopyrimidinones were measured and plotted against their JmjD2d potencies (Graph 3).

4.11.1 Synthesis of 2-substituted ether linked pyridopyrimidinones

The compounds that were found to be most potent at the JmjD2 enzymes had an aromatic ether substituent at the 2-position of the pyridopyrimidinone core. These compounds could be accessed in four steps (Scheme 37).



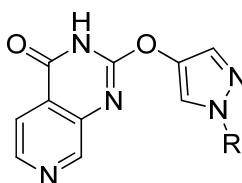
Scheme 37: Reagents and conditions: a) $\text{CS}(\text{NH}_2)_2$, 160 °C, 63%; b) aq. NaOH, EtI, MeOH, 20 °C, 92%; c) mCPBA, THF, 20 °C, 57%; d) 1,3-dimethyl-1H-pyrazol-4-ol, NaH, DMF, 100 °C, 6%.

In the first step a melt of thiourea and 3-aminoisonicotinic acid (**4.026**) were heated overnight to provide thiol example **4.138**.¹⁸¹ Thiol **4.139** was alkylated with ethyl iodide and oxidised to provide sulfone containing **4.140**.¹⁸² Some batches of sulfone compound **4.140** contained the sulfoxide as an impurity. However, the sulfoxide was found to react in the same manner as the sulfone when treated with the alkoxides of aryl compounds, which had been deprotonated with sodium hydride.¹⁸³ The methodology allowed access to compounds such as pyrazole containing **4.141**.

The methodology outlined in Scheme 37 produced a number of compounds that met the majority of the probe criteria.

4.11.2 Probe compounds for the JmjD2 family

The compounds which were found to be suitable all had an oxygen linked pyrazole present (Table 18).

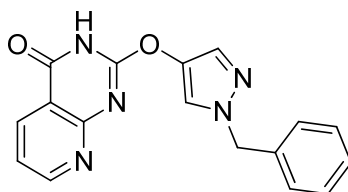


Compound	4.137*	4.142*	4.143*	Probe profile
R				
JmjD2c/d/e RapidFire™ pIC ₅₀ (LE)	6.3 / 6.4 / 6.3 (0.33 / 0.34 / 0.33)	6.2 / 6.4 / 6.3 (0.32 / 0.34 / 0.33)	6.2 ^a / 6.3 / 6.4 (0.35 / 0.36 / 0.36)	≥ 6.0
cLogP	1.5	2.2	1.7	1 – 3
AMP nm s ⁻¹	66	70	44	> 30
Aqueous solubility µg/mL	30	83	60	≥ 50
JmjD3 pIC ₅₀	< 4.0	< 4.0	< 4.0	< 4.0
EGLN3 pIC ₅₀	< 4.0	< 4.0	< 4.0	< 4.0
JmjD2c cell potency pIC ₅₀	5.3	5.3	5.7	> 5.0
Jarid1c RapidFire™ pIC ₅₀	7.2	7.1	6.9	< 4.5
Jarid1c cell potency pIC ₅₀	5.4	5.6	5.3	< 4.0

Table 18: Profiles of JmjD2 family probe compounds. ^a) Inactive on 1 of 9 test occasions.

The compounds selected meet most of the probe criteria, although they were also found to be potent inhibitors of the KDM5 family as exemplified by the Jarid1c data in Table 18. However, there is a larger drop off into the Jarid1c cell assay from the RapidFire™ assay as compared to between the JmjD2c cell assay and the RapidFire™ assay. The compounds were found to be approximately equipotent in the JmjD2c and Jarid1c cell assays. The compounds, when profiled through a selection of 43 non-related drug or liability targets were found to have no significant activity. The compounds were therefore progressed to cellular phenotypic assays to validate the KDM4 and KDM5 families of JmjC containing enzymes as viable targets for drug discovery. Crucially, an inactive control, **4.144** that

cannot chelate to the iron, was added to the collection to help to establish if any activity seen was driven by the JmjD2 family rather than by off-target activity (Table 19).



Compound	4.144*
JmjD2c/d/e RapidFire™ pIC ₅₀	≤ 4.4 ^a / < 4.0 / < 4.0
cLogP	1.5
AMP nm s ⁻¹	34
Aqueous solubility μg ml ⁻¹	≥ 179
JmjD3 pIC ₅₀	< 4.0
EGLN3 pIC ₅₀	< 4.0
JmjD2c cell potency pIC ₅₀	< 4.0
Jarid1c RapidFire™ pIC ₅₀	≤ 4.6
Jarid1c cell potency pIC ₅₀	< 4.0

Table 19: Profile of JmjD2 family inactive control **4.144**. ^a) Inactive on 5 of 6 test occasions.

The inactive control was designed to be as physicochemically similar to active **4.137** (Table 18, p 109) as possible, as **4.137** was one of the first probe compounds identified. Therefore, only the nitrogen in the pyridine ring of the pyridopyrimidinone core of **4.144** has been moved compared to active **4.137**. This disrupts the important interaction between the pyridopyrimidinone core and the iron in the JmjD2 family of enzymes and the resulting compound has a pIC₅₀ value of < 4.0 when assayed against these enzymes.

Therefore, the compounds in Table 18 and inactive control **4.144** were thought to be suitable as dual KDM4 (JmjD2) and KDM5 family probe compounds and were profiled in a range of immune cells both within our laboratories and with external collaborators. In particular, the BioMAP® (DiscoverX Corp., Fremont, CA) panel allowed a wider range of biological activities to be probed in a variety of disease relevant cellular cultures. As cyclopentyl containing **4.143** was the most potent compound seen in the JmjD2c cellular assay it was chosen to be profiled through the BioMAP® assay. However, cyclopentyl analogue **4.143** showed little biological activity outside of the grey area on the chart, which depicts the error in the assay (Fig. 49). This correlates with the data generated from the internal phenotypic assays. Due to the lack of efficacy in immuno-inflammation phenotypic assays and changes in portfolio priorities, work on inhibiting the JmjD2 family of lysine demethylases was halted.

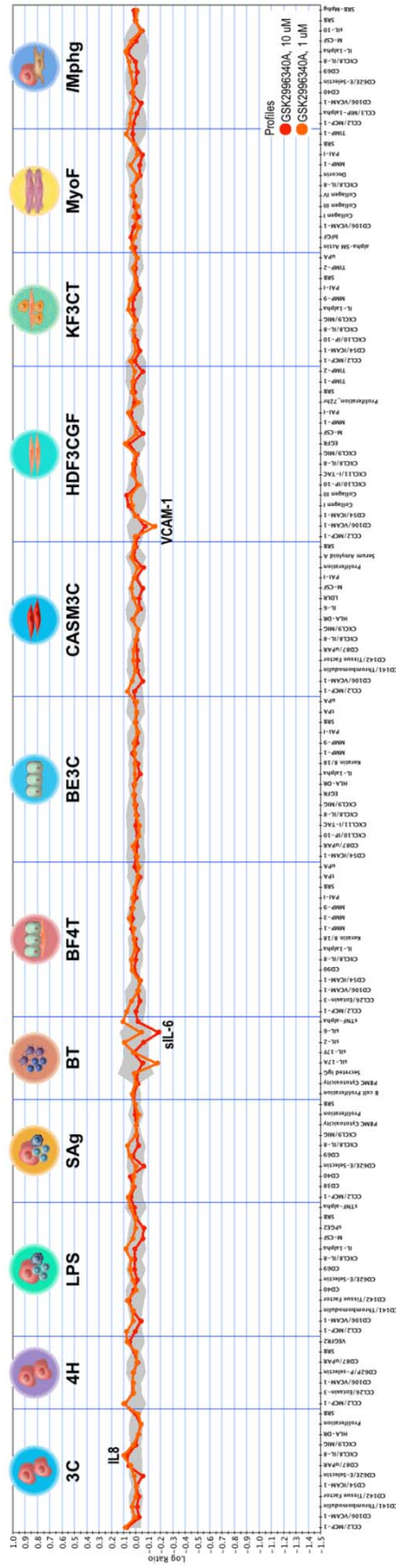
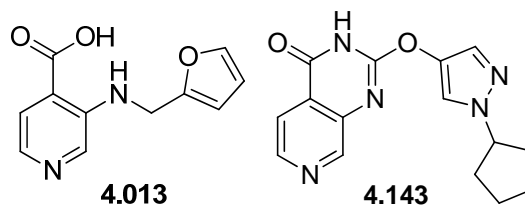


Figure 49: BioMAP® profile of cyclopyentyl containing 4.143.

4.12 JmjD2 inhibitors conclusion

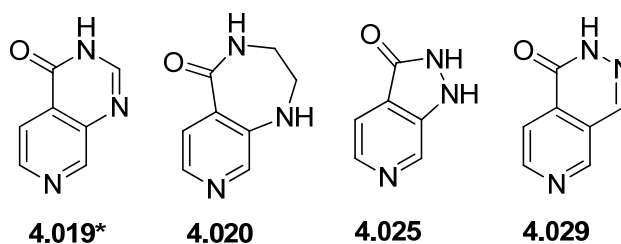
Through the work described above, a series of pyridopyrimidinone compounds was identified that showed the profile necessary to be dual KDM4 and KDM5 family probe compounds. The compounds identified were the first non-carboxylic acid compounds that inhibited the JmjD2 family of enzymes. From a very highly ligand efficient starting point with little cellular penetration were derived compounds that improved upon the potency, and through increasing the lipophilicity of the inhibitors provided cellularly penetrant molecules. Improving upon the cellular penetration over previously known carboxylic acid containing compounds (Table 20) caused lower drop off between the RapidFire™ and JmjD2c cellular assays and improved cellular potency was attained. Increasing the lipophilicity did require erosion of the high LE of the starting pyridopyrimidinone **4.019**, although the probe compounds selected did retain a respectable ligand efficiency of greater than 0.3.



JmjD2d pIC ₅₀ (LE)	6.8 (0.58)	6.3 (0.36)
JmjD3 pIC ₅₀	4.8	< 4.0
JmjD2c cell assay pIC ₅₀	5.2	5.7
AMP nm s ⁻¹	< 3	44

Table 20: Comparison of carboxylic acid **4.013** and pyridopyrimidinone **4.143** probes.

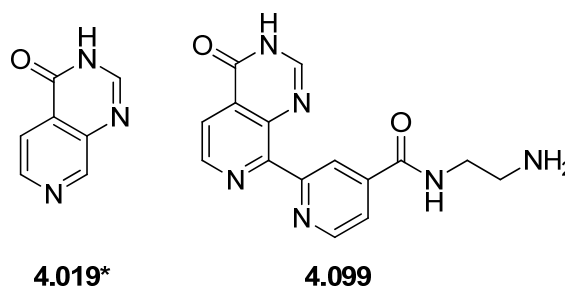
In the course of the research the author has made several key discoveries that have led to further understanding of inhibiting the JmjD2 enzymes with small molecules. Firstly deviating from a 6,6 biaryl template to either 6,5 or 6,7 ring systems is not tolerated by the JmjD2 proteins. Additionally, a H-bond acceptor at the 1-position of the 6,6 biaryl is essential for binding to the JmjD2 proteins (Table 21).



JmjD2d pIC ₅₀ (LE)	5.0 (0.62)	< 4.0	< 4.0	< 4.0
----------------------------------	------------	-------	-------	-------

Table 21: Demonstrating a 6,6 biaryl ring and an H-bond acceptor at the 1-position is essential for JmjD2 binding.

Scaffold hopping between carboxylic acid bipyridyl compounds designed by Schofield *et al.*⁷⁰ and the pyridopyrimidinone core described in this thesis was investigated. A tenfold improvement in potency was observed in the carboxylic acid template, although when repeated in the pyridopyrimidinone template no increase in potency was observed (Table 22). It was hypothesised that steric clash between the two pendant ring systems incurred on making the molecule planar was responsible for this result.



JmjD2d pIC ₅₀ (LE)	5.0 (0.62)	4.9 (0.29)
-------------------------------	------------	------------

Table 22: Potencies of original pyridopyrimidinone hit and 8-pyridyl elaborated compound.

Maintaining potency through substitution at the 8-position of the pyridopyrimidinone with an optimised group and other 8-substitutions causing at least a tenfold decrease in potency (Table 16, p 101) led to no further investigation from this vector. However, this allowed other areas of the molecule to be investigated. The author linked tuning the pK_a of the molecules with increased potency (Graph 3, p 107) by altering the atom directly substituted at the 2-position of the pyridopyrimidinone. Using this link and adding lipophilicity led to the discovery of the probe molecules with measurable cellular penetration (Table 18, p 109). These compounds had demonstrable cellular activity over compounds already known in the literature and the related pro-drugs (Fig 17, p 33).

It was thought that inhibiting the JmjD2 enzymes with the probe compounds could deliver phenotypic changes in a range of immune cells. However, upon testing these compounds in a wide range of immune cells and under different conditions, no immuno-inflammation phenotype was observed. Therefore, the high quality of the probe compounds were instrumental in allowing the programme team to make the decision to halt work on the targets. The probe compounds are undergoing further profiling elsewhere within our laboratories to better understand the biological outcome of dual KDM4/KDM5 JmjC domain inhibitors.

However, due to the probe compounds lack of efficacy in immuno-inflammation and a change in target prosecution within our laboratories, no further work is planned around this target class of “eraser” proteins of the epigenetic code (Fig. 5, p 20). The next body of work undertaken investigated the “reader proteins,” known as bromodomains and inhibiting the protein-protein interactions they form.

5 PCAF

5.1 Protein-protein interactions

Protein-protein interactions (PPI) are central to most biological processes and are involved in processes as diverse as intercellular communication and apoptosis.¹⁸⁴ Therefore, PPIs represent an important class of targets to manipulate biological responses. However, due to technological hurdles there are few small molecule inhibitors of these interactions.¹⁸⁵ Difficulties in identifying small molecule inhibitors of PPIs include having almost no natural small molecule substrates, the flatness of protein-protein interfaces and difficulty in distinguishing real from artefactual binding.

The large, relatively featureless areas across which the proteins interact with each other make it difficult for small molecules to interact with these binding domains. Proteins interact across areas of about 750 – 1500 Å² and for competitive inhibition, a small molecule must cover 800 – 1100 Å² of a protein surface.¹⁸⁶ PPI domains often lack the clefts or pockets that traditional small molecules bind to and thus any small molecule inhibitor must complement the hydrophobic and charged domains on a flat or mildly convex surface.¹⁸⁷ Despite the large surface area that PPIs span, much of the binding affinity is driven by a few key residues and is known as a “hot spot”.¹⁸⁸

Although difficult, it is possible to design and synthesise compounds that inhibit these PPIs. The inhibitors of PPIs have a higher molecular weight and are more lipophilic than typical small molecules designed within the “Rule-of-Five” parameters.¹⁸⁹ Statistical analysis of 39 PPI inhibitors has enabled the establishment of a “Rule-of-Four” for this class of molecule:

190

1. Molecular weight > 400 Da,
2. LogP > 4,
3. Number of rings > 4,
4. Number of H-bond acceptors > 4.

Despite being outside typical chemical space for oral drug-like compounds, examples of PPI inhibitors have progressed through clinical trials. Navitoclax (**5.001**), a B-cell lymphoma-2 (Bcl-2)/Bcl-2 homologous antagonist killer inhibitor was investigated for the treatment of small cell lung cancer and has a molecular weight of 975 Da and a cLogP of 12 (Fig. 50).^{185,191} Additionally RG7112 (**5.002**), a human double minute 2/p53 antagonist is

undergoing clinical trials for oncological diseases and has a molecular weight of 728 Da and a cLogP of 11 (Fig. 50).^{192,193}

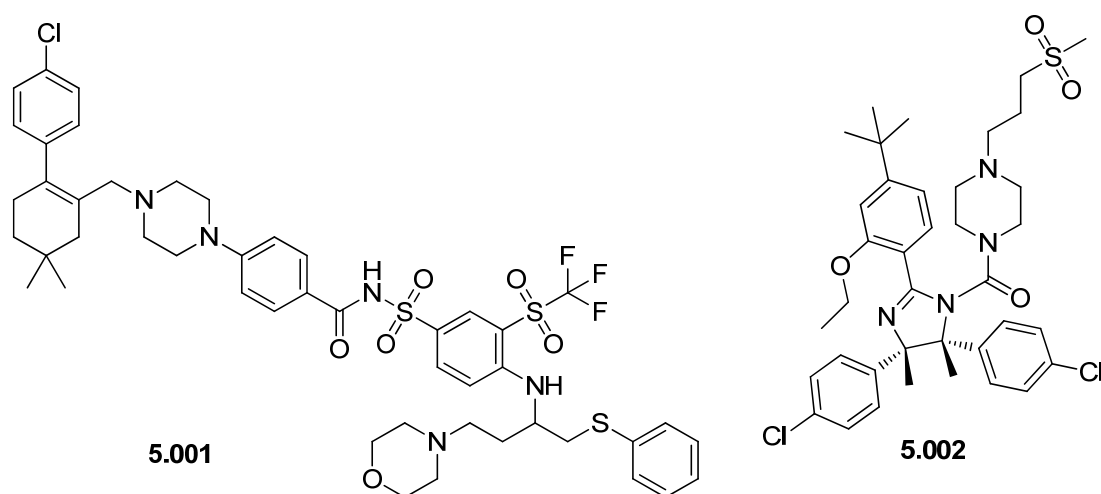


Figure 50: Examples of PPI inhibitors.

While many PPI interactions require large molecules that cover a large area of protein surface some PPIs can occur *via* a more typically druggable cleft or pocket in a protein surface. Bromodomains are one example of a PPI binding partner that has a deep binding pocket and therefore can be inhibited with “Rule-of-Five” compliant molecules as seen for characteristic orally active compounds.¹⁹⁰

5.2 Introduction to bromodomains

Bromodomains are reader domains in the read-write-erase model of the histone code (Fig. 5, p 20)¹⁹⁴ and were first identified in the drosophila gene *brahma*, hence their name.¹⁹⁵ They have been found to bind to acetylated lysines on histone tails.¹⁹⁶ Bromodomains are considerably different to the JmjC domains previously discussed as they interact with acetylated lysines rather than methylated lysines. Another difference is that bromodomains have no enzymatic function and are involved in binding protein-protein interactions, rather than adding or removing epigenetic marks.

Bromodomains all have the same tertiary structure of a four α -helix bundle with a left-handed twist, which is unusual as most four α -helix bundles have a right-handed twist.¹⁹⁶ These domains contain approximately 110 amino acid residues (Fig. 51). The α -helices are highly conserved between individual bromodomains; the majority of the differences

between bromodomains are found in the ZA and BC loops, which link the helices together.¹⁹⁷

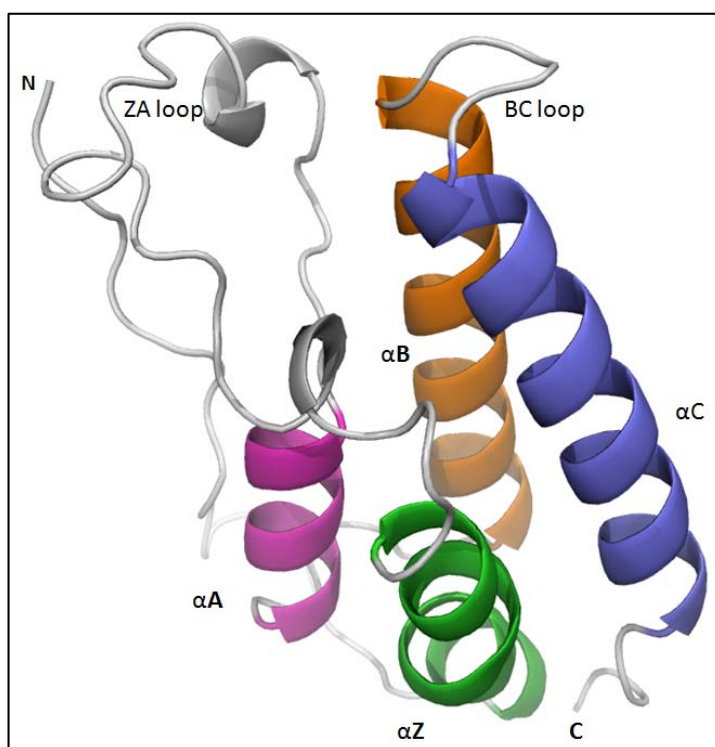


Figure 54: X-ray crystal structure of Brd4 BD1, a left-handed four α -helix bundle, resolution = 1.5 Å.

Bromodomains contain a long intervening loop between the Z and A helices with a defined conformation, termed the ZA loop, which packs against the shorter loop between helices B and C, termed the BC loop, to form a hydrophobic binding pocket.¹⁹⁶ It is within the pocket that acetylated lysines bind and form protein-protein interactions between the histone tail and the bromodomain containing protein (Fig. 52).

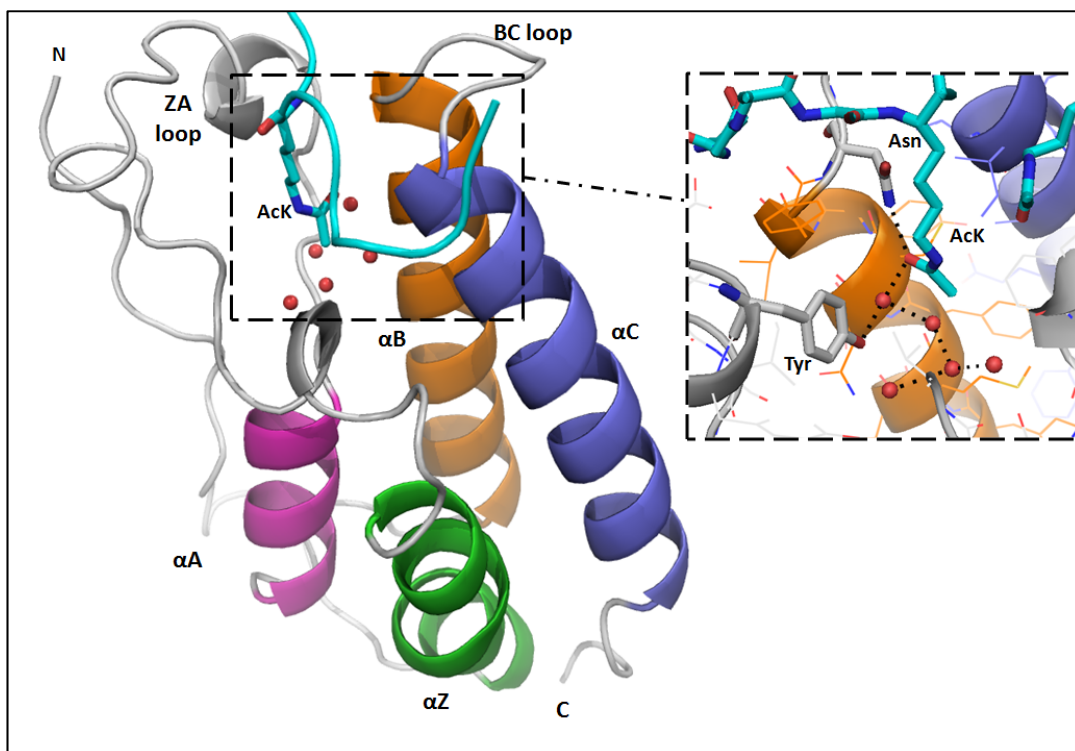


Figure 52: X-ray crystal structure demonstrating the interaction between a histone peptide (cyan) and Brd4 BD1, resolution = 1.4 Å.

The acetylated lysine from the histone peptide makes an H-bond to an asparagine and a conserved structural water, which are seen in most crystal structures of bromodomains with an acetylated lysine bound.^{198,199} The waters, shown as red spheres (Fig. 52), are highly ordered and the interaction with a conserved Tyr is believed to help in the conservation of the water molecules.¹⁹⁷

Due to the high degree of homology between bromodomains, a phylogenetic tree can be drawn showing the degree of similarity with other bromodomains. The higher the sequence similarity the individual bromodomains have, the closer they are drawn to a common branch point (Fig. 53). The groups of bromodomains that have similar sequence homology to each other can be grouped into different families which are shown through the use of colour (Fig. 53).

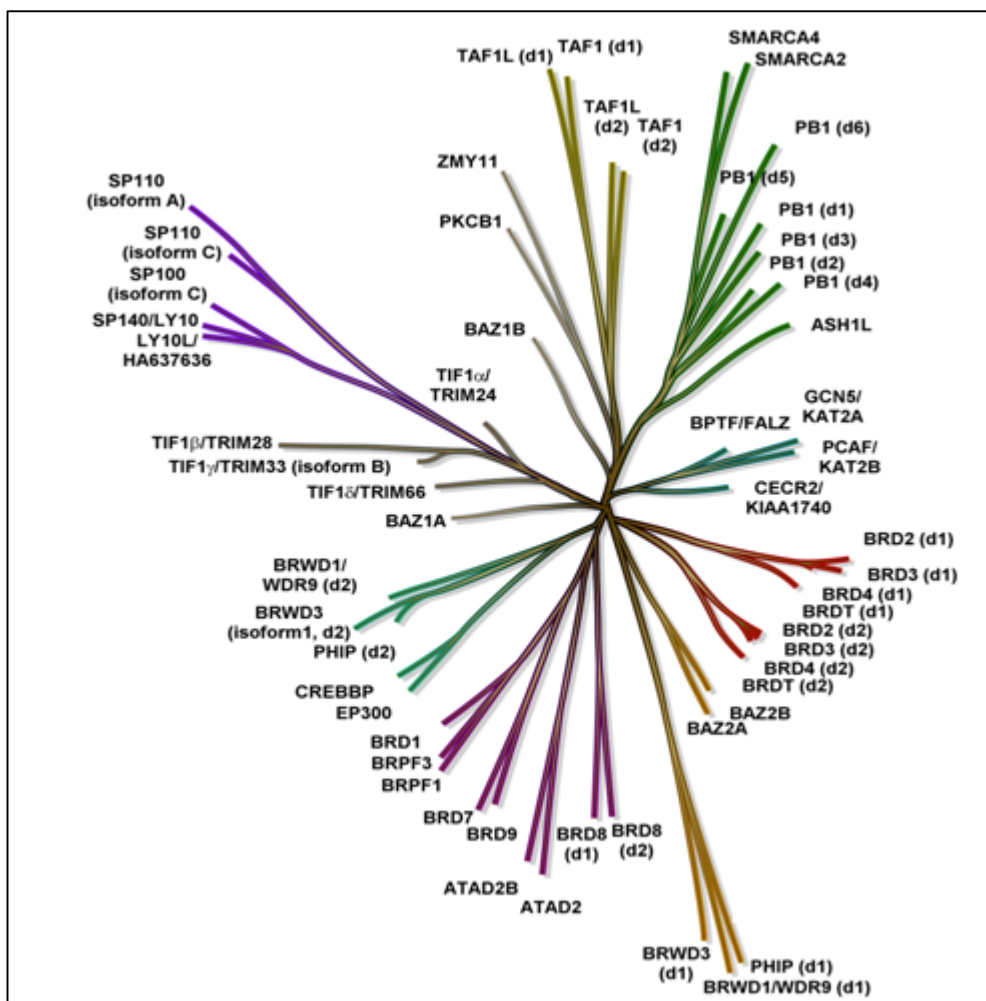


Figure 53: A phylogenetic tree of bromodomains based on sequence homology.²⁰⁰

There is disagreement in the literature on the number of bromodomain-containing proteins (BCPs) and the number of individual bromodomains. The accepted numbers vary between 41 and 46 BCPs and 56 to 61 individual bromodomains.^{201,14,202} The discrepancy between the number of bromodomains originates due to of the inclusion of bromodomain-like proteins which have low sequence homology with bromodomains. This is postulated to arise from evolution from another amino-acid sequence starting point to provide the same acetyl-lysine binding function, the translocation or insertion from the gene sequence of existing bromodomains, or a mixture of the aforementioned reasons.²⁰³ Some BCPs have more than one bromodomain, for example the BET family of bromodomains, where each protein contains two acetylated lysine binding sites,²⁰⁴ and polybromodomain-1 (PB1), which contains six bromodomains.²⁰⁵

While the lipophilic bromodomain fold is highly conserved in bromodomain containing proteins, the surface around the acetylated lysine binding site can be highly diverse. The surfaces can range from strongly positively to strongly negatively charged.²⁰⁶ Presumably the significant differences of the surfaces surrounding the bromodomain folds allows for specific binding to individual acetylated lysines on histone tails. The specific binding occurs because the amino acid residues surrounding the acetylated lysine complement the surface of the bromodomain containing protein. BCPs do not solely bind to histone proteins, PCAF is known to bind to the acetylated Tat protein of the human immunodeficiency virus.²⁰⁷

There are often multiple domains for binding to other proteins in addition to the bromodomain and BCPs usually exist as part of a chromatin modifying complex of proteins (Fig. 54).²⁰⁸

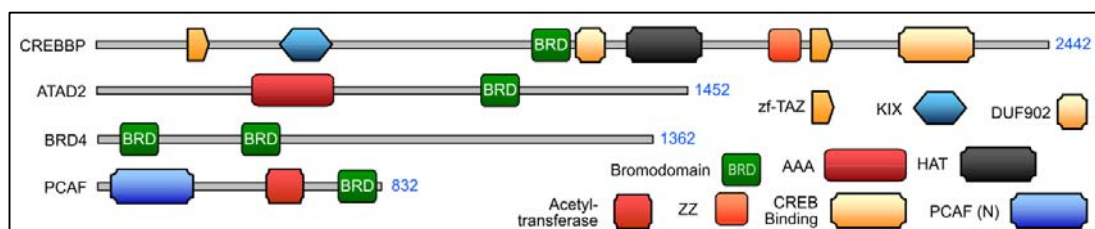


Figure 54: Schematics of representative BCPs showing a variety of domains contained within the proteins. Adapted.²⁰⁶

CREBBP has the largest number of domains shown in Fig. 54 having three zinc fingers (2 × zf-TAZ and 1 × ZZ), two other protein binding domains (KIX and CREB binding), domain of unknown function (DUF902), a HAT domain as well as a bromodomain.^{39,206} ATAD2 is simpler with an ATPase domain (AAA) and a bromodomain. Brd4 has two bromodomains in the protein. PCAF has an acetyl transferase, a EP300/CREBBP binding domain [PCAF (N)] and a bromodomain.

Currently, there are no marketed drugs that target bromodomains. However, as readers of acetylated lysines, bromodomains show potential as therapeutic targets as BCPs mediate the recruitment of proteins to macromolecular complexes. BCPs and their associated complexes can have multiple functions, such as acting as transcription factors, controlling the transcription of mRNA, or histone acetyl transferases that acetylate lysines on histone tails.²⁰⁹

For example, Brd4 uses the bromodomains present to bind to chromatin through H3K9, H3K14, H4K5 and H4K12,²¹⁰ although not all at the same time. Brd4 can also bind to positive transcription elongation factor (P-TEFb), which is involved in the transcription of DNA,²¹¹ *via* another domain present in Brd4, the P-TEFb-interacting domain (PID).²¹² Therefore, if the binding of Brd4 to chromatin is disrupted then the downstream production of associated proteins may also be altered, potentially leading to a therapeutic outcome.

5.2.1 Links between bromodomains and disease

Numerous bromodomain containing proteins have been linked to diseases and can be classified broadly into different therapeutic areas. Many BCPs are found to be overexpressed in cancerous growths compared to those in normal tissue,²¹³ which suggests that BCPs play an important role in maintaining genome integrity and suppressing the formation of tumours.¹⁹⁷ Further evidence to support the role of BCPs in cancer has come from RNA interference studies. A reduction in the expression of EP300 and CREBBP has been shown to inhibit tumour growth in prostate cancer cell lines.²¹⁴ Similar RNA interference experiments with other BCPs, for example BPTF, EP300 and SMARCA4, have shown similar results in different cancers.¹⁹⁷

There are links between BCPs and neurological diseases such as schizophrenia, epilepsy and mental retardation.¹⁹⁷ When these genetic links have been deeply studied, in all cases the diseases result from reduced or absent gene function, which probably reflects key roles for these proteins in neurological development. An example of BCPs affecting neurological development is in Rubinstein-Taybi syndrome (RTS). RTS affects approximately 1 in 100,000 newborns worldwide and is characterised by broad thumbs and toes, mental and physical retardation. Mutations in two BCPs, CREBBP and EP300, have been linked to approximately half of RTS cases.²¹⁵ BCPs are not limited to roles in developmental neurological function as reduced levels of TAF1 correlate with X-linked dystonia parkinsonism an adult onset movement disorder.²¹⁶

Metabolic diseases have been linked to BCPs through the identification of disease-associated single nucleotide polymorphisms. BAZ1B has been linked to type 2 diabetes and serum lipid levels, SMARCA4 has links with total plasma cholesterol, and Brd2 with type 2 diabetes.^{217 218,219} BET family (Brd2, Brd3, Brd4 and BrdT) inhibitor I-BET762 (**3.010**, Fig 56, p 121) was identified as a compound that increases apolipoprotein A1 (ApoA1) in a cellular

phenotypic assay (Graph 5, p 127).²²⁰ ApoA1 helps to clear fats from white blood cells within arteries and has a role in lipid metabolism.

Autoimmune and inflammatory diseases have links with BCPs. For example, SP140 and SP110 have been shown to be upregulated by the inflammatory cytokine IFN- γ .²²¹ CREBBP and EP300 are associated with immune function as individuals with systemic lupus erythematosus (SLE) and ankylosing spondylitis have reduced expression of these BCPs, respectively.^{222,223} Several BCPs including GCN5, PCAF, CREBBP and SMARCA4 are involved in the production of type 1 IFN, which drives autoimmunity in SLE.²²⁴ Brd2 has been associated with rheumatoid arthritis.²²⁵

However, the strongest link between BCPs and human disease is surrounding the BET family of bromodomains.

5.2.2 Small molecule inhibitors of BET bromodomains

The BET family of bromodomains consists of eight separate bromodomains distributed between four proteins: Brd2, Brd3, Brd4 and BrdT.⁴⁵ Each protein contains two bromodomains with the bromodomain nearest the *N*-terminal of the amino acid sequence termed BD1 and the bromodomain nearest the *C*-terminal of the amino acid sequence termed BD2 (Fig. 55).

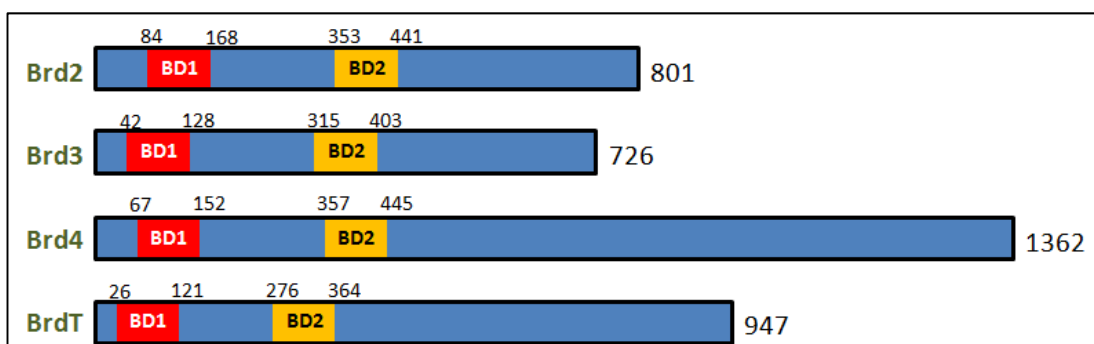


Figure 55: Schematic of the bromodomains in the BET family.²⁰¹

The BD1 domains within the BET family of bromodomains are highly conserved with few changes in the ZA and BC loops which make up the bromodomains.⁴⁵ The BD2 domains are similarly conserved between Brd2, Brd3, Brd4 and BrdT. However, there are differences between the BD1 and BD2 domains which can be exploited to identify domain selective molecules.²²⁶

Evidence for inhibiting bromodomains with small molecules to modify disease has been disclosed around (+)-JQ1 (**5.003**), I-BET762 (**3.010**) and RVX-208 (**5.004**) (Fig. 56).

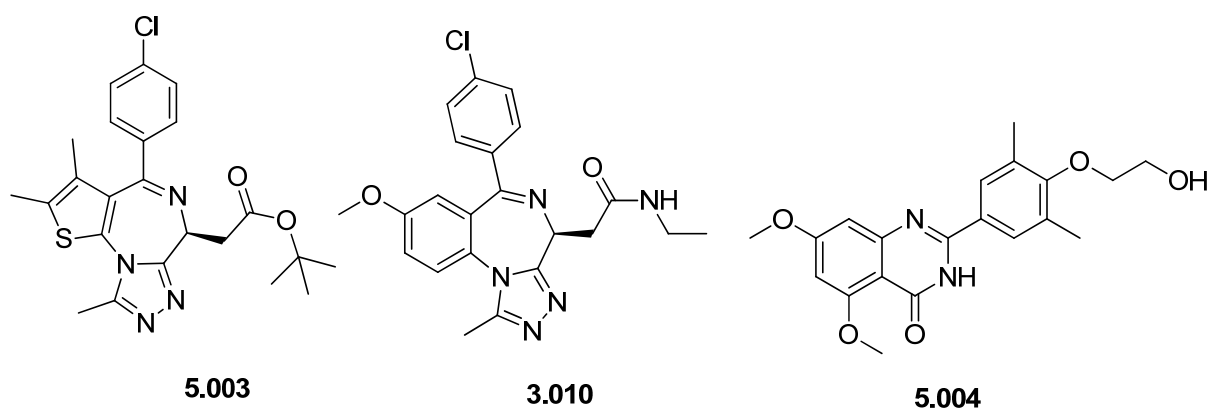
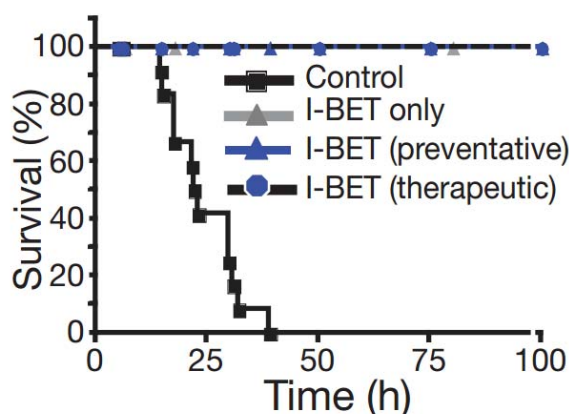


Figure 56: Inhibitors of the BET family of bromodomains.

An observation from Mitsubishi Pharmaceuticals that thienodiazepines bound to Brd4 led to the discovery of (+)-JQ1 (**5.003**).^{227,201} (+)-JQ1 (**5.003**) is a pan-inhibitor of the BET family of bromodomains, meaning that it inhibits every bromodomain of the BET family. (+)-JQ1 (**5.003**) has been shown to induce differentiation and arrests growth in nuclear protein in testes midline carcinoma (NMC).²⁰¹ (+)-JQ1 (**5.003**) has also been found to behave as an effective male contraceptive in mice, which is thought to be driven *via* inhibition of the BrdT bromodomain.²²⁸

Other biological effects have also been identified when inhibiting the BET family of bromodomains. Mice treated with I-BET762 (**3.010**) survive after being given a lethal dose of LPS, a disease model of sepsis (Graph 4).²²⁹



Graph 4: Dosing with I-BET762 enables mice to survive a lethal dose of LPS. Reprinted with permission from Macmillan Publishers Ltd, copyright 2010.²²⁹

RVX-208²³⁰ (**5.004**) is being tested for the treatment of atherosclerotic cardiovascular disease²³¹ and more recently for Alzheimer's disease and type 2 diabetes.^{232,233} I-BET762 (**3.010**) is being investigated for the treatment of NMC and clinical trials are being extended into other cancers.²³⁴ Further BET family inhibitors currently undergoing clinical trials include OncoEthix OTX015 (**5.005**), Constellation Pharmaceuticals CPI-0610 and Tensha Therapeutics TEN-010, which are investigating treatment for different cancers.²³³ The structure of OTX015 (**5.005**) is known and has a thienodiazepine core (Fig. 57), while the structures of TEN-010 and CPI-0610 are not currently in the public domain.

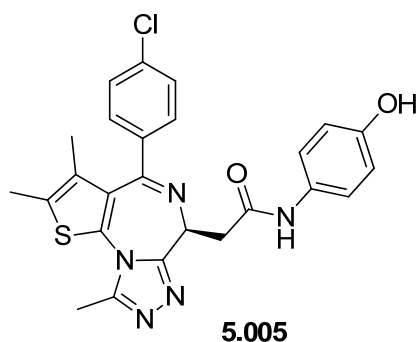
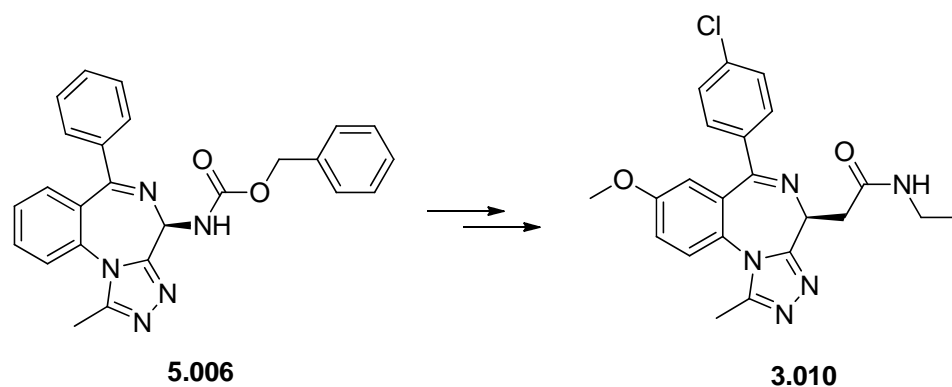


Figure 57: The structure of OTX015 (**5.005**).

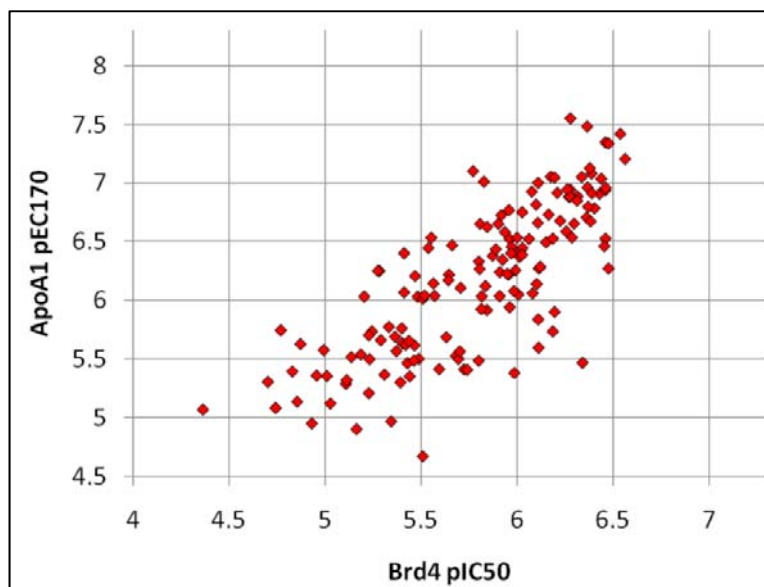
The discovery of I-BET762 (**3.010**) is an excellent case study for the discovery of a probe molecule as defined by Bunnage *et. al.* (p 24).⁴² The programme aimed to find a molecule that enhanced expression of ApoA1 with the hypothesis that increased levels of ApoA1 would prevent atherosclerosis.²³⁵ However, the mechanism of action for enhanced expression of ApoA1 was unknown. The programme, therefore, used a cell reporter assay where the DNA sequence responsible for coding for ApoA1 was replaced by the gene for the luminescent firefly luciferase.⁴⁵ This gene sequence was transfected into a suitable cell line and these cells could be used in a dose response assay where the higher the effect of the compound, the greater the luminescence from the cells. This assay helped to identify molecules which met two of the probe criteria; the compounds had to be cell penetrant and show a relevant phenotype for the assay to produce data. GW841819X (**5.006**) was found to be a potent inducer of the ApoA1 reporter gene and was optimised to I-BET762 (**3.010**) (Scheme 38).



Scheme 38: **5.006** was optimised for ApoA1 upregulation to I-BET762 (**3.010**).

An inactive control, the enantiomer of I-BET762 (**3.010**), **3.011** (Fig. 11, p 26), was identified that could be used to identify non-specific activity. However, it was unknown if the chemical series containing **3.010** was selective for one particular target or even what that target was.⁴⁵

Chemoproteomic experiments were performed, using **3.010** covalently attached to a solid support, to identify the target. The matrix was exposed to cell lysate for the same cell types as used in the luciferase assay and removed. Using LC/MS/MS, the BCP proteins Brd2, Brd3 and Brd4, members of the BET family of bromodomains, were identified as the targets for **3.010**.⁴⁵ This confirmed target engagement with the BET family. Further pharmacological profiling of I-BET762 (**3.010**) demonstrated that it had negligible activity outside of binding to the BET family, thus confirming functional pharmacology. Finally, extensive SAR analyses showed that inhibitory BET activity strongly correlated with cell potency for ApoA1 upregulation indicating a target-phenotype association in cells (Graph 5). Interestingly, interfering RNA knockdown experiments showed that only inhibiting Brd4 from the BET family was responsible for ApoA1 upregulation.⁴⁵



Graph 5: Correlation between Brd4 binding and upregulation of ApoA1.⁴⁵

5.1.3 Structural features of BET inhibitors

A common structural theme of BET inhibitors is the presence of an acetyl mimetic. It would appear that this is a necessary motif for ligands to bind to bromodomains and there are multiple functionalities which can mimic the acetyl group. The acetyl mimetics all contain an H-bond acceptor (red) with a methyl group (blue) in close proximity. The H-bond acceptor makes a hydrogen bond with a conserved asparagine and a conserved water in the binding pocket. The water hydrogen bonds to a conserved tyrosine that helps to retain the water and the methyl group is within a lipophilic pocket (Fig. 58).

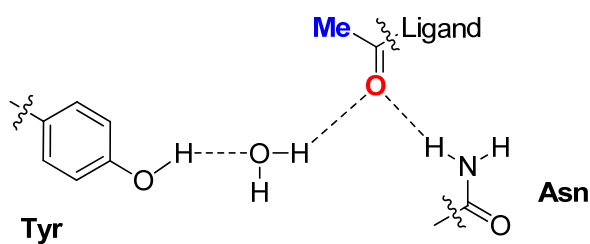
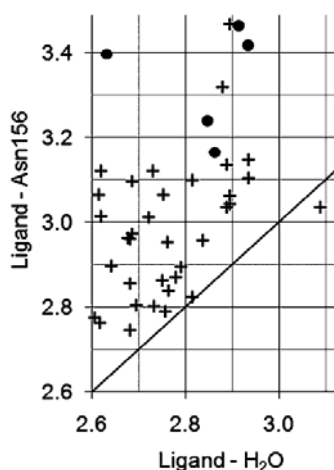


Figure 58: Binding of the H-bond acceptor to the conserved asparagine and water that is retained by a conserved tyrosine.

Analysis of X-ray crystal structures of ligands in Brd2 shows in almost all cases the hydrogen bond to the water is shorter than the hydrogen bond to the asparagine (Graph 6). This suggests the hydrogen bond to the bridging water is stronger than the hydrogen bond to the asparagine.²⁰⁰



Graph 6: Distance between the ligand and asparagine side chain nitrogen and the bridging water nitrogen for 40 Brd2 ligands. Symbols show the heavy atoms closest to the asparagine (Crosses = N or O, Circles = C).²⁰⁰

Research in this rapidly expanding area is continuing to identify inhibitors of the BET family due to the profound biological effects discussed in the previous section. Identifying a chemically diverse range of compounds that can inhibit the BET family of bromodomains allows a deep, unbiased probing of the biological systems affected by the BET family further aided by the discovery of more selective compounds. One example of a BD2 selective molecule is RVX-208 (**5.004**) which is reported to bind 20-fold selectively to BD2 of Brd2 and Brd3 compared to BD1 of these proteins.²³⁶ Conversely, a BD1 selective molecule is MS436 (**5.007**), which is reportedly at least ten-fold selective for Brd4 BD1 compared to Brd4 BD2 (Fig. 59, p 129).²³⁷ The hydrogen bond acceptors are shown in red and the methyl mimetics shown in blue.

Many of the compounds in Fig. 59 were discovered through fragment screening efforts. Compounds with molecular weights of < 250 Da were successfully soaked into apo Brd2 BD1 bromodomains and X-ray crystal structures obtained.²⁰⁰ Tetrahydroquinoline containing **5.008** and dihydroquinazolinone example **5.009** were identified directly using this method. Ketone containing **5.009** binds to a wide variety of bromodomains.²⁰⁰ The core of dihydroquinazolinone analogue PFI-1 (**5.010**) was identified in the same screen, although the molecule itself was synthesised by Fish *et al.*²³⁸ Isoxazoles as acetyl lysine mimetics were originally identified through X-ray crystal structures and **5.011** has recently been disclosed by Brennan *et al.*²³⁹ RVX-208 (**5.004**) is a derivative of the plant polyphenol resveratrol that can increase plasma levels of ApoA1. However, the mechanism was initially

unknown. Similarity to the effect of increased plasma levels of ApoA1 when dosing (+)-JQ1 (**5.003**) and I-BET762 (**3.010**) led to the investigation and identification of RVX-208 (**5.004**) as a BET inhibitor.²⁴² Interestingly, RVX-208 (**5.004**) and related phenol analogue **5.012** have different binding modes in Brd4 BD2 despite the overall similarity of structures. Removal of the hydroxyl-ethyl group causes the phenol to become the hydrogen bond acceptor motif.²⁴² The phenol is common to diazo containing **5.007** which was derived from an inhibitor of the CREBBP bromodomain (Fig. 61, p 132).²³⁷ Recent patent literature has identified compounds such as pyridinone containing **5.013** from Abbvie and triazole analogue **5.014** from Constellation Pharmaceuticals.²⁴⁰

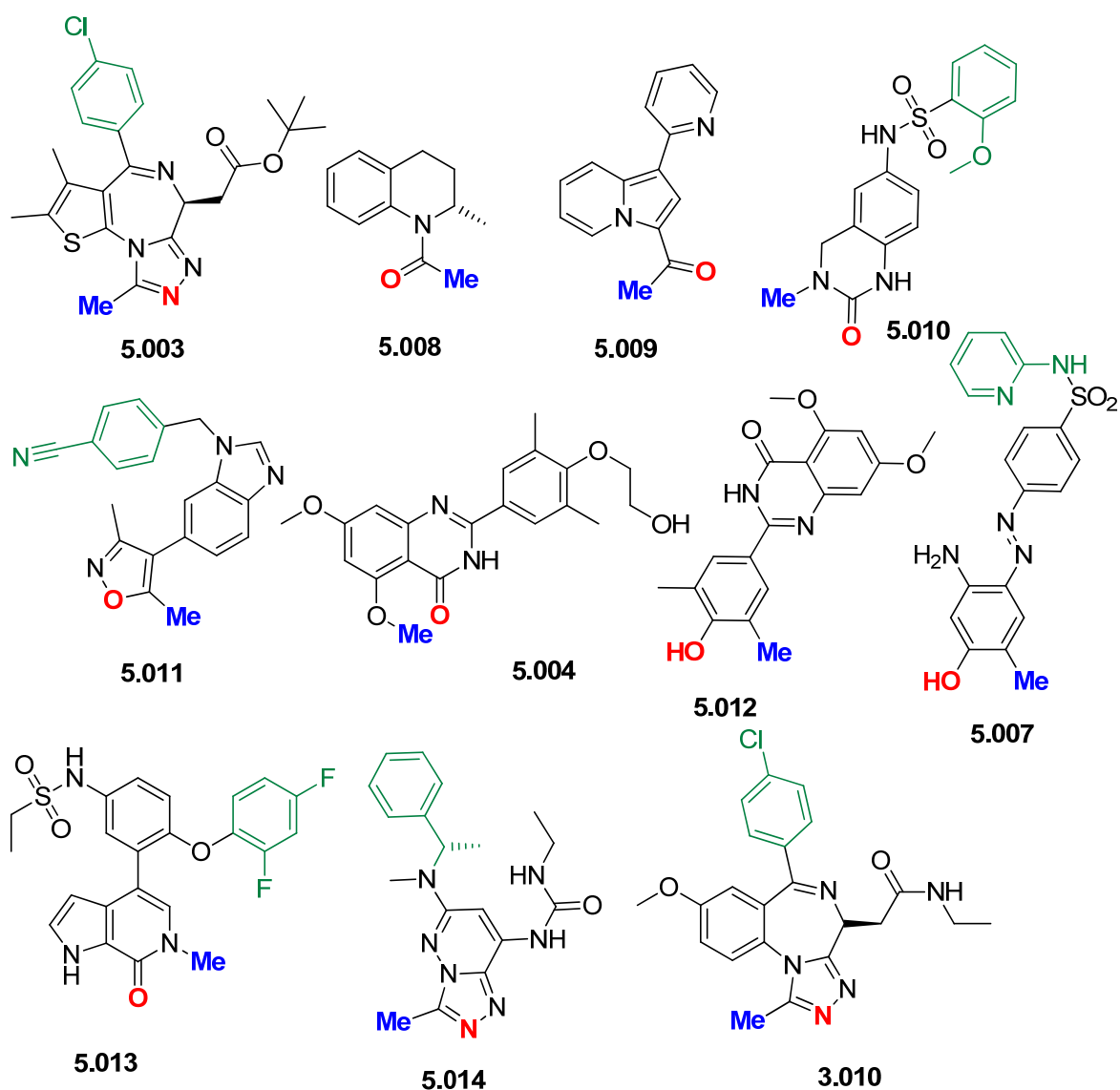


Figure 59: Examples of literature BET family inhibitors.^{241,242,240} Acetyl mimetics are shown with the methyl mimic highlighted in blue and the hydrogen bond acceptor highlighted in red. WPF shelf groups are highlighted in green.

Another feature common to many of the BET inhibitors (Fig. 59) is the presence of a group which lies on a lipophilic region of the BET protein known as the WPF shelf. The lipophilic region consists of a tryptophan (W), a proline (P) and a phenylalanine (F), thereby giving the region its name. BET inhibitors that occupy the WPF shelf usually see a large increase in binding to the bromodomain compared to those which do not.²³⁸ For example the X-ray crystal structure of I-BET762 (**3.010**) in Brd4 BD1 shows excellent shape complementarity with the bromodomain and places the 4-chlorophenyl group on the lipophilic WPF shelf (Fig. 60).

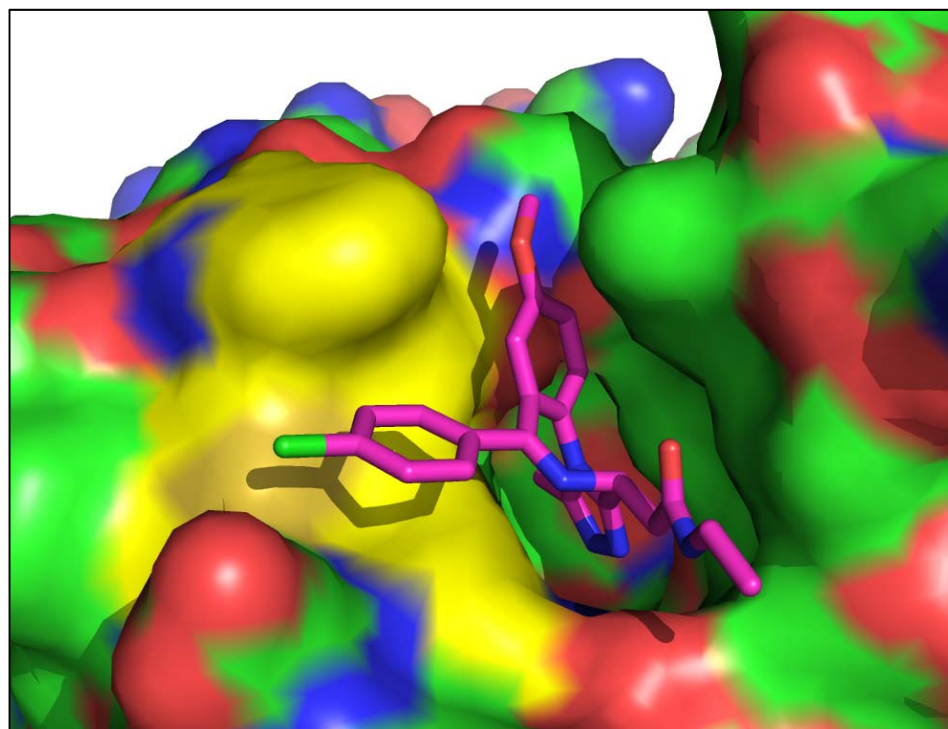


Figure 60: X-ray crystal structure of I-BET762 (**3.010**) in Brd4 BD1. The WPF shelf is highlighted in yellow, resolution = 1.6 Å.

5.3 Inhibiting non-BET family bromodomains

As inhibiting the BET family of bromodomains was found to have significant biological effects as evidenced by BET inhibitors currently undergoing clinical trials (p 121),²³³ it was postulated that inhibiting other non-BET family bromodomains could also exhibit a phenotypic response. A number of compounds have been identified as inhibitors of bromodomains other than BET (Fig. 61, p 132).

NP1 (**5.015**) was one of the first identified bromodomain inhibitors and in 2005 was found to be an inhibitor for PCAF with a reported IC_{50} of 1.6 μM .²⁴³ NP1 (**5.015**) is unusual as it does not bind in the same fashion as the compounds in Fig. 59 (p 129) as it does not form an H-bond with the conserved asparagine or water in the acetyl lysine binding site. CREBBP inhibitor MS7972 (**5.016**) also does not H-bond to the asparagine or the conserved water. However, it does show complete inhibition of binding between CREBBP and acetylated p53 at 50 μM .²⁴⁴ The binding modes of both **5.015** and **5.016** were derived *via* NMR studies.

I-CBP112 (**5.017**) returns to the conventional binding mode of an acetyl mimetic, where the oxygen of the amide is the H-bond acceptor. However, where the BET inhibitors (Fig. 59, p 129) had methyl groups I-CBP112 (**5.017**) has the larger ethyl group present.²⁴⁵ This larger group may explain why I-CBP112 (**5.017**) is selective for CREBBP and EP300 compared to the BET family of bromodomains. The reported potencies for I-CBP112 (**5.017**) is 0.15 μM at CREBBP and 0.63 μM at EP300. SGC-CBP30 (**5.018**) is known to bind to CREBBP with a K_d of 0.02 μM and EP300 with a K_d of 0.04 μM .²⁴⁶ I-CBP112 (**5.017**) has a dimethyl isoxazole group, which is present in examples of BET inhibitors (Fig. 59). SGC-CBP30 (**5.018**) has been found to be forty-fold selective for CREBBP over Brd4 BD1. Ischemin (**5.019**) is known to bind in the acetyl lysine binding site of CREBBP with a K_d of 19 μM as well as in PCAF and BAZ1B with K_d values of 40 μM .²⁴⁷ GSK2801 (**5.020**) is structurally related to **5.009** (Fig. 59) and is an inhibitor for the BAZ2A and BAZ2B bromodomains with K_d values of 0.26 and 0.14, respectively.²⁴⁸ Triazole containing **5.021** is tenfold selective over Brd4 BD1 for Brd9, CECR2 and CREBBP, where it is approximately 1 μM at those proteins.²⁴⁹ Structurally related to **5.021** is bromosporine (**5.022**), which binds to a wide range of bromodomains. As well as the BET family of bromodomains, bromosporine (**5.022**) binds to Brd7, Brd9, CECR2, EP300, PCAF, SMARCA4 and TAF making it a broad spectrum inhibitor of bromodomains.²⁵⁰

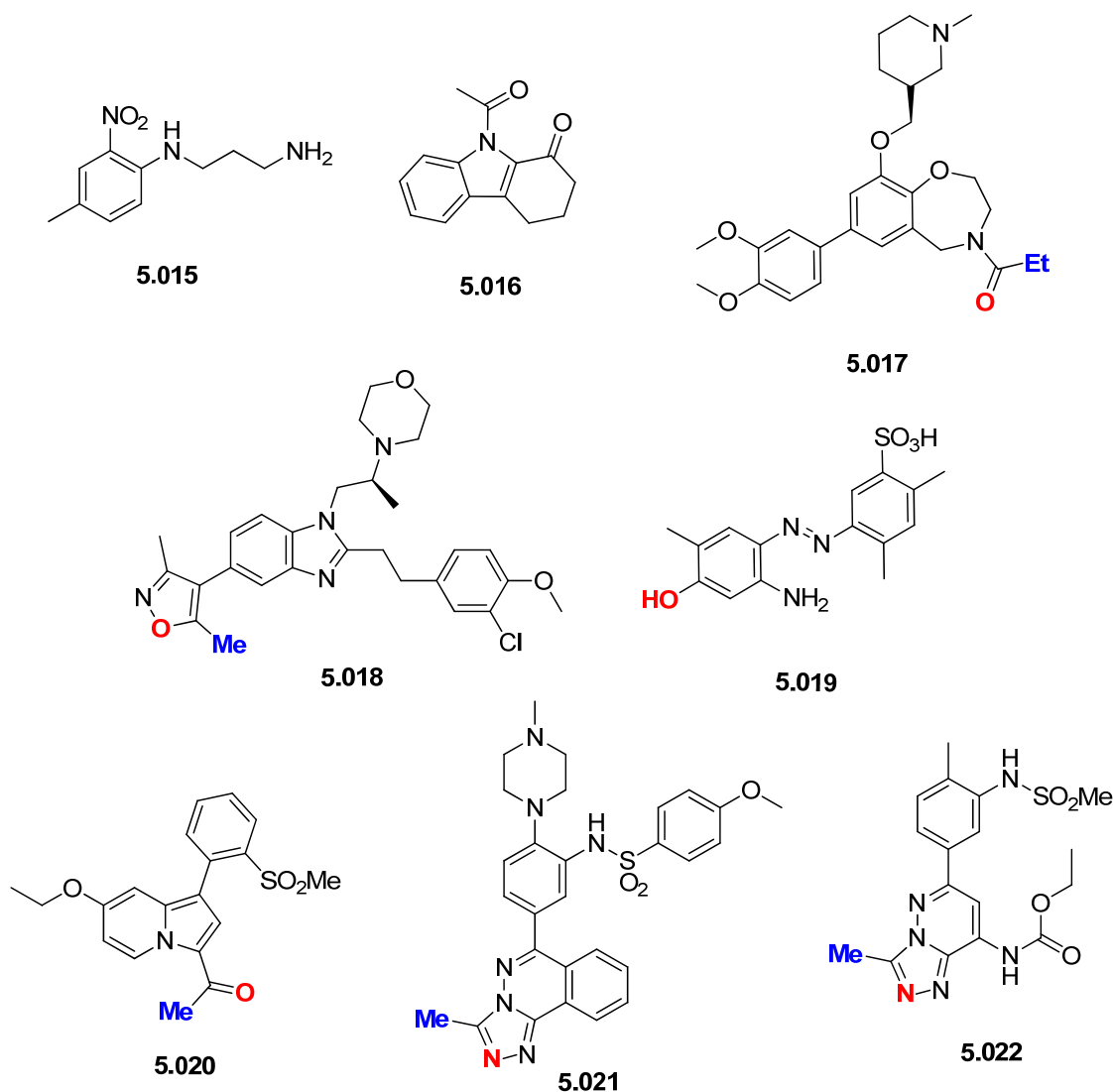


Figure 61: Known non-BET bromodomain inhibitors. The hydrogen bond acceptors are highlighted in red and the methyl mimetics highlighted in blue.

The compounds in Fig. 61 showed it was possible to inhibit bromodomains outside of the BET family. However, to date with the exception of the BET family of bromodomains, the biology of inhibiting most bromodomains has not been extensively studied. Given the profound biological impact of inhibiting the BET family of bromodomains, it was interesting to discover if inhibiting other bromodomains could have a similar effect. Therefore, a programme of work within our laboratories was begun to identify chemical probes for non-BET bromodomains to understand the consequences of selective inhibition. One of the bromodomain containing proteins of interest was PCAF.²⁵¹

5.3.1 Introduction to PCAF

PCAF or p300/CREBBP-associated factor, also known as KAT2B, is a bromodomain containing protein. PCAF, *in vivo*, exists in a complex of more than 20 polypeptides,²⁵² some of which have been identified and studied such as p300 and CBP.²⁵¹ The PCAF protein itself contains 832 amino acid residues²⁵¹ and has several domains such as an enzymatic histone acetyl transferase (HAT), a bromodomain, an E3 ligase ubiquitination domain²⁵³ and a PCAF homology domain that binds to p300 and CREBBP (Fig. 62).²⁵⁴



Figure 62: Schematic of the domains in PCAF. The PCAF homology domain where EP300 and CREBBP bind is shown in blue and includes the E3 ligase ubiquitination domain shown in grey. Adapted with permission from Macmillan Publishers Ltd, copyright 2007.²⁵⁵

The E3 ligase ubiquitination domain is known to append ubiquitin to the oncoproteins Hdm2 and Gli1, which causes Hdm2 and Gli1 to be destroyed within the cell.^{253,255} The removal of the E3 domain or knockdown of PCAF with interfering RNA causes an increase in the quantity of Hdm2 and Gli1 within the cells studied.

The HAT domain of PCAF has been extensively studied and PCAF is actually primarily known as an acetyl transferase. PCAF does not only acetylate histone lysines, it is also known to acetylate the tumour suppressor protein p53²⁵⁶ in addition to having a strong site preference for histone 3 lysine 14 (H3K14).²⁵⁷ Inhibitors of the PCAF HAT domain have shown growth inhibition in a panel of human colon and ovarian cancers.²⁵⁸ Additionally, PCAF HAT domain inhibitors have been shown to alter the expression of several genes. The acetyl transferase domain is thought to be important in the regulation of muscle cell differentiation and developmental survival.²⁵⁶

It is known that PCAF is a co-activator of the IFN regulatory factor, which transcribes interferon mRNA, and deletion of the bromodomain in PCAF prevents interaction of PCAF with IFN regulatory factors.²⁵⁹ Thus, antagonising the PCAF bromodomain could attenuate the production of the IFN family of cytokines. The PCAF bromodomain is known to bind to H4K8 and H3K15.¹⁹⁶ This may aid regulation of DNA transcription as it is known that PCAF binds to the DNA binding domain of nuclear receptors²⁶⁰ which act as transcription factors.

The closest homologue to PCAF is GCN5 which shares 73% homology with PCAF over the entire protein.²⁶¹ However, in the ZA and BC loops, which pack against each other to form the bromodomain, the sequence homology is increased to 77%.²⁶² Additionally, only one of the changes in the sequence is within the acetyl lysine binding site of the bromodomain which may mean that finding selectivity with a chemical probe over GCN5 may be challenging. Currently the effects of dual PCAF and GCN5 bromodomain inhibition are unknown so there is the possibility that inhibiting both bromodomains is beneficial and may provide a synergistic effect. Most known BET inhibitors inhibit eight bromodomains concurrently,⁴⁵ which may explain the diverse and potent biological effects these molecules show. However, the question if dual inhibition of the bromodomains of GCN5 and PCAF is desirable can only be answered if a selective inhibitor of either bromodomain can be identified.

Therefore, with evidence that the PCAF bromodomain may well regulate the expression of interferon²⁵⁹ and that PCAF is highly expressed in immune cells,^{263,264} the PCAF bromodomain became an interesting target. Currently, as there are no compounds that selectively inhibit the PCAF bromodomain, to validate the target and determine if PCAF is a valid target for drug discovery a probe compound must be identified.

5.3.2 Screening cascade

To identify a probe, certain criteria needed to be met in order to have a suitable tool compound and hence a screening cascade was designed (Fig. 63).

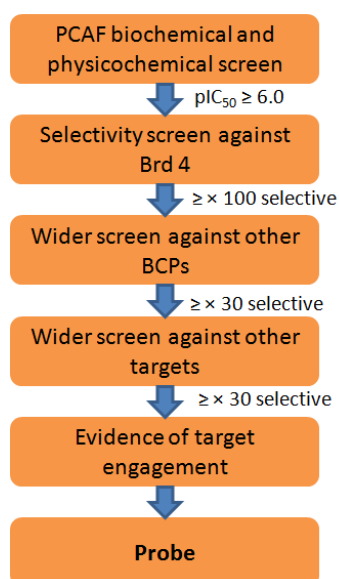


Figure 63: Screening cascade for PCAF bromodomain inhibitors.

The criteria for a probe molecule for the PCAF bromodomain were largely similar to those being used for the identification of a probe molecule for the JmjC domain of the JmjD2 family (p 38). To progress to the next level of the screening cascade the test compounds had to meet certain criteria. Initially, the compounds have to have acceptable physicochemical properties with a LogP of between 1 – 3 and a molecular weight of < 400 Da as this is considered to be a good range to obtain cellular penetration.¹⁰⁰ While increasing the lipophilicity of the compounds could aid cellular penetration, it may cause wider issues as compounds with high lipophilicity have been linked with promiscuity, poor PK and toxicology issues.¹⁰¹ These properties can be calculated prior to synthesis of the compound. However, the potency of the molecule cannot be calculated and the molecule must be synthesised and screened in the PCAF FP assay. In this case a pIC₅₀ value of ≥ 6.0 was thought to be sufficient for progression to the next level of the screening cascade along with AMP ≥ 50 nm s⁻¹ and aqueous solubility of ≥ 50 µg mL⁻¹.

The 100-fold selectivity over BET is necessary to have a window from any potential biological activity arising from antagonising the BET proteins. As mentioned previously, antagonising the BET family of bromodomains has profound biological effects (p 121) and even low levels of BET inhibition show phenotypic changes. As the bromodomains of Brd2, Brd3, Brd4 and BrdT are very similar, only the data for Brd4 will be routinely reported as it is representative for the other members of the BET family.

Taking lessons from the JmjD2 probe discovery work, where significant off-target activity was seen for the KDM5 family of enzymes a wider range of BCP will be assayed against for off-target binding. Initially using assays available in our laboratories and subsequently using external collaborators. 30-fold selectivity over other bromodomains was to ensure any biological activity observed is being caused by antagonising PCAF rather than any other bromodomain. Ideally any probe compounds identified would also be selective for GCN5 although this may not be possible and the selectivity criteria for GCN5 was relaxed. The compounds should be tested against a wide range of non-related drug and liability targets to ensure that any phenotype seen is not due to off-target activity. For any compound to inhibit PCAF, the antagonist must get to the bromodomain binding site, which is within the cell nucleus so cellular penetration is vital. Beyond this, in order to observe a phenotype the probe compound must engage the endogenous PCAF protein within the nucleus. At the

outset of this work a target engagement assay had not been developed. Generating a target engagement assay was also a key aim for the project.

5.3.3 Rationale for achieving BET selectivity

As BET selectivity was an essential goal of the programme, an analysis of the X-ray crystal structures of apo PCAF and Brd4 BD1 was carried out. The structures of the BET family of bromodomains are highly conserved, so comparison with only one of the domains is shown below (Fig. 64). From the available structural information, it was thought to be possible to get the necessary selectivity over the BET family of bromodomains due to fundamental differences in the bromodomain structure between PCAF and BET. The major structural change between PCAF and BET is brought about by a tyrosine present in PCAF, Tyr809, which blocks access to the WPF shelf in the BET family of bromodomains.²²⁹ As stated above (p 131), many BET inhibitors derive much of their potency from interacting with the WPF lipophilic region and, since access to this region is precluded in PCAF, many BET inhibitors will be unable to bind to PCAF. Additionally, there is the potential for a positive face to face aromatic interaction between Tyr809 in PCAF if the PCAF ligand contains an aromatic ring that can overlap, which is not possible in BET. This could provide a positive interaction between the ligand and the bromodomain. Comparison of the X-ray crystal structures of PCAF and BET demonstrate the inaccessibility of the WPF shelf in PCAF (Fig. 64).²²⁹

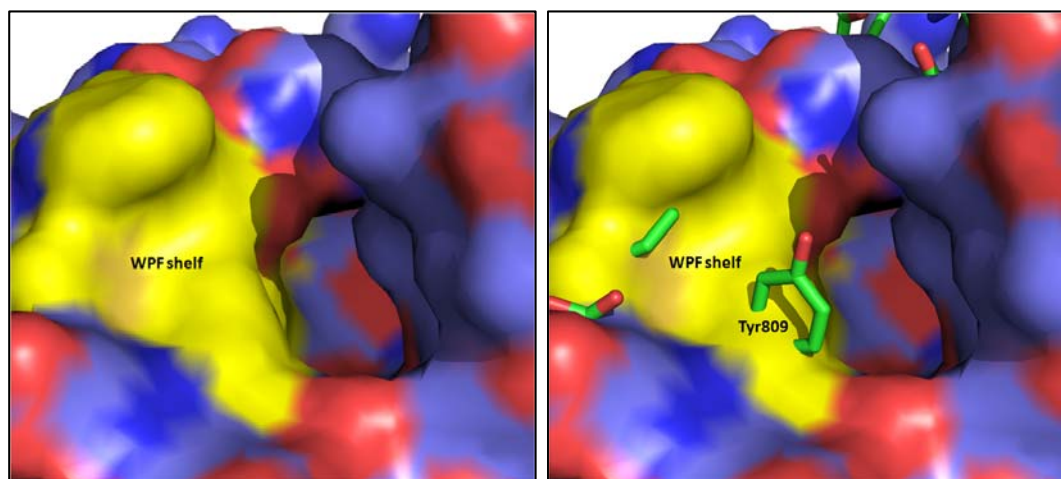


Figure 64: Left: X-ray crystal structure surface of Brd4 BD1 in blue highlighting the lipophilic WPF shelf, resolution = 1.6 Å; Right: Overlay with a PCAF X-ray crystal structure (green), resolution = 2.0 Å showing Tyr809 blocks access to the WPF shelf (yellow).

5.3.4 Known inhibitors of PCAF

Zhou *et al.* have published a range of PCAF bromodomain inhibitors based around 2-nitroanilines reporting NP1 (**5.015**) (Fig. 65) to be their most potent compound against PCAF with a pIC_{50} of 5.8.²⁴³

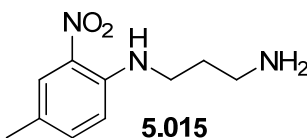


Figure 65: PCAF inhibitor NP1 (**5.015**) discovered by Zhou *et al.*²⁴³

Zhou *et al.* found that NP1 (**5.015**) could block a unique viral trans-activator protein, Tat, which is thought to be essential for the transcription of the human immunodeficiency virus (HIV).²⁴³ For the transcription of HIV to occur, the Tat protein must be acetylated on lysine 50 which binds to the co-ordinating PCAF bromodomain. Thus, by inhibiting the PCAF bromodomain and preventing Tat from binding, there is the potential for a treatment of individuals with HIV.²⁴³

As there is a clear unmet medical need for those suffering from HIV, research around this molecular series was continued. Chloroethyl analogue **5.023** (Fig. 66) was identified as binding 15-fold more strongly than NP1 (**5.015**) *in-vitro* to the PCAF bromodomain.²⁶⁵ Additionally, it was found that chloroethyl analogue **5.023** exhibited an EC_{50} of approximately 1 μ M on inhibiting Tat-mediated transcription of the viral promoter in an HIV-1 long terminal repeat (LTR) luciferase reporter gene assay.²⁶⁵ In the same luciferase assay, NP1 (**5.015**) displayed an EC_{50} of approximately 10 μ M. Recently, Zhang *et al.* have disclosed oxygen linked analogues of NP1 (**5.015**) of which **5.024** (Fig. 66) shows a 17-fold higher EC_{50} than NP1 (**5.015**) in the cell based assay of 0.6 μ M.²⁶⁶ However, upon measuring the IC_{50} of ether containing **5.024** at PCAF using an ELISA assay it was found to be 126 μ M. Due to this mismatch between the EC_{50} and the IC_{50} Zhang *et al.* conclude that the suppression in the cellular assay must be driven by off target activity.²⁶⁶ Hence, while there is interest in finding an HIV treatment, it may not be best served by these compounds.

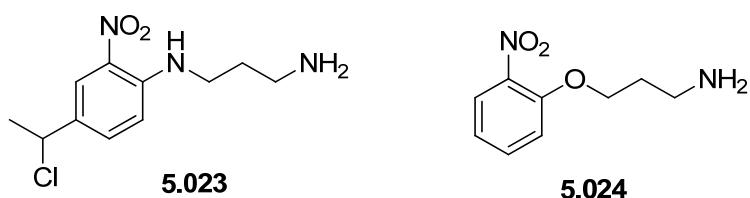


Figure 66: Molecules capable of suppressing transcription of an HIV promoter.

Another reported inhibitor of the PCAF bromodomain is ischemin (**5.019**) (Fig. 67). Ischemin was identified primarily as a binder to the CREBBP bromodomain and has been found to block apoptosis in cardiomyocytes.²⁴⁷ Ischemin is not selective for CREBBP and has a K_d of 19 μM at the CREBBP bromodomain as well as a K_d of 44 μM at the PCAF bromodomain when determined by measuring protein tryptophan fluorescence as a function of ligand concentration.²⁴⁷

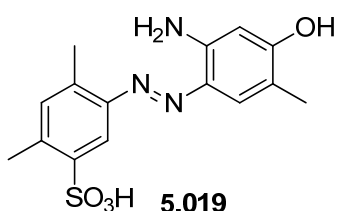


Figure 67: Ischemin (**5.019**) an inhibitor of PCAF and other bromodomains.²⁴⁷

Within the same patent which described ischemin (**5.019**) there was another compound with sub-micromolar PCAF potency, stilbene derivative **5.025** (Fig. 68).²⁶⁷ However, these reported PCAF inhibitors did not provide any selectivity over the BET family of bromodomains.

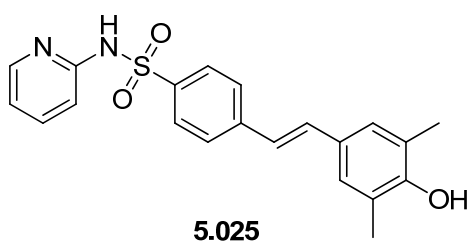


Figure 68: Reported PCAF inhibitor **5.025**.

Interestingly, none of the reported PCAF inhibitors showed evidence of binding in an FP assay or X-ray crystallography system when studied in our laboratories. However, subsequently the pan-bromodomain inhibitor bromosporine (**5.022**, Fig. 61, p 132) has

displayed a pIC_{50} of 4.7 in the PCAF FP assay, although the structure had not been disclosed upon starting this work. Zhou *et al.* have published a 3D structure of NP1 (**5.015**) bound in the PCAF bromodomain obtained by NMR methods (Fig. 69).²⁴³ However, the structure of the PCAF bromodomain with NP1 (**5.015**) bound is somewhat different from the apo structure of PCAF derived by Filippakopoulos *et al.* (Fig. 69).¹⁹⁸ The Filippakopoulos structure is almost identical to the PCAF X-ray crystal structure obtained in our laboratories.

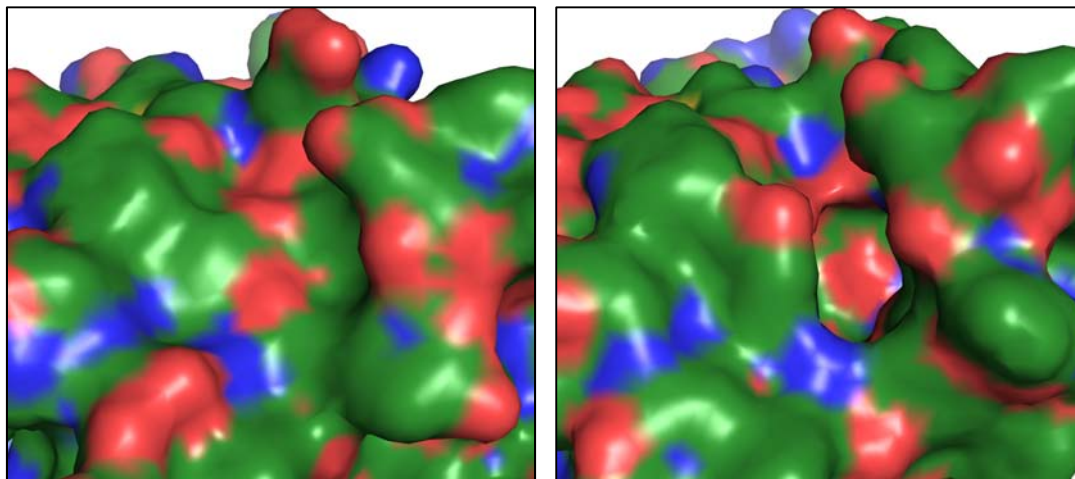


Figure 69: 3D structures of the PCAF bromodomain. Left The NMR derived Zhou PCAF structure,²⁴³ Right The Filippakopoulos PCAF structure showing the deep acetylated lysine binding pocket, resolution = 1.4 Å.¹⁹⁸

The two structures of PCAF look fundamentally different to each other, with the Zhou PCAF bromodomain showing a shallow indentation in the protein surface and the Filippakopoulos bromodomain showing the usual lipophilic groove. It may be that the binding of NP1 (**5.015**) causes a conformational shift of the residues in the protein, as different constructs had been used, or that one of the structures is inaccurate. The two structures overlay well for the majority of the protein. However, it is at the bromodomain binding site where they differ considerably. The key movements in the Zhou structure are that of Tyr802 and Tyr809 to prevent access to the acetyl lysine binding site (Fig. 70).

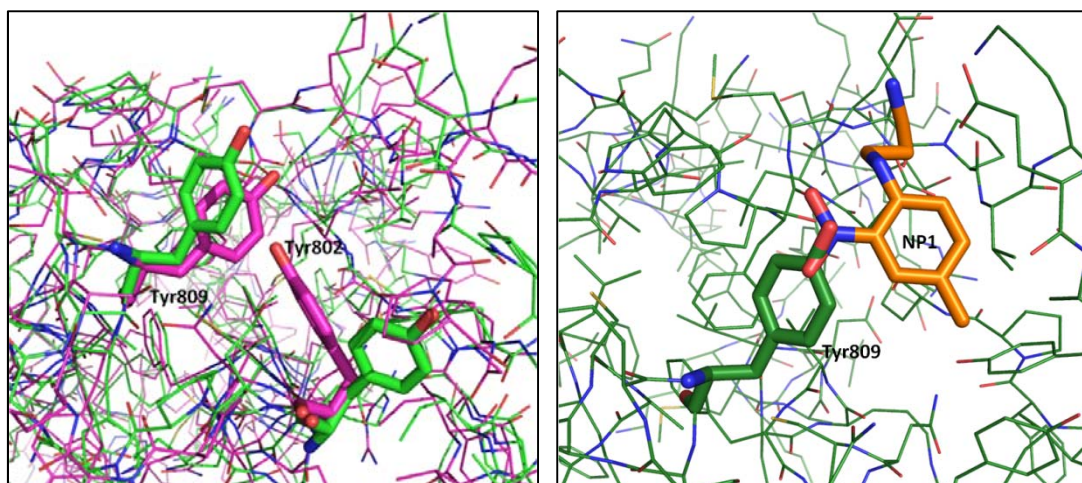


Figure 70: Left Comparison of the Zhou NMR derived structure²⁴³ in magenta and the Filippakopoulos X-ray crystal structure in green, resolution = 1.4 Å.²⁴³ Right Highlighting the clash between NP1 (**5.015**) from the NMR derived structure and Tyr809 in the Filippakopoulos X-ray crystal structure.

The major differences are between Tyr761, Tyr802, Tyr809 and Pro758. Overlaying nitro containing NP1 (**5.015**) in the Filippakopoulos X-ray crystal structure shows a major steric clash between the nitro group in NP1 (**5.015**) and Tyr809 with the nitro group superimposed through the phenolic C-O bond. With this lack of a biologically relevant binding mode in PCAF compared to other known bromodomain binders¹⁹⁹ and a lack of potency in the FP assay, other starting points were needed.

5.3.5 Bromodomain assays

Bromodomains have no enzymatic activity and therefore an assay which measures turnover of a substrate cannot be used for these proteins. Hence binding assays that use technologies such as fluorescence polarisation (FP) or fluorescence resonance energy transfer (FRET) are used.

FP assays operate by tagging a known binder of the target of interest with a fluorescent tag and allowing the resultant assay reagent to bind to the protein. Under the assay conditions, a compound is dosed and if this compound binds to the target of interest, the assay reagent is displaced. The more potent the compound, the more assay reagent is displaced and the degree of displacement can be measured by recording the degree of light scattering when plane polarised light is shone on the assay. The principle behind this is the larger the amount of displaced assay reagent, the higher the degree of scattered light and

thus a percentage inhibition can be measured.²⁶⁸ The test compound is dosed at a range of concentrations and in so doing, an IC₅₀ can be determined.

A FRET assay works in a similar manner, requiring an assay reagent with a fluorescent tag. However, the binding partner, in this case the bromodomain, must also have a fluorescent tag which is excited by the light emitted from the assay reagent, or *vice versa*, and then emits a signal which can be measured. For the light emission to be measured the tagged assay reagent and the tagged protein must be in close proximity. Hence, if an inhibitor of the bromodomain is present there will be less light emitted and a percentage inhibition can be measured (Fig. 71).²⁶⁹

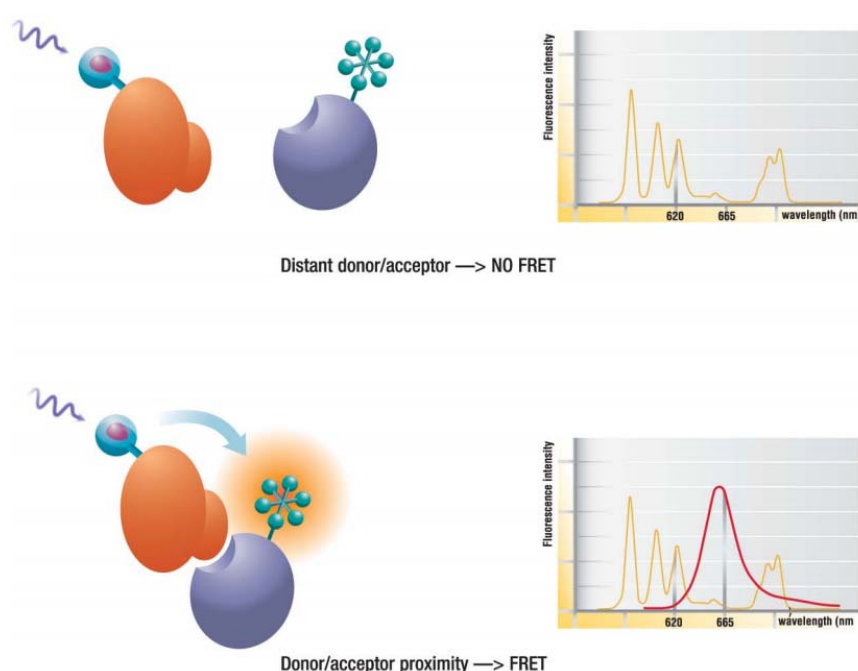


Figure 71: Schematic of a FRET assay. When the donor and acceptor are apart there is no FRET signal. When the donor and acceptor are brought into proximity a FRET signal is generated; 665 nm in this example. Reprinted courtesy of Cisbio Bioassays.²⁶⁹

5.3.6 Assay development

Earlier work in our research group to identify PCAF bromodomain inhibitors identified a fragment compound as a binder to Brd9 and CREBBP through thermal shift experiments. The fragment was identified as a BET inhibitor through X-ray crystallography and at 200 μ M was found to increase the melting point of Brd9 and CREBBP by 5.6 and 2.2 $^{\circ}$ C, respectively.

One vector from the fragment pointed directly into solvent and from this vector it was possible to append a fluorescent tag, in this case Alexa Fluor 488,²⁷⁰ to produce assay reagent **5.026** (Fig. 72).

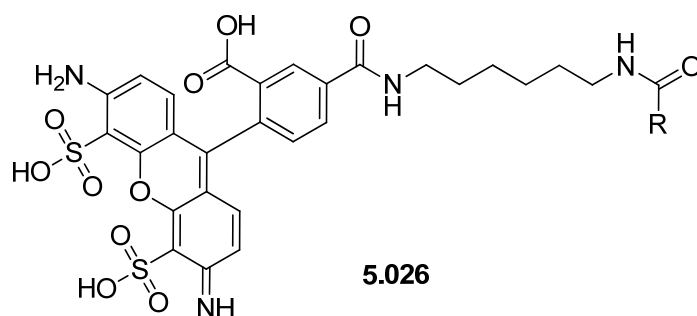
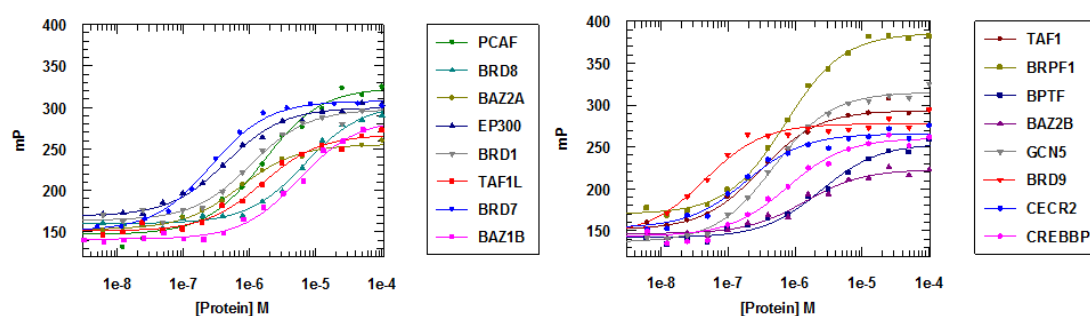


Figure 72: Assay reagent. The bromodomain binder is represented by R.

The K_d of the assay reagent **5.026** was determined for a number of bromodomains and was found to bind to sixteen examples (Table 23).



Bromodomain	K_d (μM)
Brd9	0.04
TAF1	0.17
CECR2	0.17
Brd7	0.25
GCN5	0.45
EP300	0.45
BRPF1	0.50
BAZ2A	0.65

Bromodomain	K_d (μM)
CREBBP	0.69
Brd8	6.74
Brd1	1.00
TAF1L	1.50
BPTF	2.40
PCAF	2.50
BAZ1B	5.00
BAZ2B	1.00

Table 23: K_d s of assay reagent **5.026** against different bromodomains.

Through using the assay reagent **5.026**, an FP assay was developed to measure the binding of small molecules to the PCAF bromodomain using a PCAF truncate which contained the bromodomain. The PCAF FP assay was fit for purpose as it could provide IC_{50} values for test compounds, although there were several limitations to be aware of:

- The actual pIC₅₀ of **5.009** at PCAF (Fig. 75, p 142) could not be determined with great accuracy as **5.009** was fluorescent and interfered with the readout from the assay,
- Due to the 2.50 μM K_d of **5.026** at PCAF and the low signal to noise ratio, the tight binding limit of the assay, the maximum pIC₅₀ the assay could measure, was predicted to be 5.9 assuming 100% active protein, too low to accurately measure the desired sub-micromolar compounds at PCAF,
- The assay required comparatively large amounts of protein to run. For example an HTS screen of the compound collection available within our laboratories with the PCAF FP assay would require 8 g of protein, whereas a typical HTS screen in our laboratories would require *ca.* 20 mg.

Thus, in addition to identifying a probe molecule for PCAF, a new ligand for an improved assay was required. The requirements of this ligand were:

- Requiring less PCAF bromodomain truncate protein,
- Having a smaller K_d to raise the tight binding limit of the assay,
- Ideally, not being auto-fluorescent so the readout from the assay would not be interfered with.

Once the improved assay reagent was identified, an HTS could be initiated to find other chemotypes which bound to the PCAF bromodomain and potentially find structurally diverse inhibitors of the PCAF bromodomain.

5.3.7 Comparing pIC₅₀ values across assays

Between different biochemical assays, pIC₅₀ values are typically not directly comparable as the IC₅₀ is dependent on the concentrations of the substrate used (S), in this case the assay reagent, and the affinity of the assay reagent to the protein (K_d). However, using the Cheng-Prusoff equation²⁷¹ (Equation 2) the IC₅₀s from the assays can be converted into K_i values which are directly comparable with each other, assuming competitive binding.

$$K_i = \frac{IC_{50}}{1 + \left(\frac{S}{K_d}\right)}$$

Equation 2: The Cheng-Prusoff equation.²⁷¹

By taking the negative log of the Cheng-Prusoff equation a direct, additive relationship between pK_i and pIC_{50} can be determined (Equation 3).

$$pK_i = pIC_{50} + \log\left(1 + \frac{S}{K_d}\right)$$

Equation 3: Negative log of the Cheng-Prusoff equation.

While the PCAF assay was an FP assay using assay reagent **5.026** at $S = 2.5 K_d$, due to the low signal to noise ratio, the Brd4 assays were performed in a FRET format at $S = K_d$. This difference in the substrate concentration meant that the pIC_{50} values from the two assays were not directly comparable.

Converting the values from the PCAF FP assay from pIC_{50} to pK_i gives an approximate increase of 0.5 log units for each compound while converting the values from the most relevant selectivity assay, Brd4 BD1 and Brd4 BD2, gives an increase of 0.3 log units (Equation 4).

$$PCAF\ pK_i = pIC_{50} + \log\left(1 + \frac{2.5 K_d}{K_d}\right) = pIC_{50} + \log 3.5 = pIC_{50} + 0.54$$

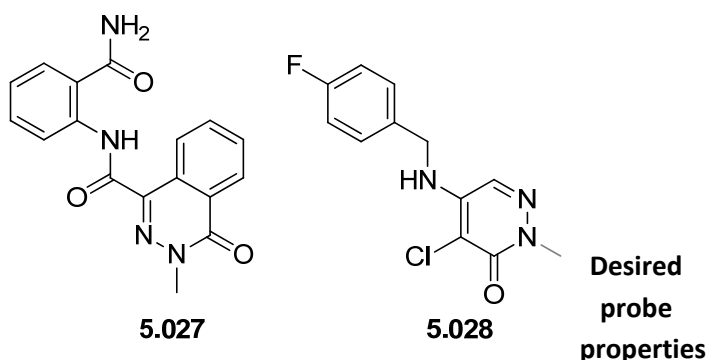
$$Brd4\ pK_i = pIC_{50} + \log\left(1 + \frac{K_d}{K_d}\right) = pIC_{50} + \log 2 = pIC_{50} + 0.30$$

Equation 4: Conversion of pIC_{50} to pK_i for the PCAF and Brd4 assays.

This means that when comparing the pIC_{50} values between the PCAF FP and the Brd4 BD1 and 2 assays the compounds will be more selective against PCAF than reported. However, as the error in the assays is approximately 0.5 log units for the PCAF FP assay and 0.3 log units for the Brd4 FRET assay the pIC_{50} values will remain uncorrected. It is worth noting that the Brd4 BD1 and BD2 data will be quoted for the selectivity against the BET family. This is based on experience of screening thousands of compounds shows that Brd4 BD1 and BD2 are good surrogates for the other BET family members due to the high homology of the bromodomains.

5.3.8 Compounds identified from a knowledge based screen

In order to identify chemical series that inhibit PCAF, a knowledge based screen of 27,000 compounds based on known bromodomain binders such as those containing a hydrogen bond acceptor close to a methyl mimetic (Fig. 59, p 128; Fig. 61, p 131) was run.



PCAF FP pIC ₅₀ (LE)	5.0 ^a (0.29)	4.7 (0.36)	≥ 6.0
Brd4 FRET BD1/BD2 pIC ₅₀	< 4.3 / < 4.3	≤ 5.0 / ≤ 4.5	≤ 4.0
MW	322	267	≤ 400
cLogP	0.65	2.1	1 – 3
Aqueous solubility μg mL ⁻¹	15	≥ 134	≥ 50
AMP nm s ⁻¹	115	630	≥ 50

Table 24: PCAF inhibitors identified from focussed screen. ^a) Inactive on 4 of 25 test occasions.

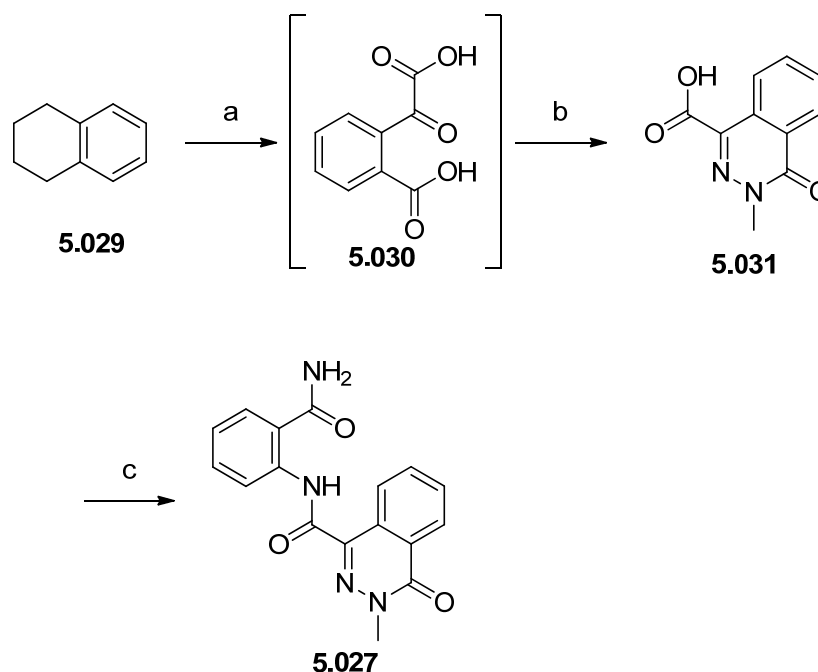
The two chemotypes identified (Table 24) have sufficient PCAF potency for initial hits, acceptable ligand efficiency as starting points for future lead optimisation and have been shown to bind in the bromodomain binding site through the use of ¹⁵N NMR.⁹³ Phthalazinone analogue **5.027** had Brd4 potencies below the level of quantification whereas the pyridazinone compound **5.028** was approximately equipotent at PCAF and Brd4. The molecular weight of phthalazinone containing **5.027** is sufficiently low for some further molecular weight to be appended as the hit is optimised, while still remaining in desired probe-like space. However, phthalazinone compound **5.027** does have low lipophilicity so lipophilic groups can be added to the molecule to aid cellular penetration.²⁷² Pyridazinone analogue **5.028** has less scope for adding lipophilic groups than phthalazinone compound **5.027** before becoming prone to being more promiscuous for other biological targets.¹³¹ However, the molecular weight of **5.028** is lower than phthalazinone containing **5.027** allowing for a considerable increase in molecular weight before the mass becomes too high

for oral bioavailability. The aqueous solubility of phthalizinone compound **5.027** is lower than desired for a probe although the AMP is well above the needed amount. The solubility and AMP of pyridazinone containing **5.028** are well above the minimum desired properties.

Phthalizinone **5.027** and aminopyridazinone **5.028** were found to be chemically stable and underwent further investigation. As for the JmjD2 family section, the programme was a team effort and the compounds reported on were not solely designed or synthesised by the author. Those compounds that were designed and synthesised by others will be identified by an asterisk (*) and those designed by the author but synthesised by others will be identified by a dagger (†). The phthalizinones will be discussed first.

5.4 Phthalizinone series

The initial phthalizinone hit **5.027** showed a promising profile with a pIC₅₀ of 5.0 at PCAF and displayed no measurable activity at Brd4. Although, these data were encouraging, phthalizinone containing **5.027** was remade to ensure the biological activity was caused by the compound itself and not a low level impurity (Scheme 39).



Scheme 39: Reagents and conditions a) KMnO₄, NaOH, H₂O, 90 °C; b) MeNHNH₂, 90 °C, 6%; c) i) DMF, (COCl)₂, 20 °C; ii) 2-aminobenzamide, NEt₃, 20 °C, 15%.

Tetrahydronaphthalene (**5.029**) was oxidised using KMnO₄ to 2-(carboxycarbonyl)benzoic acid (**5.030**) and after destruction of any residual permanganate with IPA, methyl hydrazine

was added to form the desired phthalizinone carboxylic acid **5.031**.²⁷³ The acid chloride of **5.031** was made *in situ* and coupled with 2-aminobenzenecarboxamide. Although the yields for both steps were poor, 0.8% across two steps, and would have to be improved for further analogue generation, the remade batch of amide containing **5.027** was found to have the same level of potency at PCAF and Brd4 as the historical batch. This provided the confidence necessary to continue investigating the phthalizinone series. One of the main aims with this template was to increase the potency against PCAF while maintaining the BET selectivity.

However, on repeatedly retesting the new batch of phthalizinone compound **5.027** at PCAF some concerning results came to light (Fig. 73).



Figure 73: Left: Comparison of two batches of ME on different test occasions at PCAF. Right: an example of a dose response curve for one of the inactive test occasions (red) and a successful curve (green).

Some of the assay results showed that the new batch was inactive and so the individual dose response curves were examined (Fig. 73). On the inactive test occasions there was the beginning of a dose response curve although after a concentration 3.7 μ M of phthalizinone containing **5.027** in the PCAF assay there is a drop in the percentage inhibition. This curve shape is consistent with a lack of solubility of the compound being tested in assay media. As the compound is dosed at higher concentrations the compound precipitates out of solution and is therefore unable to inhibit the bromodomain. This lack of solubility of phthalizinone analogue **5.027** was found to extend to many of the phthalizinones synthesised and was a problem which needed addressing as part of making a viable probe molecule.

The low solubility of phthalizinone **5.027** was attributed to the number of amides in the molecule, three if the embedded phthalizinone amide is included. Molecular modelling showed that the primary amide group can form an intramolecular H-bond to the secondary amide in the linker of **5.027**. The formed H-bond causes two planar sheets in the molecule when modelled thus lowering the aqueous solubility of the molecule (Fig. 76).²⁷⁴

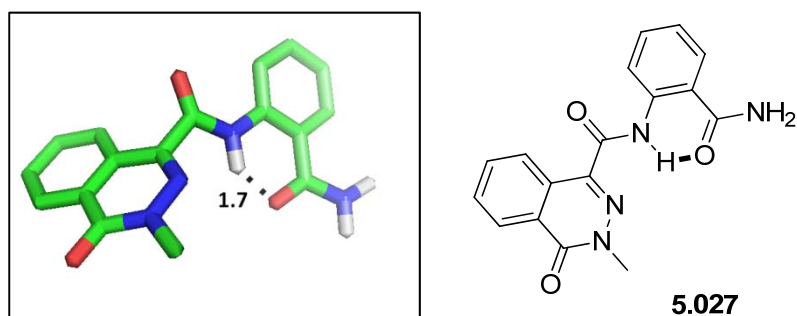


Figure 74: **5.027** showing a 1.7 Å internal H-bond. Modelled *via* a stochastic conformational search using MMFF94x and MOE 2012.10.²⁷⁵

Therefore, alternative linkers were investigated to disrupt the potential internal H-bonding and a series of analogues were targeted which remove the linking amide were designed (Fig. 75).

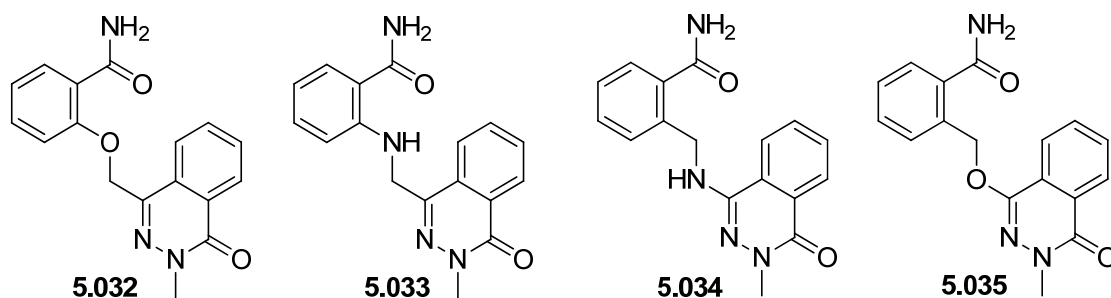
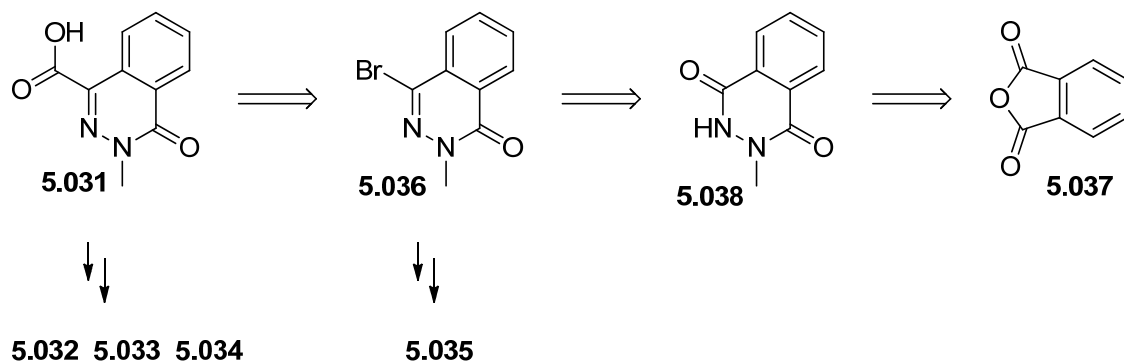


Figure 80: Target compounds with alternative linkers to **5.027**.

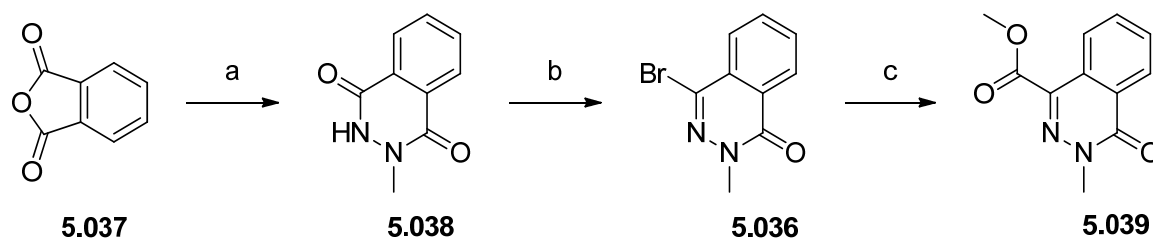
5.4.1 Development of a higher yielding route to carboxylic acid 5.027.

The target compound aryl amine **5.033**, benzyl amine containing **5.034**, phenyl ether analogue **5.032** and benzyl ether compound **5.035** all shared a phthalazinone core and thus could be synthesised using a common retrosynthetic intermediate bromo **5.036**. This key intermediate could be accessed in a straightforward manner from anhydride **5.037** *via* hydrazide **5.038** and chemoselective bromination (Scheme 40).



Scheme 40: Retrosynthesis of key intermediate **5.031**.

Dihydrophthalizindione **5.038** was accessed through the condensation of *N*-methylhydrazine with phthalic anhydride (**5.037**).²⁷⁶ **5.038** was brominated using phosphorus oxybromide and triethylamine in toluene to provide impure **5.036** contaminated with 1,4-dibromophthalazine.²⁷⁷ Bromophthalazinone **5.036** was subsequently carbonylated using catalytic palladium acetate, DPPF and carbon monoxide in MeOH to provide methyl ester **5.039** (Scheme 41).

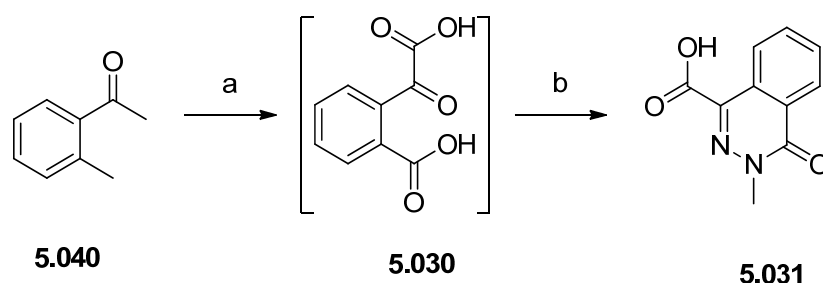


Scheme 41: Reagents and conditions a) H_2NNHMe , AcOH, 20 °C, 67% ; b) POBr_3 , NEt_3 , PhMe, 115 °C, 34%; c) CO, NEt_3 , $\text{Pd}(\text{OAc})_2$ (6 mol %), DPPF (12 mol %), MeOH, 50 °C, 41%.

While the route outlined in Scheme 41 could provide the material necessary to synthesise the alternative linker compounds (Fig. 75) and provide additional material for amide analogues of **5.027**, the overall yield of 9% to methyl ester **5.039** was deemed insufficient

to provide intermediates for multiple analogues. Thus, an effort was made to access carboxylic acid **5.031** directly from bromo **5.036** *via* halogen-lithium exchange and quenching with CO₂, however, only the des-bromo phthalizinone analogue was seen as a product by LCMS.

Therefore a re-examination of the original route to carboxylic acid **5.031** (Scheme 39, p 145) was undertaken. If an improved method of generating the dicarboxylic acid intermediate **5.030** could be identified the condensation with methyl hydrazine could give the desired carboxylic acid **5.031** in higher yield. Ketone **5.040** was oxidised with potassium permanganate in the presence of potassium carbonate to provide dicarboxylic acid **5.030** *in situ*²⁷⁸ and after destruction of the excess permanganate with ethanol, carboxylic acid **5.031** was formed by adding methyl hydrazine and acetic acid (Scheme 42).

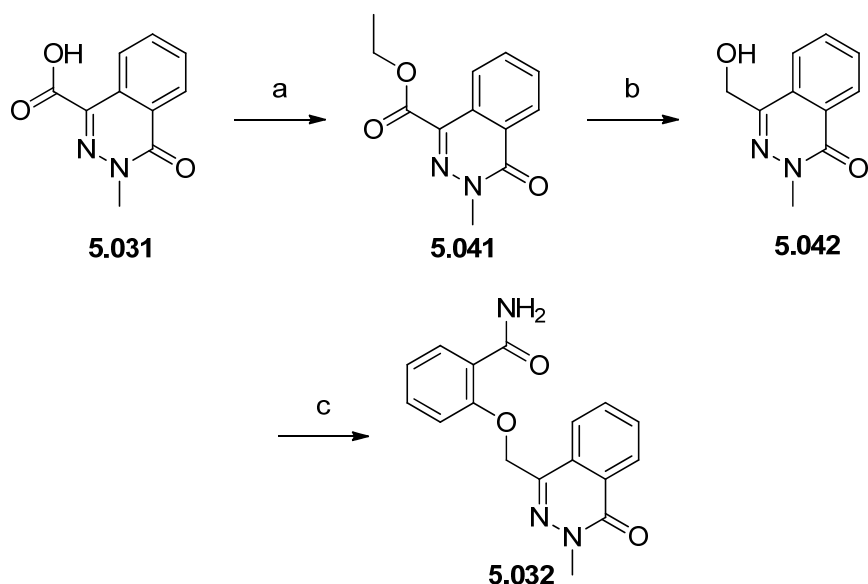


Scheme 42: Reagents and conditions a) KMnO₄, K₂CO₃, H₂O, 50 – 70 °C; b) MeNHNH₂, AcOH, 70 °C, 44% over 2 steps.

This improved synthetic route to carboxylic acid **5.031**, originating from ketone **5.040** provided sufficient material to probe alternative linkers as well as investigate other amides.

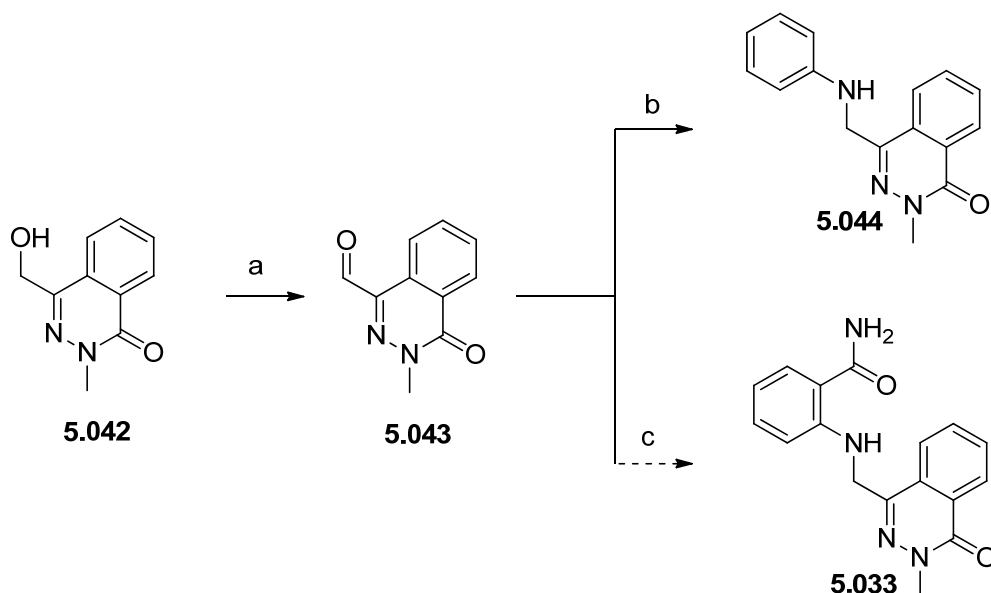
5.4.2 Synthesis of phenolic ether **5.032** and aniline **5.033**

Ethyl ester **5.041** was synthesised *via* a Fisher-Speier esterification²⁷⁹ of carboxylic acid **5.031** and was reduced using sodium borohydride to give primary alcohol **5.042**. The target molecule **5.032** was obtained using Mitsunobu conditions to give the desired phenolic ether **5.032** (Scheme 43).²⁸⁰



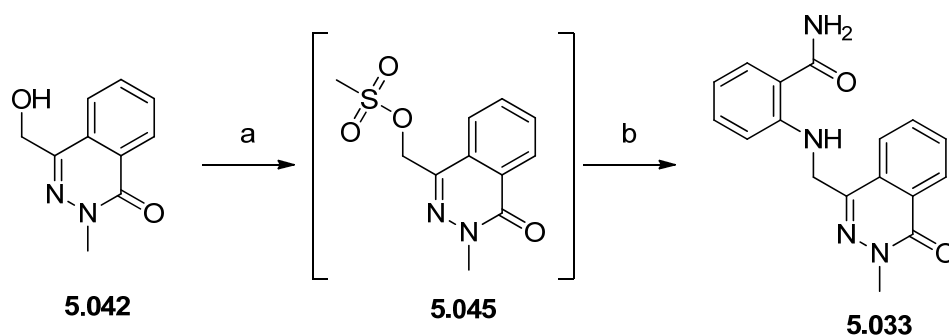
Scheme 43: Reagents and conditions a) H_2SO_4 , EtOH, 80 °C, 88%; b) NaBH_4 , THF, 60 °C, 79%; c) 2-hydroxybenzamide, DBAD, PPh_3 , 20 °C, 65%.

With the first target compound synthesised, focus was placed on the synthesis of aryl amine **5.033** which was prepared using alcohol **5.042**. Primary alcohol **5.042** was oxidised to aldehyde **5.043** using a Swern oxidation¹⁷⁶ and reductive aminations were attempted with this material. A test reaction with aniline showed this method to be successful and provided aryl amine **5.044**. However, when repeating these conditions with the electron deficient 2-aminobenzamide none of the desired aryl amine **5.033** was obtained, with the major product being the original intermediate primary alcohol **5.042** (Scheme 44).



Scheme 44: Reagents and conditions a) $(\text{COCl})_2$, DMSO, NEt_3 , DCM, $-70 - 20^\circ\text{C}$, 100%; b) PhNH_2 , $\text{NaHB}(\text{OAc})_3$, AcOH, THF, 60°C , 59%; c) 2-aminobenzamide, $\text{NaHB}(\text{OAc})_3$, AcOH, THF, 60°C , 0%.

Therefore, an alternative strategy was used to prepare 2-aminobenzamide containing **5.033**. The primary alcohol **5.042** was treated with mesyl chloride and triethylamine to form mesylate **5.045** *in situ* which alkylated 2-aminobenzamide in the presence of potassium carbonate to form aryl amine **5.033** (Scheme 45).

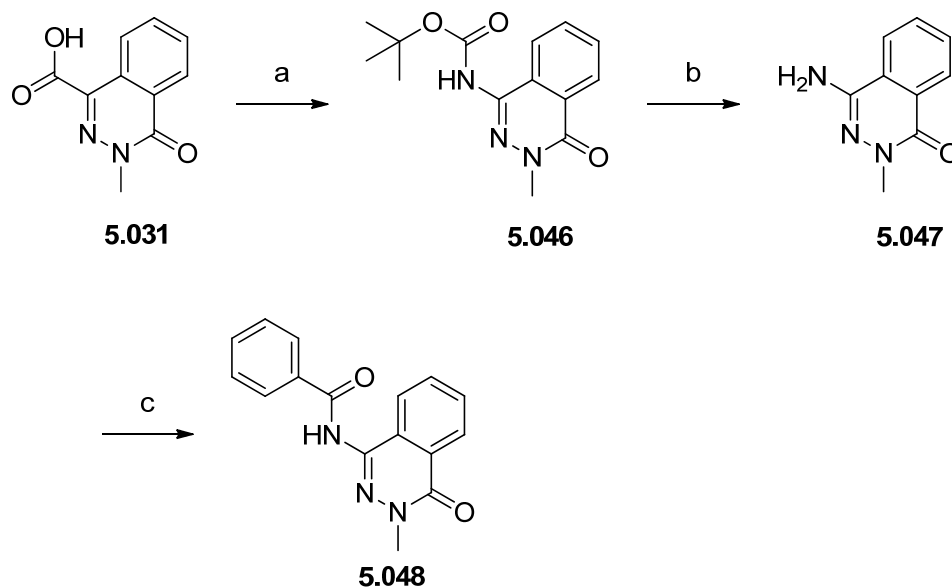


Scheme 45: Reagents and conditions a) MsCl , NEt_3 , DCM, $0 - 20^\circ\text{C}$; b) 2-aminobenzamide, K_2CO_3 , $20 - 40^\circ\text{C}$, 4%.

This provided for the target molecules with heteroatoms adjacent to the benzene ring and attention was then focussed on the remaining targets, substituted benzylamine **5.034** and benzyl ether **5.035**.

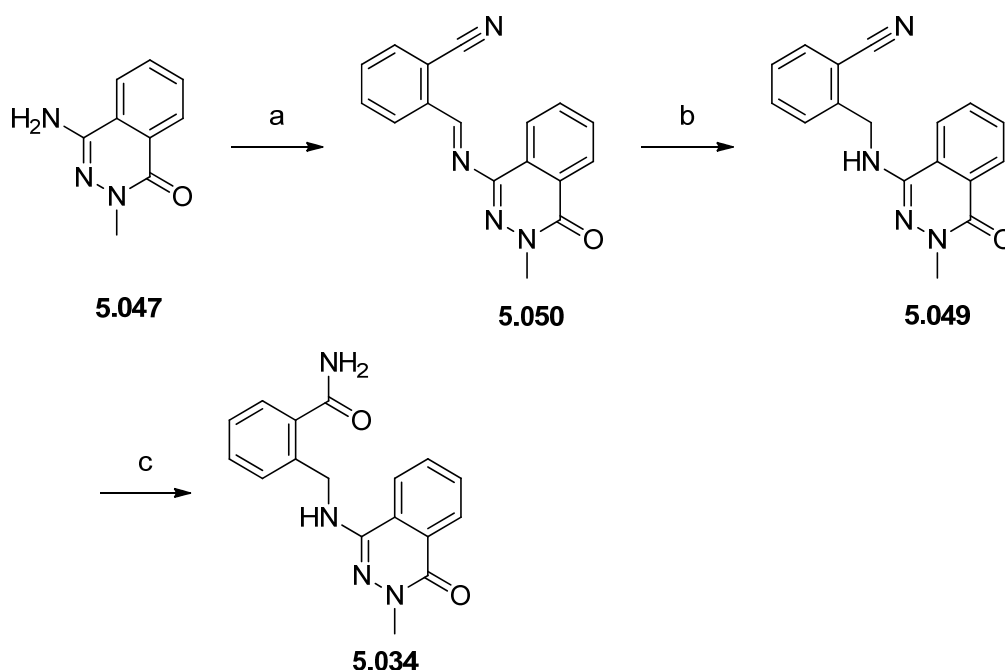
5.4.3 Synthesis of substituted benzylamine 5.034

Key intermediate carboxylic acid **5.031** was converted into carbamate **5.046** via a Curtius rearrangement²⁸¹ in *t*-BuOH.²⁸² Carbamate **5.046** was deprotected to provide amino **5.047** by treatment with HCl in IPA. The resultant amine **5.047** was opportunistically used to investigate another alternative linker in the phthalizinone series, the reverse amide of **5.027**, albeit with the simple benzamide **5.048**. **5.048** was prepared by treating amine **5.047** with benzoyl chloride in the presence of triethylamine (Scheme 46).



Scheme 46: Reagent and conditions a) $(\text{PhO})_2\text{P}(\text{O})\text{N}_3$, NEt_3 , *t*-BuOH, 30 °C, 64%; b) HCl, IPA, 20 °C, 80%; c) PhCOCl , NEt_3 , DCM, 40 °C, 17%.

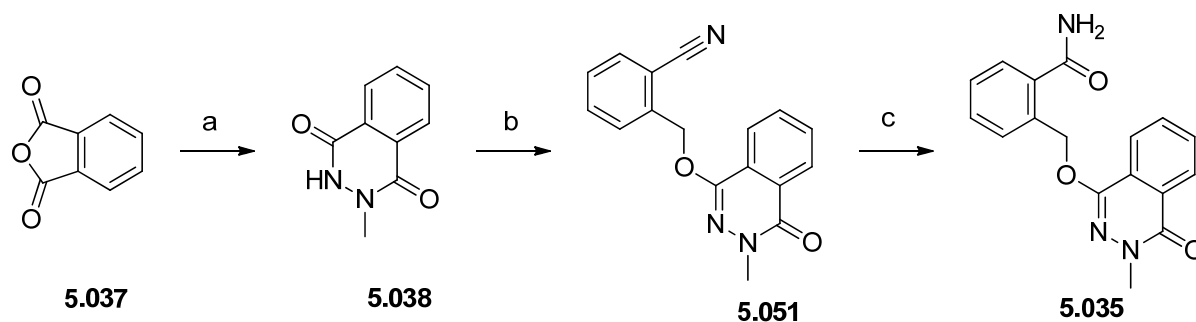
A reductive amination was attempted with commercially available 2-cyanobenzaldehyde and amine **5.047** to form benzamide analogue **5.049** with the intention to hydrolyse the nitrile to the primary amide **5.034**. This strategy was successful, although sodium triacetoxyborohydride was found to be unreactive with this system and initially imine **5.050** was isolated. Treatment of imine **5.050** with sodium borohydride reduced the imine to substituted benzylamine **5.049** which was hydrolysed using potassium carbonate and hydrogen peroxide to provide desired benzylamine containing **5.034** (Scheme 47).¹³²



Scheme 47: Reagents and conditions a) 2-cyanobenzaldehyde, AcOH, NaHB(OAc)₃, DCM, 20 °C, 42%; b) NaBH₄, MeOH, DCM, 20 °C, 61%; c) K₂CO₃, H₂O₂, DMSO, 20 °C, 59%.

5.4.4 Synthesis of benzyl ether 5.035

The final compound in the set with alternative linkers between the phthalazinone and the benzamide was accessed in an efficient manner. Phthalizindione **5.038**, which had been used as an intermediate for a trial synthetic route to key carboxylic acid **5.031**, was selectively *O*-alkylated with 2-cyanobenzyl bromide in the presence of silver carbonate to furnish ether **5.051**.²⁸³ The nitrile group on **5.051** was hydrolysed using conditions employed by Katritzky *et al.* to provide the desired primary amide **5.035** (Scheme 48).¹³²

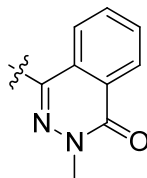


Scheme 48: Reagents and conditions a) NH₂NHMe, AcOH, 20 °C, 67%; b) 2-nitrilebenzylbromide, Ag₂CO₃, MeCN, EtOH, 80 °C, 77%; c) aq. H₂O₂, K₂CO₃, DMSO, 20 °C, 47%.

This completed the set of compounds with alternative linkers (Fig. 75, p 147), which were assayed against PCAF.

5.4.5 Assay results of phthalizinones with alternative linkers

In addition to having the potencies of the molecules measured at PCAF, the aqueous solubilities measured from DMSO were determined to establish if the compounds were more soluble than the original hit **5.027** (Table 25).



Entry	Number	Structure	PCAF pIC ₅₀	Aqueous solubility µg/mL
1	5.027		5.0 ^b	15
2	5.051		≤ 4.4	33
3	5.035		4.0	≥ 158
4	5.039	MeO ₂ C	< 4.0	≥ 197
5	5.042	HO	< 4.0	≥ 186
6	5.032[†]		< 4.0	15
7	5.044	Ph-NH	< 4.0	32
8	5.033		< 4.0	11
9	5.047	NH ₂	< 4.0	≥ 119
10	5.048	Ph-C(=O)-NH	< 4.0	≥ 137
11	5.034		4.1 ^a	22

Table 25: Potencies and solubilities of phthalizinone compounds with alternative linkers to **5.027**. ^a) Data from FRET assay (Section 5.5.8, p 191) . ^b) Inactive on 4 of 25 test occasions.

As indicated in Table 25, the measured potencies of the compounds at PCAF showed no improvement against the original amide **5.027**. Some of the compounds were more soluble than amide **5.027**, principally those unable to make a 5 or 6-membered internal H-bond: benzyl alcohol containing **5.035**, methyl ester **5.039**, amino **5.047** and benzamide analogue **5.048**. The compounds which potentially could form internal H-bonds had universally poor solubilities (Fig. 76). This supports the hypothesis outlined in Section 5.4.1 (p 150).

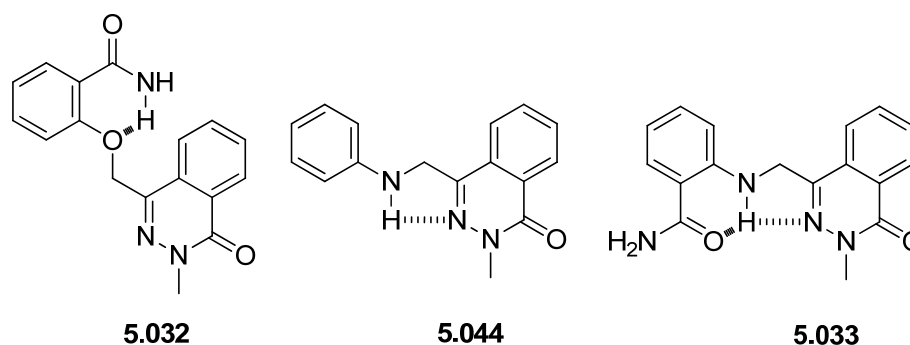
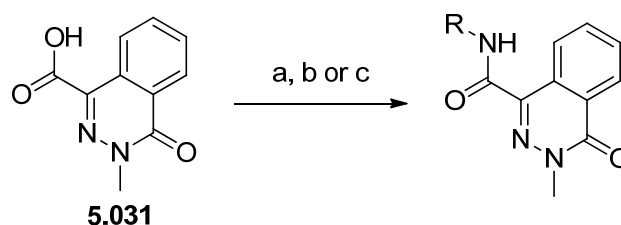


Figure 76: Potential internal H-bonds that could explain poor solubilities of these compounds.

However, only nitrile **5.035**, benzylamine analogue **5.034** and benzyl alcohol **5.051** had pIC_{50} values ≥ 4.0 at PCAF and these were approximately tenfold less potent than **5.027**. This led to the belief that the amide linker, as exemplified in the original hit **5.027**, was involved in binding to the PCAF protein. Therefore, a variety of amides were synthesised from the phthalazinone carboxylic acid **5.031** as well as screening historical compounds from the compound collection available in our laboratories.

5.4.6 Synthesis of compounds with amide linkers

A variety of amide coupling methods to vary the amide head group were used: formation of the acid chloride of **5.031**; the use of CDI to form imidazolide, or the use of T3P® to form the phosphinic anhydride intermediate (Scheme 49). None of the activated intermediates were isolated as they were used *in situ*.



Scheme 49: Reagents and conditions a) i) DMF, $(COCl)_2$, DCM, 20 °C; ii) R-NH₂, NEt₃, DMF, 20 °C; b) CDI, R-NH₂, DMSO, 20 °C; c) T3P®, R-NH₂, DIPEA, DCM, 20 °C.

Many of these phthalizinone amide compounds were profiled through the PCAF assay although ultimately no meaningful data could be gleaned for the compounds assayed. Most of the compounds synthesised were sparingly soluble in a wide variety of solvents, including water and thus within biological systems. It was difficult to determine if the compounds synthesised were inactive as inhibitors of the PCAF bromodomain or insoluble under the assay conditions. Many compounds showed inhibition curves consistent with compounds precipitating as the concentration of the compounds increased (*c.f.* Fig. 73, p 146). Examples synthesised by the author can be found in Appendix A.

An X-ray crystal structure of ortho-fluoro **5.052** was successfully obtained (Fig. 77) and this was the only X-ray crystal structure collected in PCAF for the phthalizinone series.

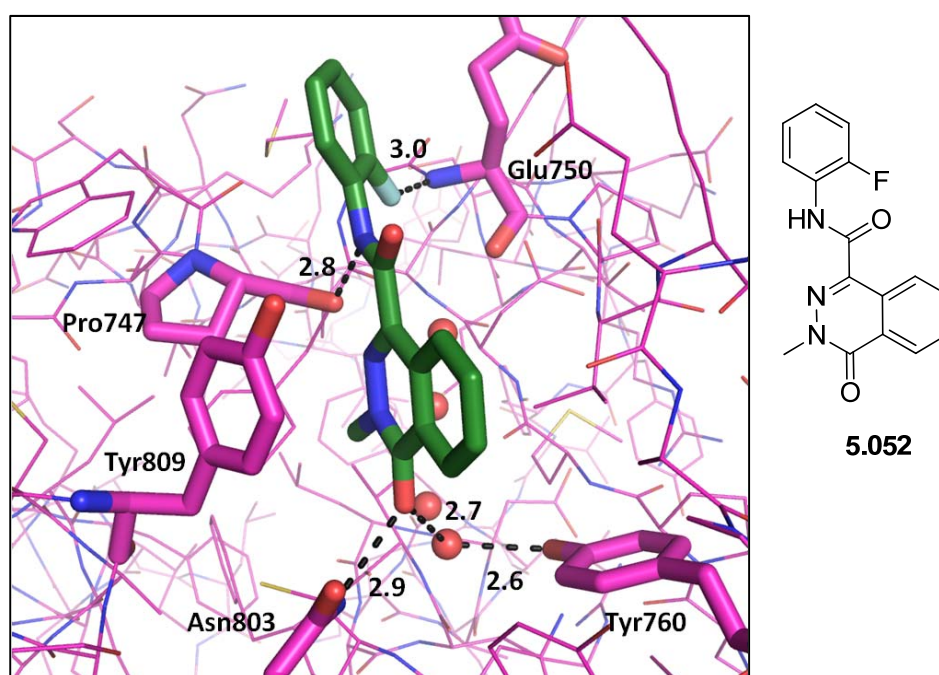


Figure 77: X-ray crystal structure of **5.052** in PCAF, resolution = 2.0 Å.

The key interactions between the PCAF protein and the ligand 2-fluoro **5.052** are highlighted in the diagram above. The majority of the interactions will be consistent for the phthalizinone amides as only the apparent H-bond²⁸⁴ between the fluorine and the N-H amide of Glu750 will be specific for 2-fluoro **5.052**. The amide N-H forms an H-bond with the carbonyl of Pro747, and the bicyclic ring system forms a face to face aromatic interaction with Tyr809. The methyl group mimics the methyl of the acetylated lysine from the histone tail binds, filling a small lipophilic pocket. The carbonyl of the phthalizinone

core is situated in the area where the carbonyl of the natural substrate, the acetylated lysine from the histone tail, binds and makes H-bonding interactions with Asn803 and a residual water.

The crystal structure is interesting beyond the interactions mentioned above as the compound is in an almost planar conformation between the amide group and the phthalizinone core, with an 8° dihedral angle. The small angle indicates that there could be an H-bonding contribution between the amide nitrogen in the 3-position of the phthalizinone ring keeping the conformation rigid. It would appear that the H-bond between the amide N-H and the carbonyl of Pro747 is key. The alternative linkers (Table 25, p 154), in general, cannot form this interaction and therefore show no potency. The exceptions to this are aryl amine compounds **5.044** and **5.033** (Fig. 78).

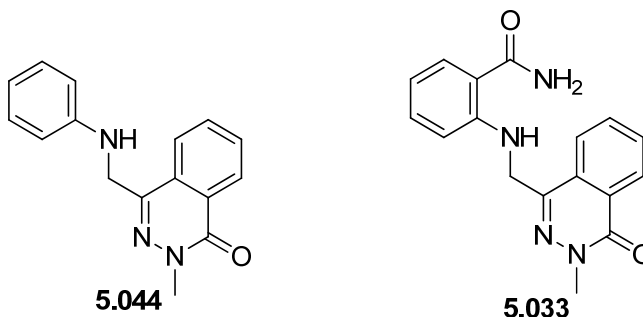


Figure 78: Aryl amine containing phthalizinones with pIC_{50} values < 4.0 at PCAF.

Aryl amines **5.044** and **5.033** could make the H-bonding interaction with Pro747 as the aniline N-H bonds will be in approximately the same position as the hit **5.027** (Table 24, p 144). The lack of measurable potency could be due to the N-H bond being insufficiently acidic or it could be due to the lack of solubility of the compounds (p 148).

The lack of aqueous solubility remained the major problem with the phthalizinone series. Hence a body of work attaching solubilising groups to the original hit **5.027** was undertaken. The addition of basic groups has proven to be an effective method to improve the aqueous solubility of some drug molecules.^{285,286} By adding a group which is charged at neutral pH the compound is made more hydrophilic and the aqueous solubility increases.

5.4.7 Addition of solubilising basic groups to the phthalizinone core

After consideration of the X-ray crystal structure of fluoro derivative **5.052** (Fig. 77, p 156) there appeared to be two vectors suitable for the incorporation of solubilising groups.

These positions were from the 4-position of the pendant benzene ring and the 6-position of the phthalizinone. Hence, compounds with basic centres were proposed: **5.053** with a basic solubilising group from the 4-position of the amide and **5.054** with a basic solubilising group originating from the 7-position of the phthalizinone core (Fig. 79).

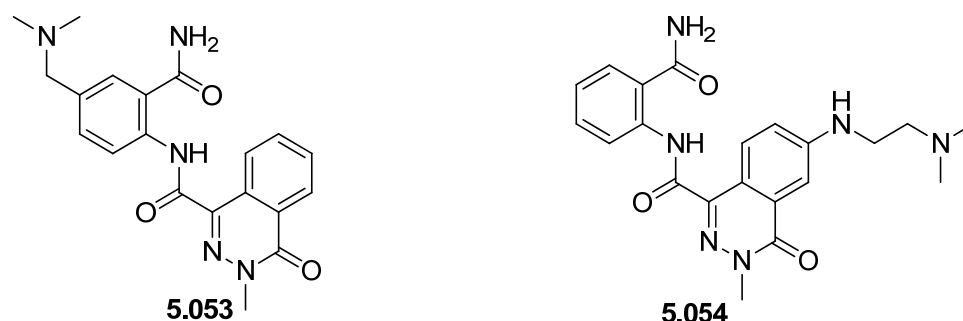
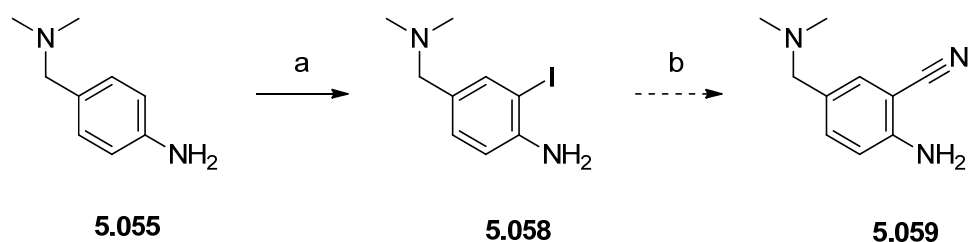


Figure 79: Phthalizinone compounds with solubilising groups.

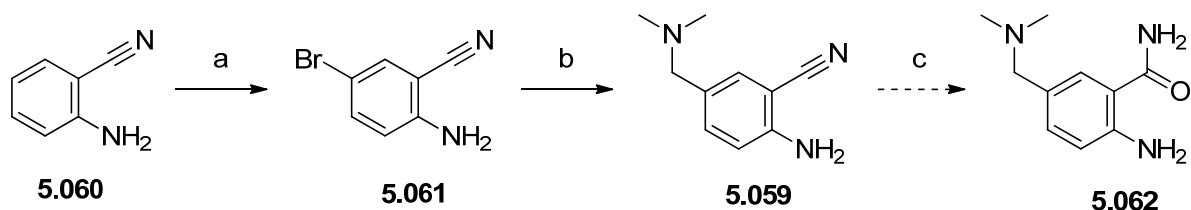
The basic groups were chosen as they will be positively charged at biological pH of 7.4 making the compounds more hydrophilic, increasing the aqueous solubility. To ensure the solubilising group would be tolerated initially, ((4-dimethylamino)methyl)aniline (**5.055**) was coupled using the CDI conditions to the phthalizinone core to give *N,N*-dimethyl benzylamine containing **5.056** (Entry 3, Table 26, p 162) and tested against PCAF. The rationale behind this was the synthesis of primary amide example **5.053** would require some synthetic commitment and if the solubilising group was not tolerated at the 4-position then there would be no cause for investing time and effort to the synthesis. *N,N*-Dimethyl benzylamine containing **5.056** was found to be equipotent with the unsubstituted aniline compound **5.057** (Entry 2, Table 26, p 162) with a potency at PCAF of 4.4 and therefore a synthesis of primary amide containing **5.053** was undertaken.

The first route attempted commenced with ((4-dimethylamino)methyl)aniline (**5.055**) and was iodinated selectively in the 2-position²⁸⁷ with Barluenga's reagent, a mild iodinating reagent,²⁸⁸ to give iodo **5.058**. The second step, a copper mediated cyanation,²⁸⁹ consumed the starting material and after aqueous work up only NMP was isolated. No further attempts to synthesise nitrile **5.059** were made *via* this 2-iodo methodology (Scheme 50).



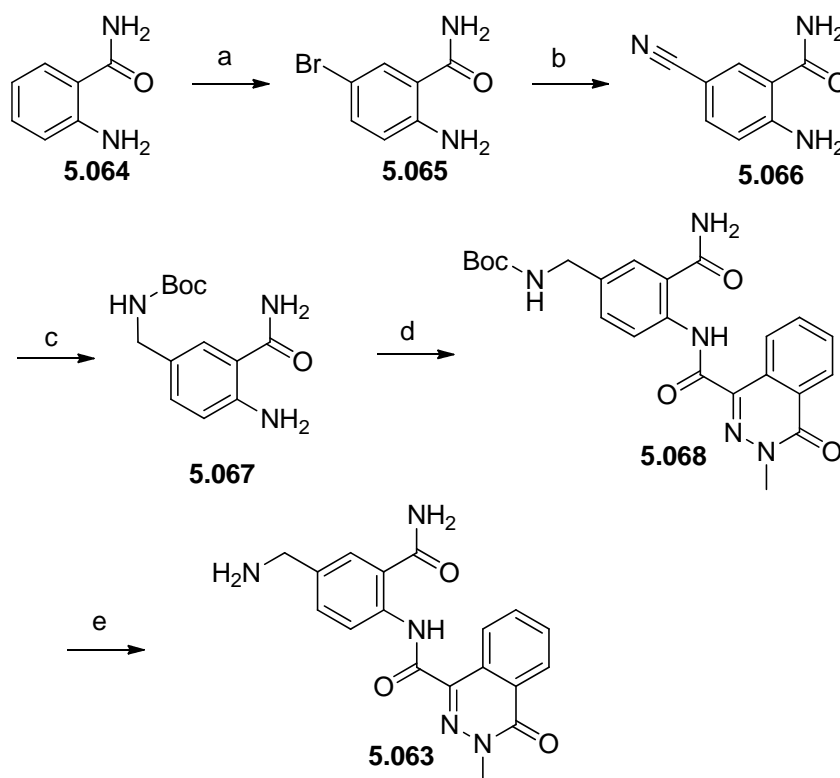
Scheme 50: Reagents and conditions a) Py_2IBF_4 , DCM, 20 °C, 37%; b) CuCN, NMP, 200 °C, 0%.

A second method was employed with the starting material containing a nitrile in place at the 2-position for later hydrolysis to the primary amide. The initial bromination of 2-aminobenzonitrile (**5.060**) with NBS was successful²⁹⁰ to give bromo nitrile **5.061**, as was the subsequent introduction of the tertiary amine using chemistry developed by Molander *et al.* albeit in poor yield.²⁹¹ However, after hydrolysing the nitrile only 12 mg of a solid was isolated, the LCMS of which did not correlate with the desired product (Scheme 51).¹³² An amide coupling with carboxylic acid **5.031** and the putative **5.062** was attempted, which did not provide evidence that the desired amide **5.053** had been formed. Therefore it was assumed that primary amide **5.062** had not been formed in the first instance.



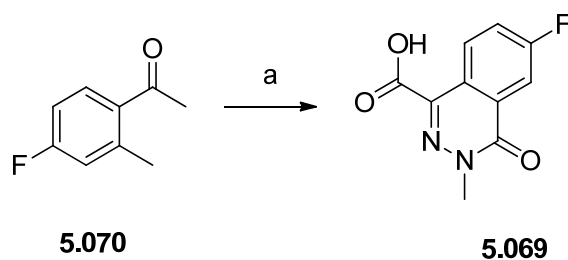
Scheme 51: Reagents and conditions a) NBS, MeCN, 0 – 20 °C, 93%; b) $\text{Me}_2\text{NCH}_2\text{BF}_3\text{K}$, XPhos, $\text{Pd}(\text{OAc})_2$, Cs_2CO_3 , CPME, H_2O , 100 °C, 8%; c) H_2O_2 , K_2CO_3 , DMSO, 20 °C, 0%.

A third method was used to try to access a close analogue of *N,N*-dimethyl benzylamine analogue **5.053**, namely primary amine **5.063**, which lacks the two methyl groups on the benzylamine functionality. Anthranilamide (**5.064**) was brominated with NBS to provide bromo **5.065**. Bromo **5.065** was cyanated with $\text{Zn}(\text{CN})_2$ in the presence of $\text{Pd}(\text{PPh}_3)_4$ to give nitrile **5.066** which was subsequently reduced and Boc protected in one synthetic step to give protected **5.067**. Aryl amine **5.067** could be coupled to carboxylic acid **5.031** using the aforementioned T3P® methodology to give amide **5.068** and finally deprotected with HCl in IPA to provide the test compound **5.063** (Scheme 52).



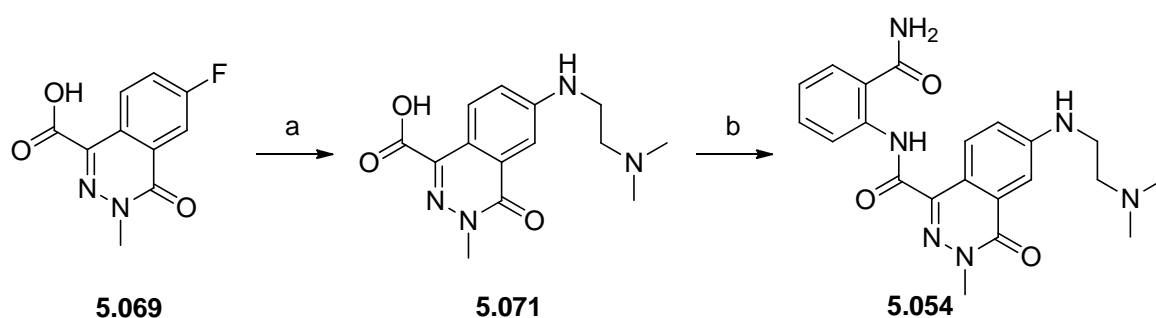
Scheme 52: Reagents and conditions a) NBS, MeCN, 0 – 20 °C, 53%; b) Zn(CN)₂, Pd(PPh₃)₄ 10 mol %, DMF, 150 °C, 87%; c) i) NiCl₂·6H₂O, NaBH₄, MeOH, 0 °C; ii) Boc₂O, 20 °C; iii) HN(CH₂CH₂NH₂)₂, 20 °C, 49%; d) **5.031**, T3P®, DIPEA, DCM, 20 °C, 77%; e) HCl, IPA, 80 °C, 87%.

The next area to investigate was to incorporate a solubilising group at the 6-position of the phthalazinone. The fluoro-phthalazinone intermediate **5.069** was a desirable intermediate so the diamine solubilising group could be installed *via* an S_NAr reaction. 6-fluoro **5.069** was synthesised using the same methodology as des-fluoro **5.031** (Scheme 42, p 149), oxidising 4'-fluoro-2'-methylacetophenone (**5.070**) with KMnO₄²⁷⁸ and condensing with methyl hydrazine (Scheme 53).²⁷³



Scheme 53: Reagents and conditions a) i) KMnO_4 , K_2CO_3 , H_2O , 50 – 70 °C; ii) MeNHNH_2 , AcOH , 70 °C, 39%.

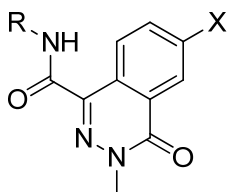
A subsequent $\text{S}_{\text{N}}\text{Ar}$ reaction²⁹² was undertaken with carboxylic acid **5.069** and N^1,N^1 -dimethylethane-1,2-diamine heating at 150 °C in DMSO in the presence of potassium carbonate as a base to give amine **5.071**. An amide forming reaction was undertaken with the most potent and selective headgroup known, 2-aminobenzamide, using T3P® conditions. This provided the desired amide **5.054** in 3% yield (Scheme 54). The yield was low due to a major *N*-acetyl impurity being formed, which was believed to be from acetic acid present in the T3P® solution in ethyl acetate.



Scheme 54: Reagents and conditions a) $\text{NH}_2\text{CH}_2\text{CH}_2\text{NMe}_2$, K_2CO_3 , DMSO, 150 °C, 40%; b) 2-aminobenzamide, T3P®, DIPEA, DCM, 20 °C, 3%.

5.4.8 Assay results of phthalazinones with solubilising groups

The compounds containing solubilising groups were investigated in the biochemical PCAF FP, Brd4 FRET, aqueous solubility assays and compared with other compounds (Table 26).



Entry	Number	R	X	PCAF pIC ₅₀	Brd4 BD1/2 pIC ₅₀	Aqueous solubility µg mL ⁻¹
1	5.027		H	5.0 ^a	< 4.3 / < 4.3	15
2	5.057		H	4.4	4.4 / 4.4	163
3	5.056		H	4.4	< 4.3 / < 4.3	≥ 224
4	5.063		H	5.4	4.6 / < 4.3	7
5	5.054			≤ 4.4	4.8 / < 4.3	≥ 235

Table 26: Potencies and solubilities of compounds at PCAF and BET. ^a) Inactive on 4 of 25 test occasions.

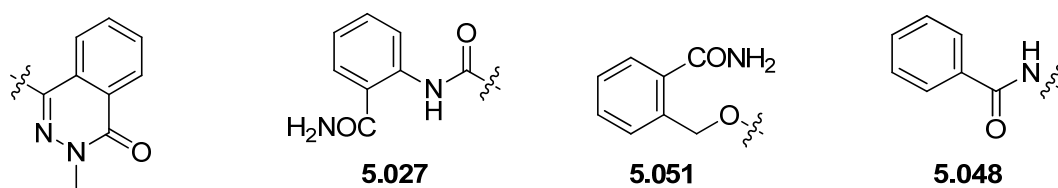
The basic groups increase the aqueous solubility of the compounds compared to those without solubilising groups, except primary amine **5.063** (Entry 4). However, pIC₅₀ values have been generated for both the PCAF and Brd4 assays so the solubility of the compound could be higher under the PCAF FP assay conditions and Brd4 FRET, than in the aqueous solubility assay. This could be caused by the addition of salts and surfactants in the biochemical assays. Primary amine **5.063** does show an increase in potency against benzylamine containing **5.056** and, surprisingly, the original hit **5.027** illustrating again that the primary amide makes a positive binding interaction with the PCAF protein. However,

benzylamine containing **5.063** also brings in Brd4 BD1 potency so solubilising groups from the pendant benzene ring are of no further interest. Why the Brd4 potency has increased is not clear. Primary amine **5.063** may be more soluble under the Brd4 assay conditions than the original phthalizinone compound **5.027** and is able to reach a sufficient concentration. Examination of the inhibition curves at Brd4 or PCAF does not support this hypothesis as the curves had the standard sigmoidal shape (Fig. 73, p 146). This leads to the belief that the amino group must be causing some form of positive binding interaction with the Brd4 BD1 bromodomain.

In substituting from the 7-position of the phthalizinone with an amine the solubility has increased with respect to the original phthalizinone compound **5.027** although the PCAF potency has decreased and tertiary amine **5.054** shows a selectivity bias towards Brd4 BD1 rather than PCAF which is not a desirable profile. Again, there is no obvious explanation as to why the Brd4 BD1 potency is increased and again the argument that the basic group is causing some form of positive binding interaction is likely to be valid.

5.4.9 Phthalizinone conclusion

Thorough SAR of the phthalizinone series could not be generated due to the insolubility of the phthalizinone compounds, which rendered them inactive in the biochemical PCAF assay. The level of insolubility also made them unsuitable as probe compounds as molecules must be in solution to penetrate cellular membranes and interact with proteins in the cell. Investigating different linkers other than the original amide improved solubility of the template, although to the detriment of PCAF potency (Table 27).

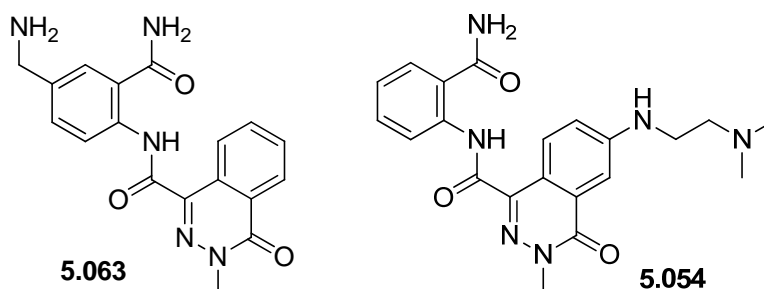


PCAF FP pIC ₅₀	5.0	4.0	< 4.0
Aqueous solubility µg mL ⁻¹	15	≥ 158	≥ 119

Table 27: Changes to the linker improves aqueous solubility of the phthalizinones at the expense of PCAF potency.

The introduction of solubilising groups successfully increased the aqueous solubility of the compounds 15-fold. However, the solubilising groups decreased PCAF potency and

additionally brought in unwanted Brd4 potency. The phthalizinones with solubilising groups **5.063** and **5.054** (Table 28) have been submitted for X-ray crystallography in Brd4 BD1 to try to understand how the basic groups are interacting with the Brd4 bromodomain. However, X-ray crystal structures of these compounds have not been obtained. Although not an aim for this project, the phthalizinones with solubilising groups **5.063** and **5.054** could provide a starting point for BET BD1 selective compounds.

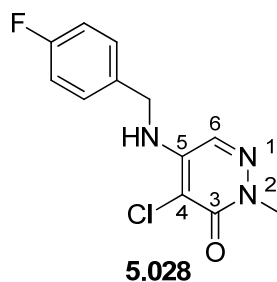


PCAF FP pIC₅₀	5.4	4.4
Brd4 BD1/2 pIC₅₀	4.6 / < 4.3	4.8 / < 4.3

Table 28: Properties of phthalizinone compounds with solubilising groups.

Based on the discussion above, the phthalizinone series was terminated and no further investigation has been carried out. Another series was investigated, the aminopyridazinones, which were more soluble and were reasoned to be better suited for delivering a PCAF probe molecule.

5.5 Aminopyridazinone series



PCAF pIC ₅₀ (LE)	4.7 (0.36)
Brd4 BD1/BD2 pIC ₅₀	≤ 4.9 / ≤ 4.5
MWt	267.7
cLogP	2.1
Aqueous solubility μg mL ⁻¹	≥ 134
Artificial membrane permeability nm s ⁻¹	630

Table 29: Original aminopyridazinone hit from the focused screen with numbering around the aminopyridazinone core.

To identify a probe molecule for the PCAF bromodomain commencing from pyridazinone **5.028**, initial efforts would need to be concentrated around improving the potency of the series and achieving selectivity over the BET family of bromodomains. The aminopyridazinone series is structurally similar to the phthalizinone series in the previous section and it was assumed that they would bind to the PCAF protein in an analogous manner with the methyl group and the carbonyl filling the acetylated lysine binding pocket (Fig. 80). It was also considered possible that the amino group was making a hydrogen bond to Pro747 similarly to the phthalizinone compound **5.052** (Fig. 77, p 156).

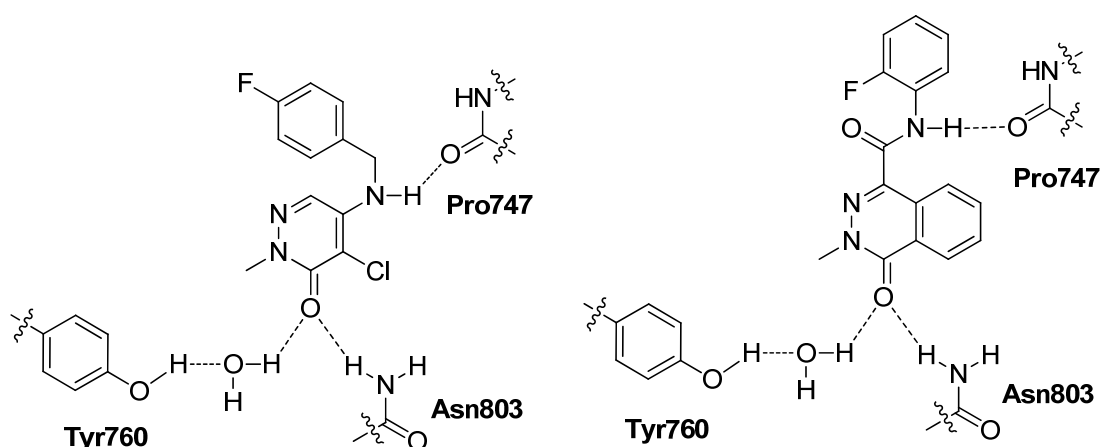


Figure 80: Potential binding mode of aminopyridazinone **5.028** compared to phthalizinone **5.052** in PCAF bromodomain.

An advantage the aminopyridazinone series had over the phthalizinone series was the core contained fewer aromatic rings; one in the aminopyridazinone system versus two in the phthalizinone system. This was attractive as it has been shown that a higher number of aromatic rings within a molecule correlates with a reduction in aqueous solubility.^{293,294} This lower aromatic ring count coupled with fewer amides in the molecule positively impacted on the solubility within the series (Table 29). However, 4-fluorobenzyl **5.028** was not as potent against PCAF as the phthalizinone hit **5.027** from the focussed screen (Table 24, p 144) and showed no selectivity against Brd4. Thus the properties which immediately needed improving upon were PCAF potency and selectivity over Brd4.

There were further examples of aminopyridazinone compounds within the compound collection available in our laboratories and these were assayed against PCAF. From the pIC₅₀ data generated from screening these compounds, broad SAR trends could be observed (Fig. 81).

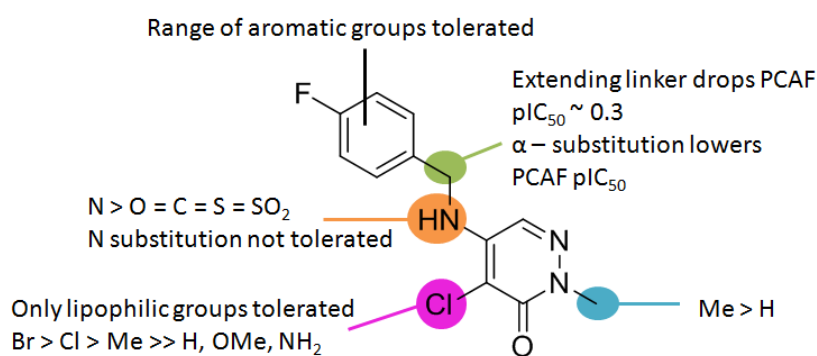


Figure 81: Initial SAR from screening aminopyridazinone compounds from GSK collection.

The SAR from screening the historical aminopyridazinone compounds showed that a wide range of aromatic groups were tolerated from the 5-position of the aminopyridazinone (Table 30, p 170). The linker between the amino group and the aromatic ring was found to be optimal with one methylene group as extending to substituted phenethyl groups caused the pIC₅₀ value to be approximately 0.3 log units lower on average than the benzyl equivalent on a number of examples. α-Methyl substitution at the benzylic carbon was not tolerated and caused the PCAF potency to drop. This is potentially due to the alpha-methyl inducing a conformational twist with the aryl ring which induces a steric clash between the PCAF protein and the test molecule.

The nitrogen linker between the pyridazinone ring was extremely important as substitution with any other atom causing a marked decrease in potency. Additionally, tri-substitution of the nitrogen with either alkyl groups or amides was not tolerated. The loss of potency upon removal of the N-H lends weight to the binding mode proposed in Fig. 80 (p 165). The N-H could be making a key hydrogen bond with the Pro747 of the PCAF protein, which would mean that the 4-chloro was the methyl mimetic of the acetylated lysine. To our knowledge, at the time, this was the first known example of a halogen being a methyl mimetic for bromodomains. While the predicted binding mode was eventually demonstrated by X-ray crystallography (Fig. 85, p 174), Vidler *et al.* have reported 3-chloropyridone compound **5.072** as an inhibitor of Brd4 where the chlorine is the methyl mimetic (Fig. 82).²⁴¹

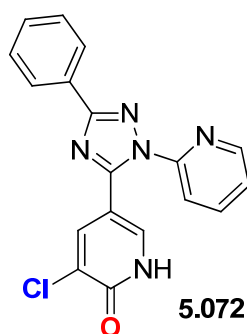


Figure 82: Structure of Brd4 inhibitor **5.072** highlighting the H-bond acceptor in red and the methyl mimetic in blue.

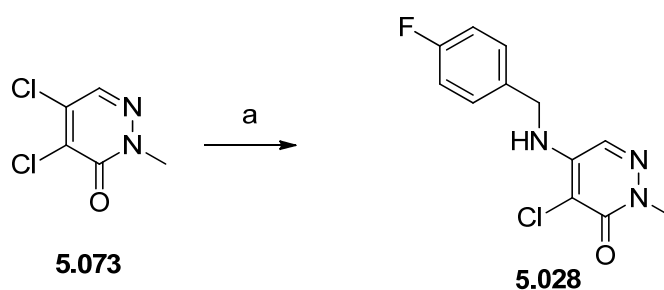
For PCAF potency, 2-methylation of the pyridazinone ring was found to be essential compared to the des-alkylated compound. The unmethylated examples had pIC_{50} values at PCAF of < 4.0. This indicated that there could be a lipophilic pocket which needed to be filled in this position and substitution from this vector is discussed later (Table 32, p 177).

Finally, other heterocyclic ring systems were investigated by other members of our research group. However, none showed the level of potency or chemical tractability needed to make analogues and hence the vast majority of the work was performed on the aminopyridazinone core.

The first area to be investigated involved aromatic analogues at the 5-position of the aminopyridazinone.

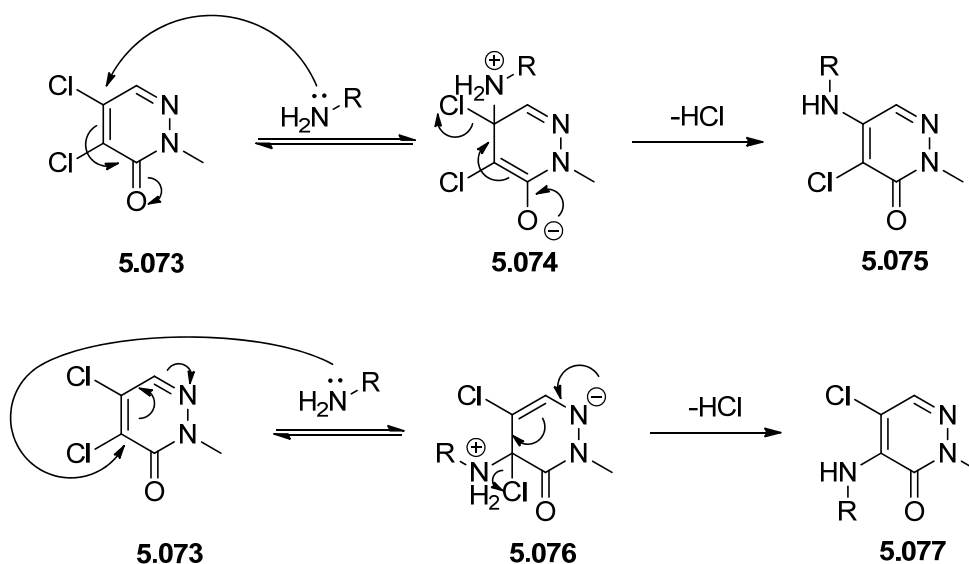
5.5.1 Benzylic aminopyridazinones

Amino analogues based around the group branching from the 5-position of the aminopyridazinone of fluoro **5.028** could be synthesised quickly in large numbers allowing for rapid expansion of SAR. This was achieved using S_NAr chemistry as the dichloropyridazinone ring is sufficiently electron deficient for the initial nucleophilic addition to occur.²⁹⁵ The conditions were optimised though experimenting with different solvents, temperatures and bases. The literature suggests that nucleophilic substitution at the desired 5-position is favoured over substitution at the 4-position in polar solvents and substitution at the 4-position is favoured in apolar solvents.^{295,296,297,298} A general procedure was used to synthesise a wide range of substrates, starting with fluoro **5.028** to confirm the data in Table 29 (Scheme 55).



Scheme 55: Reagents and conditions a) 4-F-C₆H₄CH₂NH₂, DIPEA, DMSO, 120 °C, 57%.

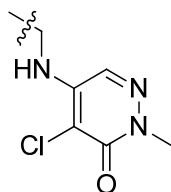
The S_NAr reaction did give a mixture of amino regioisomers substituted at the 4 and 5-positions although the desired 5-aminopyridazinone was always formed in higher abundance than the 4-substituted analogue. The ratio of the regioisomers varied for different amino substrates in the range of about 5:1 to 1.5:1. However, there was no evidence of disubstitution of the pyridazinone occurring as it would appear after having an electron donating amine on the ring the pyridazinone is no longer electron deficient enough to undergo further nucleophilic attack. The relative abundance of the 4- and 5-aminopyridazinones can be explained by considering the mechanism of formation (Scheme 56).



Scheme 56: Mechanisms of formation for the two regioisomers of the aminopyridazinones.

The intermediates of the two regioisomers **5.074** and **5.076** show the negative charge being delocalised to an oxygen and a nitrogen respectively (Scheme 56). The major regioisomer formed, 5-aminopyridazinone **5.075** is the example where the negative charge can be delocalised on to an oxygen, a more electronegative element²⁹⁹ than nitrogen, which the negative charge can only be located on during the formation of the minor regioisomer, 4-aminopyridazinone **5.077**. From the solvent effects on the distribution of the 4- and 5-isomers, intermediate **5.074** would appear to be more stable in polar solvents and **5.076** in apolar solvents.²⁹⁵⁻²⁹⁸

To further investigate the original aminopyridazinone hit **5.028** (Table 29, p 165) substitution from the 5-amino group on the pyridazinone ring was varied in order to establish an improvement in PCAF potency and Brd4 selectivity (Table 30).



Entry	Number	Structure	PCAF FP pIC ₅₀ (LE)	Brd4 FRET BD1/2 pIC ₅₀
1	5.028		4.7 (0.36)	≤ 4.9 / ≤ 4.5
2	5.078*		5.1 (0.39)	≤ 5.6 / ≤ 5.9
3	5.079*		5.0 (0.40)	< 4.3 / < 4.3
4	5.080*		4.8 (0.41)	< 4.3 / < 4.3
5	5.081*		4.8 (0.39)	< 4.3 / < 4.3

Table 30: Potencies of selected aminopyridazinone molecules at PCAF and Brd4.

Although a series of electron withdrawing, electron donating and space filling groups were investigated there was not significant effect on the PCAF potency when putting different substituents around the phenyl ring. Therefore, heteroaromatic rings were incorporated.

Thiophene containing **5.078** (Entry 2, Table 30) had a very similar profile against PCAF compared to the equivalent 4-fluorobenzyl compound **5.028** (Entry 1) which is understandable as a thiophene ring is a bioisostere of a phenyl ring.³⁰⁰ Incorporating heteroatoms into the 5-membered rings significantly lowered the Brd4 activity while maintaining PCAF potency (Entries 3 – 5). 4-Methyl-thiazole example **5.079** (Entry 3) provided the largest selectivity for PCAF over Brd4 seen so far of at least fivefold. Although it is very positive Brd4 activity can be reduced to < 4.3 while retaining PCAF potency, there is not the required increase in potency at the PCAF bromodomain to sub-micromolar levels deemed necessary for a probe molecule.

To better understand the reasons behind the selectivity for some compounds at Brd4, X-ray crystallography at Brd4 BD1 was attempted for the compounds in Table 30 that showed Brd4 activity. Ideally there would be a comparison between the PCAF and Brd4 X-ray

crystal structures. However, obtaining X-ray crystal structures in PCAF with compounds larger than fragments was not successful (*vide infra*, Section 5.5.2, p 173). An X-ray crystal structure of methyl thiophene containing **5.078** was successfully obtained in Brd4 BD1 (Fig. 83).¹⁰³

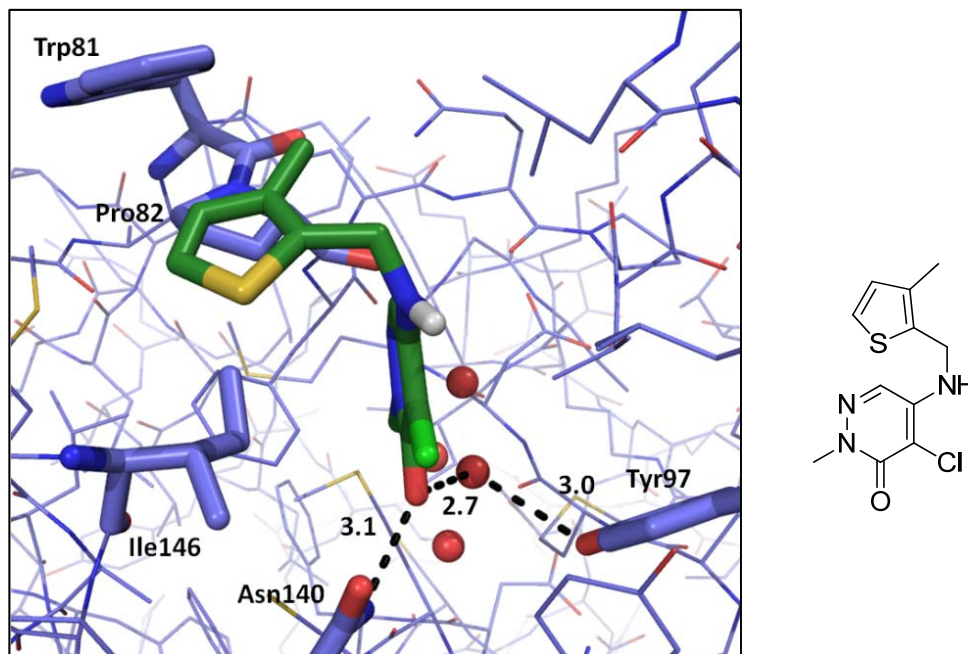


Figure 83: X-ray crystal structure of thiophene containing **5.078** in Brd4 BD1, resolution = 1.6 Å.

The core of the aminopyridazinone is orientated so the methyl group and carbonyl occupy the space that would be filled by the acetylated lysine from the histone tail as seen in the phthalizinone compounds in both PCAF and Brd4. The carbonyl makes H-bonds with Asn140 and a conserved water. There appears to be only one other major interaction between Brd4 BD1 and methyl thiophene example **5.078** which is a lipophilic interaction between the thiophene ring and a lipophilic shelf formed by Trp81, Pro82 and Ile146. There is excellent shape complementarity between the back edge of the methyl thiophene and Trp81 (Fig. 83).

From this X-ray crystal structure it can be seen that the Brd4 selectivity of the polar heterocyclic compounds likely originates from the repulsion of the polar atoms in the heterocycle and the lipophilic shelf. Another point which arises from examining the X-ray crystal structure is the orientation shown here will not allow for the key H-bonding interaction with Pro747 which looked to be essential for the phthalizinone series to bind to

PCAF. The binding mode for methyl-thiophene containing **5.078** is overlaid in PCAF (Fig. 84).

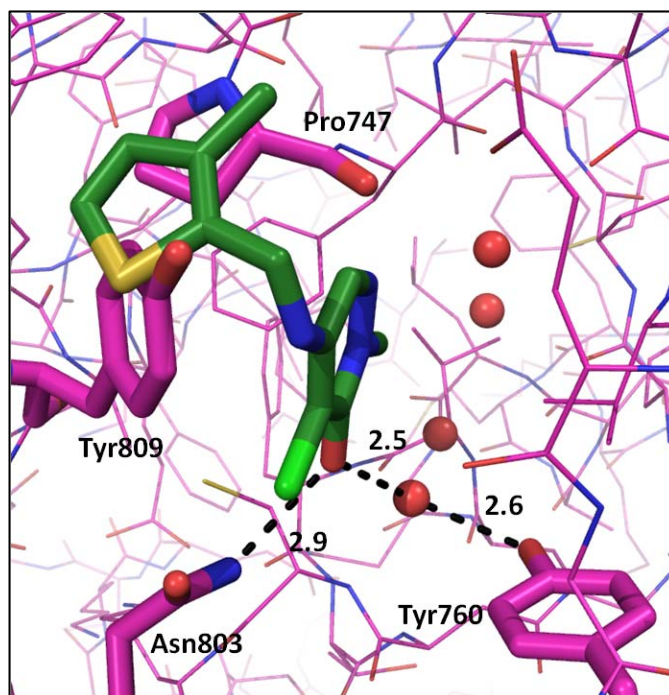
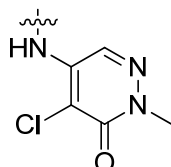


Figure 89: **5.078** in Brd4 BD1, resolution = 1.6 Å, overlaid into PCAF crystal structure, resolution = 2.0 Å.

While certain elements of this overlaid binding mode are plausible around the aminopyridazinone core of the molecule, other parts are definitely inconsistent with how the molecule would bind in PCAF. The carbonyl making H-bonds to Asn803 and a conserved water as well as the methyl group filling the space the methyl in the acetylated lysine originating from the histone tail would occupy are possible. However, the most evidently incorrect part of this overlaid binding mode is the thiophene, which is superimposed with Tyr809. Within PCAF, there does appear to be space for the thiophene group to move away from Tyr809 and occupy other areas of the bromodomain. However, there is no H-bonding interaction in this proposed binding mode with Pro747. Given this was thought to be key for the phthalizinones to bind to PCAF, it placed doubts on the applicability of the binding mode in Fig. 84. A crystal structure of an aminopyridazinone in PCAF would be helpful in determining how compounds in the series bind to the bromodomain and how to improve selectivity and potency.

5.5.2 Fragments bound to X-ray crystal structure of PCAF

The X-ray crystal structure of an apo protein was obtained and it was found that the binding site of the PCAF bromodomain was where two protein molecules met within the unit cell. Therefore, it was reasoned that the pendant aromatic groups from the aminopyridazinone core could be disrupting this crystal contact, either failing to bind into the bromodomain or preventing crystallisation. To solve this, small groups were placed at the 5-position of the aminopyridazinone in place of the aromatic ring (Table 31).



Entry	Number	Structure	PCAF pIC ₅₀ (LE)	Brd4 BD1/2 pIC ₅₀
1	5.082*	H	4.3 (0.59)	< 4.3 / < 4.3
2	5.083*	Me	4.6 (0.57)	≤ 4.4 / ≤ 4.5
3	5.084*	Et	4.6 (0.53)	< 4.3 / < 4.3

Table 31: Potencies of small aminopyridazinone compounds at PCAF and Brd4.

The data shows that the aromatic groups investigated so far are giving very little in terms of PCAF potency and may be offering little in terms of Brd4 selectivity as well. The ligand efficiency (LE) of the molecules in Table 31 is considerably higher than those for marketed drugs, which tends to be approximately 0.3.⁹³ However, to obtain higher levels of potency and selectivity it may be necessary to erode the LE. Given the high level of LE as a starting point this should not cause the LE to fall below 0.3. All of these compounds are showing Brd4 potencies of < 4.3.

An X-ray crystal structure of methyl compound **5.083** bound to PCAF was successfully obtained (Fig. 85).¹⁰³

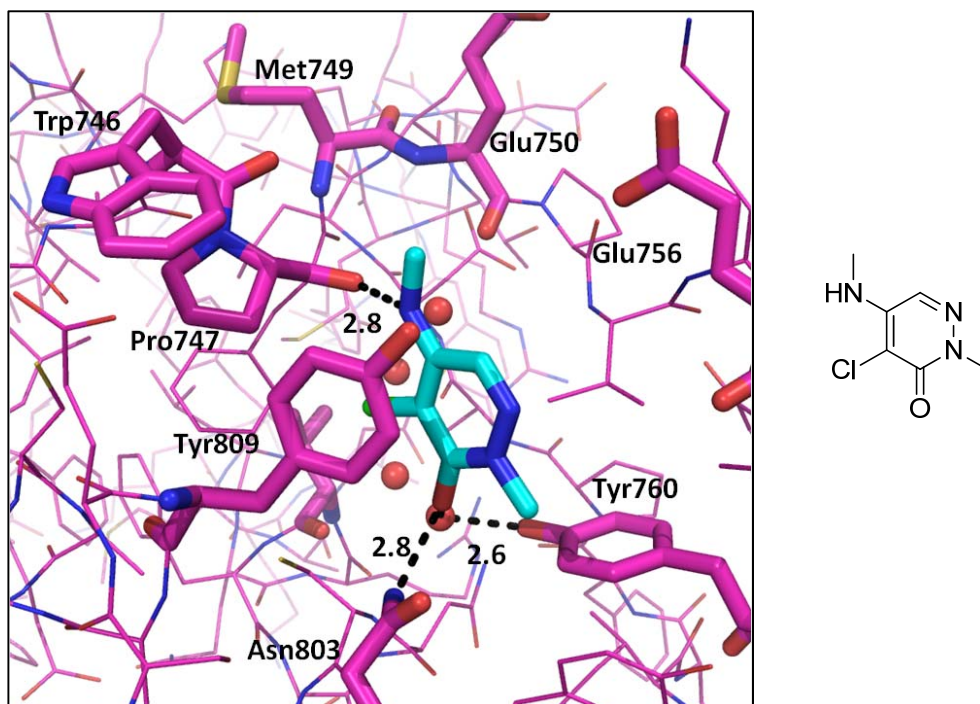


Figure 85: X-ray crystal structure of **5.083** in PCAF, resolution = 1.7 Å.

The binding mode of secondary amine **5.083** in PCAF has flipped 180° compared to the methyl thiophene **5.078** in Brd4 (Fig. 83, p 171). As predicted, the methyl binding pocket has now been filled with a chlorine atom (Fig. 80, p 165). The carbonyl makes H-bonding interactions with Asn803 and a conserved water and there is a face to face aromatic interaction with Tyr809, as there was with the phthalizinone series. There is an H-bond formed between the amino N-H and Pro747 as predicted (Fig. 80, p 165). This H-bond was thought to be vital for the potency at PCAF of the phthalizinone series and thus is expected to be important for the aminopyridazinone series also. It explains why di-substitution of the nitrogen or replacing the nitrogen with another atom is not tolerated in PCAF. Moving out from the amino methyl to the area where, presumably, the pendant aromatic groups shown in Table 30 (p 170) are bound, there is a depression in the surface of PCAF ringed by Trp746, Met 749, Glu750 and Glu756. These amino acid residues presented a good opportunity to probe for H-bonding interactions with the protein.

An X-ray structure of secondary amine **5.083** in Brd4 BD1 was also obtained and the fragment was found to bind in the same orientation as in PCAF (Fig. 86).¹⁰³

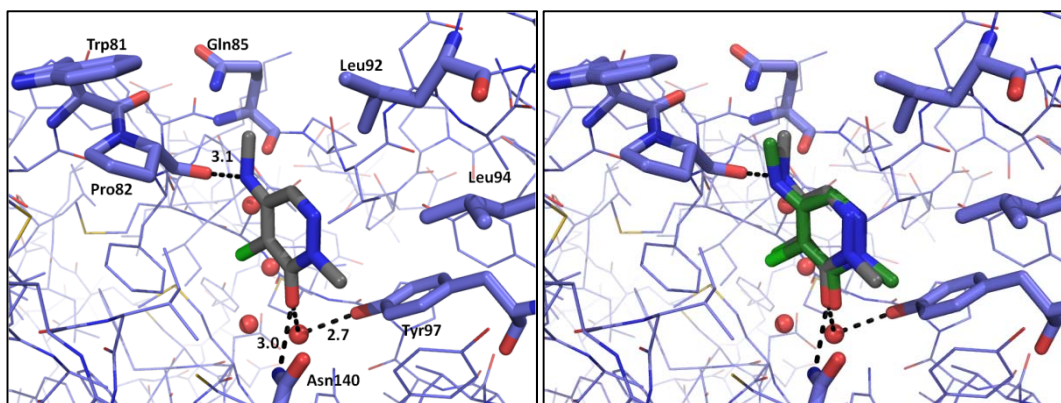


Figure 86: Left: X-ray crystal structure of methyl aminopyridazinone analogue **5.083** in Brd4 BD1 (grey), resolution = 1.6 Å. Right: the binding mode of **5.083** in PCAF overlaid (green), resolution = 1.7 Å.

Methyl aminopyridazinone **5.083** is bound flipped through 180° compared to thiophene example **5.078** in Brd4 BD1 (Fig. 84, p 172). The chlorine atom is in the methyl binding pocket of the acetylated lysine and the carbonyl is making H-bonding interactions to Asn140 and a conserved water. The amino N-H, in this orientation, can form an H-bond with Pro82 of Brd4. From further examination of the X-ray crystal structure it is possible to see why thiophene analogue **5.078** flips through 180° to bind to Brd4 BD1. The area of the Brd4 BD1 protein around the vector from the amino methyl is heavily congested with Trp81, Gln85 and Leu92 all contributing to the steric bulk in this area. Hence, thiophene compound **5.078**, and presumably the molecules with large pendant groups from the 5-position previously discussed, break the H-bond with Pro82 in Brd4 and lay the aromatic groups on the lipophilic shelf (Fig. 83, p 171).

5.5.3 Changes at the 2-position of the aminopyridazinone

Although the binding modes of methyl aminopyridazinone **5.083** are similar in Brd4 BD1 and PCAF, it was noted that a subtle change around the 2-position of the aminopyridazinone between Brd4 and PCAF offered an opportunity to find more selective PCAF compounds. What is Ala757 in PCAF is Leu94 in Brd4 BD1 and hence PCAF may be able to accommodate larger groups from the amidic nitrogen of the pyridazinone ring (Fig. 87).

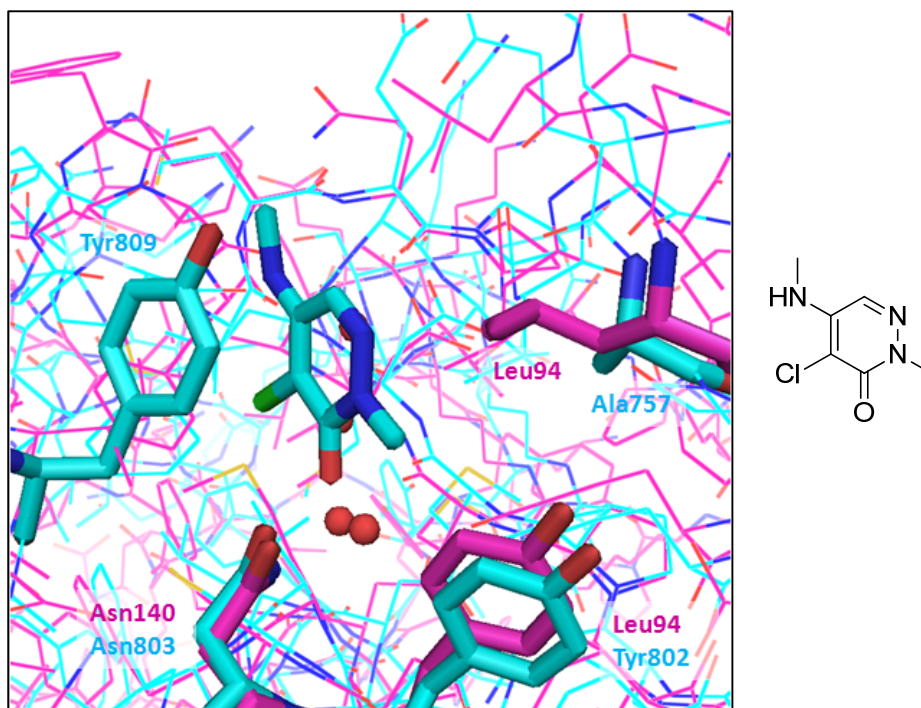
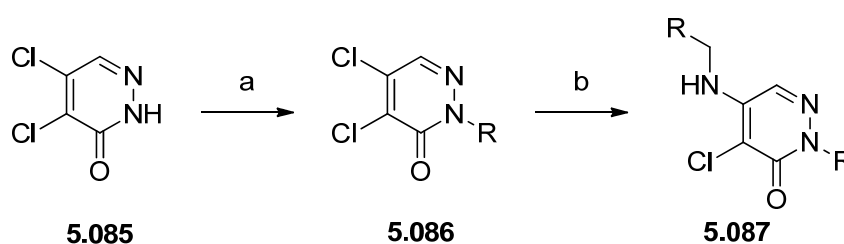


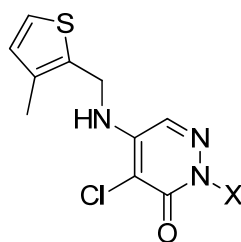
Figure 87: Comparison between the X-ray crystal structures of Brd4 (magenta), resolution = 1.6 Å and PCAF (cyan), resolution = 1.7 Å.

Therefore, compounds were synthesised with differing sterically demanding groups at the 2-position of the aminopyridazinone. One method of the initial synthesis of the core was *via* deprotonation of commercially available dichloropyridazinone **5.085** with sodium hydride and subsequent alkylation with the alkyl halide of choice.³⁰¹ Subsequently, the S_NAr conditions could be utilised to append the amino group of choice at the 5-position (Scheme 57).



Scheme 57: Reagents and conditions a) i) NaH, DMF, 20 °C; ii) R-Hal; b) RCH_2NH_2 , DIPEA, DMSO, 130 °C.

The 5-position group was standardised as the substituted 3-methylthiophene and the group at the 2-position varied. The compounds were assayed against PCAF and Brd4 (Table 32).

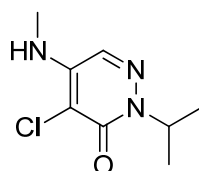
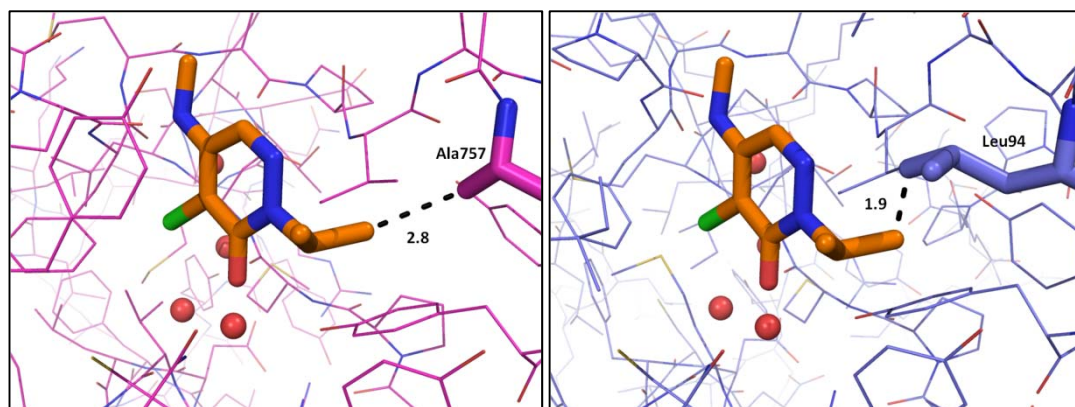


Entry	Number	X	PCAF pIC ₅₀ (LE)	Brd4 BD1/2 pIC ₅₀
1	5.078*	Me	5.1 (0.41)	≤ 5.6 / ≤ 5.9
2	5.088*	Et	4.9 (0.37)	< 4.3 / < 4.3
3	5.090*	<i>i</i> -Pr	5.2 (0.37)	< 4.3 / < 4.3
4	5.119*	<i>c</i> -Pr	4.5 (0.32)	< 4.3 / < 4.3

Table 32: Potencies of aminopyridazinones at PCAF and Brd4.

The data in Table 32 suggest there is an ideal size for the group at the 2-position between methyl and isopropyl for PCAF potency. There is a significant decrease in Brd4 potency as the size of the alkyl group coming from the nitrogen in the pyridazinone increases from methyl. This validates the hypothesis that there is limited space in Brd4 due to the change of an alanine in PCAF to a leucine in Brd4 and this can be used to drive selectivity.

Having substituents which are longer than isopropyl does decrease the PCAF potency with cyclopropyl **5.119** (Entry 4) decreasing the PCAF potency compared to the isopropyl compounds.^{302,303} The selectivity driven by the isopropyl substituted compounds can be seen by comparing the X-ray crystal structure of isopropyl containing fragment **5.091** bound to PCAF with the X-ray crystal structure of Brd4 BD1 (Fig. 88).¹⁰³



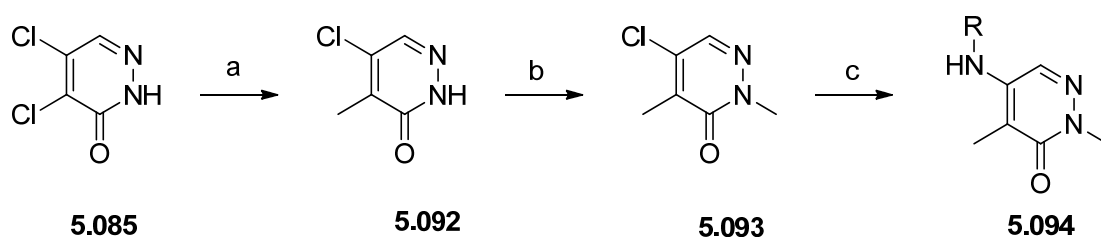
5.091

Figure 88: Left X-ray crystal structure of **5.091** in PCAF (magenta), resolution = 2.1 Å ; Right **5.091** overlaid into Brd4 BD1 (blue), resolution = 1.6 Å.

As can be seen from Fig. 88, one of the methyl groups of the isopropyl would cause a steric clash with Brd4 BD1 as it is only 1.9 Å away from Leu94. This is reflected in the potencies of the compounds with isopropyl substitution. In Brd4 BD1 a considerably different, higher energy conformation would have to be adopted for the isopropyl containing compounds to bind to the bromodomain. With investigation at the 2-position of the aminopyridazinone showing selectivity could be achieved through simple changes, other areas of the aminopyridazinone core were investigated to determine if further selectivity or potency could be derived.

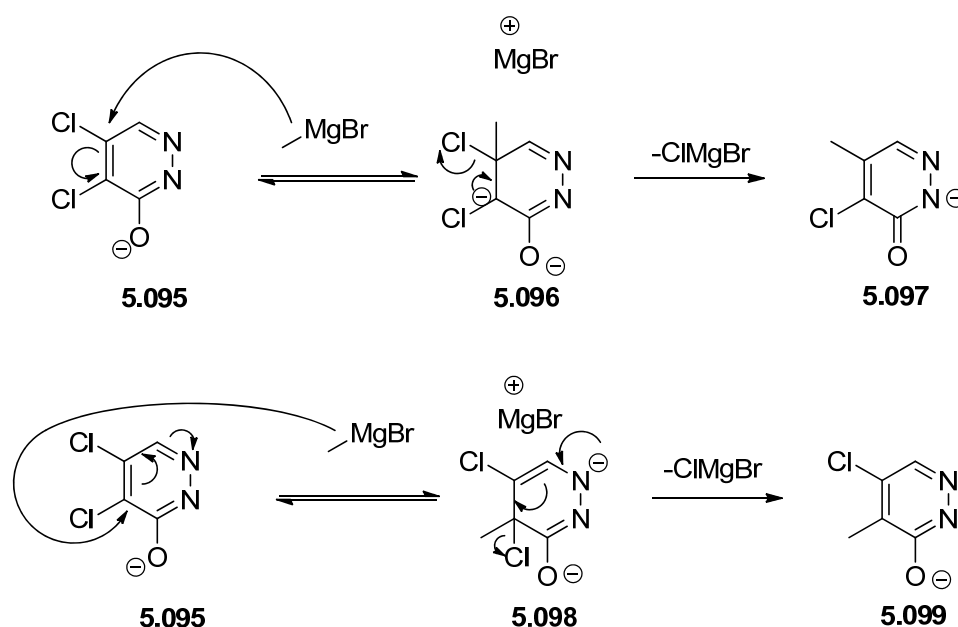
5.5.4 Synthesis of analogues at the 5-position of the 4-methyl-5-aminopyridazinone

4-Methyl aminopyridazinones could be synthesised by treating pyridazinone compound **5.085** with methylmagnesium bromide to give 4-chloro-5-methyl pyridazinone **5.092**.³⁰⁴ This was subsequently alkylated by deprotonating with sodium hydride and quenching with methyl iodide to provide methylated compound **5.093**.³⁰¹ S_NAr conditions were ineffective at appending amines to methyl containing **5.093** as the replacement of an electron withdrawing chlorine with an electron donating methyl meant the pyridazinone core was no longer sufficiently electron withdrawing for S_NAr reactions to occur. Therefore, a palladium catalysed Buchwald-Hartwig amination methodology was used (Scheme 58).³⁰⁵



Scheme 58: Reagents and conditions a) MeMgBr, THF, 0 °C, 78%; b) i) NaH, DMF, 20 °C; ii) MeI, 20 °C, 23%; c) H₂NR, BrettPhos, BrettPhos palladacycle, NaO^tBu, 1,4-dioxane, 100 °C, 7 – 69%.

In contrast to the S_NAr reaction between amines and the dichloropyridazinone (Scheme 55, p 168), the S_NAr reaction with the Grignard reagent³⁰⁶ is much more selective for the 4-substituted isomer. A ratio of 6:1 in favour of the 4-substituted isomer is formed and this can be explained by examining the mechanism (Scheme 59).

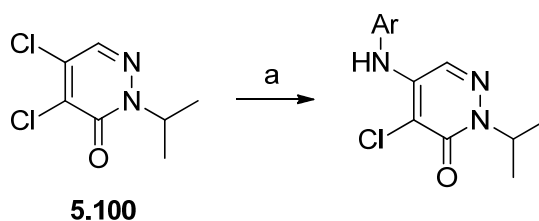


Scheme 59: Mechanism of formation of regioisomers of **5.092**.

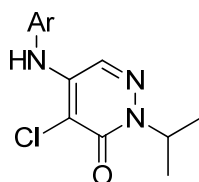
Two equivalents of methylmagnesium bromide are needed for the reaction to occur. The first equivalent presumably deprotonates dichloropyridazinone and a second equivalent can add in a nucleophilic manner at either the 4- or 5-positions. This leads to the formation of two possible intermediates, **5.096** and **5.098**. **5.096** has two negative charges β to each other and is therefore disfavoured in comparison to **5.098** which can place the two negative charges γ to each other.

Another potential reason for obtaining more of the 4-methyl pyridazinone is the reaction is performed in diethyl ether rather than DMSO. Diethyl ether is markedly less polar than DMSO and the solvent polarity has been shown (p 168)²⁹⁶⁻²⁹⁸ to affect the ratio of 4-substitution compared to 5-substitution.²⁹⁵⁻²⁹⁸ Therefore, there may be several contributory factors affecting the product ratio between 4 and 5-substitution with the Grignard reagent.

A number of benzylic analogues of type **5.094** were synthesised and these had a very similar profile to the chloro analogues shown in Table 30 (p 170) albeit with approximately twofold less potency at PCAF. The 4-methyl compounds did not show such high levels of binding at PCAF as the 4-chloro compounds although they did offer an opportunity to synthesise aminopyridazinones with less nucleophilic amines using palladium catalysed Buchwald-Hartwig conditions.³⁰⁷ The coupling of anilines and amino substituted heteroaromatics had been attempted *via* the S_NAr conditions developed for this programme (Scheme 55, p 168) and other conditions.³⁰⁸ However, these only provided sufficient quantities of desired material on one occasion in a poor yield (Scheme 60, Table 33).



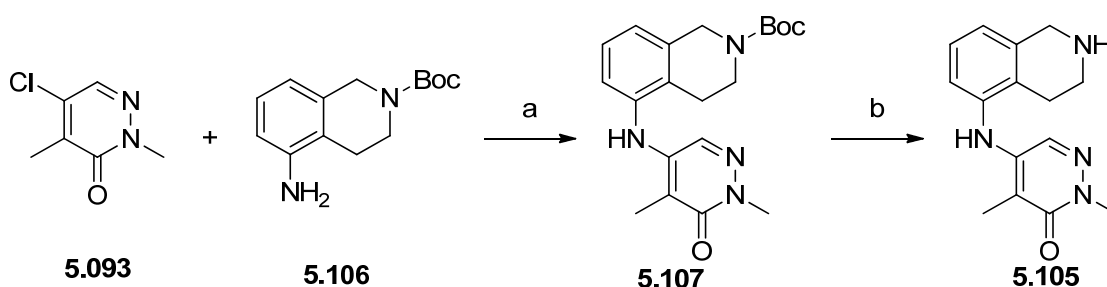
Scheme 60: Reagents and conditions a) $ArNH_2$, See Table 33.



Entry	Number	Aryl	Solvent	Base	Temperature °C	Yield
1	5.101		DMSO	DIPEA	120	3%
2	5.102		DMSO	DIPEA	140	0%
3	5.103		DMSO	DIPEA	140	0%
4	5.104		H ₂ O	-	100	0% Trace seen by LCMS

Table 33: Conditions for S_NAr reactions of aminoaryl compounds.

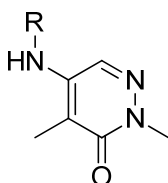
Therefore, there was an opportunity to use palladium catalysed Buchwald-Hartwig aminations to access aromatic aminopyridazinone analogues of the 4-methyl aminopyridazinone.³⁰⁵ The methodology was successful for both aromatic and heteroaromatic compounds (Scheme 61). To couple substrates with more than one amino group, as for the synthesis of tetrahydroisoquinoline containing **5.105**, a protecting group strategy was used. The more nucleophilic, basic amine was subsequently deprotected with a solution of HCl in IPA.



Scheme 61: Reagents and conditions a) BrettPhos, BrettPhos palladacycle, NaO^tBu, 1,4-dioxane, 100 °C, 69%; b) HCl, IPA, 20 °C, 91%.

5.5.5 SAR of analogues at the 5-position of the 4-methyl-5-aminopyridazinone

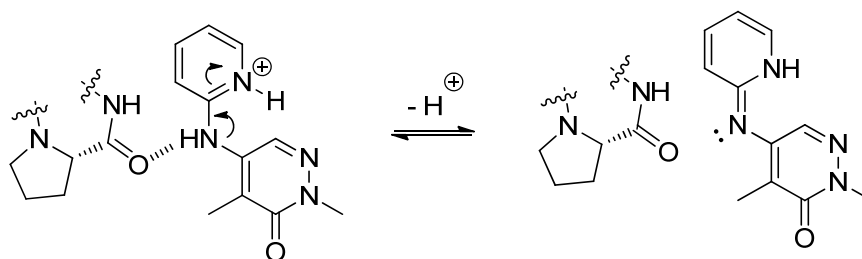
A range of compounds were synthesised to investigate the SAR around the 5-position of the aminopyridazinone. The amines at the 5-position were selected to probe for H-bonding interactions as this had proven successful in improving potency and selectivity in the phthalizinone series. The 2-methyl substituted core was chosen to investigate if Brd4 selectivity could be improved through groups at the 5-position of the aminopyridazinone (Table 34).



Entry	Number	R	PCAF pIC ₅₀ (LE)	Brd4 BD1/2 pIC ₅₀
1	5.108	Ph	4.5 (0.39)	4.6 / < 4.3
2	5.109	2-Pyr	< 4.0	< 4.3 / < 4.3
3	5.110[†]	3-Pyr	4.3 (0.37)	< 4.3 / < 4.3
4	5.111[†]	4-Pyr	< 4.0	< 4.3 / < 4.3
5	5.112*		4.3 (0.27)	4.7 / ≤ 4.6
6	5.113*		4.5 (0.32)	≤ 4.5 / ≤ 4.4
7	5.114*		4.4 (0.25)	4.8 / 4.7
8	5.115*		4.7 (0.28)	5.2 / 4.7
9	5.105		5.2 (0.36)	< 4.3 / < 4.3

Table 34: Potencies of aminopyridazinone compounds at PCAF and Brd4.

Most of the compounds in the table illustrate that the SAR at PCAF and Brd4 of the directly attached aryl compounds is largely unchanged. Phenyl substituted **5.108** (Entry 1, Table 34) shows a similar profile to 4-fluorobenzyl compound **5.028** (Entry 1, Table 30, p 170) albeit with lower potency as could be expected from the 4-methyl pyridazinone core compared to the 4-chloro core. Aniline containing **5.108** shows no selectivity for Brd4 compared to PCAF. The pyridines (Entries 2 – 4) show poor potency at PCAF and the 2 and 4-pyrido compounds, **5.109** and **5.111**, respectively have pIC₅₀ values < 4.0 at PCAF suggesting either basicity is not tolerated in these positions or the tautomer disrupts the H-bond to Pro747 (Scheme 62).



Scheme 62: Potential disruption of the essential H-bond between the 2-pyridyl ligands and Pro747.

The introduction of the primary amide in **5.112** (Entry 4) does not improve upon the PCAF potency as it did in the phthalizinones (Table 26, p 162). The introduction of polar heteroatoms into aromatic rings for isoxazole **5.113** and imidazole **5.114** (Entries 6 and 7) did not provide any Brd4 selectivity as was observed for the thiazoles, furan and pyrazoles (Table 30, p 170) which indicates they cannot bind in the same orientation as thiophene analogue **5.078** (Fig. 83, p 171). Mesityl indoline compound **5.115** (Entry 8) illustrates there is a good degree of space that can be filled from that vector with no negative effects on potency at any of the proteins of interest. Tetrahydroisoquinoline example **5.105** (Entry 9) gave a promising result as it was one of the most potent compounds seen at PCAF in the aminopyridazinone series. Tetrahydroisoquinoline compound **5.105** has Brd4 pIC₅₀ values of < 4.3, which is exciting given that the pyridazinone core is *N*-substituted with a methyl group rather than larger groups usually required for Brd4 selectivity (Table 32, p 177).

Given tetrahydroisoquinoline containing **5.105** was of considerable interest because of the selectivity over Brd4 it was profiled against further bromodomains. Of particular interest was Brd9, which has a tyrosine blocking access to the WPF shelf in the same place as Tyr809

in PCAF.²⁰⁶ Therefore, it was considered that compounds that bound to PCAF might bind to Brd9 (Table 35).

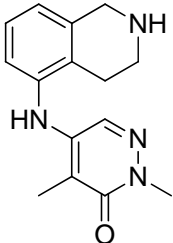
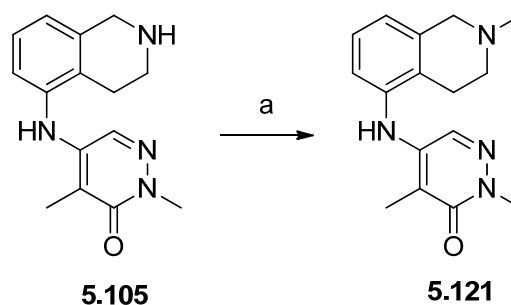
Number	Structure	PCAF pIC ₅₀ (LE)	Brd4 BD1/2 pIC ₅₀	Brd9 pIC ₅₀
5.105		5.2 (0.36)	< 4.3 / < 4.3	6.1

Table 35: Potencies of aminopyridazinone **5.105** at PCAF, Brd4 and Brd9.

The selectivity over Brd9 required improvement as it was, strikingly, eightfold more potent at Brd9 compared to PCAF. However, it was hoped that by iterating from this result it would be possible to find selective PCAF compounds.

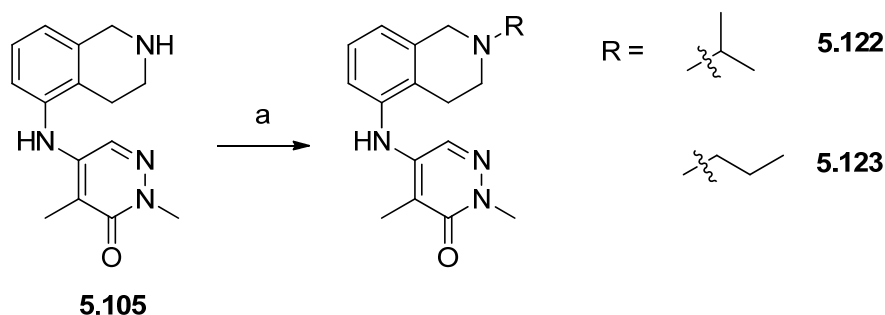
5.5.6 Variations of the tetrahydroisoquinoline containing **5.105**

A series of reductive aminations were performed using tetrahydroisoquinoline containing **5.105** as the starting material to determine if there was any space for expansion from the basic amine within the PCAF protein. These exclusively took place at the tetrahydroisoquinoline nitrogen as the aminopyridazinone nitrogen lone pair of electrons is less nucleophilic as it can be delocalised on to both the phenyl and pyridazinone aromatic rings. Methyl analogue **5.121** was synthesised using Eschweiler-Clarke conditions (Scheme 63).³⁰⁹



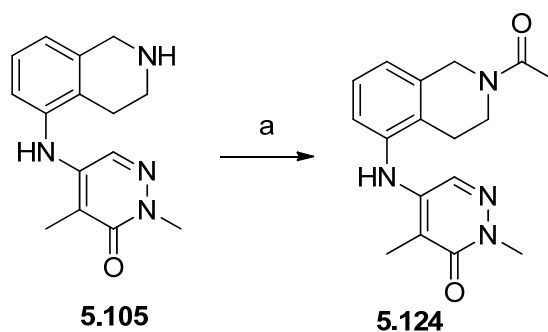
Scheme 63: Reagents and conditions a) aq. CH₂O, HCO₂H, 80 °C, 85%.

Isopropyl analogue **5.122** and *n*-propyl example **5.123** were synthesised using acetone and propionaldehyde, respectively in the presence of sodium triacetoxyborohydride and acetic acid (Scheme 64).³¹⁰



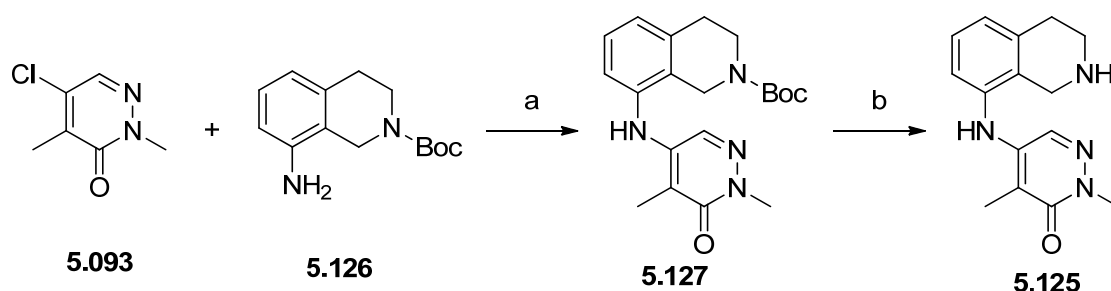
Scheme 64: Reagents and conditions a) $\text{CO}(\text{CH}_3)_2$ or $\text{CH}_3\text{CH}_2\text{CHO}$, $\text{NaBH}(\text{OAc})_3$, AcOH , DCM 20°C , **5.122** 87%, **5.123** 59%.

Acetylated tetrahydroisoquinoline compound **5.124** was synthesised to determine if the basicity of tetrahydroisoquinoline containing **5.105** was causing the increase in PCAF potency and Brd4. Acetyl **5.124** smoothly accessed *via* treating tetrahydroisoquinoline compound **5.105** with acetic anhydride in acetonitrile (Scheme 65).³¹¹



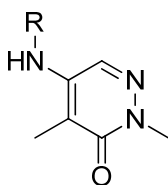
Scheme 65: Reagents and conditions a) Ac_2O , MeCN , 20°C , 69%.

Finally, to establish the effects of altering the position of the basic centre the isomeric tetrahydroisoquinoline compound **5.125** was synthesised using the same protocol as to prepare the original tetrahydroisoquinoline example **5.105** (Scheme 66).



Scheme 66: Reagents and conditions a) BrettPhos, BrettPhos palladacycle, NaO^tBu , 1,4-dioxane, 100°C , 58%; b) HCl , IPA, 20°C , 96%.

Once the tetrahydroisoquinolinyl compounds were synthesised the ligands were profiled against the bromodomains of interest, PCAF, Brd4 and Brd9 (Table 36).



Entry	Number	R	PCAF pIC ₅₀ (LE)	Brd4 BD1/2 pIC ₅₀	Brd9 pIC ₅₀
1	5.105		5.2 (0.36)	< 4.3 / < 4.3	6.1
2	5.107		< 4.0	5.6 / 5.3	6.1
3	5.124		4.1 (0.24)	5.0 / 4.6	6.2
4	5.121		5.5 (0.36)	4.4 / ≤ 4.9	5.7
5	5.122		5.1 (0.30)	< 4.3 / < 4.3	5.9
6	5.123		5.0 (0.30)	≤ 4.4 / ≤ 4.3	6.4
7	5.127		< 4.0	5.7 / 5.5	5.0
8	5.125		5.1 (0.35)	≤ 4.4 / ≤ 4.4	5.4

Table 36: Potencies of tetrahydroisoquinolinyl aminopyridazinone compounds at PCAF, Brd4 and Brd9.

Comparing *tert*-butyl carbamate protected compound **5.107** (Entry 2, Table 36) to deprotected example tetrahydroisoquinoline **5.105** (Entry 1) shows a complete swap in the

selectivity for PCAF compared to Brd4. It was considered possible that the lack of PCAF binding and micromolar Brd4 potency was being driven by the size of the *tert*-butyl carbamate. However, it was deemed more likely that the lack of a basic centre was causing the reversal in selectivity compared to basic **5.105**. Acetyl **5.124** (Entry 3) corroborates that the basic centre is vital for PCAF potency and Brd4 selectivity as comparison with isopropyl compound **5.122** (Entry 5) shows a reversal in the selectivities for PCAF and Brd4. Acetyl **5.124** is tenfold less potent at PCAF than isopropyl example **5.122** and greater than fivefold more potent at Brd4 BD1.

Entries 4-6 were synthesised to investigate the amount of steric bulk which could be accommodated in this area of the protein. Methyl substituted compound **5.121** (Entry 4) shows an increasing in Brd9 selectivity of fivefold compared to unsubstituted **5.105** (Entry 1). However, methyl example **5.121** does show potency, albeit low, at Brd4 which suggests that tetrahydroisoquinoline containing **5.105** pIC₅₀ at Brd4 is only slightly below 4.3. The absolute value could be determined by high concentration screening, although it was considered unnecessary. The more sterically demanding isopropyl compound **5.122** (Entry 5) shows similar PCAF potency of 5.1 to tetrahydroisoquinoline containing **5.105**, although with a lower ligand efficiency. Compared to unsubstituted compound **5.105**, isopropyl analogue **5.122** shows no advantage in Brd4 or Brd9 selectivity. *n*-Propyl example **5.123** (Entry 6) shows no advantages over unsubstituted **5.105** at PCAF or Brd4 and shows twofold less selectivity against Brd9. Comparing unsubstituted **5.105**, methyl **5.121**, isopropyl **5.122**, and *n*-propyl **5.123** illustrates that methyl substitution appears optimal for PCAF binding as it improves upon the PCAF potency of the unsubstituted tetrahydroisoquinoline and the larger propyl compounds reduce PCAF potency.

Altering the position of the nitrogen in the regioisomer of the tetrahydroisoquinoline was investigated with tetrahydroisoquinoline containing **5.127** and **5.123**. *tert*-Butyl protected tetrahydroisoquinoline **5.127** has a similar profile to the regioisomer **5.107** showing no PCAF activity and a pIC₅₀ at Brd4 of 5.7 and 5.5 at BD1 and BD2, respectively. This is likely to be driven chiefly by the lack of basicity with the steric bulk additionally being detrimental to the PCAF potency. However, the Brd9 potency of **5.127** is tenfold lower compared to Boc-protected example **5.107** suggesting that improved Brd9 selectivity could be achieved through substitution at this position. Unsubstituted tetrahydroisoquinoline **5.125** has an approximately equal potency of 5.1 as the tetrahydroisoquinoline regioisomer **5.105** at

PCAF, although it does show less Brd4 selectivity, displaying measurable potency of 4.4 at both BD1 and BD2.

In summary, basicity drives selectivity for PCAF over Brd4. However, basicity appears to have no effect on selectivity for PCAF over Brd9. To help try to explain this tetrahydroisoquinoline containing **5.105** was docked into the crystal structure of PCAF¹⁴⁰ which can be used to explain much of the SAR in Table 36 (Fig. 89).

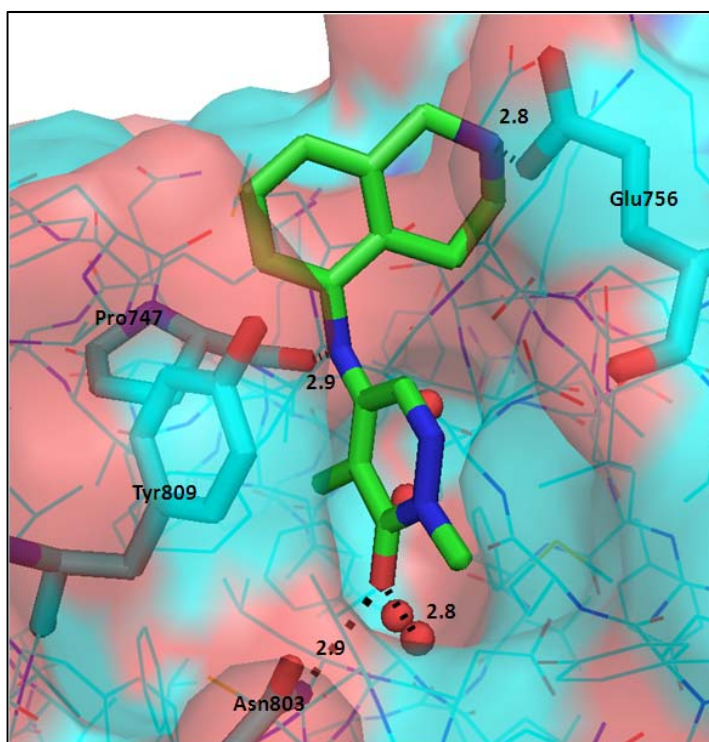
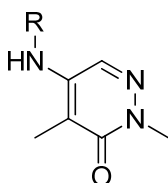


Figure 89: Glide¹⁴⁰ docking of **5.105** in PCAF.

The usual H-bonding and face to face aromatic interactions are present around the aminopyridazinone core and the tetrahydroisoquinoline has good shape complementarity with the protein. It is clear to see the basic centre could make an H-bonding interaction with Glu756 explaining the improved potency of this moiety compared to many other substituents at this position. There is space for methyl substitution from the tetrahydroisoquinoline nitrogen if the ring puckers differently which can explain the increase in potency for *N*-methylated tetrahydroisoquinoline analogue **5.121**. However, larger groups would have to move Glu750 and Lys753 to be accommodated, which indicates why isopropyl compound **5.122** and *n*-propyl analogue **5.123** are less potent. The regioisomer of tetrahydroisoquinoline compound **5.125** could also make an H-bonding

interaction between the basic nitrogen and Glu756 if the ring puckers differently to how it is shown for the tetrahydroisoquinoline regioisomer **5.105** (Fig. 89).

Two aryl amine compounds were synthesised using the methodology described in Scheme 62 (p 183)³⁰⁵ of a palladium catalysed Buchwald-Hartwig amination using the *tert*-butyl protected carbamates and subsequently deprotecting using HCl in IPA, to determine if the bicyclic ring system could be broken open and similar levels of potency at PCAF could be preserved (Table 37).



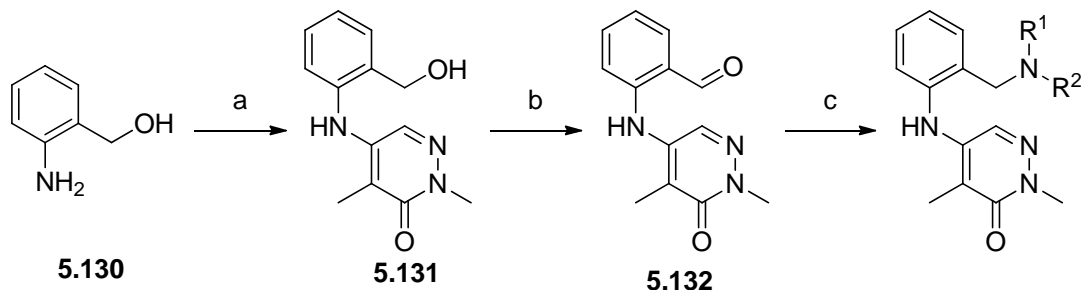
Entry	Number	R	PCAF pIC ₅₀ (LE)	Brd4 BD1/2 pIC ₅₀	Brd9 pIC ₅₀
1	5.128†		4.7 (0.36)	≤ 4.6 ^a / ≤ 5.0 ^a	5.9
2	5.129†		5.3 (0.40)	< 4.3 / ≤ 5.1 ^a	5.2

Table 37: Potencies of aminopyridazinone compounds at PCAF, Brd4 and Brd9. ^a) Active at only 1 of 3 test occasions.

There is a fourfold difference in the potencies of the two benzylamine containing compounds at PCAF. The compounds should place the basic centres in similar positions to the two tetrahydroisoquinoline regioisomers **5.105** and **5.125**. However, 2-benzylamine containing **5.129** (Entry 2, Table 37) should, in solution, have a larger dihedral angle with respect to the aminopyridazinone than 3-benzylamine example **5.128** (Entry 1) due to the 2-substitution on the aniline ring. This will aid making the 79° angle seen in Fig. 89 (p 188) between the aminopyridazinone and the tetrahydroisoquinoline ring. This indicates that exact positioning of the basic centre is crucial for increasing or maintaining PCAF potency. Therefore, no further work was undertaken on 3-substituted benzylamines such as **5.128** and changes around 2-substituted benzylamine compound **5.129** were investigated.

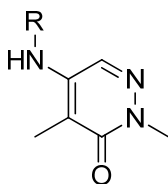
Some of the test compounds to be synthesised could be made through aryl amines, available either commercially or through the compound collection available in our laboratories, whereas others required synthesis. *N*-Substituted benzylamines were

synthesised by coupling benzyl alcohol containing **5.130** with the 4-methyl aminopyridazinone compound **5.093** using palladium catalysed Buchwald-Hartwig conditions³¹² to give primary alcohol **5.131**, oxidising with manganese dioxide to form aldehyde **5.132**³¹³ and finally reductive aminations to give the desired test compounds (Scheme 67).³¹⁴



Scheme 67: Reagents and conditions a) **5.093**, BrettPhos, BrettPhos palladacycle, NaO^tBu, 1,4-dioxane, 100 °C, 40%; b) MnO₂, OC(CH₃)₂, reflux, 73%; c) HNR¹R², NaHB(OAc)₃, AcOH, DCM, **5.133** 44%, **5.134** 8%.

The basic centre containing aryl amines were assayed against PCAF, Brd4 and Brd9 (Table 38).



Entry	Number	R	PCAF pIC ₅₀ (LE)	Brd4 BD1/2 pIC ₅₀	Brd9 pIC ₅₀
1	5.133		4.2 (0.30)	< 4.3 / < 4.3	-
2	5.134		< 4.0	< 4.3 / < 4.3	< 4.3
3	5.135[†]		4.2 (0.30)	< 4.3 / < 4.3	5.2
4	5.131		4.5 (0.34)	4.6 / < 4.3	5.5

Table 38: Potencies of aminopyridazinones at PCAF, Brd4 and Brd9.

Benzylamine analogues **5.133** and **5.134** (Entries 1 and 2, Table 38) suggest that there is insufficient space to accommodate any groups from the basic amine position as there is only a pIC₅₀ value of 4.2 seen for the mono-methylamine compound **5.133** and a pIC₅₀ value of < 4.0 for **5.134**. Interestingly, there is no measurable binding against any of the proteins of interest for dimethyl analogue **5.134**. Extending the basic group two carbons from the phenyl ring in phenethylamine compound **5.135** (Entry 3) did not give good PCAF potency as only a pIC₅₀ value of 4.2 is seen and tenfold greater potency at Brd9. Alcohol **5.131** (Entry 4) further illustrates a basic centre is needed as this compound is six-fold less potent at PCAF than the equivalent benzylamine analogue **5.129**.

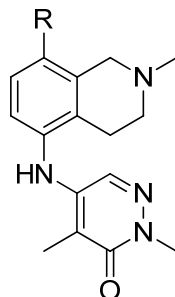
It was believed that some of these examples of aminopyridazinones with basic centres were reaching the upper limit of the FP assay and some compounds could be more potent than the data suggested. *N*-Methylated tetrahydroisoquinoline containing **5.121** was the most potent PCAF compound profiled so far and not fluorescent, an advantage over the base compound used for the PCAF FP assay reagent **5.009** (Fig. 75, p 147). Therefore, work was undertaken elsewhere in our laboratories³¹⁵ to generate an assay able to measure the difference in potency between more potent compounds and, ideally, use the same FRET format assay as used for other bromodomains. This would generally allow pIC₅₀ values to be directly compared without having to convert to pK_s. Although *N*-methylated tetrahydroisoquinoline analogue **5.121** is not selective for PCAF this is not a necessary attribute for an assay reagent as usually there will only one bromodomain present under the assay conditions. Hence, *N*-methylated tetrahydroisoquinoline analogue **5.121** was used as the basis for the synthesis of an improved assay reagent for PCAF.

5.5.7 Generation of an improved PCAF assay reagent

When generating an assay reagent tagged with a fluorophore, based on a known ligand, it is important not to induce a steric clash with the target protein. This is to ensure the assay reagent will bind to the protein of interest.

It was assumed that the *N*-methylated tetrahydroisoquinoline compound **5.121** would bind in the same orientation as the docking of unsubstituted tetrahydroisoquinoline example **5.105** (Fig. 89, p 188). The vector from the 8-position of the THIQ was identified as being unlikely to cause a steric clash with the PCAF protein as it pointed out into solvent. Therefore, substitution was investigated from this position.

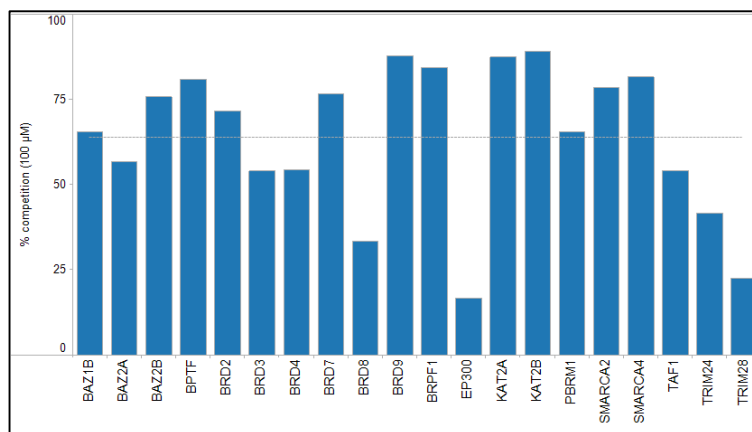
To ensure there would be no steric clash between the protein and the linker or fluorescent tag a phenyl spacer was installed at the 8-position with a Boc-protected amine to give aminopyridazinone example **5.136**. Deprotection of the Boc-group provided **5.137** which was approximately equipotent with Boc-protected compound **5.136** in the PCAF FP assay (Table 39).



Entry	Number	R	PCAF pIC ₅₀ (LE)
1	5.136*		5.6 (0.18)
2	5.137*		5.7 (0.22)

Table 39: PCAF potency profile of assay reagent intermediates.

The potencies of intermediates **5.136** and **5.137** are as high, if not higher, as any compound screened so far at PCAF. This gives confidence that there is no steric clash between the molecules and the PCAF bromodomain. The amine **5.137** was also used in chemoproteomics experiments attached to a solid support and competed with the free amine **5.137** at 100 μ M. This enabled the capture of endogenous PCAF for the first time as well as 19 other BCPs (Graph 7).³¹⁶



Graph 7: BCPs identified using **5.137** attached to a solid support.

Previous chemoproteomic experiments had attempted the pull down of PCAF. However, they had not been successful as the ligands used did not have the necessary level of selectivity over BET. The lack of BET selectivity of the ligands and the comparatively high levels of BET proteins in the nucleus compared to other BCPs it was difficult to identify non-BET bromodomain containing proteins pulled back from the cell lysate.

The amine **5.137** was tagged with the fluorescent tag Alexa Fluor® 647 and the resulting compound **5.138** (Fig. 90) was used to develop a FRET assay for PCAF.

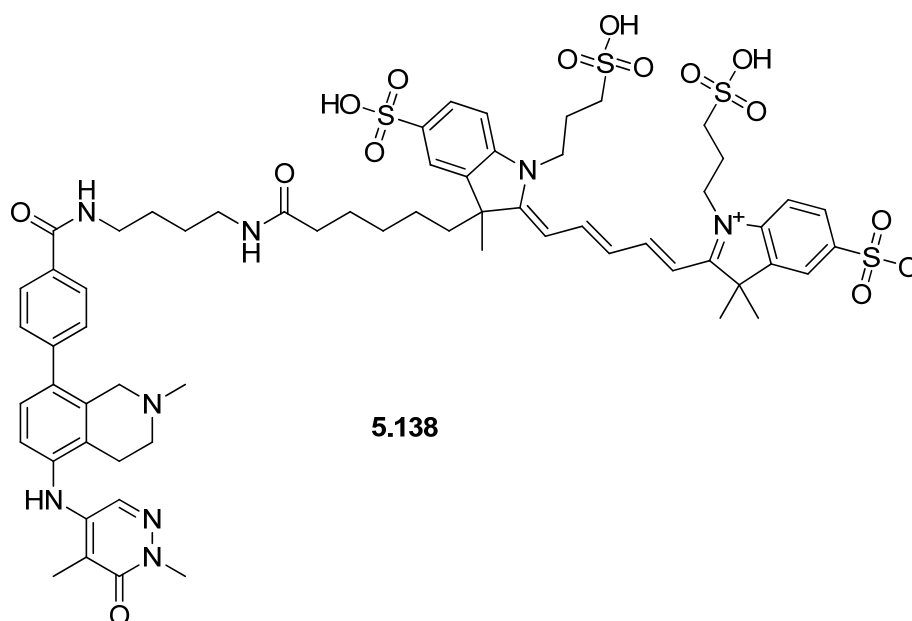


Figure 90: Fluorescent PCAF ligand used for PCAF FRET assay

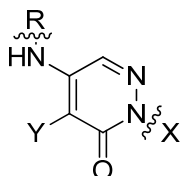
The PCAF assay that was developed using aminopyridazinone **5.138** was also suitable for an HTS as pleasingly the quantity of protein needed was 1000 times lower than for the

previous FP assay. Less protein was needed as the signal to noise ratio of the FRET assay was much higher and the K_d of the ligand to the PCAF bromodomain was 50 nM. Only 8 mg of PCAF protein would be required to screen 1.7 million compounds. The FRET assay had a higher tight binding limit than the FP assay, which enable the differentiation of compounds with pIC_{50} values > 5 (Graph 9, p 215). This allowed the identification of compounds that met the desired probe criteria of a PCAF pIC_{50} value > 6.0 . However, it took several months to optimise the assay and as such most of the pIC_{50} values below were generated using the FP assay.

While the existing tetrahydroisoquinoline aminopyridazinone compounds were of great utility as assay reagents and demonstrated high levels of PCAF potency, they did not provide selectivity over other bromodomains, most notably Brd9. Thus modifications were made to the aminopyridazinone core to try to attain selectivity.

5.5.8 Improving selectivity

The methylated tetrahydroisoquinoline example **5.121** (Entry 4, Table 36, p 186) and 2-benzylamine compound **5.129** (Entry 2, Table 37, p 189) gave the best profiles for PCAF potency and Brd4 selectivity. However, these compounds were approximately equipotent at PCAF and Brd9 so further selectivity was sought using alterations at the 2 and 4-positions of the aminopyridazinone.



Entry	Number	R	X	Y	PCAF FP pIC ₅₀ (LE)	Brd9 pIC ₅₀
1	5.078*		Me	Cl	5.1 (0.41)	6.0
2	5.079*		Me	Cl	5.0 (0.40)	6.0
3	5.090*		<i>i</i> -Pr	Cl	5.2 (0.37)	4.6
4	5.116*		<i>i</i> -Pr	Cl	4.9 (0.35)	4.6
5	5.117*		Me	Me	4.8 (0.37)	6.4
6	5.118*		Me	Cl	5.0 (0.38)	6.0
7	5.119*		Me	Me	4.7 (0.38)	6.0
8	5.120*		<i>i</i> -Pr	Me	4.6 (0.33)	4.6

Table 40: Pairwise comparisons of PCAF and Brd9 pIC₅₀ values altering groups at the 2 and 4- positions of the aminopyridazinone ring.

Through screening previously synthesised compounds it was shown that an isopropyl group at the 2-position of the aminopyridazinone helped to improve PCAF selectivity by

approximately twenty five-fold (Entries 1 and 3; 2 and 4, Table 40) compared to a methyl group. Also, having discharged the chemical instability risk of the 4-chloro aminopyridazinone compounds, they were reinvestigated. It was found that changing the 4-methyl to a 4-chloro improved the selectivity for PCAF over Brd9. This was accomplished by improving the PCAF potency while maintaining or reducing binding to Brd9 (Entries 5 and 6; 1 and 7; 3 and 8).

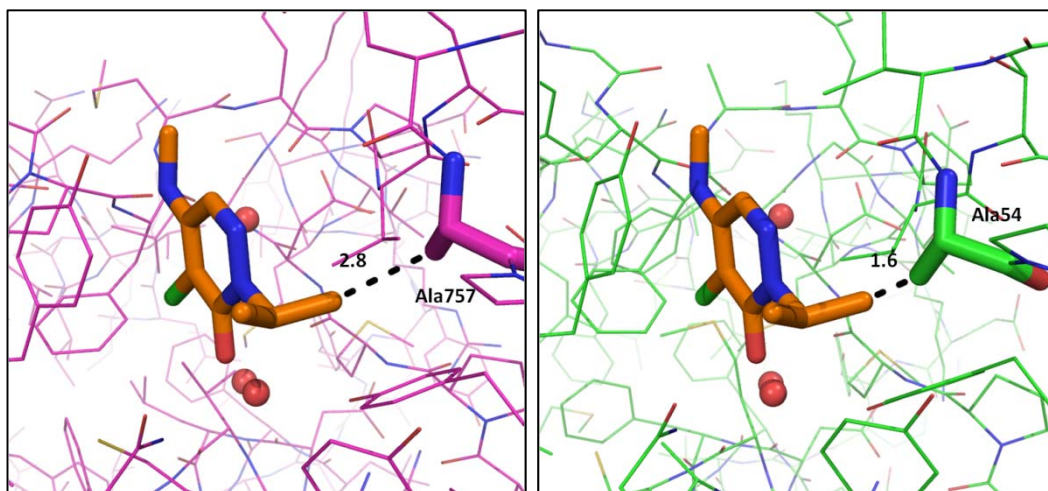


Figure 91: Left: X-ray crystal structure of 4-chloro-2-isopropyl-5-(methylamino)pyridazin-3(2H)-one (**5.091**) in PCAF, resolution = 2.1 Å; Right: overlaid into Brd9, resolution = 1.7 Å.

From the crystal structures of fragment **5.091** in PCAF and Brd9 (Fig. 91) it is possible to see that there is a greater potential for steric clash between the isopropyl group and the Brd9 bromodomain than the PCAF bromodomain.¹⁰³ Herein lies the cause of the 2-isopropyl aminopyridazinones being more potent at PCAF than Brd9.

Changing the group at the 4-position from a methyl to a chlorine has very little effect on the Brd9 potency. However, the 4-chloro compounds were more potent than the 4-methyl compounds at PCAF (Table 40).

Therefore, the combination compound **5.139** was selected as a target (Fig. 92).

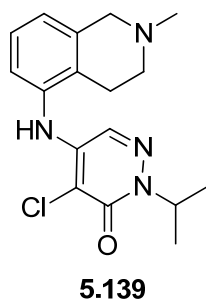
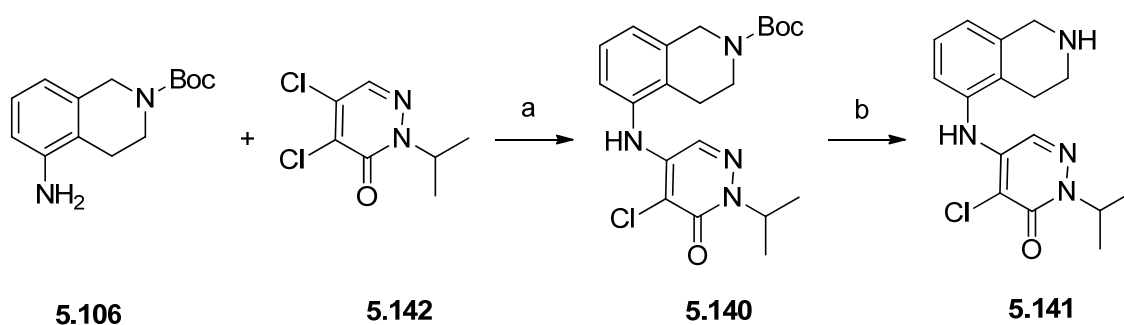


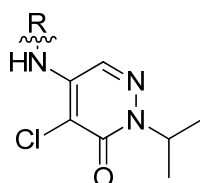
Figure 98: Combination aminopyridazinone to improve selectivity for PCAF over Brd4 and Brd9.

The compound was synthesised using the same palladium catalysed Buchwald-Hartwig conditions as used previously to synthesise the 4-methyl compounds³⁰⁵ and a 1:1 ratio of the 4 and 5-substituted aminopyridazinone was seen by LCMS in the crude reaction mixture. The desired 5-aminopyridazinone **5.140** was isolated in 7% yield and subsequently the *tert*-butyl carbamate removed with HCl in IPA to give **5.141** (Scheme 68). This provided sufficient tetrahydroisoquinoline containing **5.141** for assaying, although not enough to be confident that the subsequent methylation would give enough **5.139** for test so the reaction was not attempted.



Scheme 68: Reagents and conditions: a) BrettPhos, BrettPhos palladacycle, NaO^tBu, 1,4-dioxane, 100 °C, 7%; b) HCl, IPA, 87%.

When tested at the bromodomains of interest tetrahydroisoquinoline compound **5.141** gave some interesting results (Table 41).



Entry	Number	R	PCAF pIC ₅₀ (LE)	Brd4 BD1/2 pIC ₅₀	Brd9 pIC ₅₀
1	5.141		4.9 (0.31)	< 4.3 / < 4.3	4.4

Table 41: Potency of **5.141** at PCAF, Brd4 and Brd9.

The potency of isopropyl **5.141** for PCAF compared to Brd9 was, for the first time in an aminopyridazinone compound, threefold higher and larger than experimental error. However, the potency of tetrahydroisoquinoline containing **5.141** was lower than expected at PCAF as previously the isopropyl had no effect on PCAF potency and the 4-chlorine usually gave an approximate twofold increase in potency.

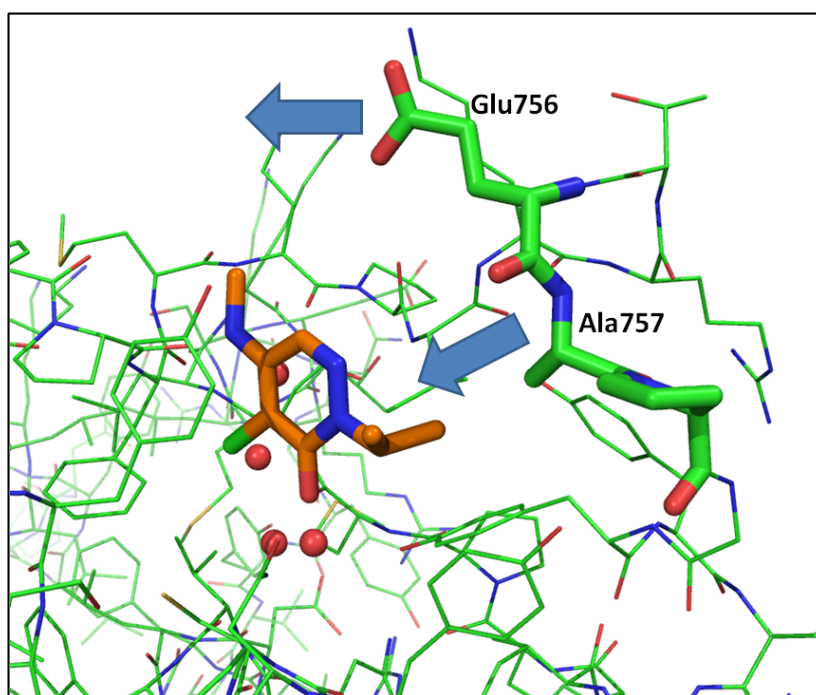


Figure 93: Movement of the highlighted chain means the isopropyl group is not tolerated, resolution = 2.1 Å.

The hypothesis for this loss in expected potency was that the interaction of the tetrahydroisoquinoline pulls Glu756 towards the ligand and this movement causes the local peptide chain to move towards the bound ligand (Fig. 93).¹⁰³ In doing so, the space around

the isopropyl group is made smaller. The bulky isopropyl group is no longer tolerated due to steric clash with Ala757. Therefore, as the 2-methyl substituted aminopyridazinone core is smaller, it was considered to be more tolerant of the predicted conformational change brought by introducing a basic centre. Compounds incorporating both a basic centre and a 2-methyl substituted aminopyridazinone core were designed and planned for synthesis to improve potency and selectivity over Brd4 (Fig. 94).

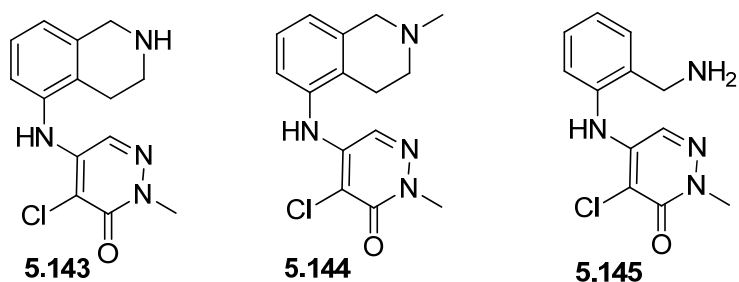
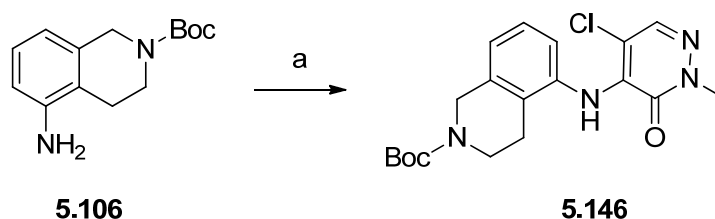


Figure 94: Compounds selected to improve potency at PCAF compared to isopropyl **5.141**.

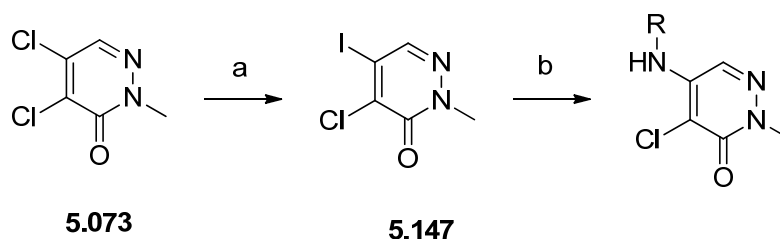
Regioselective substitution of chloropyridazinones by aromatic amines was still a problem. Several different sets of palladium catalysed Buchwald-Hartwig amination conditions were investigated. Unfortunately, conditions which gave an excess or even a 1:1 mixture of the desired 5-amino substituted products compared to the 4-amino substituted products were not identified. S_NAr reactions using the standard conditions (Scheme 55, p 168) gave none of the desired product. Therefore, S_NAr conditions were found to improve the nucleophilicity of Boc-protected compound **5.106** by deprotonating with LiHMDS. This methodology had been demonstrated on similar substrates.^{317,318} However, exclusively 4-aminopyridazinone compound **5.146** was formed (Scheme 69).



Scheme 69: Reagents and conditions a) i) LiHMDS, THF, -70 – -5 °C; ii) **5.073**, -70 – 20 °C, not isolated.

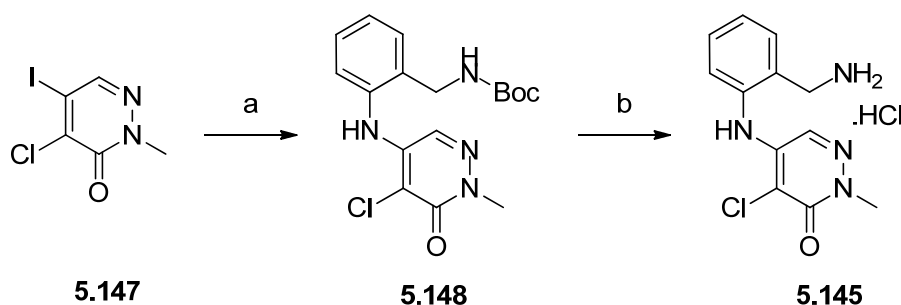
An alternative method was needed and the palladium catalysed Buchwald-Hartwig amination was revisited as it did provide some of the desired 5-substituted aminopyridazinones. To date, there had been no investigation into modification of the aryl

halide to alter the regioselectivity. If a halogen or pseudo-halogen could be incorporated at the 5-position of the pyridazinone ring that underwent oxidative addition more easily than the 4-chloro then under palladium catalysed amination conditions the desired 5-aminopyridazinone would be preferentially formed. Palladium oxidatively inserts into aryl-iodide bonds more easily than aryl-chloride bonds.³¹⁹ 4-Chloro-5-iodo-2-methylpyridazin-3(2*H*)-one (**5.147**) was synthesised *via* an aromatic Finkelstein reaction.³²⁰ Subsequently, successful palladium catalysed Buchwald-Hartwig aminations with anilines³¹⁸ were performed to exclusively provide 5-aminopyridazinone compounds (Scheme 70).



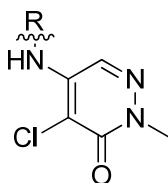
Scheme 70: Reagents and conditions a) NaI, DMF, 150 °C, 56%; b) RNH₂, BINAP, Cs₂CO₃, Pd(OAc)₂, PhMe, 80 °C.

Methylated tetrahydroisoquinoline **5.144** was synthesised directly using this method. Other examples had to be synthesised using a protecting group strategy. *tert*-Butyl carbamate 2-benzylamine containing **5.148** was synthesised using the palladium catalysed Buchwald-Hartwig amination in 14% yield and subsequently deprotected using a solution of HCl in IPA to provide the desired compound **5.145** as the HCl salt (Scheme 71).



Scheme 71: Reagents and conditions: a) *tert*-butyl 2-aminobenzylcarbamate, BINAP, Cs₂CO₃, Pd(OAc)₂, PhMe, 80 °C, 14%; b) HCl, IPA, 20 °C, 81%.

The target compounds were assayed against PCAF, Brd4 and Brd9 (Table 42).



Entry	Number	R	PCAF pIC ₅₀ (LE)	Brd4 BD1/2 pIC ₅₀	Brd9 pIC ₅₀
1	5.143		5.3 (0.33)	< 4.3 / < 4.3	5.8
2	5.144[†]		5.6 (0.33)	< 4.3 / ≤ 4.8 ^a	5.6
3	5.145		5.5 (0.42)	< 4.3 / ≤ 4.4	4.9

Table 42: Potencies of 4-chloro-5-aminopyridazinones at PCAF, Brd4 and Brd9. ^a) Inactive on 12 of 13 occasions.

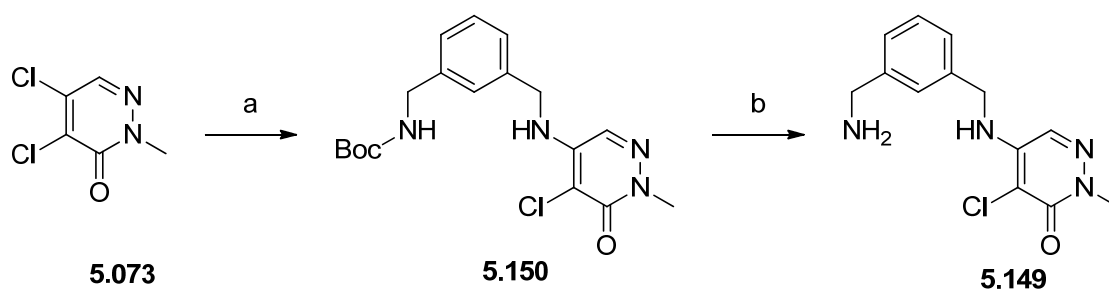
The 4-chloro compounds show a minor increase in PCAF potency; in general a minor decrease in Brd9 potency compared to the 4-methyl compounds and no Brd4 potency > 4.3. This is broadly consistent with the SAR seen when changing from the 4-methyl to the 4-chloro aminopyridazinones. The ranking of potency between the methyl and chloro examples with the R groups shown in Table 42 is consistent. Unsubstituted 4-methyl tetrahydroisoquinoline compound **5.105** (Entry 9, Table 34, p 182) and unsubstituted 4-chloro tetrahydroisoquinoline compound **5.143** (Entry 1, Table 41, p 198) are the least potent. In the 4-methyl series benzylamine analogue **5.129** (Entry 2, Table 37, p 189) is the next most potent, followed by *N*-methyl tetrahydroisoquinoline compound **5.121** (Entry 4, Table 36, p 186). The ranking does follow in the 4-chloro series with *N*-methyl tetrahydroisoquinoline example **5.144** found to be more potent than benzylamine analogue **5.145**. However it was suspected that the tight binding limit of the FP assay had been reached, which was found to be the case upon screening the compounds in Table 43 (p 203) in the PCAF FRET assay.

Although, benzylamine compound **5.145** shows the best profile seen so far with fourfold selectivity over Brd9, it does not meet the probe criteria needed of greater than micromolar potency at PCAF or greater than 30-fold selectivity over other bromodomains. It was not obvious how to progress with aryl amine compounds to find the shift needed in

PCAF potency and Brd9 selectivity. There was also the possibility that the tetrahydroisoquinoline containing compounds could have significant selectivity issues. This was highlighted by the BCPs identified to bind to tetrahydroisoquinoline containing **5.137** using chemoproteomic experiments (Graph 7, p 193). Therefore, an array of more diverse 5-aminopyridazinones containing basic nitrogens was synthesised. The aim was to try to interact with the glutamic acids in the binding site as basic centres had been seen to be beneficial for PCAF potency and Brd4 selectivity.

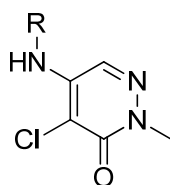
5.5.9 Basic aminopyridazinones

The S_NAr methodology used to synthesise the benzyl 5-aminopyridazinones (Scheme 55, p 168) was used to synthesise these compounds.²⁹⁵ Compounds protected with *tert*-butyl carbamates were deprotected with HCl in IPA as shown for the synthesis of benzylamine example **5.149** (Scheme 72).



Scheme 72: Reagents and conditions a) 1-(*N*-Boc-aminomethyl)-3-(aminomethyl)benzene, DIPEA, DMSO, 120 °C, 60%; b) HCl, IPA, 20 °C, 91%.

The first compounds to be investigated were intended to see if the postulated interaction with Glu756 and the tetrahydroisoquinoline substituted aminopyridazinone compounds could be found with other groups. The acetyl lysine binding site contains another more distant acidic residue, Glu750, and it was of interest if any of the target compounds could interact with this residue as well as with Glu756 (Table 43).



Entry	Number	R	PCAF pIC ₅₀ (LE)	Brd4 BD1/2 pIC ₅₀	Brd9 pIC ₅₀
1	5.151*		4.7 (0.31)	≤ 5.0 ^a / < 4.3	6.0
2	5.149†		4.5 (0.32)	< 4.3 / < 4.3	5.9
3	5.152†		4.3 (0.31)	< 4.3 / < 4.3	5.6
4	5.153†		4.8 (0.51)	< 4.3 / < 4.3	4.4
5	5.154†		4.8 (0.44)	< 4.3 / < 4.3	-
6	5.155†		5.0 (0.49)	< 4.3 / < 4.3	4.5
7	5.156†		4.6 (0.39)	< 4.3 / < 4.3	< 4.3
8	5.157†		4.6 (0.42)	< 4.3 / < 4.3	4.7

Table 43: Potencies of 4-chloro-5-aminopyridazinones at PCAF, Brd4 and Brd9. ^a) Inactive at 3 of 4 occasions.

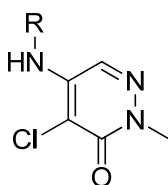
The inclusion of basic centres significantly reduces the Brd4 activity across all the compounds assayed. This is a marked change and identifies a simple and powerful way to provide BET selective compounds. This selectivity likely occurs as the lipophilic WPF shelf present in the BET family of BCPs (Fig. 64, p 135) does not accommodate polar substituents (Table 30, p 170).

2-Substituted benzylamine example **5.151** (Entry 1, Table 43) is equipotent with the 4-fluorophenyl ring containing **5.080** (Entry 4, Table 30, p 170) which indicates that the basic centre is making no positive interactions with the PCAF protein. 3-substituted compound **5.149** (Entry 2, Table 43) and 4-substituted analogue **5.152** (Entry 3) progressively shed

potency compared to phenyl containing **5.151** as the benzylamine is moved around the ring suggesting there may be limited space in this area of the protein. The lack of an increase in potency at PCAF and the, at least, tenfold higher potency at Brd9 led to no further aromatic compounds being synthesised.

Interestingly the removal of the aryl ring significantly reduces the Brd9 potency. The aliphatic chains terminating in basic amines gave a very exciting set of results. Ethylamine compound **5.153** (Entry 4) shows a similar level of PCAF potency compared to the 4-fluorophenyl ring compound **5.080** (Entry 1, Table 30, p 170) and two and half-fold selectivity over Brd9. Due to the lower number of heavy atoms the level of ligand efficiency is impressive. *N,N*-Dimethyl ethylamine analogue **5.154** (Entry 5, Table 43) shows no improvement in PCAF potency compared to the primary amine containing **5.153**. However, it suggests there is space for substitution from the basic centre. Propylamine containing **5.155** (Entry 6) improves upon the PCAF affinity shown by the ethylamine analogues **5.153** and **5.154** and has threefold selectivity over Brd9. *N,N*-Dimethyl propylamine containing **5.156** (Entry 7) causes the PCAF potency to fall two and half fold in comparison to the demethyl propylamine compound **5.155**. Possibly, there is insufficient space to accommodate the steric bulk introduced by the two methyl groups. Butylamine analogue **5.157** (Entry 8) shows a two and a half-fold fall in PCAF affinity in comparison to the propylamine containing **5.155**. This suggests that two or three carbons from the 5-aminopyridazinone is the optimal distance for the basic centre. However, this could possibly change on introducing aliphatic and heterocyclic rings to the aminopyridazinone.

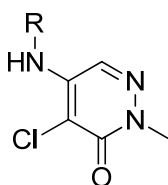
Cyclising the aliphatic chain will reduce the number of rotatable bonds and therefore reduce the entropic penalty of binding the ligand to PCAF^{321,322} thereby increasing the potency of the ligand if the basic centre can be positioned correctly. Hence, a number of basic aliphatic and heterocyclic compounds were synthesised and screened against the proteins of interest (Tables 44 and 45). The compounds have the greatest degree of selectivity observed thus far. Only one compound shown has Brd9 potency > 4.2 and there are no Brd4 pIC₅₀s > 4.2 observed for any of the compounds.



Entry	Number	R	PCAF pIC ₅₀ (LE)	Brd4 BD1/2 pIC ₅₀	Brd9 pIC ₅₀
1	5.158*		4.8 (0.41)	< 4.3 / < 4.3	< 4.3
2	5.159*		4.3 (0.35)	< 4.3 / < 4.3	4.5
3	5.160*		4.8 (0.39)	< 4.3 / < 4.3	< 4.3
4	5.161*		5.0 (0.38)	< 4.3 / < 4.3	4.3

Table 44: Potencies of 5-chloro-4-aminopyridazinones at PCAF, Brd4 and Brd9.

Pyrrolidine analogue **5.158** (Entry 1, Table 45) shows a reasonable PCAF pIC₅₀ of 4.8, although this is no improvement on the simple ethylamine compound **5.153** (Entry 4, Table 43, p 203). Expanding the ring to the 4-piperidine example **5.159** (Entry 2, Table 45) shows a significant drop, threefold, in PCAF potency and is the only molecule which displays measurable Brd9 potency. This compound mirrors butylamine containing **5.157** (Entry 8, Table 43, p 212) as there are four carbons between the nitrogen connecting to the pyridazinone ring and the basic centre. Both piperidine analogue **5.159** (Entry 2) and butylamine containing **5.157** (Entry 8, Table 43, p 203) show higher levels of Brd9 potency compared to PCAF which indicates that having a basic centre five carbons atoms away from the pyridazinone core does not give the desired selectivity profile. 2-Piperidyl **5.160** (Entry 3) shows the same level of potency at PCAF as pyrrolidine compound **5.158** (Entry 1) which illustrates that the steric bulk of the piperidine ring is tolerated in this position. Methylating the piperidine provides **5.161** (Entry 4) which shows a minor increase in PCAF potency, although with a minor decrease in ligand efficiency. This suggests the increase in potency is driven by the presence of the extra carbon atom rather than a positive interaction with the protein.



Entry	Number	R	PCAF pIC ₅₀ (LE)	Brd4 BD1/2 pIC ₅₀	Brd9 pIC ₅₀
1	5.162*		4.7 (0.40)	< 4.3 / < 4.3	< 4.3
2	5.163		4.2 (0.36)	< 4.3 / < 4.3	-
3	5.165†		4.4 (0.38)	< 4.3 / < 4.3	< 4.3
4	5.166†		5.4 (0.44)	< 4.3 / < 4.3	< 4.3
5	5.167†		5.3 (0.43)	< 4.3 / < 4.3	< 4.3
6	5.168†		5.1 (0.41)	< 4.3 / < 4.3	< 4.3

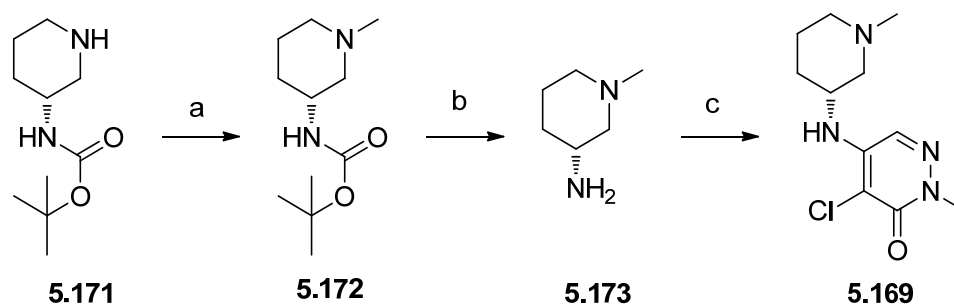
Table 45: Potencies of directly attached 5-chloro-4-aminopyridazinones at PCAF, Brd4 and Brd9.

Directly attaching the ring to the 4-aminopyridazinone is tolerated although pyrrolidine containing **5.162** (Entry 1, Table 45) with a PCAF potency of 4.7, shows no advantage over molecules already discussed. However, placing the basic centre externally to the cyclopentyl ring in a cis-configuration, as shown in cyclopentyl compound **5.163** (Entry 2), demonstrates a fall in PCAF potency and as a result no further exocyclic basic centres were investigated. Cyclopentyl compound **5.163** was synthesised *via* the *tert*-butyl carbamate example **5.164**, which was not screened as it did not contain a basic centre, using the methodology exemplified in Scheme 72 (p 202). 4-Aminopiperidine analogue **5.165** (Entry 3) suggests that this is not a good place to situate a basic centre, even though it is three

carbon atoms from the nitrogen of the aminopyridazinone. However, reinforcing the importance to PCAF potency of the positioning of the basic centre, racemic 3-aminopiperidine containing **5.166** (Entry 4) shows a pIC₅₀ of 5.4, being approximately equal in potency and with higher LE than the tetrahydroisoquinoline compounds **5.143** and **5.144** (Entries 1 and 2, Table 42, p 201). However, 3-aminopiperidine example **5.166** shows greater than 12-fold selectivity over Brd4 and Brd9 and is the most selective compound profiled so far. The 3- and 4-aminoazepane compounds **5.167** and **5.168**, respectively, (Entries 9 and 10) demonstrate a similar profile to 3-aminopiperidine **5.166** with pIC₅₀ values of greater than 5.0 at PCAF and potencies < 4.3 at Brd4 or Brd9 potency.

5.5.10 Examination of chiral examples of 3-aminopiperidine and 3-aminoazepane pyridazinones

Due to a combination of greatest selectivities and highest potencies for PCAF, 3-aminopiperidine analogue **5.166** and 3-aminoazepane containing **5.167** were selected for further study. The initial investigation was to isolate single enantiomers of the 3-aminopiperidine and 3-aminoazepane. Different strategies were employed for the enantiopure piperidines and azepanes as chiral starting materials were available for the piperidines although not for the azepanes. Both 3-(*R*) and 3-(*S*)-piperidine compounds, **5.169** and **5.170** were synthesised *via* the same method, although only the (*R*)-enantiomer is shown for clarity (Scheme 73).



Scheme 73: Reagents and conditions a) CH₂O, HCO₂H, 2-MeTHF, 80 °C, 69%; b) HCl, IPA, 80 °C, 100%; c) **5.073**, DIPEA, 130 °C, 52%.

tert-Butyl carbamate protected 3-piperidine compound **5.171** was methylated using an Eschweiler-Clarke³⁰⁹ methodology. The resulting piperidine compound **5.172** was deprotected using HCl in IPA and isolated as the bis-hydrochloride salt **5.173**. The 3-

aminopiperidine compound **5.173** could be appended to the dichloropyridazinone using the established S_NAr conditions (Scheme 72, p 202).²⁹⁵

The azepane enantiomers were synthesised by using the S_NAr reaction between azepane analogue **5.174** and dichloropyridazinone compound **5.073** (Scheme 74, p 210) to synthesise the racemic *tert*-butyl carbamate containing compound **5.175**. This was chirally separated using preparative chiral chromatography into the two enantiomers **5.176** and **5.177**. The stereochemistry of each enantiomer was unknown and both were deprotected using HCl in IPA to provide the enantiopure analogues of 3-azepane **5.167**, **5.178** and **5.179**. The unsubstituted azepanes were methylated using Eschweiler-Clarke conditions³⁰⁹ to provide enantiomers **5.180** and **5.181** which underwent vibrational circular dichroism (VCD) analysis³²³ to determine the stereochemistry of each enantiomer.

In VCD analysis, a solution of a chiral compound is irradiated with circularly polarised light in the infra red (IR) region. The absorbance of the light is measured across the IR range and the two enantiomers should have equal, but opposite spectra. The measured spectra are compared with the calculated spectrum of one of the enantiomers. When the measured and calculated spectra agree, it indicates that the chirality of the measured enantiomer is the same as the calculated enantiomer. It is possible to calculate the VCD spectrum of a chiral compound by predicting the change in dipole moment of an atom when circularly polarised light of a particular wavelength is absorbed. IR radiation is used as it does not electronically excite compounds, simplifying the calculation of the wavefunction.^{324,325} The spectrum of the (*S*)-enantiomer was calculated and used to determine the stereochemistry of **5.180** and **5.181** (Fig. 95).³²⁶

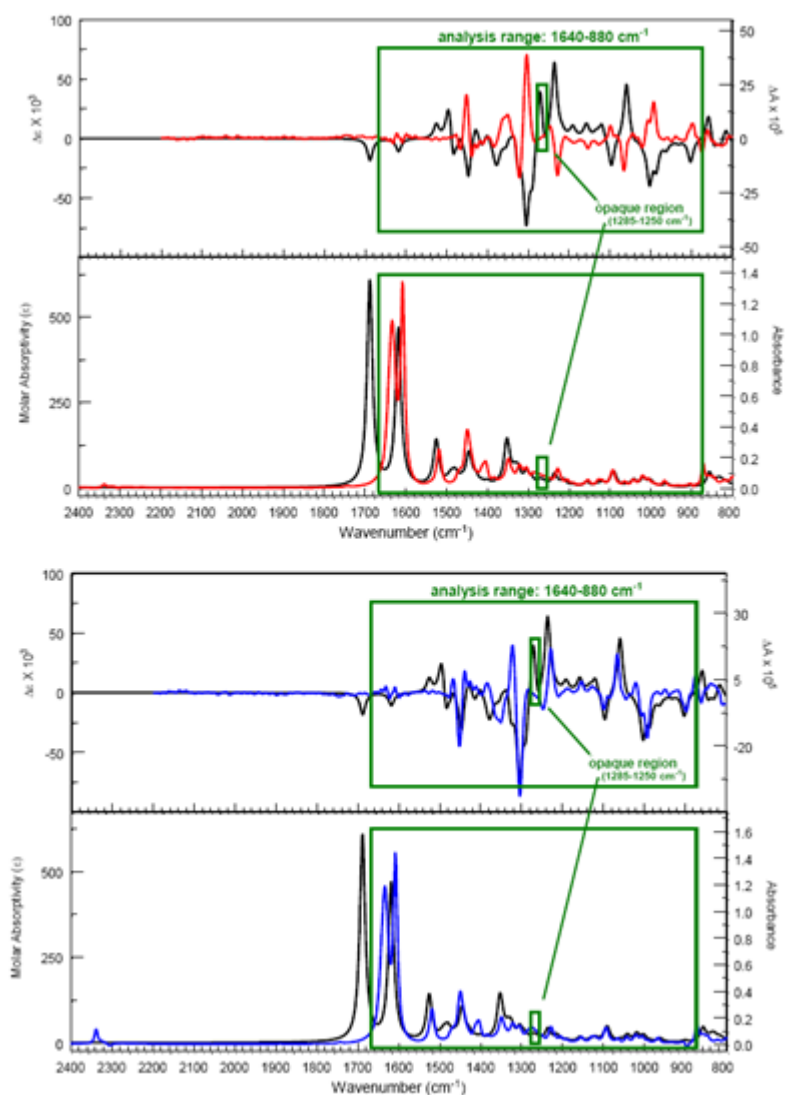
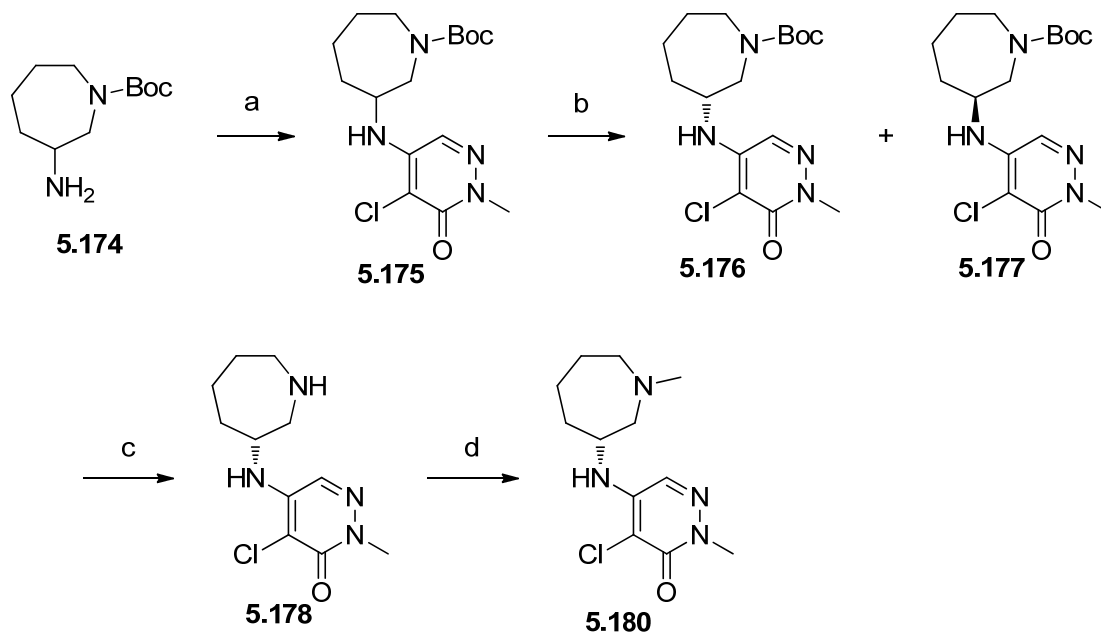


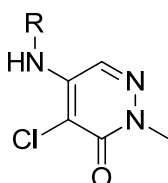
Figure 95: VCD spectra of *N*-methyl azepane compounds **5.180** and **5.181**. The black line is the calculated spectrum of the (*S*)-enantiomer **5.181**. The red line is the measured spectrum of the (*R*)-enantiomer **5.180** and the blue line is the measured spectrum of the (*S*)-enantiomer **5.181**.

After the preparative chiral chromatography only the (*R*)-enantiomer is shown as the steps were identical (Scheme 74).



Scheme 74: Reagents and conditions a) **5.073**, DIPEA, 130 °C, 31%; b) chiral chromatography: **5.176** 44%, **5.177** 38%; c) HCl, IPA, 20 °C, 95%; d) CH₂O, HCO₂H, 2-MeTHF, 80 °C, 90%.

The enantiomerically pure compounds were assayed against PCAF, Brd4 and Brd9 (Table 46).



Entry	Number	R	PCAF pIC ₅₀ (LE)	Brd4 BD1/2 pIC ₅₀	Brd9 pIC ₅₀
1	5.169	 $[\alpha]_D = +5^\circ$	5.6 (0.45)	$\leq 4.8^a / \leq 4.5^a$	< 4.3
2	5.170	 $[\alpha]_D = -10^\circ$	5.1 (0.41)	< 4.3 / < 4.3	< 4.3
3	5.178		5.4 (0.44)	$\leq 4.9^b / < 4.3$	< 4.3
4	5.179		5.0 (0.40)	< 4.3 / < 4.3	-
5	5.180	 $[\alpha]_D = +53^\circ$	5.6 (0.43)	$\leq 4.5^c / < 4.3$	< 4.3
6	5.181	 $[\alpha]_D = -48^\circ$	5.0 (0.38)	< 4.3 / < 4.3	-

Table 46: Potencies of 4-chloro-5-aminopyridazinones at PCAF, Brd4 and Brd9. ^{a)} Inactive at 6 of 7 test occasions. ^{b)} Inactive at 2 of 3 test occasions. ^{c)} Inactive at 4 of 5 test occasions.

The clear indication is that the (*R*)-enantiomers are more potent compared to the (*S*)-enantiomers. This again indicates that exact positioning of the basic centre within PCAF is key for a boost in potency. The (*S*)-enantiomers are not significantly more potent than many of the benzylic compounds (Table 30, p 170) at the 5-position of the aminopyridazinone suggesting they simply fill space in PCAF, although they are more selective with pIC₅₀s of < 4.3 at Brd4 and Brd9. It was suspected that the (*R*)-enantiomers were at the tight binding limit of the PCAF FP assay.

As the most potent and ligand efficient compound (*R*)-*N*-methyl piperidine containing **5.169** was studied further through different assays and was docked into PCAF using Glide (Fig. 96).¹⁴⁰

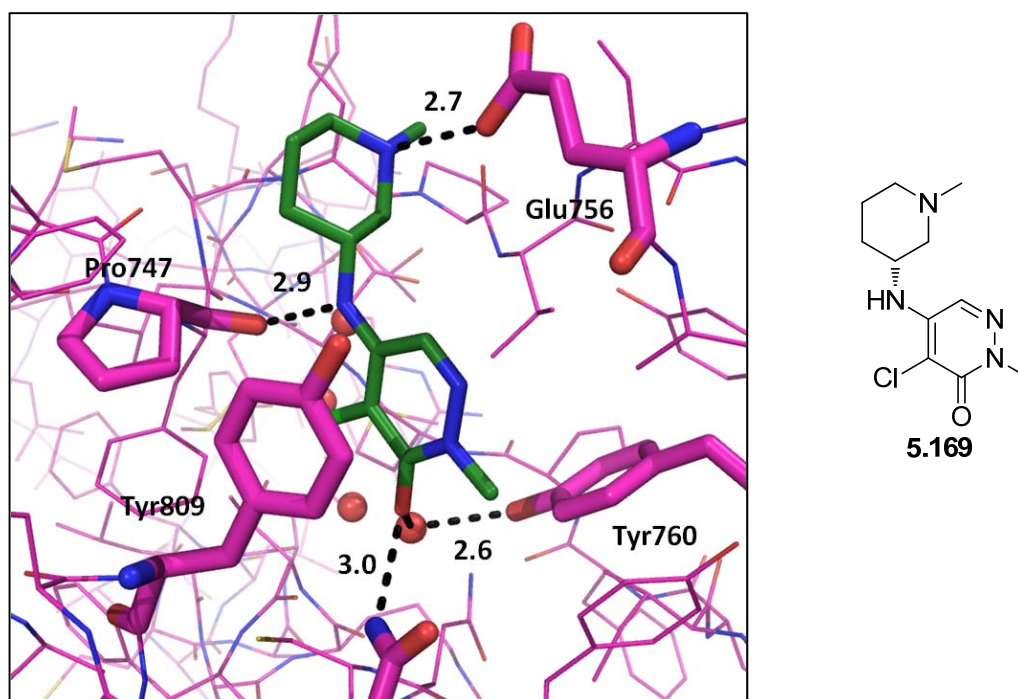
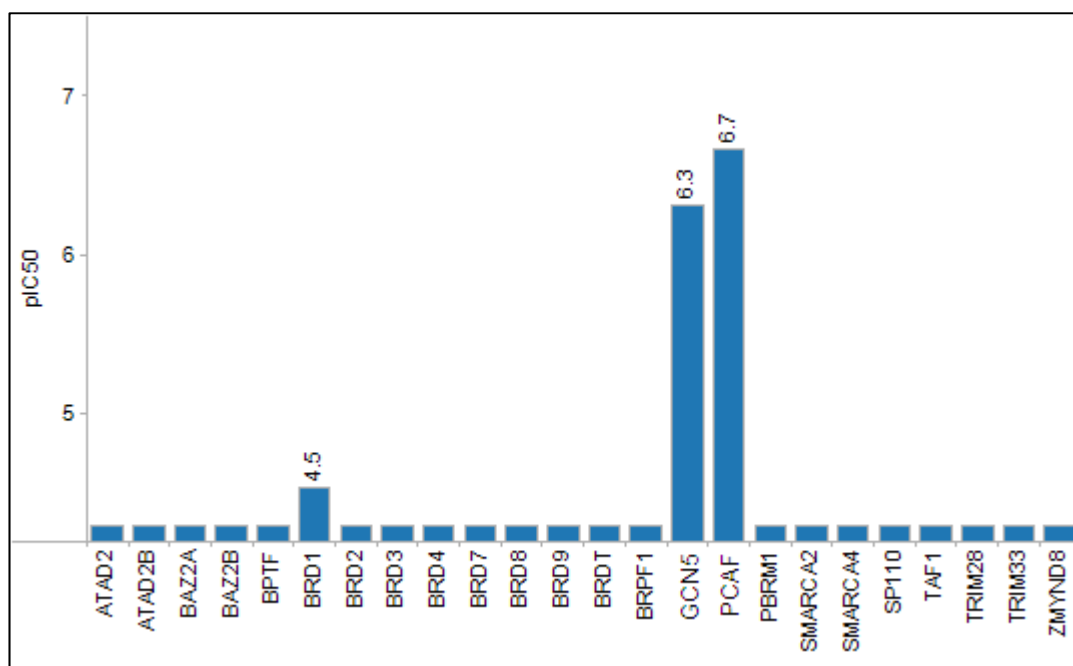


Figure 96: Glide¹⁴⁰ docking of **5.169** in PCAF.

From the docking it can be seen that piperidine compound **5.169** is likely to make the usual interactions with the PCAF protein as well as an H-bond between the basic centre and Glu756. As mentioned previously, it is believed that the H-bond between the piperidine basic centre and Glu756 gives the marked increase in PCAF potency. The basic centre provides Brd4 selectivity and the incorporation of sp^3 carbons gives Brd9 selectivity. The piperidine ring fills the available space in the PCAF pocket well, although the docking does assume the protein is rigid and the actual conformation may be considerably different.

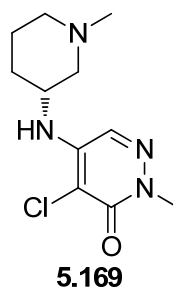
N-Methyl piperidine containing **5.169** was profiled against a number of endogenous bromodomains through multiple chemoproteomic binding experiments. Cellular lysates from different cell types were individually incubated with aminopyridazinone **5.169** and promiscuous bromodomain binder **5.137** (Entry 2, Table 39, p 192) attached to a solid support was immersed in the lysate. The beads were removed, rinsed and the BCPs bound to the beads identified which provided some interesting results (Graph 8).



Graph 8: Results from chemoproteomic experiments with **5.169** and endogenous bromodomain containing proteins.

The results showed that *N*-methyl piperidine analogue **5.169** is exceptionally selective for PCAF with greater than 100-fold selectivity over all the bromodomains studied with one exception, KAT2A also known as GCN5. As discussed previously, the homology between the bromodomains of PCAF and GCN5 is extremely high²⁵¹ and therefore it is understandable that selectivity against this bromodomain is limited. Currently there are no known inhibitors of the GCN5 bromodomain, although there are inhibitors of the GCN5 HAT domain.³²⁷ This means that *N*-Methyl piperidine containing **5.169** could be used as a dual PCAF/GCN5 probe or alternatively named as a KAT2 probe.

The other striking information from Graph 8 is that the potency of piperidine analogue **5.169** is greater than tenfold higher than measured in the PCAF FP assay. As has been expected, examples of the aminopyridazinone compounds had exceeded the maximum potency measurable by that assay. Around this time a FRET PCAF assay, using the assay reagent **5.138** (Fig. 90, p 193), was developed that was capable of determining higher pIC₅₀s. Data from the FRET and FP PCAF assays for methyl piperidine containing **5.169** was compared as well as a broader range of data (Table 47).

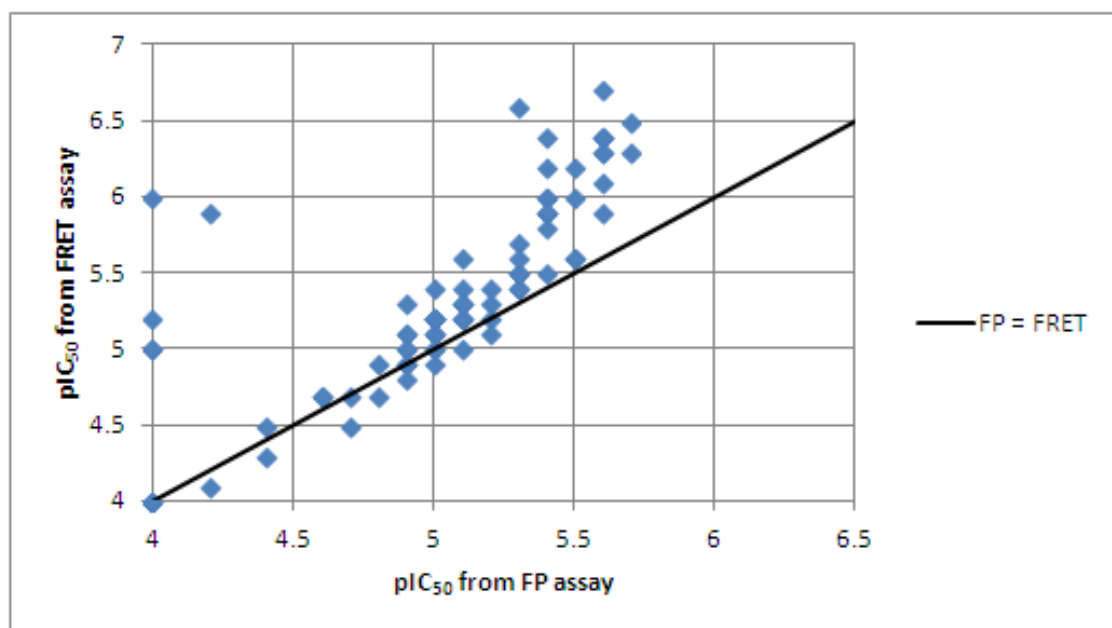


Assay	Data	Target profile
PCAF FP pIC ₅₀	5.6 (0.45)	≥ 6.0
PCAF FRET pIC ₅₀	6.3 (0.51)	
PCAF SPR pKd	6.4 (0.52)	
cLogP, MWt	1.3, 256	1 – 3, ≤ 400
Aqueous solubility µg mL ⁻¹	101	≥ 50
AMP nm s ⁻¹	320	≥ 50
MDCK2 penetration nm s ⁻¹	574	
Brd2 FRET BD1 / BD2 pIC ₅₀	< 4.3 / < 4.3	
Brd3 FRET BD1 / BD2 pIC ₅₀	< 4.3 / < 4.3	
Brd4 FRET BD1 / BD2 pIC ₅₀	≤ 4.8 ^a / ≤ 4.5 ^a	
PCAF selectivity over Brd3	≥ ×125	× 100
Brd9 FRET pIC ₅₀	< 4.3	
PCAF selectivity over Brd9	≥ ×125	× 30

Table 47: Data for piperidine **5.169**. ^a) Inactive at 6 of 7 test occasions.

Upon screening piperidine containing **5.169** in the FRET assay it was evident that, as expected, the FP assay was under-reporting the potency of the compound. The FRET, the SPR and the chemoproteomics data broadly correlate with each other. This satisfies the level of potency required for initial investigation in cellular systems.

Aminopyridazinone compounds which had pIC₅₀ values determined by both the FP and FRET PCAF assay formats were compared. There was good correlation for compounds with pIC₅₀ values of up to around 5.2 in the FP PCAF assay but beyond that there was significant deviance from the line of unity (Graph 9).



Graph 9: Comparison of pIC_{50} values of compounds between the FP PCAF assay and the FRET PCAF assay.

Theoretically, the tight binding limit was predicted to be at a pIC_{50} value of 5.9 (p 142). However, it can be seen from Graph 9 that the tight binding limit is somewhat lower. This mismatch between the observed and theoretical value is most likely due to not having entirely active protein in the assay, caused by either impurities or misfolded protein. Therefore, further examples of compounds which displayed a higher pIC_{50} than 5.2 in the FP assay were profiled through the FRET assay.

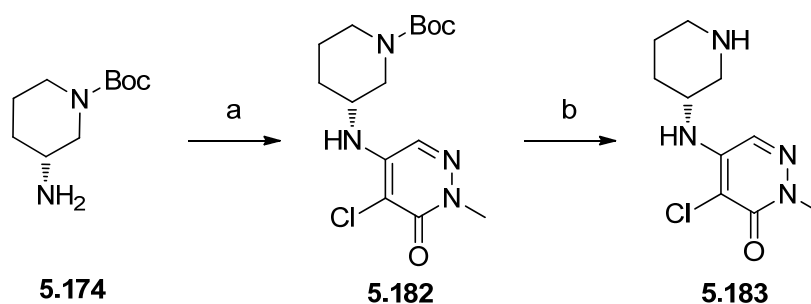
The physicochemical descriptors in Table 47 indicate that methyl piperidine analogue **5.169** is a hydrophilic, low molecular weight, water soluble compound, which correlates with the high ligand efficiency. However, due to the low molecular weight and hydrophilicity there was some debate if the molecule would penetrate cellular membranes. The data from the AMP assay suggested it would as it was shown to be highly permeable. To verify this in a cellular system the permeability of the piperidine containing **5.169** was measured in a MDCK2 permeability assay.³²⁸ Piperidine compound **5.169** was found to penetrate these cells and therefore, should enter the nucleus where the PCAF protein is located as it has a molecular weight less than 5000 Da.⁴⁴ Aminopyridazinone **5.169** was assayed through a cross screening panel of known drug safety and liability targets. From these assays, piperidine analogue **5.169** was found to have no concerning off-target liabilities. The penetration data combined with the vastly better than required selectivity over wider

bromodomains, illustrated that aminopyridazinone compound **5.169** fitted almost all the required criteria as a probe molecule. At this time the programme was without a target engagement assay so it could not be conclusively determined if *N*-methyl piperidine **5.169** was engaging endogenous PCAF in the nucleus. The 3(*R*)-aminopiperidine group was still of interest and thus a series of compounds assessing which substituents could be tolerated from the nitrogen in the piperidine ring were investigated.

5.5.11 Substitution from the 3-piperidine

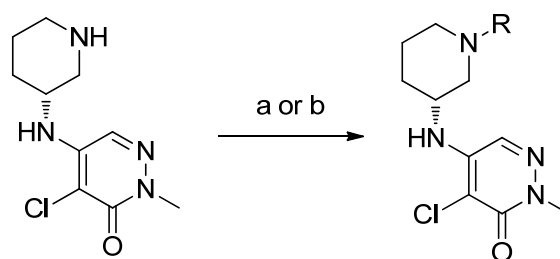
3(*R*)-Aminopiperidine compound **5.169** was a good candidate to probe the phenotypic effects of inhibiting the KAT2 family of bromodomains. However, historically molecules for other proteins have been selected as potential candidate compounds and found to not act on the predicted drug target within cells.^{329,330} For this reason, a series of compounds were designed to span a range of lipophilicities and pK_as to provide a series of chemical probes with diverse physicochemical properties. This was to give the best chance possible for penetration of the compound into the nucleus and target engagement to occur. Increasingly lipophilic compounds are more likely to be cellularly penetrant and by reducing the basicity of the piperidine less of the compound will be protonated at physiological pH. Thus there will be more neutral species to penetrate the cell and other organelles contained within.³³¹ However, the reduction in basicity could lead to the compounds losing selectivity for the BET family of bromodomains.

The 3(*R*)-aminopiperidines were synthesised by using the previously described S_NAr methodology with (*R*)-*tert*-butyl 3-aminopiperidine-1-carboxylate (**5.174**) and dichloropyridazinone compound **5.073** to provide 4-aminopyridazinone example **5.182**. The *tert*-butyl protected carbamate could be subsequently deprotected with HCl in IPA to provide the versatile intermediate **5.183** (Scheme 75).



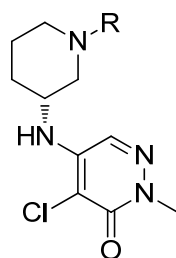
Scheme 75: Reagents and conditions a) **5.073**, DIPEA, DMSO, 130 °C, 44%; b) HCl, IPA, 20 °C, 74%.

The piperidine nitrogen of **5.183** was elaborated to investigate the effects of steric bulk coming from this vector and modulation of the pK_a . The nitrogen was alkylated using reductive aminations and alkylations with alkyl halides (Scheme 76).³³²



Scheme 76: Reagents and conditions a) R-Br, Na_2CO_3 , KI, MeCN, 130 °C; b) RCHO, $\text{NaHB}(\text{OAc})_3$, AcOH, DCM, 20 °C.

A range of compounds that investigated the area from the piperidine nitrogen with different sized substituents and functional groups were assayed against the bromodomains of interest (Table 48). All the compounds were found to have Brd4 and Brd9 $p\text{IC}_{50}$ s of ≤ 4.4 so these results are not recorded.

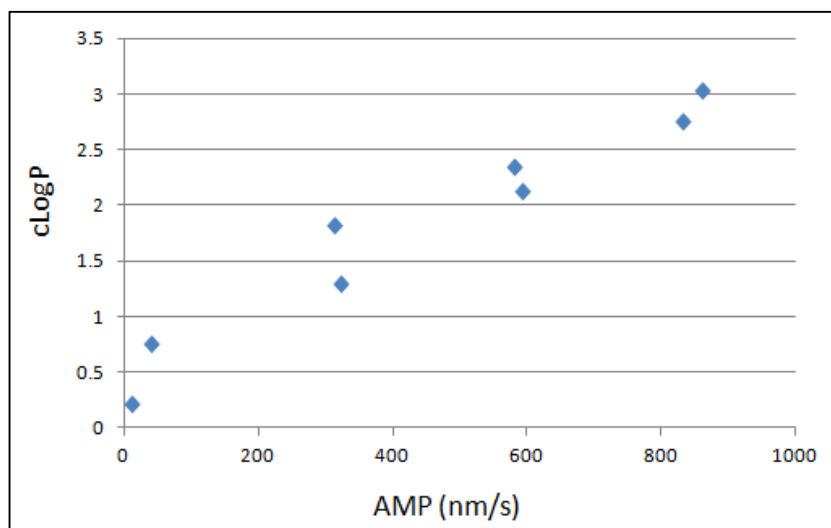


Entry	Number	R	PCAF FP $p\text{IC}_{50}$ (LE)	PCAF FRET $p\text{IC}_{50}$ (LE)	AMP nm s^{-1}	cLogP
1	5.169	Me	5.6 (0.45)	6.3 (0.51)	320	1.3
2	5.183	H	5.4 (0.46)	5.9 (0.51)	37	0.8
3	5.184†	Et	5.6 (0.43)	6.1 (0.46)	310	1.8
4	5.185*^a		4.6 (0.32)	4.7 (0.34)	10	0.2
5	5.186†	<i>i</i> -Pr	5.1 (0.37)	5.2 (0.37)	590	2.1
6	5.187†	<i>n</i> -Pr	5.2 (0.37)	5.5 (0.40)	580	2.4
7	5.188†	<i>i</i> -Bu	4.9 (0.34)	5.1 (0.35)	830	2.8
8	5.189†		5.0 (0.30)	5.2 (0.31)	860	3.0

Table 48: Potencies of aminopyridazinones at PCAF. ^a) Racemate

The levels of PCAF potency show that there is a limit to the steric bulk of groups which can be tolerated emerging from the piperidine nitrogen. The unsubstituted piperidine intermediate **5.183** (Entry 2) has a lower binding affinity for PCAF than the methyl

compound **5.169** (Entry 1) so the methyl group does provide a small improvement in binding. In the FP assay ethyl **5.184** (Entry 3) and methyl **5.169** appear to be equipotent. However, comparing the compounds in the FRET assay methyl **5.169** is marginally more potent than ethyl **5.184** which suggests the optimal size for PCAF potency is somewhere between the size of a methyl and an ethyl. Primary amide **5.185** (Entry 4) was designed to investigate if it was possible to interact with H-bond donors or acceptors. However, the PCAF potency of amide containing **5.185** is tenfold less than **5.169** when comparing the FP assay results and 50-fold less when comparing the FRET data for methyl piperidine analogue **5.169** and the FP data for amide containing **5.185**. Isopropyl **5.186** (Entry 5) and *n*-propyl **5.187** (Entry 6) show a loss in potency compared to the smaller alkyl substituents which corresponds well with the binding pose suggested by the docking (Fig. 96, p 212). This suggests that there is only a small cleft available for substituents from the piperidine nitrogen before steric clash occurs. Larger substituents from the piperidine nitrogen would have to move residues or bind in a different conformation which would not allow the H-bond between the basic centre of the piperidine and Glu756. This could be the case as Entries 5 – 8 show similar levels of PCAF potency with many of the benzyl compounds (Table 30, p 170) where it would appear no H-bonding interactions are taking place between the protein and the headgroup of the ligand. The AMP of the compounds increases in an almost linear fashion with cLogP showing that adding lipophilicity has helped cellular penetration of the molecule as predicted (Graph 10).

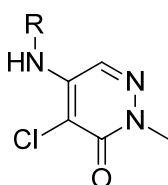


Graph 10: Illustrating the correlation between AMP and cLogP.

Only primary amide **5.185** and unsubstituted piperidine **5.183** show insufficient values of less than 50 nm s^{-1} in the AMP assay as defined by the probe criteria (p 133). The other

compounds in Table 48 are predicted to be highly permeable with values reported from the AMP assay of greater than 300 nm s^{-1} . While adding lipophilicity can have effects on the promiscuity of a compound for other protein targets³³³ these compounds have a sufficiently low cLogP, with the highest being approximately 3, for these compounds to still be within drug-like chemical space.¹⁹⁰

Next to be investigated was how the basicity of the piperidine affected binding to PCAF (Table 49). The fluoroethyl piperidine compounds **5.190** and **5.191** were synthesised using the relevant alkyl bromides as outlined in Scheme 76 (p 217).

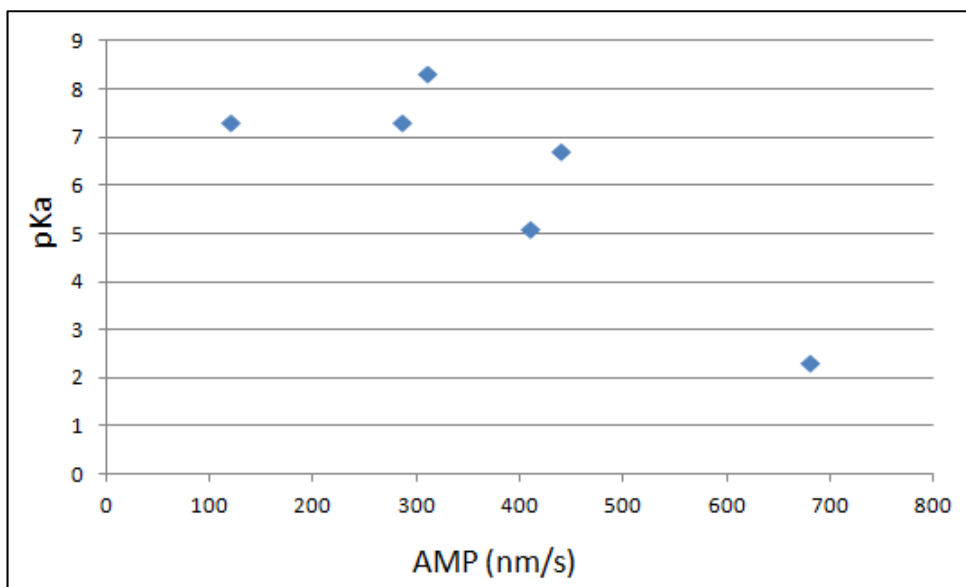


Entry	Number	R	PCAF FP pIC ₅₀ (LE)	PCAF FRET pIC ₅₀ (LE)	Calculated pK _a ^a	Measured pK _a	AMP nm s ⁻¹
1	5.169		5.6 (0.45)	6.3 (0.51)	8.2	8.1	320
2	5.190		4.8 (0.35)	5.0 (0.34)	6.7	-	440
3	5.191		4.9 (0.34)	4.7 (0.32)	5.1	5.1	410
4	5.192†		4.5 (0.29)	4.4 (0.29)	2.3	Below level of quantification	680
5	5.180		5.6 (0.43)	6.4 (0.49)	8.4	8.3	285
6	5.193†		5.2 (0.42)	5.1 (0.41)	8.6	7.3	120

Table 49: Potencies of aminopyridazinones at PCAF, and the pK_as of the protonated piperidines. ^a) Calculated by ChemAxon pK_a 5.4.1.1.

The compounds were designed to have similar steric bulk to each other and as such entries 2 – 4 are all based around an ethyl substituted piperidine. Methyl compound **5.169** (Entry 1, Table 49) is the most basic molecule of the subtype and at physiological pH of 7.2, which is typical for lymphocytes,³³⁴ will be approximately 90% protonated, that is to say 90% of the molecules will be capable of forming the putative H-bond with Glu756. However, simply introducing one electron withdrawing fluorine to the ethyl group as in monofluoro compound **5.190** (Entry 2) would cause only 20% of the molecules to be protonated and thus able to form the H-bond necessary to improve the potency of the compound. The difluoroethane containing **5.191** (Entry 3) is less basic still and will have just 0.5% protonated within the cell. Trifluoro example **5.192** (Entry 4) is essentially a neutral molecule and incapable of protonation at physiological pH. From examining the potency data around the fluorinated compounds it would appear that more than 20% of the compound needs to be protonated as monofluoro compound **5.190** is equipotent with difluoro analogue **5.191** and a number of benzylic compounds (Table 30, p 170). The reduction in potency of trifluoro compound **5.192** to a pIC₅₀ of 4.5 is not explained adequately by the protonation argument but may be answered by the increase in steric bulk of the trifluoromethyl group.³³⁵

The electronegative oxygen was introduced into oxazepane containing **5.193** (Entry 6) to reduce the basicity of the nitrogen through the inductive effect.³³⁶ There is a reduction in the measured basicity, which might explain the approximate tenfold decrease in potency. However, it could additionally be due to the oxygen present causing an unfavourable interaction with the PCAF protein. Comparing the measured pK_a, substituting for the calculated pK_a where measured data was not available, against the AMP shows a correlation between reducing basicity and increasing penetration through the artificial membrane (Graph 11).

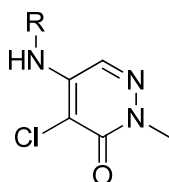


Graph 11: Illustrating the correlation between AMP and pKa.

Reducing the basicity with the intention of improving the cellular penetration has improved the transit of the molecules into the cell, although it reduced the potency to the point where the molecules were unlikely to be biologically active. Hence, the most potent molecules were selected to be further profiled in selectivity, as well as cellular assays in immune cells. The molecules selected all met the probe criteria of sub-micromolar potency in the PCAF FRET assay.

5.6 Selection of tool molecules

The molecules selected to be assayed for selectivity and in cellular systems met the probe criteria of sub-micromolar potency at PCAF. In light of the chemoproteomics data that showed piperidine containing **5.169** was approximately equipotent with GCN5 (Graph 8, p 213), a GCN5 FRET assay was developed. The GCN5 assay used the same fluorescent tagged assay ligand **5.138** as the PCAF FRET assay (Fig. 90, p 193) and was run at the same concentrations of protein and assay reagent so the pIC_{50} values generated are directly comparable. The GCN5 assay was developed to determine if any of the selected molecules showed improved PCAF selectivity over GCN5. This selectivity data and physicochemical properties are shown below (Table 50).



Compound	5.169	5.184	5.180	5.194*	Probe criteria
R					
PCAF FRET pIC ₅₀ (LE)	6.3 (0.51)	6.1 (0.46)	6.4 (0.49)	7.1 (0.42)	≥ 6.0
GCN5 FRET pIC ₅₀	6.0 (0.48)	-	5.9 (0.45)	-	≥ 6.0
PCAF SPR pK _d	6.4 (0.52)	6.4 (0.49)	6.5 (0.49)	-	≥ 6.0
cLogP, MWt	1.3, 256	1.8, 270	1.9, 270	2.9, 332	1 – 3, <400
CLND sol μg mL ⁻¹	101	≥ 151	114	109	≥ 50
AMP pH 7.4 nm s ⁻¹	320	310	285	535	≥ 10
Brd4 FRET BD1 / BD2 pIC ₅₀	≤ 4.8 ^a / ≤ 4.5 ^a	< 4.3 / < 4.3	< 4.3 / < 4.3	< 4.3 / < 4.3	
PCAF selectivity over Brd4	≥ ×125	≥ ×60	≥ ×150	≥ ×630	≥ ×100
Brd9 FRET pIC ₅₀	< 4.3	< 4.3	< 4.3	4.5	
PCAF selectivity over Brd9	≥ ×125	≥ ×60	≥ ×150	≥ ×400	≥ × 30

Table 50: Molecules selected for profiling in selectivity and cellular assays. ^a) Inactive at 6 of 7 test occasions.

What is apparent from the data is that these compounds do not have significant GCN5 selectivity compared to PCAF. As discussed earlier there is high sequence homology between GSN5 and PCAF being alternatively named KAT2A and KAT2B, respectively.^{261,262} In essence the molecules here are KAT2 family inhibitors which will be interesting to examine in their own right in the absence of solely PCAF inhibitors. Interestingly the more

sterically demanding compounds do appear to show slight bias for PCAF over GCN5. This indicates that the binding pocket in PCAF may be larger or more flexible than in GCN5.

There is one previously unmentioned compound in Table 50. Phenyl piperidine analogue **5.194** was designed through modelling iterating from piperidine compound **5.169** by Humphreys, P. The additional phenyl group was predicted to make an edge to face interaction with Trp746 as well as the other H-bonds which the core makes with the PCAF protein (Fig. 97). It was postulated that through this interaction there could be an increase in the PCAF potency as well as an increase in the lipophilicity which should aid cellular penetration of the molecule.

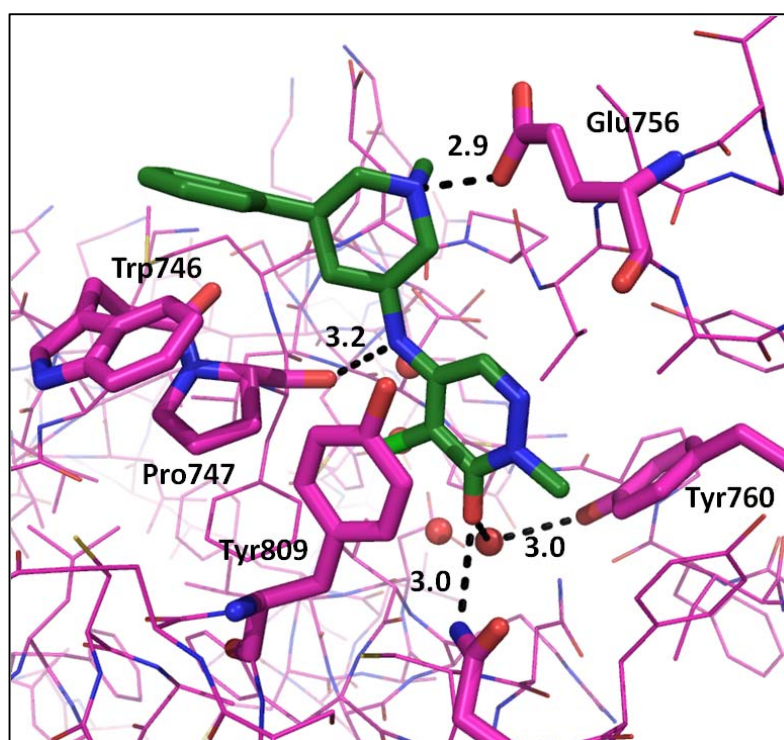
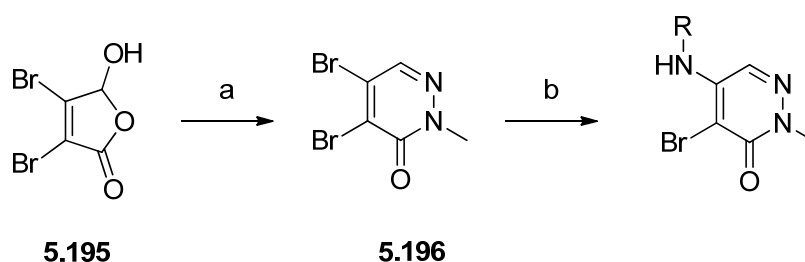


Figure 97: **5.193** docked into PCAF using Glide¹⁴⁰ showing a potential edge to face interaction with Trp746.³³⁷

On testing of the compound in the PCAF FRET assay it was found to be the most potent compound at PCAF so far with a pIC_{50} of 7.1, albeit with some erosion of the ligand efficiency. The remainder of the data showed it was suitable as a PCAF probe although with evidence of low levels of binding to Brd9. However, the compound was 400-fold selective for PCAF compared to Brd9, greater than the required 30-fold selectivity.

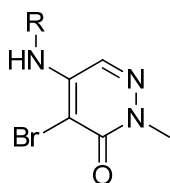
The physicochemical properties of the molecules suggested the compounds should be cellularly penetrant as they showed the compounds capable of permeating through an artificial cellular membrane as well as aqueous solubility. The molecules all displayed at least 100-fold selectivity over BET and thus met the probe criteria for cellular potency and BET selectivity.

Through the knowledge of the previously generated SAR it was known that incorporating a bromine at the 4-position of the aminopyridazinone ring gave an approximate twofold increase to the IC₅₀ value of the compound compared to the 4-chloro variant (Table 33, p 181). Therefore, the 4-bromo aminopyridazinone analogues of the compounds in Table 50 were synthesised (Scheme 77).



Scheme 77: Reagents and conditions: a) MeNHNH₂, EtOH, 45 °C, 60%; b) R-NH₂, DIPEA, DMSO, 130 °C.

Mucobromic acid (**5.195**) was condensed with methyl hydrazine to give the intermediate dibromopyridazinone analogue **5.196**.³³⁸ The desired test compounds were synthesised through the previously described S_NAr chemistry and profiled through the screening cascade (Table 51).



Compound	5.197*	5.198*	5.199*	5.200*	Probe criteria
R					
PCAF FRET pIC ₅₀ (LE)	6.5 (0.52)	6.4 (0.49)	6.7 (0.51)	7.4 (0.44)	≥ 6.0
GCN5 FRET pIC ₅₀	6.4	6.0	6.3	-	≥ 6.0
PCAF SPR pK _d	6.6	6.5	7.0	-	≥ 6.0
cLogP, MWt	1.5, 300	2.0, 315	2.0, 315	3.0, 377	1 – 3, <400
CLND sol μg mL ⁻¹	≥ 189	≥ 162	198	149	≥ 50
AMP pH 7.4 nm s ⁻¹	375	390	505	500	≥ 50
Brd4 FRET BD1 / BD2 pIC ₅₀	< 4.3 / < 4.3	< 4.3 / < 4.3	≤ 4.4 / < 4.3	≤ 4.5 / ≤ 4.6	
PCAF selectivity over Brd4	≥ ×200	≥ ×150	× 200	× 630	≥ ×100
Brd9 FRET pIC ₅₀	≤ 4.4	< 4.3	< 4.3	5.1	
Brd9 selectivity	×125	≥ ×125	≥ ×250	×250	≥ ×30

Table 51: 4-Bromo analogues of the molecules selected for profiling in selectivity and cellular assays.

The substitution of the 4-bromo for the 4-chloro in the aminopyridazinones was consistent with the known SAR for the series. The change gave the expected increase in pIC₅₀ of 0.3 log units for all the compounds with the exception of methyl piperidine containing **5.197** which showed an increase of 0.2 log units. This slightly lesser increase is within error of the assay and is consistent with the trend observed for the other compounds. Otherwise the physicochemical and selectivity data for the chloro compounds (Table 50) and the bromo

compounds (Table 51) are almost identical to each other. However, a negative control was required for the cellular assays to ensure any phenotype seen was being driven by inhibition of the KAT2 family of bromodomains. The enantiomer of the phenyl piperidine analogue **5.200**, **5.201**, was used for this purpose as **5.201** was 250-fold less potent at PCAF than **5.200** and showed no BET activity (Table 52).

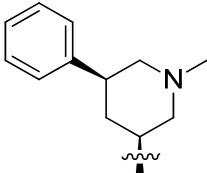
Compound	5.201*
R	
PCAF FRET pIC ₅₀ (LE)	4.9 (0.29)
GCN5 FRET pIC ₅₀	-
PCAF SPR pK _d	-
cLogP, MWt	3.0, 377
CLND sol (μg mL ⁻¹)	137
AMP pH 7.4 (nm s ⁻¹)	473
Brd4 FRET BD1 / BD2 pIC ₅₀	< 4.3 / ≤ 4.4
PCAF selectivity over Brd4	≥ ×3
Brd9 FRET pIC ₅₀	≤ 4.6
Brd9 selectivity	×3

Table 52: Profile of less active control **5.201**.

The loss of potency of **5.201**, compared to the active isomer **5.200** was believed to be due to loss of the hydrogen bond between Glu756 and the basic nitrogen in the piperidine ring (Fig. 98, p 228). Without this hydrogen bond the aminopyridazinone PCAF inhibitors profiled all tended to have a maximum pIC₅₀ value of approximately 5.0. Phenyl piperidine compound **5.201** is no exception.

Therefore, select examples were chosen for further profiling with the less active control **5.201**.

5.7 Further profiling of PCAF probe compounds

Three members of the toolset, piperidine containing **5.169**, azepane compound **5.199** and phenyl piperidine analogue **5.200** were used as exemplar compounds and profiled through a panel of 43 known safety and drug liability targets. None of the compounds displayed potency which could cause biological effects against ion channels, kinases and known targets for pro-convulsant liabilities, emesis or CV effects. In fact, in most cases the measured potency was below the level of quantification of most of the assays. This illustrates the probe molecules identified are selective for target classes other than bromodomains, which could be expected due the low lipophilicities³³⁹ and presence of chiral centres,³⁴⁰ which is known to make compounds less promiscuous. Importantly, the compounds were also found to be non-cytotoxic at concentrations up to 200 μM . Therefore, any potential phenotype observed would be through inhibition of a biological mechanism rather than through cell death.

The bromodomain selectivity of the most potent compound piperidine containing **5.200** was profiled by means of BROMOscan[®] (DiscoverX Corp., Fremont, CA, USA) against 34 bromodomain containing proteins (Table 53). The BROMOscan[®] assay measures the K_d of a test compound against a panel of immobilised bromodomains.

Bromodomain	Kd (nM)	pK _d	Bromodomain	Kd (nM)	pK _d
ATAD2A	> 30000	< 4.5	BRDT(1)	> 30000	< 4.5
ATAD2B	> 30000	< 4.5	BRDT(2)	> 30000	< 4.5
BAZ2A	20000	4.7	BRPF1	140	6.9
BAZ2B	840	6.1	BRPF3	100	7.0
BRD1	110	7.0	CECR2	11000	5.0
BRD2(1)	> 30000	< 4.5	CREBBP	> 30000	< 4.5
BRD2(2)	> 30000	< 4.5	EP300	> 30000	< 4.5
BRD3(1)	> 30000	< 4.5	FALZ	130	6.9
BRD3(2)	26000	4.6	GCN5	1.4	8.9
BRD4(1)	> 30000	< 4.5	PBRM1(2)	> 30000	< 4.5
BRD4(1,2)	> 30000	< 4.5	PBRM1(5)	< 30000	< 4.5
BRD4(2)	> 30000	< 4.5	PCAF	1.4	8.9
BRD4(full-length, short-isoform)	> 30000	< 4.5	SMARCA2	> 30000	< 4.5
BRD7	1500	5.8	TAF1(2)	> 30000	< 4.5
BRD9	1400	5.9	TAF1L(2)	> 30000	< 4.5

Table 53: Results from the BROMOscan[®] assay for phenyl piperidine compound **5.200**.

As was seen for other examples in the FRET assays (Tables 50 and 51), phenyl piperidine compound **5.200** was found to be equipotent at both PCAF and GCN5. However, phenyl piperidine analogue **5.200** has been found to have a K_d of 1.4 nM at the KAT2 family of bromodomains, which shows considerably stronger binding than was displayed in the FRET assay. The results can be visualised on a phylogenetic tree (Fig. 98).

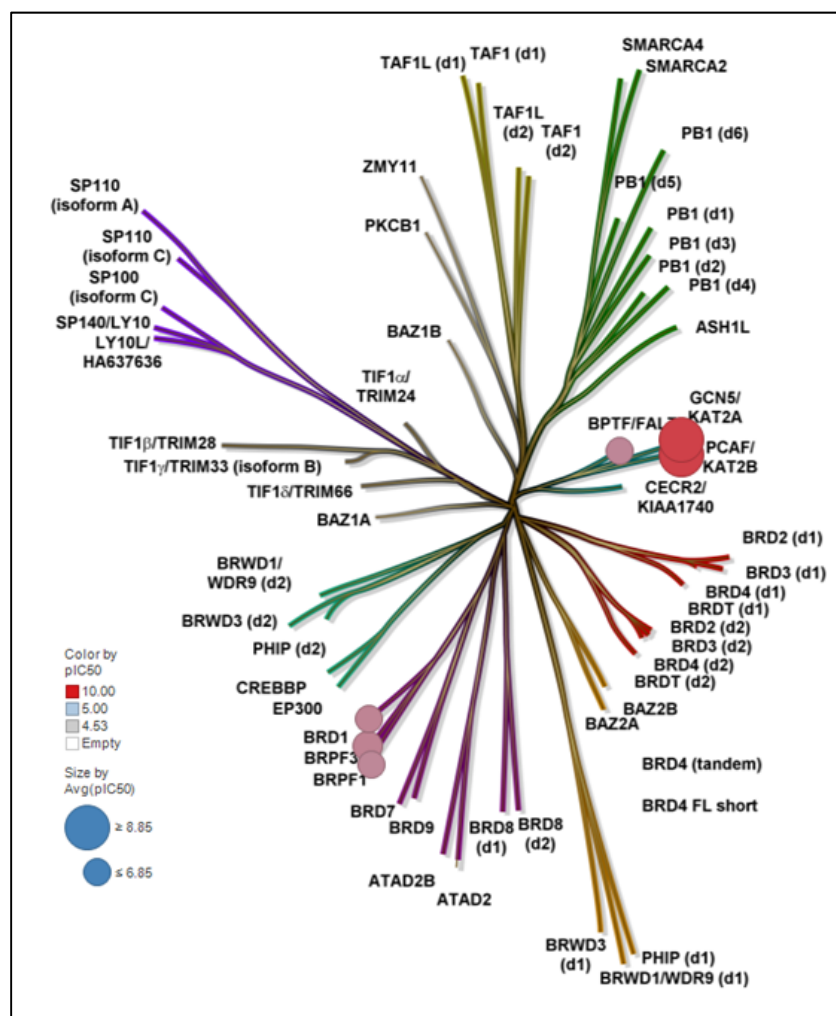


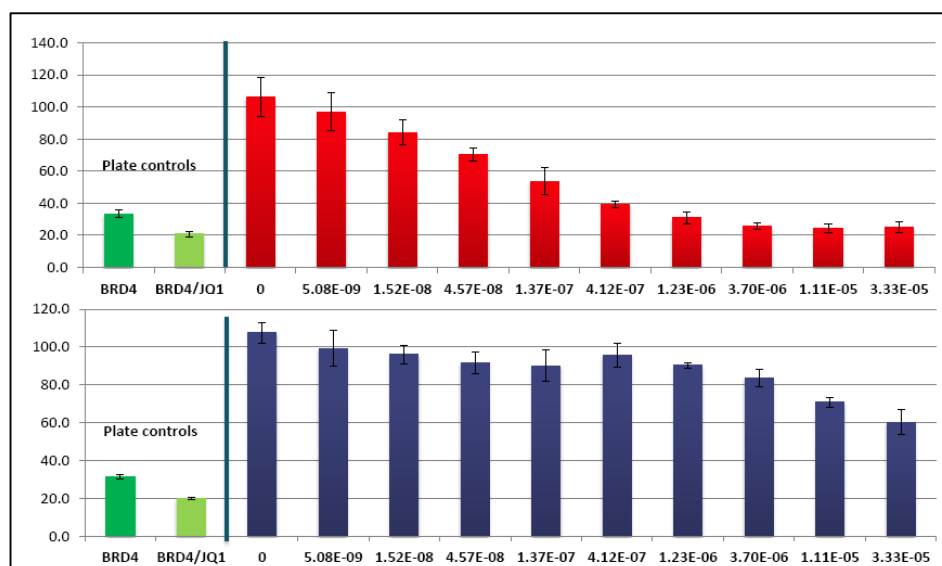
Figure 98: Phylogenetic tree showing the results from the BROMOScan assay with a six hundred-fold cut off.

Phenyl piperidine compound **5.200** has more than seventy-fold selectivity for PCAF against all the bromodomains tested against with the exception of GCN5. Gratifyingly, phenyl piperidine analogue **5.200** shows no binding to the BET family of bromodomains which correlates with the FRET assay data already collected. Using the data from the BROMOScan[®] assay shows that phenyl piperidine aminopyridazinone **5.200** is greater than 18,000-fold selective for the BET family of bromodomains. This passes one of the key probe

criteria of having greater than one hundred-fold selectivity over the BET family of bromodomains.

However, binding to other non-BET bromodomains is noted with FALZ, BRPF1, BRPF3 and Brd1 being targets. These bromodomains have phenylalanine residues present where Tyr809 is in PCAF (Fig. 97, p 223). This may cause a positive aromatic face to face interaction with the pyridazinone ring and hence binding to the off-target bromodomains. However, the level of selectivity phenyl piperidine example **5.200** shows for these bromodomains compared to the KAT2 family is close to 80-fold. According to the probe criteria (Fig. 63, p 133) this level of selectivity is higher than necessary for the compound to be selected as a probe molecule. This fulfils the greater than 30-fold selectivity probe criteria for selectivity over non-BET bromodomains. It was assumed that the other aminopyridazinone molecules in Tables 50 and 51 would have a similar, selectivity profile to phenyl piperidine compound **5.200**.

To determine if phenyl piperidine pyridazinone analogue **5.200** could engage endogenous PCAF in the nuclear environment, an in-cell bioluminescence resonance energy transfer (BRET) assay was developed by Promega (Madison, WI, USA). A BRET assay is similar to a FRET assay, although the light needed for the assay is produced by bioluminescence rather than by an external source.³⁴¹ Histone H3 and endogenous PCAF were tagged fluorescently, as for a standard FRET assay (Fig. 71, p 140), within HEK293 cells. The cells were treated with different concentrations of phenyl piperidine compound **5.200** and the less active enantiomer **5.201**. The dose response curves were measured looking at the reduction in fluorescence at different concentrations of dosed compounds (Graph 12).



Graph 12: Dose response of aminopyridazinone compounds **5.200** (red) and **5.201** (blue) from the in-cell PCAF BRET assay.

The key results from the BRET assay using endogenous full length PCAF correlated with the results from the biophysical FRET assay using truncated PCAF. The BRET assay results also showed that the bromodomain is accessible in the protein complex and demonstrated target engagement. The pIC_{50} values were found to be similar with phenyl piperidine compound **5.200** showing a pIC_{50} value of 7.4 in the PCAF FRET assay and 7.2 in the BRET assay. Less active control **5.201** showed a pIC_{50} value of 5.0 in both the biochemical FRET and in-cell BRET assays.

Therefore, the reasonable assumption was made that the other probe molecules behave in the same manner. Compounds have been found that are potent, selective, can engage endogenous PCAF and displace PCAF from chromatin and therefore are suitable to be declared as probes. The probe molecules listed in Tables 50 and 51 (p 222 and 225) were screened initially in immuno-inflammation related biological systems.

Various immune cells were exposed to solutions of the compounds, having been stimulated with substances which would give an immune response and their phenotypic response measured. However, in studies involving peripheral blood mononuclear cells (PBMCs) which had been stimulated with anti-CD3 antibodies there was no decrease in the output of IFN- γ or IL-10, 13 or 17 upon treatment with any of the probe molecules. Additionally, treatment of human B cells extracted from tonsils with the PCAF probe compounds had no effect detected upon the output of immunoglobulin G (IgG).

As the internal panel of immuno-inflammation cellular systems showed no desired change on the measured phenotypes an alternative, external approach was used. Investigating a collection of immune cell types using a BioMAP® (DiscoverX Corp., Fremont, CA) panel allowed a wider range of biological activities to be probed. As the most potent, phenyl piperidine containing **5.200** was sent for profiling through the BioMAP® panel. Even with the more diverse set of cell types no significant biological activity was seen (Fig. 99). Comparing this to data derived for BET inhibitors in the BioMAP® assay³⁴² there is a marked difference. The BET inhibitors show values significantly outside the grey area which represents a statistically significant result in the assays. However, phenyl-piperidine analogue **5.200** showed very little biological activity outside of the grey area on the chart. This led to the conclusion that inhibiting the PCAF bromodomain has no effect on immuno-inflammation phenotypes in the types of cell investigated.

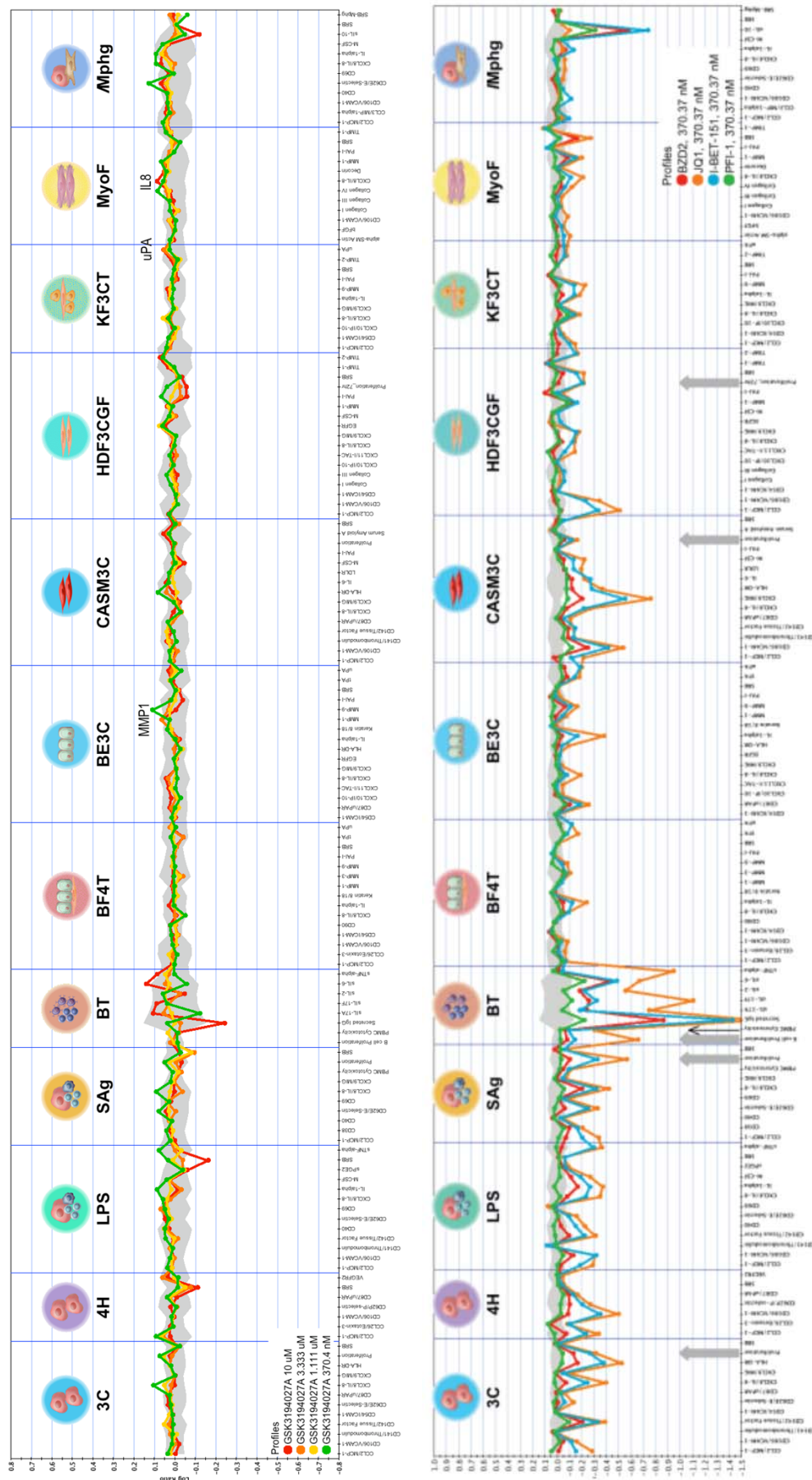


Figure 99: Top: BioMAP[®] assay readout for 5.200. Bottom: BioMAP[®] readout for published BET inhibitors. Adapted³⁴²

5.8 Conclusion

Through the work described above, a chemical series of aminopyridazinones, which displayed 20 μM potency at PCAF and was equipotent for the BET family of bromodomains, was transformed into a set of compounds that showed a K_d of 1.4 nM at PCAF and GCN5 while simultaneously reducing the BET potency. Upon testing these compounds at a wider range of bromodomains, they were found to have a greater than 70-fold selectivity against all bromodomains tested apart from the very closely related GCN5. These compounds were found to bind to displace PCAF from chromatin in the nucleus and therefore were suitable to determine if inhibiting the PCAF bromodomain had a biological effect.

The author designed and synthesised a number of important molecules to deliver chemical probes to investigate inhibition of the PCAF bromodomain. (*R*)-4-chloro-2-methyl-5-((1-methylpiperidin-3-yl)amino)pyridazin-3(2*H*)-one (**5.169**) was one such molecule as it met all of the probe criteria. Piperidine containing **5.169** has sub-micromolar potency at the KAT2 family of bromodomains, greater than 30-fold selectivity against all bromodomains tested against, no detectable off-target liabilities and is cellularly penetrant. This provided a compound suitable to investigate any phenotype driven by inhibition of the PCAF or GCN5 bromodomains (Fig. **100**). Iterations from piperidine containing **5.169** enabled the discovery of more potent compounds that were proven to have target engagement in cellular systems.

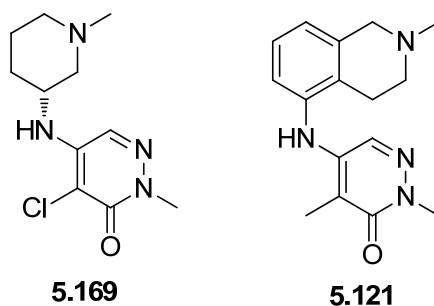


Figure 100: Key compounds for the discovery of probe PCAF inhibitors.

Tetrahydroisoquinoline **5.121** was an important compound as adding a linkable extended amino group to this compound enabled the generation of a new assay reagent that allowed the tight binding limit of the PCAF assay to be increased. Through the increase in the tight binding limit more potent compounds could be identified. The FRET assay reagent (**5.138**, Fig. 90, p 193) derived from the aminopyridazinone series has allowed an HTS to be run to identify other chemotypes that might identify novel PCAF inhibitors or new templates

capable of inhibiting BCPs. Elaborating tetrahydroisoquinoline **5.121** also enabled chemoproteomics experiments to investigate the binding of test compounds to endogenous BCPs.

The probe compounds selected show that dual PCAF and GCN5 inhibition does not show an immuno-inflammation phenotype. The aforementioned in-cell BRET assay has shown phenyl-piperidine compound **5.200** can displace PCAF from chromatin in HEK293 cells and prove cellular target engagement.

The lack of efficacy of these molecules in immuno-inflammation phenotypes does not mean they have no biological activity at all. In non-immune cell types there could be biological activity. To this end, other areas of the organisation have been notified of the profile of these molecules and are still being actively profiled through the phenotypic assay available elsewhere in our laboratories. The compounds are also being shared with the Sanger Institute to determine if the KAT2 family of bromodomains has any role in cancer.³⁴³

The compounds identified show significant improvement on the previously known PCAF inhibitors NP1 (**5.015**) and ischemin (**5.019**) (p 137) as they are over 1000-fold more potent in our assays against PCAF. The KAT2 family inhibitors also show excellent selectivity over other bromodomains, which previously reported PCAF inhibitors did not achieve. The probe compounds discovered are more amenable as starting points for potential medicines as they contain no chemical groups with known developability issues such as the nitro group in NP1 (**5.015**) or the diazo linker in ischemin (**5.019**).

In summary, selective KAT2 family inhibitors have been identified with a range of physicochemical properties. These compounds have been shown to bind to the endogenous PCAF bromodomain through the use of chemoproteomics experiments and an in-cell BRET assay. These are the first known selective molecules to achieve proven binding to the KAT2 family of bromodomains.

6 Experimental

6.1 General experimental abbreviations

a/a – percentage area of area

aq. – aqueous

decomp – decomposed

h – hour

LRMS – low resolution mass spec

MDAP – mass directed autoprep

min – minutes

mp – melting point

sat. – saturated

6.2 NMR abbreviations

app. – apparent

br. – broad

d – doublet

dd – doublet of doublets

q – quartet

quin – quintet

s – singlet

spt – septuplet

sxt – sextet

t – triplet

tt – triplet of triplets

6.3 General methods

All solvents were of analytical grade, purchased from Sigma-Aldrich in anhydrous form.

Reagents were purchased from standard suppliers and used without further purification.

Melting points were determined on a Stuart SMP10 melting point apparatus.

Infrared spectra were recorded on a Perkin Elmer Spectrum One Fourier Transform spectrometer. Selected absorptions are reported and quoted in wavenumbers (cm^{-1}).

^1H NMR were recorded on a Bruker (400 MHz) or Bruker (600 MHz) spectrometer. Chemical shifts are quoted in ppm relative to trimethylsilane and are internally referenced to the residual solvent peak. Coupling constants are given to the nearest 0.5 Hz.

^{13}C NMR were recorded on a Bruker (101 MHz) or Bruker (151 MHz) spectrometer. Chemical shifts are quoted in ppm referenced relative to the residual solvent peak.

HRMS

Chromatography and analysis conditions: An Agilent 1100 Liquid Chromatograph equipped with a model G1367A autosampler, a model G1312A binary pump and a HP1100 model G1315B diode array detector was used. The method used was generic for all experiments. All separations were achieved using a C_{18} reversed phase column (100 x 2.1 mm, 3 μm particle size) or equivalent. Gradient elution was carried out with the mobile phases as (A) water containing 0.1% (v/v) TFA and (B) acetonitrile containing 0.1% (v/v) TFA. The conditions for the gradient elution were initially 0% B, increasing linearly to 95% B over 8 min, remaining at 95% B for 0.5 min then decreasing linearly to 0% B over 0.1 min followed by an equilibration period of 1.49 min prior to the next injection. The flow rate was 1 ml/min, split to source and the temperature controlled at 40 $^{\circ}\text{C}$ with an injection volume of between 2 to 5 μL .

Mass Spectrometry conditions: Positive ion mass spectra were acquired using a Thermo LTQ–Orbitrap FT mass spectrometer, equipped with an ESI interface, over a mass range of 100 – 1100 Da, with a scan time of 1 sec. The elemental composition was calculated using

Xcalibur software and processed using RemoteAnalyzer (Spectral Works Ltd) for the [M+H]⁺ and the mass error quoted as ppm.

LRMS analysis was conducted on a Waters ZQ

Ionisation mode : Positive Electrospray

Scan Range : 100 to 1000 AMU

Scan Time : 0.27 seconds

Inter scan Delay : 0.05 seconds

Conditions for Mass Directed Auto-Preparative Chromatography (MDAP)

HPH Method A

LC Conditions

The HPLC analysis was conducted on an XBridge C18 column (100 mm x 30mm i.d. 5 µm packing diameter) at ambient temperature.

The solvents employed were:

A = 10 mM NH₄HCO₃ in water adjusted to pH 10 with aq. NH₃ solution.

B = MeCN.

The gradient employed was:

Time (min)	Flow Rate (mL/min)	%A	%B
0	40	95	5
1	40	95	5
10	40	70	30
11	40	1	99
15	40	1	99

The UV detection was an averaged signal from wavelength of 210 nm to 350 nm.

MS Conditions

MS : Waters ZQ

Ionisation mode : Alternate-scan Positive and Negative Electrospray

Scan Range : 150 to 1500 AMU

Scan Time : 0.50 seconds

Inter scan Delay : 0.25 seconds

HPH Method B

LC Conditions

The HPLC analysis was conducted on an XBridge C18 column (100 mm x 30mm i.d. 5 µm packing diameter) at ambient temperature.

The solvents employed were:

A = 10 mM NH₄HCO₃ in water adjusted to pH 10 with aq. NH₃ solution.

B = MeCN.

The gradient employed was:

Time (min)	Flow Rate (mL/min)	%A	%B
0	40	85	15
1	40	85	15
10	40	45	55
10.5	40	1	99
15	40	1	99

The UV detection was an averaged signal from wavelength of 210 nm to 350 nm.

MS Conditions

MS : Waters ZQ

Ionisation mode : Alternate-scan Positive and Negative Electrospray

Scan Range : 150 to 1500 AMU

Scan Time : 0.50 seconds

Inter scan Delay : 0.25 seconds

HPH Method C

LC Conditions

The HPLC analysis was conducted on an XBridge C18 column (100 mm x 30 mm i.d. 5 µm packing diameter) at ambient temperature.

The solvents employed were:

A = 10 mM NH_4HCO_3 in water adjusted to pH 10 with aq. NH_3 solution.

B = MeCN.

The gradient employed was:

Time (min)	Flow Rate (mL/min)	%A	%B
0	40	70	30
1	40	70	30
10	40	15	85
11	40	1	99
15	40	1	99

The UV detection was an averaged signal from wavelength of 210 nm to 350 nm.

MS Conditions

MS : Waters ZQ

Ionisation mode : Alternate-scan Positive and Negative Electrospray

Scan Range : 150 to 1500 AMU

Scan Time : 0.50 seconds

Inter scan Delay : 0.25 seconds

HPH Method E

LC Conditions

The HPLC analysis was conducted on an XBridge C18 column (100 mm x 30 mm i.d. 5 μm packing diameter) at ambient temperature.

The solvents employed were:

A = 10 mM NH_4HCO_3 in water adjusted to pH 10 with aq. NH_3 solution.

B = MeCN.

The gradient employed was:

Time (min)	Flow Rate (mL/min)	%A	%B
0	40	95	5

1	40	95	5
10	40	70	30
11	40	1	99
15	40	1	99

The UV detection was an averaged signal from wavelength of 210 nm to 350 nm.

MS Conditions

MS : Waters ZQ

Ionisation mode : Alternate-scan Positive and Negative Electrospray

Scan Range : 150 to 1500 AMU

Scan Time : 0.50 seconds

Inter scan Delay : 0.25 seconds

Formic Method A

LC Conditions

The HPLC analysis was conducted on a Sunfire C18 column (150 mm x 30 mm i.d. 5µm packing diameter) at ambient temperature.

The solvents employed were:

A = 0.1% v/v solution of CHO₂H in Water.

B = 0.1% v/v solution of CHO₂H in MeCN.

The gradient employed was:

Time (min)	Flow Rate (mL/min)	%A	%B
0	40	95	5
1	40	95	5
10	40	70	30
10.5	40	1	99
15	40	1	99

The UV detection was an averaged signal from wavelength of 210 nm to 350 nm.

MS Conditions

MS : Waters ZQ

Ionisation mode : Alternate-scan Positive and Negative Electrospray

Scan Range : 150 to 1500 AMU

Scan Time : 0.50 seconds

Inter scan Delay : 0.25 seconds

Formic Method B

LC Conditions

The HPLC analysis was conducted on a Sunfire C18 column (150 mm x 30 mm i.d. 5µm packing diameter) at ambient temperature.

The solvents employed were:

A = 0.1% v/v solution of CHO₂H in Water.

B = 0.1% v/v solution of CHO₂H in MeCN.

The gradient employed was:

Time (min)	Flow Rate (mL/min)	%A	%B
0	40	85	15
1	40	85	15
10	40	45	55
10.5	40	1	99
15	40	1	99

The UV detection was an averaged signal from wavelength of 210 nm to 350 nm.

MS Conditions

MS : Waters ZQ

Ionisation mode : Alternate-scan Positive and Negative Electrospray

Scan Range : 150 to 1500 AMU

Scan Time : 0.50 seconds

Inter scan Delay : 0.25 seconds

Formic Method C

LC Conditions

The HPLC analysis was conducted on a Sunfire C18 column (150 mm x 30 mm i.d. 5µm packing diameter) at ambient temperature.

The solvents employed were:

A = 0.1% v/v solution of CHO₂H in Water.

B = 0.1% v/v solution of CHO₂H in MeCN.

The gradient employed was:

Time (min)	Flow Rate (mL/min)	%A	%B
0	40	70	30
1	40	70	30
10	40	15	85
11	40	1	99
15	40	1	99

The UV detection was an averaged signal from wavelength of 210 nm to 350 nm.

MS Conditions

MS : Waters ZQ

Ionisation mode : Alternate-scan Positive and Negative Electrospray

Scan Range : 150 to 1500 AMU

Scan Time : 0.50 seconds

Inter scan Delay : 0.25 seconds

Formic Method D

LC Conditions

The HPLC analysis was conducted on a Sunfire C18 column (150 mm x 30 mm i.d. 5µm packing diameter) at ambient temperature.

The solvents employed were:

A = 0.1% v/v solution of CHO₂H in Water.

B = 0.1% v/v solution of CHO₂H in MeCN.

The gradient employed was:

Time (min)	Flow Rate (mL/min)	%A	%B
0	40	50	50
1	40	50	50
10	40	1	99
11	40	1	99
15	40	1	99

The UV detection was an averaged signal from wavelength of 210 nm to 350 nm.

MS Conditions

MS : Waters ZQ

Ionisation mode : Alternate-scan Positive and Negative Electrospray

Scan Range : 150 to 1500 AMU

Scan Time : 0.50 seconds

Inter scan Delay : 0.25 seconds

TFA Method B

LC Conditions

The HPLC analysis was conducted on a Sunfire C18 column (150 mm x 30 mm i.d. 5 µm packing diameter) at ambient temperature.

The solvents employed were:

A = 0.1% v/v solution of TFA in Water.

B = 0.1% v/v solution of TFA in MeCN.

The gradient employed was:

Time (min)	Flow Rate (mL/min)	%A	%B
0	40	85	15
1	40	85	15
10	40	45	55
10.5	40	1	99

The UV detection was an averaged signal from wavelength of 210 nm to 350 nm.

MS Conditions

MS : Waters ZQ

Ionisation mode : Positive Electrospray

Scan Range : 150 to 1500 AMU

Scan Time : 0.50 seconds

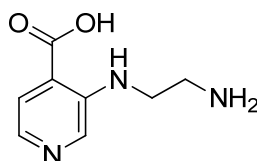
Inter scan Delay : 0.25 seconds

Under microwave conditions means heated in a Biotage® Initiator microwave synthesiser.

6.4 Procedures

6.4.1 6,7- and 6,5- sized ring systems

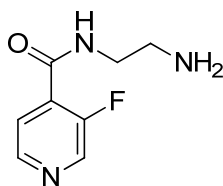
3-((2-Aminoethyl)amino)isonicotinic acid (4.021)¹⁰⁹



Chemical Formula: C₈H₁₁N₃O₂
Molecular Weight: 181.19

3-Fluoroisonicotinic acid (255 mg, 1.81 mmol) was added to ethylenediamine (1.50 mL, 22.4 mmol) and the resulting suspension heated under microwave conditions at 150 °C for 2 h. The mixture was loaded on to a preconditioned 5 g aminopropyl column, eluted with IPA (30 mL) followed by aq. 2 M HCl (25 mL). The acidic fractions were evaporated to dryness *in vacuo*, loaded on to a 10 g SCX cartridge and eluted with water:MeOH (1:1) (50 mL) followed by 2 M methanolic ammonia (50 mL). The basic fractions were evaporated to a white solid, triturated with MeOH (2 mL), filtered and dried *in vacuo* to give the title compound **4.021** as a white solid (140 mg, 41%): ¹H NMR (D₂O, 400 MHz) δ 8.09 (s, 1H), 7.90 (d, *J* = 5.0 Hz, 1H), 7.57 (d, *J* = 5.0 Hz, 1H), 3.62 (t, *J* = 6.0 Hz, 2H), 3.27 (t, *J* = 6.0 Hz, 2H); LRMS [M+H]⁺: 182; 100% a/a.

N-(2-Aminoethyl)-3-fluoroisonicotinamide (4.023)¹¹¹

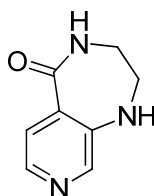


Chemical Formula: C₈H₁₀FN₃O
Molecular Weight: 183.18

Methyl 3-fluoroisonicotinate (286 mg, 1.84 mmol) was added to a solution of ethylenediamine (0.148 mL, 2.21 mmol) in ethanol (4 mL). The resulting mixture was heated under microwave conditions at 100 °C for 1 h. The resulting mixture was evaporated to dryness, triturated with DCM (2 mL), filtered and the solid recrystallised from DMSO:MeOH (1:1, 0.4 mL). The resulting solid was washed (2× MeOH, 0.4 mL) and dried *in*

vacuo to give the title compound **4.023** as a white solid (105 mg, 30%): $^1\text{H NMR}$ (CD_3CN , 400 MHz) δ 8.59 (d, $J = 2.5$ Hz, 1H), 8.53 (dd, $J = 1.0, 5.0$ Hz, 1H), 7.70 (dd, $J = 1.0, 5.0$ Hz), 7.51 (br.s, 1H), 3.62 - 3.51 (m, 2H), 3.03 - 2.90 (m, 2H); LRMS $[\text{M}+\text{H}]^+$: 184; 100% a/a.

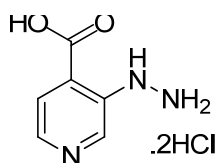
3,4-Dihydro-1H-pyrido[3,4-e][1,4]diazepin-5(2H)-one (4.020)¹⁰⁹



Chemical Formula: $\text{C}_8\text{H}_9\text{N}_3\text{O}$
Molecular Weight: 163.18

N-(2-Aminoethyl)-3-fluoroisonicotinamide (**11**) (95 mg, 0.52 mmol) was suspended in DMSO (12 mL) and heated to 160 °C under N_2 for 4 h. The resulting solution was cooled to room temperature and loaded on to a 5 g SCX cartridge. The cartridge was eluted with MeOH (40 mL), followed by 2 M methanolic ammonia (30 mL). The basic fractions were evaporated to dryness and purified by MDAP (HPH method A) to give the title compound **4.020** as a pale yellow solid (20 mg, 21%): $^1\text{H NMR}$ (CDCl_3 , 400 MHz) δ 8.08 (s, 1H), 7.98 (d, $J = 5.5$ Hz, 1H), 7.78 (d, $J = 5.5$ Hz, 1H), 6.73 (br.s, 1H), 4.62 (br.s, 1H), 3.70 - 3.62 (m, 2H), 3.57 - 3.50 (m, 2H); LRMS $[\text{M}+\text{H}]^+$: 164; 100% a/a.

3-Hydrazinylisonicotinic acid. 2 HCl (4.027)¹¹³

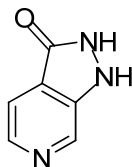


Chemical Formula: $\text{C}_6\text{H}_7\text{N}_3\text{O}_2 \cdot 2\text{HCl}$
Molecular Weight: 226.06

Conc. HCl (22.0 mL, 264 mmol) was added to a stirred suspension of 3-aminoisonicotinic acid (2.8g, 20 mmol) and the resulting suspension cooled in an ice bath. Sodium nitrite (1.6 g, 23 mmol) was added dropwise and the resulting solution stirred for 1 h. The solution was added dropwise to a solution of water sparging with gaseous sulfur dioxide and the resulting suspension stirred for 1 h and allowed to stand overnight. The suspension was stirred for 5 min, filtered, the resulting filtercake washed [2x water (20 mL), 1x water:MeOH

(20 mL, 1:1)] and dried *in vacuo* at 40 °C for 5 h to give the title compound **4.027** as a yellow solid (3.02 g, 66%): ¹H NMR (SO(CD₃)₂, 400 MHz) δ 8.92 (br.s, 1H), 8.73 (s, 1H), 8.10 - 7.99 (m, 2H), exchangeable protons not observed.

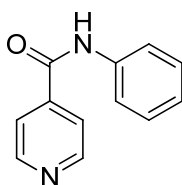
1H-Pyrazolo[3,4-c]pyridin-3(2H)-one (4.025)¹¹³



Chemical Formula: C₆H₅N₃O
Molecular Weight: 135.12

3-Hydrazinylisonicotinic acid. 2HCl (1.00 g, 4.42 mmol) was added to a stirred solution of 2M aq. HCl (50 mL, 100 mmol) and the mixture heated to reflux for 5 h and cooled to room temperature overnight. The solution was evaporated *in vacuo* to give a yellow solid. The residue was suspended in water (30 mL) and 50% aq. NaOH added until the resulting suspension was brought to pH 7. The precipitate was recrystallised from the mother liquors to give the title compound **4.025** as an orange solid (269 mg, 45%): ¹H NMR (SO(CD₃)₂, 400 MHz) δ 12.11 (br.s, 1H), 10.82 (br.s, 1H), 8.80 (d, *J* = 1.5 Hz, 1H), 8.09 (d, *J* = 5.5 Hz, 1H), 7.60 (dd, *J* = 1.5, 5.5 Hz, 1H); ¹³C NMR (SO(CD₃)₂, 100 MHz) δ 154.6, 138.0, 136.7, 134.4, 115.1, 133.7; LRMS [M+H]⁺ = 136; IR: ν 3071, 3017, 1641, 1552, 1484, 1435, 1338, 1254, 1088 cm⁻¹; mp > 250 °C.

N-Phenylisonicotinamide (4.030)¹¹⁶



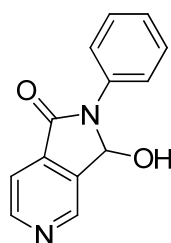
Chemical Formula: C₁₂H₁₀N₂O
Molecular Weight: 198.22

CDI (7.90 g, 48.7 mmol) was added to a stirred suspension of isonicotinic acid (5.00 g, 40.6 mmol) in 2-MeTHF (50 mL) and the resulting suspension heated to 50 °C for 30 min. Aniline (4.82 mL, 52.8 mmol) was added and the resulting solution stirred at 50 °C for 20 min. The mixture was cooled to room temperature and a precipitate formed. The suspension was

washed [3× water (10 mL), brine (10 mL)], and dried over MgSO₄. The aqueous washings were extracted [3× DCM (20 mL)], combined with the washed and dried organic layer and evaporated *in vacuo* to give a brown solid. The solid was triturated with EtOAc (5 mL) and the resulting solid washed [2x EtOAc (5 mL)] and dried *via* filtration to give the title compound **4.030** as a white crystalline solid (5.96 g, 70%): ¹H NMR (CDCl₃, 400 MHz) δ 8.79 (d, *J* = 6.0 Hz, 2H), 7.91 (br.s, 1H), 7.70 (d, *J* = 6.0 Hz, 2H), 7.63 (d, *J* = 8.0 Hz, 2H), 7.45 - 7.35 (m, 2H), 7.23 - 7.16 (m, 1H); LRMS [M+H]⁺: 199, 100% a/a.

The washings were evaporated *in vacuo* to dryness and the residue purified by silica gel chromatography cyclohexane:EtOAc (75 → 100%) to give a second crop of the title compound **4.030** as a white solid (1.14 g, 13%): Analytical data as above.

3-Hydroxy-2-phenyl-2,3-dihydro-1H-pyrrolo[3,4-c]pyridin-1-one (**4.031**)¹¹⁶



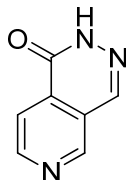
Chemical Formula: C₁₃H₁₀N₂O₂
Molecular Weight: 226.23

1.6 M *n*-Butyllithium in hexanes (7.91 mL, 12.65 mmol) was added dropwise to a stirred solution of *N*-phenylisonicotinamide (**4.030**) (1.14 g, 5.75 mmol) in dry THF (36 mL) under N₂ at -70 °C and stirred for 30 min at -70 °C and warmed to 0 °C for 5 min. The resulting solution was re-cooled to -70 °C and dry DMF (0.891 mL, 11.5 mmol) added dropwise. The mixture was allowed to come to room temperature overnight, acidified to pH 2 with 2 M aq. HCl and the organic layer separated. The aqueous layer was extracted (2x chloroform [20 mL]), the combined organic layers dried over MgSO₄ and evaporated *in vacuo* to dryness. The residue was purified by silica gel chromatography eluting with DCM:MeOH (0 → 10%) to give an impure brown solid containing the title compound **4.031** (84 mg). Used crude.

The mixed fractions from the column were evaporated *in vacuo* and triturated with EtOAc and the resulting white solid dried *in vacuo* to give an analytically pure sample of the title compound **4.031** as a white solid (32 mg, 2%): ¹H NMR (SO(CD₃)₂, 400 MHz) δ 9.00 (s, 1H),

8.88 (d, $J = 5.0$ Hz, 1H), 7.81 - 7.73 (m, 3H), 7.54 - 7.44 (m, 2H), 7.28 (t, $J = 7.5$ Hz, 1H), 7.08 (d, $J = 10.0$ Hz, 1H), 6.72 (d, $J = 10.0$ Hz, 1H); LRMS $[M+H]^+$: 227; 99% a/a

Pyrido[3,4-*d*]pyridazin-1(2*H*)-one (4.029)¹¹⁶

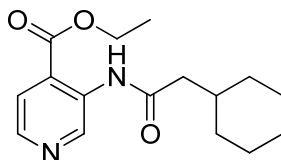


Chemical Formula: $C_7H_5N_3O$
Molecular Weight: 147.13

3-Hydroxy-2,3-dihydro-1*H*-pyrrolo[3,4-*c*]pyridin-1-one (4.031) (84 mg, 0.56 mmol) was added to a stirred solution of 35% aq. hydrazine (2.40 g, 26.2 mmol) and the mixture heated to reflux under N_2 for 2 h. The mixture was evaporated *in vacuo* and the residue purified by MDAP (HPH method A) to give the title compound 4.029 a pale brown solid (7.3 mg, 8%): 1H NMR ($SO(CD_3)_2$, 400 MHz) δ 13.00 (br.s, 1H), 9.33 (s, 1H), 8.98 (d, $J = 5.5$ Hz, 1H), 8.53 (s, 1H), 8.07 (d, $J = 5.5$ Hz, 1H); LRMS $[M-H]^-$: 146; 94% a/a

6.4.2 Pyridopyrimidinones

Ethyl 3-(2-cyclohexylacetamido)isonicotinate (4.044a)¹¹¹

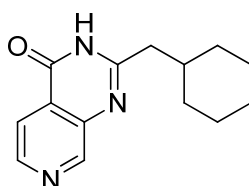


Chemical Formula: $C_{16}H_{22}N_2O_3$
Molecular Weight: 290.36

2-Cyclohexylacetic acid (171 mg, 1.20 mmol) was added to a solution of ethyl 3-aminoisonicotinate (200 mg, 1.20 mmol) and DIPEA (0.84 mL, 4.8 mmol) in DCM (10 mL), and the resulting mixture stirred at 20 °C under N_2 for 5 min. 2,4,6-Tripropyl-1,3,5,2,4,6-trioxatriphosphinane 2,4,6-trioxide (1.08 mL, 1.81 mmol) was added and the resulting mixture stirred for 18 h. 2-Cyclohexylacetic acid (100 mg, 0.703 mmol) and 2,4,6-tripropyl-1,3,5,2,4,6-trioxatriphosphinane 2,4,6-trioxide (400 mg, 1.26 mmol) were added and the reaction mixture stirred for a further 18 h under the same conditions. The reaction mixture was partitioned between sat. aq. $NaHCO_3$ (10 mL) and DCM (10 mL). The organic layer was

removed and aqueous layer extracted further with DCM (3x 20 mL). The combined organic layers were washed with water (10 mL) and filtered through a hydrophobic frit. The resulting solution was concentrated *in vacuo* to an oil. The residue was purified by silica gel chromatography eluting with DCM to give the title compound as a white solid (201 mg, 58%): $^1\text{H NMR}$ (CDCl_3 , 400 MHz) δ 10.60 (br.s, 1H), 9.99 (s, 1H), 8.36 (d, $J = 5.0$ Hz, 1H), 7.75 (d, $J = 5.0$ Hz), 4.40 (q, $J = 7.0$ Hz, 2H), 2.29 (d, $J = 7.5$ Hz, 2H), 1.95 - 1.81 (m, 1H), 1.81 - 1.56 (m, 6H), 1.40 (t, $J = 7.0$ Hz, 3H), 1.34 - 0.89 (m, 6H); LRMS $[\text{M}+\text{H}]^+$: 291; 98% a/a.

2-(Cyclohexylmethyl)pyrido[3,4-d]pyrimidin-4(3H)-one (4.044)¹²¹

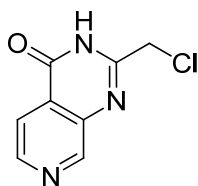


Chemical Formula: $\text{C}_{14}\text{H}_{17}\text{N}_3\text{O}$

Molecular Weight: 243.30

Ethyl 3-(2-cyclohexylacetamido)isonicotinate (200 mg, 0.689 mmol) was dissolved in 7 M methanolic ammonia (10 mL, 70 mmol) and stirred at 20 °C for 19 h. Further 7 M methanolic ammonia (10 mL, 70 mmol) was added and the solution warmed to 40 °C over the weekend. The solvent was filtered to give the title compound as a cream powder (83 mg, 50%): $^1\text{H NMR}$ ($\text{SO}(\text{CD}_3)_2$, 400 MHz) δ 12.42 (br.s, 1H), 8.99 (s, 1H), 8.60 (d, $J = 5.0$ Hz, 1H), 7.91 (d, $J = 5.0$ Hz, 1H), 2.53 (d, $J = 7.4$ Hz, 2H), 1.96 - 1.81 (m, 1H), 1.74 - 1.6 (m, 5H), 1.29 - 1.10 (m, 3H), 1.08 - 0.94 (m, 2H); LRMS $[\text{M}+\text{H}]^+$: 244, 100% a/a.

2-(Chloromethyl)pyrido[3,4-d]pyrimidin-4(3H)-one (4.047)¹³⁷



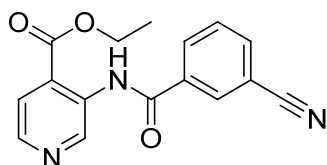
Chemical Formula: $\text{C}_8\text{H}_6\text{ClN}_3\text{O}$

Molecular Weight: 195.61

Chloroacetonitrile (1.00 mL, 15.8 mmol) was added to a stirred suspension of methyl 3-aminoisonicotinate (2.00 g, 13.1 mmol) in 4M HCl in dioxane (25 mL, 100 mmol) and the mixture heated to 80 °C for 3 h. The mixture was cooled to 50 °C, chloroacetonitrile (1.00

mL, 15.8 mmol) added and the mixture heated at this temperature for 60 h. The mixture was evaporated *in vacuo* to dryness, recharged with 4M HCl in dioxane (25 mL, 100 mmol) and chloroacetonitrile (1.00 mL, 15.8 mmol) and heated to 50 °C overnight. The mixture was evaporated *in vacuo* to dryness, recharged with 4M HCl in dioxane (25 mL, 100 mmol), chloroacetonitrile (1.00 mL, 15.8 mmol) and heated to 50 °C. The mixture was cooled to room temperature, filtered, the filtercake washed (2x dioxane (10 mL), 2x TBME (10 mL)) and dried *in vacuo* at 40 °C to give a brown solid. The residue was stirred in 5% aq. K₂CO₃ (100 mL) and the resulting solution loaded on to a Biotage 103 column (10 g). The column was eluted with water (50 mL), followed by MeOH (150 mL). The organic fractions were evaporated *in vacuo* to give the title compound **4.047** as a red solid (1.16g, 45%): ¹H NMR (SO(CD₃)₂, 400 MHz) δ 12.93 (br.s, 1H), 9.06 (s, 1H), 8.68 (d, *J* = 5.0 Hz, 1H), 7.96 (d, *J* = 5.0 Hz, 1H), 4.59 (s, 2H); ¹³C NMR (SO(CD₃)₂, 101 MHz) δ 161.1, 154.9, 151.0, 147.1, 143.4, 126.9, 118.6, 43.5 ; LRMS [M+H]⁺: 196, 198; 97% a/a; IR: solid v 2707, 1695, 1618, 1422, 1286, 1120, 1046, cm⁻¹; HRMS: C₈H₇ClN₃O [M+H]⁺ requires 196.0272, found [M+H]⁺ 196.0281; mp 240 °C (dec.).

Ethyl 3-(3-cyanobenzamido)isonicotinate (**4.052a**)¹¹¹



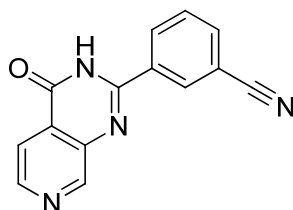
Chemical Formula: C₁₆H₁₃N₃O₃
Molecular Weight: 295.29

T3P® 50% in EtOAc (1.51 mL, 2.53 mmol) was added to a stirred suspension of ethyl 3-aminoisonicotinate (300 mg, 1.81 mmol), 3-cyanobenzoic acid (292 mg, 1.99 mmol) and DIPEA (0.95 mL, 5.42 mmol) in dry DCM (5 mL) under N₂. The reaction mixture was stirred overnight, washed with sat. aq. NaHCO₃ (5 mL), the aqueous fraction extracted with DCM (5 mL), the organic layers, combined, dried over MgSO₄ and evaporated *in vacuo* to a brown oil. The residue was purified by silica gel chromatography eluting with cyclohexane:EtOAc (0 -> 50%) to give a residue which was purified by silica gel chromatography eluting with DCM:2 M methanolic ammonia (0 -> 2%) to give the title compound **4.052a** as a pale yellow solid (55 mg, 10%): ¹H NMR (CDCl₃, 400 MHz) δ 11.81 (br.s, 1H), 10.20 (d, *J* = 5.0 Hz, 1H),

8.35 - 8.31 (m, 1H), 8.29 - 8.24 (m, 1H), 7.91 - 7.84 (m, 2H), 7.68 (app.t, $J = 8.0$ Hz, 1H), 4.50 (q, $J = 7.0$ Hz, 2H), 1.47 (t, $J = 7.0$ Hz, 3H); LRMS $[M+H]^+$: 296; 97% a/a).

The filtrate from the trituration was purified by MDAP (HPH Method A) to yield a second crop of the title compound as a pale yellow solid (33 mg, 60%): Analytical data as above.

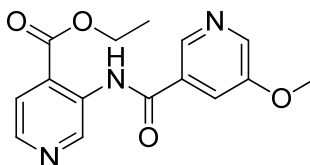
3-(4-Oxo-3,4-dihydropyrido[3,4-*d*]pyrimidin-2-yl)benzonitrile (4.052)¹²¹



Chemical Formula: $C_{14}H_8N_4O$
Molecular Weight: 248.24

3-(3-Cyanobenzamido)isonicotinate (88 mg, 0.30 mmol) was added to a solution of 7 M ammonia in MeOH (5 mL, 35.0 mmol) and the resulting solution allowed to stand overnight. 10 M aq. sodium hydroxide (0.30 mL, 3.0 mmol) was added to the solution and stirred. 2 M aq. HCl (1.5 mL, 3.0 mmol) was added, the mixture stirred for 15 min, evaporated *in vacuo* to dryness, suspended in EtOAc (10 mL) and water (5 mL) and the mixture filtered. The filtercake was washed with water (1 mL) and MeOH (1 mL). The residue was purified by MDAP (HPH Method A) to give the title compound **4.052** as a white solid (48 mg, 52%): ¹H NMR ($CDCl_3$, 400 MHz) δ 13.00 (br.s, 1H), 9.16 (s, 1H), 8.70 (d, $J = 5.0$ Hz, 1H), 8.60 (s, 1H), 8.50 (d, $J = 8.0$ Hz, 1H), 8.10 (d, $J = 8.0$ Hz, 1H), 8.00 (d, 5.0 Hz, 1H), 7.80 (app.t, $J = 8.0$ Hz, 1H); LRMS $[M+H]^+$: 249; 99% a/a.

Ethyl 3-(5-methoxynicotinamido)isonicotinate (4.053a)¹¹¹

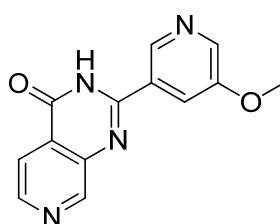


Chemical Formula: $C_{15}H_{15}N_3O_4$
Molecular Weight: 301.30

Oxalyl chloride (0.12 mL, 1.3 mmol) was added to a stirred suspension of 5-methoxynicotinic acid (185 mg, 1.21 mmol) in DCM (5 mL) under N_2 . DMF (0.01 mL, 0.129 mmol) was added and the mixture stirred for 1 h. Ethyl 3-aminoisonicotinate (183 mg, 1.10

mmol) and DIPEA (0.269 mL, 1.54 mmol) were added. The mixture was stirred for 1.5 h and allowed to stand overnight. Sat. aq. NaHCO₃ (5 mL) was added and the separated aqueous phase was extracted with DCM (2x 5 mL). The combined organic phases were dried over MgSO₄, filtered and evaporated *in vacuo* to dryness. The residue was purified by silica gel chromatography eluting with cyclohexane:EtOAc,(0 → 66 %) to give the title compound as a pale yellow solid (197 mg, 57 %): ¹H NMR (CDCl₃, 400 MHz) δ 11.78 (br.s, 1H), 10.20 (s, 1H), 8.86 (d, *J* = 2.0 Hz, 1H), 8.51 (s, 1H), 8.50 (d, *J* = 2.0 Hz, 1H), 7.88 (d, *J* = 5.0 Hz, 1H), 7.84, (dd, *J* = 2.0, 5.0 Hz, 1H), 4.48 (q, *J* = 7.0 Hz, 2H), 3.92 (s, 3H), 1.46 (t, *J* = 7.0 Hz, 3H); LRMS [M+H]⁺: 302, 100% a/a.

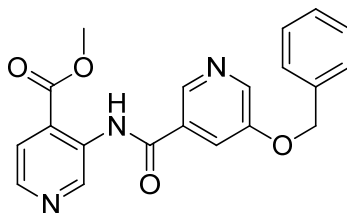
2-(5-Methoxypyridin-3-yl)pyrido[3,4-*d*]pyrimidin-4(3*H*)-one (4.053)¹²¹



Chemical Formula: C₁₃H₁₀N₄O₂
Molecular Weight: 254.24

A solution of ethyl 3-(5-methoxynicotinamido)isonicotinate (197 mg, 0.654 mmol) in 7 M aq. ammonia in MeOH (10 mL, 70.0 mmol) was stirred overnight at room temperature. 10 M aq. sodium hydroxide (0.618 mL, 6.18 mmol) was added to the resulting mixture and stirred over the weekend. 2 M aq. HCl (3.1 mL, 6.20 mmol) was added to the mixture and the resulting suspension stirred for 30 min. The suspended solid was filtered, washed [1x water (5 mL), 1x MeOH (5 mL)] and dried *in vacuo* to give the title compound **4.053** as a white solid (142 mg, 86%): ¹H NMR (SO(CD₃)₂, 400 MHz) δ 13.01 (br.s, 1H), 9.16 (d, *J* = 1.0 Hz, 1H), 8.94 (d, *J* = 2.0 Hz, 1H), 8.70 (d, *J* = 5.0 Hz, 1H), 8.50 (d, *J* = 3.0 Hz, 1H), 8.10 (dd, *J* = 2.0, 3.0 Hz, 1H), 8.01 (dd, *J* = 1.0, 5.0 Hz, 1H), 3.95 (s, 3H); ¹³C NMR (SO(CD₃)₂, 101 MHz) δ 161.8, 155.6, 153.0, 151.3, 143.9, 143.7, 141.4, 141.0, 129.4, 126.7, 119.5, 118.6, 56.4; LRMS [M+H]⁺: 255; 100% a/a; HRMS: C₁₃H₁₁N₄O₂ [M+H]⁺ requires 255.0877, found [M+H]⁺ 255.1190; IR: solid v 1698, 1584, 1418, 1217, 1032, cm⁻¹; mp > 250 °C.

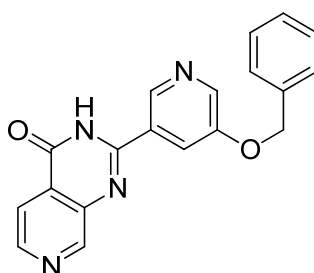
Methyl 3-(5-(benzyloxy)nicotinamido)isonicotinate (4.054a)¹¹¹



Chemical Formula: C₂₀H₁₇N₃O₄
Molecular Weight: 363.37

Oxalyl chloride (0.13 mL, 1.5 mmol) and DMF (0.01 mL) were added to a stirred suspension of sodium 5-(benzyloxy)nicotinate (**55**) (252 mg, 1.00 mmol) in DCM (10 mL). The mixture was stirred for 30 min and evaporated *in vacuo* to a white solid. The residue was suspended in DCM (10 mL), methyl 3-aminoisonicotinate (152 mg, 1.00 mmol) and DIPEA (0.44 mL, 2.5 mmol) were added and the resultant solution stirred overnight. The solution was washed [1x water (10 mL), 1x brine (10 mL)], dried over MgSO₄ and evaporated *in vacuo* to dryness. The residue was purified by silica gel chromatography eluting with DCM: 2 M methanolic ammonia (0 -> 3%). The product containing fractions were evaporated *in vacuo* to dryness and purified by MDAP (HPH Method C) to give the title compound **4.054a** as a yellow solid (87 mg, 24%): ¹H NMR (SO(CD₃)₂, 400 MHz) δ 13.00 (br.s, 1H), 9.15 (s, 1H) 8.96 (d, *J* = 2.0 Hz, 1H), 8.70 (d, *J* = 5.0 Hz, 1H), 8.57 (d, *J* = 3.0 Hz, 1H), 8.22 (m, 1H), 8.01 (dd, *J* = 0.5, 5.0 Hz, 1H), 7.54 - 7.32 (m, 5H), 5.32 (s, 2H), 3.91 (s, 3H); LRMS [M+H]⁺: 364; 95% a/a.

2-(5-(Benzyloxy)pyridin-3-yl)pyrido[3,4-*d*]pyrimidin-4(3*H*)-one (4.054)¹²¹

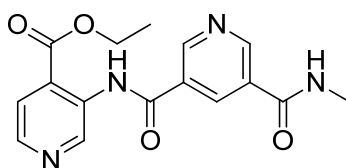


Chemical Formula: C₁₉H₁₄N₄O₂
Molecular Weight: 330.34

Methyl 3-(5-(benzyloxy)nicotinamido)isonicotinate (87 mg, 0.24 mmol) was stirred in 7 M ammonia in MeOH (10 mL, 70.0 mmol) at room temperature. The resulting suspension was stirred for 2 h, 10 M sodium hydroxide (0.239 mL, 2.394 mmol) added, the mixture stirred

for 2 days and treated with 2M HCl (0.479 mL, 2.394 mmol), evaporated *in vacuo* to dryness and purified by silica gel chromatography eluting with DCM:MeOH (0 -> 4%) to give an impure white solid. The solid was triturated with MeOH (1 mL), filtered, washed with MeOH (1 mL) and evaporated *in vacuo* to give the title compound **4.054** as a white solid (17 mg, 21%): ¹H NMR (SO(CD₃)₂, 400 MHz) δ 13.00 (br.s, 1H), 9.15 (s, 1H) 8.96 (d, *J* = 2.0 Hz, 1H), 8.70 (d, *J* = 5.0 Hz, 1H), 8.57 (d, *J* = 3.0 Hz, 1H), 8.22 (dd, *J* = 0.5, 2.0 Hz, 1H), 8.01 (dd, *J* = 0.5, 5.0 Hz, 1H), 7.56 - 7.50 (m, 2H), 7.48 - 7.41 (m, 2H), 7.41 - 7.35 (m, 1H), 5.31 (s, 2H); LRMS [M+H]⁺: 331; 100% a/a.

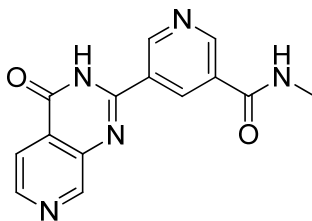
Ethyl 3-(5-(methylcarbamoyl)nicotinamido)isonicotinate (**4.056a**)¹¹¹



Chemical Formula: C₁₆H₁₆N₄O₄
Molecular Weight: 328.32

Oxalyl chloride (0.116 mL, 1.320 mmol) was added to a stirred suspension of (methylcarbamoyl)nicotinic acid (201 mg, 1.12 mmol) in DCM (5 mL) under N₂. DMF (0.010 mL, 0.13 mmol) was added and the mixture stirred for 1 h. Ethyl 3-aminoisonicotinate (183 mg, 1.10 mmol) and DIPEA (0.269 mL, 1.54 mmol) were added. The mixture was stirred for 1.5 h and allowed to stand overnight. Sat. aq. NaHCO₃ (5 mL) was added and the separated aq. phase was extracted with DCM (2x 5 mL). The combined organic phases were dried over MgSO₄, filtered and evaporated *in vacuo* to dryness. The residue was purified by silica gel chromatography eluting with DCM:2 M methanolic ammonia (0 -> 5%) to give the title compound **4.056a** as a white solid (203 mg, 56%): ¹H NMR (CDCl₃, 400 MHz) δ 11.90 (br.s, 1H), 10.18 (s, 1H), 9.37 (d, *J* = 2.5 Hz, 1H), 9.22 (d, *J* = 2.0 Hz, 1H), 8.69 (dd, *J* = 2.0, 2.5 Hz, 1H), 8.53 (d, *J* = 5.0 Hz, 1H), 7.89 (dd, *J* = 0.5, 5.0 Hz, 1H), 6.40 (br.s, 1H), 4.49 (q, *J* = 7.0 Hz, 2H), 3.09 (d, *J* = 5.0 Hz, 3H), 1.46 (t, *J* = 7.0 Hz, 3H); LRMS [M+H]⁺ 329; 100% a/a.

5-(4-Oxo-3,4-dihydropyrido[3,4-*d*]pyrimidin-2-yl)nicotinamide (4.056)¹²¹

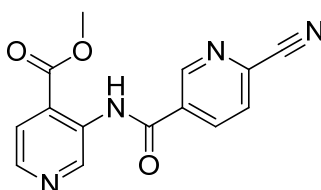


Chemical Formula: C₁₄H₁₁N₅O₂

Molecular Weight: 281.27

A solution of *N*-methyl-5-(4-oxo-3,4-dihydropyrido[3,4-*d*]pyrimidin-2-yl)nicotinamide (203 mg, 0.62 mmol) in a solution of 7 M ammonia in MeOH (10 mL, 70.0 mmol) was stirred overnight. A solution of 10 M aq. NaOH (0.618 mL, 6.18 mmol) was added to the resulting mixture and the mixture stirred over the weekend. 2 M aq. HCl (3.1 mL, 6.20 mmol) was added to the mixture and the resulting suspension stirred for 30 min. The suspended solid was filtered, washed [1x water (5 mL), 1x MeOH (5 mL)] and dried *in vacuo* to give the title compound **4.056** as a white solid (96 mg, 56%): ¹H NMR (SO(CD₃)₂, 400 MHz) δ 13.10 (br.s, 1H), 9.39 (d, *J* = 2.0 Hz, 1H), 9.21 - 9.11 (m, 2H), 8.94 - 8.86 (m, 1H), 8.82 - 8.74 (m, 1H), 8.70 (d, *J* = 5.0 Hz, 1H), 8.01 (d, *J* = 5.0 Hz, 1H), 2.87 (s, *J* = 4.5 Hz, 3H); LRMS [M+H]⁺: 282, 100% a/a.

Methyl 3-(6-cyanonicotinamido)isonicotinate (4.061)¹¹¹



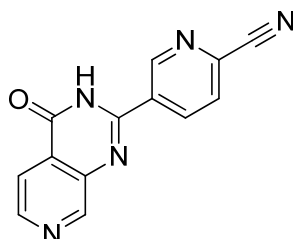
Chemical Formula: C₁₄H₁₀N₄O₃

Molecular Weight: 282.25

6-Cyanonicotinic acid (321 mg, 2.17 mmol) was suspended in dry DCM (5 mL) with stirring under N₂. Oxalyl chloride (0.21 mL, 2.4 mmol) and DMF (0.01 mL) were added, the mixture stirred for 30 min. Methyl 3-aminoisonicotinate (300 mg, 1.97 mmol) and DIPEA (0.96 mL, 5.5 mmol) were added, the mixture stirred for 5 min, further dry DCM (5 mL) added and the resulting suspension stirred for 3.5 h. The reaction mixture was partitioned between EtOAc (10 mL) and sat. aq. NaHCO₃ (5 mL). The aqueous layer was separated and the organic layer washed [1x sat. aq. NaHCO₃ (5 mL), 1x brine (5mL)], dried over MgSO₄ and evaporated *in vacuo* to dryness. The residue was purified by silica gel chromatography eluting with

DCM:2 M methanolic ammonia (0 -> 3%) to give the title compound **4.061** as a yellow solid (168 mg, 30%): $^1\text{H NMR}$ (CDCl_3 , 400 MHz) δ 11.90 (br.s, 1H), 10.19 (s, 1H), 9.36 (d, $J = 2.0$ Hz, 1H), 8.56 (d, $J = 5.5$ Hz, 1H), 8.47 (dd, $J = 2.0, 8.0$ Hz, 1H), 7.88 (m, 2H), 4.04 (s, 3H); LRMS $[\text{M}+\text{H}]^+$: 283, 98% a/a.

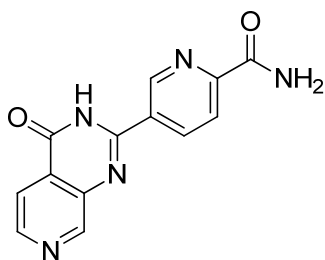
5-(4-Oxo-3,4-dihydropyrido[3,4-*d*]pyrimidin-2-yl)picolinonitrile (**4.064**)¹²¹



Chemical Formula: $\text{C}_{13}\text{H}_7\text{N}_5\text{O}$
Molecular Weight: 249.23

Methyl 3-(6-cyanonicotinamido)isonicotinate (**4.061**) (225 mg, 0.797 mmol) was stirred in 7 M aq. ammonia in MeOH (10 mL, 70 mmol) for 3 days, the mixture adsorbed on to silica and evaporated *in vacuo* to dryness. The residue was purified by silica gel chromatography eluting with DCM:2 M methanolic ammonia (5 -> 20%) to give the title compound **4.064** as an off white solid (89 mg, 45%): $^1\text{H NMR}$ ($\text{SO}(\text{CD}_3)_2$, 400 MHz) δ 13.22 (br.s, 1H), 9.45 (dd, $J = 1.0, 2.0$ Hz, 1H), 9.16 (d, $J = 1.0$ Hz, 1H), 8.74 (dd, $J = 2.0, 8.0$ Hz, 1H), 8.70 (d, $J = 5.0$ Hz, 1H), 8.26 (dd, $J = 1.0, 8.0$ Hz, 1H), 8.00 (dd, $J = 1.0$ Hz, 5.0 Hz, 1H); LRMS $[\text{M}+\text{H}]^+$ 250; 97% a/a.

5-(4-Oxo-3,4-dihydropyrido[3,4-*d*]pyrimidin-2-yl)picolinamide (**4.055**)¹³²

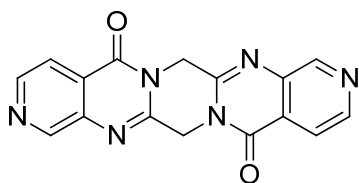


Chemical Formula: $\text{C}_{13}\text{H}_9\text{N}_5\text{O}_2$
Molecular Weight: 267.24

35% aq. Hydrogen peroxide (0.31 mL, 3.6 mmol) was added to a stirred suspension of 5-(4-oxo-3,4-dihydropyrido[3,4-*d*]pyrimidin-2-yl)picolinonitrile (**4.061**) (89 mg, 0.36 mmol) and potassium carbonate (99 mg, 0.71 mmol) at 0 °C in DMSO (10 mL). The resulting mixture was stirred for 3 h and 10% aq. sodium thiosulfate (10 mL) added. The mixture was

adjusted to pH 7 with 2M aq. HCl, the resulting suspension filtered, washed [2x water (20 mL), 1x MeOH:water (1:1, 5 mL), 1x MeOH (5 mL)] and the mixture dried *in vacuo* to give the title compound **4.055** as an almost white solid (54 mg, 57%): ^1H NMR ($\text{SO}(\text{CD}_3)_2$, 400 MHz) δ 13.15 (br.s, 1H), 9.33 (dd, $J = 1.0, 2.5$ Hz, 1H), 9.17 (d, $J = 0.5$ Hz, 1H), 8.71 (m, 2H), 8.26 (br.s, 1H), 8.21 (dd, $J = 0.5, 8.0$ Hz, 1H), 8.02 (dd, $J = 1.0, 5.0$ Hz, 1H), 7.79 (br.s, 1H); ^{13}C NMR (101 MHz, $\text{SO}(\text{CDCl}_3)_2$) δ 165.3, 161.3, 152.3, 152.2, 150.8, 147.8, 146.4, 143.2, 137.3, 130.6, 126.3, 121.7, 118.1; LRMS $[\text{M}+\text{H}]^+$ 268, 100% a/a; HRMS: $\text{C}_{13}\text{H}_{10}\text{N}_5\text{O}_2$ $[\text{M}+\text{H}]^+$ requires 268.0829, found $[\text{M}+\text{H}]^+$ 268.0832; IR solid: ν 3307, 1704, 1592, 1423, 1310 cm^{-1} ; mp > 250 $^\circ\text{C}$.

Pyrido[3,4-*d*]pyrido[3'',4'':4',5']pyrimido[1',2':4,5]pyrazino[1,2-*a*]pyrimidine-5,13(7*H*,15*H*)-dione (**4.075**)



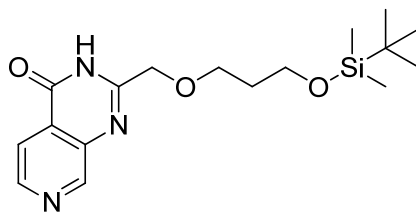
Chemical Formula: $\text{C}_{16}\text{H}_{10}\text{N}_6\text{O}_2$

Molecular Weight: 318.29

3-((*tert*-Butyldimethylsilyl)oxy)propan-1-ol (0.22 mL, 1.0 mmol) was added to a stirred suspension of potassium carbonate (106 mg, 0.77 mmol) and 2-(chloromethyl)pyrido[3,4-*d*]pyrimidin-4(3*H*)-one (**4.047**) (100 mg, 0.51 mmol) in the acetone (5 mL) and the resulting suspensions heated at 50 $^\circ\text{C}$ overnight. The reaction mixture was cooled to room temperature, partitioned between 2-MeTHF (50 mL) and water (10 mL). The aqueous layer was separated and the organic layer washed (2x water [10 mL], 1x brine [10 mL]). The aqueous layer was extracted with DCM (2x 20 mL), all the organic portions combined, dried over MgSO_4 and evaporated *in vacuo* to dryness. The residue was purified by silica gel chromatography eluting with DCM:2 M methanolic ammonia to give the title compound **4.075** as a white solid (9 mg, 5%): ^1H NMR ($\text{SO}(\text{CD}_3)_2$, 400 MHz) δ 9.13 (s, 2H), 8.74 (d, $J = 5.0$ Hz, 2H), 8.05 (d, $J = 5.0$ Hz, 2H), 5.37 (s, 4H); LRMS $[\text{M}+\text{H}]^+$: 319; 97% a/a.

2-((3-((tert-Butyldimethylsilyl)oxy)propoxy)methyl)pyrido[3,4-d]pyrimidin-4(3H)-one

(4.077)¹³⁹

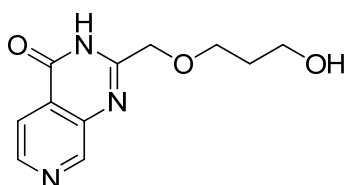


Chemical Formula: C₁₇H₂₇N₃O₃Si

Molecular Weight: 349.50

Sodium hydroxide (184 mg, 4.60 mmol) was added to a stirred suspension of 2-(chloromethyl)pyrido[3,4-d]pyrimidin-4(3H)-one (**4.047**) (288 mg, 1.47 mmol) in 3-((tert-butyl dimethylsilyl)oxy)propan-1-ol (3.0 mL, 14 mmol) and the mixture heated to 90 °C for 1 h and the resulting suspension cooled to room temperature, partitioned between water (10 mL) and EtOAc (60 mL). The aqueous layer was separated and the organic layer washed [3x water (10 mL), 1x brine (10 mL)], dried over MgSO₄ and evaporated *in vacuo* to a pale yellow oil. The oil was purified by silica gel chromatography eluting with cyclohexane:EtOAc (10 -> 100%) to give the title compound **4.077** as a white solid (53 mg, 10%): ¹H NMR (CDCl₃, 400 MHz) δ 9.73 (br.s, 1H), 9.10 (s, 1H), 8.70 (d, *J* = 5.0 Hz, 1H), 8.06 (d, *J* = 5.0 Hz, 1H), 4.57 (s, 2H), 3.83 - 3.71 (m, 4H), 1.90 (app. quin, *J* = 6.0 Hz, 2H), 0.91 (s, 9H), 0.08 (s, 6H); LRMS [M+H]⁺: 350; 100% a/a.

2-((3-Hydroxypropoxy)methyl)pyrido[3,4-d]pyrimidin-4(3H)-one (4.076)



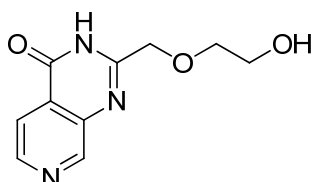
Chemical Formula: C₁₁H₁₃N₃O₃

Molecular Weight: 235.24

1M TBAF in THF (0.23 mL, 0.23 mmol) was added to a solution of 2-((3-((tert-butyl dimethylsilyl)oxy)propoxy)methyl)pyrido[3,4-d]pyrimidin-4(3H)-one (**4.077**) (53 mg, 0.15 mmol) in THF (2 mL) and the resulting solution stirred overnight. The mixture was evaporated *in vacuo* to dryness and the residue purified by silica gel chromatography eluting with DCM:2 M methanolic ammonia to give the title compound **4.076** as a white solid (25 mg, 70%): ¹H NMR (SO(CD₃)₂, 400 MHz) δ 12.50 (br.s, 1H), 9.04 (s, 1H), 8.65 (d, *J* =

5.0 Hz, 1H), 7.95 (d, $J = 5.0$ Hz, 1H), 4.63 - 4.21 (m, 3H), 3.61 (t, $J = 6.5$ Hz, 2H), 3.50 (t, $J = 6.5$ Hz, 2H), 1.72 (app. quin, $J = 6.5$ Hz, 2H); ^{13}C NMR ($\text{SO}(\text{CD}_3)_2$, 101 MHz) δ 161.1, 156.7, 150.9, 146.5, 143.5, 127.0, 118.6, 70.5, 68.6, 58.2, 32.9; LRMS $[\text{M}+\text{H}]^+$: 236; 100% a/a; HRMS: $\text{C}_{11}\text{H}_{14}\text{N}_3\text{O}_3$ $[\text{M}+\text{H}]^+$ requires 236.1030, found $[\text{M}+\text{H}]^+$ 236.1029; IR: solid v 3322, 1685, 1619, 1494, 1450, 1423, 1332, 1120, cm^{-1} ; mp 159 – 162 °C.

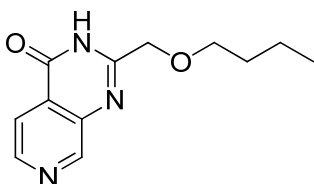
2-((2-Hydroxyethoxy)methyl)pyrido[3,4-*d*]pyrimidin-4(3*H*)-one (4.083)¹³⁹



Chemical Formula: $\text{C}_{10}\text{H}_{11}\text{N}_3\text{O}_3$
Molecular Weight: 221.21

Sodium hydroxide (78 mg, 2.0 mmol) was added to a stirred solution of 2-(chloromethyl)pyrido[3,4-*d*]pyrimidin-4(3*H*)-one (4.047) (100 mg, 0.511 mmol) in ethane-1,2-diol (5.0 mL, 89 mmol) at 100 °C and the mixture heated for 3 h. The solution was allowed to cool to room temperature, evaporated *in vacuo* to dryness, 2 M aq. HCl added (2 mL), evaporated *in vacuo* to dryness and purified by MDAP (HPH, Method A, Xbridge column) to give the title compound 4.083 as a brown solid (55 mg, 49%): ^1H NMR ($\text{SO}(\text{CD}_3)_2$, 400 MHz) δ 12.41 (br.s, 1H), 9.03 (s, 1H), 8.65 (d, $J = 5.5$ Hz, 1H), 7.94 (d, $J = 5.5$ Hz, 1H), 4.88 (br.s, 1H), 4.50 (s, 2H), 3.53 - 3.67 (m, 4H); ^{13}C NMR ($\text{SO}(\text{CD}_3)_2$, 101 MHz) δ 161.0, 156.8, 150.8, 146.4, 143.5, 127.0, 118.6, 73.3, 70.4, 60.6; LRMS $[\text{M}+\text{H}]^+$: 222; 100% a/a; HRMS: $\text{C}_{10}\text{H}_{12}\text{N}_3\text{O}_3$ $[\text{M}+\text{H}]^+$ requires 222.0873, found $[\text{M}+\text{H}]^+$ 222.0874; IR: solid v 3149, 1679, 1618, 1423, 1127, 1061 cm^{-1} ; mp 182 – 186 °C.

2-(Butoxymethyl)pyrido[3,4-*d*]pyrimidin-4(3*H*)-one (4.084)¹³⁹



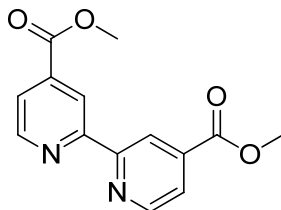
Chemical Formula: $\text{C}_{12}\text{H}_{15}\text{N}_3\text{O}_2$
Molecular Weight: 233.27

Sodium hydroxide (92 mg, 2.3 mmol) was added to a stirred suspension of 2-(chloromethyl)pyrido[3,4-*d*]pyrimidin-4(3*H*)-one (4.047) (150 mg, 0.767 mmol) and 3-((*tert*-

butyldimethylsilyloxy)propan-1-ol (0.245 mL, 1.15 mmol) in 1-butanol (5 mL). The mixture was heated to 75 °C for 30 min. The mixture was cooled to room temperature, partitioned between 1 M aq. citric acid (10 mL) and 2-MeTHF (60 mL) and the aqueous layer separated. The organic layer was washed [2x water (10 mL), 1x brine (10 mL)], dried over MgSO₄ and evaporated *in vacuo* to dryness. The residue was purified by silica gel chromatography eluting with cyclohexane:EtOAc (0 -> 100%) to give the title compound **4.084** as an off white solid (49 mg, 29%): ¹H NMR (SO(CD₃)₂, 400 MHz) δ 12.52 (br.s, 1H), 9.04 (s, 1H), 8.65 (d, *J* = 5.0 Hz, 1H), 7.95 (d, *J* = 5.0, 1H), 4.40 (s, 2H), 3.53 (t, *J* = 6.5 Hz, 2H), 1.61 - 1.5 (m, 2H), 1.42 - 1.29 (m, 2H), 0.89 (t, *J* = 7.5 Hz, 3H); ¹³C NMR (SO(CD₃)₂, 101 MHz) δ 161.1, 156.6, 150.9, 146.5, 143.5, 127.0, 118.5, 70.8, 70.5, 31.6, 19.2, 14.2; LRMS [M+H]⁺: 234; 100% a/a; HRMS: C₁₂H₁₆N₃O₂ [M+H]⁺ requires 234.1107, found [M+H]⁺ 234.1106; IR: solid v 1689, 1621, 1417, 1278, 1090, 1046 cm⁻¹; mp 155 – 157 °C.

6.4.3 Schofield type compounds

Dimethyl [2,2'-bipyridine]-4,4'-dicarboxylate (4.089)¹⁴⁶

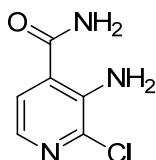


Chemical Formula: C₁₄H₁₂N₂O₄
Molecular Weight: 272.26

Thionyl chloride (3.77 mL, 51.7 mmol) was added dropwise to a suspension of [2,2'-bipyridine]-4,4'-dicarboxylic acid (5.05 g, 20.7 mmol) in methanol (410 mL). The resulting suspension refluxed overnight, cooled in an ice bath, filtered, the filtercake washed (3x MeOH [20 mL], 1x MeOH:TBME [1:1, 20 mL], 1x TBME [20 mL]) and dried *in vacuo* at 40 °C to give a white solid. The solid was partitioned between DCM (150 mL) and sat. aq. NaHCO₃ (50 mL). The organic layer was removed, the aqueous layer extracted (3x DCM [100 mL]), the organic portions combined, dried over MgSO₄ and evaporated to give the title compound **4.089** a as white solid (1.39 g, 25%): ¹H NMR (CDCl₃, 400 MHz) δ 8.99 (s, 2H), 8.88 (d, *J* = 5.0 Hz, 2H), 7.96 - 7.89 (m, 2H), 4.02 (s, 6H); LRMS [M+H]⁺: 273, 100% a/a.

The filtrate from the initial filtration was evaporated *in vacuo* to a pink solid and the residue partitioned between sat. aq. NaHCO₃ (200 mL) and DCM (100 mL). The organic layer was removed and the aqueous portion extracted with DCM (4 x 100mL), the organic portions combined, dried and evaporated *in vacuo* to an off white solid. The residue was purified by silica gel chromatography eluting with DCM:2 M methanolic ammonia (0 -> 2 %). The product containing fractions were evaporated *in vacuo* to give the title compound **4.089** as a white solid (2.28 g, 40%): Analytical data as above.

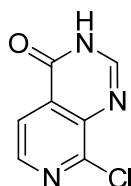
3-Amino-2-chloroisonicotinamide (4.096)¹⁴⁸



Chemical Formula: C₆H₆ClN₃O
Molecular Weight: 171.58

35% aq. Hydrogen peroxide (2.06 mL, 23.6 mmol) was added dropwise over 45 min to a stirred suspension of 3-aminoisonicotinamide (2.81g, 20.5 mmol) in fuming HCl (60 mL, 730 mmol). The mixture was allowed to stir overnight, cooled in an ice bath and basified to pH 8 with 50% aq. NaOH. The resulting suspension was stirred for 30 min at room temperature, filtered, the collected solid washed with water (5 mL) and dried *in vacuo*. The filtrate was evaporated to dryness, combined with the dried, filtered solid and the mixture slurried in MeOH. The suspension was filtered, the filtrate adsorbed on to silica, evaporated *in vacuo* and purified by silica gel chromatography eluting with cyclohexane:EtOAc to give the title compound **4.096** as a white solid (852 mg, 24%): ¹H NMR (SO(CD₃)₂, 400 MHz) δ 8.16 (br.s, 1H), 7.61 (m, 2H), 7.52 (d, *J* = 5.1 Hz, 1H), 6.73 (br.s, 2H); LRMS [M+H]⁺: 172, 174; 92% a/a.

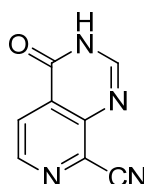
8-Chloropyrido[3,4-*d*]pyrimidin-4(3*H*)-one (4.095)¹⁴⁹



Chemical Formula: C₇H₄ClN₃O
Molecular Weight: 181.58

Tosic acid monohydrate (7 mg, 0.04 mmol) was added to a stirred suspension of 3-amino-2-chloroisonicotinamide (**4.096**) (132 mg, 0.769 mmol) in triethyl orthoformate (2.5 mL, 15.03 mmol) and ethanol (2.5 mL). The suspension was heated to reflux for 1 h, cooled to room temperature and the suspension evaporated to dryness *in vacuo*. The residue was triturated [2x EtOAc (1 mL)], filtered and dried *in vacuo* to give the title compound **4.095** as a white solid (132 mg, 95%): ¹H NMR (SO(CD₃)₂, 400 MHz) δ 12.84 (br.s, 1H), 8.45 (d, *J* = 5.1 Hz, 1H), 8.32 (s, 1H), 7.98 (d, *J* = 5.1 Hz, 1H); LRMS [M+H]⁺: 182, 184; 100% a/a.

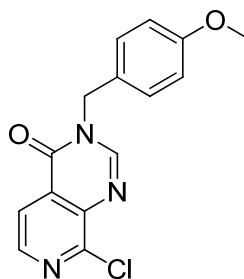
4-Oxo-3,4-dihydropyrido[3,4-*d*]pyrimidine-8-carbonitrile (4.094)¹⁵⁰



Chemical Formula: C₈H₄N₄O
Molecular Weight: 172.14

Zinc cyanide (69 mg, 0.58 mmol) was added to stirred mixture of 8-chloropyrido[3,4-*d*]pyrimidin-4(3*H*)-one (**4.095**) (106 mg, 0.583 mmol) in DMF (3 mL) under N₂. The resulting suspension was degassed under vacuum and backfilled with N₂ (x3), tetrakis-(triphenylphosphine)-palladium (38 mg, 0.033 mmol) added, the mixtures degassed under vacuum and backfilled with N₂ (x2), heated to 90 °C overnight and concentrated *in vacuo* to dryness. The residue was suspended in water, filtered, the filtercake washed [2x 2 M methanolic ammonia (2 mL), 1x Et₂O (2 mL)] and air dried to give the title compound **4.094** as a white solid. (96 mg, 96%, contained 20% 8-chloropyrido[3,4-*d*]pyrimidin-4(3*H*)-one (**4.095**) w/w): ¹H NMR (SO(CD₃)₂, 400 MHz) δ 8.28 (d, *J* = 5.0 Hz, 1H), 8.24 (s, 1H), 7.87 (d, *J* = 5.0 Hz, 1H); LRMS [M+H]⁺: 173; 100% a/a.

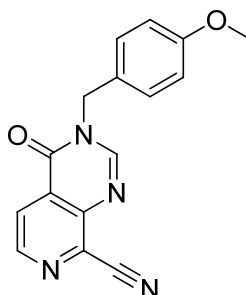
8-Chloro-3-(4-methoxybenzyl)pyrido[3,4-*d*]pyrimidin-4(3*H*)-one (**4.098**)



Chemical Formula: C₁₅H₁₂ClN₃O₂
Molecular Weight: 301.73

4-Methoxybenzyl chloride (0.84 mL, 6.2 mmol) was added to a stirred suspension of 8-chloropyrido[3,4-*d*]pyrimidin-4(3*H*)-one (**4.095**) (1.02g, 5.62 mmol), K₂CO₃ (0.99 g, 7.2 mmol) and potassium iodide (9.32 mg, 0.056 mmol) and the suspension heated to 50 °C overnight. The resulting suspension was partitioned between 2-MeTHF (50 mL) and water (10 mL). The aqueous layer was separated, the organic layer washed [2x sat. aq. NaHCO₃ (10 mL), 1x brine (5 mL)], dried over MgSO₄ and evaporated *in vacuo* to an off white solid. The residue was slurried in refluxing EtOAc (16 mL), cooled in an ice bath with stirring, filtered, the filter cake washed [1x EtOAc (16 mL), 1x EtOAc (8 mL)] and dried *in vacuo* to give the title compound **4.098** as a white solid (1.46 g, 86%): ¹H NMR (CDCl₃, 400 MHz) δ 8.47 (d, *J* = 5.1 Hz, 1H), 8.28 (s, 1H), 8.07 (d, *J* = 5.1 Hz, 1H), 7.31 (d, *J* = 8.6 Hz, 2H), 6.92 (d, *J* = 8.6 Hz, 2H), 5.16 (s, 2H), 3.81 (s, 3H); LRMS [M+H]⁺: 302; 100% a/a.

3-(4-Methoxybenzyl)-4-oxo-3,4-dihydropyrido[3,4-*d*]pyrimidine-8-carbonitrile (4.099)¹⁵⁰



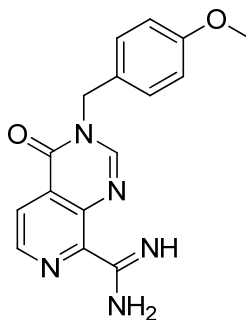
Chemical Formula: C₁₆H₁₂N₄O₂

Molecular Weight: 292.29

Tetrakis triphenyl phosphine palladium (249 mg, 0.215 mmol) was added to a vacuum degassed solution of zinc cyanide (278 mg, 2.370 mmol) and 8-chloro-3-(4-methoxybenzyl)pyrido[3,4-*d*]pyrimidin-4(3*H*)-one (**4.098**) (650 mg, 2.15 mmol) in DMF (20 mL) under N₂. The resulting suspension was vacuum degassed and backfilled with N₂ (x3), heated to 90 °C overnight and cooled to room temperature. The reaction mixture was partitioned between 2-MeTHF (15 mL) and water (5 mL). The aqueous layer was separated, the organic washed [1x water (30 mL), 1x brine (30 mL)], dried over MgSO₄ and evaporated to dryness. The residue was purified by silica gel chromatography eluting with cyclohexane:EtOAc (10 → 100%) to give a white solid containing the title compound **4.099** and triphenylphosphine oxide. The residue purified again by silica gel chromatography eluting with DCM:MeOH (0 → 2%). The residue purified by silica gel chromatography eluting with DCM:EtOAc (0 → 10) gave the title compound **4.099** as a white solid (572 mg, 91%): ¹H NMR (CDCl₃, 400 MHz) δ 8.80 (d, *J* = 5.0 Hz, 1H), 8.31 - 8.26 (m, 2H), 7.33 (d, *J* = 8.5 Hz, 2H), 6.92 (d, *J* = 8.5 Hz, 2H), 5.17 (s, 2H), 3.82 (s, 3H); LRMS [M+H]⁺: 293; 100% a/a.

3-(4-Methoxybenzyl)-4-oxo-3,4-dihydropyrido[3,4-*d*]pyrimidine-8-carboximidamide

(4.100)¹⁵³

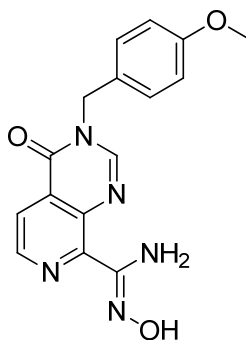


Chemical Formula: C₁₆H₁₅N₅O₂

Molecular Weight: 309.32

Acetic anhydride (0.082 mL, 0.87 mmol) was added to a stirred solution of *N'*-hydroxy-3-(4-methoxybenzyl)-4-oxo-3,4-dihydropyrido[3,4-*d*]pyrimidine-8-carboximidamide (**4.101**) (0.188 g, 0.578 mmol) in acetic acid (5 mL) and the resulting solution stirred for 30 min. 10% palladium on carbon (0.031 g, 0.029 mmol) was added and the resulting suspension stirred under an atmosphere of hydrogen for 24 h. The mixture was filtered through celite and washed with acetic acid. The filtrate was evaporated *in vacuo* to dryness, the residue purified by silica gel chromatography eluting with DCM:2 M methanolic ammonia to give the title compound **4.100** as a brown solid (34 mg, 19%): ¹H NMR (SO(CD₃)₂, 400 MHz) δ 10.03 (br.s, 3H), 8.86 (s, 1H), 8.81 (d, *J* = 5.0 Hz, 1H), 8.28 (d, *J* = 5.0 Hz, 1H), 7.38 (d, *J* = 8.5 Hz, 2H), 6.94 (d, *J* = 8.5 Hz, 2H), 5.18 (s, 2H), 3.73 (s, 3H); LRMS [M+H]⁺: 310; 91% a/a.

N'-Hydroxy-3-(4-methoxybenzyl)-4-oxo-3,4-dihydropyrido[3,4-*d*]pyrimidine-8-carboximidamide (**4.101**)¹⁵¹

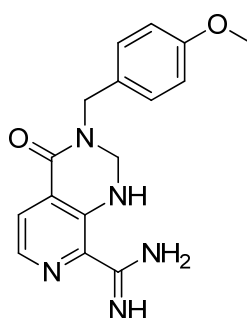


Chemical Formula: C₁₆H₁₅N₅O₃

Molecular Weight: 325.32

A solution of 2 M aq. sodium hydroxide (0.34 mL, 0.68 mmol) was added to a stirred suspension of 3-(4-methoxybenzyl)-4-oxo-3,4-dihydropyrido[3,4-*d*]pyrimidine-8-carbonitrile (**4.099**) (200 mg, 0.684 mmol) and hydroxylamine hydrochloride (48 mg, 0.68 mmol) in ethanol (10 mL). The resulting suspension was stirred overnight at room temperature and heated to 60 °C for 7 h. Further hydroxylamine hydrochloride (48 mg, 0.68 mmol) and 2 M aq. NaOH (0.34 mL, 0.68 mmol) were added, the mixture heated overnight, water (1 mL) added and the mixture cooled to room temperature. The resulting suspension was filtered, the filtercake washed [2x EtOH (5 mL), 2x TBME (5 mL)] and pulled to dryness under vacuum to give the title compound **4.101** (188 mg, 84%): ¹H NMR (SO(CD₃)₂, 400 MHz) δ 9.74 (s, 1H) 8.70 - 8.65 (m, 2H), 8.03 (d, 5.0 Hz, 1H), 7.37 (d, 8.5 Hz, 2H), 6.91 (d, 8.5 Hz, 2H), 5.90 (s, 2H), 5.15 (s, 2H), 3.73 (s, 3H); LRMS [M+H]⁺: 326; 100% a/a.

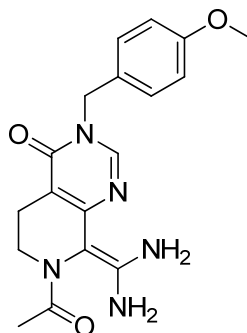
3-(4-Methoxybenzyl)-4-oxo-1,2,3,4-tetrahydropyrido[3,4-*d*]pyrimidine-8-carboximidamide
(4.102)



Chemical Formula: C₁₆H₁₇N₅O₂
Molecular Weight: 311.34

Prepared by the same method as **4.100** to give the title compound **4.102** as a brown solid (42 mg, 23%): ¹H NMR (SO(CD₃)₂, 600 MHz): δ 10.09 (br.s, 1H), 7.96 (d, *J* = 4.5 Hz, 1H), 7.68 (d, *J* = 4.5 Hz, 1H), 7.26 (d, *J* = 8.5 Hz, 1H), 7.31 (br.s, 2H), 6.91 (d, *J* = 8.5 Hz, 2H), 6.52 (br.s, 2H), 4.71 (s, 2H), 4.57 (s, 2H), 3.73 (s, 3H); LRMS [M+H]⁺ = 312; 100% a/a.

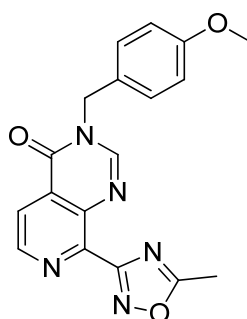
7-acetyl-8-(diaminomethylene)-3-(4-methoxybenzyl)-5,6,7,8-tetrahydropyrido[3,4-d]pyrimidin-4(3H)-one (4.103)



Chemical Formula: C₁₈H₂₁N₅O₃
Molecular Weight: 355.39

Prepared by the same method as **4.100** to give the title compound **4.103** as a brown solid (59 mg, 29%): ¹H NMR (SO(CD₃)₂, 600 MHz): δ 8.25 (s, 1H), 7.29 (d, *J* = 8.5 Hz, 2H), 7.00 (br. s, 2H), 6.88 (d, *J* = 8.5 Hz, 2H), 5.86 (s, 2H), 4.96 - 4.90 (m, 1H), 4.88 (d, *J* = 14.0 Hz, 1H), 4.56 - 4.48 (m, 1H), 3.72 (s, 3H), 2.44 (d, *J* = 12.5 Hz, 1H), 2.33 - 2.26 (m, 1H), 2.28 - 2.21 (m, 1H), 1.86 (s, 3H); LRMS [M+H]⁺: 356; 100% a/a.

3-(4-Methoxybenzyl)-8-(5-methyl-1,2,4-oxadiazol-3-yl)pyrido[3,4-d]pyrimidin-4(3H)-one (4.106)¹⁶¹

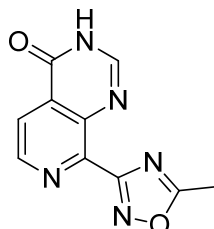


Chemical Formula: C₁₈H₁₅N₅O₃
Molecular Weight: 349.34

Acetic anhydride (3.2 mL, 34 mmol) was added to a stirred suspension of *N'*-hydroxy-3-(4-methoxybenzyl)-4-oxo-3,4-dihydropyrido[3,4-*d*]pyrimidine-8-carboximidamide (**4.100**) (117 mg, 0.360 mmol) in acetic acid (2 mL) and the resulting solution stirred at room temperature for 2 h, heated to 100 °C for 1.5 h and cooled to room temperature. The solution was evaporated *in vacuo* and purified by silica gel chromatography eluting with DCM:2 M methanolic ammonia to give the title compound **4.106** as a white solid (114 mg,

91%): ^1H NMR (CDCl_3 , 400 MHz) δ 8.92 (d, $J = 5.0$ Hz, 1H), 8.33 (s, 1H), 8.30 (d, $J = 5.0$ Hz, 1H), 7.32 (d, $J = 8.5$ Hz, 2H), 6.92 (d, $J = 8.5$ Hz, 2H), 5.17 (s, 2H), 3.81 (s, 3H), 2.76 (s, 3H); LRMS $[\text{M}+\text{H}]^+$: 350; 100% a/a.

8-(5-Methyl-1,2,4-oxadiazol-3-yl)pyrido[3,4-*d*]pyrimidin-4(3*H*)-one (4.107)¹⁶³

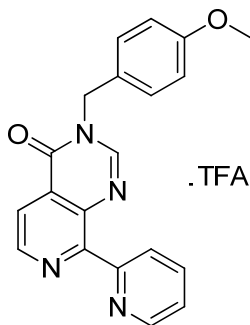


Chemical Formula: $\text{C}_{10}\text{H}_7\text{N}_5\text{O}_2$
Molecular Weight: 229.19

A solution of 3-(4-methoxybenzyl)-8-(5-methyl-1,2,4-oxadiazol-3-yl)pyrido[3,4-*d*]pyrimidin-4(3*H*)-one (**4.106**) (115 mg, 0.329 mmol) in TFA (5 mL) was heated at 70 °C for 1 h, cooled to room temperature and evaporated *in vacuo* to dryness. The residue was triturated with a THF:water:conc. aq. ammonia mix, evaporated *in vacuo* to dryness, triturated with THF:water, filtered, washed (MeOH, 5 mL) and the filtercake dried *in vacuo* at 40 °C overnight to give the title compound **4.107** as an almost white solid (19 mg, 25%): ^1H NMR ($\text{SO}(\text{CD}_3)_2$, 400 MHz) δ 12.74 (br.s, 1H), 8.78 (d, $J = 5.0$ Hz, 1H), 8.23 (s, 1H), 8.19 (d, $J = 5.0$ Hz, 1H), 2.72 (s, 3H); LRMS $[\text{M}+\text{H}]^+$ = 230; 98% a/a.

A second crop was isolated *via* the following method. The filtrate was evaporated *in vacuo* to dryness, dissolved in THF:water (1:1), and passed through a preconditioned 5 g aminopropyl cartridge. The cartridge was eluted with MeOH (20 mL) and the filtrate evaporated *in vacuo* to a pale brown solid. The residue was purified by MDAP (Formic method A) to give the title compound **4.107** as a white solid (8 mg, 11%): Analytical data as above.

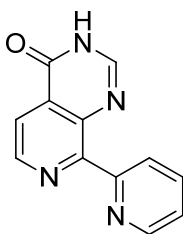
3-(4-Methoxybenzyl)-8-(pyridin-2-yl)pyrido[3,4-*d*]pyrimidin-4(3*H*)-one .TFA (4.110)¹⁶⁷



Chemical Formula: C₂₀H₁₆N₄O₃ .TFA
Molecular Weight: 441.38

Tetrakis-(palladium)-triphenylphosphine (57 mg, 0.050 mmol) was added under N₂ to a vacuum degassed suspension of 8-chloro-3-(4-methoxybenzyl)pyrido[3,4-*d*]pyrimidin-4(3*H*)-one (**4.098**) (150 mg, 0.497 mmol) and 0.5 M 2-pyridylzinc bromide in THF (1.09 mL, 0.547 mmol) in THF (4 mL). The resulting suspension was vacuum degassed, heated to reflux overnight and cooled to room temperature. The mixture was partitioned between sat. aq. NaHCO₃ (5 mL) and 2-MeTHF (10 mL). The aqueous layer was separated, the organic layer washed (2x sat. aq. NaHCO₃), dried over MgSO₄ and evaporated *in vacuo* to a brown solid. The residue was purified by silica gel chromatography eluting with DCM:2 M methanolic ammonia to give impure **4.110** which was purified by MDAP (TFA method B) to give the TFA salt of title compound **4.110** as a colourless gum (81 mg, 36%): ¹H NMR (CDCl₃, 400 MHz) δ 9.67 (d, *J* = 5.5 Hz, 1H), 9.21 (d, *J* = 8.5 Hz, 1H), 8.99 (s, 1H), 8.92 (d, *J* = 5.0 Hz, 1H), 8.59 - 8.53 (m, 1H), 8.36 (d, *J* = 5.0 Hz, 1H), 8.00 - 7.95 (m, 1H), 7.44 (d, *J* = 8.5 Hz, 2H), 6.92 (d, *J* = 8.5 Hz, 2H), 5.26 (s, 2H), 3.81 (s, 3H); LRMS [M+H]⁺: 345; 100% a/a.

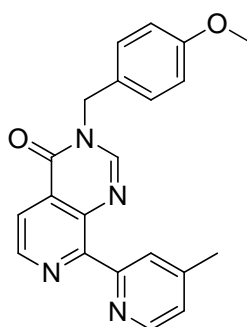
8-(Pyridin-2-yl)pyrido[3,4-*d*]pyrimidin-4(3*H*)-one (4.108)¹⁶³



Chemical Formula: C₁₂H₈N₄O
Molecular Weight: 224.22

3-(4-Methoxybenzyl)-8-(pyridin-2-yl)pyrido[3,4-*d*]pyrimidin-4(3*H*)-one.TFA (**4.110**) (79 mg, 0.17 mmol) was stirred in TFA (2 mL) and the mixture heated to 75 °C for 4 days, cooled to room temperature, evaporated *in vacuo* to a dark red gum and purified by MDAP (HPH method A). The product containing fractions were evaporated *in vacuo* to give the title compound **4.108** as a white solid (12 mg, 31%): ¹H NMR (SO(CD₃)₂, 400 MHz) δ 12.65 (br.s, 1H), 8.78 - 8.68 (m, 2H), 8.21, (s, 1H), 8.04 (d, *J* = 5.0 Hz, 1H), 8.00 - 7.82 (m, 2H), 7.51 - 7.44 (m, 1H); LRMS [M+H]⁺: 225; 100% a/a.

3-(4-Methoxybenzyl)-8-(4-methylpyridin-2-yl)pyrido[3,4-*d*]pyrimidin-4(3*H*)-one (**4.113**)¹⁶⁷



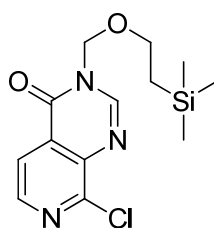
Chemical Formula: C₂₁H₁₈N₄O₂
Molecular Weight: 358.39

2-Bromo-4-methylpyridine (0.56 mL, 5.0 mmol) was added dropwise to a stirred solution of 2 M isopropylmagnesium chloride in Et₂O (2.75 mL, 5.50 mmol) under N₂ in an ice bath keeping the internal temperature below 20 °C. Once the addition was complete the ice bath was removed and the suspension stirred at room temperature for 2 h. Further 2M isopropylmagnesium chloride in Et₂O (2.50 mL, 5.00 mmol) was added dropwise, keeping the internal temperature below 20 °C. The resulting suspension was stirred for 2 h, further 2 M isopropylmagnesium chloride in Et₂O (2.75 mL, 5.50 mmol) added at room temperature and the mixture stirred for 1 h. The resulting brown solution was cooled in an ice bath and 0.5 M zinc chloride in THF (35.0 mL, 17.5 mmol) added dropwise to give the organozinc compound **4.115** as a brown stock suspension at 0.11 M in THF:Et₂O (4.4:1).

Tetrakis-(palladium)-triphenylphosphine (57 mg, 0.050 mmol) was added to a vacuum degassed suspension of 8-chloro-3-(4-methoxybenzyl)pyrido[3,4-*d*]pyrimidin-4(3*H*)-one (**4.098**) (150 mg, 0.497 mmol) in the previously prepared suspension of (4-methylpyridin-2-yl)zinc(II) chloride in THF and Et₂O (6.78 mL, 0.746 mmol). The resulting suspension was vacuum degassed and heated to reflux overnight and cooled to room temperature,

partitioned between water (10 mL) and EtOAc (30 mL). The aqueous layer was separated, the organic layer extracted [2x water (10 mL), 1x brine (5 mL)], the combined aqueous portions combined, extracted [4x DCM (20 mL)], the combined DCM portions dried over MgSO₄ and evaporated *in vacuo* to dryness. The residue was purified by silica gel chromatography eluting with DCM:2 M methanolic ammonia (0 -> 5%) to give the title compound **4.113** as a pale brown solid (40 mg, 22%): ¹H NMR (CDCl₃, 400 MHz) δ 9.66 (d, *J* = 6.0 Hz, 1H), 9.47 (s, 1H), 8.90 (s, 1H), 8.84 (d, *J* = 5.0 Hz, 1H), 8.28 (d, *J* = 5.0 Hz, 1H), 7.70 (d, *J* = 6.0 Hz, 1H), 7.52 (d, *J* = 8.5 Hz, 2H), 6.84 (d, *J* = 8.5 Hz, 2H), 5.28 (s, 2H), 3.76 (s, 3H), 2.74 (s, 3H); LRMS [M+H]⁺: 359; 88% a/a.

8-Chloro-3-((2-(trimethylsilyl)ethoxy)methyl)pyrido[3,4-*d*]pyrimidin-4(3*H*)-one (**4.116**)

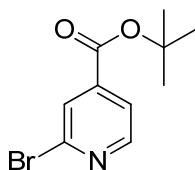


Chemical Formula: C₁₃H₁₈ClN₃O₂Si
Molecular Weight: 311.84

2-(Trimethylsilyl)ethoxymethyl chloride (2.19 mL, 12.4 mmol) was added to a stirred suspension of potassium carbonate (2.28 g, 16.5 mmol) and 8-chloropyrido[3,4-*d*]pyrimidin-4(3*H*)-one (**4.095**) (1.5 g, 8.3 mmol) in acetone (20 mL) and DMF (20 mL). The resulting suspension was heated to 50 °C for 4 h and further potassium carbonate (2.28 g, 16.5 mmol) and 2-(trimethylsilyl)ethoxymethyl chloride (2.19 mL, 12.4 mmol) added. The mixture was heated at 50 °C overnight, cooled to room temperature and partitioned between water (20 mL) and 2-MeTHF (100 mL). The aqueous layer was separated and the organic layer washed [2x water (20 mL), 1x brine (10 mL)], dried over MgSO₄ and evaporated *in vacuo* to a pale brown oil. The residue was purified by silica gel chromatography eluting with cyclohexane:EtOAc (0 -> 33%) to give the title compound **4.116** as a white solid (2.11 g, 82%): ¹H NMR (CDCl₃, 400 MHz) δ 8.49 (d, *J* = 5.0 Hz, 1H), 8.33 (s, 1H), 8.06 (d, *J* = 5.0 Hz, 1H), 5.45 (s, 2H), 3.69 (t, *J* = 8.0 Hz, 2H), 0.98 (t, *J* = 8.0 Hz, 2H), -0.01 (s, 9H); ¹³C NMR (CDCl₃, 101 MHz) δ 159.4, 151.0, 148.0, 145.8, 140.6, 129.4, 118.8, 75.1, 68.0, 18.0, -1.4; LRMS [M+H]⁺: 312; 100% a/a; HRMS: C₁₃H₁₉ClN₃O₂ [M+H]⁺ requires

312.0935, found $[M+H]^+$ 312.0930; IR: solid v 1699, 1602, 1378, 1248, 1152, 1089 cm^{-1} ; mp 86 – 89 °C.

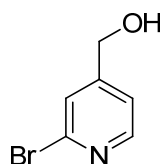
tert-Butyl 2-bromoisonicotinate (4.117)¹⁷³



Chemical Formula: $\text{C}_{10}\text{H}_{12}\text{BrNO}_2$
Molecular Weight: 258.11

DCC (2.54 mL, 16.3 mmol) at 40 °C was added to a stirred solution of 2-bromoisonicotinic acid (3.00 g, 14.9 mmol), *tert*-butanol (2.13 mL, 22.3 mmol) and DMAP (0.181 g, 1.49 mmol) in DCM (70 mL) and DMF (20 mL) under N_2 . The resulting suspension was stirred over the weekend and evaporated *in vacuo* to a brown residue. The residue was partitioned between EtOAc (200 mL) and sat. aq. NaHCO_3 (30 mL). The aqueous layer was separated, the organic layer washed [2x sat. aq. NaHCO_3 (30 mL)], dried over MgSO_4 and evaporated *in vacuo* to a pale brown solid. The residue was purified by silica gel chromatography, eluting with cyclohexane:EtOAc (5 -> 33%) to give the title compound **4.117** as a white solid (2.23 g, 58%): ^1H NMR (CDCl_3 , 400 MHz) δ 8.51 (d, J = 5.0 Hz, 1H), 7.99 (d, J = 1.5 Hz, 1H), 7.77 (dd, J = 1.5, 5.0 Hz, 1H), 1.62 (s, 9H); LRMS $[M+H]^+$: 258 & 260; 100% a/a

(2-Bromopyridin-4-yl)methanol (4.120)¹⁷⁵

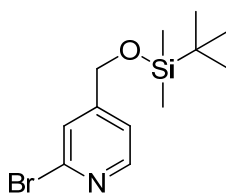


Chemical Formula: $\text{C}_6\text{H}_6\text{BrNO}$
Molecular Weight: 188.02

A solution of 1 M borane:THF complex in THF (24.6 mL, 24.6 mmol) was added dropwise to a stirred suspension of 2-bromoisonicotinic acid (1.98 g, 9.82 mmol) in THF (40 mL) under N_2 at 0 °C. Upon completion of the addition the resulting suspension was stirred at room temperature for 2 h and heated to 60 °C for 2 h. Further 1M borane:THF complex in THF (24.6 mL, 24.6 mmol) added at 60 °C and stirred for 60 h under N_2 . The resulting mixture was cooled to room temperature, water added dropwise until no further gas evolution was

noticed. NaOH (0.39 g, 9.8 mmol) was added and the mixture was refluxed for 1 h. The resulting suspension was cooled to room temperature, evaporated *in vacuo* to a white solid, dissolved with sat. aq. NaHCO₃ (20 mL) and extracted with DCM (20 mL x 8). The combined organic extractions were dried over MgSO₄ and evaporated *in vacuo* to a colourless oil. The residue was purified by silica gel chromatography eluting with cyclohexane:EtOAc (10 -> 66%) to give the title compound **4.120** as a white solid (485 mg, 26%): ¹H NMR (CDCl₃, 400 MHz) δ 8.34 (d, *J* = 5.0 Hz, 1H), 7.55 (s, 1H), 7.27 (d, *J* = 5.0 Hz, 1H), 4.76 (s, 2H); LRMS [M+H]⁺: 188 and 190; 100% a/a

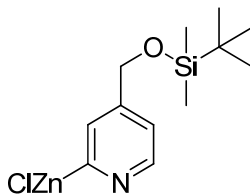
2-Bromo-4-(((*tert*-butyldimethylsilyl)oxy)methyl)pyridine (**4.121**)



Chemical Formula: C₁₂H₂₀BrNOSi
Molecular Weight: 302.28

TBDMS-Cl (504 mg, 3.35 mmol) was added to a stirred solution of (2-bromopyridin-4-yl)methanol (**4.120**) (484 mg, 2.57 mmol) and 1*H*-imidazole (280 mg, 4.12 mmol) in dry DMF (10 mL) under N₂. The resulting solution was allowed to stand overnight, evaporated *in vacuo* to dryness and the residue partitioned between TBME (50 mL) and water (10 mL). The aqueous layer was separated, the organic layer washed [2x water (10 mL)], dried over MgSO₄ and evaporated *in vacuo* to a colourless oil. The residue was purified by silica gel chromatography, eluting with cyclohexane:EtOAc (0 -> 10%) to give the title compound **4.121** as a colourless oil (811 mg, 96%): ¹H NMR (CDCl₃, 400 MHz) δ 8.30 (d, *J* = 5.0 Hz, 1H), 7.47 (s, 1H), 7.21 (d, *J* = 5.0 Hz, 1H), 4.72 (s, 2H), 0.97 (s, 9H), 0.13 (s, 6H); LRMS [M+H]⁺: 302 & 304; 100% a/a.

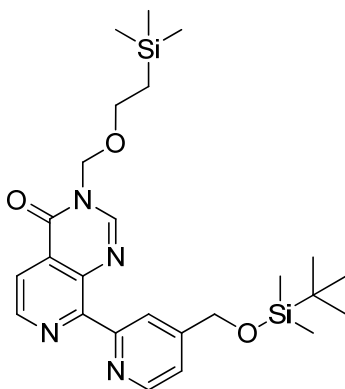
4-(((tert-Butyldimethylsilyl)oxy)methyl)pyridin-2-yl)zinc chloride (4.122)¹⁷⁴



Chemical Formula: C₁₂H₂₀ClNOSiZn
Molecular Weight: 323.21

2-Bromo-4-(((tert-butyl dimethylsilyl)oxy)methyl)pyridine (**4.121**) (2 g, 6.62 mmol) was added dropwise to a stirred solution of 2 M isopropylmagnesium chloride in Et₂O (9.9 mL, 20 mmol) under N₂ in an ice bath and the resulting orange suspension warmed to room temperature. The suspension was stirred for 30 min, cooled in an ice bath and 0.5 M zinc chloride in THF (43.7 mL, 21.8 mmol) added dropwise, the mixture stirred for 1 h and used as a stock suspension without further manipulation.

8-(4-(((tert-Butyldimethylsilyl)oxy)methyl)pyridin-2-yl)-3-((2-(trimethylsilyl)ethoxy)methyl)pyrido[3,4-d]pyrimidin-4(3H)-one (4.123)¹⁶⁷



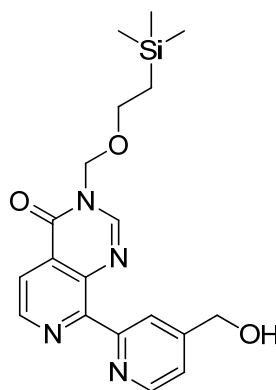
Chemical Formula: C₂₅H₃₈N₄O₃Si₂
Molecular Weight: 498.77

A suspension of 4-(((tert-butyl dimethylsilyl)oxy)methyl)pyridin-2-yl)zinc(II) chloride in THF and Et₂O (**4.122**) (40.8 mL, 4.81 mmol) filtered through a 0.2 μm PES syringe filter was added to 8-Chloro-3-((2-(trimethylsilyl)ethoxy)methyl)pyrido[3,4-d]pyrimidin-4(3H)-one (**4.116**) (1.00 g, 3.21 mmol) under N₂. The resulting solution was vacuum degassed under N₂, tetrakis-(triphenylphosphine)-palladium (0.37 g, 0.32 mmol) added, the resulting solution vacuum degassed, heated to 64 °C for 2 h and further tetrakis-(triphenylphosphine)-palladium (0.371 g, 0.321 mmol) added. The mixture was vacuum

degassed and heated at 64 °C for 2 h and allowed to cool to room temperature overnight. The resulting suspension was eluted through a silica plug with first THF (250 mL), followed by 10% 2 M methanolic ammonia in DCM (250 mL) and the basic fractions evaporated *in vacuo* to dryness. The residue was purified by silica gel chromatography eluting with DCM:2 M methanolic ammonia to give a crude sample of the title compound **4.123** (1.16 g): LRMS [M+H]⁺: 499; 72% a/a.

Crude **4.123** (60 mg, 0.09 mmol, correcting for purity) was sub-sampled and purified by MDAP for characterisation data (HPH method E) to give the title compound **4.123** (18 mg): ¹H NMR (SO(CD₃)₂, 400 MHz) δ 8.78 (d, *J* = 5.0 Hz, 1H), 8.64 (d, *J* = 5.0 Hz, 1H), 8.45 (s, 1H), 8.12 (d, *J* = 5.0 Hz, 1H), 7.71 (s, 1H), 7.40 (d, *J* = 5.0 Hz, 1H), 5.40 (s, 2H), 4.85 (s, 2H), 3.64 (t, *J* = 8.0 Hz, 2H), 0.97 - 0.84 (m, 11H), 0.12 (s, 6H), -0.04 (s, 9H); LRMS [M+H]⁺: 499; 96% a/a.

8-(4-(Hydroxymethyl)pyridin-2-yl)-3-((2-(trimethylsilyl)ethoxy)methyl)pyrido[3,4-*d*]pyrimidin-4(3*H*)-one (**4.124**)

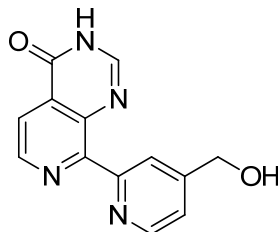


Chemical Formula: C₁₉H₂₄N₄O₃Si
Molecular Weight: 384.50

A solution of 1M TBAF in THF (2.2 mL, 2.2 mmol) was added dropwise to a stirred solution of 8-(4-(((*tert*-butyldimethylsilyl)oxy)methyl)pyridin-2-yl)-3-((2-(trimethylsilyl)ethoxy)methyl)pyrido[3,4-*d*]pyrimidin-4(3*H*)-one (**4.123**) (1.1g, 2.2 mmol) in THF (42 mL) and the resulting orange suspension stirred for 1 h. The suspension was partitioned between EtOAc (100 mL) and aq. NaCl (20 mL). The aqueous layer was separated and the organic layer washed [2x aq. NaCl (10 mL), 1x brine (10 mL)], dried over MgSO₄ and evaporated *in vacuo* to a yellow gum. The residue was purified by silica gel chromatography eluting with DCM:2 M methanolic ammonia (0 -> 7%) giving the title compound **4.124** as a pale yellow solid (519 mg, 61%): ¹H NMR (SO(CD₃)₂, 400 MHz) δ 8.78

(s, $J = 5.5$ Hz, 1H), 8.62 (d, $J = 5.0$ Hz, 1H), 8.47 (s, 1H), 8.12 (d, $J = 5.0$ Hz, 1H), 7.68 (s, 1H), 7.43 - 7.39 (m, 1H), 5.48 (t, $J = 6.0$ Hz, 1H), 5.39 (s, 2H), 4.64 (d, $J = 6.0$ Hz, 2H), 3.65 (t, $J = 8.0$ Hz, 2H), 0.89 (t, $J = 8.0$ Hz, 2H), -0.03 (s, 9H); LRMS $[M+H]^+$: 385; 100% a/a.

8-(4-(Hydroxymethyl)pyridin-2-yl)pyrido[3,4-*d*]pyrimidin-4(3*H*)-one (4.125)

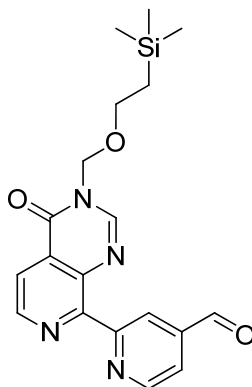


Chemical Formula: $C_{13}H_{10}N_4O_2$

Molecular Weight: 254.24

A solution of 1M TBAF in THF (0.150 mL, 0.150 mmol) was added to a stirred solution of 8-(4-(((*tert*-butyldimethylsilyl)oxy)methyl)pyridin-2-yl)-3-((2-(trimethylsilyl)ethoxy)methyl)pyrido[3,4-*d*]pyrimidin-4(3*H*)-one (4.123) (25 mg, 0.050 mmol) in THF (1 mL), the resulting solution was allowed to stand for 4 days. The reaction mixture was warmed to 60 °C overnight, evaporated *in vacuo* to dryness and purified by MDAP (formic method A) to give the title compound 4.125 as a grey solid (7 mg, 55%): 1H NMR ($SO(CD_3)_2$, 600 MHz) δ 9.08 (d, $J = 1.5$ Hz, 1H), 8.99 (d, $J = 6.0$ Hz, 1H), 8.95 (d, $J = 5.0$ Hz, 1H), 8.45 (s, 1H), 8.29 (d, $J = 5.0$ Hz, 1H), 8.08 (dd, $J = 1.5, 6.0$ Hz, 1H), 4.91 (s, 2H), exchangeable protons not observed; ^{13}C NMR ($SO(CD_3)_2$, 151 MHz) δ 163.8, 159.2, 148.8, 147.1, 145.9, 144.0, 142.7, 141.9, 130.1, 124.4, 123.8, 122.4, 61.6; LRMS $[M+H]^+$: 255; 100% a/a; HRMS: $C_{13}H_{11}N_4O_2$ $[M+H]^+$ requires 255.0877, found $[M+H]^+$ 255.0874.

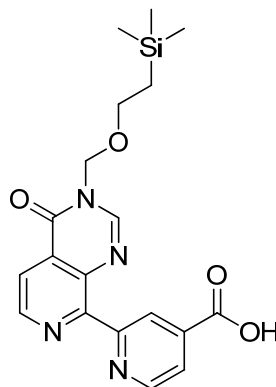
2-(4-Oxo-3-((2-(trimethylsilyl)ethoxy)methyl)-3,4-dihydropyrido[3,4-*d*]pyrimidin-8-yl)isonicotinaldehyde (4.126)¹⁷⁷



Chemical Formula: C₁₉H₂₂N₄O₃Si
Molecular Weight: 382.49

Oxalyl chloride (0.23 mL, 2.7 mmol) was added to a stirred solution of DMSO (0.19 mL, 2.7 mmol) in dry DCM (6 mL) under N₂ at -78 °C. The resulting solution was stirred for 15 min, a solution of 8-(4-(hydroxymethyl)pyridin-2-yl)-3-((2-(trimethylsilyl)ethoxy)methyl)pyrido[3,4-*d*]pyrimidin-4(3*H*)-one (**4.124**) (511 mg, 1.33 mmol) in dry DCM (19 mL) was added dropwise keeping the internal temperature below -60 °C. The resulting suspension was stirred for 15 min and triethylamine (0.74 mL, 5.3 mmol) dried over MgSO₄ added. The resulting solution was warmed with stirring to room temperature over 1 h and partitioned between DCM (50 mL) and water (10 mL). The aqueous layer was removed and the organic layer washed [2x water (10 mL)], dried over MgSO₄ and evaporated with PhMe *in vacuo* to give the title compound **4.126** as a brown oil (514 mg, 81%): ¹H NMR (SO(CD₃)₂, 400 MHz) δ 10.18 (s, 1H), 9.03 (d, *J* = 5.0 Hz, 1H), 8.83 (d, *J* = 5.0 Hz, 1H), 8.51 (s, 1H), 8.22 (s, 1H), 8.16 (d, *J* = 5.0 Hz, 1H) 7.93 (dd, *J* = 1.5, 5.0 Hz, 1H), 5.40 (s, 2H), 3.65 (t, *J* = 8.0 Hz, 2H), 0.90 (t, *J* = 8.0 Hz, 2H), -0.03 (s, 9H); LRMS of MeOH hemiacetal [M+H]⁺: 414.

2-(4-Oxo-3-((2-(trimethylsilyl)ethoxy)methyl)-3,4-dihydropyrido[3,4-d]pyrimidin-8-yl)isonicotinic acid (**4.127**)¹⁷⁸

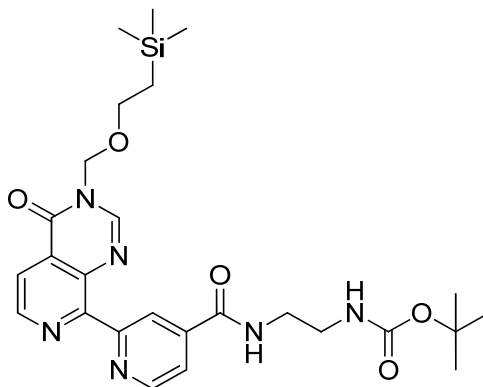


Chemical Formula: C₁₉H₂₂N₄O₄Si
Molecular Weight: 398.49

Sodium chlorite (483 mg, 5.34 mmol) was added to a stirred solution of 2-(4-oxo-3-((2-(trimethylsilyl)ethoxy)methyl)-3,4-dihydropyrido[3,4-d]pyrimidin-8-yl)isonicotinaldehyde (**4.126**) (511 mg, 1.34 mmol), 2-methyl-2-butene (1.0 mL, 9.4 mmol) and sodium phosphate monobasic (817 mg, 6.81 mmol) in *tert*-butanol (19.3 mL) and water (6.4 mL). The resulting orange solution turned to a yellow solution over 1 h, was evaporated *in vacuo* to dryness, partitioned between EtOAc (20 mL) and aq. formic acid at pH 4 (5 mL). The aqueous layer was separated, the organic layer washed (3x aq. formic acid at pH 4 [5 mL]), passed through a hydrophobic frit and evaporated *in vacuo* to give the title compound **4.127** as a white solid (252 mg, 47%): ¹H NMR (SO(CD₃)₂, 400 MHz) δ 13.73 (br.s, 1H), 8.91 (d, *J* = 5.0 Hz, 1H), 8.81 (d, *J* = 5.0 Hz, 1H), 8.51 (s, 1H), 8.23 (s, 1H), 8.16 (d, *J* = 5.0 Hz, 1H), 7.92 (dd, *J* = 1.5, 5.0 Hz, 1H), 5.39 (s, 2H), 3.65 (t, *J* = 8.0 Hz, 2H), 0.90 (t, *J* = 8.0 Hz, 2H), -0.03 (s, 9H); LRMS [M+H]⁺: 399; 100% a/a.

A second crop was isolated by combining the water portions, concentrating *in vacuo* to dryness and slurrying with EtOAc. The organic portion was decanted and evaporated *in vacuo* to give *carboxylic acid* **4.127** as a white solid (59 mg, 11%): Analytical data as above.

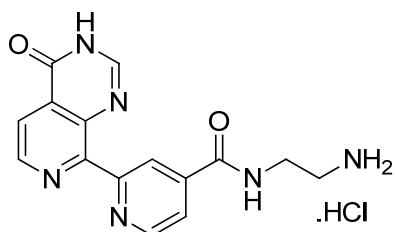
tert-Butyl (2-(2-(4-oxo-3-((2-(trimethylsilyl)ethoxy)methyl)-3,4-dihydropyrido[3,4-d]pyrimidin-8-yl)isonicotinamido)ethyl)carbamate (4.128)¹¹¹



Chemical Formula: C₂₆H₃₆N₆O₅Si
Molecular Weight: 540.69

Oxalyl chloride (37 μ L, 0.42 mmol) was added to a stirred suspension of 2-(4-oxo-3-((2-(trimethylsilyl)ethoxy)methyl)-3,4-dihydropyrido[3,4-d]pyrimidin-8-yl)isonicotinic acid (**4.127**) (120 mg, 0.301 mmol) in DCM under N₂. DMF (5 μ L, 0.07 mmol) was added to the resulting orange suspension and the suspension stirred for 40 min. The orange suspension was concentrated *in vacuo* to dryness and resuspended in dry DCM (5 mL). *N*-Boc-ethylenediamine (67 μ L, 0.42 mmol) was added to the stirred suspension followed by triethylamine (42 μ L, 0.30 mmol) dried over MgSO₄. The resulting solution was stirred for 30 min and evaporated *in vacuo* to a brown oil. The residue was purified by silica gel chromatography eluting with DCM:2 M methanolic ammonia (0 -> 5%) to give the title compound **4.128** as a pale yellow solid (140 mg, 86%): ¹H NMR (SO(CD₃)₂, 400 MHz) δ 8.90 - 8.74 (m, 3H), 8.49 (s, 1H), 8.21 - 8.08 (m, 2H), 7.85 (d, *J* = 5.0 Hz, 1H), 6.94 - 6.84 (m, 1H), 5.39 (s, 2H), 3.65 (t, *J* = 8.0 Hz, 2H), 3.37 - 3.29 (m, 2H), 3.16 - 3.08 (m, 2H), 1.35 (s, 9H), 0.90 (t, *J* = 8.0 Hz, 2H), -0.03 (s, 9H); LRMS [M+H]⁺: 541; 98% a/a.

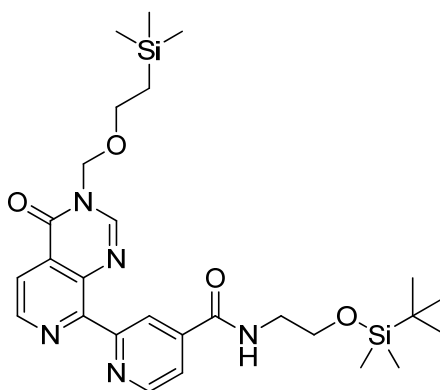
N-(2-Aminoethyl)-2-(4-oxo-3,4-dihydropyrido[3,4-*d*]pyrimidin-8-yl)isonicotinamide.
hydrochloride (**4.086**)



Chemical Formula: C₁₅H₁₄N₆O₂ .HCl
Molecular Weight: 346.77

A solution of 5 N HCl in 2-propanol (5.0 mL, 25 mmol) was added to a flask containing *tert*-butyl (2-(2-(4-oxo-3-((2-(trimethylsilyl)ethoxy)methyl)-3,4-dihydropyrido[3,4-*d*]pyrimidin-8-yl)isonicotinamido)ethyl)carbamate (**4.128**) (136 mg, 0.252 mmol) and the resulting suspension stirred for 2 h. The suspension was heated to 60 °C for 3 h and allowed to cool to room temperature overnight. The resulting suspension was filtered, washed [1x IPA (1 mL), 1x TBME (1 mL)] and dried *in vacuo* at 40 °C for 1 h to give the title compound **4.086** as the mono HCl salt as an almost white solid (79 mg, 91%): ¹H NMR (SO(CD₃)₂, 400 MHz) δ 9.26 (t, *J* = 5.5 Hz, 1H), 8.94 (d, *J* = 5.5 Hz, 1H), 8.82 (d, *J* = 5.5 Hz, 1H), 8.54 (s, 1H), 8.34 (s, 1H), 8.23 - 8.03 (m, 5H), 3.59 (app.q, *J* = 6.0 Hz, 2H), 3.11 - 2.93 (m, 2H); ¹³C NMR (SO(CD₃)₂, 101 MHz) δ 164.0, 159.6, 152.8, 148.8, 148.6, 147.0, 145.5, 144.6, 140.5, 129.4, 124.1, 123.0, 120.9, 38.2, 37.4; LRMS [M+H]⁺: 311; 100% a/a; HRMS: C₁₅H₁₅N₆O₂ [M]⁺ requires 311.1251, found [M]⁺ 311.1253; IR solid: ν 3317, 3042, 1645, 1539, 1448, 1295, 1121 cm⁻¹; mp Decomp. 210 °C.

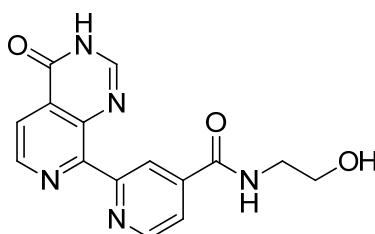
N-(2-((*tert*-Butyldimethylsilyl)oxy)ethyl)-2-(4-oxo-3-((2-(trimethylsilyl)ethoxy)methyl)-3,4-dihydropyrido[3,4-*d*]pyrimidin-8-yl)isonicotinamide (4.129)¹¹¹



Chemical Formula: C₂₇H₄₁N₅O₄Si₂
Molecular Weight: 555.82

Oxalyl chloride (40 μ L, 0.45 mmol) was added to a stirred suspension of 2-(4-oxo-3-((2-(trimethylsilyl)ethoxy)methyl)-3,4-dihydropyrido[3,4-*d*]pyrimidin-8-yl)isonicotinic acid (**4.127**) (129 mg, 0.324 mmol) in DCM. DMF (5 μ L, 70 μ mol) was added to the resulting suspension, the suspension stirred for 1 h and evaporated *in vacuo* to dryness. The residue was resuspended in DCM (5 mL) and 2-((*tert*-butyldimethylsilyl)oxy)ethanamine (114 mg, 0.647 mmol) and triethylamine (68 μ L, 0.49 mmol) added. The resulting suspension was stirred for 1 h and evaporated to dryness. The residue was purified by silica gel chromatography eluting with DCM:2 M methanolic ammonia (0 \rightarrow 4%) to give the title compound **4.129** as a colourless gum (63 mg, 35%): ¹H NMR (SO(CD₃)₂, 400 MHz) δ 8.92 - 8.78 (m, 3H), 8.49 (s, 1H), 8.23 - 8.06 (m, 2H), 7.84 (dd, *J* = 1.5, 5.0 Hz, 1H), 5.40 (s, 2H), 3.72 (t, *J* = 6.5 Hz, 2H), 3.65 (t, *J* = 8.0 Hz, 2H), 3.43 - 3.36 (m, 2H), 0.96 - 0.82 (m, 11H), 0.03 (s, 6H), -0.03 (s, 9H); LRMS [M+H]⁺: 556; 83% a/a.

N-(2-Hydroxyethyl)-2-(4-oxo-3,4-dihydropyrido[3,4-*d*]pyrimidin-8-yl)isonicotinamide (4.130)



Chemical Formula: C₁₅H₁₃N₅O₃
Molecular Weight: 311.30

A solution of 1 M TBAF in THF (0.34 mL, 0.34 mmol) was added to a stirred solution of *N*-(2-((*tert*-butyldimethylsilyloxy)ethyl)-2-(4-oxo-3-((2-(trimethylsilyloxy)methyl)-3,4-dihydropyrido[3,4-*d*]pyrimidin-8-yl)isonicotinamide (**4.129**) (63 mg, 0.11 mmol) in THF (5 mL), the resulting solution heated to 60 °C for 5 h and further 1 M TBAF in THF (0.34 mL, 0.34 mmol) was added, the mixture heated at 110 °C under microwave conditions for 6 h and cooled to room temperature. The reaction mixture was evaporated *in vacuo* to dryness and purified by MDAP (HPH method A) to give the title compound **4.130** as a white solid (5 mg, 14%): ¹H NMR (SO(CD₃)₂, 400 MHz) δ 12.76 (br.s, 1H), 8.83 (d, *J* = 5.0 Hz, 1H), 8.81 - 8.75 (m, 1H), 8.73 (d, *J* = 5.0 Hz, 1H), 8.27 - 8.15 (m, 2H), 8.07 (d, *J* = 5.0 Hz, 1H), 7.85 (dd, *J* = 1.5, 5.0 Hz, 1H), 4.76 - 4.67 (m, 1H), 3.53 (dd, *J* = 6.0, 11.0 Hz, 2H), 3.37 (app. q, *J* = 6.0 Hz, 2H); LRMS [M+H]⁺: 312; 100 a/a.

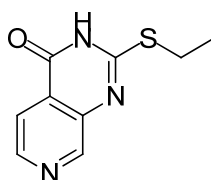
2-Mercaptopyrido[3,4-*d*]pyrimidin-4(3*H*)-one (**4.138**)¹⁸¹



Chemical Formula: C₇H₅N₃OS
Molecular Weight: 179.20

3-Aminoisonicotinic acid (12.1 g, 88.0 mmol) and thiourea (8.02 g, 105 mmol) were mixed together as solids and heated to 160 °C overnight. Water (120 mL) was added, the mixture cooled to 100 °C and then cooled slowly to room temperature. The resulting suspension was filtered, washed [water (20 mL), water:MeOH (1:1, 10 mL), MeOH (10 mL), TBME (20mL)] and dried *in vacuo* to give a the title compound as a pale brown solid (9.85 g, 63%). ¹H NMR (SO(CD₃)₂, 400 MHz) δ 12.87 (br.s, 1H), 12.68 (br.s, 1H), 8.72 (s, 1H), 8.47 (d, *J* = 5.0 Hz, 1H), 7.78 (d, *J* = 5.0 Hz, 1H); LRMS [M+H]⁺: 180; 99% a/a.

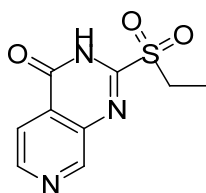
2-(Ethylthio)pyrido[3,4-*d*]pyrimidin-4(3*H*)-one (**4.139**)¹⁸²



Chemical Formula: C₉H₉N₃OS
Molecular Weight: 207.25

1 M aq. sodium hydroxide (146 mL, 146 mmol) was added to a fine suspension of 2-mercaptopyrido[3,4-*d*]pyrimidin-4(3*H*)-one (9.85g, 55.0 mmol) in methanol (146 mL) and the resulting suspension stirred for 5 min. Ethyl iodide (5.33 mL, 66.0 mmol) was added, the resulting solution stirred for 2.5 hours, and 2 M aq. HCl (73 mL) added. The resulting suspension was filtered, washed [MeOH (20 mL), TBME (20 mL)] and dried *in vacuo* to give the title compound as an almost white solid (10.6 g, 92%): ¹H NMR (SO(CD₃)₂, 400 MHz) δ 12.86 (br.s, 1H), 8.90 (s, 1H), 8.55 (d, *J* = 5.0 Hz, 1H), 7.87 (dd, *J* = 1.0, 5.0 Hz, 1H), 3.24 (q, *J* = 7.5 Hz, 2H), 1.36 (t, *J* = 7.5 Hz, 3H); LRMS [M+H]⁺: 208; 99% a/a.

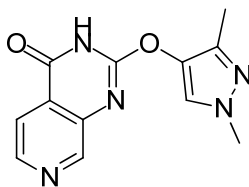
2-(Ethylsulfonyl)pyrido[3,4-*d*]pyrimidin-4(3*H*)-one (4.140)¹⁸²



Chemical Formula: C₉H₉N₃O₃S
Molecular Weight: 239.25

mCPBA (8.99 g, 52.1 mmol) was added to a ground suspension of 2-(ethylthio)pyrido[3,4-*d*]pyrimidin-4(3*H*)-one (3.60 g, 17.4 mmol) in THF (180 mL) and the resulting suspension stirred under nitrogen overnight. The solvent was replaced by IPA (50 mL) and the resulting solid filtered, washed [IPA (10 mL), TBME (10 mL)] and the solid dried *in vacuo* at 40 °C overnight to give an almost white solid. The solid was sonicated in THF (15 mL) for 10 min and evaporated *in vacuo* to give the title compound as a white solid (2.34 g, 57%): ¹H NMR (SO(CD₃)₂, 400 MHz) δ 9.19 (d, *J* = 0.5 Hz, 1H), 8.81 (d, *J* = 5.0 Hz, 1H), 8.03 (dd, *J* = 0.5, 5.0 Hz, 1H), 3.66 (q, *J* = 7.5 Hz, 2H), 1.31 (t, *J* = 7.5 Hz, 3H); LRMS [M+H]⁺: 240; 80% a/a.

2-((1,3-dimethyl-1H-pyrazol-4-yl)oxy)pyrido[3,4-*d*]pyrimidin-4(3*H*)-one (4.141)¹⁸³

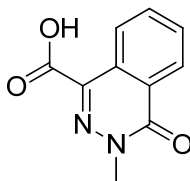


Chemical Formula: C₁₂H₁₁N₅O₂
Molecular Weight: 257.25

60% w/w Sodium hydride in mineral oil (115 mg, 2.88 mmol) was added to a solution of 1,3-dimethyl-1*H*-pyrazol-4-ol (105 mg, 0.936 mmol) in DMF (5 mL) under N₂ and the resulting suspension stirred for 5 min. 2-(Ethylsulfonyl)pyrido[3,4-*d*]pyrimidin-4(3*H*)-one (150 mg, 0.568 mmol) was added, the resulting suspension heated to 110 °C for 1.5 h. The mixture was cooled to room temperature, acidified to pH 4 with a solution of 2 M HCl and diluted with ethyl acetate (20 mL). The aqueous layer was removed and the organic layer washed [3x water (5 mL), 1x brine (5 mL)], dried over MgSO₄ and evaporated *in vacuo* to a dark red solid. The residue was purified by silica gel chromatography eluting with DCM:MeOH (0 -> 6%) to give the title compound as a white solid (9 mg, 6%): ¹H NMR (SO(CD₃)₂, 400 MHz) δ 13.05 (br.s, 1H), 8.80 (s, 1H), 8.52 (d, J = 5.0 Hz, 1H), 7.90 (s, 1H), 7.88 (d, J = 5.0 Hz, 1H), 3.78 (s, 3H), 2.07 (s, 3H); LRMS [M+H]⁺: 258; 100% a/a.

6.4.5 Phthalazinones

3-Methyl-4-oxo-3,4-dihydrophthalazine-1-carboxylic acid (5.031)



Chemical Formula: C₁₀H₈N₂O₃
Molecular Weight: 204.18

Method 1:²⁷³

Potassium permanganate (58.0 g, 367 mmol) was added portionwise over 45 min to a stirred emulsion of Decon® 90 (4 drops), 1,2,3,4-tetrahydronaphthalene (6.78 mL, 49.9 mmol) and sodium hydroxide (1 g, 25.00 mmol) in water (100 mL). The mixture was heated to 90 °C for 1 h and cooled to room temperature overnight. The resulting suspension was filtered through celite, IPA added with stirring until no purple colour remained, filtered and evaporated *in vacuo* to ~120 mL of a brown suspension. Methylhydrazine (4.14 mL, 79.0 mmol) was added cautiously and the resulting colourless solution was heated to 90 °C for 1 h. The solution was cooled in an ice bath and acidified with conc. aq. HCl until a white precipitate formed (~ pH 3). The suspension was filtered, washed [1x water (20 mL), 1x water:acetone (1:1, 10 mL), 1x acetone (5 mL)] and dried under suction to give the title compound **5.031** as a white solid (343 mg, 3.4%). ¹H NMR (SO(CD₃)₂, 400 MHz) δ 13.67 (br.s, 1H), 8.56 (d, *J* = 7.5 Hz, 1H), 8.32 (dd, *J* = 1.0, 8.0 Hz, 1H), 8.02 - 7.94 (m, 1H), 7.94 - 7.86 (m, 1H), 3.79 (s, 3H); LRMS [M+H]⁺: 205, 99% a/a.

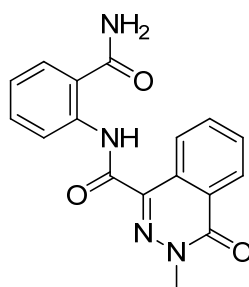
Further acetone (50 mL) was added to the filtrate, evaporated *in vacuo* to dryness and stirred in methanol (50 mL) for 1 h. The resulting suspension was filtered. The filtrate was evaporated to dryness, suspended in water (2 mL) and filtered. The filtered solid was washed [3x water (10 mL)] and pulled to dryness under vacuum to give the title compound **5.031** as a white solid (241 mg, 2.4%): Analytical data as above.

Method 2:²⁷⁸

Potassium permanganate (24.7 g, 157 mmol) was added dropwise over 45 min to a stirred emulsion of 2'-methyl-acetophenone (4.87 mL, 37.3 mmol) and potassium carbonate (3.22 g, 23.29 mmol) in water (150 mL) at 50 °C. The resulting solution was heated to 70 °C for 2

h, ethanol (10 mL) added and cooled to room temperature. The resulting black suspension was filtered, washed [2x water (100 mL)], evaporated at 40 bar at 35 °C for 10 min and methylhydrazine (2.54 mL, 48.4 mmol) added. The colourless solution was heated to 90 °C for 15 min, and acetic acid (15 mL) added. The resulting solution was stirred for 2 hours at 70 °C and cooled in an ice bath. The resulting solution was acidified to pH 0 with 37% aq. HCl (18 mL) and the formed suspension filtered. The filtered solid was washed [2x water (20 mL), 1x water:acetone (1:1, 10 mL), 1x acetone (10 mL), 1x TBME (5 mL)], pulled to dryness under vacuum and dried *in vacuo* at 40 °C to give the title compound **5.031** as a white solid (3.317 g, 44%): ¹H NMR and LRMS data as above; ¹³C NMR (SO(CD₃)₂, 101 MHz) δ 164.9, 159.1, 136.1, 134.2, 132.5, 128.0, 127.4, 126.7, 126.6, 40.0; HRMS: C₁₀H₉N₂O₃ [M+H]⁺ requires 205.0608, found [M+H]⁺ 205.0611; IR: ν 3319, 1717, 1622, 1416, 1347, 1186 cm⁻¹.

N-(2-Carbamoylphenyl)-3-methyl-4-oxo-3,4-dihydrophthalazine-1-carboxamide (**5.027**)¹¹¹

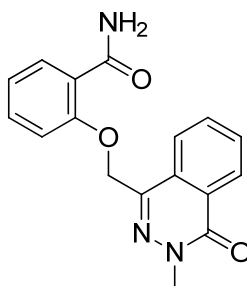


Chemical Formula: C₁₇H₁₄N₄O₃
Molecular Weight: 322.32

Oxalyl chloride (51.4 μL, 0.588 mmol) was added to a suspension of DMF (5 μL, 0.065 mmol) and 3-methyl-4-oxo-3,4-dihydrophthalazine-1-carboxylic acid (100 mg, 0.490 mmol) in DCM (5 mL) under N₂. The suspension was stirred for 30 min, triethylamine (102 μL, 0.735 mmol) added, stirred for 5 min and 2-aminobenzamide (133 mg, 0.979 mmol) added. The resulting suspension was stirred for 10 min and stood overnight. The reaction mixture was diluted with EtOAc (15 mL) and 2-MeTHF (15 mL) and washed [3x sat. aq. sodium hydrogen carbonate (5 mL), 1x brine (5 mL)], dried over MgSO₄ and evaporated *in vacuo* to dryness. The residue was purified by silica gel chromatography eluting with cyclohexane:ethyl acetate (10 -> 100%) to give the title compound **5.027** as a white solid (23 mg, 15%): ¹H NMR (SO(CD₃)₂, 400 MHz) δ 13.20 (s, 1H), 9.06 (d, *J* = 8.0 Hz, 1H), 8.73 (d, *J*

= 7.5 Hz, 1H), 8.41 - 8.27 (m, 2H), 8.05 - 7.96 (m, 1H), 7.96 - 7.79 (m, 3H), 7.59 (dd, $J = 1.0$, 8.5 Hz, 1H), 7.21 (dd, $J = 1.0$, 8.0 Hz, 1H), 3.86 (s, 3H); LRMS $[M+H]^+$: 323, 91% a/a.

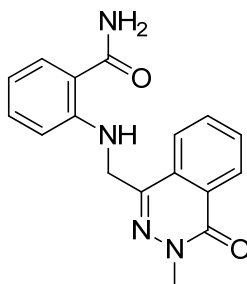
2-((3-Methyl-4-oxo-3,4-dihydrophthalazin-1-yl)methoxy)benzamide (5.032)²⁸⁰



Chemical Formula: $C_{17}H_{15}N_3O_3$
Molecular Weight: 309.32

DBAD (91 mg, 0.39 mmol) was added to a stirred solution of 4-(hydroxymethyl)-2-methylphthalazin-1(2H)-one (50 mg, 0.26 mmol), 2-hydroxybenzamide (40 mg, 0.29 mmol) and triphenylphosphine (103 mg, 0.394 mmol) in THF (5 mL) under N_2 . The reaction mixture was stirred at 20 °C for 41 h. The resultant suspension was filtered under vacuum and the white solid rinsed with Et_2O (5 mL) and pulled to dryness under vacuum for 20 min, to give the title compound **5.032** as a white solid (53 mg, 65%): 1H NMR ($SO(CD_3)_2$, 400 MHz) δ 8.32 (dd, $J = 0.5$, 8.0 Hz, 1H), 8.14 (d, $J = 7.5$ Hz, 1H), 8.01 – 7.89 (m, 3H), 7.86 (dd, $J = 1.5$, 7.5 Hz, 1H), 7.59 – 7.50 (m, 2H), 7.47 – 7.42 (m, 1H), 7.13 – 7.07 (m, 1H), 5.59 (s, 2H), 3.76 (s, 3H); ^{13}C NMR ($SO(CD_3)_2$, 101 MHz) δ 166.5, 159.0, 156.4, 141.1, 133.9, 132.9, 132.6, 131.4, 128.4, 127.5, 126.6, 125.6, 123.5, 121.6, 114.0, 68.0, 39.5; LRMS $[M+H]^+$: 310, 100% a/a; HRMS: $C_{17}H_{16}N_3O_3$ $[M+H]^+$ requires 310.1186, found $[M+H]^+$ 310.1195 ; IR: solid v 3403, 1688, 1647, 1591, 1573, 1484, 1456 cm^{-1} ; mp > 250 °C.

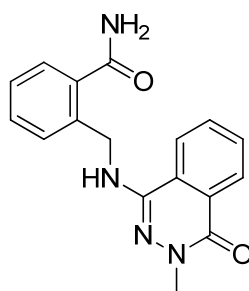
2-(((3-methyl-4-oxo-3,4-dihydrophthalazin-1-yl)methyl)amino)benzamide (5.033)



Chemical Formula: $C_{17}H_{16}N_4O_2$
Molecular Weight: 308.33

A solution of 4-(hydroxymethyl)-2-methylphthalazin-1(2*H*)-one (50 mg, 0.26 mmol) and triethylamine (0.073 mL, 0.53 mmol) in DCM (5 mL) was cooled in an ice bath. Methanesulfonyl chloride (0.023 mL, 0.29 mmol) was added over 1 min and the reaction mixture stirred under N₂ for 30 min. Further methanesulfonyl chloride (0.010 mL, 0.13 mmol) was added and the reaction mixture stirred for 10 min. The reaction mixture was warmed to 20 °C and 2-aminobenzamide (54 mg, 0.39 mmol) and potassium carbonate (55 mg, 0.39 mmol) were added in single portions. The resulting suspension was stirred for 1.5 h and heated at 40 °C for 3 h. The reaction mixture was partitioned between DCM (10 mL) and water (20 mL). The organic portion was removed and washed with water (20 mL) and evaporated *in vacuo* to a cream residue. The residue was purified by MDAP (Formic method B) to give the title compound **5.033** as a white solid (3 mg, 4%): ¹H NMR (SO(CD₃)₂, 400 MHz) δ 8.89 (t, *J* = 5.0 Hz, 1H), 8.31 (dd, *J* = 8.0 Hz, 1H), 8.16 (d, *J* = 8.0 Hz, 1H), 7.96 (ddd, *J* = 1.5, 8.0, 8.0 Hz, 1H), 7.91 – 7.71 (m, 2H), 7.62 (dd, *J* = 1.5, 8.0 Hz, 1H), 7.36 – 7.29 (m, 1H), 7.16 (br.s, 1H), 7.00 (d, *J* = 8.0 Hz, 1H), 6.59 (t, *J* = 7.0 Hz, 1H), 4.69 (d, *J* = 5.0 Hz, 2H), 3.76 (s, 3H); LRMS [M+H]⁺: 309, 100% a/a.

2-(((3-methyl-4-oxo-3,4-dihydrophthalazin-1-yl)amino)methyl)benzamide (**5.034**)¹³²

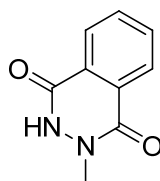


Chemical Formula: C₁₇H₁₆N₄O₂
Molecular Weight: 308.33

A solution of 30% hydrogen peroxide in water (0.056 mL, 0.55 mmol) was added to a stirred suspension of potassium carbonate (15 mg, 0.11 mmol) and 2-(((3-methyl-4-oxo-3,4-dihydrophthalazin-1-yl)amino)methyl)benzamide (16 mg, 0.055 mmol) in DMSO (1 mL). The resulting suspension was stirred for 4 h and evaporated under a stream of nitrogen. The residue was suspended in water (1 mL), filtered, washed (water [1 mL]) and dried *in vacuo* at 40 °C to give the title compound **5.034** as a white solid (10 mg, 59%): ¹H NMR (SO(CD₃)₂, 400 MHz) δ 8.24 (dd, *J* = 1.0, 7.5 Hz, 1H), 8.13 (d, *J* = 8.0 Hz, 1H), 7.94 - 7.79 (m,

3H), 7.53 - 7.42 (m, 3H), 7.38 (td, $J = 1.5, 7.5$ Hz, 1H), 7.32 - 7.24 (m, 2H), 4.64 (d, $J = 5.5$ Hz, 2H), 3.51 (s, 3H); LRMS $[M+H]^+$: 309, 97% a/a.

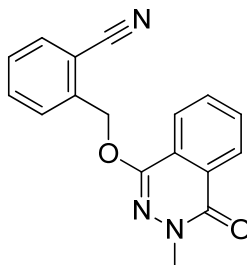
2-Methyl-2,3-dihydrophthalazine-1,4-dione (5.038)²⁷⁶



Chemical Formula: $C_9H_8N_2O_2$
Molecular Weight: 176.17

Phthalic anhydride (2.00 g, 13.5 mmol) was added to acetic acid (12.8 mL) and the suspension stirred for 5 min. *N*-Methylhydrazine (0.778 mL, 14.9 mmol) was added cautiously and the resulting suspension stirred for 3 h, filtered, the solid washed [2x AcOH (10 mL), 1x AcOH:TBME (1:1, 10 mL), 2x TBME (10 mL)] and pulled to dryness under vacuum to give the title compound **5.038** as a white solid (1.602 g, 67%): 1H NMR ($SO(CD_3)_2$, 400 MHz) δ 11.63 (br.s, 1H), 8.29 - 8.18 (m, 1H), 8.01 - 7.93 (m, 1H), 7.93 - 7.83 (m, 2H), 3.57 (s, 3H); LRMS $[M+H]^+$: 177, 100% a/a.

2-(((3-Methyl-4-oxo-3,4-dihydrophthalazin-1-yl)oxy)methyl)benzonitrile (5.051)²⁸³

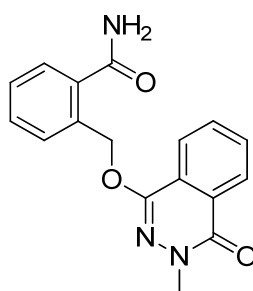


Chemical Formula: $C_{17}H_{13}N_3O_2$
Molecular Weight: 291.30

α -Bromo-2-tolunitrile (117 mg, 0.596 mmol) was added to a stirred suspension of Ag_2CO_3 (172 mg, 0.624 mmol) and 2-methyl-2,3-dihydrophthalazine-1,4-dione (100 mg, 0.568 mmol) in ethanol (0.1 mL) and acetonitrile (5 mL). The resulting suspension was stirred at room temperature for 16 h and the resulting suspension heated to 80 °C for 24 h. The resulting black suspension was cooled to room temperature, partitioned between ethyl acetate (20 mL) and water (5 mL), filtered and the aqueous layer removed. The organic layer was washed (1x water [5 mL], 1x brine [5 mL]), dried over $MgSO_4$ and evaporated *in*

vacuo to dryness. The residue was purified by silica gel chromatography eluting with cyclohexane:ethyl acetate (10 -> 50%) to give the title compound **5.051** as a white solid (128 mg, 77%): $^1\text{H NMR}$ ($\text{SO}(\text{CD}_3)_2$, 400 MHz) δ 8.28 - 8.24 (m, 1H), 8.05 - 7.99 (m, 1H), 7.98 - 7.88 (m, 3H), 7.88 - 7.82 (m, 1H), 7.78 (td, $J = 1.5, 7.5$ Hz, 1H), 7.60 (td, $J = 1.5, 7.5$ Hz, 1H), 5.54 (s, 2H), 3.65 (s, 3H); LRMS: $[\text{M}+\text{H}]^+$: 292, 92% a/a.

2-(((3-methyl-4-oxo-3,4-dihydrophthalazin-1-yl)oxy)methyl)benzamide (5.035)¹³²

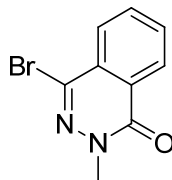


Chemical Formula:
 $\text{C}_{17}\text{H}_{15}\text{N}_3\text{O}_3$
Molecular Weight: 309.32

30% aq. hydrogen peroxide (0.400 mL, 3.91 mmol) was added to a stirred suspension of 2-(((3-methyl-4-oxo-3,4-dihydrophthalazin-1-yl)oxy)methyl)benzamide (114 mg, 0.391 mmol) and potassium carbonate (108 mg, 0.783 mmol) in DMSO (5 mL). The resulting suspension was stirred for 30 min, and partitioned between water (5 mL) and ethyl acetate (20 mL). The aqueous layer was run off and the organic layer washed (3x water [5 mL], 1x brine [5 mL]), dried over MgSO_4 and evaporated *in vacuo* to a white solid. The residue was purified by silica gel chromatography eluting with cyclohexane:ethyl acetate (50 -> 100%) to give a white powder. The solid was triturated in hot methanol, cooled to 4 °C and filtered to give the title compound **5.035** as a white crystalline solid (33 mg, 27%): $^1\text{H NMR}$ ($\text{SO}(\text{CD}_3)_2$, 400 MHz) δ 8.29 - 8.22 (m, 1H), 8.06 - 7.99 (m, 1H), 7.97 - 7.85 (m, 3H), 7.71 - 7.64 (m, 1H), 7.58 - 7.47 (m, 2H), 7.47 - 7.38 (m, 2H), 5.55 (s, 2H), 3.63 (s, 3H); $^{13}\text{C NMR}$ ($\text{SO}(\text{CD}_3)_2$, 101 MHz) δ 170.8, 158.0, 149.1, 136.6, 135.0, 133.7, 132.9, 130.2, 129.1, 128.8, 128.3, 128.0, 126.8, 124.5, 123.9, 66.6, 38.8; LRMS: $[\text{M}+\text{H}]^+$: 310, 100% a/a; HRMS: $\text{C}_{17}\text{H}_{16}\text{N}_3\text{O}_3$ $[\text{M}+\text{H}]^+$ requires 310.1186, found $[\text{M}+\text{H}]^+$ 310.1181; IR: solid v 3324, 1640, 1585, 1390, 1332, 1132, 1100 cm^{-1} ; mp 217 - 222 °C.

The filtrate gave further solid on standing overnight. The filtrate was filtered to give a second crop of the title compound **5.035** as a white crystalline solid (25 mg, 20%): Analytical data as above.

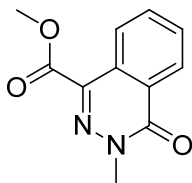
4-bromo-2-methylphthalazin-1(2H)-one (5.036)²⁷⁷



Chemical Formula: C₉H₇BrN₂O
Molecular Weight: 239.07

Phosphorus(V) oxybromide (1.67 g, 5.83 mmol) was added to a stirred suspension of 2-methyl-2,3-dihydrophthalazine-1,4-dione (342mg, 1.94 mmol) and triethylamine (0.95 mL, 6.8 mmol) in toluene (10 mL) under N₂. The resulting suspension was heated to 115 °C overnight and cooled to room temperature. The reaction mixture was partitioned between water (15 mL) and ethyl acetate (80 mL), the aqueous layer run off and the organic washed [3x water (20 mL), 1x brine (10 mL)], dried over MgSO₄ and evaporated *in vacuo* to a brown solid. The residue was purified by silica gel chromatography and eluted with cyclohexane:ethyl acetate (5 -> 35%) to give the title compound **5.036** as a white solid (228 mg, 34%, correcting for 30% 1,4-dibromophthalazine present): ¹H NMR (SO(CD₃)₂, 400 MHz) δ 8.44 (dd, *J* = 1.0, 7.5 Hz, 1H), 7.97 - 7.93 (m, 1H), 7.88 (td, *J* = 1.5, 7.5 Hz, 1H), 7.82 (td, *J* = 1.5, 7.5 Hz, 1H), 3.85 (s, 3H); LRMS [M+H]⁺: 239 & 241, 76% a/a.

Methyl 3-methyl-4-oxo-3,4-dihydrophthalazine-1-carboxylate (5.039)²⁷⁷

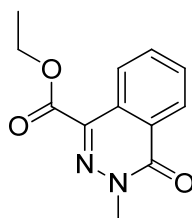


Chemical Formula: C₁₁H₁₀N₂O₃
Molecular Weight: 218.21

A solution of 4-bromo-2-methylphthalazin-1(2H)-one (100 mg, 0.418 mmol), DPPF (28 mg, 0.050 mmol) and Pd(OAc)₂ (5.6 mg, 0.025 mmol) in DMF (2.5 mL) and methanol (2.5 mL) was vacuum degassed with nitrogen, sparged with carbon monoxide for 5 min, heated to

50 °C and triethylamine (0.12 ml, 0.84 mmol) added. The solution was stirred overnight, further DPPF (28 mg, 0.050 mmol), Pd(OAc)₂ (5.6 mg, 0.025 mmol) and triethylamine (0.12 ml, 0.84 mmol) were added in DMF (0.5 mL) and methanol (0.5 mL) and the resulting suspension stirred for 4 days. The resulting black solution was cooled to room temperature and partitioned between ethyl acetate (10 mL) and water (3 mL). The aqueous layer was removed, the organic layer washed (2x water [3 mL], 1x brine [3 mL]), dried over MgSO₄ and evaporated *in vacuo* to dryness. The residue was purified by silica gel chromatography eluting with cyclohexane:ethyl acetate (5 -> 33%) to give the title compound **5.039** as a white solid (37 mg, 41%): ¹H NMR (CDCl₃, 400 MHz) δ 8.64 (d, *J* = 8.0 Hz, 1H), 8.47 (dd, *J* = 1.0, 8.0 Hz, 1H), 7.90 - 7.73 (m, 3H), 7.94 - 7.86 (m, 3H), 4.03 (s, 3H), 3.94 (s, 3H); LRMS [M+H]⁺: 219, 95 % a/a.

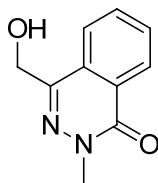
Ethyl 3-methyl-4-oxo-3,4-dihydrophthalazine-1-carboxylate (**5.041**)²⁷⁹



Chemical Formula:
C₁₂H₁₂N₂O₃
Molecular Weight: 232.24

Sulfuric acid (0.026 mL, 0.49 mmol) was added to a stirred suspension of 3-methyl-4-oxo-3,4-dihydrophthalazine-1-carboxylic acid (1.00 g, 4.90 mmol). The suspension was heated at 80 °C for 2 days. The resulting solution was cooled to room temperature, partitioned between EtOAc (40 mL) and sat. aq. NaHCO₃ (40 mL). The aqueous portion was removed and the organic layer washed (2x sat. aq. NaHCO₃ [40 mL]). The combined aqueous portions were extracted with EtOAc (30 mL). The combined organic phases were evaporated *in vacuo* to a colourless oil which crystallised overnight. The residue was purified by silica gel chromatography eluting with cyclohexane:EtOAc (0 -> 50%) to give the title compound **5.041** as a white solid (1.00 g, 88%): ¹H NMR (SO(CD₃)₂, 400 MHz) δ 8.48 (d, *J* = 7.5 Hz, 1H), 8.33 (dd, *J* = 1.0, 8.0 Hz, 1H), 8.03 – 7.96 (m, 1H), 7.95 – 7.89 (m, 1H), 4.43 (q, *J* = 7.0 Hz, 2H), 3.79 (s, 3H), 1.37 (t, *J* = 7.0 Hz, 3H); LRMS [M+H]⁺: 233, 100% a/a.

4-(Hydroxymethyl)-2-methylphthalazin-1(2H)-one (5.042)

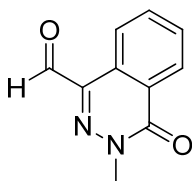


Chemical Formula: C₁₀H₁₀N₂O₂

Molecular Weight: 190.20

Sodium borohydride (435 mg, 11.5 mmol) was added in to a stirred solution of ethyl 3-methyl-4-oxo-3,4-dihydrophthalazine-1-carboxylate (100 mg, 0.431 mmol) in THF (2.5 mL) under N₂. The reaction mixture was stirred for 1 h under N₂ at 20 °C and heated to reflux for 65 h. The reaction mixture was cooled to room temperature and evaporated *in vacuo* to a white solid. The residue was partitioned between DCM (30 mL) and 2M HCl (20 mL). The organic portion was removed and the aqueous layer extracted with DCM (2x 30 mL). The combined organic layers were washed with water (50 mL) and evaporated *in vacuo* to a white solid. The residue was purified by silica gel chromatography eluting with DCM:MeOH (0 → 8%) to give the title compound **5.042** as a white solid (574 mg, 79%): ¹H NMR (SO(CD₃)₂, 400 MHz) δ 8.29 (dd, *J* = 1.0, 8.0 Hz, 1H), 8.14 (d, *J* = 8.0 Hz, 1H), 7.94 (td, *J* = 1.5, 8.0 Hz, 1H), 7.90 – 7.81 (m, 1H), 5.52 (t, *J* = 5.5 Hz, 1H), 4.71 (d, *J* = 5.5 Hz, 2H), 3.72 (s, 3H); LRMS [M+H]⁺: 191, 91% a/a.

3-Methyl-4-oxo-3,4-dihydrophthalazine-1-carbaldehyde (5.043)¹⁷⁶



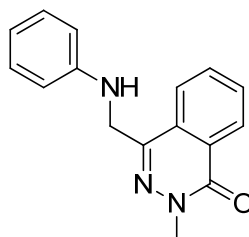
Chemical Formula: C₁₀H₈N₂O₂

Molecular Weight: 188.18

A solution of oxalyl chloride (0.276 mL, 3.15 mmol) in DCM (12.5 mL) was cooled to -70 °C under N₂. DMSO (0.448 mL, 6.31 mmol) was added over a period of 1 min and the reaction mixture stirred at -70 °C for 30 min. A solution of 4-(hydroxymethyl)-2-methylphthalazin-1(2H)-one (300 mg, 1.58 mmol) in DCM (12.5 mL) was added dropwise over 15 min and the reaction mixture stirred for a further 15 min at -70 °C. Triethylamine (1.32 mL, 9.46 mmol) was added in a single portion and the reaction mixture warmed to 20 °C and stirred for 1.5

h. The reaction mixture was diluted with DCM (10 mL) and washed with water (30 mL). The separated aqueous portion was further extracted with DCM (2x 30 mL) and the combined organic phases were washed with water (100 mL). The resulting solution was evaporated *in vacuo* to give the title compound **5.043** as a cream solid (296 mg, 100%): $^1\text{H NMR}$ ($\text{SO}(\text{CD}_3)_2$, 400 MHz) δ 9.86 (s, 1H), 8.91 (d, $J = 8.0$ Hz, 1H), 8.33 (dd, $J = 0.5, 8.0$ Hz, 1H), 8.03 (ddd, $J = 1.5, 8.0, 8.0$ Hz, 1H), 7.97 – 7.90 (m, 1H), 3.88 (s, 3H); LRMS $[\text{M}+\text{H}]^+$: 189, 97% a/a.

2-Methyl-4-((phenylamino)methyl)phthalazin-1(2H)-one (**5.044**)

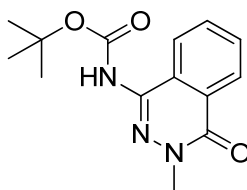


Chemical Formula: $\text{C}_{16}\text{H}_{15}\text{N}_3\text{O}$

Molecular Weight: 265.31

Acetic acid (11 μL , 0.19 mmol) was added to a stirred solution of aniline (0.019 mL, 0.21 mmol) and 3-methyl-4-oxo-3,4-dihydrophthalazine-1-carbaldehyde (39 mg, 0.19 mmol) in THF (5 mL) at 20 $^\circ\text{C}$. The reaction mixture was stirred for 10 min and sodium triacetoxyborohydride (79 mg, 0.37 mmol) was added and the resulting solution stirred for 30 min. The reaction mixture was heated at 60 $^\circ\text{C}$ under N_2 for 1.5 h and further sodium triacetoxyborohydride (79 mg, 0.37 mmol) added and heated at 60 $^\circ\text{C}$ for a further 30 min. A further portion of sodium triacetoxyborohydride (79 mg, 0.37 mmol) was added, the reaction mixture stirred at 60 $^\circ\text{C}$ for 1 h and cooled to 20 $^\circ\text{C}$. The reaction mixture was partitioned between sat. aq. NaHCO_3 (10 mL) and EtOAc (20 mL). The organic portion was removed and the aqueous portion was extracted with EtOAc (2x 10 mL). The organic portions were combined, washed with water (20 mL) and evaporated *in vacuo* to a solid. The residue was purified by silica gel chromatography eluting with cyclohexane:EtOAc (0 -> 75%) to give the title compound **5.044** as a white solid (29 mg, 59%): $^1\text{H NMR}$ ($\text{SO}(\text{CD}_3)_2$, 400 MHz) δ 8.30 (dd, $J = 1.0, 8.0$ Hz, 1H), 8.15 (d, $J = 7.5$ Hz, 1H), 7.93 (ddd, $J = 1.5, 7.5, 7.5$ Hz, 1H), 7.90 – 7.83 (m, 1H), 7.10 (dd, $J = 7.5, 8.5$ Hz, 2H), 6.75 (d, $J = 7.5$ Hz, 2H), 6.60 – 6.54 (m, 1H), 6.17 (t, $J = 5.5$ Hz, 1H), 4.53 (d, $J = 5.5$ Hz, 2H), 3.75 (s, 3H); LRMS $[\text{M}+\text{H}]^+$: 266, 100% a/a.

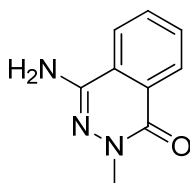
tert-Butyl (3-methyl-4-oxo-3,4-dihydrophthalazin-1-yl)carbamate (5.046)²⁸²



Chemical Formula: C₁₄H₁₇N₃O₃
Molecular Weight: 275.30

3-Methyl-4-oxo-3,4-dihydrophthalazine-1-carboxylic acid (200 mg, 0.980 mmol) was stirred at 30 °C under N₂ in *t*-BuOH (10 mL) and triethylamine (0.68 mL, 4.9 mmol). Diphenyl phosphorazidate (0.42 mL, 2.0 mmol) was added in a single portion and the reaction mixture stirred for 1.5 h. The reaction mixture was heated to 75 °C for a further 3 h, cooled to 20 °C and partitioned between EtOAc (20 mL) and sat. aq. NaHCO₃ (20 mL). The aqueous layer was removed and the organic portion was washed sat. aq. NaHCO₃ (20 mL). The combined aqueous phases were extracted with EtOAc (40 mL) and the combined organic portions evaporated *in vacuo*. The residue was purified by silica gel chromatography eluting with cyclohexane:EtOAc (20 → 70%) to give the title compound **5.046** as a white solid (173 mg, 64 %): ¹H NMR (SO(CD₃)₂, 400 MHz) δ 9.49 (s, 1H), 8.27 (d, *J* = 1.0, 8.0 Hz, 1H), 7.98 - 7.92 (m, 1H), 7.91 - 7.86 (m, 1H), 7.77 (d, *J* = 8.0 Hz, 1H), 3.69 (s, 3H), 1.45 (s, 9H); LRMS [M+H]⁺: 276, 93% a/a.

4-Amino-2-methylphthalazin-1(2H)-one (5.047)

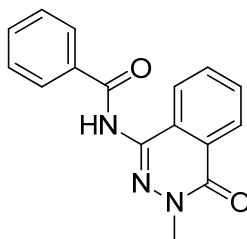


Chemical Formula: C₉H₉N₃O
Molecular Weight: 175.19

tert-Butyl (3-methyl-4-oxo-3,4-dihydrophthalazin-1-yl)carbamate (169 mg, 0.614 mmol) was stirred in 5 M HCl in IPA (5 mL) at 20 °C for 2 h. The reaction mixture was evaporated *in vacuo* to a white solid. The residue was dissolved in MeOH, loaded onto a preconditioned SCX cartridge and eluted with MeOH, followed by 2 M methanolic ammonia. The basic fractions were evaporated *in vacuo* to give the title compound **5.047** as a white solid (86 mg, 80%): ¹H NMR (SO(CD₃)₂, 400 MHz) δ 8.24 (dd, *J* = 1.5, 7.5 Hz, 1H),

8.07 (d, $J = 8.0$ Hz, 1H), 7.91 - 7.79 (m, 2H), 6.15 (s, 2H), 3.54 (s, 3H); LRMS $[M+H]^+$: 176, 100% a/a.

N-(3-Methyl-4-oxo-3,4-dihydrophthalazin-1-yl)benzamide (5.048)

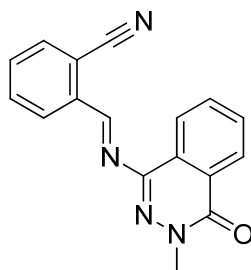


Chemical Formula: $C_{16}H_{13}N_3O_2$

Molecular Weight: 279.29

Benzoyl chloride (0.022 mL, 0.19 mmol) was added to a stirred solution of 4-amino-2-methylphthalazin-1(2*H*)-one (30 mg, 0.17 mmol) and triethylamine (0.048 mL, 0.34 mmol) in DCM (5 mL) at 20 °C under N_2 . The reaction mixture was stirred at 20 °C for 16 h. A further benzoyl chloride (0.022 mL, 0.19 mmol) and triethylamine (0.048 mL, 0.34 mmol) were added and the reaction mixture stirred at 20 °C for 1 h and heated to 40 °C for 6 h. Further benzoyl chloride (0.022 mL, 0.19 mmol) and triethylamine (0.048 mL, 0.34 mmol) were added and the reaction mixture stirred for 16 h. Further portion of benzoyl chloride (0.022 mL, 0.19 mmol) and triethylamine (0.048 mL, 0.34 mmol) were added and the reaction stirred for 6 h. Upon cooling to 20 °C, the reaction mixture was partitioned between DCM (10 mL) water (10 mL). The aqueous layer was removed and the organic portion was washed with water (2x 10 mL) and evaporated *in vacuo* to dryness. The residue was purified by MDAP (Formic method B) to give the title compound **5.048** as a white solid (8 mg, 17%): 1H NMR ($SO(CD_3)_2$, 600 MHz) δ 10.77 (s, 1H), 8.34 - 8.30 (m, 1H), 8.06 (d, $J = 7.5$ Hz, 2H), 7.94 - 7.88 (m, 2H), 7.77 - 7.74 (m, 1H), 7.68 - 7.63 (m, 1H), 7.60 - 7.55 (m, 2H), 3.74 (s, 3H); ^{13}C ($SO(CD_3)_2$, 151 MHz) δ 167.2, 158.5, 138.5, 133.3, 133.0, 132.2, 132.1, 128.5, 127.8, 127.6, 126.1, 125.5, 38.8 (carbon signals superimposed at 127.8); LRMS $[M+H]^+$: 280, 100% a/a.

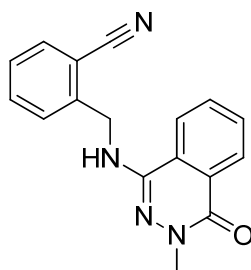
2-(((3-methyl-4-oxo-3,4-dihydrophthalazin-1-yl)imino)methyl)benzonitrile (5.050)



Chemical Formula: C₁₇H₁₂N₄O
Molecular Weight: 288.30

2-Cyanobenzaldehyde (42.7 mg, 0.325 mmol) was added to a stirred suspension of 4-amino-2-methylphthalazin-1(2H)-one (38 mg, 0.22 mmol) and acetic acid (0.015 mL, 0.26 mmol) in DCM (3 mL). The resulting solution was allowed to stand overnight under N₂ and sodium triacetoxyborohydride (46.0 mg, 0.217 mmol) added. The resulting solution was stirred for 8 h and allowed to stand overnight. The reaction mixture was purified by silica gel chromatography eluting with cyclohexane:EtOAc (5 -> 40%) to give the title compound **5.050** as a yellow solid (26 mg, 42%): ¹H NMR (SO(CD₃)₂, 400 MHz) δ 9.26 (s, 1H), 8.41 - 8.29 (m, 3H), 8.05 - 7.88 (m, 4H), 7.84 - 7.76 (m, 1H), 8.81 (s, 3H); LRMS [M+H]⁺: 289, 100% a/a; IR: ν 2225, 1661, 1623, 1580, 1329, 1260 cm⁻¹.

2-(((3-methyl-4-oxo-3,4-dihydrophthalazin-1-yl)amino)methyl)benzonitrile (5.049)



Chemical Formula: C₁₇H₁₄N₄O
Molecular Weight: 290.32

Sodium borohydride (3.4 mg, 0.090 mmol) was added to a stirred suspension of 2-(((3-methyl-4-oxo-3,4-dihydrophthalazin-1-yl)imino)methyl)benzonitrile (26 mg, 0.090 mmol) in a mixture of methanol (1.0 mL) and DCM (1.0 mL). The resulting suspension was stirred for 1 h and evaporated to dryness under a stream of N₂. The residue was purified by silica gel chromatography eluting with cyclohexane:EtOAc (10 -> 50%) to give the title compound **5.049** as a white solid (16 mg, 61%): ¹H NMR (SO(CD₃)₂, 400 MHz) δ 8.24 (dd, J = 1.0, 8.0 Hz,

1H), 8.17 (d, $J = 8.0$ Hz, 1H), 7.91 (td, $J = 1.5, 7.5$ Hz, 1H), 7.87 - 7.79 (m, 2H), 7.67 - 7.58 (m, 3H), 7.47 - 7.40 (m, 1H), 4.63 (d, $J = 5.5$ Hz, 2H), 3.49 (s, 3H); LRMS $[M+H]^+$: 291, 100% a/a.

Methods used for the synthesis of phthalizinone amides (Appendix A)

General Method A: Amide coupling using acid chloride intermediate. (5.057)

Oxalyl chloride (2.4 eq.) was added to a stirred suspension of 3-methyl-4-oxo-3,4-dihydrophthalazine-1-carboxylic acid (1.0 eq.) in DCM (10 mL) under nitrogen. The suspension was stirred for 2 min, DMF (0.05 mL) added and the suspension stirred for 30 min. The reaction mixture was evaporated *in vacuo* to dryness and resuspended in DMF (5.0 mL). The relevant aniline (1.2 eq.) and triethylamine (1.0 eq.) were added, the mixtures stirred for 15 min, allowed to stand overnight. The mixture was evaporated to dryness and dissolved in a 2-MeTHF and DCM mixture (1:1, 50 mL). The mixture was washed (2x sat. aq. NaHCO_3 [10 mL], 2x water [10 mL], 2x 2M HCl [10 mL], 1x brine [10 mL]), dried over MgSO_4 and evaporated *in vacuo* to dryness. The residues were purified by silica gel chromatography to give the *amide* product.

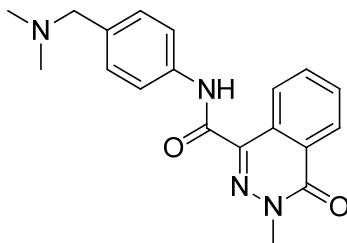
General Method B: Amide coupling using CDI. (5.056)

CDI (1.2 eq.) was added to a stirred solution of 3-methyl-4-oxo-3,4-dihydrophthalazine-1-carboxylic acid (1.0 eq.) in DMSO (5 mL). The resulting solution was stirred for 2 h, and the relevant aniline added (1.5 eq.). The resulting solution was stirred for 5 min and allowed to stand overnight. The reaction mixture was partitioned between ethyl acetate (50 mL) and sat. aq. NaHCO_3 (10 mL). The aqueous layer was removed and the organic layer washed (3x sat. aq. NaHCO_3 [10 mL], 1x brine [10 mL]), dried over MgSO_4 and evaporated *in vacuo* to dryness. The residue was purified by silica gel chromatography to give the *amide* product.

General Method C: Amide coupling using T3P®.

50% w/v T3P® in ethyl acetate (2.0 eq.) was added to stirred mixtures of DIPEA (3.3 eq.), 3-methyl-4-oxo-3,4-dihydrophthalazine-1-carboxylic acid (100 mg, 0.490 mmol) and the relevant amine (1.2 eq.) in DCM (5 mL). The resulting mixture was stirred for 45 min. The reaction mixtures were partitioned between sat. aq. NaHCO_3 (30 mL) and ethyl acetate (5 mL). The aqueous layer was removed and the organic layer washed (2x aq. NaHCO_3 [5 mL], 1x brine [5 mL]), dried over MgSO_4 and evaporated *in vacuo* to dryness. The residues were purified by silica gel chromatography.

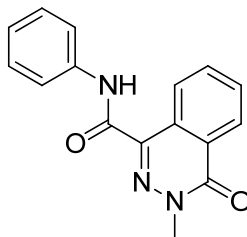
N-(4-((Dimethylamino)methyl)phenyl)-3-methyl-4-oxo-3,4-dihydrophthalazine-1-carboxamide (5.056)



Chemical Formula: C₁₉H₂₀N₄O₂
Molecular Weight: 336.39

Synthesised using general method B. The silica gel chromatography was eluted with DCM:2 M methanolic ammonia (0 -> 5%) to give the title compound **5.056** as a white solid (79 mg, 51%): ¹H NMR (SO(CD₃)₂, 400 MHz) δ 10.58 (s, 1H), 8.49 (d, *J* = 7.5 Hz, 1H), 8.35 (dd, *J* = 1.0, 8.0 Hz, 1H), 8.01 - 7.89 (m, 2H), 7.74 (d, *J* = 8.5 Hz, 2H), 7.30 (d, *J* = 8.5 Hz, 2H), 3.84 (s, 3H), 3.31 (s, 2H), 2.15 (s, 6H); LRMS [M+H]⁺: 337, 100% a/a.

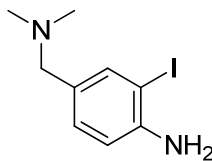
3-Methyl-4-oxo-*N*-phenyl-3,4-dihydrophthalazine-1-carboxamide (5.057)



Chemical Formula: C₁₆H₁₃N₃O₂
Molecular Weight: 279.29

Synthesised using general method A. The silica gel chromatography was eluted with cyclohexane:EtOAc (10 -> 50%) to give the title compound **5.057** as a white solid (53 mg, 26%): ¹H NMR (SO(CD₃)₂, 400 MHz) δ 10.63 (s, 1H) 8.49 (dd, *J* = 0.5, 8.0 Hz, 1H) 8.35 (dd, *J* = 1.0, 8.0 Hz, 1H) 7.89 - 8.03 (m, 2H) 7.80 (dd, *J* = 1.0, 8.5 Hz, 2H) 7.40 (app.t, *J* = 8.0 Hz, 2H) 7.16 (app.t, *J* = 7.5 Hz, 1H) 3.85 (s, 3H); LRMS [M+H]⁺: 280, 100% a/a.

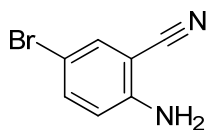
4-((Dimethylamino)methyl)-2-iodoaniline (5.058)²⁸⁷



Chemical Formula: C₉H₁₃IN₂
Molecular Weight: 276.12

Barluenga's reagent (0.996 g, 2.68 mmol) was added to a vigorously stirred suspension of 4-((dimethylamino)methyl)aniline, hydrochloride (0.500 g, 2.68 mmol) in DCM (7 mL) under N₂. The resulting suspension was stirred for 1 h, and sat. aq. NaHCO₃ (2 mL) and 10% w/v Na₂S₂O₃ (2 mL) added. The organic layer was removed, the aqueous layer was extracted (3x DCM [10 mL]), the organic layers combined, dried over MgSO₄ and evaporated *in vacuo* to a black oil. The residue was purified by silica gel chromatography eluting with DCM:2 M methanolic ammonia (0 -> 10%) to give the title compound **5.058** as a brown oil (275 mg, 37%): ¹H NMR (SO(CD₃)₂, 400 MHz) δ 7.59 (d, *J* = 2.0 Hz, 1H), 7.12 (dd, *J* = 2.0, 8.0 Hz, 1H), 6.71 (d, *J* = 8.0 Hz, 1H), 4.08 (br.s, 2H), 3.35 (s, 2H), 2.27 (s, 6H); LRMS [M+H]⁺: 277, 83% a/a.

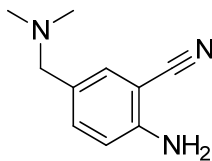
2-Amino-5-bromobenzonitrile (5.061)²⁹⁰



Chemical Formula: C₇H₅BrN₂
Molecular Weight: 197.03

NBS (753 mg, 4.23 mmol) dissolved in acetonitrile (7.5 mL) was added dropwise to a solution of 2-aminobenzonitrile (500 mg, 4.23 mmol) dissolved in acetonitrile (5 mL), stirring in an ice bath. The resulting solution was stirred for 1 h and evaporated to dryness over 2 days open to the atmosphere. The residue was purified by silica gel chromatography eluting with cyclohexane:DCM (5 -> 20%) to give the title compound **5.061** as a white solid (779 mg, 93%): ¹H NMR (SO(CD₃)₂, 400 MHz) δ 7.59 (d, *J* = 2.5 Hz, 1H), 7.42 (dd, *J* = 2.5, 9.0 Hz, 1H), 6.74 (d, *J* = 9.0 Hz, 1H), 6.25 (br.s, 2H); LRMS [M+H]⁺: 197 & 199, 96% a/a.

2-Amino-5-((dimethylamino)methyl)benzonitrile (5.059)²⁹¹

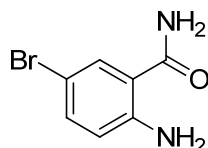


Chemical Formula: C₁₀H₁₃N₃

Molecular Weight: 175.23

XPhos (44 mg, 0.091 mmol) was added to a vacuum degassed suspension of 2-amino-5-bromobenzonitrile (300 mg, 1.52 mmol), potassium dimethylaminomethyltrifluoroborate (276 mg, 1.68 mmol), palladium(II) acetate (10 mg, 0.046 mmol) and cesium carbonate (1.49 mg, 4.57 mmol) in a mixture of CPME (5.5 mL) and water (0.550 mL). The resulting suspension was vacuum degassed and heated to 100 °C with stirring under nitrogen for 40 h. Further XPhos (44 mg, 0.091 mmol) added. The resulting suspension was heated to 95 °C for 5 h and palladium(II) acetate (10 mg, 0.046 mmol), potassium dimethylaminomethyltrifluoroborate (276 mg, 1.675 mmol) and cesium carbonate (1488 mg, 4.57 mmol) added. The reaction was heated at 95 °C over the weekend, and partitioned between water (10 mL) and ethyl acetate (40 mL). The aqueous layer was removed, the organic layer washed (2x aq. NaHCO₃ [5 mL], 1x brine [10 mL]), dried over MgSO₄ and evaporated *in vacuo* to an orange gum. The residue was purified on a preconditioned SCX cartridge eluting with MeOH followed by 2 M methanolic ammonia. The basic fractions were evaporated *in vacuo* to dryness and the residue purified by silica gel chromatography eluting with DCM:2 M methanolic ammonia (0 -> 5%) to give the title compound **5.059** as a brown gum (20 mg, 8%): ¹H NMR (SO(CD₃)₂, 400 MHz) δ 7.26 - 7.18 (m, 2H), 6.78 - 6.72 (m, 1H), 5.94 (br.s, 2H), 3.20 (s, 2H), 2.09 (s, 6H); LRMS [M+H]⁺: 176, 93% a/a.

2-Amino-5-bromobenzamide (5.065)²⁸⁷

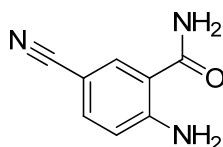


Chemical Formula: C₇H₇BrN₂O

Molecular Weight: 215.05

NBS (1.31 g, 7.34 mmol) dissolved in MeCN (15 mL) was added to an ice cold stirred solution of anthranilamide (1.00g, 7.34 mmol) in MeCN (10 mL) and warmed to 20 °C. The solution was stirred for 5 min, the resulting suspension warmed to room temperature, filtered, washed (1x MeCN [5 mL], 1x TBME [5 mL]) and dried *in vacuo* to give the title compound **5.065** as a pale grey solid (834 mg, 53%): ¹H NMR (CDCl₃, 400 MHz) δ 7.83 (br.s, 1H), 7.69 (d, *J* = 2.5 Hz, 1H), 7.24 (dd, *J* = 2.5, 9.0 Hz, 1H), 7.15 (br.s, 1H), 6.70 (br.s, 2H), 7.25 (d, *J* = 9.0 Hz, 1H); LRMS [M+H]⁺: 215 & 217, 100% a/a.

2-Amino-5-cyanobenzamide (5.066)¹⁵⁰

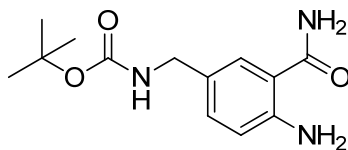


Chemical Formula: C₈H₇N₃O

Molecular Weight: 161.16

Zinc cyanide (1.64 g, 14.0 mmol) and Pd(PPh₃)₄ (1.08 g, 0.930 mmol) were added to a solution of 2-amino-5-bromobenzamide (2.00 g, 9.30 mmol) in DMF (10 mL). The mixture was heated to 150 °C under microwave conditions for 30 min. The mixture was filtered and the filtrate diluted with EtOAc (50 mL) washed with brine (3 x 50 mL), dried over Na₂SO₄ and evaporated *in vacuo*. The residue was purified by silica gel chromatography eluting with pet ether:EtOAc (0 -> 30%) to give the title compound **5.066** as a white solid (1.30 g, 87%): ¹H NMR (SO(CD₃)₂, 400 MHz) δ 8.00 (d, *J* = 1.5 Hz, 1H), 7.93 (br.s, 1H), 7.50 – 7.46 (m, 3H), 7.46 (br.s, 1H), 6.77 (d, *J* = 8.5 Hz, 1H); LRMS [M+H]⁺: 162, 100% a/a.

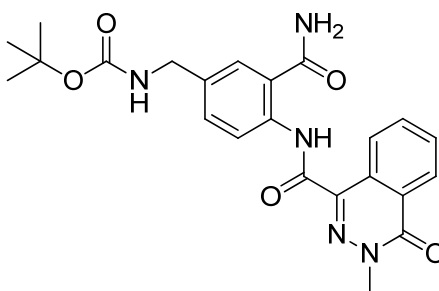
tert-Butyl 4-amino-3-carbamoylbenzylcarbamate (5.067)



Chemical Formula: C₁₃H₁₉N₃O₃
Molecular Weight: 265.31

NaBH₄ (1.88 g, 49.6 mmol) was added to a solution of 2-amino-5-cyanobenzamide (1.00 g, 6.20 mmol) and NiCl₂·6H₂O (1470 mg, 6.20 mmol) in MeOH (10 mL) at 0 °C over 30 min. Di-*tert*-butyl dicarbonate (1.35 g, 6.20 mmol) was added at 0 °C and stirred at 20 °C for 30 min. *N*¹-(2-Aminoethyl)ethane-1,2-diamine (0.640 g, 6.20 mmol) was added at 0 °C and stirred at 20 °C for 30 min. The mixture was diluted with aq. NH₄Cl (100 mL) and extracted (2x EtOAc [50 mL]). The combined organic phases were washed (2x brine [50 mL]), dried over Na₂SO₄, and evaporated *in vacuo* to dryness. The residue was purified by silica gel chromatography eluting with pet ether:EtOAc (0 → 60%) to obtain a crude product, which was washed with DCM (5 mL) to give the title compound **5.067** as a white solid (814 mg, 49%): ¹H NMR (CD₃OD, 400 MHz) δ 7.41 (s, 1H), 7.14 (dd, *J* = 2.5, 11.0 Hz, 1H), 6.72 (d, *J* = 11.0 Hz, 1H), 4.08 (s, 2H), 1.44 (s, 9H), exchangeable protons not seen; LRMS [M+H]⁺: 266, 99% a/a.

tert-Butyl 3-carbamoyl-4-(3-methyl-4-oxo-3,4-dihydrophthalazine-1-carboxamido)benzylcarbamate (5.068)

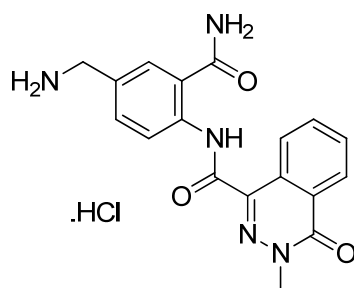


Chemical Formula: C₂₃H₂₅N₅O₅
Molecular Weight: 451.48

50% T3P[®] in ethyl acetate (312 mg, 0.980 mmol) was added to a stirred suspension of 3-methyl-4-oxo-3,4-dihydrophthalazine-1-carboxylic acid (100 mg, 0.490 mmol), *tert*-butyl 4-amino-3-carbamoylbenzylcarbamate (156 mg, 0.588 mmol) and DIPEA (0.28 mL, 1.6 mmol) in DCM (5 mL). The reaction mixture was stirred for 2 h and the resulting suspension

diluted with EtOAc (5 mL), filtered and the solid washed with EtOAc (5 mL) and dried *in vacuo* to give the title compound **5.068** as a white solid (170 mg, 77%): ^1H NMR ($\text{SO}(\text{CD}_3)_2$, 400 MHz) δ 13.01 (s, 1H), 9.06 (d, $J = 8.0$ Hz, 1H), 8.64 (d, $J = 8.5$ Hz, 1H), 8.34 (dd, $J = 1.0$, 8.0 Hz, 1H), 8.26 (br.s, 1H), 8.03 - 7.96 (m, 1H), 7.95 - 7.89 (m, 1H), 7.80 (br.s, 1H), 7.75 (d, $J = 1.5$ Hz, 1H), 7.45 (dd, $J = 1.5$, 8.5 Hz, 1H), 7.34 (t, $J = 5.5$ Hz, 1H), 4.16 (d, $J = 5.5$ Hz, 2H), 3.85 (s, 3H), 1.41 (s, 9H); LRMS $[\text{M}+\text{H}]^+$: 452, 100% a/a.

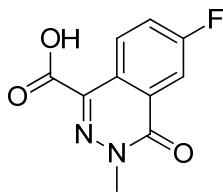
N-(4-(Aminomethyl)-2-carbamoylphenyl)-3-methyl-4-oxo-3,4-dihydrophthalazine-1-carboxamide, hydrochloride salt (**5.063**)



Chemical Formula: $\text{C}_{18}\text{H}_{17}\text{N}_5\text{O}_3 \cdot \text{HCl}$
Molecular Weight: 387.82

5 M HCl in IPA (5.0 mL, 25 mmol) was added to *tert*-butyl 3-carbamoyl-4-(3-methyl-4-oxo-3,4-dihydrophthalazine-1-carboxamido)benzylcarbamate (170 mg, 0.377 mmol) and the resulting suspension stirred for 3 h. The suspension was heated to 80 °C for 30 min, cooled to 20 °C and evaporated under a stream of nitrogen. The residue was stirred in TBME (3 mL) for 2 h and filtered. The resulting solid was washed (2x TBME [3 mL]) and dried *in vacuo* to give the title compound as the HCl salt of **5.063** as a white solid (127 mg, 87%): ^1H NMR ($\text{SO}(\text{CD}_3)_2$, 400 MHz) δ 13.13 (s, 1H), 9.08 (d, $J = 8.0$ Hz, 1H), 8.73 (d, $J = 8.5$ Hz, 1H), 8.41 (br.s, 3H), 8.35 (dd, $J = 1.0$, 8.0 Hz, 1H), 8.29 (br.s, 1H), 8.16 (d, $J = 2.0$ Hz, 1H), 8.04 - 7.89 (m, 3H), 7.69 (dd, $J = 2.0$, 8.5 Hz, 1H), 4.04 (q, $J = 5.0$ Hz, 2H), 3.86 (s, 3H); ^{13}C NMR ($\text{SO}(\text{CD}_3)_2$, 101 MHz) δ 170.8, 162.0, 159.3, 139.3, 135.5, 134.1, 133.3, 132.5, 130.7, 128.7, 128.1, 127.7, 127.1, 126.6, 120.6, 120.2, 42.4, 40.3; LRMS $[\text{M}+\text{H}]^+$: 352, 100% a/a; HRMS: $\text{C}_{18}\text{H}_{18}\text{N}_5\text{O}_3$ $[\text{M}]^+$ requires 352.1404, found $[\text{M}]^+$ 352.1416; IR: solid v 2990, 1670, 1638, 1591, 1527, 1389, 1355, 1306 cm^{-1} ; mp > 250 °C.

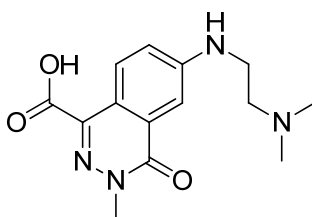
6-Fluoro-3-methyl-4-oxo-3,4-dihydrophthalazine-1-carboxylic acid (5.069)²⁷⁸



Chemical Formula: C₁₀H₇FN₂O₃
Molecular Weight: 222.17

Potassium permanganate (21.3 g, 135 mmol) was added portionwise over 45 min to an emulsion of 4'-fluoro-2'-methylacetophenone (4.88 g, 32.1 mmol) and potassium carbonate (2.77 g, 20.04 mmol) in water (150 mL) at 50 °C. The resulting mixture was heated to 70 °C overnight, ethanol (10 mL) added and the mixture cooled to room temperature. The suspension was filtered, the filtercake washed (1x water (10 mL) , 1x ethanol:water (1:1 [10 mL]), 1x water [10 mL]), partially evaporated *in vacuo* (20 min at 40 mbar), acidified with acetic acid (15 mL), methylhydrazine (2.18 mL, 41.7 mmol) added and the solution heated to 70 °C for 4 h. The solution was cooled in an ice bath, acidified with conc. HCl to pH 0 and the suspension filtered. The filtercake was washed [1x water (5 mL), 1x water:acetone (1:1, 5 mL), 1x acetone (5 mL)] and dried *in vacuo* at 40 °C to give the title compound **5.069** as a pale yellow solid (2.74 g, 39%): ¹H NMR (SO(CD₃)₂, 400 MHz) δ 13.72 (br.s, 1H), 8.70 (dd, *J* = 5.5, 9.0 Hz, 1H), 7.98 (dd, *J* = 3.0, 9.0 Hz, 1H), 7.86 (td, *J* = 3.0, 9.0 Hz, 1H), 3.79 (s, 3H); LRMS [M+H]⁺: 223, 98% a/a.

6-((2-(Dimethylamino)ethyl)amino)-3-methyl-4-oxo-3,4-dihydrophthalazine-1-carboxylic acid (5.071)²⁹²

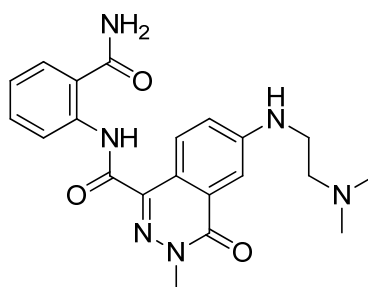


Chemical Formula: C₁₄H₁₈N₄O₃
Molecular Weight: 290.32

N,N-Dimethylethyleneamine (0.1 mL, 0.9 mmol) was added to a suspension of 6-fluoro-3-methyl-4-oxo-3,4-dihydrophthalazine-1-carboxylic acid (100 mg, 0.450 mmol) and potassium carbonate (156 mg, 1.13 mmol) in DMSO (2.5 mL). The resulting suspension was

stirred under microwave conditions at 150 °C for 1 h. The reaction mixture was stirred under microwave conditions at 200 °C for 1 h and stirred under microwave conditions at 150 °C for 8 h. The resulting mixture was dissolved in MeOH:Water (10 mL) and loaded on to a preconditioned SCX cartridge. The cartridge was eluted with MeOH followed by 2 M methanolic ammonia. The basic fractions were evaporated *in vacuo* to a brown gum, dissolved in MeOH and loaded on to a preconditioned aminopropyl cartridge. The column was eluted with MeOH, followed by acetic acid. The acetic acid fractions were evaporated *in vacuo* to give the title compound **5.071** as a pale brown solid (52mg, 40%): ¹H NMR (SO(CD₃)₂, 400 MHz) δ 8.07 (d, *J* = 9.0 Hz, 1H), 7.22 (d, *J* = 2.5 Hz, 1H), 7.13 (dd, *J* = 2.5, 9.0 Hz, 1H), 6.82 - 6.75 (m, 1H), 3.65 (s, 4H), 3.47 - 3.38 (m, 2H), 2.84 (t, *J* = 6.5 Hz, 2H), 1.91 (s, 6H); LRMS [M+H]⁺: 291, 99% a/a.

N-(2-Carbamoylphenyl)-6-((2-(dimethylamino)ethyl)amino)-3-methyl-4-oxo-3,4-dihydrophthalazine-1-carboxamide (5.054)

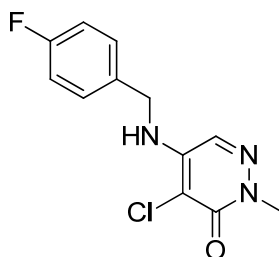


Chemical Formula: C₂₁H₂₄N₆O₃
Molecular Weight: 408.45

Synthesised using general method C. The silica gel chromatography was eluted with DCM:2 M methanolic ammonia (0 -> 6%) to give an impure product. The residue was purified by MDAP (HPH method B) to give the title compound **5.054** as a brown gum (2.2 mg, 3%): ¹H NMR (SO(CD₃)₂, 400 MHz) δ 13.02 (s, 1H), 8.77 - 8.66 (m, 2H), 8.28 (br.s, 1H), 7.85 (dd, *J* = 1.5, 8.0 Hz, 1H), 7.79 (br.s, 1H), 7.57 (ddd, *J* = 1.5, 7.5, 8.5 Hz, 1H), 7.28 - 7.22 (m, 2H), 7.19 (td, *J* = 1.0 Hz, 7.5 Hz, 1H), 6.84 (t, *J* = 5.5 Hz, 1H), 3.79 (s, 3H), 3.30 - 3.23 (m, 2H), 2.50 - 2.46 (peak obscured by DMSO), 2.21, (s, 6H); LRMS [M+H]⁺: 409, 88% a/a.

6.4.6 Aminopyridazinones

4-Chloro-5-((4-fluorobenzyl)amino)-2-methylpyridazin-3(2H)-one (5.028)²⁹⁵

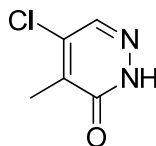


Chemical Formula: C₁₂H₁₁ClFN₃O

Molecular Weight: 267.69

4-Fluorobenzylamine (0.114 mL, 1.01 mmol) was added to a suspension of 4,5-dichloro-2-methyl-3(2H)-pyridazinone (0.15g, 0.838 mmol) in DIPEA (0.468 mL, 2.68 mmol) and DMSO (0.5 mL). The resulting suspension was heated to 130 °C for 1 h under microwave conditions. The reaction mixture was partitioned between water (10 mL) and DCM (10 mL). The organic layer was removed and the aqueous layer extracted [2x DCM (10 mL)]. The combined organic layers were dried over MgSO₄ and evaporated in vacuo to a brown solid. The residue was purified by silica gel chromatography eluting with cyclohexane:EtOAc (10 -> 80%) to give the title compound **5.028** as a white solid (129 mg, 57%): ¹H NMR (SO(CD₃)₂, 400 MHz) δ 7.72 (s, 1H), 7.37 (dd, *J* = 5.5, 8.5 Hz, 2H), 7.30 (t, *J* = 6.5 Hz, 1H), 7.21 - 7.14 (m, 2H), 4.55 (d, *J* = 6.5 Hz, 2H), 3.55 (s, 3H); ¹³C NMR (SO(CD₃)₂, 101 MHz) δ 161.3 (d, ¹*J*_{CF} = 244Hz), 156.7, 144.4, 135.2, 128.8 (d, ³*J*_{CF} = 8.0 Hz), 126.3, 115.3 (d, ²*J*_{CF} = 21 Hz), 105.2, 44.4, 39.4; LRMS [M+H]⁺: 268, 100% a/a; HRMS: C₁₂H₁₁ClFN₃O [M+H]⁺ requires 268.0647, found [M+H]⁺ 268.0643; IR: ν 3283, 1642, 1604, 1506, 1455, 1312, 1220 cm⁻¹; mp 211 - 213 °C.

5-Chloro-4-methylpyridazin-3(2H)-one (5.092)³⁰⁴

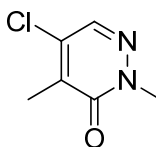


Chemical Formula: C₅H₅ClN₂O

Molecular Weight: 144.56

A solution of 3 M methylmagnesium bromide in diethyl ether (91.0 mL, 273 mmol) was added dropwise over 15 min to a stirred suspension of 4,5-dichloropyridazin-3(2H)-one (15 g, 91 mmol) in THF (300 mL) was cooled in an ice/water bath under N₂. The resulting solution was stirred for 10 min, warmed to 20 °C and stirred for 6 h. Sat. aq. NH₄Cl (150 mL) was added dropwise over 10 min. The reaction mixture was partitioned EtOAc (400 mL) and 2 M aq. hydrochloric acid (350 mL). The organic portions were removed, the aqueous portions extracted [EtOAc (2x 200 mL)] and the organic portions combined and evaporated *in vacuo*. The resulting dark orange solid was triturated with Et₂O (600 mL), filtered and the filtrate evaporated *in vacuo* to give the title compound **5.092** as an orange solid (10.20 g, 78%): ¹H NMR (CDCl₃, 400 MHz) δ 11.67 (br.s, 1H), 7.78 (s, 1H), 2.30 (s, 3H); LRMS [M+H]⁺: 145, 97% a/a.

5-Chloro-2,4-dimethylpyridazin-3(2H)-one (5.093)³⁰¹



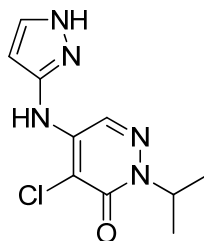
Chemical Formula: C₆H₇ClN₂O

Molecular Weight: 158.59

60% w/w Sodium hydride in mineral oil (0.899 g, 22.48 mmol) was added portionwise to a stirred solution of 5-chloro-4-methylpyridazin-3(2H)-one (2.5 g, 17 mmol) in DMF (60 mL) under N₂. The resulting purple suspension was stirred for 10 min and iodomethane (1.5 ml, 24 mmol) added dropwise over 1 min. The resulting solution was stirred for 2 h, quenched with sat. aq. NH₄Cl and 2 M aq. HCl (100 mL) added. The resulting green solution was extracted with EtOAc (3x 30 mL), the combined organic portions dried over MgSO₄ and evaporated *in vacuo* to a brown oil. The residue was purified by silica gel chromatography eluting with cyclohexane:EtOAc (0 -> 30%) to give an impure solid. The residue was purified

by silica gel chromatography eluting with DCM:MeOH (0 -> 2%) to give the title compound **5.093** as a white solid (640 mg, 23%): $^1\text{H NMR}$ ($\text{SO}(\text{CD}_3)_2$, 400 MHz) δ 7.98 (s, 1H), 3.64 (s, 3H), 2.15 (s, 3H); LRMS $[\text{M}+\text{H}]^+$: 159, 100% a/a.

5-((1H-Pyrazol-3-yl)amino)-4-chloro-2-isopropylpyridazin-3(2H)-one (5.101)²⁹⁵



Chemical Formula: $\text{C}_{10}\text{H}_{12}\text{ClN}_5\text{O}$

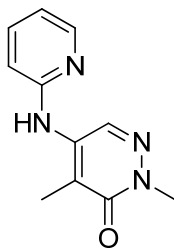
Molecular Weight: 253.69

4,5-Dichloro-2-isopropylpyridazin-3(2H)-one (100 mg, 0.483 mmol), DIPEA (200 mg, 1.545 mmol) and DIPEA (200 mg, 1.545 mmol) were suspended in DMSO (0.4 mL) and heated under microwave conditions at 120 °C for 4.5 h. The reaction mixture was purified by MDAP (HPH method B) to give an impure yellow solid which was purified by silica gel chromatography eluting with cyclohexane:EtOAc (40 -> 80%) to give the title compound **5.101** as a white solid (4 mg, 3%): $^1\text{H NMR}$ (CDCl_3 , 400 MHz) δ 9.90 (br.s, 1H), 8.83 - 8.52 (m, 1H), 7.56 (d, $J = 2.5$ Hz, 1H), 6.59 (br.s, 1H), 6.13 (d, $J = 2.5$ Hz, 1H), 5.32 (spt, $J = 6.5$ Hz, 1H), 1.35 (d, $J = 6.5$ Hz, 6H); LRMS: 254, 100% a/a.

Method used for the synthesis of 4-methyl substituted aminopyridazinones *General method E*³⁰⁵ (**5.109**, **5.127**, **5.131**, **5.140**)

5-Chloro-2,4-dimethylpyridazin-3(2H)-one (1.0 eq.), the amine (1.5 eq.), Brettphos palladacycle (0.1 eq.), Brettphos (0.1 eq.) and sodium *tert*-butoxide (1.2 eq.) in 1,4-Dioxane (0.16 M) were heated under microwave conditions at 100 °C for 1 h. The reaction mixture was cooled to 20 °C, diluted with water (20 mL) and extracted with DCM (3x 20 mL). The organic phases were dried over MgSO_4 , evaporated *in vacuo* to dryness and purified.

2,4-Dimethyl-5-(pyridin-2-ylamino)pyridazin-3(2H)-one (5.109)

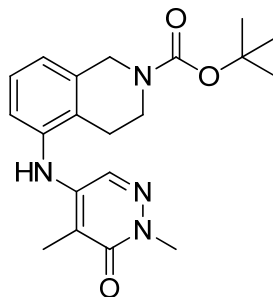


Chemical Formula: C₁₁H₁₂N₄O

Molecular Weight: 216.24

Synthesised using general method E. Heated for 30 min. Purified by MDAP (Formic method A) to give the title compound **5.109** as a white solid (51 mg, 37%): ¹H NMR (SO(CD₃)₂, 400 MHz) δ 8.71 (br.s, 1H), 8.49 (s, 1H), 8.17 (dd, *J* = 1.0, 5.0 Hz, 1H), 7.68 (ddd, *J* = 2.0, 7.5, 8.5 Hz, 1H), 7.06 (d, *J* = 8.5 Hz, 1H), 6.93 – 6.88 (m, 1H), 3.60 (s, 3H), 2.04 (s, 3H); LRMS [M+H]⁺: 217, 98% a/a.

tert-Butyl 5-((1,5-dimethyl-6-oxo-1,6-dihydropyridazin-4-yl)amino)-3,4-dihydroisoquinoline-2(1H)-carboxylate (5.107)

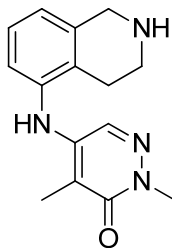


Chemical Formula: C₂₀H₂₆N₄O₃

Molecular Weight: 370.45

Synthesised using general method E. Purified by silica gel chromatography eluting with cyclohexane:EtOAc (50 -> 80%) to give the title compound **5.107** as a white solid (323 mg, 69%): ¹H NMR (CDCl₃, 400 MHz) δ 7.40 - 7.35 (m, 1H), (t, *J* = 8.0 Hz, 1H), 7.02 (app. d, *J* = 7.5 Hz, 2H), 5.30 (br.s, 1H), 4.61 (s, 2H), 3.73 (s, 3H), 3.66 (t, *J* = 6.0 Hz, 2H), 2.70 (t, *J* = 6.0 Hz, 2H), 2.12 (s, 3H), 1.49 (s, 9H); LRMS [M+H]⁺: 371, 100% a/a.

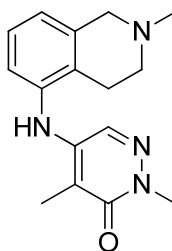
2,4-Dimethyl-5-((1,2,3,4-tetrahydroisoquinolin-5-yl)amino)pyridazin-3(2H)-one (5.105)



Chemical Formula: C₁₅H₁₈N₄O
Molecular Weight: 270.33

tert-Butyl 5-((1,5-dimethyl-6-oxo-1,6-dihydropyridazin-4-yl)amino)-3,4-dihydroisoquinoline-2(1H)-carboxylate (320 mg, 0.864 mmol) was stirred in a solution of 5 M HCl in IPA (5.00 mL, 25.0 mmol) at 20 °C for 3 h. The resulting solution was evaporated *in vacuo* to a brown solid and dissolved in THF:water (1:1). The solution was loaded on to a preconditioned SCX cartridge and eluted with MeOH, followed by 2 M methanolic ammonia. The basic fractions were evaporated *in vacuo* to give the title compound **5.105** as a pale brown solid (212 mg, 91%): ¹H NMR (CDCl₃, 400 MHz) δ 7.44 (s, 1H), 7.20 - 7.12 (m, 1H), 6.99 (d, *J* = 8.0 Hz, 1H), 6.93 (d, *J* = 8.0 Hz, 1H), 5.28 (br.s, 1H), 4.05 (s, 2H), 3.73 (s, 3H), 3.17 (t, *J* = 6.0 Hz, 2H), 2.62 (t, *J* = 6.0 Hz, 2H), 2.12 (s, 3H); LRMS [M+H]⁺: 271, 100% a/a.

2,4-Dimethyl-5-((2-methyl-1,2,3,4-tetrahydroisoquinolin-5-yl)amino)pyridazin-3(2H)-one (5.121)³⁰⁹

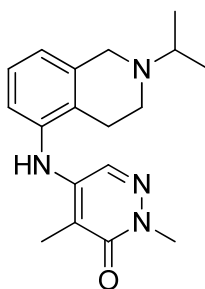


Chemical Formula: C₁₆H₂₀N₄O
Molecular Weight: 284.36

A solution of 37% formaldehyde in water with 10-15 % methanol (15 μL, 0.20 mmol) and formic acid (30 μL, 0.78 mmol) were added to 2,4-dimethyl-5-((1,2,3,4-tetrahydroisoquinolin-5-yl)amino)pyridazin-3(2H)-one (50 mg, 0.19 mmol) in a sealed tube and heated to 80 °C in an oven for 24 h. The solution was cooled to room temperature and diluted with MeOH (1 mL). The solution was loaded on to a 2 g SCX cartridge and eluted with MeOH (10 mL), followed by 2 M methanolic ammonia (10 mL). The basic fractions

were evaporated *in vacuo* to give the title compound **5.121** as an almost white solid (45 mg, 85%): ^1H NMR (CDCl_3 , 400 MHz) δ 7.43 (s, 1H), 7.18 (dd, $J = 7.5, 8.0$ Hz, 1H), 7.00 (d, $J = 8.0$ Hz, 1H), 6.96 ($J = 7.5$ Hz, 1H), 5.31 (s, 1H), 3.74 (s, 3H), 3.62 (s, 2H), 2.81 – 2.68 (m, 4H), 2.49 (s, 3H), 2.13 (s, 3H); ^{13}C NMR (CDCl_3 , 101 MHz): 161.8, 142.8, 137.1, 137.0, 128.9, 128.6, 126.6, 124.2, 122.2, 112.8, 58.0, 52.5, 46.0, 39.9, 25.5, 9.1; LRMS $[\text{M}+\text{H}]^+$: 285, 100% a/a; HRMS: $\text{C}_{16}\text{H}_{21}\text{N}_4\text{O}$ $[\text{M}+\text{H}]^+$ requires 285.1340, found $[\text{M}+\text{H}]^+$ 285.1345; IR: solid v 3226, 1583, 1428, 1397, 1315, 1128 cm^{-1} ; mp 211 – 216 $^\circ\text{C}$.

5-((2-Isopropyl-1,2,3,4-tetrahydroisoquinolin-5-yl)amino)-2,4-dimethylpyridazin-3(2H)-one
(5.122)³¹⁰

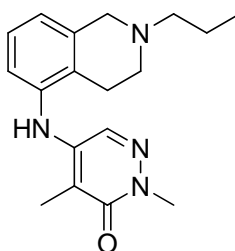


Chemical Formula: $\text{C}_{18}\text{H}_{24}\text{N}_4\text{O}$
Molecular Weight: 312.41

Sodium triacetoxyborohydride (78.0 mg, 0.370 mmol) was added to a stirred suspension of 2,4-dimethyl-5-((1,2,3,4-tetrahydroisoquinolin-5-yl)amino)pyridazin-3(2H)-one (50.0 mg, 0.185 mmol), acetic acid (0.012 mL, 0.20 mmol) and acetone (0.027 mL, 0.37 mmol) in DCM (4 mL). The resulting suspension was stirred overnight. Further acetone (0.027 mL, 0.37 mmol) and sodium triacetoxyborohydride (78 mg, 0.370 mmol) were added and the resulting suspension stirred for 4 h. The reaction mixture was quenched with water (2 mL) and MeOH (3 mL). The resulting solution was loaded on to a preconditioned SCX cartridge and eluted with MeOH (20 mL), followed by 2 M methanolic ammonia (20 mL). The basic fractions were evaporated *in vacuo* to give the title compound **5.122** as a white solid (48 mg, 87%): ^1H NMR ($\text{SO}(\text{CD}_3)_2$, 400 MHz) δ 7.59 (s, 1H), 7.19 - 7.11 (m, 2H), 6.98 (d, $J = 7.5$ Hz, 1H), 6.92 (d, $J = 8.0$ Hz, 1H), 3.66 (s, 2H), 3.54 (s, 3H), 2.84 (spt, $J = 6.5$ Hz, 1H), 2.72 - 2.58 (m, 4H), 1.93 (s, 3H), 1.05 (d, $J = 6.5$ Hz, 6H); LRMS $[\text{M}+\text{H}]^+$: 313, 100% a/a.

2,4-Dimethyl-5-((2-propyl-1,2,3,4-tetrahydroisoquinolin-5-yl)amino)pyridazin-3(2H)-one

(5.123)³¹⁰



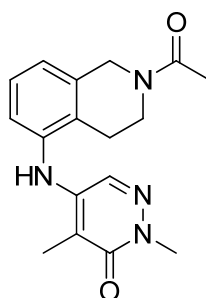
Chemical Formula: C₁₈H₂₄N₄O

Molecular Weight: 312.41

Sodium triacetoxyborohydride (78 mg, 0.37 mmol) was added to a stirred suspension of 2,4-dimethyl-5-((1,2,3,4-tetrahydroisoquinolin-5-yl)amino)pyridazin-3(2H)-one (50.0 mg, 0.185 mmol), acetic acid (0.012 mL, 0.20 mmol) and propionaldehyde (0.027 mL, 0.37 mmol) in DCM (4 mL). The resulting solution was stirred for 30 min and sat. aq. NaHCO₃ (5 mL) was added to the reaction mixture. The resulting biphasic mixture was extracted with EtOAc (10 mL). The organic portion was washed [1x sat. aq. NaHCO₃ (2 mL) , 1x brine (2 mL)], dried over MgSO₄ and evaporated *in vacuo* to dryness. The residue was purified by silica gel chromatography eluting with DCM:2 M methanolic ammonia (0 -> 5%) to give the title compound **5.123** as a white solid (34 mg, 59%): ¹H NMR (SO(CD₃)₂, 400 MHz) δ 7.58 (s, 1H), 7.19 - 7.13 (m, 2H), 6.97 (d, *J* = 7.5 Hz, 1H), 6.93 (d, *J* = 8.0 Hz, 1H), 3.55 (s, 2H), 3.54 (s, 3H), 2.69 - 2.58 (m, 2H), 2.43 - 2.36 (m, 2H), 1.93 (s, 3H), 1.54 (app.sxt, *J* = 7.5 Hz, 2H), 0.89 (t, *J* = 7.5 Hz, 3H); LRMS [M+H]⁺: 313, 97% a/a.

5-((2-acetyl-1,2,3,4-tetrahydroisoquinolin-5-yl)amino)-2,4-dimethylpyridazin-3(2H)-one

(5.124)³¹¹

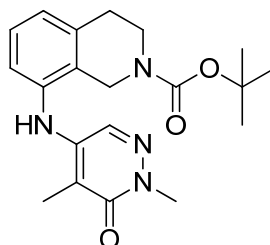


Chemical Formula: C₁₇H₂₀N₄O₂

Molecular Weight: 312.37

Acetic anhydride (0.021 mL, 0.22 mmol) was added to a stirred suspension of 2,4-dimethyl-5-((1,2,3,4-tetrahydroisoquinolin-5-yl)amino)pyridazin-3(2H)-one (50.0 mg, 0.185 mmol) in acetonitrile (1 mL). The resulting suspension was stirred for 1 h and partitioned between EtOAc (10 mL) and aq. NaHCO₃ (2 mL). The aqueous layer was separated, the organic layer washed [1x aq sat. NaHCO₃ (2 mL), 1x brine (2 mL)], dried over MgSO₄ and evaporated *in vacuo* to a white foam. The residue was purified by silica gel chromatography eluting with DCM:MeOH (0 -> 5%) to give the title compound **5.124** as a white solid (40 mg, 69%): ¹H NMR (SO(CD₃)₂, 400 MHz) δ 7.29 (br.s, 1H), 7.20 (app.t, *J* = 7.5 Hz, 1H), 7.17 (s, 1H), 7.05 (d, *J* = 7.5 Hz, 1H), 6.95 (d, *J* = 7.5 Hz, 1H), 4.62 (s, 2H), 3.64 (t, *J* = 6.0 Hz, 2H), 2.71 (t, *J* = 6.0 Hz, 2H), 2.05 (s, 3H), 1.94 (s, 3H); LRMS [M+H]⁺: 313, 100% a/a.

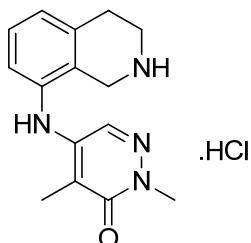
tert-Butyl 8-((1,5-dimethyl-6-oxo-1,6-dihydropyridazin-4-yl)amino)-3,4-dihydroisoquinoline-2(1H)-carboxylate (**5.127**)



Chemical Formula: C₂₀H₂₆N₄O₃
Molecular Weight: 370.45

Synthesised using general method E. Purified by silica gel chromatography eluting with cyclohexane:EtOAc (0 -> 80%) to give the title compound **5.127** as a brown solid (135 mg, 58%): ¹H NMR (SO(CD₃)₂, 400 MHz) δ 7.71 (s, 1H), 7.28 – 7.20 (m, 1H), 7.17 (s, 1H), 7.09 (d, *J* = 7.0 Hz, 1H), 6.99 (d, *J* = 7.0 Hz, 1H), 4.40 (s, 2H), 3.61 – 3.48 (m, 5H), 1.95 (s, 3H), 1.39 (s, 9H); LRMS [M+H]⁺: 371, 100% a/a.

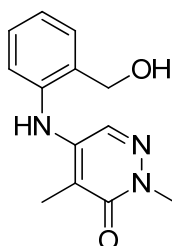
2,4-Dimethyl-5-((1,2,3,4-tetrahydroisoquinolin-8-yl)amino)pyridazin-3(2H)-one, hydrochloride salt (5.125)



Chemical Formula: C₁₅H₁₈N₄O .HCl
Molecular Weight: 306.79

tert-Butyl 8-((1,5-dimethyl-6-oxo-1,6-dihydropyridazin-4-yl)amino)-3,4-dihydroisoquinoline-2(1*H*)-carboxylate (128 mg, 0.346 mmol) was added to a solution of 5 M HCl in IPA (2.00 mL, 10.0 mmol) and stirred at 20 °C overnight. The reaction mixture was evaporated *in vacuo* to give the hydrochloride salt of the title compound **5.125** as a brown solid (102 mg, 96%): ¹H NMR (SO(CD₃)₂, 400 MHz) δ 9.57 (br.s, 2H), 7.81 (s, 1H), 7.37 - 7.22 (m, 2H), 7.10 (d, *J* = 7.5 Hz, 1H), 6.99 (d, *J* = 7.5 Hz, 1H), 3.56 (s, 3H), 3.40 - 3.26 (m, 2H), 3.11 - 2.98 (m, 2H), 1.94 (s, 3H); ¹³C NMR (SO(CD₃)₂, 101 MHz) δ 161.4 143.5, 137.9, 134.3, 129.8, 128.3, 126.2, 125.2, 123.7, 113.3, 41.2, 25.3, 10.9 (some peaks obscured by DMSO); LRMS [M+H]⁺: 271, 100% a/a; HRMS: C₁₅H₁₉N₄O [M]⁺ requires 271.1534, found [M]⁺ 271.1533; IR: solid v 3282, 2746, 1594, 1581, 1429, 1396, 1276, 1181 cm⁻¹; mp > 250 °C.

5-((2-(hydroxymethyl)phenyl)amino)-2,4-dimethylpyridazin-3(2H)-one (5.131)

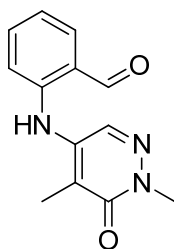


Chemical Formula: C₁₃H₁₅N₃O₂
Molecular Weight: 245.28

Synthesised by general method E. Purified by silica gel chromatography eluting with DCM:2 M methanolic ammonia (0 -> 10%) to give the title compound **5.131** as a brown gum (61 mg, 40%): ¹H NMR (SO(CD₃)₂, 400 MHz) δ 7.71 (br.s, 1H), 7.47 (dd, *J* = 1.0, 7.5 Hz, 1H), 7.37

(s, 1H), 7.32 – 7.26 (m, 1H), 7.22 – 7.16 (m, 1H), 7.12 (dd, $J = 1.0, 8.0$ Hz), 5.35 (t, $J = 5.0$ Hz, 1H), 4.52 (d, $J = 5.0$ Hz, 2H), 3.56 (s, 3H), 1.94 (s, 3H); LRMS: $[M+H]^+$: 246, 100% a/a.

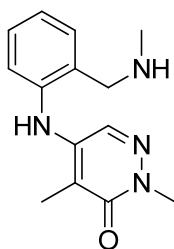
2-((1,5-Dimethyl-6-oxo-1,6-dihydropyridazin-4-yl)amino)benzaldehyde (5.132)³¹³



Chemical Formula: $C_{13}H_{13}N_3O_2$
Molecular Weight: 243.26

Manganese dioxide (256 mg, 2.50 mmol) was added to a solution of 5-((2-(hydroxymethyl)phenyl)amino)-2,4-dimethylpyridazin-3(2H)-one (61 mg, 0.25 mmol) in acetone (25 mL). The reaction was heated to reflux stirred overnight and filtered through celite and concentrated *in vacuo*. The residue purified by silica gel chromatography eluting with cyclohexane:EtOAc (10 → 60%) to give the title compound **5.132** as a yellow solid (45 mg, 73%): 1H NMR ($SO(CD_3)_2$, 400 MHz) δ 10.04 (s, 1H), 9.47 (br.s, 1H), 7.94 (s, 1H), 7.86 (dd, $J = 1.5, 7.5$ Hz, 1H), 7.62 - 7.56 (m, 1H), 7.19 - 7.10 (m, 2H), 3.64 (s, 3H), 2.01 (s, 3H); LRMS $[M+H]^+$: 244, 100% a/a.

2,4-dimethyl-5-((2-((methylamino)methyl)phenyl)amino)pyridazin-3(2H)-one (5.133)³¹⁴

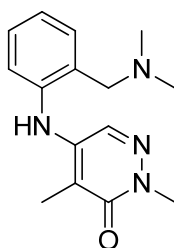


Chemical Formula: $C_{14}H_{18}N_4O$
Molecular Weight: 258.32

Sodium triacetoxyborohydride (434 mg, 2.05 mmol) was added to a solution of 2-((1,5-dimethyl-6-oxo-1,6-dihydropyridazin-4-yl)amino)benzaldehyde (83 mg, 0.34 mmol) methylamine hydrochloride (46 mg, 0.68 mmol) and acetic acid (2 μ L, 0.04 mmol) in DCM (5 mL). The reaction mixture was stirred at 20 °C for 3 h. Methylamine 33% w/v in ethanol (85 μ L, 0.68 mmol) was added, the reaction mixture was stirred under N_2 overnight. The

reaction mixture was diluted with EtOAc (20 mL), washed [1x sat. aq. NaHCO₃ (10 mL)], the aqueous portion was extracted with [2x EtOAc (10 mL)] and the combined organic layers were dried over MgSO₄ and evaporated *in vacuo*. The residue was purified by silica gel chromatography eluted with DCM: 2 M methanolic ammonia (0 -> 7.5%) to give the title compound **5.133** as a white solid (39 mg, 44%): ¹H NMR (SO(CD₃)₂, 400 MHz) δ 9.35 (br.s, 1H), 7.77 (s, 1H), 7.32 - 7.23 (m, 2H), 7.20 - 7.14 (m, 1H), 7.02 (app.td, *J* = 1.0, 7.5 Hz, 1H), 3.71 (s, 2H), 3.59 (s, 3H), 2.29 (s, 3H), 1.96 (s, 3H); LRMS [M+H]⁺: 259, 100% a/a.

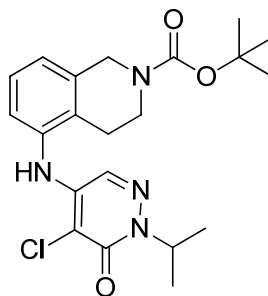
5-((2-((dimethylamino)methyl)phenyl)amino)-2,4-dimethylpyridazin-3(2H)-one (5.134)³¹⁴



Chemical Formula: C₁₅H₂₀N₄O
Molecular Weight: 272.35

Sodium triacetoxyborohydride (233 mg, 1.10 mmol) was added to a mixture of 2-((1,5-dimethyl-6-oxo-1,6-dihydropyridazin-4-yl)amino)benzaldehyde (45 mg, 0.18 mmol), dimethylamine hydrochloride (30 mg, 0.37 mmol) and acetic acid (1 μL, 0.02 mmol) in DCM (5 mL). The reaction mixture was stirred under N₂ 2.5 h and further dimethylamine hydrochloride (30 mg, 0.37 mmol) added. The reaction mixture was stirred for 30min and sodium triacetoxyborohydride (233 mg, 1.10 mmol) was added. The reaction was stirred for 2 h and 2 M dimethylamine solution in THF (0.2 mL, 0.4 mmol) was added and the reaction was stirred for 30 min. Further sodium triacetoxyborohydride (233 mg, 1.10 mmol) was added, the reaction mixture was stirred for 3.5 h and concentrated *in vacuo*, loaded on to a preconditioned SCX cartridge and eluted with MeOH (20 mL) followed by 2 M methanolic ammonia (20 mL). The basic fractions were concentrated *in vacuo* and the white residue purified by silica gel chromatography eluting with DCM: 2 M methanolic ammonia (0 -> 5%) to give the title compound **5.134** as a white solid (4 mg, 8%): ¹H NMR (SO(CD₃)₂, 400 MHz) δ 9.21 (br.s, 1H), 7.84 (s, 1H), 7.33 - 7.23 (m, 2H), 7.23 - 7.17 (m, 1H), 7.02 (app.td, *J* = 1.0, 7.5 Hz, 1H), 3.59 (s, 3H), 3.49 (s, 2H), 2.20 (s, 6H), 1.96 (s, 3H); LRMS [M+H]⁺: 273, 100% a/a.

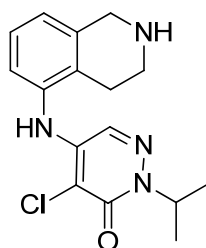
tert-Butyl 5-((5-chloro-1-isopropyl-6-oxo-1,6-dihydropyridazin-4-yl)amino)-3,4-dihydroisoquinoline-2(1H)-carboxylate (5.140)



Chemical Formula: C₂₁H₂₇ClN₄O₃
Molecular Weight: 418.92

Synthesised using general method E. Purified by MDAP (Formic method D) to give the title compound **5.140** as a white solid (10 mg, 7%): ¹H NMR (SO(CD₃)₂, 400 MHz) δ 8.33 (s, 1H), 7.31 – 7.24 (m, 2H), 7.21 – 7.12 (m, 2H), 5.09 (spt, *J* = 6.5 Hz, 1H), 4.55 (s, 2H), 3.53 (t, *J* = 6.0 Hz, 2H), 2.66 (t, *J* = 6.0 Hz, 2H), 1.43 (s, 9H), 1.22 (d, *J* = 6.5 Hz, 6H); LRMS [M+H]⁺: 419, 100%, a/a.

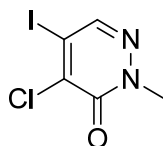
4-Chloro-2-isopropyl-5-((1,2,3,4-tetrahydroisoquinolin-5-yl)amino)pyridazin-3(2H)-one (5.141)



Chemical Formula: C₁₆H₁₉ClN₄O
Molecular Weight: 318.80

tert-Butyl 5-((5-chloro-1-isopropyl-6-oxo-1,6-dihydropyridazin-4-yl)amino)-3,4-dihydroisoquinoline-2(1H)-carboxylate (10 mg, 0.024 mmol) was stirred in a 5 M solution of HCl in IPA (5.0 mL, 25 mmol) at 20 °C for 1.5 h. The volatiles were removed *in vacuo* and the residue was purified on a preconditioned SCX cartridge eluting with MeOH (20 mL) followed by 2 M methanolic ammonia (20 mL) to give the title compound **5.141** as a white solid (6.6 mg, 87%). ¹H NMR (SO(CD₃)₂, 400 MHz) δ 8.30 (s, 1H), 7.25 - 7.17 (m, 2H), 7.12 - 7.03 (m, 2H), 6.60 (spt, *J* = 6.5 Hz, 1H), 3.94 (s, 2H), 2.98 (t, *J* = 6.0 Hz, 2H), 2.57 (t, *J* = 6.0 Hz, 2H), 1.22 (d, *J* = 6.5 Hz, 6H); LRMS [M+H]⁺: 319, 100%, a/a.

4-Chloro-5-iodo-2-methylpyridazin-3(2H)-one (5.147)³²⁰

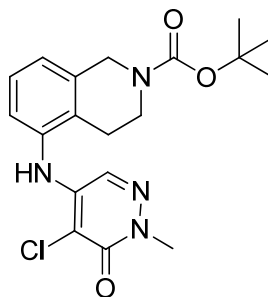


Chemical Formula: C₅H₄ClIN₂O

Molecular Weight: 270.46

Sodium iodide (3.00 g, 20.0 mmol) was added to a stirred solution of 4,5-dichloro-2-methylpyridazin-3(2H)-one (1.79 g, 10.0 mmol) in DMF (20 mL) under N₂. The reaction mixture was heated to 150 °C for 24 h. Further sodium iodide (3.00 g, 20.0 mmol) was added and the reaction mixture stirred overnight. The resulting solution was slurried with water (20 mL), filtered and washed [2x water (5 mL), 1x TBME (4 mL)]. The solid was dried *in vacuo* to give the title compound **5.147** as a pale brown solid (1.528 g, 56%): ¹H NMR (SO(CD₃)₂, 400 MHz) δ 8.22 (s, 1H), 3.65 (s, 3H); LRMS [M+H]⁺: 271, 86% a/a.

tert-Butyl 5-((5-chloro-1-methyl-6-oxo-1,6-dihydropyridazin-4-yl)amino)-3,4-dihydroisoquinoline-2(1H)-carboxylate (5.143a)³¹⁸



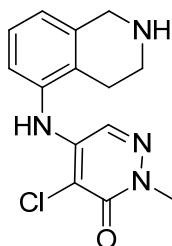
Chemical Formula: C₁₉H₂₃ClN₄O₃

Molecular Weight: 390.86

tert-Butyl 5-amino-3,4-dihydroisoquinoline-2(1H)-carboxylate (92 mg, 0.370 mmol), 4-chloro-5-iodo-2-methylpyridazin-3(2H)-one (100 mg, 0.370 mmol), palladium(II) acetate (11 mg, 0.048 mmol), cesium carbonate (205 mg, 0.629 mmol) and BINAP (41 mg, 0.067 mmol) were suspended in toluene (3 mL). The suspension was heated under microwave conditions at 80 °C for 16 h. The resulting black solution was diluted with toluene (20 mL), washed [2x water (10 mL), 1x brine (5 mL)], dried over MgSO₄ and evaporated *in vacuo* to dryness. The residue was purified by MDAP (Formic method C) to give the title compound **5.143a** as white solid (96 mg, 66%): ¹H NMR (SO(CD₃)₂, 400 MHz) δ 8.33 (s, 1H), 7.30 - 7.23

(m, 1H), 7.21 - 7.25 (m, 2H), 7.13 (d, $J = 7.5$ Hz, 1H), 4.54 (s, 2H), 3.59 (s, 3H), 3.52 (t, $J = 5.5$ Hz, 2H), 2.64 (t, $J = 5.5$ Hz, 2H), 1.42 (s, 9H); LRMS $[M+H]^+$: 391, 100% a/a.

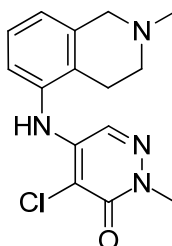
4-Chloro-2-methyl-5-((1,2,3,4-tetrahydroisoquinolin-5-yl)amino)pyridazin-3(2H)-one (5.143)



Chemical Formula: $C_{14}H_{15}ClN_4O$
Molecular Weight: 290.75

tert-Butyl 5-((5-chloro-1-methyl-6-oxo-1,6-dihydropyridazin-4-yl)amino)-3,4-dihydroisoquinoline-2(1H)-carboxylate (16 mg, 0.041 mmol) was stirred in a 5 M solution of HCl in IPA (2.0 mL, 10 mmol) for 2 h. The reaction mixture was evaporated *in vacuo* to dryness and purified on to a 2 g SCX cartridge eluting with MeOH followed by 2 M methanolic ammonia to give unsubstituted the title compound **5.143** as a brown solid (6.4 mg, 54%): 1H NMR ($SO(CD_3)_2$, 400 MHz) δ 8.29 (s, 1H), 7.24 - 7.17 (m, 1H), 7.11 (s, 1H), 7.08 - 7.01 (m, 2H), 3.89 (s, 2H), 3.58 (s, 3H), 2.92 (t, $J = 6.0$ Hz, 2H), 2.53 (peak obscured by DMSO); LRMS $[M+H]^+$: 291, 99% a/a.

4-Chloro-2-methyl-5-((2-methyl-1,2,3,4-tetrahydroisoquinolin-5-yl)amino)pyridazin-3(2H)-one (5.144)³¹⁸

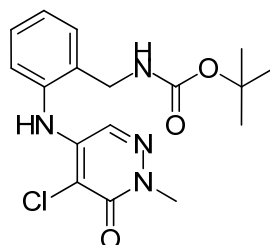


Chemical Formula: $C_{15}H_{17}ClN_4O$
Molecular Weight: 304.77

2-methyl-1,2,3,4-tetrahydroisoquinolin-5-amine (70 mg, 0.43 mmol), 4-chloro-5-iodo-2-methylpyridazin-3(2H)-one (117 mg, 0.431 mmol), palladium (II) acetate (11 mg, 0.048 mmol), cesium carbonate (205 mg, 0.629 mmol) and BINAP (41 mg, 0.067 mmol) were suspended in toluene (3 mL) and heated to 80 °C under microwave conditions for 4 h. The

reaction mixture was partitioned between EtOAc (10 mL) and water (3 mL) and the aqueous layer removed. The organic layer was washed (1x water [3 mL], 1x brine [3 mL]), dried over MgSO₄ and evaporated *in vacuo* to a brown gum. The residue was purified by MDAP (HPH method B) to give the title compound **5.144** as a white solid (19 mg, 14%): ¹H NMR (SO(CD₃)₂, 400 MHz) δ 8.29 (br.s, 1H), 7.22 (app.t, *J* = 8.0 Hz, 1H), 7.12 (s, 1H), 7.10 - 7.05 (m, 2H), 3.59 (s, 3H), 3.52 (s, 2H), 2.66 (t, *J* = 5.5 Hz, 2H), 2.56 (t, *J* = 5.5 Hz, 2H), 2.33 (s, 3H); ¹³C NMR (CDCl₃)₂, 101 MHz) δ 157.8, 142.6, 137.4, 135.4, 130.4, 126.8, 126.7, 125.7, 123.8, 109.3, 57.9, 52.4, 45.9, 40.3, 25.6; LRMS [M+H]⁺: 305, 100% a/a; HRMS: C₁₅H₁₈ClN₄O [M+H]⁺ requires 305.1162, found [M+H]⁺ 305.1164; IR: solid v 2789, 1635, 1610, 1334, 1301, 1127 cm⁻¹; mp 167 - 171 °C.

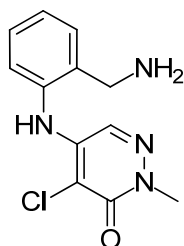
tert-Butyl 2-((5-chloro-1-methyl-6-oxo-1,6-dihydropyridazin-4-yl)amino)benzylcarbamate
(5.148)³¹⁸



Chemical Formula: C₁₇H₂₁ClN₄O₃
Molecular Weight: 364.83

tert-Butyl 2-aminobenzylcarbamate (99 mg, 0.44 mmol), 4-chloro-5-iodo-2-methylpyridazin-3(2*H*)-one (100 mg, 0.370 mmol), palladium (II) acetate (11 mg, 0.048 mmol), cesium carbonate (205 mg, 0.629 mmol) and BINAP (41 mg, 0.067 mmol) were suspended in toluene (3 mL) and heated to 80 °C under microwave conditions for 4 h. The reaction mixture was partitioned between EtOAc (10 mL) and water (3 mL) and the aqueous layer removed. The organic layer was washed (1x water [3 mL], 1x brine [3 mL]), dried over MgSO₄ and evaporated *in vacuo* to a brown gum. The residue was purified by silica gel chromatography eluting with cyclohexane:EtOAc (10 -> 50%) to give the title compound **5.148** as a pale brown solid (19 mg, 14%): ¹H NMR (SO(CD₃)₂, 400 MHz) δ 8.50 (br.s, 1H), 7.42 - 7.29 (m, 4H), 7.28 - 7.17 (m, 2H), 4.11 (d, *J* = 6.0 Hz, 2H), 3.59 (s, 3H), 1.35 (s, 9H); LRMS [M+H]⁺: 365, 99% a/a.

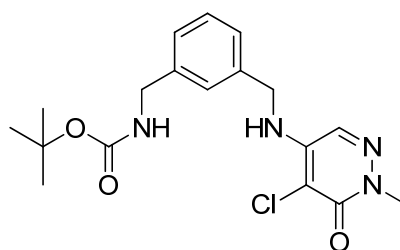
5-((2-(aminomethyl)phenyl)amino)-4-chloro-2-methylpyridazin-3(2H)-one, hydrochloride salt (5.145)



Chemical Formula: C₁₂H₁₃ClN₄O .HCl
Molecular Weight: 301.17

A solution of 5 M HCl in IPA (3.00 mL, 15.0 mmol) was added to *tert*-butyl 2-((5-chloro-1-methyl-6-oxo-1,6-dihydropyridazin-4-yl)amino)benzylcarbamate (42 mg, 0.115 mmol) and the suspension stirred for 2 h. The resulting solution was evaporated to dryness, triturated with TBME (2 mL), filtered, the solid washed (1x TBME [2 mL]) and dried *in vacuo* to give the title compound **5.145** as a pale brown solid (28 mg, 81%): ¹H NMR (SO(CD₃)₂, 400 MHz) δ 8.48 (s, 1H), 8.31 (br.s, 3H), 7.63 (d, *J* = 7.5 Hz, 1H), 7.52 – 7.38 (m, 2H), 7.34 (d, *J* = 7.5 Hz, 1H), 7.27 (s, 1H), 4.05 (s, 2H), 3.61 (s, 3H), ¹³C NMR (SO(CD₃)₂, 101 MHz) δ 157.5, 143.9, 137.6, 131.4, 131.3, 130.3, 128.3, 128.2, 127.6, 108.5, 38.6 (peak obscured by DMSO); LRMS [M+H]⁺: 265, 99% a/a; HRMS: C₁₂H₁₄ClN₄O [M]⁺ requires 265.0851, found [M]⁺ 265.8052; IR: solid v 3226, 2860, 1600, 1578, 1494, 1390, 1315 cm⁻¹; mp > 250 °C.

tert-Butyl 3-(((5-chloro-1-methyl-6-oxo-1,6-dihydropyridazin-4-yl)amino)methyl)benzylcarbamate (5.150)²⁹⁵

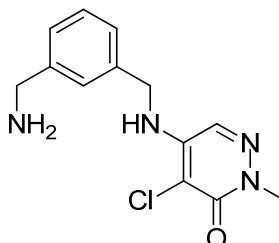


Chemical Formula: C₁₈H₂₃ClN₄O₃
Molecular Weight: 378.85

4,5-Dichloro-2-methyl-3(2H)-pyridazinone (100 mg, 0.559 mmol), DIPEA (0.31 mL, 1.8 mmol) and 1-(*N*-Boc-aminomethyl)-3-(aminomethyl)benzene (0.171 mL, 0.766 mmol) were heated to 120 °C for 45 min. The reaction mixture was diluted with MeOH (1 mL) to give a

homogenous solution and purified by MDAP (Formic method C) to give the title compound **5.150** as a white solid (126 mg, 60%): $^1\text{H NMR}$ ($\text{SO}(\text{CD}_3)_2$, 400 MHz) δ 7.60 (s, 1H), 7.31 - 7.23 (m, 1H), 7.22 (s, 1H), 7.19 - 7.12 (m, 2H), 6.83 - 6.61 (m, 2H), 4.55 (d, $J = 6.5$ Hz, 2H), 4.12 (d, $J = 6.5$ Hz, 2H), 3.55 (s, 3H), 1.37 (s, 9H); LRMS $[\text{M}+\text{H}]^+$: 379, 100% a/a.

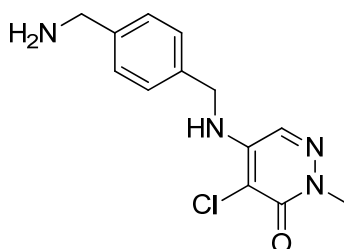
5-((3-(Aminomethyl)benzyl)amino)-4-chloro-2-methylpyridazin-3(2H)-one (5.149)



Chemical Formula: $\text{C}_{13}\text{H}_{15}\text{ClN}_4\text{O}$
Molecular Weight: 278.74

tert-Butyl 3-(((5-chloro-1-methyl-6-oxo-1,6-dihydropyridazin-4-yl)amino)methyl)benzylcarbamate (98 mg, 0.26 mmol) was stirred in a solution of 5 M HCl in IPA (5.0 mL, 25 mmol) for 2 h, evaporated *in vacuo* to dryness, dissolved in MeOH and loaded on to a preconditioned SCX cartridge. The SCX cartridge was eluted with MeOH (20 mL) followed by 2 M methanolic ammonia (20 mL) and the basic fractions evaporated *in vacuo* to a colourless gum. The gum was triturated with TBME (2 mL) and dried *in vacuo* to give the title compound **5.149** a white solid (65 mg, 91%): $^1\text{H NMR}$ ($\text{SO}(\text{CD}_3)_2$, 400 MHz) δ 7.68 (s, 1H), 7.33 - 7.19 (m, 4H), 7.16 - 7.10 (m, 1H), 4.54 (d, $J = 6.5$ Hz, 2H), 3.70 (s, 2H), 3.54 (s, 3H), 1.87 (br.s, 2H); LRMS $[\text{M}+\text{H}]^+$: 279, 100% a/a.

5-((4-(Aminomethyl)benzyl)amino)-4-chloro-2-methylpyridazin-3(2H)-one (5.152)²⁹⁵

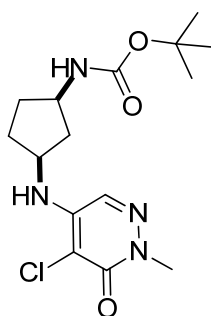


Chemical Formula: $\text{C}_{13}\text{H}_{15}\text{ClN}_4\text{O}$
Molecular Weight: 278.74

A solution of 4,5-dichloro-2-methyl-3(2H)-pyridazinone (100 mg, 0.559 mmol), DIPEA (0.312 mL, 1.788 mmol) and 4-xylylenediamine (152 mg, 1.117 mmol) in DMSO (0.4 mL) were

heated to 120 °C for 45 min under microwave conditions. The resulting biphasic solution was partitioned between EtOAc (15 mL) and water (5 mL). The aqueous layer was separated and the organic layer washed (2x sat. aq. NaHCO₃ [5 mL], 1x brine [5 mL]), dried over MgSO₄ and evaporated *in vacuo* to dryness. The combined aqueous portions were extracted (3 x DCM [10 mL]), combined and evaporated *in vacuo* to a white gum. The two residues were combined, dissolved in DCM:MeOH (1:1, 5 mL) and loaded on to a preconditioned SCX cartridge. The cartridge was eluted with MeOH (20 mL) followed by 2 M methanolic ammonia (20 mL). The basic fractions were evaporated *in vacuo* to a colourless gum and purified by MDAP (HPH method B) to give the title compound **5.152** to a white solid (54 mg, 35%): ¹H NMR (SO(CD₃)₂, 400 MHz) δ 8.38 (s, 1H), 7.67 (s, 1H), 7.38 - 7.25 (m, 5H), 4.55 (d, *J* = 6.5 Hz, 2H), 3.81 (s, 2H), 3.54 (s, 3H); LRMS [M+H]⁺: 279, 100% a/a.

tert-Butyl ((*cis*)-3-((5-chloro-1-methyl-6-oxo-1,6-dihydropyridazin-4-yl)amino)cyclopentyl)carbamate (**5.164**)²⁹⁵

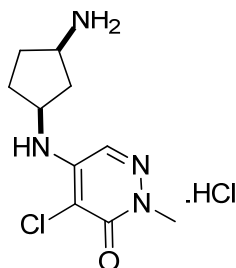


Chemical Formula: C₁₅H₂₃ClN₄O₃
Molecular Weight: 342.82

DIPEA (0.516 mL, 2.96 mmol) was added to a stirred suspension of 4,5-dichloro-2-methylpyridazin-3(2*H*)-one (126 mg, 0.704 mmol), and *tert*-butyl (3-aminocyclopentyl)carbamate, hydrochloride (217 mg, 0.915 mmol) in DMSO (0.4 mL). The reaction mixture was heated to 110 °C under microwave conditions for 3 h. Methanol (1 mL) was added to the biphasic reaction mixture until a homogeneous solution formed and the mixture was purified by MDAP (TFA method B) and the product containing fractions evaporated to a brown residue. TLC analysis (EtOAc) indicated the presence of two products - likely to be *cis* and *trans* isomers. The residue was purified by silica gel chromatography eluting with cyclohexane:EtOAc (75 -> 100%) to give the title compound **5.164** as a white solid (28 mg, 12%): ¹H NMR (SO(CD₃)₂, 600 MHz) δ 7.86 (s, 1H), 6.97 (d, *J* = 5.5 Hz, 1H), 6.68 - 6.73 (m, 1H), 6.27 (d, *J* = 8.0 Hz, 1H), 4.10 (app.sxt, *J* = 7.5 Hz, 1H), 3.79

(d, $J = 6.5$ Hz, 1H), 3.58 (s, 3H), 2.31 (dt, $J = 7.5, 13.5$ Hz, 1H), 1.88 - 1.96 (m, 1H), 1.70 - 1.79 (m, 1H), 1.61 - 1.67 (m, 1H), 1.55 - 1.60 (m, 1H), 1.47 (dt, $J = 7.0, 13.5$ Hz, 1H), 1.38 (s, 9H); LRMS $[M+H]^+$: 343, 100% a/a.

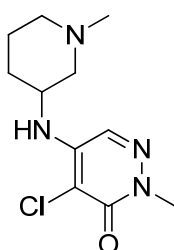
5-(((*cis*)-3-Aminocyclopentyl)amino)-4-chloro-2-methylpyridazin-3(2*H*)-one, hydrochloride salt (5.163)



Chemical Formula: $C_{10}H_{15}ClN_4O \cdot HCl$
Molecular Weight: 279.17

A solution of 5 M HCl in IPA (3.00 mL, 15.0 mmol) was added to *tert*-butyl ((*cis*)-3-((5-chloro-1-methyl-6-oxo-1,6-dihydropyridazin-4-yl)amino)cyclopentyl)carbamate (22 mg, 0.064 mmol) and the resulting solution stirred for 2 h. The reaction mixture was evaporated under a stream of nitrogen, stirred in TBME (3 mL), evaporated under a stream of nitrogen and dried *in vacuo* to give the title compound **5.163** as a white solid (16 mg, 89%): 1H NMR ($SO(CD_3)_2$, 400 MHz) δ 8.07 (br.s, 3H), 7.77 (s, 1H), 5.99 (d, $J = 6.0$ Hz, 1H), 4.19 (app.sxt, $J = 7.0$ Hz, 1H), 3.59 (s, 3H), 3.57 - 3.48 (m, 1H), 2.55 - 2.49 (m, partially obscured by DMSO), 2.10 - 1.82 (m, 4H), 1.72 (dt, $J = 7.0, 14.0$ Hz, 1H); LRMS $[M+H]^+$: 243, 92% a/a.

4-Chloro-2-methyl-5-((1-methylpiperidin-3-yl)amino)pyridazin-3(2*H*)-one (5.166)²⁹⁵

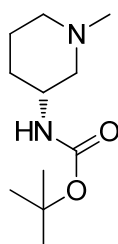


Chemical Formula: $C_{11}H_{17}ClN_4O$
Molecular Weight: 256.73

DIPEA (0.29 mL, 1.7 mmol) was added to a solution of 1-methylpiperidin-3-amine (96 mg, 0.84 mmol) and 4,5-dichloro-2-methylpyridazin-3(2*H*)-one (100 mg, 0.56 mmol) in DMSO (2

mL). The solution was heated under microwave conditions at 130 °C for 1 h. The resulting biphasic solution was made homogenous by the addition of DMSO (1 mL) and purified by MDAP (HpH method B) to give the title compound as a yellow solid (37 mg, 26%): ¹H NMR (SO(CD₃)₂, 400 MHz) δ 7.90 (s, 1H), 5.89 (d, *J* = 9.0 Hz, 1H), 3.94 – 3.80 (s, 1H), 3.58 (s, 3H), 2.60 - 2.52 (m, 1H), 2.42 - 2.11 (m, 6H), 1.72 - 1.39 (m, 4H); LRMS [M+H]⁺: 257, 100% a/a

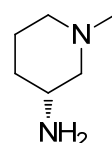
(R)-tert-Butyl (1-methylpiperidin-3-yl)carbamate (5.172)³⁰⁹



Chemical Formula: C₁₁H₂₂N₂O₂
Molecular Weight: 214.30

Formic acid (1.94 mL, 50.5 mmol) was added to a solution of (R)-tert-butyl piperidin-3-ylcarbamate (5.06 g, 25.3 mmol) and 37% w/v formaldehyde in water (3.88 mL, 52.1 mmol) in 2-MeTHF (135 mL). The resulting solution was stirred for 1 h at room temperature, heated to 80 °C for 30 min and cooled to room temperature. The solution was evaporated *in vacuo* to a colourless oil and purified by silica gel chromatography eluting with DCM:2 M methanolic ammonia (0 → 10%) to give the title compound **5.172** as a white solid (3.71 g, 69%): ¹H NMR (SO(CD₃)₂, 400 MHz) δ 6.66 (d, *J* = 8.0 Hz, 1H), 3.52 - 3.34 (m, obscured by water peak), 2.68 (dd, *J* = 3.0, 10.0 Hz, 1H), 2.55 (d, *J* = 11.0 Hz, 1H), 2.13 (s, 3H), 1.81 - 1.71 (m, 1H), 1.71 - 1.54 (m, 3H), 1.48 - 1.32 (m, 10H), 1.14 - 1.02 (m, 1H); LRMS [M+H]⁺: 215.

(R)-1-methylpiperidin-3-amine, 2 hydrochloride (5.173)

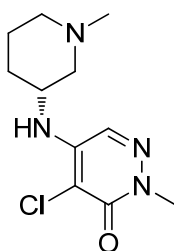


Chemical Formula: C₆H₁₄N₂ · 2HCl
Molecular Weight: 187.11

A solution of 5 M HCl in IPA (55.0 mL, 275 mmol) was added to (R)-tert-butyl (1-methylpiperidin-3-yl)carbamate (3.70 g, 17.3 mmol) and the resulting suspension heated to 80 °C for 1 h. The resulting suspension was cooled to room temperature and TBME (55 mL)

added. The suspension was filtered, washed (2x TBME [30 mL]) and dried *in vacuo* to give the title compound **5.173** as a white solid (3.213 g, 100%): $^1\text{H NMR}$ ($\text{SO}(\text{CD}_3)_2$, 400 MHz, 120 $^\circ\text{C}$) δ 3.65 (tt, $J = 4.5, 9.5$ Hz, 1H), 3.54 - 3.45 (m, 1H), 3.31 - 3.19 (m, 1H), 3.18 - 3.08 (m, 1H), 3.02 - 2.89 (m, 1H), 2.75 (s, 3H), 2.18 - 2.02 (m, 1H), 2.01 - 1.84 (m, 2H), 1.81 - 1.61 (m, 1H), exchangeable protons not observed; LRMS $[\text{M}+\text{H}]^+$: 115.

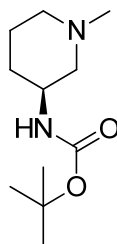
(R)-4-Chloro-2-methyl-5-((1-methylpiperidin-3-yl)amino)pyridazin-3(2H)-one (5.169)²⁹⁵



Chemical Formula: $\text{C}_{11}\text{H}_{17}\text{ClN}_4\text{O}$
Molecular Weight: 256.73

DIPEA (3.28 mL, 18.8 mmol) was added to a suspension of 4,5-dichloro-2-methyl-3(2H)-pyridazinone (0.8 g, 4.47 mmol) and (*R*)-1-methylpiperidin-3-amine, 2 hydrochloride (1.00 g, 5.36 mmol) in DMSO (2.4 mL). The mixture was heated to 130 $^\circ\text{C}$ for 4 h under microwave conditions. The reaction mixture was partitioned between DCM (20 mL) and aq. NaHCO_3 (20 mL). The organic layer was removed and the aqueous layer extracted (3x DCM [20 mL]). The organic portions were combined, dried over MgSO_4 and evaporated *in vacuo* to an orange oil. The residue was purified by silica gel chromatography eluting with DCM:2 M methanolic ammonia (0 \rightarrow 5%) to give the title compound **5.169** as a crystalline brown solid (600 mg, 52%): $^1\text{H NMR}$ (CDCl_3 , 400 MHz) δ 7.54 (s, 1H), 5.24 (br.s, 1H), 3.79 – 3.67 (m, 4H), 2.67 – 2.52 (m, 1H), 2.52 – 2.36 (m, 2H), 2.36 – 2.22 (m, 4H), 1.84 – 1.66 (m, 2H), 1.65 – 1.47 (m, 2H); $^{13}\text{C NMR}$ (CDCl_3 , 101 MHz) δ 157.9, 143.2, 125.5, 107.6, 60.6, 55.5, 48.5, 46.4, 40.1, 29.2, 22.0; LRMS $[\text{M}+\text{H}]^+$: 257, 100% a/a; HRMS: $\text{C}_{11}\text{H}_{18}\text{ClN}_4\text{O}$ $[\text{M}+\text{H}]^+$ requires 257.1164, found $[\text{M}+\text{H}]^+$ 257.1160.; IR: solid v 2938, 1630, 1602, 1445, 1345 cm^{-1} ; mp 111 – 115 $^\circ\text{C}$; $[\alpha]_D = +5^\circ$ at 23.9 $^\circ\text{C}$ at $c = 1$ in chloroform.

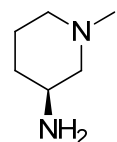
(S)-tert-Butyl (1-methylpiperidin-3-yl)carbamate (5.170a)



Chemical Formula: C₁₁H₂₂N₂O₂
Molecular Weight: 214.30

Formic acid (0.391 mL, 10.2 mmol) was added to a suspension of (S)-tert-butyl piperidin-3-ylcarbamate (1.02 g, 5.09 mmol) and 37% w/v formaldehyde in water (0.827 mL, 10.2 mmol) in 2-MeTHF (50 mL). The suspension was heated to 80 °C for 45 min and cooled to room temperature. The reaction mixture was evaporated *in vacuo* to a colourless oil. The residue purified by silica gel chromatography eluting with DCM:2 M methanolic ammonia (0 -> 8%) to give the title compound **5.170a** as a white solid (985 mg, 90%): ¹H NMR (SO(CD₃)₂, 400 MHz, 120 °C) δ 6.65 (d, *J* = 8.0 Hz, 1H), 3.50 - 3.34 (m, obscured by water peak), 2.68 (dd, *J* = 3.0, 10.0 Hz, 1H), 2.55 (d, *J* = 11.0 Hz, 1H), 2.13 (s, 3H), 1.81 - 1.71 (m, 1H), 1.71 - 1.54 (m, 2H), 1.48 - 1.32 (m, 10H), 1.14 - 1.02 (m, 1H); LRMS [M+H]⁺: 215; [α]_D = -17° at 21.5 °C at c = 1 in MeOH.

(S)-1-methylpiperidin-3-amine, 2 hydrochloride (5.170b)

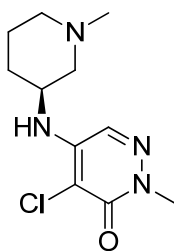


Chemical Formula: C₆H₁₄N₂ · 2HCl
Molecular Weight: 187.11

A solution of 5 M HCl in IPA (15 mL, 75 mmol) was added to (S)-tert-butyl (1-methylpiperidin-3-yl)carbamate (985 mg, 4.60 mmol) and the mixture heated to 50 °C for 5 min and cooled to 20 °C. The resulting suspension was allowed to stand for 1 h, diluted with TBME (20 mL) and filtered. The resulting solid was washed (2x TBME [5 mL]) and dried *in vacuo* to give the title compound **5.170b** as a white solid (709 mg, 84%): ¹H NMR (SO(CD₃)₂, 400 MHz, 120 °C) δ 3.65 (tt, *J* = 4.5, 9.5 Hz, 1H), 3.54 - 3.45 (m, 1H), 3.31 - 3.19 (m, 1H), 3.18 - 3.08 (m, 1H), 3.02 - 2.89 (m, 1H), 2.75 (s, 3H), 2.18 - 2.02 (m, 1H), 2.01 - 1.84

(m, 2H), 1.81 - 1.61 (m, 1H), exchangeable protons not observed; LRMS [M+H]⁺: 115; [α]_D = +2° at 22.0 °C at c = 1 in MeOH.

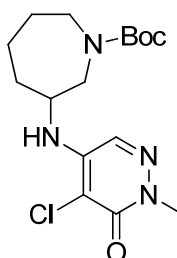
(S)-4-Chloro-2-methyl-5-((1-methylpiperidin-3-yl)amino)pyridazin-3(2H)-one (5.170)²⁹⁵



Chemical Formula: C₁₁H₁₇ClN₄O
Molecular Weight: 256.73

DIPEA (0.41 mL, 2.4 mmol) was added to a stirred suspension of 4,5-dichloro-2-methylpyridazin-3(2H)-one (100 mg, 0.559 mmol), and (S)-1-methylpiperidin-3-amine, 2 hydrochloride (136 mg, 0.726 mmol) in DMSO (0.4 mL). The resulting suspension was heated to 130 °C for 5 h under microwave conditions and cooled to 20 °C. The reaction mixture was diluted with MeOH (2 mL) and loaded on to a preconditioned SCX cartridge. The cartridge was eluted with MeOH (40 mL), followed by 2 M methanolic ammonia (50 mL). The basic fractions were evaporated *in vacuo* to a brown oil and purified by MDAP (HPH method B) to give the title compound **5.170** as a pale brown solid (13 mg, 9%): ¹H NMR (SO(CD₃)₂, 400 MHz) δ 7.90 (s, 1H), 5.89 (d, *J* = 9.0 Hz, 1H), 3.94 - 3.80 (s, 1H), 3.58 (s, 3H), 2.60 - 2.52 (m, 1H), 2.42 - 2.11 (m, 6H), 1.72 - 1.39 (m, 4H); LRMS [M+H]⁺: 257, 100% a/a; HRMS: C₁₁H₁₈ClN₄O [M+H]⁺ requires 257.1164, found [M+H]⁺ 257.1161; [α]_D = -10° at 23.2 °C at c = 1 in chloroform.

tert-Butyl 3-((5-chloro-1-methyl-6-oxo-1,6-dihydropyridazin-4-yl)amino)azepane-1-carboxylate (5.175)²⁹⁵

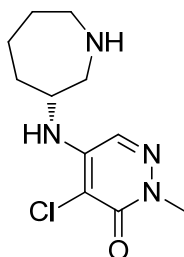


Chemical Formula: C₁₆H₂₅ClN₄O₃
Molecular Weight: 356.85

DIPEA (1.61 mL, 9.22 mmol) was added to a solution of 4,5-dichloro-2-methylpyridazin-3(2H)-one (0.50 g, 2.79 mmol) and 3-amino-1-N-Boc-azepane (0.898 g, 4.19 mmol) in DMSO (1.6 mL). The resulting mixture was heated to 130 °C under microwave conditions for 2 h. The reaction mixture was partitioned between water (20 mL) and DCM (20 mL). The organic layer was separated and the aqueous layer extracted (2x DCM [20 mL]). The combined organic portions were combined, dried over MgSO₄ and evaporated *in vacuo* to a brown oil. The residue was purified by silica gel chromatography eluting with cyclohexane:DCM (25 -> 100%) followed by cyclohexane:EtOAc (25 -> 75%) to give a brown solid which was triturated with TBME to give the title compound **5.175** as a white solid (260 mg, 26%): ¹H NMR (SO(CD₃)₂, 400 MHz) δ 7.83 (s, 1H), 5.72 (br.s, 1H), 3.89 (m, 1H), 3.63 - 3.54 (m, 4H), 3.43 - 3.30 (m, 3H), 1.96 - 1.85 (m, 1H), 1.82 - 1.52 (m, 4H), 1.49 - 1.34 (m, 10H); LRMS [M+H]⁺: 357, 93% a/a.

The filtrate was stood overnight and a precipitate formed. The filtrate was evaporated under a stream of nitrogen, triturated with TBME (2 mL) and washed with TBME (1 mL). The resulting solid was dried *in vacuo* to give the title compound **5.175** as a white solid (53 mg, 5%): Analytical data as above.

(R)-5-(azepan-3-ylamino)-4-chloro-2-methylpyridazin-3(2H)-one (5.178)

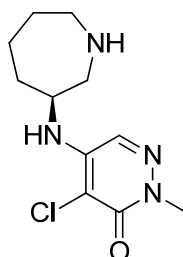


Chemical Formula: C₁₁H₁₇ClN₄O
Molecular Weight: 256.73

A solution of 5 M HCl in IPA (5.0 mL, 25 mmol) was added to (*R*)-*tert*-butyl 3-((5-chloro-1-methyl-6-oxo-1,6-dihydropyridazin-4-yl)amino)azepane-1-carboxylate (126 mg, 0.353 mmol) and the resulting solution stirred for 1 h. The reaction mixture was evaporated *in vacuo* to dryness, dissolved in MeOH and loaded on to a preconditioned SCX cartridge. The cartridge was eluted with MeOH (50 mL), followed by 2 M methanolic ammonia (50 mL). The basic fractions were evaporated *in vacuo* to give the title compound **5.178** as a colourless gum (86 mg, 95%): ¹H NMR (SO(CD₃)₂, 400 MHz) δ 7.87 (s, 1H), 6.19 (d, *J* = 9.0 Hz,

1H), 3.97 - 3.81 (m, 1H), 3.58 (s, 3H), 2.94 - 2.67 (m, 4H), 1.80 - 1.38 (m, 6H); LRMS [M+H]⁺: 257, 100% a/a.

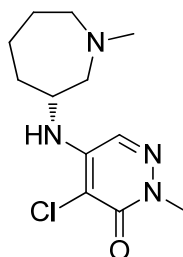
(S)-5-(azepan-3-ylamino)-4-chloro-2-methylpyridazin-3(2H)-one (5.179)



Chemical Formula: C₁₁H₁₇ClN₄O
Molecular Weight: 256.73

A solution of 5 M HCl in IPA (5.00 mL, 25.0 mmol) was added to (*S*)-*tert*-butyl 3-((5-chloro-1-methyl-6-oxo-1,6-dihydropyridazin-4-yl)amino)azepane-1-carboxylate (110 mg, 0.353 mmol) and the resulting solution stirred for 1 h. The reaction mixture was evaporated *in vacuo* to dryness, dissolved in MeOH (5 mL) and loaded on to a preconditioned SCX cartridge. The cartridge was eluted with MeOH (50 mL), followed by 2 M methanolic ammonia (50 mL). The basic fractions were evaporated *in vacuo* to give the title compound **5.179** as a colourless gum (74 mg, 94%): ¹H NMR (SO(CD₃)₂, 400 MHz) δ 7.87 (s, 1H), 6.19 (d, *J* = 9.0 Hz, 1H), 3.97 - 3.81 (m, 1H), 3.58 (s, 3H), 2.94 - 2.67 (m, 4H), 1.80 - 1.38 (m, 6H); LRMS [M+H]⁺: 257, 100% a/a.

(R)-4-Chloro-2-methyl-5-((1-methylazepan-3-yl)amino)pyridazin-3(2H)-one (5.180)³⁰⁹

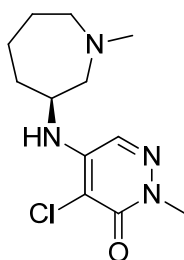


Chemical Formula: C₁₂H₁₉ClN₄O
Molecular Weight: 270.76

Formic acid (0.019 mL, 0.506 mmol) was added to a solution of 37% w/w formaldehyde in water (0.038 mL, 0.51 mmol) and (*R*)-5-(azepan-3-ylamino)-4-chloro-2-methylpyridazin-3(2H)-one (65 mg, 0.253 mmol) in 2-MeTHF (5 mL). The resulting suspension was heated to reflux overnight and evaporated *in vacuo* to dryness. The residue was dissolved in MeOH

(10 mL) and loaded on to a preconditioned SCX cartridge and eluted with MeOH (50 mL) followed by 2 M methanolic ammonia (50 mL). The basic fractions were evaporated *in vacuo* to give the title compound **5.180** as a colourless gum (62 mg, 90%): ^1H NMR ($\text{SO}(\text{CD}_3)_2$, 400 MHz) δ 7.86 (s, 1H), 6.18 (d, $J = 9.0$ Hz, 1H), 4.02 - 3.87 (m, 1H), 3.59 (s, 3H), 2.79 - 2.57 (m, 3H), 2.48 - 2.41 (m, 1H), 2.36 (s, 3H), 1.78 - 1.41 (m, 6H); ^{13}C NMR (CDCl_3 , 101 MHz) δ 158.0, 143.2, 126.1, 107.4, 58.6, 57.4, 50.6, 47.9, 40.1, 35.1, 28.2, 21.1; LRMS $[\text{M}+\text{H}]^+$: 271, 100% a/a; HRMS: $\text{C}_{12}\text{H}_{20}\text{ClN}_4\text{O}$ $[\text{M}+\text{H}]^+$ requires 271.1320, found $[\text{M}+\text{H}]^+$ 271.1315; IR: solid ν 3431, 1602, 1519, 1447, 1203, 1155, 1089 cm^{-1} ; mp 71 - 73 $^\circ\text{C}$, $[\alpha]_{\text{D}} = -48^\circ$ at 23.2 $^\circ\text{C}$ at $c = 1$ in chloroform.

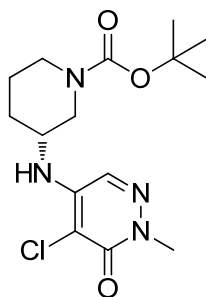
(S)-4-Chloro-2-methyl-5-((1-methylazepan-3-yl)amino)pyridazin-3(2H)-one (5.181)³⁰⁹



Chemical Formula: $\text{C}_{12}\text{H}_{19}\text{ClN}_4\text{O}$
Molecular Weight: 270.76

Formic acid (15 μL , 0.39 mmol) was added to a solution of 37% w/w formaldehyde in water (29 μL , 0.39 mmol) and (S)-5-(azepan-3-ylamino)-4-chloro-2-methylpyridazin-3(2H)-one (50.0 mg, 0.195 mmol). The resulting suspension was heated to reflux overnight and evaporated *in vacuo* to dryness. The residue was dissolved in MeOH and loaded on to a preconditioned SCX cartridge and eluted with MeOH (50 mL) followed by 2 M methanolic ammonia (50 mL). The basic fractions were evaporated *in vacuo* to give the title compound **5.181** as a colourless gum (47 mg, 89%): ^1H NMR ($\text{SO}(\text{CD}_3)_2$, 400 MHz) δ 7.86 (s, 1H), 6.18 (d, $J = 9.0$ Hz, 1H), 4.02 - 3.87 (m, 1H), 3.59 (s, 3H), 2.79 - 2.57 (m, 3H), 2.48 - 2.41 (m, 1H), 2.36 (s, 3H), 1.78 - 1.41 (m, 6H); LRMS $[\text{M}+\text{H}]^+$: 271, 100% a/a; mp 67 - 69 $^\circ\text{C}$; $[\alpha]_{\text{D}} = +53^\circ$ at 23.2 $^\circ\text{C}$ at $c = 1$ in chloroform.

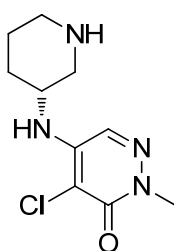
(R)-tert-Butyl 3-((5-chloro-1-methyl-6-oxo-1,6-dihydropyridazin-4-yl)amino)piperidine-1-carboxylate (5.182)²⁹⁵



Chemical Formula: C₁₅H₂₃ClN₄O₃
Molecular Weight: 342.82

DIPEA (1.56 mL, 8.94 mmol) was added to a suspension of 4,5-dichloro-2-methyl-3(2H)-pyridazinone (0.500g, 2.79 mmol) and (R)-(-)-3-amino-1-Boc-piperidine (0.671 g, 3.35 mmol) in DMSO (1.6 mL). The mixture was heated to 130 °C for 2 h under microwave conditions and the reaction mixture partitioned between DCM (20 mL) and water (20 mL). The organic layer was removed and the aqueous layer extracted [2x DCM (20 mL)]. The combined organic layers were dried over MgSO₄ and evaporated *in vacuo* to dryness. The residue was purified by silica gel chromatography eluting with cyclohexane:EtOAc (40 -> 80%) to give the title compound **5.182** as a brown oil (425 mg, 44%): ¹H NMR (SO(CD₃)₂, 400 MHz) δ 7.89 (s, 1H), 6.04 (br.s, 1H), 3.74 - 3.61 (m, 2H), 3.59 (s, 3H), 3.20 - 2.75 (m, 2H), 1.95 - 1.79 (m, 1H), 1.72 - 1.56 (m, 2H), 1.54 - 1.26 (m, 11H); LRMS [M+H]⁺: 343, 100% a/a.

(R)-4-Chloro-2-methyl-5-(piperidin-3-ylamino)pyridazin-3(2H)-one (5.183)

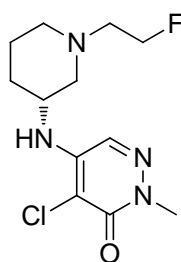


Chemical Formula: C₁₀H₁₅ClN₄O
Molecular Weight: 242.71

A solution of 5 M HCl in IPA (5.00 mL, 25.0 mmol) was added to (R)-tert-butyl 3-((5-chloro-1-methyl-6-oxo-1,6-dihydropyridazin-4-yl)amino)piperidine-1-carboxylate (420 mg, 1.23 mmol), the resulting solution stirred for 1.5 h and evaporated *in vacuo* to dryness. The

residue was dissolved in the minimum amount of MeOH and loaded on to a preconditioned SCX cartridge. The cartridge was eluted with MeOH (50 mL) followed by 2 M methanolic ammonia (50 mL) and the basic fractions were evaporated *in vacuo* to give the title compound **5.183** as a brown gum (220 mg, 74%): ^1H NMR ($\text{SO}(\text{CD}_3)_2$, 400 MHz) δ 7.88 (s, 1H), 6.01 (d, $J = 9.0$ Hz, 1H), 3.73 - 3.63 (m, 1H), 3.58 (s, 3H), 2.88 (dd, $J = 3.0, 12.0$ Hz, 1H), 2.75 - 2.65 (m, 2H), 2.60 - 2.46 (m, partially obscured), 1.82 - 1.71 (m, 1H), 1.63 - 1.49 (m, 2H), 1.47 - 1.34 (m, 1H); LRMS $[\text{M}+\text{H}]^+$: 243, 100% a/a.

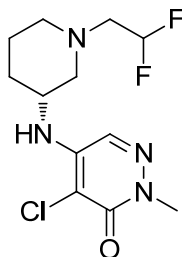
(R)-4-Chloro-5-((1-(2-fluoroethyl)piperidin-3-yl)amino)-2-methylpyridazin-3(2H)-one (5.190)



Chemical Formula: $\text{C}_{12}\text{H}_{18}\text{ClFN}_4\text{O}$
Molecular Weight: 288.75

(R)-4-Chloro-2-methyl-5-(piperidin-3-ylamino)pyridazin-3(2H)-one (70 mg, 0.29 mmol) was added to a stirred suspension of 1-bromo-2-fluoroethane (0.064 mL, 0.87 mmol), sodium carbonate (45.9 mg, 0.433 mmol) and potassium iodide (4.8 mg, 0.029 mmol) in acetonitrile (5 mL). The resulting suspension was heated to 130 °C for 2 h under microwave conditions and cooled to 20 °C. The reaction mixture was evaporated *in vacuo* and purified by silica gel chromatography eluting with DCM:2 M methanolic ammonia (0 -> 5%) to give the title compound **5.190** as a colourless gum (59 mg, 71%): ^1H NMR ($\text{SO}(\text{CD}_3)_2$, 400 MHz) δ 7.89 (s, 1H), 5.94 (d, $J = 9.0$ Hz, 1H), 4.53 (dt, $J = 5.0, 48.0$ Hz, 2H), 3.93 - 3.78 (m, 1H), 3.59 (s, 3H), 2.77 - 2.59 (m, 3H), peak obscured by DMSO, 2.44 - 2.33 (m, 2H), 1.76 - 1.41 (m, 4H); LRMS $[\text{M}+\text{H}]^+$: 289, 100% a/a.

(R)-4-Chloro-5-((1-(2,2-difluoroethyl)piperidin-3-yl)amino)-2-methylpyridazin-3(2H)-one
(5.191)



Chemical Formula: C₁₂H₁₇ClF₂N₄O
Molecular Weight: 306.74

(R)-4-chloro-2-methyl-5-(piperidin-3-ylamino)pyridazin-3(2H)-one (70 mg, 0.29 mmol) was added to a stirred suspension of 2-bromo-1,1-difluoroethane (0.037 mL, 0.420 mmol), sodium carbonate (45.9 mg, 0.433 mmol) and potassium iodide (4.79 mg, 0.029 mmol) in acetonitrile (5 mL). The resulting suspension was heated to 60 °C for 4 h. Further 2-bromo-1,1-difluoroethane (0.037 mL, 0.42 mmol) was added, the reaction heated overnight. The reaction mixture was heated to 100 °C for 21 h under microwave conditions. The temperature was increased to 130 °C for 2 h under microwave conditions. The temperature was increased to 140 °C for 6 h and cooled to room temperature. The reaction mixture was evaporated *in vacuo* to dryness and purified by silica gel chromatography eluting with cyclohexane:EtOAc (50 -> 100%) to give the title compound **5.191** as a colourless gum (59 mg, 77%): ¹H NMR (SO(CD₃)₂, 400 MHz) δ 7.89 (s, 1H), 6.14 (tt, *J* = 4.5, 55.5 Hz, 1H), 5.94 (d, *J* = 9.0, 1H), 3.91 - 3.87 (m, 1H), 3.59 (s, 3H), 2.87 - 2.17 (m, 3H), 2.69 - 2.57 (m, 1H), 2.58 - 2.31 (m, partially obscured by DMSO); LRMS [M+H]⁺: 307; 100% a/a.

7 References

- 1 Steinbrook, R. *N. Engl. J. Med.* **2008**, *359*, 1977 – 1981.
- 2 Munos, B. M. *Nat. Rev. Drug Discov.* **2009**, *8*, 959 – 968.
- 3 Scannell, J. W.; Blanckley, A.; Boldon, H.; Warrington, B. *Nat. Rev. Drug Discov.* **2012**, *11*, 191 – 200.
- 4 Kola, I.; Landis, J. *Nat. Rev. Drug Discov.* **2004**, *3*, 711 – 715.
- 5 Grabowski, H. G.; Vernon, J. M. *Int. J. Technology Management* **2000**, *19*, 98 – 120.
- 6 Simon, W. A.; Herrmann, M.; Klein, T.; Shin, J. M.; Huber, R.; Senn-Bilfinger, J.; Postius, S. J. *Pharmacol. Exp. Ther.* **2007**, *321*, 866 – 874.
- 7 Kotz, J. *SciBX* **2012**, *5*, 1 – 3.
- 8 Chanda, S. K.; Caldwell, J. S. *Drug Discov. Today* **2003**, *8*, 168 – 174.
- 9 Swinney, D. C.; Anthony, J. *Nat. Rev. Drug Discov.* **2011**, *10*, 507 – 519.
- 10 Cook, D.; Brown, D.; Alexander, R.; March, R.; Morgan, P.; Satterthwaite, G.; Pangalos, M. N. *Nat. Rev. Drug Discov.* **2014**, *13*, 419 – 431.
- 11 Annunziato, A. T. *Nature Educ.* **2008**, *1*, 1 – 3.
- 12 Widom, J. *Annu. Rev. Biophys. Biomol. Struct.* **1998**, *27*, 285 – 327.
- 13 Georgopoulos, K. *Nat. Rev. Immunol.* **2002**, *2*, 162 – 174.
- 14 Arrowsmith, C. H.; Bountra, C.; Fish, P. V.; Lee, K.; Schapira, M. *Nat. Rev. Drug Discov.* **2012**, *11*, 384 – 400.
- 15 Jenuwein, T.; Allis, C. D. *Science* **2001**, *293*, 1074 – 1080.
- 16 Robinson, P. J.; Fairall, L.; Huynh, V. A.; Rhodes, D. *Proc. Natl. Acad. Sci. U.S.A.* **2006**, *103*, 6506 – 6511.
- 17 Woodcock, C. L.; Ghosh, R. P. *Cold Spring Harb. Perspect. Biol.* **2010**, *2*, 1 – 25.
- 18 Tonna, S.; El-Osta, A.; Cooper, M. E.; Tikellis, C. *Nat. Rev. Nephrol.* **2010**, *6*, 332 – 341.
- 19 Kouzarides, T. *Cell* **2007**, *128*, 693 – 705.
- 20 Dekker, F. J.; Haisma, H. J. *Drug Discov. Today* **2009**, *14*, 942 – 948.
- 21 Josling, G. A.; Selvarajah, S. A.; Petter, M.; Duffy, M. F. *Genes* **2012**, *3*, 320 – 343.
- 22 Bannister, A. J.; Kouzarides, T. *Cell Res.* **2011**, *21*, 381 – 395.
- 23 Zhang, Y.; Reinberg, D. *Genes Dev.* **2001**, *15*, 2343 – 2360.
- 24 Martin, C.; Zhang, Y. *Nat. Rev. Mol. Cell Biol.* **2005**, *6*, 838 – 849.
- 25 Xiao, B.; Jing, C.; Wilson, J. R.; Walker, P. A.; Vasisht, N.; Kelly, G.; Howell, S.; Taylor, I. A.; Blackburn, G. M.; Gamblin, S. J. *Nature* **2003**, *421*, 652 – 656.
- 26 Hofjfeld, J. W.; Agger, K.; Helin, K. *Nat. Rev. Drug Discov.* **2013**, *12*, 917 – 930.
- 27 Zeng, L.; Zhou, M. M. *FEBS Lett.* **2002**, *513*, 124 – 128.

- 28 Herold, J. M.; Wigle, T. J.; Norris, J. L.; Lam, R.; Korboukh, V. K.; Gao, C.; Ingerman, L. A.; Kireev, D. B.; Senisterra, G.; Vedadi, M.; Tripathy, A.; Brown, P. J.; Arrowsmith, C. H.; Jin, J.; Janzen, W. P.; Frye, S. V. *J. Med. Chem.* **2011**, *54*, 2504 – 2511.
- 29 De Ruijter, A. J. M.; Van Gennip, A. H.; Caron, H. N.; Kemp, S. Van Kuilenburg, A. B. P. *Biochem J.* **2003**, *370*, 737 – 749.
- 30 Dokmanovic, M. Clarke, C.; Marks, P. A. *Mol. Cancer Res.* **2007**, *5*, 981 – 989.
- 31 Finnin, M. S.; Donigian, J. R.; Cohen, A.; Richon, V. M.; Rifkind, R. A.; Marks, P. A.; Breslow, R.; Pavletich, N. P. *Nature* **1999**, *401*, 188 - 193.
- 32 Pedersen, M. T.; Helin, K. *Trends Cell Biol.* **2010**, *20*, 662 – 671.
- 33 Martin-Puig, S.; Temes, E.; Olmos, G.; Jones, D. R.; Aragones, J.; Landazuri, M. O. *J. Biol. Chem.* **2004**, *279*, 9504 – 9511.
- 34 Butler, L. M.; Zhou, X.; Xu, W.-S.; Scher, H. I.; Rifkind, R. A.; Marks, P. A.; Richon, V. M. *P. Natl. Acad. Sci. U.S.A.* **2002**, *99*, 11700 – 11705.
- 35 Nakajima, H.; Kim, Y. B.; Terano, H.; Yoshida, M.; Horinouchi, S. *Exp. Cell Res.* **1998**, *241*, 126 - 133.
- 36 Huang, L.; Pardee, A. B. *Molecular Medicine* **2000**, *6*, 849 – 866.
- 37 Nasevicius, A.; Ekker, S. C. *Nat. Genet.* **2000**, *26*, 216 – 220.
- 38 Hamilton, A. J.; Baulcombe, D. C. *Science* **1999**, *286*, 950 – 952.
- 39 Mulligan, C. G.; Zhang, J.; Kasper, L. H.; Lerach, S.; Payne-Turner, D.; Phillips, L. A.; Heatley, S. L.; Holmfeldt, L.; Collins-Underwood, R.; Ma, J.; Buetow, K. H.; Pui, C.-H.; Baker, S. D.; Downing, J. R. *Nature* **2011**, *471*, 235 – 241.
- 40 Hury, D. M.; Resnick, L. O.; Wipf, P. *J. Med. Chem.* **2013**, *56*, 7161 – 7176.
- 41 Frye, S. V. *Nat. Chem. Biol.* **2010**, *6*, 159 – 161.
- 42 Bunnage, M. E.; Piatnitski, C.; Jones, L. H. *Nat. Chem. Biol.* **2013**, *9*, 195 – 199.
- 43 Morgan, P.; Van Der Graaf, P. H.; Arrowsmith, J.; Feltner, D. E.; Drummond, K. S.; Wegner, C. D.; Street, S. D. A. *Drug Discov. Today* **2012**, *17*, 419 – 424.
- 44 Alberts, B.; Johnson, A. Lewis, J.; Raff, M.; Roberts, K.; Walter, P. *Molecular Biology of the Cell*, 5th ed.; Garland Science: New York, **2004**; pp 704 – 712.
- 45 Chung, C.-W.; Coste, H.; White, J. H.; Mirguet, O.; Wilde, J.; Gosmini, R. L.; Delves, C.; Magny, S. M.; Woodward, R.; Hughes, S. A.; Boursier, E. V.; Flynn, H.; Bouillot, A. M.; Bamborough, P.; Brusq, J.-M. G.; Gellibert, F. J.; Jones, E. J.; Riou, A. M.; Homes, P.; Martin, S. L.; Uings, I. J.; Toum, J.; Clément, C. A.; Boullay, A.-B.; Grimley, R. L.; Blandel, F. M.; Prinjha, R. K.; Lee, K.; Kirilovsky, J.; Nicodeme, E. *J. Med. Chem.* **2011**, *54*, 3827 – 3838.
- 46 D'Arcy, P.; Brnjic, S.; Olofsson, M. H.; Frysknas, M.; Lindsten, K.; De Cesare, M.; Perego, P.; Sadeghi, B.; Hassan, M.; Larsson, R.; Linder, S. *Nat. Med.* **2011**, *17*, 1636 – 1641.
- 47 Ju, K.-S.; Parales, R. E. *Microbiol. Mol. Biol. R.* **2010**, *74*, 250 – 272.

- 48 Ishizaki, M.; Muromoto, R.; Akimoto, T.; Sekine, Y.; Kon, S.; Diwan, M.; Maeda, H.; Togi, S.; Shimoda, K.; Oritani, K.; Matsuda, T. *Int. Immunol.* **2013**, *26*, 257 – 267.
- 49 Du, C.; Bright, J. J.; Sriram, S. *J. Neuroimmunol.* **2001**, *114*, 69 – 79.
- 50 Vlahos, C. J.; Matter, W. F.; Hui, K. Y.; Brown, R. F. *J. Biol. Chem.* **1994**, *269*, 5241 – 5248.
- 51 Dittmann, A.; Werner, T.; Chung, C.-W.; Savitski, M. M.; Savitski, M. F.; Grandi, P.; Hopf, C.; Lindon, M.; Neubauer, G.; Prinjha, R. K.; Bantscheff, M.; Drewes, G. *ACS Chem. Biol.* **2014**, *9*, 495 – 502.
- 52 Abdul-Ghani, R.; Serra, V.; Gyorffy, B.; Jurchott, K. Solf, A.; Dietel, M.; Schafer, R. *Oncogene* **2006**, *25*, 1743 – 1752.
- 53 Takeuchi, T.; Yamazaki, Y.; Katoh-Fukui, Y.; Tsuchiya, R.; Kondo, S.; Motoyama, J.; Higashinakagawa, T. *Gene Dev.* **1995**, *9*, 1211 – 1222.
- 54 Johansson, C.; Tumber, A.; Che, K.; Cain, P.; Nowak, R. Gileadi, C. Oppermann, U. *Epigenomics* **2014**, *6*, 89 – 120.
- 55 Hublitz, P.; Albert, M.; Peters, A. H. F. M. *Int. J. Dev. Biol.* **2009**, *53*, 335 – 354.
- 56 Klose, R. J.; Kallin, E. M.; Zhang, Y. *Nat. Rev. Genet.* **2006**, *7*, 715 – 727.
- 57 Shi, Y.; Whetstone, J. R. *Mol. Cell* **2007**, *25*, 1 – 14.
- 58 Tsukada, Y.; Fang, J.; Erdjument-Bromage, H.; Warren, M. E.; Borchers, C. H.; Tempst, P.; Zhang, Y. *Nature* **2006**, *439*, 811 – 816.
- 59 Livolsi, A.; Busuttill, V.; Imbert, V.; Abraham, R. T.; Peyron, J.-F. *Eur. J. Biochem.* **2001**, *268*, 1508 – 1515.
- 60 Brauchle, M.; Yao, z.; Arora, R.; Thigale, S.; Clay, I.; Inverardi, B.; Fletcher, J.; Taslimi, P.; Acker, M. G.; Gerrits, B.; Voshol, J.; Bauer, A.; Schübeler, D.; Bouwmeester, T.; Ruffner, H. *PLoS ONE* **2013**, *8*, e60549 – e60549.
- 61 Hillringhaus, L.; Yue, W. W.; Rose, N. R.; Ng, S. S.; Gileadi, C.; Loenarz, C.; Bello, S. H.; Bray, J. E.; Schofield, C. J.; Oppermann, U. *J. Biol. Chem.* **2011**, *286*, 41616 – 41625.
- 62 Zhu, Y.; Van Essen, D.; Sacconi, S. *Mol. Cell* **2012**, *46*, 408 – 423.
- 63 Patsialou, A.; Wilsker, D.; Moran, E. *Nucl. Acids Res.* **2005**, *33*, 66 – 80.
- 64 Pointon, J. J.; Harvey, D.; Karaderi, T.; Appleton, L. H.; Farrar, C.; Wordsworth, B. P. *Genes Immun.* **2011**, *12*, 395 – 398.
- 65 Sieper, J.; Braun, J.; Rudwaleit, M.; Boonen, A.; Zink, A. *Ann. Rheum. Dis.* **2002**, *61*, iii8 – iii18.
- 66 Hong, S.; Cho, Y. W.; Yu, L. R.; Yu, H.; Veenstra, T. D.; Ge, K. *Proc. Natl Acad. Sci. U.S.A.* **2007**, *104*, 18439 – 18444.
- 67 Horton, J. R.; Upadhyay, A. K.; Qi, H. H.; Zhang, X.; Shi, Y.; Cheng, X. *Nat. Struct. Mol. Biol.* **2010**, *17*, 38 – 43.
- 68 Arteaga, M. F.; Mikesch, J.-H.; Qiu, J.; Christensen, J.; Helin, K.; Kogan, S. C.; Dong, S.; So, C. W. E. *Cancer Cell* **2013**, *23*, 376 – 389.

- 69 Stender, J. D.; Pascual, G.; Liu, W.; Kaikkonen, M. U.; Do, K.; Spann, N. J.; Boutros, M.; Perrimon, N.; Rosenfeld, M. G.; Glass, C. K. *Mol. Cell* **2012**, *48*, 28 – 38.
- 70 Chang, K.-H.; King, O. N. F.; Tumber, A.; Woon, E. C. Y.; Heightman, T. D.; McDonough, M. A.; Schofield, C. J.; Rose, N. R. *ChemMedChem* **2011**, *6*, 759 – 764.
- 71 Horton, J. R.; Upadhyay, A. K.; Qi, H. H.; Zhang, X.; Shi, Y.; Cheng, X. *Nat. Struct. Mol. Biol.* **2010**, *17*, 38 – 43.
- 72 Berry, W. L.; Janknecht, R. *Cancer Res.* **2013**, *73*, 2936 – 2942.
- 73 Krishnan, S.; Trievel, R. C. *Structure* **2013**, *21*, 98 – 108.
- 74 Cloos, P. A.; Christensen, J.; Agger, K.; Maiolica, A.; Rappsilber, J.; Antal, T.; Hansen, K. H.; Helin, K. *Nature* **2006**, *442*, 307 - 311.
- 75 Hamada, S.; Kin, T.-D.; Suzuki, T.; Itoh, Y.; Tsumoto, H.; Nakagawa, H.; Janknecht, R.; Miyata, N. *Bioorg. Med. Chem. Lett.* **2009**, *19*, 2852 – 2855.
- 76 McDonough, M. A.; McNeill, L. A.; Tilliet, M.; Papamicael, C. A.; Chen, Q.-Y.; Banerji, B.; Hewitson, K. S.; Schofield, C. J. *J. Am. Chem. Soc.* **2005**, *127*, 7680 – 7681.
- 77 Rose, N. R.; Ng, S. S.; Mecinovic, J.; Lienard, B. M. R.; Bello, S. H.; Sun, Z.; McDonough, M. A.; Oppermann, U.; Schofield, C. J. *J. Med. Chem.* **2008**, *51*, 7053 – 7056.
- 78 Loenarz, C.; Rose, N. R.; Schofield, C. J.; Thalhammer, A.; Mecinovic, J.; Heightman, T. D.; Tumber, A. *Org. Biomol. Chem.* **2011**, *9*, 127 – 135.
- 79 King, O. N. F.; Li, X. S.; Sakurai, M.; Kawamura, A.; Rose, N. R.; Ng, S. S.; Quinn, A. M.; Rai, G., Mott; B. T.; Beswick, P.; Klose, R. J.; Oppermann, U.; Jadhav, A.; Heightman, T. D.; Maloney, D. J.; Schofield, C. J.; Simeonov, A. *PLoS ONE* **2010**, *5*, e15535 - e15535.
- 80 Kruidenier, L.; Chung, C.-W.; Cheng, Z.; Liddle, J.; Che, K.-H.; Joberty, G.; Bantscheff, M.; Bountra, C.; Bridges, A.; Diallo, H.; Eberhard, D.; Hutchinson, S.; Jones, E.; Katso, R.; Leveridge, M.; Mander, P. K.; Mosley, J.; Ramirez-Molina, C.; Rowland, P.; Schofield, C. J.; Sheppard, R. J.; Smith, J. E.; Swales, C.; Tanner, R.; Thomas, P.; Tumber, A.; Drewes, G.; Oppermann, U.; Patel, D. J.; Lee, K.; Wilson, D. M. *Nature* **2012**, *488*, 404 - 408.
- 81 Rose, N. R.; McDonough, M. A.; King, O. N. F.; Kawamura, A.; Schofield, C. J. *Chem Soc. Rev.* **2011**, 4364 – 4397.
- 82 Hamada, S.; Itoh, Y.; Miyata, N.; Nakagawa, H.; Ogasawara, D.; Ozasa, H.; Suzuki, T.; Tsumoto, H.; Suzuki, T.; Hasegawa, M.; Kato, A.; Komaarashi, H.; Koseki, K.; Mino, K.; Mizukami, T.; Flamme, I.; Oehme, F.; Sasaki, R. *J. Med. Chem.* **2010**, *53*, 5629 – 5638.
- 83 Luo, X.; Liu, Y.; Kubicek, S.; Myllyharju, J.; Tumber, A.; Ng, S.; Che, K. H.; Podoll, J.; Heightman, T. D.; Oppermann, U.; Scriber, S. L.; Wang, X. *J. Am. Chem. Soc.* **2011**, *133*, 9451 – 9456.

- 84 Fang, T. C.; Schaefer, U.; Mecklenbrauker, I.; Stienen, A.; Dewell, S.; Chen, M. S.; Rioja, I.; Parravicini, V.; Prinjha, R. K.; Chandwani, R.; MacDonald, M. R.; Lee, K.; Rice, C. M.; Tarakhovsky, A. *J. Exp. Med.* **2012**, *209*, 661 – 669.
- 85 Golding, A.; Rosen, A.; Petri, M.; Akhter, E.; Andrade F. *Immunology* **2010**, *131*, 107- 117.
- 86 Campbell, I. L.; Kay, T. W. H.; Oxbrow, L.; Harrison, L. C. *J. Clin. Invest.* **1991**, *87*, 739 – 742.
- 87 Schindler, U.; Beckmann, H.; Cashmore, A. R. *Plant J.* **1993**, *4*, 137 – 150.
- 88 Shin, S.; Janknecht, R. *Biochem. Bioph. Res. Co.* **2006**, *353*, 973 – 977.
- 89 Katoh, M.; Katoh, M. *Int. J. Oncol.* **2004**, *24*, 1623 – 1628.
- 90 Vanin, E. F. *Annu. Rev. Genet.* **1985**, *19*, 253 – 272.
- 91 Ozbal, C. C.; LaMarr, W. A.; Linton, J. R.; Green, D. F.; Katz, A.; Morrison, T. B.; Brenan, C. J. H. *Assay Drug Dev. Techn.* **2004**, *2*, 373 – 381.
- 92 Fitch, D. M.; Shaw, A. N.; Wigall, K. *Int. Patent* 150011, 15 October, **2013**.
- 93 Hopkins, A. L.; Groom, C. R.; Alex, A. *Drug Discov. Today* **2004**, *9*, 430 – 431.
- 94 Reynolds, C. H.; Tounge, B. A.; Bembenek, S. D. *J. Med. Chem* **2008**, *51*, 2432 – 2438.
- 95 Kuntz, I. D.; Chen, K.; Sharp, K. A.; Kollman, P. A. *Proc. Natl. Acad. Sci. USA* **1999**, *96*, 9997 – 10002.
- 96 Carr, R. A. E.; Congreve, M.; Murray, C. W., Rees, D. C. *Drug Discov. Today* **2005**, *10*, 987 – 992.
- 97 Alberts, B.; Johnson, A. Lewis, J.; Raff, M.; Roberts, K.; Walter, P. *Molecular Biology of the Cell*, 4th ed.; Chapter 11. Garland Science: New York, **2002**; pp 704 – 712
- 98 Gleeson, M. P. *J. Med. Chem.* **2008**, *51*, 817 – 834.
- 99 Zhu, C.; Jiang, L.; Chen, T.-M.; Hwang, K.-K. *Eur. J. Med. Chem.* **2002**, *37*, 399 -407.
- 100 Waring, M. J. *Bioorg. Med. Chem. Lett.* **2009**, *19*, 2844 – 2851.
- 101 Hughes, J. D.; Blagg, J.; Price, D. A.; Bailey, S.; DeCrescenzo, G. A.; Devraj, R. V.; Ellsworth, E.; Fobian, Y. M.; Gibbs, M. E.; Gilles, R. W.; Greene, N.; Huang, E.; Krieger-Burke, T.; Loesel, J.; Wager, T.; Whiteley, L.; Zhang, Y. *Bioorg. Med. Chem. Lett.* **2008**, *18*, 4872 – 4875.
- 102 Los, G. V.; Encell, L. P.; McDougall, M. G.; Hartzell, D. D.; Karassina, N.; Zimprich, C.; Wood, M. G.; Learish, R.; Ohana, R. F.; Urh, M.; Simpson, D.; Mendez, J.; Zimmerman, K.; Otto, P.; Vidugiris, G.; Zhu, J.; Darzins, A.; Klaubert, D. H.; Bulleit, R. F.; Wood, K. V. *ACS Chem. Biol.* **2008**, *3*, 373 – 382.
- 103 X-ray crystallography performed by Biomolecular Sciences, GSK Stevenage.
- 104 Substructure searching performed by Humphreys, P.
- 105 Malik, M. A.; Wani, M. Y.; Al-Thabaiti, S. A.; Shiekh, R. A. *J. Incl. Phenom. Macrocycl. Chem.* **2014**, *78*, 15 – 37.
- 106 Ballatore, C.; Huryn, D. M.; Smith, A. B. *ChemMedChem* **2013**, *8*, 385 – 395.
- 107 Farkas, E.; Enyedy, E. A.; Csoka, H. *Polyhedron* **1999**, *18*, 2391 – 2398.

- 108 O'Brien, E. C.; Farkas, E.; Gil, M. J.; Fitzgerald, D.; Castineras, A.; Nolan, K.B. *J. Inorg. Biochem.* **2000**, *79*, 47 – 51.
- 109 Asakawa, H.; Matano, M. *Chem. Pharm. Bull.* **1979**, *27*, 1287 – 1298.
- 110 Baldwin, J. E. *J. Chem. Soc., Chem. Commun.* **1976**, 734 – 736.
- 111 Montalbetti, C. A. G. N.; Falque, V. *Tetrahedron* **2005**, *61*, 10827 – 10852.
- 112 Valeur, E.; Bradley, M. *Chem. Soc. Rev.* **2009**, *38*, 606 – 631.
- 113 Sekikawa, I.; Nishie, J.; Tono-oka, S.; Tanaka, Y.; Kakimoto, S. *J. Het. Chem.* **1973**, *10*, 931 – 932.
- 114 McGaughey, G. B.; Gagne, M., Rappe, A. K. *J. Biol. Chem.* **1998**, *273*, 15458 – 15463.
- 115 Rodgers, M. T. *J. Phys. Chem. A.* **2001**, *105*, 8145 – 8153.
- 116 Epsztajna, J.; Jóźwiaka, A.; Szcześniaka, A. K. *Synth. Commun.* **1994**, *24*, 1789 – 1798.
- 117 Snieckus, V. *Chem. Rev.* **1990**, *90*, 879 – 933.
- 118 Amunugama, R.; Rodgers, M. T. *Int. J. Mass Spectrom.* **2000**, *195/196*, 439 – 457.
- 119 Albrecht, M.; Witt, K.; Frohlich, R.; Kataeva, O. *Tetrahedron* **2002**, *58*, 561 – 567.
- 120 Abraham, M. H.; Duce, P. P.; Prior, D. V. *J. Chem. Soc. Perkin Trans. II* **1989**, 1355 – 1375.
- 121 Khan, K. M.; Maharvi, G. M.; Choudhary, M. I.; Rahman, A.; Perveen, S. *J. Heterocyclic Chem.* **2005**, *42*, 1085 – 1093.
- 122 Gellibert, F.; Fouchet, M.-H.; Nguyen, V.-L.; Krysa, G.; de Gouville, A.-C.; Huet, S.; Dodic, N.; Wang, R. *Bioorg. Med. Chem. Lett.* **2009**, *19*, 2277 – 2281.
- 123 Kabri, Y.; Gellis, A.; Vanelle, P. *Eur. J. Org. Chem.* **2009**, 4059 – 4066.
- 124 Kostakis, I. K.; Elomri, A.; Seguin, E.; Iannelli, M.; Besson, T. *Tetrahedron Lett.* **2007**, *48*, 6609 – 6613.
- 125 Meredith, E. L.; Beattie, K.; Burgis, R.; Capparelli, M.I.; Dipietro, L.; Gamber, G.; Enyedy, I.; Hosagrahara, V.; Jewell, C.; Lee, W.; Miranda, K.; Rao, C.; Rozhitskaya, O.; Springer, C.; Vega, R. B.; Yan, W.; Zhu, Q.; Monovich, L. G.; Chapo, J.; Hood, D. B.; Koch, K. A.; Lemon, D. D.; Mckinsey, T. A.; Pagratis, N.; Phan, D.; Plato, C.; Soldermann, N.; Van Eis, M. *J Med. Chem.* **2010**, *53*, 5422 – 5438.
- 126 Gelling, I. R.; Wibberley, D. G. *J. Chem. Soc. (C)* **1969**, 931 – 934.
- 127 Shvedov, V. I.; Sycheva, T. P.; Sakovich, T. V. *Chem. Heterocycl. Compd.* **1979**, *15*, 1074 – 1077.
- 128 Allred, A. L. *J. Inorg. Nucl. Chem.* **1961**, *17*, 215 – 221.
- 129 True, J. E.; Thomas, T. D.; Winter, R. W.; Gard, G. L. *Inorg. Chem.* **2003**, *42*, 4437 – 4441.
- 130 Tanford, C. *The Hydrophobic Effect*, **1973**: Wiley, New York, Chapter 2.
- 131 Gleeson, M. P.; Hersey, A.; Montanari, D.; Overington, J. *Nat. Rev. Drug. Discov.* **2011**, *10*, 197 – 208.
- 132 Katritzky, A. R.; Pilarski, B.; Urogdi, L. *Synthesis* **1989**, 949 – 950.
- 133 Kukushkin, V. Y.; Pombeiro, A. J. L. *Inorg Chim Acta* **2005**, *358*, 1 – 21.

- 134 Muller, C. W.; Schlauderer, G. J.; Reinstein, J.; Schulz, G. E. *Structure* **1996**, *4*, 147 – 156.
- 135 Kempner, E. S. *FEBS Lett.* **1993**, *326*, 4 – 10.
- 136 Wissner, A.; Berger, D. M.; Boschelli, D. H.; Brawner, F.; Greenberger, L. M.; Gruber, B. C.; Johnson, B. D.; Mamuya, N.; Nilakantan, R.; Reich, M. F.; Shen, R.; Tsou, H.-W.; Upeslakis, E.; Wu, B.; Ye, F.; Wang, Y. F.; Zhang, N. *J. Med. Chem.* **2000**, *43*, 3244 – 3256.
- 137 Perrissin, M.; Favre, M.; Duc, C. L.; Huguet, F.; Gaultier, C.; Narcisse, G. *Eur. J. Med. Chem.* **1988**, *23*, 453 – 456.
- 138 Bauer, P. H.; Wright, S. W.; Schnur, R. C. *U.S. Patent* 144308, July 31, **2003**.
- 139 Kabri, Y.; Gellis, A.; Vanelle, P. *Eur. J. Org. Chem.* **2009**, *24*, 4059 – 4066.
- 140 Glide, version 5.5, Schrödinger Inc., New York, NY, **2009**.
- 141 Benfield, A. P.; Teresk, M. G.; Plake, H. R.; DeLorbe, J. E.; Millspaugh, L. E.; Martin, S. F. *Angew. Chem. Int. Ed.* **2006**, *45*, 6830 – 6835.
- 142 CCG *The Molecular Operating Environment (MOE)* **2012** [Windows XP] version 2012.10;
<http://www.chemcomp.com>.
- 143 Miyaura, N.; Yamada, K.; Suzuki, A. *Tetrahedron Lett.* **1979**, *36*, 3437 - 3440
- 144 Miyaura, N.; Suzuki, A. *Chem. Rev.* **1995**, *95*, 2457 – 2483.
- 145 Dick, G. R.; Woerly, E. M.; Burke, M. D. *Angew. Chem. Int. Ed.* **2012**, *51*, 2667 – 2672.
- 146 Schofield, C. J.; McDonough, M.; Rose, N.; Thalhammer, A. *Int. Patent* 043866, 22 April, **2010**.
- 147 Bakke, J. M.; Ranes E. *Synthesis*, **1997**, 281 – 283.
- 148 Bakke, J. M.; Riha, J. *J. Heterocyclic Chem.* **2001**, *38*, 99 – 104.
- 149 Fisher, R.; Lund, A. *Int. Patent* 059103, 8 June, **2006**.
- 150 Burgey, C. S.; Robinson, K. A.; Lyle, T. A.; Sanderson, P. E. J.; Lewis, D. S.; Lucas, B. J.; Krueger, J. A.; Singh, R.; Miller-Stein, C.; White, R. B.; Wong, Bradley; Lyle, E. A.; Williams, P. D.; Coburn, C. A.; Dorsey, B. D.; Barrow, J. C.; McDonough, C. M.; Stranieri, M. T.; Holahan, M. A.; Sitko, G. R.; Cook, J. J.; McMasters, D. R.; Sanders, W. M.; Wallace, A. A.; Clayton, F. C.; Bohn, D.; Leonard, Y. M.; Detwiler, T. J.; Lynch, J. J.; Yan, Y.; Chen, Z.; Kuo, L.; Gardell, S. J.; Shafer, J. A.; Vacca, J. P. *J. Med. Chem.* **2003**, *46*, 461 – 473.
- 151 Shen, H. C.; Ding, F.-X.; Wang, S.; Deng, Q.; Zhang, X.; Chen, Y.; Zhou, G.; Xu, Suoyu; Chen, H.-S.; Tong, X.; Tong, V.; Mitra, K.; Kumar, S.; Tsai, C.; Stevenson, A. S.; Pai, L.-Y.; Alonso-Galicia, M.; Chen, X.; Soisson, S. M.; Roy, S.; Zhang, B.; Tata, J. R.; Berger, J. P.; Colletti, S. L. *J. Med. Chem.* **2009**, *52*, 5009 - 5012
- 152 Fina, N. J.; Edawrds, J. O. *Int. J. Chem. Kin.* **1973**, *5*, 1 – 26.
- 153 Childs, B. J.; Craig, D. C.; Scudder, M. L.; Goodwin, H. A. *Aust. J. Chem.* **1999**, *52*, 673 – 680.
- 154 Escalante, J.; Flores, P.; Ortiz-Nava, C.; Priego, J. M.; Garcia-Martinez, C. *Molecules* **2007**, *12*, 173 – 182.

- 155 Carson, D. A.; Chao, Q.; Cottam, H. B.; Deng, L.; Genini, D.; Leoni, L. M.; Shih, H. *J. Med. Chem.* **1999**, *42*, 3860 – 3873.
- 156 Meyer, M. D.; Altenbach, R. J.; Bai, H.; Basha, F. Z.; Carroll, W. A.; Kerwin, J. F.; Lebold, S. A.; Lee, E.; Pratt, J. K.; Sippy, K. B.; Tietje, K.; Wendt, M. D.; Brune, M. E.; Buckner, S. A.; Hancock, A. A.; Drizin, I. *J. Med. Chem.* **2001**, *44*, 1971 – 1985.
- 157 Escalante, J.; Flores, P.; Priego, J. M. *Heterocycles* **2004**, *63*, 2019 - 2032
- 158 Bernabeu, M. C.; Diaz, J. L.; Jimenez, O.; Lavilla, R. *Synth. Comm.* **2004**, *34*, 137 – 149.
- 159 Notte, G. T.; Sammakia, T. *J. Am. Chem. Soc.* **2006** *128*, 4230 – 4231.
- 160 Gronowitz, S.; Liljefors, S. *Acta Chem. Scand. B* **1977**, *31*, 771 – 780.
- 161 Dosa, S.; Daniels, J.; Gutschow, M. *J. Heterocyclic Chem.* **2011**, *48*, 407 – 413.
- 162 Wright, J. A.; Yu, J.; Spencer, J. B. *Tetrahedron Lett.* **2001**, *42*, 4033 – 4036.
- 163 Iwamua, H.; Naka, T. *Int. Patent 51924*, 9 June, **2005**.
- 164 Deng, J. Z.; Paone, D. V.; Ginnetti, A. T.; Kurihara, H.; Dreher, S. D.; Weissman, S. A.; Stauffer, S. R.; Burgey, C. S. *Org. Lett.* **2009**, *11*, 345 – 347.
- 165 Knapp, D. M.; Gillis, E. P.; Burke, M. D. *J. Am. Chem. Soc.* **2009**, *131*, 6961 – 6963.
- 166 Kinzel, T.; Zhang, Y.; Buchwald, S. L. *J. Am. Chem. Soc.* **2010**, *132*, 14073 – 14075.
- 167 Murata, N.; Sugihara, T.; Kondo, Y.; Sakamoto, T. *Synlett.* **1997**, 298 – 300.
- 168 Adam, W.; Grimison, A.; Rodriguez, G. *Tetrahedron* **1967**, *23*, 2513 – 2521.
- 169 Kim, S.-H.; Rieke, R. D.; Slocum, T. B. *Synthesis* **2009**, *22*, 3823-3827.
- 170 Zhang, D.; Dufek, E. J.; Clennan, E. L. *J. Org. Chem.* **2006**, *71*, 315 – 319.
- 171 Do, H.-Q.; Fu, G. C.; Chandrashekar, E. R. R.; Fu, G. C. *J. Am. Chem. Soc.* **2013**, *135*, 16288 – 16291.
- 172 Jackson, R. W. *Tetrahedron Lett.* **2001**, *42*, 5163 – 5165.
- 173 Drewe, W. C.; Nanjunda, R.; Gunaratnam, M.; Beltran, M.; Parkinson, G. N.; Reszka, A. P.; Wilson, W. D.; Niedle, S. *J. Med. Chem.* **2008**, *51*, 7751 – 7767.
- 174 Luzung, M. R.; Patel, J. S.; Yin, J. *J. Org. Chem.* **2010**, *75*, 8330 – 8332.
- 175 Amb, C. M.; Rasmussen, S. C. *J. Org. Chem.* **2006**, *71*, 4696 – 4699.
- 176 Omura, K.; Swern, D. *Tetrahedron* **1978**, *34*, 1651 – 1660.
- 177 Mello, J. V.; Finney, N. S. *J. Am. Chem. Soc.* **2005**, *127*, 10124 – 10125.
- 178 Berlin, M.; Aslanian, R.; de Lera Ruiz, M.; McCormick, K. D. *Synthesis* **2007**, *16*, 2529 – 2533.
- 179 Calculations performed by Thomas, P.
- 180 Childs, B. J.; Craig, D. C.; Scudder, M. L.; Goodwin, H. A. *Aust. J. Chem.* **1999**, *52*, 673 – 680.
- 181 Cox, C. D.; Raheem, I. T.; Flores, B. A.; Whitman, D. B. *US Patent*, 29 December, **2011**.
- 182 Somers, F.; Ouedraogo, R.; Antoine, M.-H.; de Tullio, P.; Becker, B.; Fontaine, J.; Damas, J.; Dupont, L.; Rigo, B.; Delarge, J.; Lebrun, P.; Pirotte, B. *J. Med. Chem.* **2001**, *44*, 2575 – 2585.

- 183 Font, D.; Heras, M.; Villalgordo, J. M. *Synthesis* **2002**, 1833 – 1842.
- 184 Arkin, M. R.; Wells, J. A. *Nat. Rev. Drug Discov.* **2004**, *3*, 301 – 317.
- 185 Mullard, A. *Nat. Rev. Drug Discov.* **2012**, *11*, 173 – 175.
- 186 Wilson, A. J. *Chem. Soc. Rev.* **2009**, *38*, 3289 – 3300.
- 187 Scott, D. E.; Ehebauer, M. T.; Pukala, T.; Marsh, M.; Blundell, T. L.; Venkitaraman, A. R.; Abell, C.; Hyvonen, M. *ChemBioChem* **2013**, *14*, 332 – 342.
- 188 Clackson, T.; Wells, J. A. *Science* **1995**, *267*, 383 – 386.
- 189 Morelli, X.; Bourgeas, R.; Roche, P. *Curr. Opin. Chem. Biol.* **2011**, *15*, 475 – 481.
- 190 Lipinski, C. A. *Drug Discov. Today Tech.* **2004**, *1*, 337 – 341.
- 191 Rudin, C. M.; Hann, C. L.; Garon, E. B.; Ribeiro de Oliveira, M.; Bonomi, P. D.; Camidge, D. R.; Chu, Q.; Giaccone, G.; Khaira, D.; Ramalingam, S. S.; Ranson, M. R.; Dive, C.; McKeegan, E. M.; Chyla, B. J.; Dowell, B. L.; Chakravartty, A.; Nolan, C. E.; Rudersdorf, N.; Busman, T. A.; Mabry, M. H.; Krivoshik, A. P.; Humerickhouse, R. A.; Shapiro, G. I.; Gandhi, L. *Clin. Cancer Res.* **2012**, *18*, 3163 – 3169.
- 192 Biswas, S.; Killick, E.; Jochemsen, A. G.; Lunec, J. *Expert Opin. Investig. Drugs* **2014**, *23*, 629 – 645.
- 193 Vu, B.; Wovkulich, P.; Pizzolato, G.; Lovey, A.; Ding, Q.; Jiang, N.; Liu, J.-J.; Zhao, C.; Glenn, K.; Wen, Y.; Tovar, C.; Packman, K.; Vassilev, L.; Graves, B. *ACS Med. Chem. Lett.* **2013**, *4*, 466 – 469.
- 194 Strahl, B. D.; Allis, C. D. *Nature* **2000**, *403*, 41 – 45.
- 195 Tamkun, J. W.; Deuring, R.; Scott, M. P.; Kissinger, M. Pattatucci, A. M.; Kaufman, T. C.; Kennison, J. A. *Cell* **1992**, *68*, 561 – 572.
- 196 Dhalluin, C.; Carlson, J. E.; Zeng, L.; He, C.; Aggarwal, A. K.; Zhou, M.-M. *Nature* **1999**, *399*, 491 – 496.
- 197 Chung, C.; Tough, D. F. *Drug Discov. Today. Ther. Strat.* **2012**, *9*, e111 – e120.
- 198 Filippakopoulos, P.; Picaud, S.; Mangos, M.; Keates, T.; Lambert, J. P.; Barysytte-Lovejoy, D.; Felletar, I.; Volkmer, R.; Muller, S.; Pawson, T.; Gingras, A. C.; Arrowsmith, C. H.; Knapp, S. *Cell* **2012**, *149*, 214 – 231.
- 199 Hewings, D. S.; Rooney, T. P.C.; Jennings, L. E.; Hay, D. A.; Schofield, C. J.; Brennan, P. E.; Conway, S. J.; *J. Med. Chem.* **2012**, *55*, 9393 – 9413.
- 200 Chung, C.-W.; Dean, A. W.; Woolven, J. M.; Bamborough, P. *J. Med. Chem.* **2012**, *55*, 576 – 586.
- 201 Filippakopoulos, P.; Qi, J.; Picaud, S.; Shen, Y.; Smith, W. B.; Fedorov, O.; Morse, E. M. Keates, T.; Hickman, T. T.; Felletar, I.; Philpott, M.; Munro, S.; McKeown, M. R.; Wang, Y.; Christie, A. L.; West, N.; Cameron, M. J.; Schwartz, B.; Heightman, T. D.; La Thangue, N.; French, C. A.; Wiest, O.; Kung, A. L.; Knapp, S.; Bradner, J. E. *Nature* **2010**, *468*, 1067 – 1073.
- 202 Sanchez, R.; Zhou, M.-M. *Curr. Opin. Drug Discov. Devel.* **2009**, *12*, 659 – 665.
- 203 Bamborough, P. Personal communication.

- 204 Wu, S.-Y.; Chiang, C.-M. *J. Biol. Chem.* **2007**, *282*, 13141 – 13145.
- 205 Thompson, M. *Biochimie* **2009**, *91*, 309 – 319.
- 206 Filippakopoulos, P.; Picaud, S.; Mangos, M.; Keates, T.; Lambert, J.P.; Barsyte-Lovejoy, D.; Felletar, I.; Volkmer, R.; Muller, S.; Pawson, T.; Gingras, A.C.; Arrowsmith, C.H.; Knapp, S. *Cell* **2012**, *149*, 214 – 231.
- 207 Dorr, A.; Kiermer, V.; Pedal, A.; Rackwitz, H.-R.; Henklein, P.; Schubert, U.; Zhou, M.-M.; Verdin, E.; Ott, M. *EMBO J.* **2002**, *21*, 2715 – 2723.
- 208 Hassan, A. H.; Prochasson, P.; Neely, K. E.; Galasinski, S. C.; Chandy, M.; Carrozza, M. J.; Workman, J. L. *Cell* **2002**, *111*, 369 – 379.
- 209 Muller, S.; Filippakopoulos, P.; Knapp, S. *Expert Rev. Mol. Med.* **2011**, *13*, 1 – 21.
- 210 Philpott, M.; Yang, J.; Tumber, T.; Fedorov, O.; Uttarkar, S.; Filippakopoulos, P.; Picaud, S.; Keates, T.; Felletar, I.; Ciulli, A.; Knapp, S.; Heightman, T. D. *Mol. Biosyst.* **2011**, *7*, 2899 – 2908.
- 211 Zhou, Q.; Li, T.; Price, D. H. *Annu. Rev. Biochem.* **2012**, *81*, 119 – 143.
- 212 Schroder, S.; Cho, S.; Zeng, L.; Zhang, Q.; Kaehlcke, K.; Mak, L.; Lau, J.; Bisgrove, D.; Schnlzer, M.; Verdin, E.; Zhou, M.-M.; Ott, M. *J. Biol. Chem.* **2012**, *287*, 1090 – 1099.
- 213 Kalashnikova, E. V.; Revenko, A. S.; Gemo, A. T.; Andrews, N. P.; Tepper, C. G.; J Zou, J. X.; Cardiff, R. D.; Borowsky, A. D.; Chen, H.-W. *Cancer Res.* **2010**, *70*, 9402 – 9412.
- 214 Santer, F. R.; Höschele, P. P. S.; Oh, S. J.; Erb, H. H. H.; Bouchal, J.; Cavarretta, I. T.; Parson, W.; Meyers, D. J.; Cole, P. A.; Culig Z. *Mol. Cancer Ther.* **2011**, *10*, 1644 – 1655.
- 215 Roelfsema, J. H.; Peters, D. J. *Expert Rev. Mol. Med.* **2007**, *9*, 1 – 16.
- 216 Makino, S.; Kaji, R.; Ando, S.; Tomizawa, M.; Yasuno, K.; Goto, S.; Matsumoto, S.; Tabuena, M. D.; Maranon, E.; Dantes, M.; Lee, L. V.; Ogasawara, K.; Tooyama, I.; Akatsu, H.; Nishimura, M.; Tamiya, G. *Am. J. Hum. Genet.* **2007**, *80*, 393 – 406.
- 217 Aulchenko, Y. S.; Ripatti, S.; Lindqvist, I.; Boomsma, D.; Heid, I. M.; Pramstaller, P. P.; Penninx, B. W. J. H.; Janssens, A. C. J. W.; Wilson, J. F.; Spector, T.; Martin, N. G.; Pederson, N. L.; Kyvik, K. O.; Kaprio, J.; Hofman, A.; Freimer, N. B.; Jarvelin, M.-R.; Gyllensten, U.; Campbell, H.; Rudan, I.; Johansson, I.; Pattaro, C.; Wright, A.; Hastie, N.; Pichler, Hicks, A. A.; Falchi, M.; Willemsen, G.; Hottenga, J.-J.; de Geus, E. J.C.; Montgomery, G. W.; Whitfield, J.; Magnusson, P.; Saharinen, J.; Perola, M.; Silander, K.; Isaacs, A.; Sijbrands, E. J. G.; Uitterlinden, A. G.; Witteman, J. C. M.; Oostra, B. A.; Elliot, P.; Ruukonen, A.; Sabatti, C.; Gieger, C.; Meitinger, Kronenberg, F.; Doring, A.; Wichmann, H.-E.; Smit, J. H.; McCarthy, M. I.; van Duijn, C. M.; Peltonen, L. *Nat. Genet.* **2009**, *41*, 47 – 55.
- 218 Chidambaram, M.; Venkatesan, R.; Mohan, V. *Metabolism* **2010**, *59*, 1760 – 1766.
- 219 Lu, Y.; Feskens, E. J.; Boer, J. M.; Imholz, S.; Verschuren, W. M.; Wijmenga, C.; Vaarhost, A.; Slagboom, E.; Muller, M.; Dollé, M. E. *Atherosclerosis* **2010**, *213*, 200 – 205.

- 220 Mirguet, O.; Gosmini, R.; Toum, J.; Clement, C. A.; Barnathan, M.; Brusq, J.-M.; Mordaunt, J. E.; Grimes, R. M.; Crowe, M.; Pineau, O.; Ajakane, M.; Daugan, A.; Jeffrey, P.; Cutler, L.; Haynes, A. C.; Smithers, N. N.; Chung, C.-W.; Bamborough, P.; Uings, I. J.; Lewis, A.; Witherington, J.; Parr, N.; Prinjha, R. K.; Nicodeme, E. *J. Med. Chem.* **2013**, *56*, 7501 – 7515.
- 221 Bloch, D. B.; Nakajima, A.; Gulick, T.; Chiche, J.-D.; Orth, D.; de la Monte, S. M.; Bloch, K. D. *Mol. Cell Biol.* **2000**, *20*, 6138 – 6146.
- 222 Hu N.; Qiu, X.; Luo, Y.; Yuan, J.; Li, Y.; Lei, W.; Zhang, G.; Zhou, Y.; Su, Y.; Lu, Q. *J. Rheumatol* **2008**, *35*, 804 – 810.
- 223 Pimentel-Santos F. M.; Ligeiro, D.; Matos, M.; Mourão, A. F.; Costa, J.; Santos, H.; Barcelos, A.; Godinho, F.; Pinto, P.; Cruz, M.; Fonseca, J. E.; Guedes-Pinto, H.; Branco, J. C.; Brown, M. A.; Thomas, G. P. *Arthritis Res. Ther.* **2011**, *13*, R57.
- 224 Ford, E.; Thanos, D. *Biochim. Biophys. Acta* **2010**, *1799*, 328 – 336.
- 225 Mahdi, H. Benjamin A Fisher, B. A.; Källberg, H.; Plant, D.; Malmström, V.; Rönnelid, J.; Charles, P.; Ding, B.; Alfredsson, L.; Padyukov, L.; Symmons, D. P. M.; Venables, P. J.; Klareskog, L.; Lundberg, K. *Nat. Genet.* **2009**, *41*, 1319 – 1324.
- 226 Wang, L.; Pratt, J. K.; McDaniel, K. F.; Dal, Y.; Fidanze, S. D.; Hasvold, L.; Holms, J. H.; Kati, W. M.; Liu, D.; Mantei, R. A.; McClellan, W. J.; Pard, G. S. Wada, C. K. *Int. Patent* 097601, 4 July, **2013**.
- 227 Miyoshi, S., Ooike, S., Iwata, K., Hikawa, H. & Sugaraha, K. *Int. Patent* 084693, 26 Decemeber, **2009**.
- 228 Matzuk, M. M.; McKeown, M. R.; Filippakopoulos, P. Li, Q.; Ma, L.; Agno, J. E.; Lemieux, M. E.; Picaud, S.; Yu, R. N.; Qi, J.; Knapp, S.; Bradner, J. E. *Cell* **2012**, *150*, 673 – 684.
- 229 Nicodeme, E.; Jeffrey, K. L.; Schaefer, U.; Beinke, S.; Dewell, S.; Chung C.; Chandwani, R.; Marazzi, I.; Wilson, P.; Coste, H.; White, J.; Kirilovsky, J.; Rice, C. M.; Lora, J. M.; Prinjha, R. K.; Lee, K.; Tarakhovsky, A. *Nature* **2010**, *468*, 1119 – 1123.
- 230 Khmelnitsky, Y. L.; Mozhaev, V. V.; Cotterill, I. C.; Michels, P. C.; Boudjabi, S.; Khlebnikov, V.; Reddy, M. M.; Wagner, G. S.; Hansen, H. C. *Eur. J. Med. Chem.* **2013**, *64*, 121 – 128.
- 231 Bailey, D.; Jahagirdar, R.; Gordon, A.; Hafiane, A.; Cambell, S.; Chatur, S.; Wagner, G. S.; Hansen, H. C.; Chiacchia, F. S.; Johansson, J.; Krimbou, L.; Wong, N. C. W.; Genest, J. *J. Am. Coll. Cardiol.* **2010**, *55*, 2580 – 2589.
- 232 McNeill, E. *Curr. Opin. Investig. Drugs* **2010**, *11*, 357 – 364.
- 233 Filippakopoulos, P., Knapp, S. *Nat. Rev. Drug Discov.* **2014**, doi:10.1038/nrd4286
- 234 Dawson, M. A.; Kouzarides, T.; Huntly, B. J. P. *N. Eng. J. Med.* **2012**, *367*, 647 – 657.
- 235 Barter, P. J.; Nicholls, S.; Rye, K.; Anantharamaiah, G. M.; Navab, M.; Fogelman, A. M. *Circ. Res.* **2004**, *95*, 764 – 772.

- 236 Knapp, S. *Selective Targeting of Protein Interactions Mediated by Epigenetic Effector Domains*. Presented at SGC-DiscoverX Symposium, Oxford, UK, September 12, **2013**.
- 237 Zhang, G.; Plotnikov, A. N.; Rusinova, E.; Shen, T.; Morohashi, K.; Joshua, .; Zeng, L.; Mujtaba, S.; Ohlmeyer, M.; Zhou, M.-M. *J. Med. Chem.* **2013**, *56*, 9251 – 9264.
- 238 Fish, P. V.; Bish, G.; Bunnage, M. E.; Cook, A. S.; Owen, D. R.; Ralph, M. J.; Sciammetta, N.; Filippakopoulos, P.; Brennan, P. E.; Federov, O.; Knapp, S.; Marsden, B.; Philpott, M.; Picaud, S.; Gerstenberger, B. S.; Jones, H.; Nocka, K.; Primiano, M. J.; Trzupek, J. D.; Owen, D. R. *J. Med. Chem.* **2012**, *55*, 9831 - 9837.
- 239 Hay, D.; Fedorov, O.; Filippakopoulos, P.; Martin, S.; Philpott, M.; Picaud, S.; Hewings, D. S.; Uttakar, S.; Heightman, T. D.; Conway, S. J.; Knapp, S.; Brennan, P. E.; *Med. Chem. Commun.* **2013**, *4*, 140 – 144.
- 240 Garnier, J.-M.; Sharp, P. P.; Burns, C. J. *Expert Opin. Ther. Patents* **2014**, *24*, 185 – 199.
- 241 Vidler, L. R.; Filippakopoulos, P.; Fedorov, O.; Picaud, S.; Martin, S.; Tomsett, M.; Woodward, H.; Brown, N.; Knapp, S.; Hoelder, S. *J. Med. Chem.* **2013**, *56*, 8073 – 8088.
- 242 Picaud, S.; Wells, C.; Felletar, I.; Brotherton, D.; Martin, S.; Savitsky, P.; Diez-Dacal, B.; Philpott, M.; Bountra, C.; Lingard, H.; Fedorov, O.; Muller, S. Brennan, P. E.; Knapp, S.; Filippakopoulos, P. *Proc. Natl. Acad. Sci. U.S.A.* **2013**, *110*, 19754 – 19759.
- 243 Zeng, L.; Li, J.; Muller, M.; Yan, S.; Mujtaba, S.; Pan, C.; Wang, Z.; Zhou, M.-M. *J. Am. Chem. Soc.* **2005**, *127*, 2376 – 2377.
- 244 Sachchidanand; Silverman-Resnick, L.; Yan, S.; Mutjaba, S.; Liu, W.-J.; Zeng, L.; Manfredi, J. J.; Zhou, M.-M. *Chem. Biol.* **2006**, *13*, 81 – 90.
- 245 Filippakopoulos, P., Picaud, S., Felletar, I., Hay, D., Fedorov, O., Martin, S., Chaikuad, A., Von Delft, F., Brennan, P., Arrowsmith, C.H., Edwards, A.M., Bountra, C., Knapp, S. In press.
- 246 Hay, D. A.; Fedorov, O.; Martin, S. Singleton, D. C.; Tallant, C.; Wells, C.; Picaud, S.; Philpott, M.; Monteiro, O. P.; Rogers, C. M.; Conway, S. J.; Rooney, T. P. C.; Tumber, A.; Yapp, C.; Filippakopoulos, P.; Bunnage, M. E.; Müller, S. Knapp, S.; Schofield, C. J.; Brennan, P. E. *J. Am. Chem. Soc.* **2014**, *136*, 9308 – 9319.
- 247 Borah, J. C.; Mujtaba, S.; Karakikes, I.; Zeng, L.; Muller, M.; Patel, J.; Moshkina, N.; Morohashi, K.; Zhang, W.; Gerona-Navarro, G.; Hajjar, R. J.; Zhou, M.-M. *Chem. Biol.* **2011**, *18*, 531 – 541.
- 248 Chaikuad, A., Felletar, I., Chung, C.W., Drewry, D., Chen, P., Filippakopoulos, P., Fedorov, O., Krojer, T., von Delft, F., Arrowsmith, C.H., Edwards, A.M., Bountra, C., Knapp, S. In press
- 249 Fedorov, O.; Lingard, H.; Wells, C.; Monteiro, O. P.; Picaud, S.; Keates, T.; Yapp, C.; Philpott, M.; Martin, S.J.; Felletar, I.; Marsden, B. D.; Filippakopoulos, P.; Müller, S.; Knapp, S.; Brennan, P. E. *J. Med. Chem.* **2014**, *57*, 462 - 476.

- 250 Salcius, M.; Bauer, A. J.; Hao, Q.; Li, S.; Tutter, A.; Raphael, J.; Jahnke, W.; Rondeau, J.-M.; Bourgier, E.; Tallarico, J.; Michaud, G. A. *J. Biomol. Screen.* **2014**, *19*, 917 – 927.
- 251 Yang, X.-J.; Ogryzko, V. V.; Nishikawa, J.-I.; Howard, B. H.; Nakatani, Y. *Nature* **1996**, *382*, 319 – 324.
- 252 Vassilev, A.; Yamauchi, J.; Kotani, T.; Prives, C.; Avantaggiati, M. L.; Qin, J.; Nakatani, Y. *Mol. Cell* **1998**, *2*, 869 – 875.
- 253 Linares, L. K.; Kiernan, R.; Triboulet, R.; Chable-Bessa, C.; Latrielle, D.; Cuvier, O.; Lacroix, M.; Le Cam, L.; Coux, O. Benkirane, M. *Nat. Cell Biol.* **2007**, *9*, 331 – 338.
- 254 Schiltz, R. L.; Nakatani, Y. *Biochim Biophys Acta* **2000**, *1470*, M37 – M53.
- 255 Tora, L.; Nagy, Z. *Oncogene* **2007**, *26*, 5341 – 5357.
- 256 Modak, R.; Basha, J.; Bharathy, N.; Maity, K.; Mizar, P.; Bhat, A. V.; Vasudevan, M.; Rao, V. K.; Kok, W. K.; Natesh, N.; Taneja, Kundu, T. K. *ACS Chem. Biol.* **2013**, *8*, 1311 – 1323.
- 257 Roth, S. Y.; Denu, J. M.; Allis, C. D. *Annu. Rev. Biochem.* **2001**, *70*, 81 – 120.
- 258 Stimson, L.; Rowlands, M. G.; Newbatt, Y. M.; Smith, N. F.; Raynaud, F. I.; Rogers, P.; Bavetsias, V.; Gorsuch, S.; Jarman, M.; Bannister, A.; Kouzarides, T.; McDonald, E.; Workman, P.; Aherne, G. W. *Mol. Cancer Ther.* **2005**, *4*, 1521 – 1532.
- 259 Masumi, A.; Wang, I.-M.; Lefebvre, B.; Yang, X.-J.; Nakatani, Y.; Ozato, K. *Mol. Cell Biol.* **1999**, *19*, 1810 – 1820.
- 260 Blanco, J. C. G.; Minucci, S.; Lu, J.; Yang, X.-J.; Walker, K. K.; Chen, H.; Evans, R. M.; Nakatani, Y.; Ozato, K. *Genes & Dev.* **1998**, *12*, 1638 – 1651.
- 261 Nagy, Z.; Tora, L. *Oncogene* **2007**, *26*, 5341 – 5357.
- 262 Marmorstein, R.; Berger, S. L. *Gene* **2001**, *272* 1 – 9.
- 263 Wu, C.; Orozco, C.; Boyer, J.; Leglise, M.; Goodale, J.; Batalov, S.; Hodge, C. L.; Haase, J.; Janes, J.; Huss, J. W.; Su, A. I. *Genome Biol.* **2009**, *10*, R130.1 – R130.8.
- 264 Su, A. I.; Wiltshire, T.; Batalov, S.; Lapp, H.; Ching, K. A.; Block, D.; Zhang, J.; Soden, R.; Hayakawa, M.; Kreiman, G.; Cooke, M. P.; Walker, J. R.; Hogenesch, J. B. *P. Natl. Acad. Sci. U.S.A.*, **2004**, *101*, 6062 – 6067.
- 265 Pan, C.; Mezei, M.; Mujtaba, S.; Muller, M.; Zeng, L.; Li, J.; Wang, Z.; Zhou, M.-M. *J. Med. Chem.* **2007**, *50*, 2285 – 2288.
- 266 Wang, Q.; Wang, R.; Zhang, B.; Zhang, S.; Zheng, Y.; Wang, Z. *Med. Chem. Comm.* **2013**, *4*, 737 – 740.
- 267 Zhou, M.-M.; Ohl-Meyer, M.; Mujtaba, S.; Plotnikov, A.; Kastriusky, D.; Zhang, G. Borah, J. *Int. Patent* 116170 A1 23 February, **2012**.
- 268 Lea, W. A.; Simeonov, A. *Expt. Opin. Drug Discov.* **2011**, *6*, 17 – 32.

- 269 Degorce, F.; Card, A.; Soh, S.; Trinquet, E.; Knapik, G. P.; Xie, B. *Curr. Chem. Genom.* **2009**, *3*, 22 – 32.
- 270 Panchuk-Voloshina, N.; Haugland, R. P.; Bishop-Stewart, J.; Bhalgat, M. K.; Millard, P. J.; Mao, F.; Leung, W.-Y.; Haugland, R. P. *J. Histochem. Cytochem.* **1999**, *47*, 1179 – 1188.
- 271 Cheng, Y.-C.; Prusoff, W. H. *Biochem. Pharmacol.* **1973**, *22*, 3099 – 3108.
- 272 Lui, X.; Testa, B.; Fahr, A. *Pharm. Res.* **2011**, *28*, 962 – 977.
- 273 van Braun, J. *Ber. Dtsch. Chem. Ges.* **1923**, *56*, 2332 – 2343.
- 274 Ishikawa, M.; Hasimoto, Y. *J. Med. Chem.* **2011**, *54*, 1539 – 1554.
- 275 CCG *The Molecular Operating Environment (MOE)* **2012** [Windows XP] version 2012.10;
<http://www.chemcomp.com>.
- 276 Prime, M. E.; Courtney, S. M.; Brookfield, F. A.; Marston, R. W.; Walker, V.; Warne, J.; Boyd, A. E.; Kairies, N. A.; von der Saal, W.; Limberg, A.; Georges, G.; Engh, R. A.; Goller, B.; Rueger, P.; Rueth, M. *J. Med. Chem.* **2011**, *54*, 312 – 319.
- 277 Prime, M. E.; Courtney, S. M.; Brookfield, F. A.; Marston, R. W.; Walker, V.; Warne, J.; Boyd, A. E.; Kairies, N. A.; von der Saal, W.; Limberg, A.; Georges, G.; Engh, R. A.; Goller, B.; Rueger, P.; Rueth, M. *J. Med. Chem.* **2011**, *54*, 312 – 319.
- 278 Sugimoto, A.; Sakamoto, K.; Fujino, Y.; Takashima, Y.; Ishikawa, M. *Chem. Pharm. Bull.* **1985**, *33*, 2809 – 2820.
- 279 Fischer, E.; Speier, A. *Ber. Dtsch. Chem. Ges.* **1895**, *28*, 3252 – 3258.
- 280 Mitsunobu, O.; Yamada, M.; Mukaiyama, T. *Bull. Chem. Soc.* **1967**, *40*, 935 – 939.
- 281 Curtius, T. *Ber. Dtsch. Chem. Ges.* **1890**, *23*, 3023 – 3033.
- 282 Wacker, D. A.; Rossi, K. A.; Wang, Y.; Wu, G. *Int. Patent* 009183 A1 21 Jan, **2008**.
- 283 Saga, Y.; Motoki, R.; Makino, S.; Shimizu, Y.; Kanai, M.; Shibasaki, M. *J. Am. Chem. Soc.* **2010**, *132*, 7905 – 7907.
- 284 Böhm, H.-J.; Banner, D.; Bendels, S.; Kansy, M.; Kuhn, B.; Müller, K. Obst-Sander, U.; Stahl, M. *ChemBioChem* **2004**, *5*, 637 – 643.
- 285 Milbank, J. B. J.; Tercel, M.; Atwell, G. J.; Wilson, W. R.; Hogg, A.; Denny, W. A. *J. Med. Chem.* **1999**, *42*, 649 – 658.
- 286 Bavetsias, V.; Skelton, L. A.; Yafai, F.; Mitchell, F.; Wilson, S. C.; Allan, B.; Jackman, A. L. *J. Med. Chem.* **2002**, *45*, 3692 – 3702.
- 287 Ezquerra, J.; Pedregal, C.; Lamas, C. *J. Org. Chem.* **1996**, *61*, 5804-5812.
- 288 Barluenga, J.; Campos, P. J.; Gonzalez, J. M.; Suarez, J. L.; Asensio, G. *J. Org. Chem.* **1991**, *56*, 2234.
- 289 Koreeda, T.; Kochi, T.; Kakiuchi, F. *J. Am. Chem. Soc.* **2009**, *131*, 7238 – 7239.
- 290 Zysman-Colman, E.; Arias, K.; Siegel, J. S. *Can. J. Chem.* **2009**, *87*, 440 – 447.
- 291 Molander, G. A.; Sandrock, D. L.; *Org. Lett.* **2007**, *9*, 1597 – 1600.

- 292 McQueen, A. J.; Green, C.; Butlin, R. J.; Graeme, R. R.; Wood, J. M.; McCoull, W. *Int. Patent* 047558, 16 April, **2009**.
- 293 Ritchie, T. J.; Macdonald, D. J. F. *Drug Discov. Today* **2009**, *14*, 1011 – 1020.
- 294 Young, R. J.; Green, D. V. S.; Luscombe, C. N.; Hill A. P. *Drug Discov. Today* **2011**, *16*, 822 – 830.
- 295 Polonka-Balint, A.; Saraceno, C.; Matyus, P.; Ludanyi, K.; Benyei, A. *Synlett* **2008**, 2846 – 2850.
- 296 Betti, L.; Corelli, F.; Floridi, M.; Giannaccini, G.; Maccari, L.; Manetti, F.; Stappaghetti, G.; Botta, M. *J. Med. Chem.* **2003**, *46*, 3555 – 3558.
- 297 Varga, I.; Jerkovich, G.; Matyus, P. *J. Het. Chem.* **1991**, *28*, 493 – 496.
- 298 Kaji, K.; Nagashima, H.; Oda, H. *Chem. Pharm. Bull.* **1984**, *32*, 1423 – 1432.
- 299 Atkins, P. W. *The Elements of Physical Chemistry*, 2nd ed.; Oxford University Press: Oxford, U.K., **1996**; pp 356.
- 300 Vega, A.; Alonso, J.; Diaz, J. A.; Junquera, F.; Perez, C.; Darias, V.; Bravo, L.; Abdallah, S. *Eur. J. Med. Chem.* **1991**, *26*, 323 – 329.
- 301 Lim, C. J.; Kim, S. H.; Lee, B. H.; Oh, K.-S.; Yi, K. Y. *Bioorg. Med. Chem. Lett.*, **2012**, *22*, 427 – 430.
- 302 Huang, D.; Wang, H.; Xue, F.; Guan, H.; Li, L.; Peng, X.; Shi, Y. *Org. Lett.* **2011**, *13*, 6350 – 6353.
- 303 Bernal, I.; Levendis, D. C.; Fuchs, R.; Reisner, G. M.; Cassidy, J. M. *Struct. Chem.* **1997**, *8*, 275 – 285.
- 304 Purohit, A.; Radeke, H.; Azure, M.; Hanson, K.; Su, F.; Yu, M.; Hayes, M.; Guaraldi, M.; Kagan, M.; Robinson, S.; Casebier, D.; Benetti, R.; Yalamanchili, P. *J. Med. Chem.* **2008**, *51*, 2954 – 2970.
- 305 Biscoe, M. R.; Fors, B. P.; Buchwald, S. L. *J. Am. Chem. Soc.* **2008**, *130*, 6686 – 6687.
- 306 Grignard, V. *C. R. Hebd. Acac. Sci.* **1900**, 1322 – 1324.
- 307 Paul, F.; Patt, J.; Hartwig, J. F. *J. Am. Chem. Soc.* **1994**, *116*, 5969–5970.
- 308 Lee, H.-G.; Kim, M.-J.; Lee, I.-H.; Kim, E. J.g; Kim, B. R.; Yoon, Y.-J. *B. Kor. Chem. Soc.* **2010**, *31*, 1061 – 1063.
- 309 Edben, M. R.; Simpkins, N. S.; Fox, D. N. A. *Tetrahedron*, **1998**, *54*, 12923-12952
- 310 Betschmann, P.; Carroll, W. A.; Ericsson, A. M.; Fix-Stenzel, S. R.; Friedman, M.; Hirst, G. C.; Josephson, N. S.; Li, B.; Perez-Medrano, A.; Morytko, M. J.; Rafferty, P. *US Patent* 015192, 10 January, **2008**.
- 311 Woodward, R. B.; Doering, W. E. *J. Am. Chem. Soc.* **1945**, *67*, 860 – 874.
- 312 Surry, D. S.; Buchwald, S. L. *Chem. Sci.* **2011**, *2*, 27 – 50.
- 313 Feng, S.; Panetta, C. A.; Graves, D. E. *J. Org. Chem.* **2001**, *66*, 612 – 616.
- 314 Koshio, H.; Hirayama, F.; Ishihara, T.; Shiraki, R.; Shigenaga, T.; Taniuchi, Y.; Sato, K.; Moritani, Y.; Iwatsuki, Y.; Kaku, S.; Katayama, N.; Kawasakia, T.; Matsumotoa, Y.; Sakamotoc, S.; Tsukamoto, S. *Bioorg. Med. Chem.* **2005**, *13*, 1305 – 1323.
- 315 Assay generation performed by Biological Sciences, GSK Stevenage.

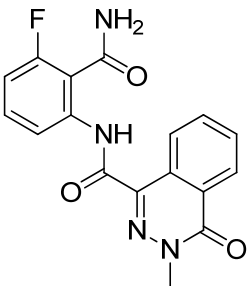
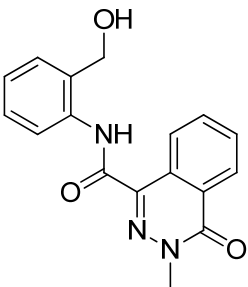
- 316 Chemoproteomic experiments performed by Cellzome (GSK), Heidelberg, Germany.
- 317 Garnier, E.; Audoux, J.; Pasquinet, E.; Suzenet, F.; Poullain, D.; Lebret, B.; Guillaumet, G. *J. Org. Chem.* **2004**, *69*, 7809 – 7815.
- 318 Marlow, A. L.; Wallace, E.; Seo, J.; Lyssikatos, J. P.; Yang, H. W.; Blake, J.; Storey, R. A.; Booth, R. J.; Pittam, J. D.; Leonard, J.; Fielding, M. R. *Int. Patent* 044084, 19 April, **2007**.
- 319 Fitton, P.; Rick, E. A. *J. Organomet. Chem.* **1971**, *28*, 287 – 291.
- 320 Krajsovsky, G.; Karolyhazy, L.; Reidl, Z.; Csampai, A.; Dunkel, P.; Lerner, A.; Dajka-Halasz, B.; Hajos, G.; Matyus, P. *J. Mol. Struct. (THEOCHEM)* **2005**, *713*, 235 – 243.
- 321 Andrews, P. R.; Craik, D. J.; Martin, J. L. *J. Med. Chem.* **1984**, *27*, 1648 – 1657.
- 322 Hann, M. M.; Leach, A. R.; Harper, G. *J. Chem. Inf. Comput. Sci.* **2001**, *41*, 856 – 864.
- 323 Atkins, P. W. *Physical Chemistry*, 6th Ed.; Oxford University Press: Oxford, U.K., 2000.
- 324 Stephens, P. J. *J. Phys. Chem.* **1985**, *85*, 748 – 752.
- 325 Buckingham, A. D.; Fowler, P. W.; Galwas, P. A. *Chem. Phys.* **1987**, *112*, 1 – 14.
- 326 VCD experiments and calculation performed by Minick, D.
- 327 Biel, M.; Kretsovali, A.; Karatzali, E.; Papamatheakis, J.; Giannis, A. *Angew. Chem. Int. Ed.* **2004**, *43*, 3974 – 3976.
- 328 Cheng, K.-C.; Li, C.; Uss, A. S. *Expert Opin. Drug Metab. Toxicol.* **2008**, *4*, 581 – 590.
- 329 Auld, D. S.; Thorne, N.; Maguire, W. F.; Inglese, J. *Proc. Natl. Acad. Sci. U.S.A.* **2009**, *106*, 3585 – 3590.
- 330 Guha, M. *Nat. Biotechnol.* **2011**, *29*, 373 – 374.
- 331 Sugano, K.; Kansy, M.; Artursson, P.; Avdeef, A.; Bendels, S.; Di, L.; Ecker, G. F.; Faller, B.; Fischer, H.; Gerebtzoff, G.; Lennernaes, H.; Senner, F. *Nat. Rev. Drug Discov.* **2010**, *9*, 597 – 614.
- 332 Veach, D. R.; Namavari, M.; Pillarsetty, N.; Santos, E. B.; Beresten-Kochetkov, T.; Lambek, C.; Punzalan, B. J.; Antczak, C.; Smith-Jones, P. M.; Djaballah, H.; Clarkson, B.; Larson, Steven M. *J. Med. Chem.* **2007**, *50*, 5853 – 5857.
- 333 Leeson, P. D.; Springthorpe, B. *Nat. Rev. Drug Discov.* **2007**, *6*, 881 – 890.
- 334 Deutch, C.; Taylor, J. S.; Wilson, D. F. *Proc. Natl. Acad. Sci. U.S.A.* **1982**, *79*, 7944 – 7948.
- 335 Schlosser, M.; Michel, D. *Tetrahedron* **1996**, *52*, 99 – 108.
- 336 Atkins, P. W. *The Elements of Physical Chemistry*, 2nd Ed.; Chapter 9.6; Oxford University Press: Oxford, U.K., **1996**.
- 337 Docking by Hussein, J.
- 338 Santagati, N. A.; Duro, F.; Caruso, A.; Trombadore, S.; Amico-Roaxas, M. *Farmaco Sci.* **1985**, *40*, 921 – 929.
- 339 Price, D. A.; Blagg, J.; Jones, L.; Greene, N.; Wager, T. *Expert Opin. Drug Metab. Toxicol.* **2009**, *5*, 921 – 931.

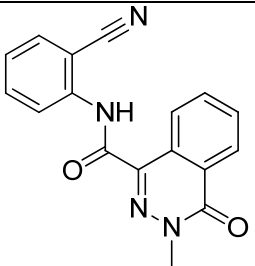
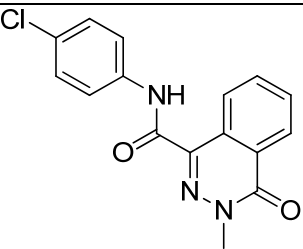
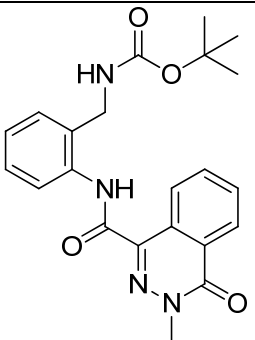
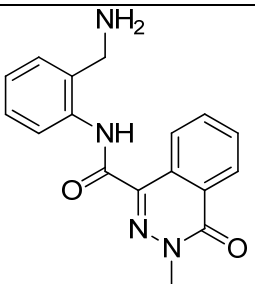
- 340 Lovering, F. *Med. Chem. Commun.* **2013**, *4*, 515 – 519.
- 341 Boute, N.; Jockers, R.; Issad, T. *Trends Pharmacol. Sci.* **2002**, *23*, 351 – 354.
- 342 O'Mahony, A.; Treiber, D. *Novel Assays and Human Model Systems for Epigenetic Drug Discovery*, Presented at SGC-DiscoverX Symposium, Oxford, UK, September 12, **2013**.
- 343 Forbes, S. A.; Bhamra, G.; Bamford, S.; Dawson, E.; Kok, C.; Clements, J.; Menzies, A.; Teague, J. W.; Futreal, P. A.; Stratton, M. R. *Current Protocols in Human Genetics*; John Wiley & Sons: Chicester, U.K. **2008**; Unit 10.11.

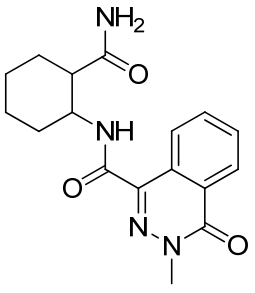
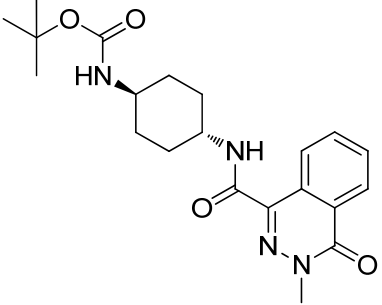
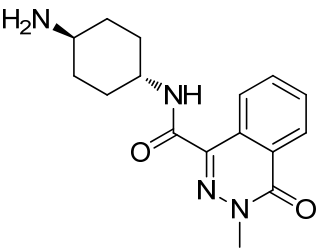
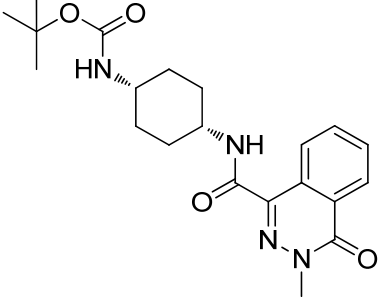
Appendix A Phthalizinone amide compounds

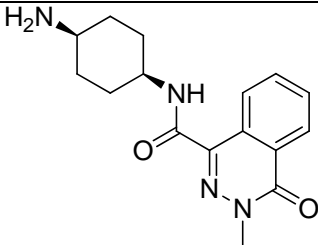
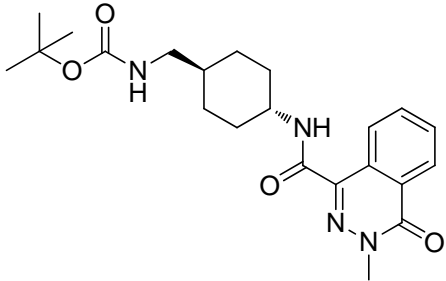
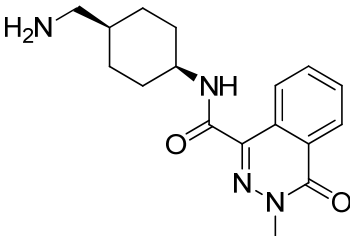
Removal of Boc groups *General method D.*

A solution of 5 M HCl in IPA was added to the starting material and heated to 80 °C for 1 h. The reaction mixture was cooled, sufficient MeOH added to form a solution and the solution loaded on to an SCX cartridge. The cartridge was eluted with MeOH followed by a solution of 2 M methanolic ammonia. The basic fractions were evaporated *in vacuo* to give the title compounds.

Number	Structure	General method used	Analytical data
A.001	 <p>Chemical Formula: C₁₇H₁₃FN₄O₃ Molecular Weight: 340.31</p>	A	¹ H NMR (SO(CD ₃) ₂ , 400 MHz) δ 11.79 (s, 1H), 9.09 - 9.00 (m, 1H), 8.38 - 8.30 (m, 2H), 8.21 (br.s, 1H), 8.15 (br.s, 1H), 8.04 - 7.97 (m, 1H), 7.96 - 7.90 (m, 1H), 7.57 (td, J = 6.5, 8.5 Hz, 1H), 7.15 - 7.06 (m, 1H), 3.85 (s, 3H); LRMS [M+H] ⁺ : 341, 96% a/a.
A.002	 <p>Chemical Formula: C₁₇H₁₅N₃O₃ Molecular Weight: 309.32</p>	A	¹ H NMR (SO(CD ₃) ₂ , 400 MHz) δ 10.74 (br.s, 1H), 8.92 (d, J = 8.0 Hz, 1H), 8.35 (dd, J = 1.0, 8.0, 1H), 8.06 - 7.96 (m, 2H), 7.95 - 7.89 (m, 1H), 7.42 - 7.31 (m, 2H), 7.17 (td, J = 1.0, 7.5 Hz, 1H), 5.70 (br.s, 1H), 4.65 (s, 2H), 3.84 (s, 3H); LRMS [M+H] ⁺ : 310, 99% a/a.

A.003	 <p>Chemical Formula: C₁₇H₁₂N₄O₂ Molecular Weight: 304.30</p>	A ¹ H NMR (SO(CD ₃) ₂ , 400 MHz) δ 10.82 (s, 1H), 8.74 (d, <i>J</i> = 9.0 Hz, 1H), 8.36 (dd, <i>J</i> = 1.0, 9.0 Hz, 1H), 8.00 (td, <i>J</i> = 1.5, 7.5 Hz, 1H), 7.97 - 7.90 (m, 2H), 7.82 - 7.75 (m, 2H), 7.49 - 7.43 (m, 1H), 3.87 (s, 3H); LRMS [M+H] ⁺ : 305, 100% a/a.
A.004	 <p>Chemical Formula: C₁₆H₁₂ClN₃O₂ Molecular Weight: 313.74</p>	C ¹ H NMR (SO(CD ₃) ₂ , 400 MHz) δ 10.74 (s, 1H), 8.51 (d, <i>J</i> = 8.0 Hz, 1H), 3.85 (dd, <i>J</i> = 1.0, 7.5 Hz, 1H), 8.03 - 7.88 (m, 2H), 7.88 - 7.80 (m, 2H), 7.49 - 7.42 (m, 2H), 3.85 (s, 3H); LRMS [M+H] ⁺ : 314, 100% a/a.
A.005	 <p>Chemical Formula: C₂₂H₂₄N₄O₄ Molecular Weight: 408.45</p>	C ¹ H NMR (SO(CD ₃) ₂ , 400 MHz) δ 10.50 (br.s, 1H), 8.73 (d, <i>J</i> = 8.0 Hz, 1H), 8.35 (dd, <i>J</i> = 1.0, 8.0 Hz, 1H), 8.02 - 7.88 (m, 2H), 7.66 (d, <i>J</i> = 7.5 Hz, 1H), 7.55 - 7.40 (m, 1H), 7.38 - 7.30 (m, 2H), 7.29 - 7.21 (m, 1H), 4.18 (d, <i>J</i> = 6.0 Hz, 2H), 3.87 (s, 3H), 1.35 (s, 9H); LRMS [M+H] ⁺ : 409, 100% a/a.
A.006	 <p>Chemical Formula: C₁₇H₁₆N₄O₂ Molecular Weight: 308.33</p>	D ¹ H NMR (SO(CD ₃) ₂ , 400 MHz) δ 8.96 (d, <i>J</i> = 8.0 Hz, 1H), 8.35 (d, <i>J</i> = 8.0 Hz, 1H), 8.17 (d, <i>J</i> = 8.0 Hz, 1H), 8.03 - 7.95 (m, 1H), 7.95 - 7.88 (m, 1H), 7.35 - 7.24 (m, 2H), 7.12 - 7.05 (m, 1H), 3.91 (s, 2H), 3.85 (s, 3H), exchangeable protons not observed; LRMS [M+H] ⁺ : 309, 99% a/a.

<p>A.007</p>	 <p>Chemical Formula: C₁₇H₂₀N₄O₃ Molecular Weight: 328.37</p>	<p>C</p> <p>¹H NMR (SO(CD₃)₂, 400 MHz) δ 8.61 (d, <i>J</i> = 8.0 Hz, 1H), 8.42 (d, <i>J</i> = 8.5 Hz, 1H), 8.30 (dd, <i>J</i> = 8.0, 1.0 Hz, 1H), 7.98 - 7.83 (m, 2H), 7.36 (br.s, 1H), 6.94 (br.s, 1H), 4.30 - 4.20 (m, 1H), 3.76 (s, 3H), 2.61 (dt, <i>J</i> = 4.0, 8.0 Hz, 1H), 2.09 - 1.97 (m, 1H), 1.95 - 1.82 (m, 1H), 1.67 - 1.30 (m, 6H); LRMS [M+H]⁺: 329, 100% a/a.</p>
<p>A.008</p>	 <p>Chemical Formula: C₂₁H₂₈N₄O₄ Molecular Weight: 400.47</p>	<p>C</p> <p>¹H NMR (SO(CD₃)₂, 400 MHz) δ 8.51 (d, <i>J</i> = 8.0 Hz, 1H), 8.43 (d, <i>J</i> = 7.5 Hz, 1H), 8.30 (dd, <i>J</i> = 1.0, 8.0 Hz, 1H), 7.97 - 7.86 (m, 2H), 6.74 (br.d, <i>J</i> = 8.0 Hz, 1H), 3.78 (s, 3H), 3.76 - 3.67 (m, 1H), 3.26 - 3.15 (m, 1H), 1.93 - 1.79 (m, 4H), 1.49 - 1.37 (m, 11H), 1.33 - 1.22 (m, 2H); LRMS [M+H]⁺: 401, 100% a/a.</p>
<p>A.009</p>	 <p>Chemical Formula: C₁₆H₂₀N₄O₂ Molecular Weight: 300.36</p>	<p>D</p> <p>¹H NMR (SO(CD₃)₂, 400 MHz) δ 8.46 (d, <i>J</i> = 8.0 Hz, 1H), 8.42 (d, <i>J</i> = 7.5 Hz, 1H), 8.30 (dd, <i>J</i> = 1.0, 7.5 Hz, 1H), 7.98 - 7.84 (m, 2H), 3.80 - 3.67 (m, 4H), 2.57 - 2.52 (m, 1H), 1.91 - 1.75 (m, 4H), 1.52 (br.s, 2H), 1.43 - 1.31 (m, 2H), 1.20 - 1.06 (m, 2H); LRMS [M+H]⁺: 301, 100% a/a.</p>
<p>A.010</p>	 <p>Chemical Formula: C₂₁H₂₈N₄O₄ Molecular Weight: 400.47</p>	<p>C</p> <p>¹H NMR (SO(CD₃)₂, 400 MHz) δ 8.42 (d, <i>J</i> = 8.0 Hz, 1H), 8.35 - 8.28 (m, 2H), 7.99 - 7.86 (m, 2H), 6.67 (br.s, 1H), 3.95 - 3.84 (m, 1H), 3.79 (s, 3H), 3.52 - 3.40 (m, 1H), 1.80 - 1.52 (m, 8H), 1.39 (s, 9H); LRMS [M+H]⁺: 401, 97% a/a.</p>

<p>A.011</p>	 <p>Chemical Formula: C₁₆H₂₀N₄O₂ Molecular Weight: 300.36</p>	<p>D</p> <p>¹H NMR (SO(CD₃)₂, 400 MHz) δ 8.46 - 8.34 (m, 2H), 8.31 (d, J = 8.5 Hz, 1H), 8.00 - 7.84 (m, 2H), 3.95 - 3.84 (m, 1H), 3.78 (s, 3H), 2.92 - 2.83 (m, 1H), 1.86 - 1.72 (m, 2H), 1.65 - 1.39 (m, 8H); LRMS [M+H]⁺: 301, 98%.</p>
<p>A.012</p>	 <p>Chemical Formula: C₂₂H₃₀N₄O₄ Molecular Weight: 414.50</p>	<p>C</p> <p>¹H NMR (SO(CD₃)₂, 400 MHz) δ 8.48 (d, J = 8.0 Hz, 1H), 8.43 (d, J = 7.5 Hz, 1H), 8.31 (dd, J = 1.0, 8.0 Hz, 1H), 7.97 - 7.85 (m, 2H), 6.86 - 6.79 (m, 1H), 3.81 - 3.68 (m, 4H), 2.80 (t, 6.0 Hz, 2H), 1.96 - 1.86 (m, 2H), 1.79 - 1.67 (m, 2H), 1.43 - 1.25 (m, 12H), 1.07 - 0.89 (m, 2H); LRMS [M+H]⁺: 415, 99% a/a.</p>
<p>A.013</p>	 <p>Chemical Formula: C₁₇H₂₂N₄O₂ Molecular Weight: 314.38</p>	<p>D</p> <p>¹H NMR (SO(CD₃)₂, 400 MHz) δ 8.48 (d, J = 8.0 Hz, 2H), 8.43 (d, J = 8.0 Hz, 1H), 8.31 (dd, J = 1.0, 7.5 Hz, 1H), 8.00 - 7.84 (m, 2H), 3.80 - 3.61 (m, 4H), 2.40 (d, J = 6.5 Hz, 2H), 1.97 - 1.64 (m, 5H), 1.33 (qd, 3.0, 12.5 Hz, 2H), 1.26 - 1.11 (m, 1H), 1.06 - 0.91 (m, 2H); LRMS [M+H]⁺: 315, 99% a/a.</p>

Appendix B Copyright permissions

Graph 5: Reprinted with permission from Chung, C.-W.; Coste, H.; White, J. H.; Mirguet, O.; Wilde, J.; Gosmini, R. L.; Delves, C.; Magny, S. M.; Woodward, R.; Hughes, S. A.; Boursier, E. V.; Flynn, H.; Bouillot, A. M.; Bamborough, P.; Brusq, J.-M. G.; Gellibert, F. J.; Jones, E. J.; Riou, A. M.; Homes, P.; Martin, S. L.; Uings, I. J.; Toum, J.; Clément, C. A.; Boullay, A.-B.; Grimley, R. L.; Blandel, F. M.; Prinjha, R. K.; Lee, K.; Kirilovsky, J.; Nicodeme, E. *J. Med. Chem.* **2011**, *54*, 3827 – 3838. Copyright 2011 American Chemical Society."

Graph 6: Reprinted with permission from Chung, C.-W.; Dean, A. W.; Woolven, J. M.; Bamborough, P. *J. Med. Chem.* **2012**, *55*, 576 – 586. Copyright 2012 American Chemical Society."

Figure 3: From Jenuwein, T.; Allis, C. D. *Science* **2001**, *293*, 1074 – 1080. Reprinted with permission from AAAS.

Figure 15: From Johansson, C.; Tumber, A.; Che, K.; Cain, P.; Nowak, R. Gileadi, C. Oppermann, U. *Epigenomics* **2014**, *6*, 89 – 120. Republished with permission from Future Medicine Ltd.

Figure 19: Adapted from Berry, W. L.; Janknecht, R. *Cancer Res.* **2013**, *73*, 2936 – 2942 KDM4/JMJD2 histone demethylases: epigenetic regulators in cancer cells, with permission from AACR.

Figure 57: Adapted from Histone Recognition and Large-Scale Structural Analysis of the Human Bromodomain Family, Filippakopoulos, P., Picaud, S., Mangos, M., Keates, T., Lambert, J.P., Barsyte-Lovejoy, D., Felletar, I., Volkmer, R., Muller, S., Pawson, T., Gingras, A.C., Arrowsmith, C.H., Knapp, S. *Cell* **2012**, *149*, 214 – 231. Used under a Creative Commons licence - <http://creativecommons.org/licenses/by/3.0/legalcode>.